

The Role of STATs in TLR Signalling

A thesis submitted for the degree of

Doctor of Philosophy (PhD)

To the

Faculty of Medicine, Nursing and Health Sciences

Monash University

By

Kevin Luu

B. Biomed. Sc. (Hons)

Centre for Innate Immunity and Infectious Diseases

Monash Institute of Medical Research

Monash University, Australia

2014

Table of Contents

Abstract	vi
Declaration	viii
Copyright	ix
Acknowledgements	x
Abbreviations	xi
List of Figures	xx
Chapter 1	xx
Chapter 3	xxii
Chapter 4	xxiv
Chapter 5	xxv
List of Tables	xxvi
Chapter 1	xxvi
Chapter 2	xxvi
Chapter 3	xxvi
Chapter 5	xxvi
Presentations at Meetings and Conferences	xxvii
Chapter 1: Literature Review	1
1.1 – Immune system	2
1.2 - Toll-like receptors	3
1.2.1 - Toll-like receptors structure and function	4
1.2.2 - Cell surface TLRs	9
1.2.3 - Intracellular TLRs	20
1.2.4 – Cellular localisation of TLRs	28
1.3 - Toll-like receptor ligands	34
1.3.1 – Endogenous ligands	35
1.4 - Toll-like receptor signalling	38
1.4.1 - MyD88-dependent pathway	39
1.4.2 - MyD88-independent pathway	45
1.4.3 - Signalling molecules	50
1.5 - JAK-STAT pathway	65
1.5.1 – STAT structure	65
1.5.2 - STAT1	75

1.5.3 - STAT3.....	79
1.6 – Rationale and aims of my PhD project.....	83
Chapter 2: Materials and Methods.....	85
2.1 - Tissue culture.....	86
2.1.1 - Cell line passaging.....	86
2.1.2 - Generation of Mouse Embryonic Fibroblasts (MEFs).....	87
2.1.3 – Generation of Bone Marrow-derived Macrophages (BMMs).....	87
2.1.4 - Viable cell counting.....	88
2.1.5 - Thawing cells.....	88
2.1.6 - Freezing cells.....	88
2.2 – TLR stimulation of RAW264.7 murine macrophages.....	89
2.2.1 - Preparation of RAW264.7 murine macrophages.....	89
2.2.2 - Cell harvesting.....	89
2.2.3 - Nuclear protein extracts.....	91
2.3 – Mitochondrial isolation.....	91
2.3.1 – THP1 cell preparation.....	91
2.3.2 – Cell harvesting and mitochondria isolation.....	92
2.4 - Sodium Dodecyl Sulfate-Polyacrylamide Gel Electrophoresis (SDS-PAGE).....	92
2.5 - Western blot.....	94
2.5.1 - Wet transfer.....	94
2.5.2 - Immunoblotting.....	94
2.5.3 - Enhanced Chemiluminescence (ECL) detection.....	96
2.5.4 - Odyssey infrared system.....	96
2.5.5 - Membrane stripping.....	96
2.5.6 – Densitometry analysis.....	96
2.6 - DNA manipulation.....	97
2.6.1 - Mini-preparations of plasmid DNA.....	97
2.6.2 - Midi-preparations of plasmid DNA.....	97
2.6.3 – Restriction endonuclease digest.....	98
2.6.4 – Agarose gel electrophoresis.....	98
2.6.5 – Site-directed mutagenesis.....	99
2.6.6 – DNA quantification.....	101
2.6.7 - Glycerol stocks.....	101
2.6.8 - DNA sequencing.....	101

2.7 - Immunoprecipitation	101
2.7.1 - Cell transfection	101
2.7.2 - Ectopic immunoprecipitation.....	102
2.7.3 – Semi-endogenous immunoprecipitation.....	103
2.8 - Expression and purification of murine-GST-TRAF6 and GST	103
2.8.1 - Batch purification of proteins	104
2.8.2 - Coomassie R250 blue staining.....	104
2.9 - GST pull-down assay	105
2.10 - Confocal microscopy	105
2.10.1 - Coverslip and cell preparation	105
2.10.2 - Cell fixation.....	106
2.10.3 - Cell permeabilization	106
2.10.4 - Immunostaining	106
2.11 - High content screen	107
2.12 - Small Interfering RNA (siRNA) transfection	108
2.13 - Enzyme-linked Immunosorbent Assay (ELISA).....	108
2.14 – MTT cell proliferation assay	109
2.15 - Luciferase reporter assay	109
2.16 – TRANSFAC promoter analysis.....	110
2.17 - Statistical analysis	110
Chapter 3: Demonstrating the Cross-talk Between TLR and JAK-STAT Signalling	111
3.1 – Introduction.....	112
3.2 – Results	115
3.2.1 – Serine phosphorylation of STAT1 following TLR ligand stimulation.....	115
3.2.2 - Serine phosphorylation of STAT1 is dependent on MyD88/TRIF but not IRF3/7	123
3.2.3 – Serine phosphorylation of STAT3 following TLR stimulation	126
3.2.4 – Serine phosphorylation of STAT3 is dependent on MyD88/TRIF and not IRF3/7	135
3.2.5 – TRAF6 binding motifs in STAT1 and STAT3.....	139
3.2.6 – Production of recombinant GST-TRAF6 fusion protein.....	139
3.2.7 – STAT1 and STAT3 interact with recombinant GST-TRAF6 fusion protein	139
3.2.8 – Semi-endogenous immunoprecipitation of TRAF6 and STAT1	143
3.2.9 – STAT3 interaction with TRAF6 following TLR4 and TLR2 stimulation	147
3.2.10 – Identifying the kinase that phosphorylates STAT1 and STAT3.....	150
3.2.11 – STAT3 Ser-727 phosphorylation is not attenuated in PKR-deficient cells.....	154

3.3 - Discussion.....	156
Chapter 4: Ser-727 STAT3, Mitochondria and Innate Immunity.....	165
4.1 – Introduction.....	166
4.2 – Results	168
4.2.1 – TLR-induced mitochondrial membrane destabilisation	168
4.2.2 – TLR stimulation induces mitochondrial reactive oxygen species production	171
4.2.3 – Mitochondrial destabilisation is also observed in fibroblasts.....	171
4.2.4 – TLR stimulation increases nuclear localisation of STAT3	174
4.2.5 – TLR-induced pSer-727 STAT3 doesn't localise to the nucleus.....	174
4.2.6 – Rapid nuclear localisation of pTyr-705 STAT3 is not observed in TLR stimulated cells	179
4.2.7 – pSer-727 STAT3 localises to mitochondria.....	179
4.2.8 – Total STAT3 does not localise to mitochondria and remains in the nucleus	181
4.2.9 – TRAF6 colocalises with pSer-727 STAT3, but this complex is not detected in mitochondria	186
4.2.10 – pSer-727 STAT3 and TRAF6 can be detected in mitochondrial extracts.....	190
4.2.11 –STAT3 S727A mutant inhibits NFκB activation.....	190
4.2.12 – STAT3 depletion using siRNA.....	193
4.2.13 – IL-6 is attenuated in STAT3-depleted macrophages, but TNF-α production is not affected	193
4.3 - Discussion.....	197
Chapter 5 – The Role of STAT1 Ser-727 in TLR-mediated Inflammation	205
5.1 – Introduction.....	206
5.2 – Results	210
5.2.1 – STAT1 localises to the nucleus following LPS stimulation.....	210
5.2.2 – LPS induces pSer-727 STAT1 nuclear translocation	210
5.2.3 – Nuclear pTyr-701 STAT1 is only detected 60 minutes post-LPS stimulation	214
5.2.4 – pSer-727 STAT1 does not colocalise with mitochondria.....	214
5.2.5 – Nuclear localisation of pSer-727 STAT1 can be induced by multiple TLRs.....	216
5.2.6 – Hyperactive F/F MEFs display decreased cytokine expression in the absence of STAT1.	219
5.2.7 – STAT1 S727A mutant suppresses TLR2-mediated NFκB promoter activity.	219
5.2.8 – Nuclear localisation of STAT1 is not affected in STAT1 S727A BMMs	222
5.2.9 – TNF-α, but not IL-6 or RANTES production is diminished in STAT1 S727A BMMs.....	228
5.3 - Discussion.....	239

Chapter 6: Discussion and Conclusion	249
Appendix I – Formulation of Buffers and Solutions	258
Appendix II – Primer Sequences.....	270
Appendix III – List of Manufacturers	272
Bibliography	275

Abstract

Innate immunity is crucial to living beings as it allows both multi-cellular and single cellular organisms to detect and eradicate invading pathogens. The Toll-like receptors (TLRs) are pivotal to the innate immune response as they bind microbial components and activate the prototypic proinflammatory molecule, Nuclear Factor κ B (NF κ B). The activation of NF κ B is critical to initiating an anti-pathogenic state enabling the clearance of pathogens and the instigation of the adaptive immune response.

Whilst the downstream signalling mechanisms of TLR signalling have been studied in great detail, more focus on cross-talk between signalling pathways is required. The main aim of this thesis is the examination of cross-talk between Janus Kinase-Signal Transducer and Activator of Transcription (JAK-STAT) and TLR pathways, and the role STAT1 and STAT3 have in TLR-induced inflammatory responses.

Following stimulation with TLR ligands, STAT1 and STAT3 were demonstrated to undergo a rapid Ser-727 phosphorylation independent of tyrosine phosphorylation. The Ser-727 phosphorylation of STAT1 and STAT3 was found to be dependent on Myeloid Differentiation Primary Response Gene 88 (MyD88) and Toll/Interleukin-1 Receptor (TIR) Domain-containing Adapter Inducing Interferon- β (TRIF) signalling but not secretion of Interferon- β (IFN- β). Bioinformatic analyses of STAT1 and STAT3 identified putative Tumour Necrosis Factor Receptor-associated Factor 6 (TRAF6) Binding Motifs (T6BMs), a well-documented site important for association with TRAF6, a central molecule in TLR signalling. STAT1 and STAT3 were shown to interact with TRAF6 through overexpression assays and endogenous immunoprecipitations.

TLR stimulation was found to induce mitochondrial reactive oxygen species (mtROS) production thought to be a result of STAT3 mitochondrial localisation. STAT3 and TRAF6 were found to localise to mitochondria separately, although the two proteins colocalised in the cytoplasm. STAT3 S727A mutants also failed to drive activation of the NF κ B promoter Tripalmitoyl-S-glycerol-L-Cys (Pam₃Cys) stimulation demonstrating the ability of Phosphoserine (pSer)-727 STAT3 to modulate cytokine production. Examination of cytokine production following TLR stimulation showed that siRNA depletion of STAT3 abolished Interleukin-6 (IL-6) production and diminished Tumour Necrosis Factor- α (TNF- α) levels. The findings here suggest that pSer-727 STAT3 colocalises to the mitochondria, where it is proposed to interact with the Electron Transport

Chain (ETC) and generate ROS production, this in turn drives expression of proinflammatory cytokines.

Confocal microscopy conducted on TLR-stimulated cells displayed rapid nuclear localisation of pSer-727 STAT1, with Tyr-701 STAT1 only translocating to the nucleus at 60 minutes. A range of TLR ligands was able to induce pSer-727 STAT1 nuclear localisation demonstrating this to be a board TLR-induced response. Interestingly, STAT1 S727A mutants failed to drive NFκB and IL-6 activation, but not TNF-α following Pam₃Cys stimulation. STAT1 S727A Bone Marrow-derived Macrophages (BMMs) however, were found to produce less TNF-α, but not IL-6 or Regulated on Activation Normal T Cell Expressed and Secreted (RANTES). Nuclear translocation of STAT1 was not observed to be different in WT and STAT1 S727A BMMs, but may be an issue with being unable to directly detect pSer-727 STAT1. To further assess STAT1s role in driving inflammatory responses Glycoprotein 130 (gp130)^{Y757F/Y757F} (F/F) STAT1-deficient Mice Embryonic Fibroblasts (MEFs) were employed. Following TLR stimulation, TNF-α production was severely ablated, whilst IL-6 production was not affected. This aligns with the BMM data, suggesting the pSer-727 STAT1 predominately regulates TLR-induced inflammatory responses through regulation of TNF-α production.

My findings propose a new and novel means of regulating inflammatory responses by TLRs. The rapid serine phosphorylation of STAT1 and STAT3 may be used by the TLRs as a means of fine-tuning the innate immune response, with STAT1 acting upon TNF-α and STAT3 predominately regulating IL-6. Serine phosphorylation of the STATs is traditionally thought to increase transcriptional activity, but this study is the first in demonstrating its ability to modulate proinflammatory responses.

Declaration

This is to certify that this thesis contains no material that has been accepted for the award of any other degree or diploma in any university or other institution, and to the best of my knowledge, contains no material previously published or written by another person, except where due reference is made in the text of the thesis.

Kevin Luu

Copyright

Notice 1

Under the Copyright Act 1968, this thesis must be used only under the normal conditions of scholarly fair dealing. In particular no results or conclusions should be extracted from it, nor should it be copied or closely paraphrased in whole or in part without the written consent of the author. Proper written acknowledgement should be made for any assistance obtained from this thesis.

Notice 2

I certify that I have made all reasonable efforts to secure copyright permissions for third-party content included in this thesis and have not knowingly added copyright content to my work without the owner's permission.

Acknowledgements

The completion of this PhD would not have been possible without my main supervisor, Dr. Ashley Mansell. Your vast knowledge of cell signalling pathways and specific scientific papers has never ceased to amaze me. Thank you for your patience and guidance over the years. Our meetings were always inspiring and motivating, giving me hope when the results were not always as predicted.

A special thanks to all the members of the Mansell group (Dr Kristie Jenkins, Dr Brett Verstak, Dr Tali Lang, Kathryn Hjerrld, Dr Jing Jing Khoo and Matthew Mangan) throughout the years for their help with troubleshooting problems and random bits of wisdom. Also thank you to all past and present members of the CIID for their help, expertise and reagents. Thanks to Dr. Trevor Wilson with his help on the high content screen and Dr Camden Lo on all things microscopy related.

My PhD would not have being as fun and enjoyable without Louise McLeod, Jodee Gould, Dr Ka Yee Fung, Dr Alec Drew, Sebastian Stifter and Sam Forster. Lou, our discussions of fashion was always insightful and entertaining. And thanks for making me get my haircut, though a \$7 haircut will always be a bargain. Jodee, your ability to break programs and computers just perplexes me; I guess I will just never understand how you manage to do it. Ka Yee, you were always are joy to hang around with and I'm sorry for being mean to you. Alec, you always have interesting stories to tell and our discussions were always stimulating. Seb, Friday night gaming will need to come back now that I have time. We still need to finish the Borderlands 2 DLC! Sam, for all our conversations on all things geek including computers, phones and all other gadgets and tech. Thanks everyone for all the entertaining lunch times and discussion topics. Coming into the lab would not have been as pleasant without any of you guys.

To my uni friends Anna, Benny, Brendan, Marty, Pete, Polly and Shaan thanks for all the social outings, annual trip to EP and the very memorable trips to Tasmania to visit Kizza. It was always good to have some time away from my PhD and I hope we can continue to have many more social outings.

Last but not least, thanks to Dad, Mum (for packing me lunch everyday), Billy and Andy for the never-ending support. Although you guys may never know exactly what I do, at least I can finally say yes when you ask "Are you finished studying yet?" A special thank you to Polly for always being so supportive, understanding and making me work on my thesis instead of procrastinating.

Abbreviations

°C	Degree Celsius
aa	Amino acid
ANOVA	Analysis of variance
AP-1	Activator protein 1
AP3	Adaptor protein 3
APS	Ammonium persulfate
ARM	Armadillo repeat motif
ASC	Apoptosis-associated speck-like protein containing a CARD
ASOs	Antisense oligonucleotides
Asp	Asparagine
ATP	Adenosine triphosphate
BMDCs	Bone marrow-derived dendritic cells
BME	2-Mercaptoethanol
BMMs	Bone marrow derived macrophages
bp	Base pair
BPI	Bactericidal and permeability-increasing protein
BRCA1	Breast cancer 1, early onset
BSA	Bovine serum albumin
Btk	Bruton's tyrosine kinase
cAMP	Cyclic adenosine monophosphate
CARD	Caspase activation and recruitment domains
CBP	CREB-binding protein
CCR2	Chemokine receptor type 2
CD	Cluster of differentiation
CDK	Cyclin-dependent kinase
CETP	Cholesterol ester transfer protein
CHO	Chinese hamster ovary
ciAP	Cellular inhibitor of apoptosis
CK	Casein Kinase
CLL	Chronic lymphocytic leukaemia
CLR	C-type lectin receptor
CMV	Cytomegalovirus

CO₂	Carbon dioxide
CpG	2'-deoxyribo(cytidine-phosphate-guanosine)
CREB	cAMP response element binding protein
CRP	C-reactive protein
CSF	Colony stimulating factor
CUE	Coupling of Ubiquitin Conjugation to ER Degradation
DAMP	Damage-associated molecular patterns
DCs	Dendritic cells
DD	Death domain
DHE	Dihydroethidium
DMEM	Dulbecco's modified Eagle's medium
DMSO	Dimethyl sulfoxide
DNA	Deoxyribonucleic acid
DNase	Deoxyribonuclease
dNTP	Deoxyribonucleotide triphosphate
DPBS	Dulbecco's phosphate buffered saline
dsDNA	Double-stranded deoxyribonucleic acid
dsRNA	Double-stranded ribonucleic acid
DTT	Dithiothreitol
EBV	Epstein-Barr virus
ECL	Enhanced chemiluminescence
ECSIT	Evolutionarily conserved signalling intermediate in Toll pathways
EDTA	Ethylenediaminetetraacetic acid
EGF	Epidermal growth factor
ELISA	Enzyme-linked immunosorbent assay
ER	Endoplasmic reticulum
ERGIC	ER-Golgi intermediate compartment
ERK	Extracellular signal-regulated kinases
ETC	Electron transport chain
EtOH	Ethanol
F/F	gp130 ^{Y757F/Y757F}
FADD	Fas-associated death domain
FasL	Fas ligand
FBS	Fetal bovine serum

FliC	Flagella filament protein
GAS	γ -IFN activation site
Gbp2	Guanylate Binding Protein 2
G-CSF	Granulocyte colony stimulating factor
GF	Glial fibrillary
Glu	Glutamic acid
GOLD	Golgi dynamics
gp130	Glycoprotein 130
GPI	Glycosylphosphatidylinositol
GRIM-19	Gene associated with retinoic-interferon-induced mortality-19
GRP94	Glucose-regulated protein of 94 kDa
GST	Glutathione S-transferase
GTP	Guanosine triphosphate
H₂SO₄	Sulphuric acid
HCl	Hydrochloric acid
HEK	Human embryonic kidney
HEPES	Hydroxyethyl piperazineethanesulfonic acid
HLA-B27	Human leukocyte antigen-subtypes B*2701-2759
HMEC	Human microvascular endothelial cell
HMGB1	High mobility group box 1
HRP	Horseradish peroxidase
HSP	Heat shock proteins
HSSB	High salt soluble buffer
I/U	International units
IFN	Interferon
IFNAR	Interferon α/β receptor
IGF	Insulin growth factor
IKK	I κ B kinase
IL	Interleukin
IL-1R	Interleukin-1 receptor
IP-10	IFN- γ -induced protein 10 kDa
IPTG	Isopropyl- β -D-thiogalactopyranoside
IRAK	IL-1 receptor-associated kinase
IRF	IFN-regulatory factor

ISGF	IFN-stimulated gene factor
ISRE	IFN-stimulated response element
IκB	Inhibitor of NFκB
JAK	Janus kinase
JNK	c-Jun NH ₂ -terminal kinase
K48	Lysine 48
K63	Lysine 63
KCl	Potassium chloride
kDa	Kilodalton
KH₂KPO₄	Potassium dihydrogen phosphate
L	Litres
LAMP2	Lysosome-associated membrane glycoprotein 2
LB	Luria-Bertani
LBP	LPS-binding protein
LGP2	Laboratory of genetics and physiology 2
LMCV	Lymphocytic choriomeningitis virus
LMP2	Low molecular mass polypeptide 2
LPS	Lipopolysaccharide
LROs	Lysosomal-related organelles
LRR	Leucine-rich repeat
LRRCT	Leucine-rich repeat C-terminal
LRRNT	Leucine-rich repeat N-terminal
LSSB	Low salt soluble buffer
LTA	Lipoteichoic acid
LT-LBP	Lipid transfer or lipopolysaccharide binding protein
M	Molar
Mal	MyD88 adaptor-like
MAP	Mitogen-activated protein
MAPK	Mitogen-activated protein kinases
MAPKKK	Mitogen-activated protein kinase kinase kinase
MAR1	Mouse IFN-α/β receptor 1
MCL-1	Myeloid cell leukaemia sequence 1
MDA5	Melanoma differentiation-associated gene 5
mDCs	Myeloid dendritic cells

MEFs	Mouse embryonic fibroblasts
MEK	Mitogen-activated protein kinase kinase
MeOH	Methanol
mg/ml	Milligrams per millilitre
MgCl₂	Magnesium chloride
MgSO₄	Magnesium sulphate
MKK	MAP kinase kinase
ml	Millilitre
mM	Millimolar
MQ.H₂O	MilliQ water
mRNA	Messenger ribonucleic acid
MS	Myristoylation site
mtROS	Mitochondrial ROS
MTT	Methylthiazolyldiphenyl-tetrazolium bromide
MyD88	Myeloid differentiation primary response gene 88
Na₂CO₃	Sodium carbonate
Na₂HPO₄	Disodium hydrogen phosphate
NAC	N-acetyl-cysteine
NaCl	Sodium chloride
NADPH	Nicotinamide adenine dinucleotide phosphate
NaF	Sodium fluoride
NaHCO₃	Sodium hydrogen carbonate
NALP	NACHT, LRR and PYD domains-containing protein
NaOH	Sodium hydroxide
NAP1	NAK-associated protein 1
NaV	Sodium vanadate
NBD	NEMO-binding domain
NDUFAF1	NADH dehydrogenase (ubiquinone) complex I, assembly factor 1
NEMO	NFκB essential modulator
NFκB	Nuclear factor κB
ng	Nanogram
ng/ml	Nanograms per millilitre
NK	Natural killer
NLR	NOD-like receptor

NLRP	NOD-like receptor protein
NLS	Nuclear localisation sequence
nM	Nanomolar
nm	Nanometer
NO	Nitric oxide
NOD	Nuclear oligomerisation domain
Nox2	NADPH oxidase 2
NRLP3	NOD-like Receptor Family, Pyrin Domain Containing 3
NS	Not significant
NZF	Novel zinc finger
OD	Optical density
ODN	Oligodeoxynucleotide
Pam₂CSK₄	Dipalmitoyl-S-glycerol-L-Cys-Ser-(Lys) ₄
Pam₃CSK₄	Tripalmitoyl-S-glycerol-L-Cys-Ser-(Lys) ₄
Pam₃Cys	Tripalmitoyl-S-glycerol-L-Cys
PAMP	Pathogen-associated molecular pattern
PBS	Phosphate buffered saline
PBST	Phosphate buffered saline tween
PCR	Polymerase chain reaction
pDCs	Plasmacytoid dendritic cells
PDGF	Platelet-derived growth factor
PI3K	Phosphoinositide 3-kinase
PIP₂	Phosphatidylinositol-4, 5-bisphosphate
PKC	Protein kinase C
PKR	Protein kinase R
PLTP	Phospholipid transfer protein
pM	Picomolar
PMI	Peptidomimetic inhibitors
PMSF	Phenylmethylsulphonyl fluoride
Poc	Pococurante
Poly (I:C)	Polyinosinic-polycytidylic acid
PRAT4A	Protein-associated with TLR4 A
Pro	Proline
ProST	Proline, serine and threonine

PRR	Pattern recognition receptor
pSer	Phosphoserine
psi	Pounds per square inch
pTyr	Phosphotyrosine
PVDF	Polyvinylidene fluoride
PYD	Pyrin domain
RAGE	Receptor for advanced glycation end-products
RANTES	Regulated and normal T cell expressed and secreted
RecA	Reactive arthritis
RHIM	RIP homotypic interaction motif
RIG-1	Retinoic acid-inducible gene-1
RING	Really interesting new gene
RIP	Receptor-interacting protein
RIPK1	Receptor-interacting protein kinase 1
RLR	RIG-1-like receptors
RNA	Ribonucleic acid
RNAi	Ribonucleic acid interference
ROS	Reactive oxygen species
RPM	Revolutions per minute
RPMI	Roswell park memorial institute
S	Svedberg unit
SAM	Sterile α motifs
SARM	Sterile α and armadillo motif-containing protein
SDS	Sodium dodecyl sulphate
SDS-PAGE	Sodium dodecyl sulphate - polyacrylamide gel electrophoresis
Ser	Serine
Ser/Thr	Serine/threonine
SH2	Src-homology 2
siRNA	Short interfering ribonucleic acid
SLF	Steel factor
SMDD	Small-molecule dimerisation disruptors
SOCS	Suppressor of cytokine signalling
ssDNA	Single-stranded deoxyribonucleic acid
ssRNA	Single-stranded ribonucleic acid

STAT	Signal transducer and activators of transcription
T6BM	TRAF6 binding motif
TAB	TAK1-binding protein
TAD	Transactivation domain
TAE	Tris-acetate-EDTA
TAG	TRAM adaptor with GOLD domain
TAK	TGF- β -activated-kinase
TANK	TRAF-family-member-associated NF κ B activator
TBK	TANK binding kinase
TBS	Tris buffered saline
TBST	Tris-buffered saline tween
TEMED	Tetramethylethylenediamine
TGF	Transforming growth factor
T_H1	T helper type 1
TICAM	TIR domain-containing molecule
TIR	Toll/IL-1R homology domain
TIRAP	TIR domain-containing adaptor protein
TK	Thymidine kinase
TLR	Toll-like receptor
TM	Transmembrane
TNFR	Tumour necrosis factor receptor
TNF-α	Tumour necrosis factor- α
TOM22	Translocase of the outer mitochondrial membrane 22
TRADD	TNFR type 1-associated death domain protein
TRAF	Tumour necrosis factor receptor-associated factor
TRAM	TRIF-related adaptor molecule (aka TICAM2)
TRANCER	TNF-related activation-induced cytokine receptor
TRIF	TIR domain containing adaptor inducing interferon β (aka TICAM1)
TRIKA	TRAF6-regulated IKK activator
TRIL	TLR4 interactor with LRRs
Tris	Tris (hydroxymethyl) aminomethane
TXNIP	Thioredoxin-interacting protein
TYK2	Tyrosine kinase 2
Tyr	Tyrosine

U/ml	Units per millilitre
UNC93B1	Unc-93 homolog B1
UV	Ultraviolet
V	Volts
v/v	Volume per volume
VDAC1	Voltage-dependent anion channels 1
VEGF	Vascular endothelial growth factor
VLR	Variable lymphocyte receptor
w/v	Weight per volume
WCL	Whole cell lysate
Wild-type	WT
zVAD	Benzyloxycarbonyl-Val-Ala-Asp
µg	Microgram
µg/ml	Micrograms per millilitre
µl	Microlitre
µM	Micromolar

List of Figures

Chapter 1

Figure	Title	Page Number
1.1	Interleukin-1 receptor and Toll-like receptor	5
1.2	Structure of the TIR domain of TLR10 as a Dimer	7
1.3	Ribbon diagram of the LRR domain of TLR3.	8
1.4	Overall TLR structure	10
1.5	Overall Structure of TLR2/TLR1 bound to Pam ₃ CSK ₄ lipopeptide	12
1.6	Overall structure of mouse TLR2/TLR6 bound to Pam ₂ CSK ₄ lipoprotein	13
1.7	Overall structure of mouse TLR4-MD2 complex and MD2	15
1.8	Overall structure of human MD2 bound to eritoran	16
1.9	Overall structure of the TLR4-MD2-LPS complex	17
1.10	Overall structure of human and mouse CD14	19
1.11	Overall structure of zebrafish TLR5 bound to flagellin	21
1.12	Overall structure of TLR3	23
1.13	Crystal Structure of TLR3 bound to dsRNA	24
1.14	Toll-like receptor ligands	37
1.15	Schematic representation of Toll-like Receptors and TIR containing adaptors	40
1.16	TLR-mediated signalling	41
1.17	IRAK family members	53 & 54
1.18	TRAF family members	58
1.19	Structural analysis of TRAF6	59
1.20	Structure of the N-terminal region of TRAF6	62
1.21	Dimerization of the TRAF6 N-terminal domain	63
1.22	JAK-STAT signalling in type I, II interferon and Interleukin-6	66
1.23	STAT domains	67
1.24	Structure of STAT1 homodimer	69
1.25	Structure of STAT3 homodimer	70
1.26	Structure of STAT1 tetramer	71
1.27	Structure of STAT1 dimer interfaces	72
1.28	Two possible STAT1 dimer conformations	73
1.29	Structure of monomeric STAT3	74

1.30	Interaction between TLR4 and type 1 IFN receptor via production of IFN- β and subsequent activation of JAK-STAT signalling	77
1.31	TLR9 mediated activation of STAT1 in DC vs. macrophages	80

Chapter 3

Figure	Title	Page Number
3.1	IFN- α stimulation induces rapid Ser-727 and Tyr-701 phosphorylation of STAT1	116
3.2	The TLR2 ligand, Pam ₃ Cys, induces rapid Ser-727 phosphorylation of STAT1	117
3.3	STAT1 Ser-727 phosphorylation shows delayed kinetics in response to the TLR3 ligand, poly (I:C)	118
3.4	Rapid Ser-727 phosphorylation with no corresponding Tyr-701 phosphorylation is observed in RAW 264.7 cells stimulated with the TLR4 ligand, LPS	120
3.5	TLR7 ligand, loxoribine, induces Ser-727 phosphorylation of STAT1 albeit with delayed kinetics	121
3.6	Ser-727 phosphorylation of STAT1 is delayed when stimulated with the TLR9 ligand, CpG DNA	122
3.7	Wild-type C57/BL6 immortalised macrophages stimulated with TLR agonists demonstrate Ser-727 phosphorylation of STAT1	124
3.8	MyD88/TRIF ^{-/-} immortalised macrophages fail to induce Ser-727 phosphorylation of STAT1 when stimulated with TLR agonists	125
3.9	Ser-727 phosphorylation of STAT1 is independent of JAK-STAT signalling as IRF3/7 ^{-/-} immortalised macrophages still induce Ser-727 phosphorylation of STAT1 following TLR agonists stimulation	127
3.10	IFN- α induces rapid Tyr-705 and Ser-727 phosphorylation of STAT3	128
3.11	Rapid induction of pSer-727 STAT3 following stimulation with Pam ₃ Cys	129
3.12	Poly (I:C) induces rapid Ser-727 phosphorylation of STAT3 with pTyr-705 STAT3 being detected at 120 minutes post-stimulation	131
3.13	LPS induces rapid Ser-727 phosphorylation of STAT3 and pTyr-705 STAT3 can be detected at 120 minutes post-stimulation	132
3.14	Stimulation with loxoribine induces rapid phosphorylation of STAT3 at Ser-727	133
3.15	CpG DNA induces rapid Ser-727 phosphorylation of STAT3 with no corresponding Tyr-705 phosphorylation	134

3.16	Stimulation with TLR agonists induces Ser-727 phosphorylation of STAT3 in wild-type C57/BL6 immortalised macrophages	136
3.17	In MyD88/TRIF ^{-/-} immortalised macrophages stimulation with TLR agonists fails to induce Ser-727 phosphorylation of STAT3	137
3.18	Ser-727 phosphorylation of STAT3 is not abolished in IRF3/7 ^{-/-} immortalised macrophages following stimulation with TLR agonists	138
3.19	Coomassie stain of recombinant GST-TRAF6 fusion protein	141
3.20	STAT1 interacts with recombinant TRAF6	142
3.21	STAT3 interacts with recombinant TRAF6	144
3.22	STAT1 interacts with TRAF6 at basal levels and following LPS stimulation	145
3.23	In THP1 cells, STAT1 interacts with TRAF6 in unstimulated and Pam ₃ Cys stimulated cells	146
3.24	STAT3 interaction with TRAF6 occurs in resting cells and following LPS stimulation	148
3.25	THP1 cells demonstrate interaction of STAT3 and TRAF6 in unstimulated and Pam ₃ Cys stimulated cells	149
3.26	Serine phosphorylation of STAT1 is not affected by treatment with MEK1/2, p38k, JNK, PI3K and PKR inhibitors	152
3.27	STAT3 Ser-727 phosphorylation is not affected by MEK1/2, p38k, JNK and PI3K, but PKR may be involved in STAT3 serine phosphorylation	153
3.28	Ser-727 phosphorylation and STAT3 is not inhibited in PKR KO cells	155

Chapter 4

Figure	Title	Page Number
4.1	Mean Mitotracker Red intensity decreases following TLR stimulation	169
4.2	Mean Mitotracker Red intensity decreases marginally in macrophages	170
4.3	TLR stimulations induces production of ROS	172
4.4	Mitochondrial ROS increases following TLR stimulation	173
4.5	Mean Mitotracker Red intensity decreases greatly in fibroblasts following TLR stimulation	175
4.6	LPS stimulation increase STAT3 detection in the cytoplasm	176 & 177
4.7	pSer-727 STAT3 can be detected in the cytoplasm following LPS stimulation	178
4.8	pTyr-705 STAT3 increases following LPS stimulation and can be detected in the nucleus 60 minutes post-stimulation	180
4.9	LPS stimulation results in pSer-727 STAT3 co-localisation with mitochondria	182 & 183
4.10	Intensity profile plot demonstrates co-localisation of Mitotracker Red and pSer-727 STAT3	184
4.11	Unphosphorylated STAT3 does not co-localise with mitochondria	185
4.12	LPS stimulation results in pSer-727 STAT3 co-localisation with TRAF6 and pSer-727 STAT3 and TRAF6 can be observed to co-localise with mitochondria individually	187 & 188
4.13	pSer-727 STAT3 co-localises with TRAF6 and mitochondria, TRAF6 also co-localises with mitochondria however of a complex of pSer-727 STAT3/TRAF6 in mitochondria is not observed	189
4.14	pSer-727 STAT3 and TRAF6 can be detected in mitochondria	191
4.15	STAT3 S727A acts as a dominant negative inhibiting activation of <i>Nfkb</i>	192
4.16	STAT3 can be effectively silenced in macrophages	194
4.17	IL-6 production is severely attenuated in STAT3 knockdown RAW 264.7 cells	195
4.18	TNF- α production is not diminished in STAT3 knockdown RAW 264.7 cells, whilst TLR stimulation fails to induce IL-12 production	196

Chapter 5

Figure	Title	Page Number
5.1	LPS stimulation induces nuclear localisation of STAT1	211 & 212
5.2	Rapid nuclear localisation of pSer-727 STAT1 following LPS stimulation	213
5.3	Nuclear localisation of pTyr-701 STAT1 is only induced 60 minutes post LPS stimulation	215
5.4	pSer-727 STAT1 does not localise to mitochondria following LPS stimulation	217
5.5	pSer-727 STAT1 can be detected in both cytoplasm and nucleus following TLR stimulation	218
5.6	F/F STAT1 ^{-/-} MEFs are impaired in their ability to induce TNF production in response to TLR stimulation	220
5.7	IL-6 production is not reduced in F/F STAT1 ^{-/-} MEFs in response to Pam ₃ Cys and LPS except following CpG DNA treatment	221
5.8	STAT1 S727A acts as a dominant negative to inhibit TLR2-mediated NFκB activation	223
5.9	STAT1 S727A does not suppress TLR2-induced TNF-α activation	224
5.10	STAT1 S727A suppresses <i>Il-6</i> promoter activity following Pam ₃ Cys challenge	225
5.11	Nuclear localisation of STAT1 can be observed in both WT and STAT1 S727A BMMs following Pam ₃ Cys stimulation	226 & 227
5.12	Following LPS stimulation, STAT1 is observed to translocate to nuclei in both WT and STAT1 S727A BMMs	229 & 230
5.13	Nuclear localisation of STAT1 is similar between WT and STAT1 S727A BMMs post-CpG DNA stimulation	231 & 232
5.14	Nuclear localisation of STAT1 is not affected in STAT1 S727A BMMs	233
5.15	TNF production in STAT1 S727A BMMs is attenuated in response to TLR ligands	234
5.16	Production of IL-6 is not affected in STAT1 S727A BMM compared to WT BMMs when stimulated with TLR ligands	236
5.17	RANTES production is not inhibited in STAT1 S727A BMMs in response to TLR stimulation	237
5.18	TLR stimulation does not induce IL-12 production in BMMs	238

List of Tables

Chapter 1

Table	Title	Page Number
1.1	Toll-like receptors and their ligands	36
1.2	Putative TRAF6 binding motifs in immune signalling molecules	60

Chapter 2

Table	Title	Page Number
2.1	TLR ligands and the concentrations used	90
2.2	Compositions of separating and stacking gels.	93
2.3	List of antibodies and dilutions	95
2.4	Cycle parameters for PCR	100

Chapter 3

Table	Title	Page Number
3.1	Putative TRAF6 binding motifs in immune signalling molecules	114
3.2	Putative TRAF6 binding motifs in STAT1 and STAT3	140
3.3	Kinases responsible for STAT1 and STAT3 Ser-727 phosphorylation	151

Chapter 5

Table	Title	Page Number
5.1	Promoter analysis indicating potential STAT1 binding sites	246

Presentations at Meetings and Conferences

2012 TLROZ Conference.

STATs in TLR Signalling.

Kevin Luu, Trevor Wilson, Brendan Jenkins, Paul Hertzog & Ashley Mansell.

2012 Southern Health Research Week.

The Role of STATs in TLR Signalling.

Kevin Luu, Trevor Wilson, Brendan Jenkins, Paul Hertzog & Ashley Mansell.

2012 Monash Institute of Medical Research Scientific Retreat.

The Role of STATs in TLR Signalling.

Kevin Luu, Trevor Wilson, Brendan Jenkins, Paul Hertzog & Ashley Mansell.

2011 Monash Institute of Medical Research Student Symposium.

The Role of STATs in TLR Signalling.

Kevin Luu, Kathryn Hjerrild, Tali Lang, Jing Jing Khoo, Brendan Jenkins & Ashley Mansell.

2011 WEHI and CIID Symposium.

The Role of STATs in TLR Signalling.

Kevin Luu, Trevor Wilson, Kathryn Hjerrild, Tali Lang, Jing Jing Khoo, Brendan Jenkins & Ashley Mansell.

2011 Victorian Infection and Immunity Network.

STATs in Innate Immunity.

Kevin Luu, Marcin Ciula, Kristie Jenkins, Paul Hertzog & Ashley Mansell.

2011 Southern Health Research Week.

STATs in Innate Immunity.

Kevin Luu, Marcin Ciula, Kristie Jenkins, Paul Hertzog & Ashley Mansell.

2010 Victorian Infection and Immunity Network.

Investigating the Interaction of TRAF6, STAT1 and STAT3.

Kevin Luu, Marcin Ciula, Kristie Jenkins, Kathryn Hjerrild, Jodee Gould, Paul Hertzog & Ashley Mansell.

2010 Southern Health Research Week.

Investigating the Interaction of TRAF6, STAT1 and STAT3.

Kevin Luu, Marcin Ciula, Kristie Jenkins, Kathryn Hjerrild, Jodee Gould, Paul Hertzog & Ashley Mansell.

Chapter 1: Literature Review

Chapter 1: Literature Review

1.1 – Immune system

The immune system is essential to the survival of all living organisms, as it allows them to eliminate pathogen threats from the host. The immune system in vertebrates consists of two branches: the innate immune system which is also known as the first line of defence and the adaptive immune system, known as the second line of defence. Innate immunity is a rapid response that is mediated by white blood cells such as macrophages and neutrophils (Aderem and Ulevitch, 2000). Whilst adaptive immunity primarily involves the elimination of pathogens and occurs in the late phase of the immune response. The adaptive immune system is highly sophisticated and involves the generation of specific receptors to antigens found within the body. This is mediated through T and B cells and incorporates deoxyribonucleic acid (DNA) rearrangement, giving the adaptive immune system the potential to recognise a wide range of antigens (Akira and Takeda, 2004). Adaptive immunity differs from innate immunity through the specificity of the response and the generation of immunological memory (Akira et al., 2006).

Unlike adaptive immunity which is only found in vertebrates, innate immunity is highly conserved and is present in almost all multi-cellular organisms (Zhu et al., 2007). The innate immune response has always been regarded as a non-specific system that destroys pathogens and presents them to cells of the adaptive immune system. However, studies in the past decade have shown that the innate immune response is far more specific than once thought, with a highly developed ability to discriminate between self and foreign antigens (Akira and Takeda, 2004).

The innate immune system recognises microorganisms through a finite number of germ-line encoded Pattern Recognition Receptors (PRRs). All PRRs share common characteristics, they detect microorganisms through Pathogen Associated Molecular Patterns (PAMPs) and can identify pathogens at any life cycle stage (Akira et al., 2006, Zhu et al., 2007). These PAMPs have three common characteristics that make them ideal targets for innate immunity recognition. First, they are produced by microorganisms, but not the host in which they reside; this allows discrimination between “self” and “non-self” when PAMPs are detected. Second, PAMPs do not vary among microbes of the same class, allowing a limited number of PRRs to identify the existence of a microbial infection. Third, PAMPs are highly conserved among pathogens and these

motifs are essential to the biology of the pathogen, therefore they are not subject to high mutation rates (Medzhitov, 2001). PRRs are also constitutively expressed on cells of a certain type that function independently of immunological memory. Different PRRs interact with specific PAMPs, and these activate specific signalling pathways which lead to varied immune responses. The basic mechanisms involving pathogen recognition in innate immunity is highly conserved, even amongst different species (Akira et al., 2006).

With the discovery of the Toll-like Receptors (TLRs) came a renewed interest in innate immunity. TLRs are now recognised as having an essential role in the innate immune systems recognition of PAMPs, and the activation of the adaptive immune response in mammals (Schnare et al., 2001). TLRs are pivotal in early host defence against microbial invasion, and it is now accepted that activation of innate immunity is a prerequisite for the initiation of adaptive immunity (Akira and Takeda, 2004).

Following the discovery of the TLRs, further families of PRRs have been identified that also recognise PAMPs and shape the immune response. These include the membrane bound C-type Lectin Receptors (CLRs), Cytoplasmic Protein-like the Nuclear Oligomerisation Domain (NOD)-like Receptors (NLRs), and Retinoic Acid-inducible Gene 1 (RIG-1)-like Receptors (RLRs). The CLRs are a family of membrane bound proteins that contain one or more C-type lectin domains and mainly recognise PAMPs from fungi and bacteria (Robinson et al., 2006). The RLR family is made up of three members; RIG-1, Melanoma Differentiation-associated Gene 5 (MDA5) and Laboratory of Genetics and Physiology 2 (LGP2) (Yoneyama and Fujita, 2007). They recognise viruses and activate type I interferons (IFNs) to aid in viral clearance. The NLR family contains more than 20 proteins, with some of these recognising various PAMPs. Some NLR members like NAcHT Leucine-rich Repeat Protein 1 (NALP1) and NALP3 form components of the inflammasome, leading to the cleavage of pro-interleukin (IL)-1 β to its mature form IL-1 β (Martinon et al., 2009). In this review I will be focusing on the function, structure and signalling pathways of the TLRs.

1.2 - Toll-like receptors

The TLR family were discovered through the identification of the gene *Toll* identified in *Drosophila melanogaster*. Initially the *Toll* gene was found to regulate embryonic dorsoventral polarity in the fruit fly (Hashimoto et al., 1988). *Toll* mutant flies were also shown to be highly susceptible to

fungal infections, which demonstrated the importance of innate immunity as a means of detecting invasion by microorganisms (Lemaitre et al., 1996). It was demonstrated that the *Toll* gene and its extracellular ligand, spätzle, also activated an antifungal peptide gene, Drosomycin. (Lemaitre et al., 1996)

Mammalian homologues of the *Toll* gene were subsequently discovered through expressed sequence tags and database searches (Medzhitov et al., 1997). Functional studies performed in vertebrates have not, thus far, uncovered a role for TLRs in development. Rather mammalian TLRs have vital roles in the direct recognition of pathogens, the initiation of the Nuclear Factor κ B (NF κ B) signalling pathway and the commencement of both innate and adaptive immunity (Leulier and Lemaitre, 2008). To date, 13 mammalian TLRs have been discovered (Uematsu and Akira, 2007). Each member of the family detects distinct PAMPs and also signal through their respective pathways resulting in varied immune responses that eliminate or halt the progression of an infection (Takeda and Akira, 2004).

Ten functional TLRs have been identified in humans, each recognising different PAMPs (Werts et al., 2006). An eleventh human TLR does exist; however it contains a stop codon in the gene rendering the receptor non-functional. TLRs are expressed on various immune cells: including macrophages, dendritic cells (DCs), B cells and certain types of T cells. Even non-immune cells such as fibroblasts, mucosal epithelial and endothelial cells also express TLRs (Akira et al., 2006, Verstak et al., 2007).

1.2.1 - Toll-like receptors structure and function

The TLRs are type I integral membrane glycoproteins, where all members of the TLR family contain three domains; cytoplasmic, transmembrane and extracellular domains (Akira et al., 2006, Kobayashi et al., 2006, Bowie and O'Neill, 2000). The cytoplasmic domain of the TLRs is characterized by a common motif termed the Toll/interleukin-1 Receptor (TIR) domain that is homologous to the Interleukin-1 Receptor (IL-1R) (Gay and Keith, 1991). The cytoplasmic domain functions as a signalling component, recruiting signal adaptor molecules via TIR-TIR homotypic interactions (Kobayashi et al., 2006). Within the TIR domain there are three motif sequences (terminal boxes) that are conserved between TLRs and IL-1Rs; this region is crucial for signalling and is ~200 residues in length (Figure 1.1) (Bowie and O'Neill, 2000). Sequence conservation is relatively low between TIR domains, ranging between 20-30%, with domains varying in length

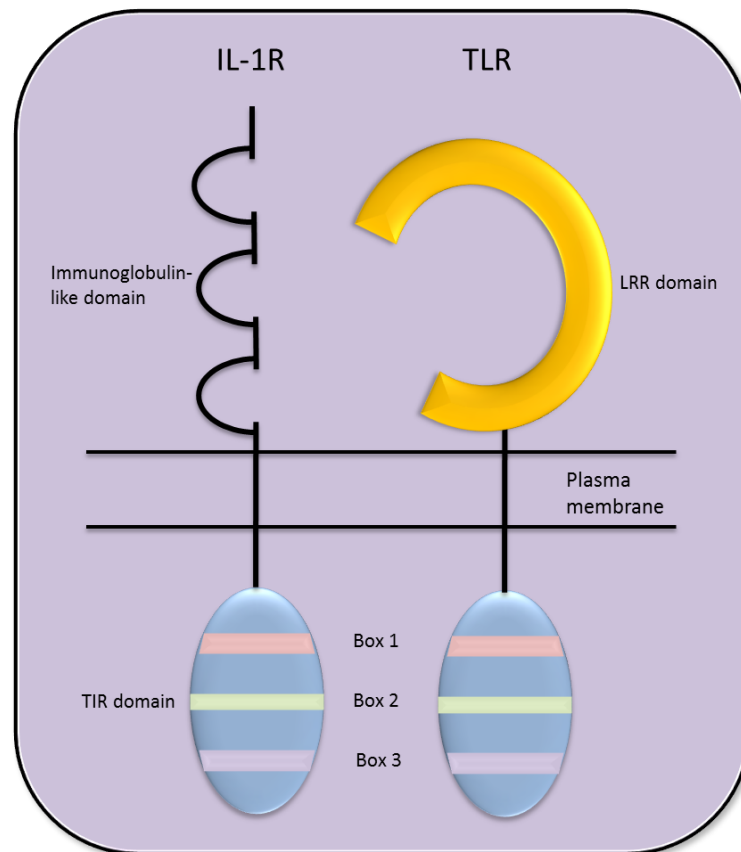


Figure 1.1: Interleukin-1 receptor and Toll-like receptor.

The IL-1 receptor and TLR have a conserved cytoplasmic domain, known as the TIR domain. The TIR domain is characterized by the presence of three highly homologous regions (Box 1, 2 and 3).

Adapted from Akira, S. and K. Takeda (2004). "Toll-Like Receptors Signalling." Nature Reviews: Immunology. 4: 499-511.

from 135 to 160 residues. This is a result of deletions and insertions in the loop regions (Song and Lee, 2012). The monomeric structures of the TIR domains of TLR1, 2 and 10 have also been determined (Xu et al., 2000, Nyman et al., 2008). They have similar structural homology and mutagenesis studies have revealed several key regions that are crucial for signalling. Box 1 and box 2 are essential for signalling as demonstrated through mutagenesis studies (Croston et al., 1995). Other studies have found that box 3 may also play a role in signalling, though its role may not be as important as boxes 1 and 2 (Slack et al., 2000). Crystal structures of the TIR domains of TLR1 and TLR2 have revealed a central five stranded parallel β sheet that is surrounded by five α -helices on each side (Khan et al., 2004). These secondary structures are connected by loops, and the conserved boxes 1 and 2 display their side chains for interaction with other adaptor proteins (Xu et al., 2000). These repeats are comprised of an α -helix and a β sheet, which is connected by loops. The loops are named according to the secondary structures that they connect i.e. the BB loop joins strand β B and helix α B (Xu et al., 2000) (Figure 1.2). It has been published that the interactions between the TIR domains take place at the BB loop regions between the second α -helix and second β -strand (Huyton et al., 2007). Mutations to this region in TLR2 abolished signal transduction in response to yeast and Gram-positive bacteria, demonstrating the importance of the BB loop (Underhill et al., 1999). The intracellular TIR domain and extracellular Leucine-rich Repeat (LRR) domain is linked by a short transmembrane region (~2-10 residues) and a single transmembrane α -helix.

The extracellular domains are characterized by a varying number of LRR motifs, each containing 24-29 amino acids (aa) and hydrophobic residues spaced at regular intervals. This LRR domain contains the motif L-X-X-L-X-L-X-N-X-L and is directly involved in the recognition of pathogens (Kajava, 1998). The LRRs form a solenoid structure with the hydrophobic residues in the interior, and each repeat is a turn of the solenoid. This hydrophobic core confers stability to the LRR solenoid, and the capping structures that form the ends of the first and last LRR residues are thought to protect the hydrophobic core by further stabilizing this structure (Bella et al., 2008) (Figure1.3). The central L-X-L motif forms the core of the β -strand, the two leucine residues point towards the centre of the structure, forming the hydrophobic core. The different X residues in the motif are exposed to solvent and are thought to interact with ligands (Song and Lee, 2012). The β -strands all align forming a parallel β sheet, as the β -strands are packed so closely, this causes the solenoid to curve, producing a horseshoe like structure (Botos et al., 2011). The LRR solenoid is protected by two modules called the LRRNT and LRRCT, which are respectively in the N- and C-terminal domains of the protein. These two modules have a different sequence to the LRR motif

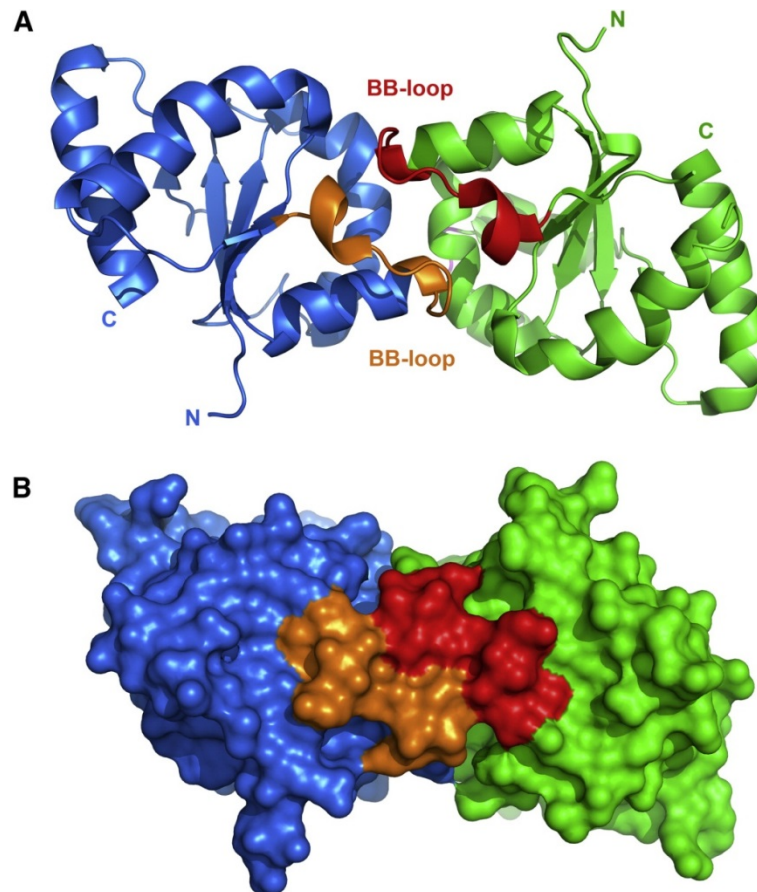


Figure 1.2: Structure of the TIR domain of TLR10 as a Dimer.

(A) Ribbon diagram of the TIR domain of TLR10. The two interacting BB loops are in gold and red.

(B) Molecular surface of TLR10 dimer.

Botos et al. (2011). "The Structural Biology of Toll-like Receptors." *Structure*. 4: 447-459.

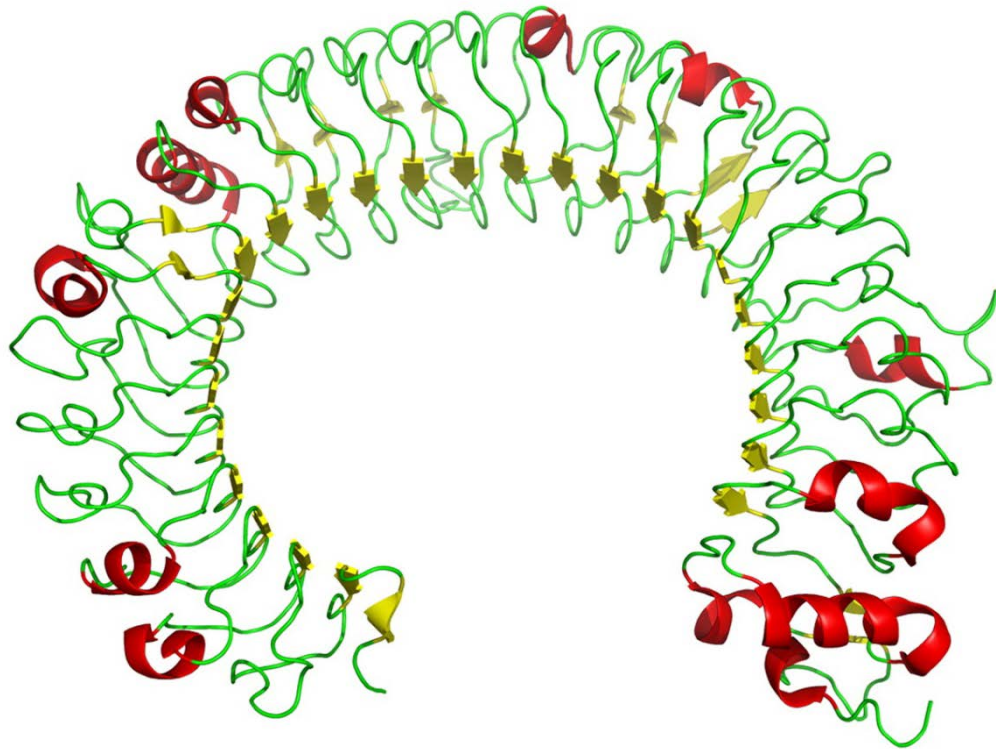


Figure 1.3: Ribbon diagram of the LRR domain of TLR3.

The LRR motifs together form a solenoid structure, with the hydrophobic residues pointing towards the centre, thus forming a stable core. The β -strands all align and form a parallel β sheet that is held together by hydrogen bonds. As the β -strands are packed more closely together than the LRR region, the solenoid adopts a curved shape.

Botos et al. (2011). "The Structural Biology of Toll-like Receptors." *Structure*. 4: 447-459.

and the LRRNT motif contains an anti-parallel β hairpin, which is stabilized through disulphide bonds (Song and Lee, 2012). The LRRCT is a globular structure that is made up of two α -helices and is further stabilized by two disulphide bonds (Botos et al., 2011) (Figure 1.4).

Despite the conservation of the LRR domains, they surprisingly recognise structurally unrelated ligands. Structural studies have provided new insights to the mechanisms of TLR ligand recognition. The family of TLRs can be very versatile in the way ligand recognition occurs as they can practically use all the LRR motifs on them to identify PAMPs. In addition to this, the location and variations in shape of the bound LRRs aids in ligand diversity (Lu and Sun, 2012). This flexibility allows the limited number of TLRs to recognise a wide variety of ligands.

Unlike insect *Toll* which has a role in both embryonic development and immunity, the main function of mammalian TLRs is the initiation of inflammation and induction of the adaptive immune response (Kaisho and Akira, 2006). Signalling from TLRs can sustain a more vigorous inflammatory state, inducing an increased production of inflammatory cytokines such as IL-6 and Tumour Necrosis Factor- α (TNF- α). The production of these cytokines leads to activation of the surrounding cells which in turn produce chemokines and adhesion molecules. The production of these proteins recruits inflammatory cells to the site of infection. Macrophages and neutrophils that are recruited to the area will become activated and phagocytose foreign antigens leading to the internalization of PAMPs. These activated leukocytes will kill the pathogens through the generation of nitric oxide (NO) and reactive oxygen species (ROS). The local inflammatory response in this situation is pivotal to the resolution of the infection. However, inflammation itself can be a double-edged sword, excessive amounts of cytokines can have detrimental effects on the host, and thus tight regulation of inflammation is also an important component of the immune response (Kaisho and Akira, 2006).

1.2.2 - Cell surface TLRs

1.2.2.1 - TLR2

TLR2 can form heterodimers with TLR1 or TLR6 and recognises a wide range of PAMPs from bacteria, viruses, fungi and parasites (Takeuchi et al., 2001, Takeuchi et al., 2002). The TLR2/1 heterodimer recognises triacylated lipoproteins, whereas the TLR2/6 heterodimer recognises

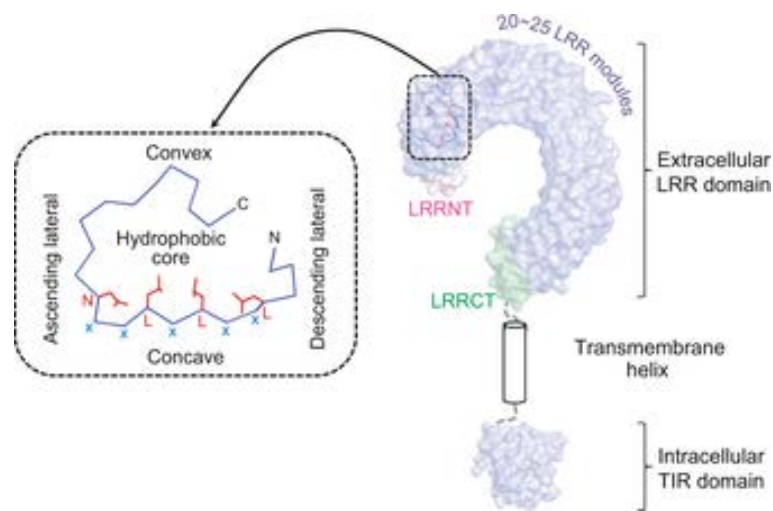


Figure 1.4: Overall TLR structure.

The extracellular domain and cytoplasmic domain of the TLR are in blue. The LLRNT and LLRCT are in pink and green, respectively. The C- α trace displays the LRR loop, with the central hydrophobic core and side chains from the conserved leucine and asparagine residues.

Song et al. (2012). "Sensing of microbial molecular patterns by Toll-like receptors." Immunological Reviews. 250: 216-229.

diacylated lipoproteins. Jin et al. (2007) was able to show the crystal structures of the TLR1-TLR2 complex bound to a synthetic lipoprotein agonist, tripalmitoyl-S-glycerol-L-Cys-Ser-(Lys)₄ (Pam₃CSK₄). Binding of a triacylated lipoprotein to TLR2 occurs in a lipid-binding pocket that is on the convex face of the extracellular LRR domains. Two of the three acyl groups bind to the pocket of TLR2, whilst the remaining acyl group binds to a similar lipid-binding pocket of TLR1 (Jin et al., 2007) (Figure 1.5). It is this structure that explains the heterodimerisation of TLR1 and TLR2. Modelling of TLR6 by Jin et al. (2007) suggests that TLR6 does not contain a lipid-binding pocket, therefore this may explain the differences in lipoprotein recognition.

TLR6 shares 56% sequence homology with TLR1 however, there are structural differences in its ligand binding and dimerisation that is attributed to the variations in ligand binding specificity. Binding of dipalmitoyl-S-glycerol-L-Cys-Ser-(Lys)₄ (Pam₂CSK₄) induces a “M” shaped dimerisation of TLR2 and TLR6, where the N termini extends out to their opposite ends, and the C termini meet in the middle (Kang et al., 2009) (Figure 1.6). In fact, this “M” shaped dimerization is found in all TLR homo- or heterodimers and supports previous theories suggesting that dimerisation allows activation of the intracellular TIR domains (Jin et al., 2007). Unlike the way Pam₃CSK₄ interacts with the TLR2/1 heterodimer, the lipid chains of Pam₂CSK₄ are submerged in the TLR2 hydrophobic pocket, whereas the peptide portion forms hydrogen bonds with both TLR2 and TLR6 (Botos et al., 2011).

TLR10 has recently been demonstrated to require TLR2 for ligand recognition (Guan et al., 2010). TLR10 shares a variety of agonists with TLR1 as both receptors recognise triacylated lipopeptides (Guan et al., 2010). It was further demonstrated that structurally, TLR2/TLR10 bound to lipopeptide was similar to TLR2/TLR1/lipopeptide complex. TLR10 and TLR1 share 43% aa identity in their ectodomains and similar to TLR1, TLR10 contains a hydrophobic channel which runs along its convex side which facilitates interaction with ligands (Guan et al., 2010). LRRs 6-17 of TLR10 were demonstrated to be responsible for ligand specificity as substitution studies conducted with the TLR1's LRRs 6-17 retained lipopeptide recognition (Guan et al., 2010).

TLR2 also has two cofactors, CD14 (discussed later) and CD36 that have been shown to be critical in activating downstream signalling for specific ligands. CD36 is a 476 aa membrane protein that is part of the scavenger receptor class B family and is found in lipid rafts (Calvo et al., 1995). Using fluorescent imaging techniques Triantafyllou et al. (2006) demonstrated that the heterodimer

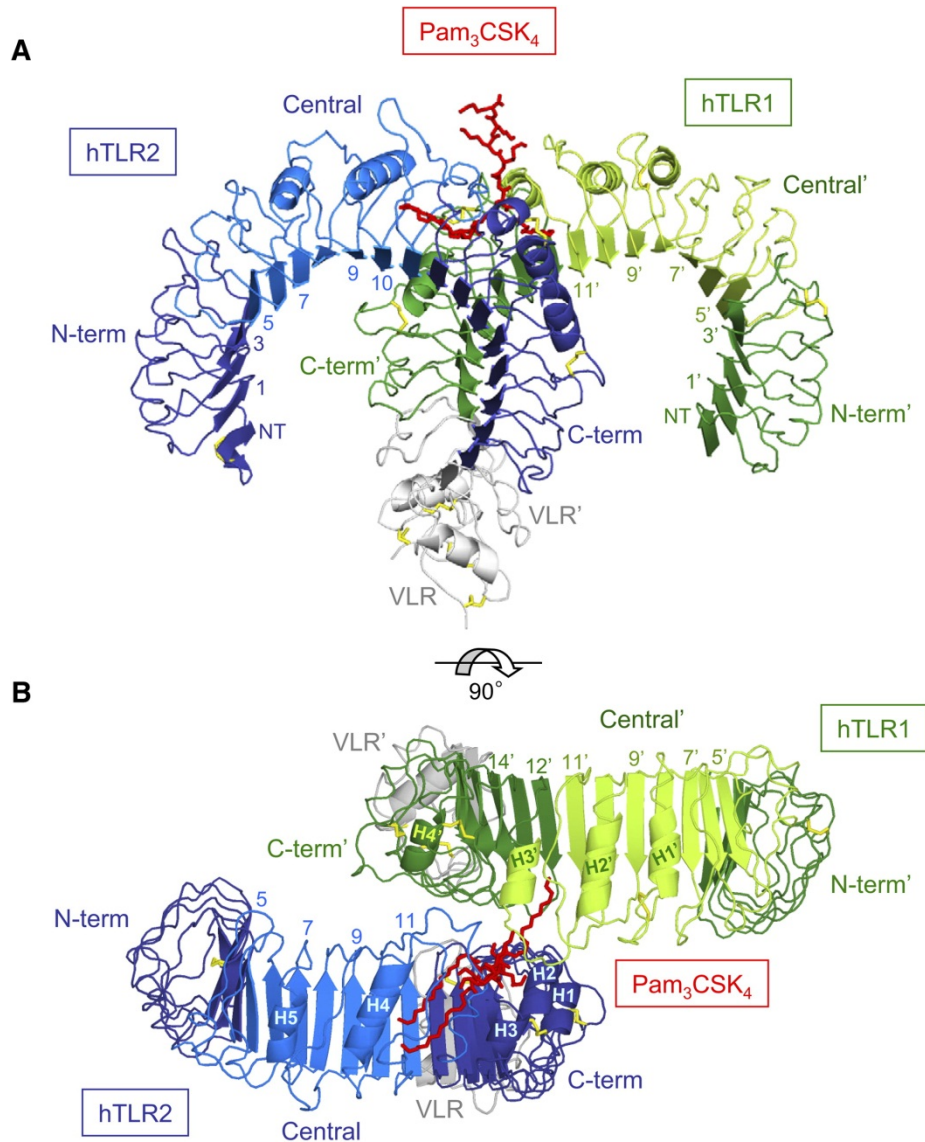


Figure 1.5: Overall structure of TLR2/TLR1 bound to Pam₃CSK₄ lipopeptide.

TLR1 is represented in green, TLR2 in blue, the Variable Lymphocyte Receptor (VLR) fragment in grey and Pam₃CSK₄ lipopeptide in red. The central domains of TLR1 and TLR2 are coloured in green and blue, respectively. Disulphide bridges are represented in yellow. **(A)** Side view. **(B)** Top view.

Jin et al. (2007). "Crystal structure of the TLR1-TLR2 heterodimer induced by binding of a tri-acylated lipopeptide." *Cell*. 130: 1071-82.

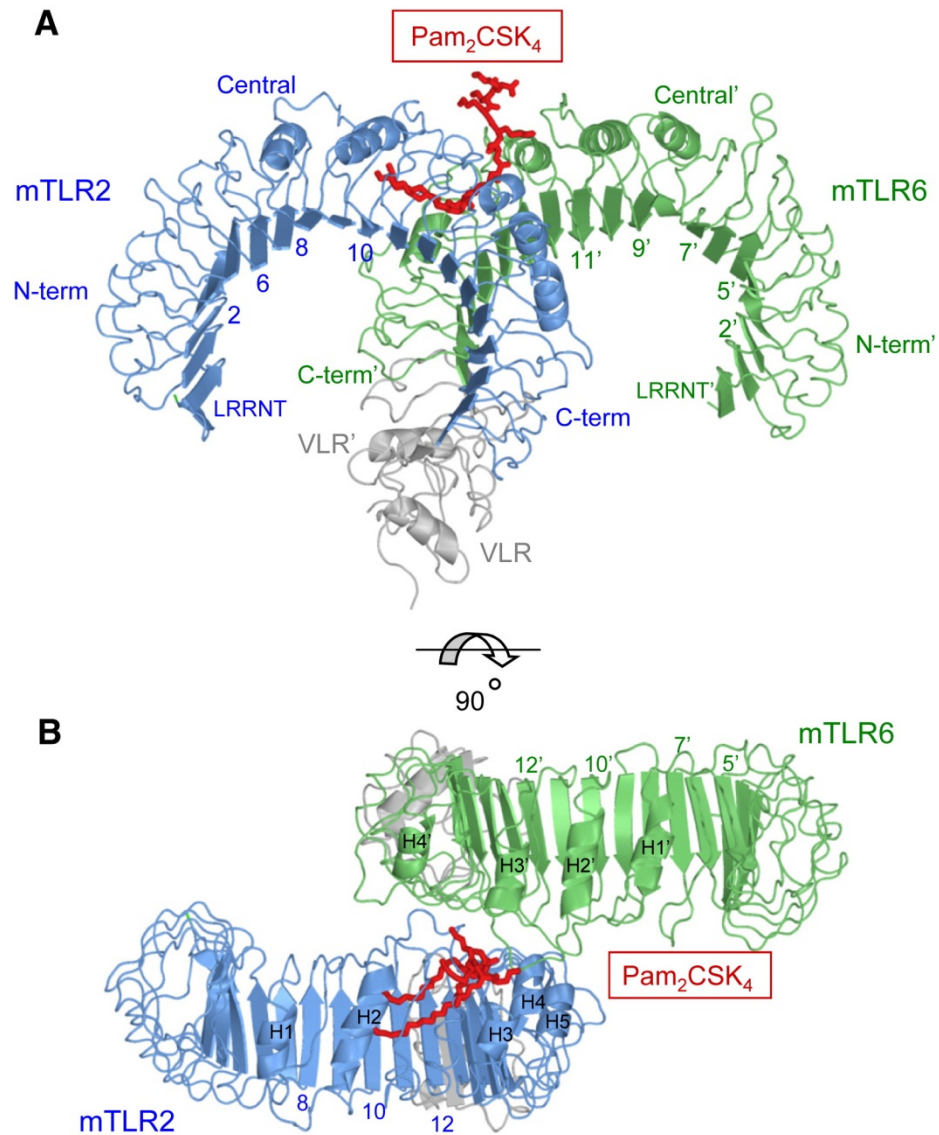


Figure 1.6: Overall structure of mouse TLR2/TLR6 bound to Pam₂CSK₄ lipopeptide.

TLR2 is represented in light green, TLR6 in light blue, VLR fragments in grey and Pam₂CSK₄ lipopeptide in red. **(A)** Side view. **(B)** Top view.

Kang et al. (2009). "Recognition of Lipopeptide Patterns by Toll-like Receptor 2-Toll-like Receptor 6 Heterodimer." *Immunity*. 31: 873-884.

TLR2/TLR6 directly interacted with CD36 in response to lipoteichoic acid (LTA) and diacylated lipoproteins. TLR2 ligands induced formation of this receptor complex near the cell surface in lipid rafts. The heterodimer TLR2/TLR1 however did not interact with CD36 following triacylated lipoprotein activation. Recently, CD36 has been shown to be important for the full activation of the NOD-like Receptor Family, Pyrin Domain Containing 3 (NLRP3) inflammasome in atherosclerosis through engagement of oxidised low-density lipoprotein and the TLR2/TLR6 heterodimer (Sheedy et al., 2013). The two heterodimers TLR2/TLR1 and TLR2/TLR6 pre-exist in the cell, upon ligand binding the receptors are internalised and then targeted to the Golgi apparatus. As ligand recognition for TLR2 occurs on the surface, CD36 and CD14 must bind and present the ligand to the receptor on the cell surface, allowing it to be internalised and trafficked to the Golgi apparatus (Nilsen et al., 2008).

1.2.2.2 - TLR4

TLR4 is unique amongst all the TLRs as it is the only one capable of signalling through all four adaptor molecules. TLR4 recognises lipopolysaccharide (LPS), an essential component of the bacterial outer membrane (Raetz, 1990). Using the hybrid LRR technique, Kim et al. (2007a) demonstrated that TLR4 bound to an accessory protein MD-2 (Figure 1.7). The TLR4-MD-2 complex is shown bound to eritoran, one of its ligands and an analogue of LPS. Eritoran was demonstrated to bind within an internal hydrophobic pocket of MD-2 (Kim et al., 2007a). Kim et al. (2007a) were able to demonstrate that there was no direct contact between eritoran and TLR4. The four acyl groups of eritoran occupy nearly 90% of the space inside the hydrophobic pocket, and the two phosphate groups of the diglucosamine backbone of eritoran form ionic bonds with positively charged residues at the opening of the pocket (Figure 1.8).

LPS signals through TLR4 by binding to its co-receptor MD-2. MD-2 contains two anti-parallel β sheets that are sandwiched together. The space between the two sheets enables it to form a large internal pocket where hydrophobic ligands like LPS can be bound (Song and Lee, 2012). Park et al. (2009) demonstrated that when LPS is complexed to TLR4-MD-2, five of its six lipid chains bind the hydrophobic pocket of MD-2, and the remaining chain binds to TLR4 (Figure 1.9). Other accessory proteins are also involved in the interaction of LPS and the TLR4-MD-2 complex (Kawai and Akira, 2010). LPS-binding Protein (LBP) and CD14 bind LPS and deliver it to the TLR4-MD-2 complex, causing dimerisation of two TLR4-MD-2-LPS complexes, which initiates downstream

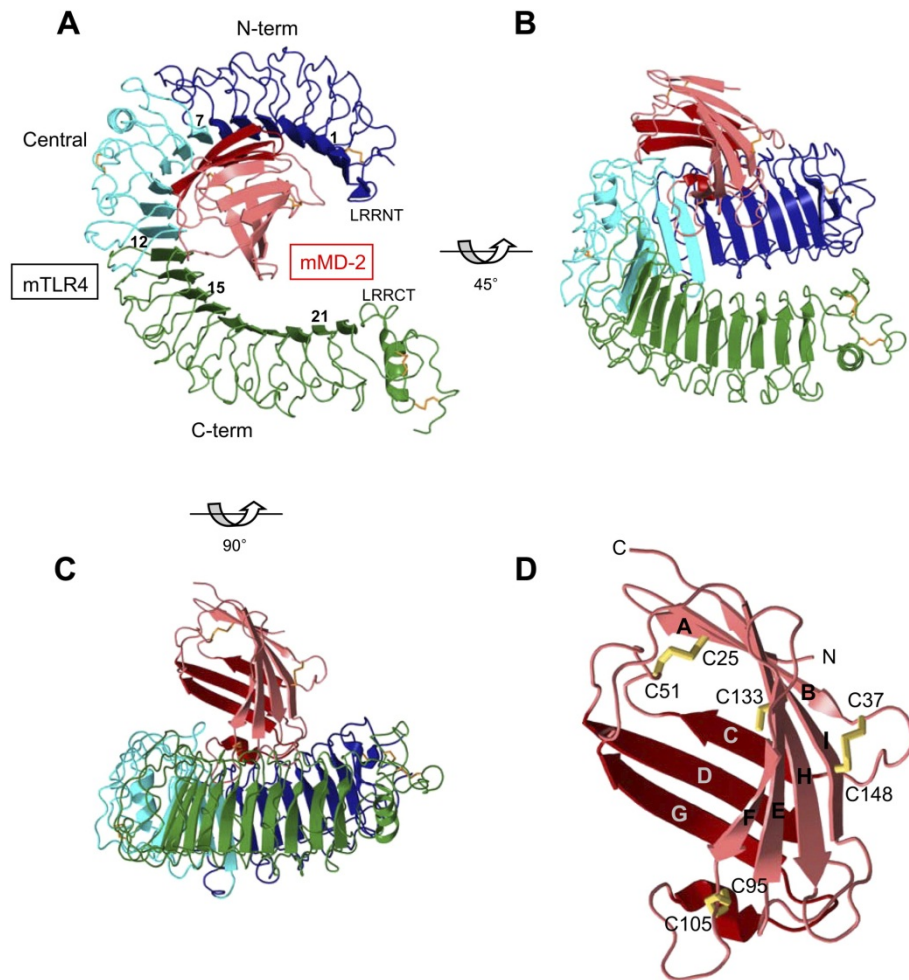


Figure 1.7: Overall structure of mouse TLR4-MD-2 complex and MD-2.

The N-terminal domain is in blue, central domain in cyan and C-terminal domain in green. The β -strands are represented in red and pink. Disulphide bridges are shown in yellow. **(A)** Side view. **(B)** Lateral view. **(C)** Top view. **(D)** Close view of mouse MD2, with cysteine residues labelled. Cys-133 is not used in the formation of a disulphide bridge.

Kim et al. (2007). "Crystal structure of the TLR4-MD-2 complex with bound endotoxin antagonist Eritoran." *Cell*. 130: 906-17.

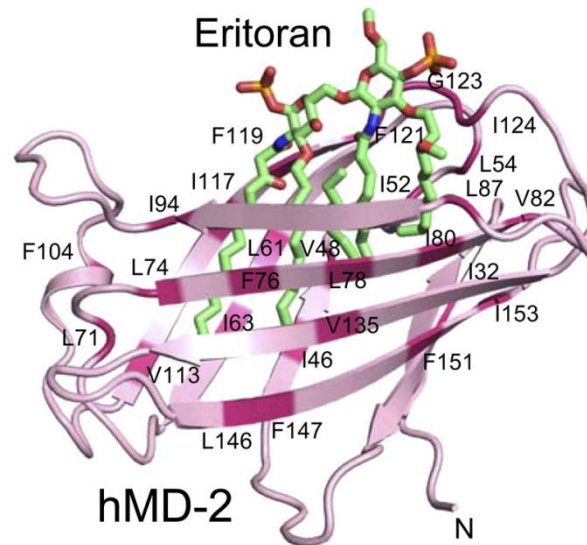


Figure 1.8: Overall structure of human MD-2 bound to eritoran.

Close up view of human MD-2 bound to eritoran. The carbon, oxygen and phosphorus atoms in eritoran are coloured green, red and orange, respectively. The MD-2 residues that interact with eritoran are coloured in magenta and are labelled.

Kim et al. (2007). "Crystal structure of the TLR4-MD-2 complex with bound endotoxin antagonist Eritoran." *Cell*. 130: 906-17.

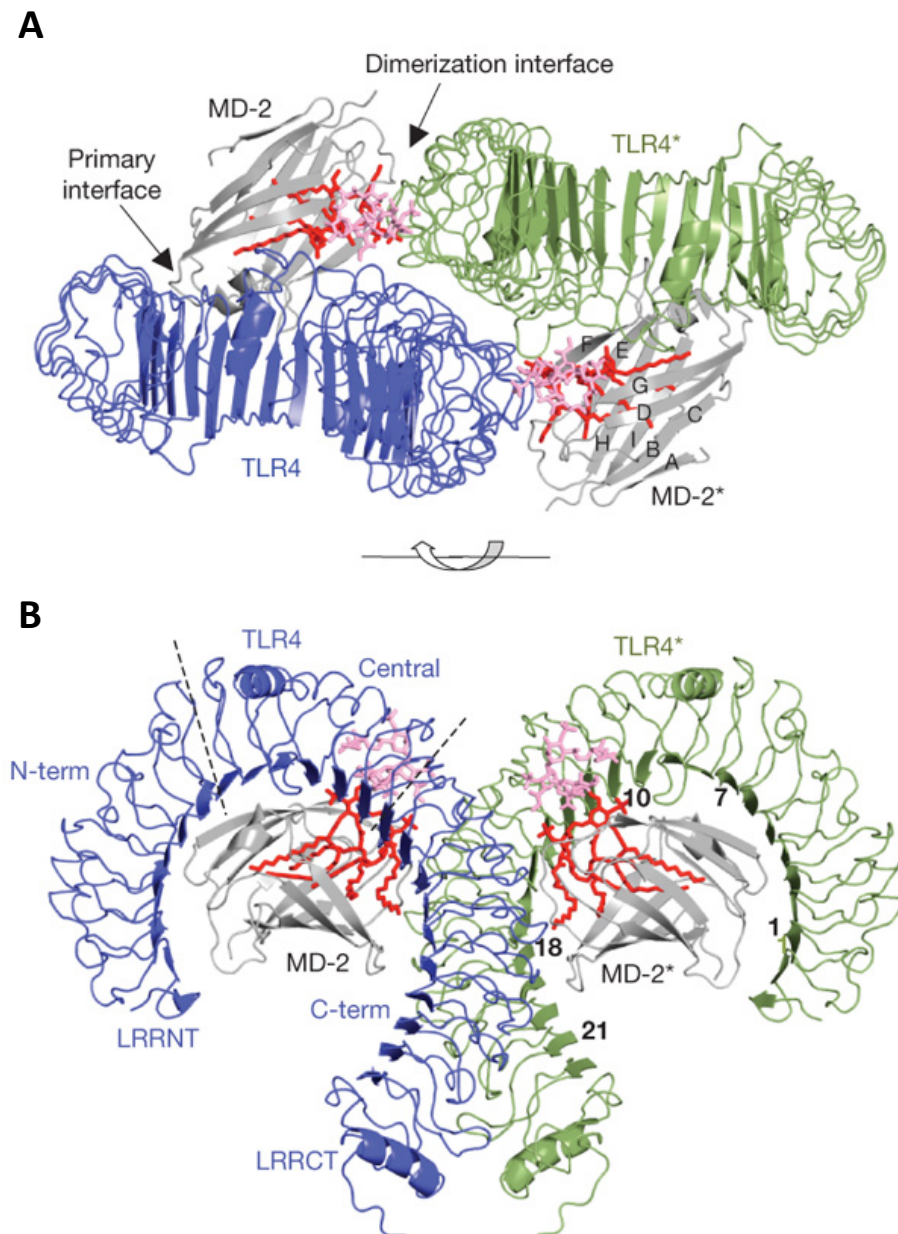


Figure 1.9: Overall structure of the TLR4-MD-2-LPS complex.

TLR4 is represented as a dimer in blue and green, MD-2 in grey, the lipid A component of LPS is red and its inner core highlighted in pink. **(A)** Top view of the TLR4-MD-2-LPS complex as a dimer. TLR4 and MD-2 are formed before binding of LPS occurs and binding of LPS induces dimerisation of the receptor. **(B)** Side view of the complex. The N- and C-terminal domains of TLR4 are capped off by the LRRNT and LRRCT modules, respectively.

Park et al. (2009). "The structural basis of lipopolysaccharide recognition by the TLR4-MD-2 complex." *Nature*. 458: 1191-1195.

signal transduction (Fujihara et al., 2003, Akashi et al., 2003). LBP is required for binding LPS from the outer membranes of bacteria or vesicles and then transferring the bound LPS to a monomeric form of CD14. CD14 itself cannot initiate downstream signalling, therefore this complex of LBP, CD14 and LPS must be delivered to TLR4-MD-2 in order to activate immune responses.

LBP belongs to the Lipid Transfer or LBP (LT-LBP) family, its other members include Bactericidal and Permeability-increasing Protein (BPI), Phospholipid Transfer Protein (PLTP) and Cholesterol Ester Transfer Protein (CETP) (Mulero et al., 2002). Whilst the structure of LBP bound to LPS is yet to be resolved, BPI has been used for homology modelling of LBP. Both BPI and LBP have a conserved and characteristic boomerang-shaped structure, which is comprised of a central β sheet, with the N-terminal and C-terminal sharing little sequence homology. (Beamer et al., 1999). The N-terminus is where the LPS binding occurs, although the precise site of LPS binding is still unknown (Krasity et al., 2011). The C-terminal domain is responsible for transferring LPS to CD14 (Iovine et al., 2002).

CD14 can be found as a glycosylphosphatidylinositol (GPI)-anchored cell surface protein or in a soluble form that can be found in serum (Jin and Lee, 2008). It is a monocyte differentiation antigen, and is unique as it can bind multiple microbial products including LPS, peptidoglycan, polyinosinic-polycytidylic acid (poly (I:C)) and 2'-deoxyribo(cytidine-phosphate-guanosine) (CpG) DNA (Dziarski et al., 1998, Baumann et al., 2010, Hailman et al., 1994, Lee et al., 2006, Nakata et al., 2006). It can therefore interact with multiple TLRs. The binding site for different TLR ligands appears to overlap in CD14, as different TLR ligands can compete with each other for CD14 binding (Dziarski et al., 1998, Baumann et al., 2010, Lee et al., 2006). It belongs in the LRR family of proteins, and binding of LPS by CD14 is slow without the presence of LBP to catalyse the interaction (Hailman et al., 1994). Kelley et al. (2012) resolved the crystal structure of CD14 and found it to have a bent solenoid shape formed by 11 LRRs. The structure also revealed five α -helices on the convex side, with eleven β sheets forming the concave side of the solenoid. In the N-terminus of CD14 there exists a cavity that is believed to function as the LPS binding site. The cavity is mainly comprised of hydrophobic residues, with some positively charged residues in and around the rim of the cavity (Figure 1.10).

TLR4 Interactor with LRRs (TRIL) is an 811 aa type 1 transmembrane protein that contains 13 LRRs in its extracellular domain (Carpenter et al., 2009). The LRR motif is similar to that of TLRs and has

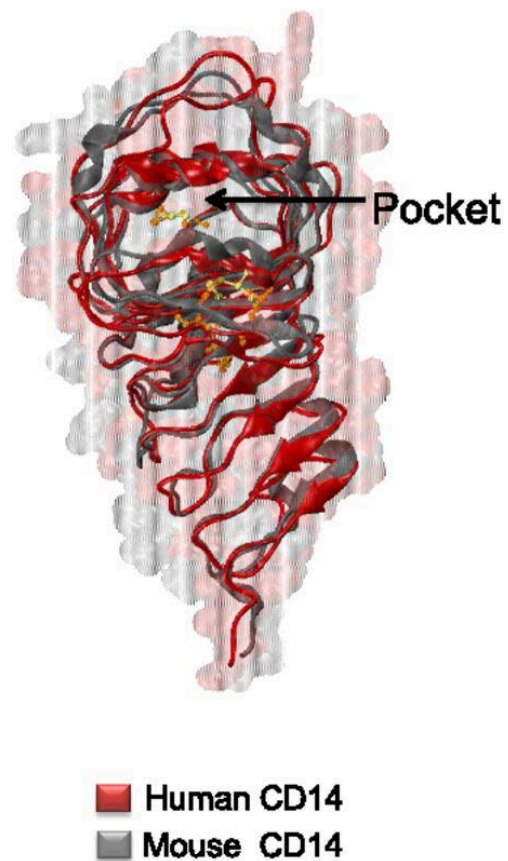


Figure 1.10: Overall structure of human and mouse CD14.

Human CD14 (red) is overlaid over mouse CD14 (grey). The N-terminal binding pocket of CD14 is highlighted and it thought to bind LPS and other TLR ligands.

Kelley et al. (2012) "The Crystal Structure of Human Soluble CD14 Reveals a Bent Solenoid with a Hydrophobic Amino-Terminal Pocket." [The Journal of Immunology.](#)

notably high expression in the brain. LPS upregulates the expression of TRIL and this greatly increases the interaction between TLR4 and TRIL. TRIL can also interact with LPS, and knockdown of TRIL attenuates TLR4 signalling (Carpenter et al., 2009). Carpenter et al. (2011) later found that TRIL can also interact with TLR3, and its expression can also be induced by poly (I:C). TRIL appears to act like CD14 however it is unclear whether TRIL can bind double-stranded ribonucleic acid (dsRNA).

1.2.2.3 - TLR5

TLR5 recognises the bacterial PAMP, flagellin (Hayashi et al., 2001). Flagellae are made up of three substructures, a long flagellin fibre and a hook which connects the fibre to the basal body. This flagellin fibre comprises of a large number of fliC flagellin. The crystal structure of a zebrafish TLR5 has been resolved in complex with a truncated part of *Salmonella* fliC (Yoon et al., 2012). TLRs between fish and humans share a high sequence homology, thus allowing prediction of similar structures and ligand binding mechanisms. The crystal structures revealed the D1 domain of flagellin is involved in binding and the dimerisation of TLR5. Similar to when other TLRs bind their ligands, the D1 domain binds two TLR5 molecules forming the characteristic “M” shape, with the two C-termini joined at the centre and the two N-termini facing outwards (Song and Lee, 2012) (Figure 1.11).

1.2.3 - Intracellular TLRs

1.2.3.1 - TLR3

TLR3 is located in intracellular compartments like endosomes, and recognises poly (I:C), which is a synthetic analog of dsRNA (Alexopoulou et al., 2001). Studies performed by Wang et al. (2010) reveal that TLR3 is monomeric in solution, but forms dimers with 45 base pair (bp) segments of RNA, the minimum length required for TLR3 binding and activation. Binding of RNA is also independent of its sequence and only occurs at a pH of 6.5 or lower (Leonard et al., 2008).

The structure of TLR3 was first elucidated by analysis of the ectodomain of TLR3 bound to dsRNA. Similar to other TLRs, TLR3 also has a horseshoe like structure, but the solenoid has a lack of twist

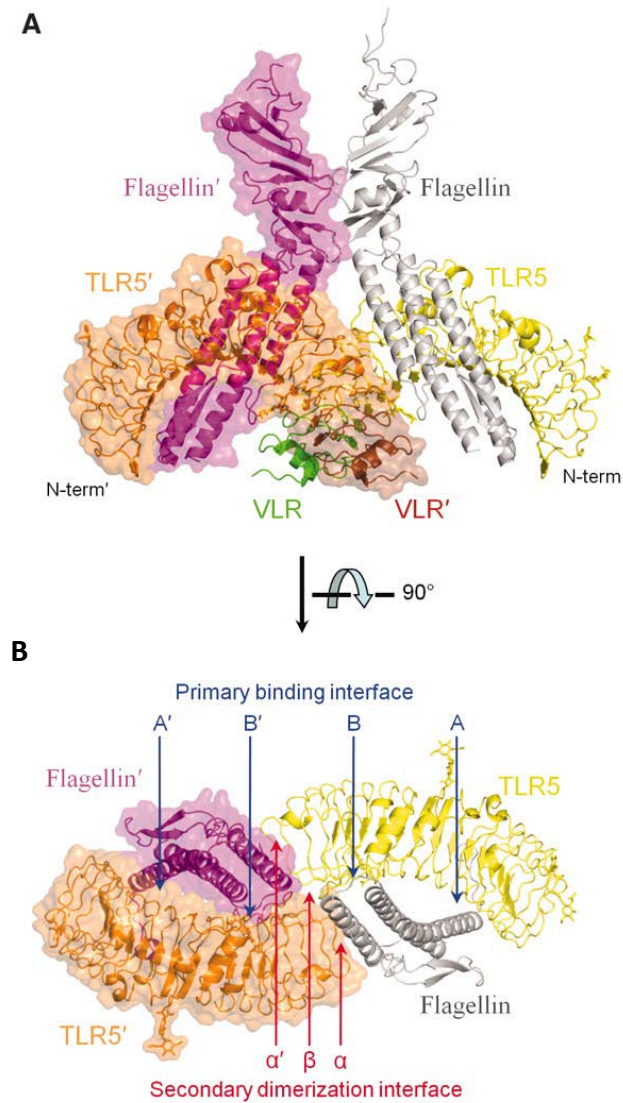


Figure 1.11: Overall structure of zebrafish TLR5 bound to flagellin.

TLR5 fragments are represented in orange and yellow, VLR fragments in green and brown and flagellin in magenta and grey. **(A)** Side view. TLR5 interacts with *Salmonella* fliC flagellin in a 2:2 ratio. This interaction brings the C-terminal domains of TLR5 inwards forming the characteristic “M” shape. **(B)** Top view.

Yoon et al. (2012). “Structural Basis of TLR5-Flagellin Recognition and Signalling.” *Science*. 335: 859-864.

due to irregular LRR motifs (Bell et al., 2006b) (Figure 1.12). At LRR12 and 20, TLR3 contains two large insertions that follow the β -strand (Choe et al., 2005). This is unique among TLRs and is conserved in all mammalian TLR3 orthologs. Deletion of LRR12 did not effect TLR3 stimulation, but deletion of LRR20 resulted in significant loss of activity (Bell et al., 2006a). The TLR3 ectodomain is heavily glycosylated, except for the C-terminal side of the β sheet. This side interacts with dsRNA and in the crystal structure, it is shown that dsRNA is sandwiched between two TLR3 molecules, forming the “M” shape arrangement (Liu et al., 2008) (Figure 1.13). When bound to ligand, TLR3 does not undergo any conformational change. dsRNA interacts with TLR3 at two sites, one is close to the N-terminal domain and the other is near the C-terminal domain. The ectodomains of both TLR3 molecules also interact at the LRRCT motif and mutation studies have demonstrated that all three binding sites are crucial for dsRNA binding (Wang et al., 2010). The interaction between the LRRCT motifs is mainly hydrophilic, comprised of hydrogen bonds and salt bridges. This site is vital for dsRNA binding as it aligns the other four dsRNA binding sites and also brings the C-termini of both TLR3 molecules close together (Wang et al., 2010). It is hypothesised that within a cell, the interaction between the LRRCT motifs may occur on the luminal side of the endosome, allowing two TIR domain containing proteins to come together, forming a platform for adaptor molecules to bind and initiate downstream signalling.

The reason TLR3 can only recognise dsRNA at a length of 45 bp is due to the distance between the N-termini of two TLR3 molecules (Leonard et al., 2008). As cells normally contain short segments of dsRNA (micro RNA and transfer RNA), the inability of TLR3 to recognise anything shorter helps avoid autoreactive immune responses to self dsRNA (Botos et al., 2011). When binding dsRNA, TLR3 only interacts with the ribose-phosphate backbone, this is the reason behind the lack of RNA sequence specificity. In addition, it also confers an advantage when detecting viruses, as mutation of its own sequence still cannot aid it in avoiding TLR3 recognition.

Most of the interactions between TLR3 and dsRNA are hydrophilic and these include hydrogen bonds and salt bridges. Of particular importance are the interactions between the phosphate groups of the dsRNA backbone and the imidazole rings of four histidine residues, three found in the N-terminal domain and one located in the C-terminal domain of TLR3 (Botos et al., 2011). Mutation of the H39 and H60 residues to alanine abolishes binding to dsRNA demonstrating the importance of the salt bridges that are formed between these molecules. These interactions may also explain the pH dependency of dsRNA binding, as these side chains would only become

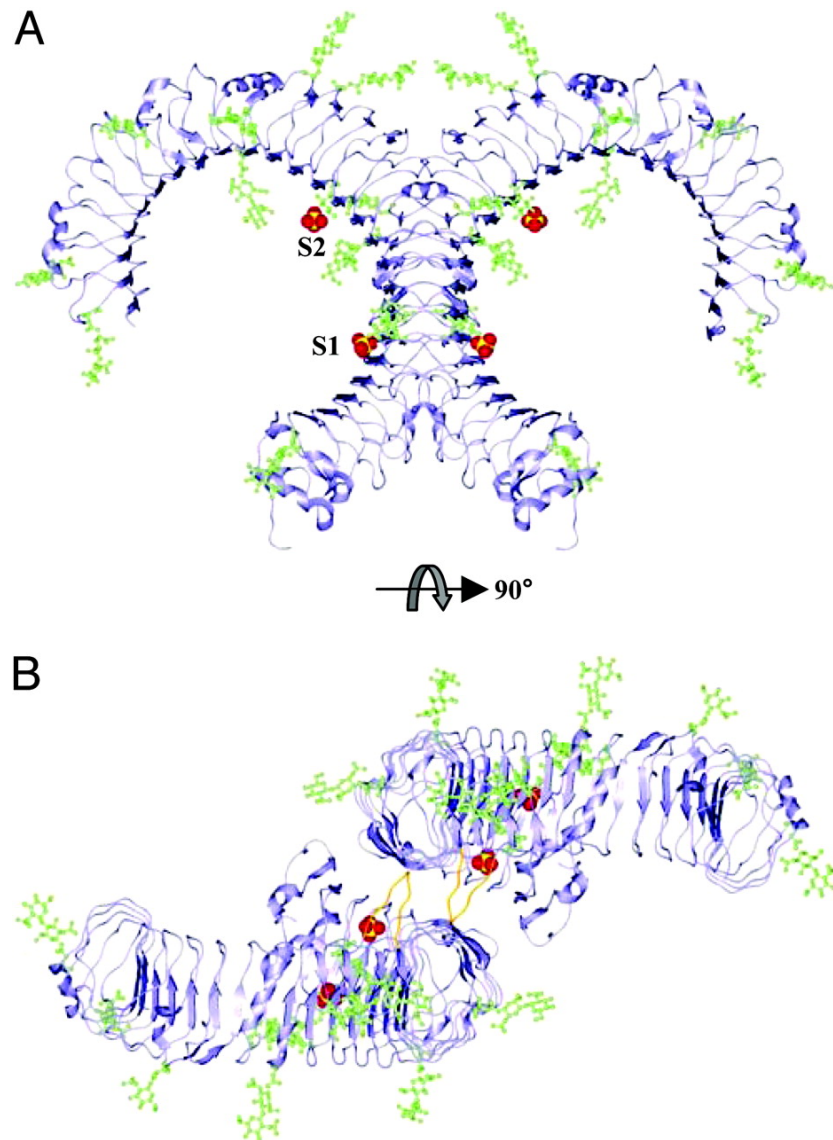


Figure 1.12: Overall structure of TLR3.

TLR3 is represented in blue, N-glycosylation is green and the two sulphate ions are depicted in red and yellow. **(A)** Side view. TLR3 is glycosylated along the lateral surfaces of the molecule. **(B)** Top view. The dimerisation domain between the two TLR3 dimers displays a region with no glycan groups that allows binding of dsRNA.

Bell et al. (2005). "The molecular structure of the Toll-like receptor 3 ligand-binding domain." Proceedings of the National Academy of Sciences. 102: 10976-80.

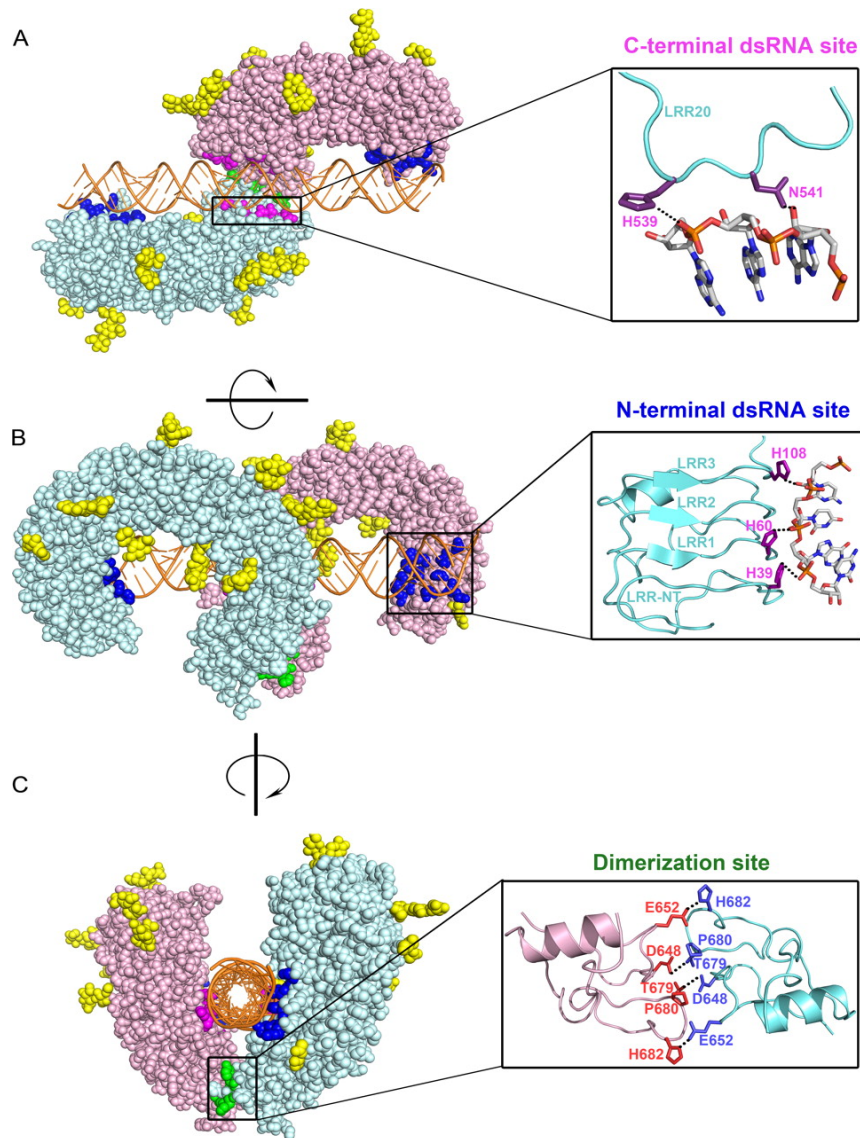


Figure 1.13: Crystal structure of TLR3 bound to dsRNA.

TLR3 is represented in pink and light blue, dsRNA is in orange and N-linked glycans are in yellow. Binding sites of dsRNA at the N- and C-terminus are shown in dark blue and magenta, respectively. The dimerisation site of TLR3 is coloured in green. **(A)** Top view of the complex displaying the dsRNA bound to TLR3 and running the span of the receptors. **(B)** Side view illustrating the characteristic “M” shape induced upon ligand binding. **(C)** View of the complex looking down the dsRNA.

Wang et al. (2010). “Dimerization of Toll-like Receptor 3 (TLR3) is required for ligand binding.” *Journal of Biology Chemistry*. 285: 36836-41.

positively charged below pH 6.5, allowing them to interact with the RNA backbone. The inability of TLR3 to bind dsDNA can also be explained from its structure. dsDNA forms in a B form, whereas dsRNA adopts an A form. Thus dsDNA would be structurally unable to bind into the two termini binding sites (Botos et al., 2011).

1.2.3.2 - TLR7 & 8

Structures of TLR7 and 8 have yet to be achieved, but like TLR3, both TLR7 and 8 are found intracellularly. Compared to the cell surface TLRs, TLR7 and TLR8 have a higher molecular mass and therefore longer ectodomains. The aa sequence of TLR7 and TLR8 suggests that it is quite different from TLR3. The ectodomains of both TLRs contain 25 LRR motifs and are heavily glycosylated. TLR7 and TLR8 contain large insertions at LRR2, 5 and 8, which would form structures that extend out from the ectodomains and may be involved in nucleic acid binding (Bell et al., 2003). The ectodomains of TLR7 and 8 also contain segments of ~40 residues between LRRs 14 and 15 that don't have a defined structure. These are the only segments that have the greatest variability between species (Botos et al., 2011). TLR7 and 8 also have differential expression, with TLR7 found in the lung, placenta and spleen, whereas TLR8 is more abundant in the lung and peripheral blood leukocytes (Sandor and Buc, 2005).

TLR7 was first discovered to recognise imidazoquinoline derivatives such as resiquimod and imiquimod, and guanine analogs like loxoribine (Akira et al., 2006). TLR7 also recognises single-stranded RNA (ssRNA) from RNA viruses like influenza A virus and human immunodeficiency virus (HIV) (Kawai and Akira, 2006). Synthetic poly (U) RNA and certain small interfering RNAs (siRNAs) can also be detected by TLR7 (Hornung et al., 2005). TLR7 is highly expressed on plasmacytoid dendritic cells (pDCs), which are able to produce large amounts of type I IFNs following viral infection. This would suggest that TLR7 is the main sensor for ssRNA viruses.

TLR8 is similar to TLR7 and recognises resiquimod and viral ssRNA (Akira et al., 2006). Mice lacking TLR8 respond normally to TLR8 agonist, unlike TLR7-deficient mice which fail to mount an immune response (Akira et al., 2006, Kawai and Akira, 2006).

1.2.3.1 - TLR9

TLR9 recognises unmethylated CpG DNA, which is found in bacteria and viruses, but is low in mammalian cells. CpG DNA drives a strong T helper type 1 (T_H1) response and is used as a vaccine adjuvant (Kawai and Akira, 2006). TLR9 can also detect non DNA components like hemozoin, a by-product of haemoglobin digested by *Plasmodium falciparum* (Coban et al., 2010).

Similar to TLR7 and 8, TLR9 contains 25 LRR motifs, is heavily glycosylated, and also contains large insertions at LRR2, 5 and 8 (Botos et al., 2011). In addition, unstructured regions can be found within TLR9 that span between LRR14 and 15 and these stretches can be ~40 residues long. There is high expression of TLR9 on pDCs, where TLR9 serves as the sensor for ssDNA virus infection. Studies have shown that TLR9 moves into early endosomes where it is transferred into lysosomal compartments. TLR9 can also redistribute itself from the endoplasmic reticulum (ER) into CpG DNA containing compartments. In order for recognition CpG DNA and activation of TLR9, internalization and acidification of the receptor is necessary (Latz et al., 2004).

Latz et al. (2007) demonstrated that upon binding to CpG DNA, TLR9 undergoes a conformational change in the ectodomain, making it very different to TLR3. This ligand-induced conformational change may occur at the ~40 residue span between LRR14 and 15, as this unstructured region could allow for changes in the receptor. Several other studies have suggested that proteases are required for TLR9 function. It is thought that TLR9 is cleaved between LRR14 and 15, within the undefined region (Matsumoto et al., 2008, Park et al., 2008). Park et al. (2008) also found that the C-terminus, containing LRR15 to LRR25 was active by itself, however a conflicting study by Peter et al. (2009) demonstrated that N-terminal mutations inactivated TLR9. It would be unlikely that such a large portion of the TLR9 ectodomain would be highly conserved, but not crucial in TLR9 ligand recognition. Further studies into the structure of TLR9 are needed to further elucidate the mechanism of ssDNA binding and activation of this receptor.

TLR9, like TLR4, also has a variety of cofactors that aid in the delivery of its ligand to the receptor. These include granulins, High Mobility Group Box 1 (HMGB1) and LL37. Granulin is produced from the proteolytic cleavage of its precursor form, pro-granulin a 593 aa protein (Kessenbrock et al., 2008). In its pro-form, granulin has anti-inflammatory properties, but when degraded by neutrophil elastase, granulin peptides exhibit proinflammatory properties (Zhu et al., 2002). Park et al. (2011) found that granulin fragments are able to interact with TLR9, and the addition of pro-

granulin in cells increased production of TNF- α . Addition of elastase inhibitors attenuated TLR9 signalling, but did not have an effect on TLR9 cleavage, demonstrating that proteolytic cleavage of granulin is required for TLR9 signalling. Granulin was also found to bind to CpG oligonucleotides, and via fluorescent microscopy was shown to colocalise with CpG oligonucleotides. It is thought that granulin may facilitate the delivery of CpG oligonucleotides to TLR9 in endolysosomes, and TLR9 interaction with CpG oligonucleotides was also enhanced in the presence of granulin (Park et al., 2011). It is still unclear whether granulin can bind dsDNA, though the structure is known and further analysis is required to answer this question.

The family of HMGB molecules are nuclear proteins that interact with chromatin and are involved in allowing several other regulatory proteins to complex with DNA (Lotze and Tracey, 2005). HMGB1 is a 215 aa protein that contains two DNA binding domains. HMGB1 exhibits proinflammatory properties when it is secreted by the cell in response to cytokine stimulation (Wang et al., 1999). CpG oligonucleotides have been shown to interact with HMGB1, which potentiates the immune response through a TLR9-dependent manner. In unstimulated cells, HMGB1 binds to TLR9 and this complex localises to the ER-Golgi Intermediate Compartment (ERGIC) (Ivanov et al., 2007). Stimulation with TLR9 ligand leads to the complex of CpG oligonucleotides, HMGB1 and TLR9 localising with the early endosome marker EEA1. Their data suggests that HMGB1 does not affect uptake of CpG oligonucleotides or its entry in early endosomes, but rather it hastens TLR9s trafficking to early endosomes in response to CpG oligonucleotides (Ivanov et al., 2007). Tian et al. (2007) found that CpG oligonucleotides bound to HMGB1 and this augmented IFN- α production. IFN- α secretion was dependent on HMGB1 interacting with Receptor for Advanced Glycation End-products (RAGE) and TLR9. The absence of HMGB1 attenuated the ability of CpG oligonucleotides to induce type I IFN production and the secretion of other inflammatory cytokines (Ivanov et al., 2007).

In pDCs, LL37 has been reported to be another cofactor of TLR9 and has shown to be involved in presenting self DNA to TLR9 (Lande et al., 2007). LL37 is a 37 aa antimicrobial peptide produced from its precursor, cathelicidin following cleavage by serine proteases (Zanetti et al., 1997). In psoriasis, LL37 can be detected at high levels in keratinocytes (Lande et al., 2007). LL37 breaks tolerance to self DNA by forming a complex with it and triggering IFN production. The complexes of LL37 and DNA cannot be broken down by deoxyribonucleases (DNases), and are taken up by pDCs (Lande et al., 2007). These complexes are relocated to early endosomes where they come into contact with TLR9 and induce IFN- α production (Lande et al., 2007). There is no evidence

which suggests that LL37 binds to TLR9, instead LL37 is thought to function as a delivery molecule bringing into contact self DNA and TLR9 during cell damage. LL37 has also been shown to form complexes with self RNA and may also be cofactors to TLR7 and TLR8 (Ganguly et al., 2009). It has further been reported that LL37 can bind self RNA from dying cells and transport it into endosomal compartments, activating both TLR7 and 8 and inducing IFN- α , TNF- α and IL-6 production (Ganguly et al., 2009). Like HMGB1, LL37 can bind and deliver DNA/RNA to intracellular TLRs, but whether it has a role in host defences is unknown.

1.2.4 – Cellular localisation of TLRs

The maturation and folding of the TLRs is dependent on two proteins, Glucose-regulated Protein of 94 kDa (GRP94) and Protein-associated with TLR4 A (PRAT4A). GRP94 is an 803 aa ER protein, and is a paralog of Heat Shock Protein 90 (HSP90), which facilitates protein folding (Lee et al., 2012). GRP94 is ubiquitously expressed, and exists as a homodimer. GRP94 has been shown to chaperone several cell surface TLRs, as well as several intracellular TLRs. It is also required for the function of TLR1, 2, 4, 5, 7 and 9, but not TLR3 (Liu and Li, 2008, Randow and Seed, 2001, Yang et al., 2007b). GRP94-deficient macrophages lack the ability to respond to ligands of TLR2, 4, 5, 7 and 9 (Yang et al., 2007b). The surface expression of TLR1, TLR2 and TLR4 requires GRP94, and it is also involved in TLR9 maturation and cleavage (Randow and Seed, 2001, Yang et al., 2007b, Liu et al., 2010). GRP94 must therefore facilitate TLR folding and maturation, and allow the receptors to be trafficked from the ER. However, it is unknown where in the process GRP94 acts in TLR folding and how it carries out this role. Similar to HSP90, GRP94 also requires co-chaperones to aid in its action and this molecule is PRAT4A.

PRAT4A, like GRP94, is ubiquitously expressed. PRAT4A is a 276 aa protein that can be found in the ER, and has been shown to interact with TLR4. PRAT4A associates with the premature form of TLR4, though it does not interact with MD-2, and regulates the cell surface expression of TLR4 (Wakabayashi et al., 2006). Cells isolated from PRAT4A-deficient mice had lower levels of inflammatory cytokine production in response to TLR1, TLR2, TLR4, TLR7 and TLR9 ligands. Cytokine levels in response to TLR3 ligands however, were not affected (Takahashi et al., 2007). This suggests that the trafficking of TLR3 and TLR9 from the ER are regulated by different molecules. Takahashi et al. (2007) also found that PRAT4A^{-/-} mice inhibited the trafficking of TLR1 and TLR4 to the plasma membrane and TLR9s translocation to lysosomes following ligand stimulation. Like GRP94, PRAT4A is also crucial to the maturation of multiple TLRs in the ER.

GRP94 was thought to act independently without the need of co-chaperones however, Liu et al. (2010) discovered that GRP94 directly interacts with PRAT4A, and this complex dissociates in the presence of Adenosine Triphosphate (ATP). Single aa substitutions of GRP94 (E103A) and PRAT4A (M145K) rendered them unable to associate and in addition their TLR chaperoning function was abolished (Liu et al., 2010). TLR9 can also form a complex with PRAT4A and GRP94, and knockdown of either GRP94 or PRAT4A ablated TLR9s interaction with either molecule. GRP94 and PRAT4A alone cannot fold the TLRs, allowing them to reach full maturation (Liu et al., 2010). This suggests that TLR9s interaction with either molecule is dependent on the presence of the other, where both are critical to the folding and maturation of the receptor. It is thought that other TLRs may also share a similar mechanism when being folded, though why this doesn't affect TLR3 is still unknown. TLR3 is heavy glycosylated, and this alone may serve as an effective chaperoning method. Another possibility is that there may be a set of TLR3 specific chaperones which have similar roles to PRAT4A and GRP94.

1.2.4.1 - TLR2

In unstimulated monocytes, TLR2 is expressed on the cell membrane, early endosomes and lysosomes. TLR2 however, is not found in the Golgi apparatus and ER (Nilsen et al., 2008). Upon stimulation TLR2 accumulates in lipid rafts and is then rapidly relocated to phagosomes (Triantafyllou et al., 2006, Underhill et al., 1999). Similar to TLR2, TLR1 and TLR6 are also expressed on the plasma membrane, and following stimulation will gather in phagosomes (Underhill et al., 1999). In contrast, TLR10 is highly expressed in B cell lines and pDCs (Hasan et al., 2005). The complexes of TLR2/TLR1 and TLR2/TLR6 are gathered to the phagosomes, regardless of the presence of Gram-positive bacteria, thus allowing them the potential to detect the existence of other pathogens (Ozinsky et al., 2000). In response to zymosan, TLR10 and TLR2 can also be detected to colocalise to phagosomes, suggesting that TLR2/TLR10 functions similar to the TLR2/TLR1 complex (Guan et al., 2010).

Staphylococcus aureus needs to be engulfed before TLR2 activation can occur, as inhibition of this process prevents TNF- α and IL-6 production (Ip et al., 2008). However, engulfment isn't mandatory for Gram-positive bacterial wall components zymosan and LTA when activating TLR2 signalling (Nilsen et al., 2008). This suggests that whole bacteria are engulfed and their individual outer membrane components must be separated before TLR2 can recognise them.

Inflammatory monocytes, which are rapidly recruited to sites of infection in a Chemokine Receptor Type 2 (CCR2) -dependent manner, have been shown by Barbalat et al. (2009) to induce type I IFN production through TLR2 signalling. This TLR2-induced type I IFN production is only activated upon viral but not bacterial ligand stimulation. TLR2 internalisation is required for IFN production but not for TNF- α , this demonstrates that like TLR4, cellular localisation of the receptor can induce production of a different set of inflammatory cytokines.

1.2.4.2 - TLR4

Cells responsiveness to LPS is partly dependent on the levels of TLR4 expressed on the plasma membrane. These levels of TLR4 receptor are regulated by the amount of TLR4 that is trafficked from the Golgi apparatus to the cell surface and the levels of TLR4 inside of endosomes (McGettrick and O'Neill, 2010). Surface expression of TLR4 is dependent on MD-2, as fibroblast lacking MD-2 have TLR4 predominantly in the Golgi apparatus (Nagai et al., 2002).

In resting human monocytes, TLR4 can be detected in the Golgi apparatus and on the plasma membrane (Husebye et al., 2006, Latz et al., 2002). Confocal studies conducted by Latz et al. (2002) revealed that the TLR4-MD-2-CD14 complex is rapidly recycled between the Golgi apparatus and the plasma membrane. Interestingly, LPS is also trafficked between the two areas alongside the receptor complex. Trafficking of the TLR4-MD-2-CD14-LPS complex to the Golgi apparatus was originally thought to be critical for TLR4 signalling, however inhibition of this trafficking had no effect on the TLR4 pathway (Latz et al., 2002).

Following LPS stimulation, the TLR4-MD-2-LPS complex is translocated from the plasma membrane to the endosome (Tanimura et al., 2008). This translocation occurs within 15 minutes of LPS stimulation, and both MD-2 and CD14 greatly increased the binding and uptake of LPS (Husebye et al., 2006). Inhibition of LPS internalisation leads to LPS-induced NF κ B activation, and it was therefore thought that TLR4 relocation to the endosome was for its subsequent degradation. Where in fact, it was revealed that the internalisation of TLR4 was required for complete signalling from this receptor. Kagan et al. (2008) also inhibited internalisation of LPS and found that it had no effect on NF κ B activation, but demonstrated that Interferon Regulatory Factor 3 (IRF3) did not undergo phosphorylation. The internalisation of TLR4 was revealed to not only dampen the LPS response; it was also required for TLR4 to signal through TRIF Related Adaptor Molecule (TRAM) and TIR Domain-containing Adaptor Protein Inducing IFN- β (TRIF)

(Kagan et al., 2008). This relocation of the TLR4 was required to induce type I IFN production. In resting cells, TRIF is found diffusely in the cytoplasm (Honda et al., 2004). Upon LPS stimulation, TRIF is relocated to lipid rafts close to the cell surface, it is also trafficked to early endosomes where it localises with TRAM (Wong et al., 2009, Tanimura et al., 2008). In resting cells, TRAM is found at the plasma membrane and early endosomes: in endosomes TRAM can colocalise with CD14, but does not interact with TLR4 (Rowe et al., 2006, Tanimura et al., 2008). Within 30 minutes of LPS stimulation, TRAM is trafficked from the cell surface to early endosomes where it colocalises with TLR4 (Palsson-McDermott et al., 2009). TLR4, MD-2 and CD14 are all required for the translocation of TRAM, as cells that lack the expression of all three molecules fail to shuttle TRAM from the plasma membrane to early endosomes (Tanimura et al., 2008).

TRAM Adaptor with Golgi Dynamics (GOLD) Domain (TAG) is a splice variant of TRAM. It has been shown to negatively regulate TLR4 signalling by displacing TRIF from TRAM (Palsson-McDermott et al., 2009). The GOLD domain is found in several proteins that are involved in the Golgi apparatus secretion and localisation of proteins into vesicles (Anantharaman and Aravind, 2002). In resting cells, TAG is found in the ER and early endosomes. Upon LPS stimulation, TAG relocates to the membrane of late endosomes, there it interacts with TLR4 and TRAM. (Palsson-McDermott et al., 2009). The complex TRIF and TRAM is disrupted by TAG and subsequently inhibits type I IFN production (Palsson-McDermott et al., 2009). TAG also causes the degradation of TLR4, though it is unknown if TLR4s translocation to late endosomes is dependent on TAG.

TLR4 internalisation and its requirement for inducing type I IFN production ended the controversy involving TLR4 interaction with TRAM and Myeloid Differentiation Primary Response Gene 88 (MyD88) Adaptor-like (Mal). Following LPS stimulation, TLR4 dimerises and is recruited to phosphatidylinositol-4,5-bisphosphate (PIP₂) rich lipid rafts (Triantafilou et al., 2002). As Mal contains a PIP₂ binding domain, it is also trafficked to lipid rafts, where it colocalises with TLR4 (Kagan and Medzhitov, 2006). Following LPS stimulation, MyD88 is translocated to lipid rafts at the plasma membrane where it colocalises with Mal and TLR4, and activates NFκB signalling. Levels of PIP₂ drop during the process of endocytosis, and this causes Mal to dissociate from TLR4 (McGettrick and O'Neill, 2010). TRAM can then bind TLR4 and initiate IRF3 signalling (Kagan et al., 2008).

TLR4s ability to activate type I IFNs is unique among the cell surface TLRs. Whilst TLR4-mediated MyD88-dependent signalling occurs at the plasma membrane, MyD88-independent signalling

requires endocytosis of TLR4. In the endosome TLR4 can interact with TRIF and TRAM, which recruits TNF Receptor(TNFR)-associated Factor 3 (TRAF3) (Kagan et al., 2008). TRAF3 then undergoes TRIF-dependent lysine 63 (K63)-linked polyubiquitination, which is required for the activation of TRAF-family-member-associated NFκB Activator (TANK) Binding Kinase 1 (TBK1) and IκB kinase ε (IKKε) and phosphorylation of IRF3, resulting in IRF3 translocation to the nucleus and induction of type 1 IFN production (Tseng et al., 2010). In contrast TLR2 is unable to induce IFN production, as its expression is confined to the plasma membrane and TRAF3 is unable to be recruited to the cell surface, furthermore internalisation of TLR2 would cause dissociation of MyD88 and Mal disabling the receptors ability to propagate signalling (Kagan et al., 2008).

1.2.4.3 - Intracellular TLRs

TLR3, 7, 8 and 9 are found in intracellular compartments where they are needed to sense foreign nucleic acids. Blockage of endolysosome acidification prevents TLR7 and TLR9 induced immune responses (Kawai and Akira, 2010). This finding reveals that the internalising of nucleic acids is crucial for the activation of intracellular TLRs. TLR7 and 9 are found in the ER of unstimulated cells, and upon ligand stimulation they are promptly trafficked to endolysosomes (Kim et al., 2008). These intracellular TLRs possess retention signals that allow them to remain in the ER. These retention signals vary from TLR to TLR. For TLR9 either the ectodomain or the transmembrane is required for intracellular retention (Leifer et al., 2006). TLR7 only requires its transmembrane domain to retain it internally, whereas TLR3 has a 23 aa sequence in its cytoplasmic region that retains the receptor intracellularly (Nishiya et al., 2005). It is still unknown whether the cell surface TLRs contain either an export signal or the lack of a retention signal that determines their cellular localisation.

Following ligand stimulation, TLRs 3, 7 and 9 are trafficked from the ER to endosomes (Latz et al., 2004, Johnsen et al., 2006). Trafficking of TLR7 and 9 however, isn't ligand specific as LPS stimulation also causes the relocation of these two TLRs to endosomes (Kim et al., 2008). Endosomal localisation of TLR3 and TLR9 are however essential for dsRNA-induced and CpG-induced signalling in cells, respectively (Yi et al., 1998, Johnsen et al., 2006). For TLR9 to bind its ligand it must first undergo cleavage by cathepsin L. Inhibition of lysosomal proteolysis renders TLR9 inactive, although its importance at this point is not understood (Park et al., 2008). Much controversy surrounds the cleavage of TLR9 as deletion of specific LRRs in the N-terminus renders it unable to bind to its ligands. The N-terminus is also positively charged and has been proposed

to bind negatively charged DNA (Peter et al., 2009). This interaction site mimics that of TLR3's interaction site, and suggests that the endosomal TLRs may bind their cognate ligands in a similar fashion.

The localisation of these TLRs is important as it may help prevent recognition of self DNA. Barton et al. (2006) replaced the native transmembrane of TLR9 with that of TLR4 and found that the chimeric TLR9 receptor localised to the cell surface. It was able to respond to synthetic ligands, but failed to illicit a response to viral nucleic acids. The relocated chimeric receptor was also able to recognise self DNA, which wild-type (WT) TLR9 normally isn't exposed to. Normally self-nucleic acids are degraded rapidly before reaching the endolysosome, while viral DNA is protected by capsid proteins. TLR7 and TLR9 are therefore able to detect viral DNA, and this also serves as a safety mechanism, by limiting these receptors to compartments where self DNA doesn't normally exist (McGettrick and O'Neill, 2010).

The trafficking of TLRs from the ER to endolysosome is facilitated by the protein UNC93B1. This multi-transmembrane ER protein plays an important role in the localisation of intracellular TLRs, but doesn't have a role in the regulation of cell surface TLRs. Triple D mice which have a single missense mutation in the UNC93B1 gene, are unable to mount a proper immune reaction in response to TLR3, TLR7 and TLR9 ligands (Tabeta et al., 2006). As a result these mice are highly susceptible to bacterial and viral infection. UNC93B1 interacts with the transmembrane domains of TLRs 3, 7 and 9 and a single point mutation at residue 421 (H412R) abolishes signalling through these TLR pathways (Brinkmann et al., 2007). UNC93B1 appears to be involved in the delivery of TLR7 and TLR9 from the ER to endosomes; however its role may be more complex. Fukui et al. (2009) found that UNC93B1 has a bias towards DNA detection. A mutation of UNC93B1 upregulated its interaction with TLR7, which conversely caused a decrease in association with TLR9. This also led to an increase in ligand-induced trafficking of TLR7 and a decrease in TLR9 ligand-induced trafficking. Misregulation of TLR7 has been known to exacerbate autoimmune diseases, whilst TLR9 appears to confer a protective function in autoimmune diseases (Christensen et al., 2006). Previous studies have shown that overexpression of TLR9 suppresses TLR7, thus revealing that UNC93B1's bias towards TLR9 response may in fact be a protective mechanism against autoimmune diseases (Wang et al., 2006).

Adaptor Protein 3 (AP3) is another protein that has been shown to play a role in the trafficking of TLR9. Members of the AP family are involved in selecting cargo to be placed in vesicles part of the

late secretory and endocytic pathway (Nakatsu and Ohno, 2003). AP3 consists of four subunits, δ , μ 3A, β 3A and σ 3, and it is found on endosomal membranes, serving a role in recruiting proteins into endosomes for trafficking to lysosomes and Lysosomal-related Organelles (LROs) (Bonifacino and Traub, 2003). Cells lacking AP3 had reduced IFN production in response to CpG oligonucleotides and TLR9 was also not observed in Lysosome-associated Membrane Glycoprotein 2 (LAMP2)-expressing compartments, following treatment with CpG-A oligonucleotides coupled to a liposomal transfection reagent, DOTAP (Sasai et al., 2010). This suggests a role for AP3 in recruiting TLR9 to lysosomes or LROs. The failure of AP3-deficient cells to induce IFN production can also be attributed to the lack of IRF7 recruitment to lysosomes. These findings demonstrate the crucial role AP3 plays in inducing IFN secretion through TLR9 signalling.

TLR trafficking and localisation represents an important part of the receptors ability to sense ligands. Improper trafficking of the TLRs can potentially lead to autoimmune diseases; therefore these processes must be tightly regulated to ensure no recognition of “self” antigen occurs. As the trafficking of the TLRs is essential in the detection of pathogens, targeting these pathways may provide therapeutic benefits in downregulating inflammation.

1.3 - Toll-like receptor ligands

The expression of TLRs is not fixed; rather it is affected by the presence of pathogens, cytokines and environmental stresses. In addition, TLRs can be expressed intra- and extracellularly, and believed to correlate with the specific ligands they bind (Akira and Takeda, 2004). TLRs 1, 2, 4, 5, 6 and 10 are expressed on the cell surface, whilst TLRs 3, 7, 8 and 9 are found exclusively in intracellular compartments such as endosomes. As the ligands of these latter TLRs are mainly nucleic acids, they require internalisation before signalling can commence (Akira et al., 2006). Based on their primary sequence the TLRs can be further divided into subfamilies each recognising related PAMPs.

TLRs 1, 2, 4, 5, 6 and 10 recognise lipid based structures (O'Neill, 2006, Guan et al., 2010). TLR1 is known to recognise both triacylated lipoproteins and mycobacterial products (Takeuchi et al., 2002). Studies have shown that TLR2 ligands are peptidoglycan and LTA from Gram-positive bacteria (Schwandner et al., 1999). Subsequent studies have revealed that TLR2 heterodimerises

with either TLR1 or TLR6 in order to recognise triacylated and diacylated lipoproteins, such as Pam₃CSK₄ and zymosan respectively, further reiterating the high degree of specificity in the innate immune response (Takeuchi et al., 2001, Lin et al., 2000, Jin et al., 2007). TLR10 also recognises triacylated lipoproteins, similar to TLR1, and requires TLR2 to initiate signalling (Guan et al., 2010). It was once thought that the ligand for TLR2 was LPS, however further studies revealed that in fact it was TLR4 that recognised LPS from Gram-negative bacteria and TLR2 recognised lipoprotein contamination of LPS (Politorak et al., 1998, Hirschfeld et al., 2000). TLR4 can also recognise several structurally unrelated ligands, such as fibronectin and HSPs, however endogenous proteins contaminated with bacterial products cannot be discounted (Akira et al., 2006). The TLR5 ligand, profilin, a component of bacterial flagellin, allows the host to detect motile pathogens (See Table 1.1 and Figure 1.14) (Hayashi et al., 2001).

TLRs 3, 7, 8 and 9 recognise nucleic acids from invading pathogens (O'Neill, 2006). TLR3 recognises dsRNA, however, subsequent studies have shown that TLR3 may form multimers in response to poly (I:C), viral RNA, messenger RNA (mRNA) and siRNA (Jiang et al., 2003, Bell et al., 2005, Alexopoulou et al., 2001). In contrast to TLR3, TLRs 7 and 8 recognise ssRNA, and as these receptors are localised intracellularly, they are dependent on endosomal acidification before they can bind their targets (Diebold et al., 2004, Heil et al., 2004). TLR9 recognises unmethylated CpG dinucleotide containing sequences, which is found primarily in bacterial and viral genomic DNA (Table 1.1 and Figure 1.14) (Krug et al., 2004, Lund et al., 2003).

1.3.1 – Endogenous ligands

In response to a fungal infection, *D. melanogaster* activates protease cascades which lead to generation of the protein spätzle, an endogenous ligand of Toll. Spätzle binds to Toll and causes a signalling cascade. In contrast, mammalian TLRs interact directly with microbial proteins to generate an immune response and do not rely on endogenous ligands similar to Toll (Akira et al., 2001). There is however, increasing evidence that suggests TLRs can be stimulated by endogenous ligands which, in turn, activate the immune response.

Damaged or stressed cells can release signals that have the potential to trigger an immune response, even in the absence of an infection, this is known as the “danger model” (Matzinger, 1994). Cells that are entering programmed cell death (apoptosis) are usually scavenged by surrounding cells and macrophages before they disintegrate, whereas cells that die via the

Table 1.1: Toll-like receptors and their ligands.

Basith et al. (2012). "Roles of Toll-like receptors in Cancer: A Double-edged Sword for Defense and Offense." *Archives of Pharmacal Research*. 35: 1297-1316

Receptor	DAMPs (Danger-associated molecular patterns)	PAMPs (Pathogen-associated molecular patterns)	Synthetic analog
TLR1		Triacyl lipopeptides: Bacteria and mycobacteria. Soluble factors: <i>Neisseria meningitidis</i> .	Triacyl lipopeptides
TLR2	Heat-shock protein 60 (HSP60), HSP70, HSP96. High-mobility group protein B1 (HMGB1) Hyaluronic acid	Lipoprotein/lipopeptides: Gram-positive bacteria, Mycoplasma, Mycobacteria & Spirochetes. Peptidoglycan: Gram-positive bacteria. Lipoteichoic acid: Gram-positive bacteria. Lipoarabinomannan: Mycobacteria. Phenol-soluble modulin: <i>Staphylococcus epidermidis</i> . Glycoinositolphospholipids: <i>Trypanosoma cruzi</i> . Glycolipids: <i>Treponema maltophilia</i> . Porins: <i>Neisseria</i> . Atypical lipopolysaccharide: <i>Leptospira interrogans</i> , <i>Porphyromonas gingivalis</i> . Zymosan: <i>Saccharomyces</i> . Heat-killed bacteria: <i>Listeria monocytogenes</i> . Outer membrane protein A: <i>Klebsiella pneumoniae</i> . Phospholipomannan: <i>Candida albicans</i> . Structural viral proteins: Herpes simplex virus, Cytomegalovirus. Hemagglutinin: Measles viruses. Lipoarabinomannan: Mycobacteria.	Diacyl and triacyl lipopeptides
TLR3	Self double-stranded RNA (dsRNA), messenger RNA (mRNA)	Double-stranded RNA: Viruses.	Poly (I:C), Poly (I:C ₁₂ U)
TLR4	HSP22, HSP60, HSP70, HSP96, HMGB1β-defensin 2 Extra domain A of fibronectin Hyaluronic acid Heparan sulfate Fibrinogen surfactant-protein A	Lipopolysaccharide: Gram-negative bacteria. HSP60: <i>Chlamydia pneumoniae</i> . Taxol: plants. Fusion protein: Respiratory syncytial virus. Envelope protein: Respiratory syncytial virus & mouse mammary-tumour virus. Glycoinositolphospholipids: <i>Trypanosoma cruzi</i> .	Lipid A mimetics (monophosphoryl lipid A, aminoalkyl glucosamine 4-phosphate), E6020, E5531, E5564
TLR5		Flagellin: Bacteria.	Discontinuous 13 amino acid peptide CBLB502
TLR6		Diacyl lipopeptides: Mycoplasma. Lipoteichoic acid: Gram-positive bacteria. Zymosan: <i>Saccharomyces</i> . Phenol-soluble modulin: <i>Staphylococcus epidermidis</i> . Heat-labile soluble factor: Group B streptococcus.	Diacyl lipopeptides
TLR7	Endogenous RNA	Single-stranded RNA: Viruses.	Oligonucleotides, Imidazoquinoline (Imiquimod, Resiquimod), Guanosine nucleotides (Loxoribine, Istaribine), Bropirimine
TLR8	Endogenous RNA	Single-stranded RNA.	Imidazoquinolines (Resiquimod)
TLR9	Endogenous DNA	CpG-containing DNA: Bacteria and viruses. Hemozoin: <i>Plasmodium</i> .	CpG oligodeoxynucleotides
TLR10		Triacyl lipopeptides: Bacteria and mycobacteria.	Triacyl lipopeptides
TLR11		Profilin-like molecule: <i>Toxoplasma gondii</i> .	

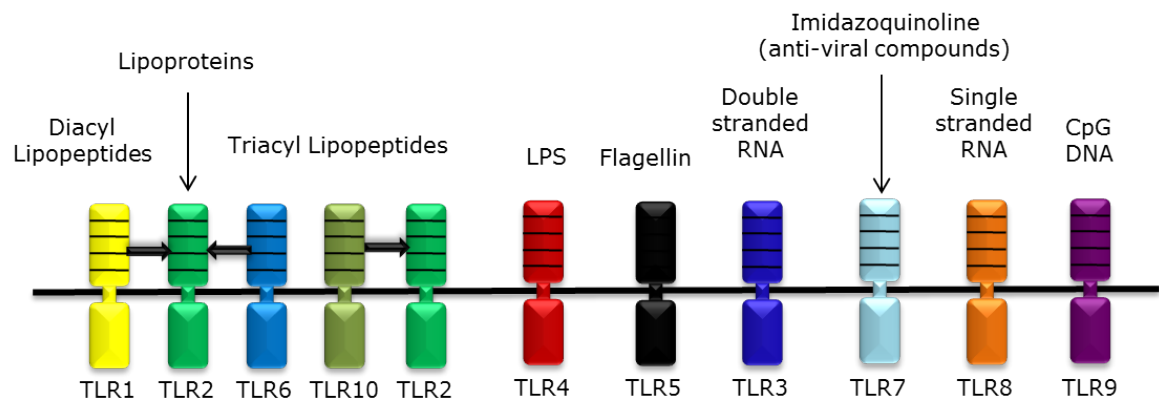


Figure 1.14: Toll-like receptor ligands.

Adapted from Akira, S. (2003). "Toll-like Receptor Signalling." *Journal of Biological Chemistry*. 278(40): 38105-38108.

necrotic pathway release their contents into the surrounding environment. Any intracellular substance can be a potential danger signal, as anything made or altered by the stressed or injured cell can be an inducible alarm signal (Matzinger, 2002). Proteins such as HSPs, which function as molecular chaperones, can alter their expression and sub-cellular localisation in response to stress. The trafficking of these proteins into an extracellular environment in response to stress is a key factor in activating DCs that eventually leads to the induction of adaptive immunity against both self and non-self antigens (Liu et al., 2003). The list of endogenous ligands for TLR2 and TLR4 continue to grow and these include the HSPs (GRP94, HSP22, HSP70 and HSP72), HMGB1 extracellular matrix molecules (biglycan, tenascin-C and versican), hyaluronic acid and heparin sulphate (Wheeler et al., 2009, Schaefer et al., 2005, Midwood et al., 2009, Kim et al., 2009, Termeer et al., 2002, Johnson et al., 2002, Vabulas et al., 2002a, Vabulas et al., 2002b, Roelofs et al., 2006, Klune et al., 2008). The presence of these Damage-associated Molecular Patterns (DAMPs) normally alerts the organism to tissue damage and this in turn initiates a tissue repair response (Piccinini and Midwood, 2010). DAMPs are analogous to a double-edged sword, on one hand they promote tissue repair, but at the same time may also contribute to the pathogenesis of inflammation and autoimmune diseases. Whether TLRs activate the immune response in the presence of these danger signals has yet to be determined. Though extensive work has been carried out on recombinantly generated endogenous ligands from *Escherichia coli*, contamination from endotoxin has been identified as an issue. Gao and Tsan (2003) found that in commercially available HSP70, LPS contamination was responsible for inducing TNF- α production, thus demonstrating the importance of purification steps and proper removal of endotoxin. Perhaps the most convincing evidence of endogenous ligands is from a study conducted by Curtiss and co-workers (Mullick et al., 2005), where it was shown that mice deficient in TLR2 had reduced atherosclerotic disease progression, whereas systemic exposure to TLR2 ligands resulted in increased atherosclerotic lesions.

1.4 - Toll-like receptor signalling

TLR ligand recognition triggers the activation of a signalling cascade, leading to the expression of genes that have antimicrobial properties. Following binding of a ligand to the receptor, TLRs dimerise and undergo conformational changes, which are essential to the recruitment of TIR-domain containing adaptor proteins (Akira et al., 2006). There are five adaptor molecules that the TLRs recruit to their TIR domain. These are MyD88, TIR Domain-containing Adaptor Protein

(TIRAP)/**Mal**, **TRIF**/TIR Domain-containing Molecule 1 (TICAM1), **TRAM**/TICAM2 and Sterile α and Armadillo Motif-containing Protein (**SARM**) (Figure 1.15) (Adachi et al., 1998, Kawai et al., 1999, Fitzgerald et al., 2001, Yamamoto et al., 2003a, Yamamoto et al., 2002a, O'Neill et al., 2003, Liberati et al., 2004). Genetic data has allowed the classification of TLRs into groups based on their use of adaptors. The first group consists of TLRs 5, 7, 8 and 9 which signal only via MyD88, the second group containing TLR2, uses both MyD88 and Mal, whilst the third group comprising only TLR3 utilizes TRIF; the fourth group that contains TLR4 makes use of all four adaptor molecules (Hacker et al., 2006, Gohda et al., 2004). The differences in responses from the TLRs can be attributed to the selection of these adaptor molecules. There are two common pathways that TLRs use for signal transduction, the first is the MyD88-dependent pathway also known as the canonical pathway, and the second is the MyD88-independent pathway, also known as the TRIF-dependent pathway (Figure 1.16).

1.4.1 - MyD88-dependent pathway

With the exception of TLR3, all TLRs make use of the MyD88-dependent pathway. As the cytoplasmic domains of the TLRs are homologous to that of IL-1R it is of no surprise that the relay of downstream signals is mediated by similar proteins. Activation of TLRs leads to the recruitment of MyD88 to the dimerised receptor. This complex then interacts with IL-1R-associated Kinases 1 (IRAK1), IRAK2, IRAK4 and IRAK-M. The interaction of the Death Domain (DD) of six MyD88, four IRAK4 and four IRAK2 molecules forms the Myddosome complex. As the complex is formed, IRAK4 becomes activated and phosphorylates IRAK1 which induces autophosphorylation of IRAK1, leading to interaction of the complex TRAF6 (Akira et al., 2003). Activation of IRAK2 is also required for robust activation of NF κ B and Mitogen-Activated Protein Kinases (MAPKs) (Kawagoe et al., 2008). The IRAKs and TRAF6 dissociate from the receptor complex and associate with another complex comprised of Transforming Growth Factor- β -activated Kinase 1 (TAK1), TAK1-binding proteins 1 (TAB1) and TAB2 (Uematsu and Akira, 2007). TRAF6 is critical in TLR signal transduction and can also act as a point of bifurcation between the canonical pathway and activation of the MAPKs. TRAF6 is a Really Interesting New Gene (RING)-domain E3 ubiquitin ligase and together with E2 ubiquitin conjugating enzyme Ubc13 and Ubc-like protein Uev1A, promotes K63-linked polyubiquitination of itself and IRAK1 (Kawai and Akira, 2010). The interaction of these two complexes induces phosphorylation of TAB2 and TAK1, which together with TRAF6 and TAB1 are translocated to the cytosol. TAK1 is then activated in the cytoplasm

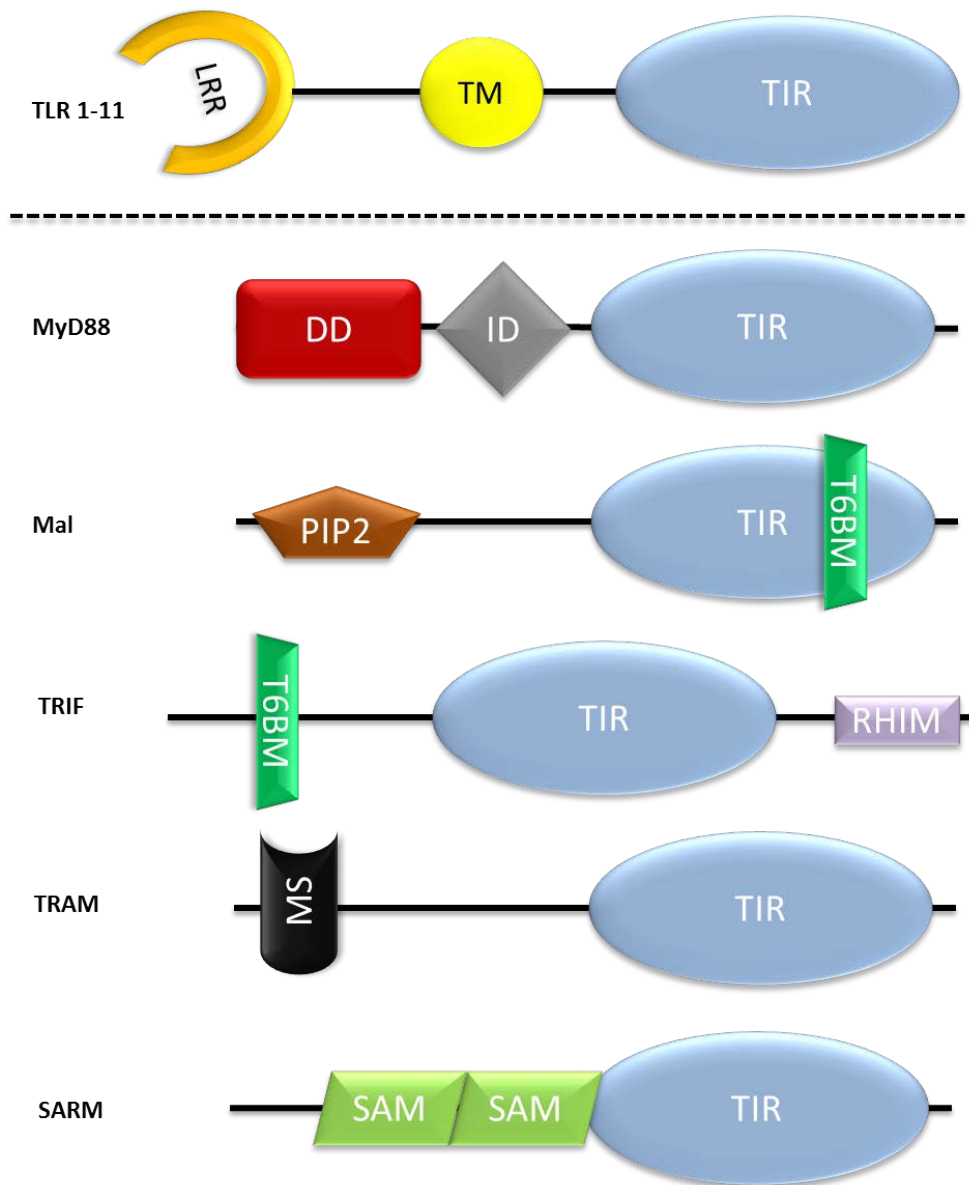


Figure 1.15: Schematic representation of Toll-like receptors and TIR containing adaptors.

TIR - Toll/IL-1R domain, DD - death domain, TM - transmembrane domain, LRR - leucine-rich repeats, ID - intermediary domain, PIP₂ - phosphatidylinositol-4,5-bisphosphate-binding motif, T6BM - TRAF6 binding motif, RHIM – Receptor-interacting Protein (RIP) homotypic interaction motif, MS - myristoylation site, SAM - Sterile α Motif (SAM) domain.

Adapted from O’Neill & Bowie. (2007). “The family of five: TIR-domain-containing adaptors in Toll-like receptor signalling.” *Nature Reviews: Immunology*. 7: 353-364.

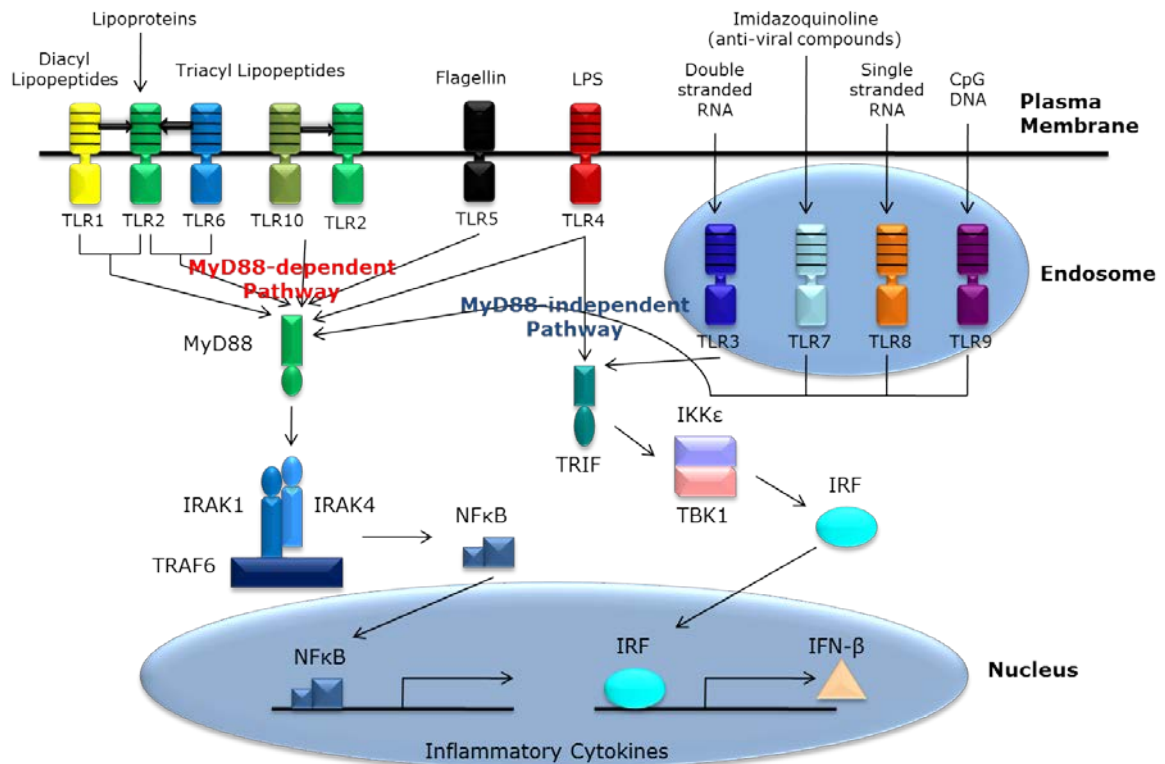


Figure 1.16: TLR-mediated signalling.

TLR3 utilises the MyD88-independent pathway (TRIF-dependent pathway). TLR4 uses both MyD88-dependent and -independent pathway. All other TLRs signal via the MyD88-dependent pathway.

where it activates the IKKs, IKK α and IKK β via serine phosphorylation (Kaisho and Akira, 2006). Normally I κ B sequesters NF κ B in the cytoplasm, but activation of the IKKs leads to phosphorylation and degradation of I κ B and the subsequent release of NF κ B into the nucleus (Wu and Arron, 2003). Activation of TAK1 also induces activation of MAPK, Extracellular Signal-regulated Kinases 1 (ERK1), ERK2, p38 MAPK (p38k) and c-Jun NH₂-terminal Kinase (JNK) (Wang et al., 2001).

1.4.1.1 - MyD88

MyD88 was originally isolated as a gene rapidly induced in response to IL-6 stimulated differentiation of M1 myeloleukemic cells into macrophages (Adachi et al., 1998). It was the first adaptor molecule found to be crucial for TLR and IL-1 signalling, where it is required to induce the expression of inflammatory cytokines such as TNF- α , IL-1 and IL-6 (Muzio et al., 1997, Adachi et al., 1998, Wesche et al., 1997, Gohda et al., 2004). MyD88 consists of an N-terminal DD and a C-terminal TIR domain that is separated by a short linker sequence (Akira et al., 2003, Adachi et al., 1998). The DD was originally identified in apoptosis promoting proteins. In most proteins the DDs are located in the extreme C-terminus of the protein, however in MyD88 and IRAKs they are found within the N-terminus (Janssens and Beyaert, 2002). Following further experimentation, MyD88 was cloned as an adaptor molecule, which recruits IRAK4 to the IL-1R complex following IL-1 stimulation. MyD88 recruits IRAK4 via homotypic interaction between their DDs. When recruited to the receptor complex, MyD88 itself forms homodimers through the interaction of its DD and TIR domain (Akira and Takeda, 2004).

MyD88 is crucial to the induction of type I IFNs following TLR7, TLR8 and TLR9 stimulation. In pDCs, TLR-mediated IFN- α production occurs through the formation of a complex consisting of MyD88, TRAF6 and IRF7, and activation of IRF7 is dependent on TRAF6 ubiquitin ligase activity (Kawai et al., 2004). Subsequent studies also found that MyD88 is vital in the activation of IRF7 by TLRs 7, 8 and 9, resulting in IFN- α production (Honda et al., 2004, Honda et al., 2005). A complex comprising of MyD88, IRAK1, IRAK4, TRAF6 and IRF7 has been reported in pDCs (Hochrein et al., 2004). IRAK1 phosphorylates IRF7, which is essential for TLR7, 8 and 9 induction of IRF7. IRAK1-deficient cells fail to induce IRF7, although NF κ B activation is only slightly impaired (Uematsu et al., 2005).

MyD88 can also interact with IRF1 and IRF5 and this has been shown to be vital to their activation. IFN- γ was required to induce IRF1 production and IRF1 translocated to the nucleus more efficiently with MyD88, where it was required for the induction of several TLR-dependent genes (Negishi et al., 2006). Takaoka et al. (2005) found IRF5 is generally required for TLR-MyD88-induced proinflammatory cytokine production, and IRF5-deficient mice failed to induce these cytokines in response to TLR ligands.

TRAF3 has also been demonstrated to interact with MyD88. Cells lacking TRAF3 were unable to induce type I IFNs and IL-10, but were still able to produce proinflammatory cytokines. TRAF3 is recruited to TRIF and is required for recruitment of TBK1 into contact with TIR domain containing complexes (Hacker et al., 2006). Oganessian et al. (2006) found that TRAF3 associates with TRIF and IRAK1 as well as TBK1 and IKK ϵ suggesting that it is a critical link between TLR signalling and IRF activation.

Mice with a random germ-line mutagenesis in MyD88 have revealed new insights into MyD88 function. This mutation termed Pocurante (Poc) site, results in an I179N mutation, rendering mice unable to respond to TLR ligands that signal through the MyD88-dependent pathway (Jiang et al., 2006). Interestingly, these mice were able to respond to diacylated lipopeptides demonstrating that TLR2/TLR6 may interact with MyD88 differently. Jiang et al. (2006) proposed that the Poc site of MyD88 interacts with BB loop from the TLRs and this surface is critical in signal transduction.

In humans who have a MyD88 deficiency, these patients suffer from life threatening recurrent pyogenic bacterial infections, however, they were otherwise healthy and had resistance to other types of microbes (von Bernuth et al., 2008). In contrast, MyD88-deficient mice are more susceptible to pathogens, suggesting that TLRs are the primary PRR in mice. Without antibiotics most MyD88-deficient patients would succumb to infection in early life, however, TLR signalling is less important in adult life, this is likely attributable to the development of the adaptive immune response.

1.4.1.2 - Mal

Mal was the second TIR-containing adaptor molecule described that is involved in TLR signalling (Fitzgerald et al., 2001, Horng et al., 2001). It was originally proposed that Mal participates in

TLR4-induced MyD88-independent pathway. However subsequent studies revealed its role in both TLR2 and TLR4 signalling as cytokine production via MyD88-dependent pathway was affected in Mal-deficient mice (Yamamoto et al., 2002a, Yamamoto et al., 2004, Horng et al., 2002). In MyD88-deficient mice, TLR4 is still able to activate NF κ B and MAPKs, albeit with delayed kinetics and this was thought to involve Mal (Horng et al., 2001, Horng et al., 2002). MyD88 and Mal were thought to function redundantly in the MyD88-independent pathway, but this was disproven with the generation of double MyD88/Mal-deficient mice which had impaired expression of inflammatory cytokines, but produced normal levels of IFN-inducible genes following LPS stimulation (Akira and Takeda, 2004). Similar to the MyD88/Mal-deficient mice, Mal knockout mice did not have impaired expression of TLR4-mediated IFN production confirming Mal's role in MyD88-dependent signalling and not MyD88-independent signalling (Akira and Takeda, 2004). Thus, genetic studies suggested that Mal was not dissimilar to MyD88, acting solely as a "bridging" adaptor by recruiting MyD88 to the TLR2 or TLR4 complex. Subsequent research has shown that Mal contains a PIP₂ binding domain, which facilitates Mal recruitment to the plasma membrane (Kagan and Medzhitov, 2006). This data distinguishes Mal from MyD88, as MyD88 functions solely as a signalling adaptor, whilst Mal primarily functions as a sorting adaptor allowing the recruitment of MyD88 to TLR2 and TLR4. Ectopic expression of Mal however is able to activate NF κ B, JNK, ERK1 and ERK2, and can form both homodimers and heterodimers with MyD88 (Fitzgerald et al., 2001).

Recent studies have demonstrated a novel role for Mal via an interaction between Mal and TRAF6. It was found that similar to TRIF (Ye et al., 2002), Mal also contains a TRAF6 Binding Motif (T6BM); this putative binding motif is required for interaction with TRAF6 and Mal-induced serine phosphorylation of the p65 subunit of NF κ B (Mansell et al., 2004). More importantly, MyD88 does not contain a T6BM and therefore cannot interact directly with TRAF6, meaning it can only interact with the signalling pathway via the IRAKs. Mal can also undergo tyrosine phosphorylation by Bruton's tyrosine kinase (Btk), which has a role in TLR2 and TLR4 signalling (Jefferies et al., 2003, Liljeroos et al., 2007, Gray et al., 2006). Tyrosine phosphorylation of Mal is required for it to signal, but also subjects it to Suppressor of Cytokine Signalling 1 (SOCS1)-mediated degradation (Mansell et al., 2006). Miggin and co-workers (2007) further found that Mal associated with caspase-1 which mediates its cleavage at Asp-190. Although the function of this cleavage event is unclear, it does affect Mal-mediated signalling. These studies therefore demonstrate a novel role for Mal in TLR2 and TLR4 signalling via this unique interaction with TRAF6, a function distinct from that of a bridging adaptor for MyD88.

1.4.2 - MyD88-independent pathway

The MyD88-independent pathway was discovered in MyD88^{-/-} mice that displayed delayed NFκB nuclear translocation but no NFκB-dependent gene expression in response to LPS (Kawai et al., 1999). The delayed responses failed to induce gene expression of inflammatory cytokines such as TNF-α and IL-1 but were sufficient for the induction of IFN-β and IFN-inducible genes (Kaisho and Akira, 2006). Unlike the MyD88-dependent pathway that is used by all the TLRs except TLR3; the MyD88-independent pathway's use is limited strictly to TLR3 and TLR4.

Upon binding of the cognate ligands of TLR3 and TLR4, TRIF is recruited via its TIR domain. Whilst TLR3 can directly interact with TRIF, TLR4 requires the adaptor molecule, TRAM. Signalling through TRIF causes activation of NFκB and IRF3, leading to production of IFN-β and other inflammatory genes (Yamamoto et al., 2002b, Oshiumi et al., 2003a). TRIF can also interact with non-canonical IκB kinases IKKε and TBK1 (Pandey and Agrawal, 2006). Both of these kinases serine phosphorylate IRF3 (Sharma et al., 2003), allowing it to translocate to the nucleus to induce the production of IFN-β and subsequently IFN-inducible genes via the IFN-α/β Receptor (IFNAR) and Janus Kinase-Signal Transducer and Activators of Transcription (JAK-STAT) pathway (Youn et al., 2005). The activation of IKKε and TBK1 by TRIF requires interaction with TRAF3 as TRAF3-deficient cells fail to induce IFN-β by TLR3, as well as TLR7 and TLR9 (Hacker et al., 2006, Oganessian et al., 2006).

In TLR4 signalling, TRAF3 can also associate with the MyD88-IRAK signalling complex. This causes TRAF3 to undergo lysine 48 (K48)-linked polyubiquitination and degradation via Cellular Inhibitor of Apoptosis 1 (cIAP1) and cIAP2 (Vallabhapurapu et al., 2008). Degradation of TRAF3 causes the signalling complex to move from the plasma membrane to the cytoplasm, allowing activation of TAK1 (Tseng et al., 2010). During MyD88-dependent signalling, degradation of TRAF3 via ubiquitination is essential for induction of proinflammatory cytokines and activation of MAPKs (Tseng et al., 2010). On the contrary, in MyD88-independent signalling, TRAF3 self-ubiquitination is important for induction of the IFN response (Tseng et al., 2010).

TRIF can also lead to the activation of NFκB via TRAF6; this interaction takes place via the T6BM. The mechanisms of NFκB activation are proposed to be similar to MyD88-dependent signalling. There is also a TRAF6-independent pathway, whereby TRIF interacts with the DD kinase Receptor-interacting Protein 1 (RIP1), through a RIP Homotypic Interaction Motif (RHIM) (Hernance et al.,

2005). RIP1 undergoes K63-linked polyubiquitination and this modification has been shown to be crucial for NF κ B activation (Meylan et al., 2004, Kawai and Akira, 2010). The adaptor, TNFR Type 1-associated Death Domain Protein (TRADD) can also interact with RIP1. TRADD-deficient cells show a loss of RIP1 ubiquitination which impairs NF κ B activation (Pobezinskaya et al., 2008, Ermolaeva et al., 2008). Pellino-1, a member of the E3 ubiquitin ligases, also plays a role in MyD88-independent signalling, as Pellino-1-deficient cells fail to ubiquitinate RIP1 and activate NF κ B (Chang et al., 2009). Upon poly (I:C) stimulation, TRIF forms a complex with TRAF6, TRADD, Pellino-1 and RIP1, thus activating NF κ B and MAPK pathways.

1.4.2.1 - TRIF

TRIF was the third adaptor protein described following database searches. Enforced expression of TRIF leads to the activation of the IFN- β promoter and NF κ B, whereas dominant negative forms of TRIF lead to inhibited TLR3-induced activation of IFN- β (Oshiumi et al., 2003a). The biological function of TRIF was discovered through the generation of TRIF-deficient mice, which when exposed to TLR3 and TLR4 ligands, displayed impaired activation of IRF3 and subsequent decreased production of IFN-inducible genes (Yamamoto et al., 2003a). Interestingly, in TRIF-deficient mice, the expression of cytokines is impaired in TLR4 signalling, despite normal function of the MyD88-dependent pathway. These findings show that TLR4 requires coordination of the MyD88-dependent and -independent pathways to induce cytokine production (Yamamoto et al., 2003a). In cells deficient in both TRIF and MyD88, LPS-mediated NF κ B activation was completely eliminated, demonstrating TRIFs role in mediating MyD88-independent signalling. These MyD88/TRIF double knockout cells also demonstrated no upregulation of LPS-inducible genes (Hirotsu et al., 2005).

Further studies generated a germ-line mutation in mice known as *Lps2*, which confirmed the role of TRIF. This mutation completely abolished poly (I:C)-induced signalling and LPS-induced cytokine production was severely impaired (Hoebe et al., 2003). Analysis of this mutation revealed that it caused a frame shift in TRIF, resulting in production of an unstable or inactive protein. Whilst these mice were resistant to a lethal dose of LPS, they were more susceptible to cytomegalovirus (CMV) infection suggesting TRIFs role in type I IFN production (Hoebe et al., 2003).

All molecules that interact with TRAF6 contain a T6BM and like Mal, TRIF also contains a T6BM. Sato et al. (2003) showed that disruption of the T6BM disabled TRIF and TRAF6 interaction. This

resulted in a decrease in TRIF-induced NF κ B activation, but did not affect IFN- β production. The N-terminus of TRIF was necessary for induction of IFN- β production through TBK1. McWhirter et al. (2004) demonstrated that in TBK1^{-/-} cells, TRIF was unable to activate IRF3 gene expression, supporting the importance of the TRIF N-terminus in recruiting TBK1 for IFN- β production.

The interaction of TRIF and TRAF3 has been shown to be crucial for type I IFN induction through IRF3 (Oganesyan et al., 2006). Whilst it was proposed that the N-terminal region of TRIF engaged TBK1 and mediated IRF-3 activation, it is now thought that TRIF binds TBK1 through NAK-associated Protein 1 (NAP1) and possibly TRAF3 (Sasai et al., 2005). Overexpression of NAP1 resulted in increased TBK1-mediated IFN- β production. The activation of NF κ B can occur via two different pathways involving TRIF. As stated previously, TRIF contains a T6BM in the N-terminal region that has been shown to be crucial for NF κ B activation (Sato et al., 2003). However, the role of TRAF6 is still unclear in MyD88-independent signalling as in TRAF6^{-/-} macrophages TLR3 signalling was not affected (Gohda et al., 2004). In contrast, TRAF6-deficient Mouse Embryonic Fibroblasts (MEFs), NF κ B activation was completely abolished (Jiang et al., 2003). The C-terminus of TRIF can also activate NF κ B through its interaction with RIP1. Following poly (I:C) stimulation, TRIF recruits both RIP1 and RIP3 to this domain, and in the absence of RIP1, NF κ B activation was attenuated, but not IFN- β production (Meylan et al., 2004). RIP3 in contrast negatively regulates TRIF and RIP1-induced NF κ B signalling. Therefore TLR3-mediated NF κ B activation is dependent on TRIF and RIP1 interaction (Meylan et al., 2004).

Other than NF κ B and IRF3 activation, TRIF can also activate a third signalling pathway. In response to *Yersinia*, signalling via TRIF induces apoptosis through interaction with Fas-associated Death Domain (FADD) and caspase-8 (Ruckdeschel et al., 2004). Kaiser and Offermann (2005) reported that TRIF is able to induce apoptosis through the RHIM. Though the domain containing the RHIM can activate NF κ B and IRF3, it is the presence of this motif that gives TRIF this pro-apoptotic property.

1.4.2.2 - TRAM

TRAM is the fourth TIR adaptor molecule that has been identified. *In vitro* studies have shown that TRAM interacts only with TRIF and TLR4, but not TLR3 (Oshiumi et al., 2003b, Fitzgerald et al., 2003). TRAM-deficient mice also demonstrate defects in cytokine expression in response to TLR4 ligands specifically, but not to ligands of other TLRs, whilst TLR3-mediated IFN- β production via

MyD88-independent pathway was not abolished (Yamamoto et al., 2003b). These studies therefore demonstrated that TRAM is essential for TLR4 signalling via the MyD88-independent pathway.

TRAM undergoes myristoylation at the N-terminus, a form of protein modification where myristic acid is covalently bound to an aa (Boutin, 1997), and this has been shown to be required for membrane association (Rowe et al., 2006). Mutation of this domain abrogated TRAM binding to the plasma membrane and localised it to the cytosol, and this mutant was unable to reconstitute LPS signalling in TRAM-deficient mice. TRAM is also phosphorylated at the Ser-16 residue by Protein Kinase C- ϵ (PKC- ϵ) (McGettrick et al., 2006). In PKC- ϵ -deficient cells, induction of IFN- β and Regulated and Normal T cell Expressed and Secreted (RANTES) expression was impaired, demonstrating the importance of serine phosphorylation of TRAM for signalling.

Studies by Kagan et al. (2008) have shown that TRAM functions as a sorting adaptor, similar to Mal. Their study proposed a new model of TLR4 Mal-MyD88 and TRAM-TRIF signalling. TLR4 first activates Mal-MyD88 at the plasma membrane following ligand binding, this then results in endocytosis of the receptor. As the endosome becomes acidified, the Mal-MyD88 complex dissociates from the receptor, allowing the TRAM-TRIF complex to interact with TLR4 via their TIR domains, resulting in the induction of IFN- β production (Kagan et al., 2008).

1.4.2.3 – SARM

SARM is the fifth TIR containing adaptor molecule, and has been demonstrated to negatively regulate TLR signalling (Liberati et al., 2004). SARM was originally identified as an orthologue of *D. melanogaster* protein (Mink et al., 2001). It also has an orthologue in *Caenorhabditis elegans* that has been implicated in TLR signalling and has been shown to regulate expression of two anti-microbial peptides, NLP-29 and NLP-31 (Couillault et al., 2004). SARM is a 690 aa protein that contains a TIR domain, two Sterile α Motifs (SAM) and an Armadillo Repeat Motif (ARM) (O'Neill et al., 2003).

In *C. elegans* only two genes encode TIR domain containing proteins, *tol-1* (TLR homolog) and *tir-1* (SARM orthologue). It was shown that RNA interference (RNAi) of *tir-1* increased *C. elegans* susceptibility to bacterial and fungal infection, demonstrating its importance in worm innate immunity (Couillault et al., 2004, Liberati et al., 2004). Liberati et al. (2004) also found that

overexpression of SARM did not activate NF κ B or IRF3 signalling. In humans, SARM acts as a negative regulator of TLR signalling. Bowie and co-workers (Carty et al., 2006) demonstrated that SARM expression did not inhibit MyD88-dependent NF κ B activation, however it did inhibit TRIF-dependent NF κ B activation. SARM was shown to inhibit signalling through TLR3 and TLR4, as both poly (I:C) and LPS stimulation impaired RANTES expression. SARM exerts its inhibitory effects on TLR signalling by targeting TRIF. Carty et al. (2006) found that the inhibition of TRIF required the TIR and SAM domains of SARM, as truncated constructs lacking either the TIR or both SAM domains failed to inhibit NF κ B activation. Whilst LPS can induce expression of SARM, deletion of the N-terminus of SARM inhibited its ability to regulate LPS-induced signalling. In *C. elegans*, the N-terminal domain also appears to have a regulatory or inhibitory function, and similar to SARM the TIR and SAM domains are important for TIR-1 function (Chuang and Bargmann, 2005).

In human and mice myeloid cells, SARM is found to be expressed at very low levels (Kim et al., 2007b). SARM was identified to be expressed mainly in neuronal cells, where it can interact with mitochondria, microtubules and JNK3 to regulate the death of neuronal cells during oxygen and glucose deprivation. Ding and colleagues (Kim et al., 2007b) found that murine SARM has a nonredundant role in macrophages. SARM-deficient Bone Marrow-derived Macrophages (BMMs) were stimulated with Pam₃Cys, poly (I:C), LPS and CpG DNA and produced similar levels of cytokines compared to WT BMMs. In macrophages, perhaps SARM does not regulate responses to TLR ligands. SARM was also detected in T lymphocytes, and this may be the site where SARM exerts its inhibitory effects.

The horseshoe crab, *Carcinoscopius rotundicauda*, also expresses SARM (CrSARM), and similar to human SARM it too acts as a negative regulator. In the presence of CrSARM, overexpression of TRIF failed to activate NF κ B (Belinda et al., 2008). Comparable to human SARM, deletion of the SAM, ARM and TIR domains impaired the inhibitory properties of CrSARM. This study demonstrated how evolutionary conserved SARM is, with its function conserved from arthropod to human.

SARM was demonstrated to be able to inhibit LPS-induced MyD88 and TRIF-mediated Activator Protein 1 (AP-1) activation (Peng et al., 2010). siRNA knockdown of SARM enhanced expression of AP-1, further supporting the role of SARM inhibition of AP-1. SARM expression was shown to reduce phosphorylation of p38k, independent of TRIF and MyD88, although it is thought that this is not a secondary effect of SARM-TRIF interaction (Peng et al., 2010). Confocal microscopy

studies demonstrated that in humans, full length SARM was found in the nucleus and cytoplasm, whereas the N-terminal deletion mutant was only found in the cytoplasm. On the contrary, in mice SARM is found localised to mitochondria. As mouse and human SARM have different tissue expression and subcellular localisation, this may explain the different functions SARM has.

1.4.3 - Signalling molecules

1.4.3.1 - NFκB

Ultimately, TLR signalling leads to the activation of the prototypic inflammatory transcription factor family NFκB. The NFκB family control a wide variety of physiological and pathological functions, including immunity, inflammation and cell survival (Adhikari et al., 2007). The NFκB transcription factors all contain a Rel-homology domain that bind to specific DNA sequences known as κB consensus sites (Kawai and Akira, 2007). In mammals there are five members of the NFκB family: RelA (p65), RelB, C-Rel, p105/NFκB1 (a precursor of p50) and p100/NFκB2 (a precursor of p52) (Akira and Takeda, 2004). The transcription factors form homo- and heterodimers that regulate the expression of overlapping genes involving a variety of cellular processes. The NFκB dimers are normally sequestered in the cytosol of unstimulated cells. This is achieved through the interaction of the inhibitory protein of the NFκB family, IκB (Nolan et al., 1991). In TLR signalling, the most common inflammatory form of NFκB is the heterodimer p65 and p50 (Hayden et al., 2006). Upon TLR ligand binding, IκB is phosphorylated at specific serine residues by the IKK complex, made up of IKKα, IKKβ and a regulatory subunit NFκB Essential Modifier (**NEMO**)/IKKγ (Kawai and Akira, 2007). IKKα and IKKβ are structurally similar; both contain a kinase domain, a leucine zipper domain, helix-loop-helix structures and a NEMO-binding Domain (NBD). Phosphorylated IκB is targeted for ubiquitination and undergoes 26S proteasome degradation, thus allowing NFκB to translocate to the nucleus where it induces the expression of inflammatory genes. This pathway is known as the “canonical pathway” and is the pathway utilised by TLRs to induce inflammatory cytokines such as TNF-α and IL-6 (Hayden et al., 2006). DiDonato et al. (1997) found that it is IKKβ that plays a pivotal role in the activation of NFκB in TLR signalling. IKKα in contrast, is important in the termination of NFκB signalling (Li et al., 2005). Transactivation of the p65 subunit via phosphorylation enhances the overall transcriptional activity of NFκB and this is regulated by several kinases and occurs inside the nucleus (Vermeulen et al., 2002).

Baeuerle and co-workers (Schreck et al., 1991) first demonstrated that Jurkat cells stimulated with hydrogen peroxide (H_2O_2) could activate NF κ B. Subsequent studies focused on T cells, which during inflammation, are subjected to ROS produced from macrophages and neutrophils (Lander, 1997). ROS-induced activation of NF κ B is dependent on tyrosine phosphorylation of I κ B α , rather than classical serine phosphorylation by the IKK complex (Schoonbroodt et al., 2000). Furthermore, studies have suggested that ROS may also be involved in activation of NF κ B by proinflammatory cytokines. In lymphoid and monocytic cells, NF κ B activation by IL-1 β was reported to require ROS (Bonizzi et al., 2000). In addition, Li et al. (2006) further demonstrated in epithelial cells ROS production was crucial for NF κ B activation by IL-1 β . ROS generation was dependent on the small GTPase, Rac-1 and allowed TRAF6 to associate with the endocytosed IL-1 receptor, resulting in IKK and NF κ B activation (Li et al., 2006). Other studies have implicated ROS in the activation of NF κ B by LPS through the use of antioxidants. Neutrophils treated with the antioxidants, N-Acetyl-Cysteine (NAC) and α -tocopherol, displayed impaired LPS-induced NF κ B activation and expression of cytokines (Asehnoune et al., 2004). In a subsequent study, human monocyte cells, THP1, were also treated with NAC and Dimethyl Sulfoxide (DMSO), and LPS-induced NF κ B activation was also blocked, along with IL-8 production (Ryan et al., 2004). In response to LPS, activation of Rac-1 and generation of ROS was demonstrated to be crucial to the activation of NF κ B and production of TNF- α (Sanlioglu et al., 2001). This indicates that ROS production is a key mediator in activating immune response. Park et al. (2004) was able to identify the source of ROS generation in HEK293Ts. Following LPS stimulation, TLR4 was found to interact with Nicotinamide Adenine Dinucleotide Phosphate (NADPH) Oxidase 2 (Nox2) and mediate ROS production. Collectively, these studies indicate that ROS generation serves as another signalling paradigm that induces robust NF κ B activation and expression of proinflammatory cytokines.

1.4.3.2 - IRAK family

The IRAK family are a group of serine/threonine kinases (Cao et al., 1996b), which in mammals, four different IRAK molecules have been identified; IRAK1, IRAK2, IRAK4 and IRAK-M. IRAK4 is most significantly involved in the MyD88-dependent pathway, made evident by IRAK4-deficient mice exhibiting severely impaired immune responses when challenged with TLR ligands (Suzuki et al., 2002). The expression patterns of these IRAKs differ in that IRAKs 1 and 4 are expressed in all tissues, whereas IRAK2 has a small cellular distribution and IRAK-M expression is limited to cells of myeloid origin (Akira et al., 2003). All IRAKs contain a DD at the N-terminus, a proST domain, a

central serine/threonine kinase domain and a C-terminal domain (except IRAK4) (Feinstein et al., 1995, Kollwee et al., 2004) (Figure 1.17). The DD is required for interaction with DD containing molecules such as MyD88 (Muzio et al., 1997). The proST domain is rich in serine, proline and threonine, and it is reported that IRAK1 undergoes hyperphosphorylation here (Kollwee et al., 2004). IRAK1 is reported to contain two P-E-S-T sequences in this domain, which mediates its degradation, whilst IRAK2 does not contain these P-E-S-T sequences and is therefore not degraded (Martin and Kollwee, 2001). The central domain contains the activation loop which is vital for kinase activity. The kinase domain of each IRAK also contains a conserved lysine residue in the ATP binding site that is pivotal to its catalytic ability (Meylan and Tschopp, 2008). The C-terminal domain contains T6BMs which are important for interaction with TRAF6 (Ye et al., 2002). IRAK1 contains three T6BMs; IRAK2 has two T6BMs and IRAK-M one.

A study by Gay and co-workers (Motshwene et al., 2009) demonstrated that MyD88 and IRAK4 can assemble into a complex through their DDs and this was further confirmed by Lin et al. (2010) who reported the crystal structure. This complex, termed the Mydosome is thought to be important for TLR4 signalling and may serve to recruit IRAK2 or IRAK-M to the signalling complex. MyD88 serves as an adaptor for IRAK4 and IRAK1 interaction. IRAK4 has been reported to phosphorylate IRAK1, allowing it to autophosphorylate itself. IRAK4 has also been implicated in inducing the degradation of IRAK1. Expression of IRAK4 was sufficient in causing IRAK1 degradation, demonstrating a negative feedback loop that can regulate MyD88-dependent signalling (Kubo-Murai et al., 2008). IRAK4 has also been demonstrated to be important in inducing type I IFN production by TLR7, TLR8 and TLR9. Although IRAK4-deficient cells could still produce type I IFNs, showing that in response to viruses they can signal alternatively through TLR3 and TLR4 signalling pathways.

The kinase activity of the IRAK1 increases greatly following IL-1 stimulation and is required for signalling through to NFκB. However, kinase activity itself is not essential for signalling function as NFκB activation is still detectable in cells containing IRAK1 kinase defective mutants. In contrast, kinase defective mutants of IRAK4 inhibit IL-1-induced NFκB activation, revealing that the kinase activity in IRAK4 is crucial to TLR signalling (Suzuki et al., 2002).

Following ligand binding by the TLRs, MyD88 recruits and binds IRAK4 via DD-DD homotypic dimerisation; this allows the phosphorylation of critical residues in the kinase activation loop of IRAK1. Thr-66 has been indicated as an important residue in the DD, as it is crucial for formation

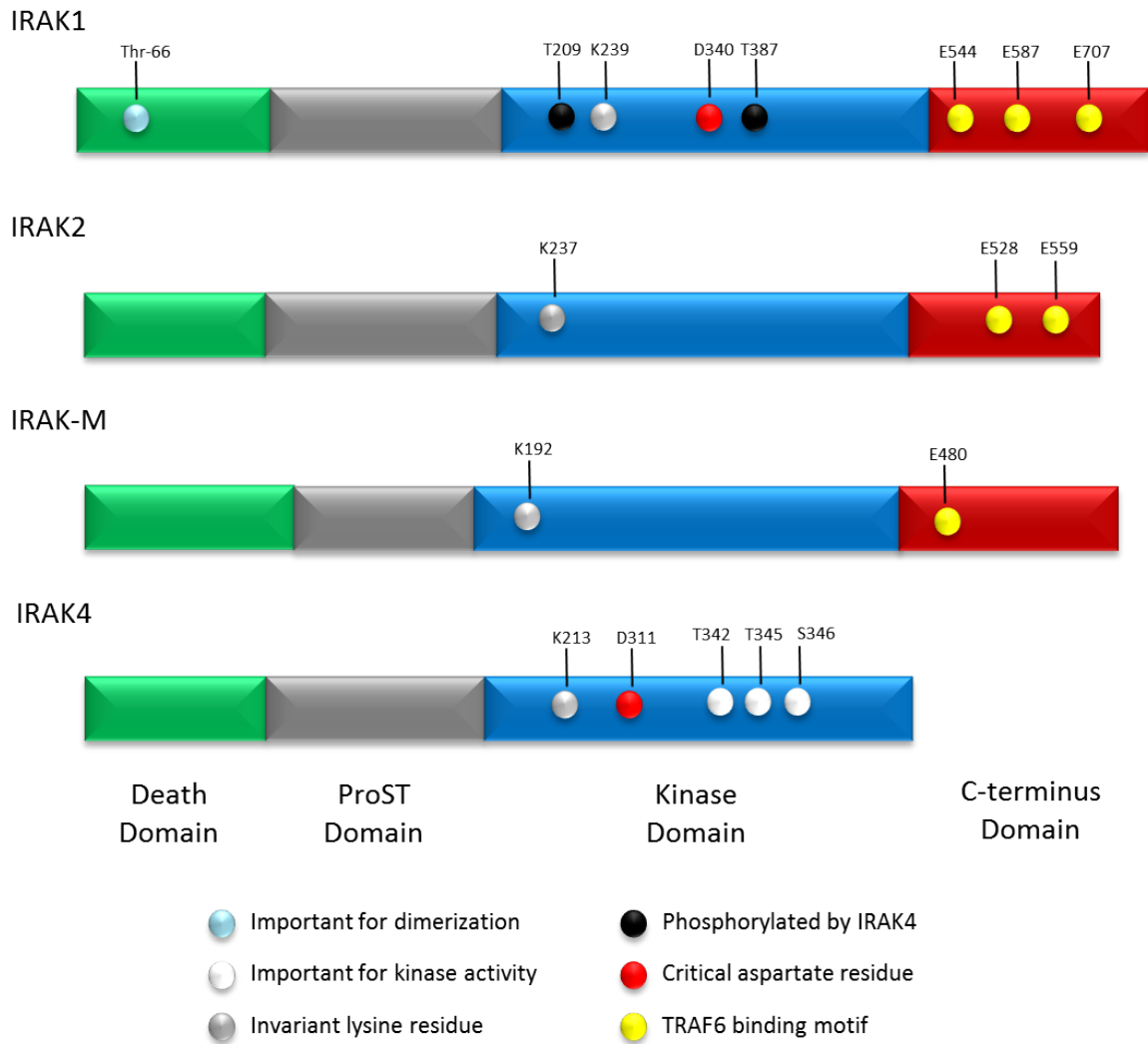


Figure 1.17: IRAK family members.

The domains of IRAK family members. All members possess a death domain, proST domain, a conserved kinase domain and a C-terminal domain. Only IRAK4 does not contain a C-terminal domain. IRAK1 contains a critical residue at Thr-66 that is required for signalling. It undergoes hyperautophosphorylation in the proST domain. Thr-209 and Thr-387 are also located in the activation loop and are potential phosphorylation sites for IRAK4. The invariant lysine residue of IRAK1 is located in the ATP binding pocket at K239, there is also a critical aspartate residue at D340 and these are important for IRAK1 kinase function. IRAK1 contains three T6BMs in the C-terminus at E544, E587 and E707. IRAK2s invariant lysine residue is located at K237 in the ATP binding pocket, and this is critical for its kinase activity. IRAK2 also contains two T6BMs in its C-terminus located at E528 and E559. The invariant lysine residue of IRAK-M is located at K192. IRAK-M's T6BM is found at the C-terminus at E480. IRAK4 which lacks a C-terminus has its invariant lysine residue at K213. The aspartate residue at D311 is crucial for IRAK4 kinase activity. The residues at T342, T345 and T346 are also important for IRAK4 function.

Adapted from Flannery et al. (2010). "The interleukin-1 receptor-associated kinases: Critical regulators of innate immune signalling." Biochemical Pharmacology. 80: 1981-1991.

of IRAK1 homodimers. Mutation of this residue did not ablate interaction with IRAK2 or IRAK-M, but did impair NF κ B activation (Ross et al., 2002). Activated IRAK1 is believed to autophosphorylate residues in its N-terminus and TRAF6 is also recruited to the receptor complex, via T6BMs (Ye et al., 2002). Extensive studies have revealed that IRAK1 is a direct substrate for IRAK4, and that IRAK1-deficient mice demonstrated only reduced cytokine expression in response to LPS and IL-1 (Thomas et al., 1999, Swantek et al., 2000, Li et al., 2002). In contrast, IRAK4-deficient mice demonstrate almost no response to LPS and IL-1 stimulation (Suzuki et al., 2002). IRAK4 has been shown to play a pivotal role in signal transduction as IRAK4 knockout mice and humans with IRAK4 deficiency exhibit defects in the IL-1/TLR signalling pathway (Cheng et al., 2007). Humans deficient in IRAK4 have indistinguishable clinical features from MyD88-deficient patients (Picard et al., 2010). They too are susceptible to life threatening infections, although the severity of these infections decrease with age probably due to the development of an adaptive immune response (von Bernuth et al., 2012).

Following TLR stimulation, IRAK1 has been reported to undergo phosphorylation. Kollwe et al. (2004) found that, *in vitro*, IRAK1 first undergoes phosphorylation at Thr-209, which induces a conformational change of the kinase domain allowing further phosphorylation to take place. Next, Thr-387 is phosphorylated in the activation loop and this gives it maximal enzymatic activity (Kollwe et al., 2004). This residue has been suggested as a site for phosphorylation by IRAK4. IRAK1 then autophosphorylates in the proST domain; hyperphosphorylation of this domain permits IRAK1 to dissociate from MyD88 but IRAK1 remains bound to TRAF6 (Kollwe et al., 2004). How TRAF6 is activated by IRAK1 is still unknown. IRAK1 has been reported to undergo both ubiquitination and SUMOylation (Conze et al., 2008). Following activation and the subsequent phosphorylation events, IRAK1 has been found to undergo K48-linked ubiquitination resulting in its degradation by proteasomes (Yamin and Miller, 1997). Other studies have reported that IRAK1 also undergoes K63-linked ubiquitination, which has been shown to be required for signal transduction rather than degradation (Conze et al., 2008, Windheim et al., 2008, Ordureau et al., 2008). Windheim et al. (2008) reported that IRAK1 undergoes K63-linked ubiquitination and this enables it to interact with NEMO, the regulatory subunit of NF κ B. Mutation of the ubiquitination sites ablates NEMO binding and TLR-induced NF κ B signalling. Other studies propose that TRAF6 and Pellino act as the E3 ubiquitin ligase inducing K63-linked ubiquitination of IRAK1 (Conze et al., 2008, Windheim et al., 2008, Ordureau et al., 2008). Newton et al. (2008) has further found that RIP1 and IRAK1 can also both undergo polyubiquitin editing. Both proteins firstly undergo K63-linked polyubiquitination, at later time points they are targeted to the

proteasome through K48-linked ubiquitination and this is mediated by A20 (Wertz et al., 2004). This demonstrates that polyubiquitin editing is a means of regulating the innate immune system.

IRAK1 and IRAK4 contain a functional catalytic site with a critical aspartate residue, whilst IRAK2 and IRAK-M have inactive kinase domains, due to a substitution of the critical aspartate residue to a serine or asparagine residue. However it is unclear whether IRAK2 functions as an active kinase as it cannot undergo autophosphorylation like IRAK1 and IRAK4 (Wesche et al., 1999). IRAK-M has been demonstrated to negatively regulate TLR signalling, following TLR stimulation. IRAK2 does contain an ATP-binding pocket with the conserved lysine residue in the kinase domain, and it has been proposed that this may be sufficient for kinase activity (Meylan and Tschopp, 2008, Kawagoe et al., 2008). Kawagoe et al. (2008) found that IRAK2 is phosphorylated following stimulation with TLR2 ligands, and it is thought that IRAK4 can phosphorylate IRAK2, activating its kinase function. Whilst overexpression of IRAK1 and IRAK4 kinase dead mutants still activated NF κ B, overexpression of an IRAK2 kinase dead mutant abolished NF κ B activation revealing that IRAK2 has the potential to be a kinase important for NF κ B activation (Kawagoe et al., 2008).

IRAK2 was initially demonstrated to interact with TRAF6 and MyD88 and activate NF κ B, suggesting that its function is similar to IRAK1 (Muzio et al., 1997). Other studies have suggested that IRAK2 interacts with Mal (Fitzgerald et al., 2001). The importance of IRAK2 in TLR-induced NF κ B signalling was revealed in studies using Vaccinia virus. Vaccinia produces a protein called A52, that interacts with IRAK2 and TRAF6 thus inhibiting NF κ B activation (Harte et al., 2003). As the virus only targeted IRAK2, this highlighted its importance in activating NF κ B. siRNA studies in human cell lines have also demonstrated that IRAK2 participates in the NF κ B response for a number of TLRs, including TLR3 (Keating et al., 2007). Kawagoe et al. (2008) demonstrated that both IRAK1 and IRAK2 act redundantly at early time points following TLR stimulation, however IRAK2 is crucial in sustaining the response at later time points. In macrophages, IRAK2 was necessary in order to mount an optimal immune response by most TLRs and for IL-1 signalling (Kawagoe et al., 2008). Interestingly, Jiang et al. (2003) found that IRAK2 is recruited to TLR3, although further studies are required to fully elucidate the role of IRAK2 in MyD88-independent signalling.

1.4.3.3 - TRAF6

The TRAF family of intracellular proteins function as adaptor molecules. To date, there are seven known mammalian TRAFs (Kobayashi et al., 2004). Except for TRAF1, all the TRAF proteins are characterized by the presence of an N-terminus, containing a RING finger followed by several zinc fingers (Chung et al., 2002, Naito et al., 1999). The C-terminus of TRAF contains a coiled-coil domain known as the TRAF-N domain and a highly conserved TRAF-C domain (Wu and Arron, 2003) (Figure 1.18). The N-terminal domain is essential for signalling, and deletion of this section of the protein renders it unable to signal (Lomaga et al., 1999). Studies have revealed that the RING finger domain is required for NF κ B activation and that the zinc fingers in the N-terminus have been demonstrated to mediate DNA binding and/or protein-protein interactions (Arch et al., 1998, Rothe et al., 1995). The RING finger has also been proposed to modulate protein levels via the ubiquitination and subsequent degradation of proteins by proteasomes (Lorick et al., 1999). Structural studies of the C-terminal TRAF domain reveal that it forms a mushroom like structure, with the coiled-coil TRAF-N domain as the stalk and the TRAF-C domain as the head (Park et al., 1999) (Figure 1.19). The TRAF domain allows the molecule to self-associate and interact with receptors and other signalling molecules (Takeuchi et al., 1996).

The TRAF proteins are able to interact with and transduce signals from multiple receptors, and each receptor is also able to utilize multiple TRAFs for particular roles (Arch et al., 1998). Unlike the other TRAFs that mediate signalling from the TNFR super-family, TRAF6 mediates signal transduction in the IL-1R/TLR super-family (Chung et al., 2002). Structural analysis has revealed a 40° difference in the directions of the bound peptides in TRAF6 and TRAF2, demonstrating the remarkable differences in receptor recognition between TRAF6 and the other TRAF molecules (Ye et al., 2002). The T6BM also allows TRAF6 to interact with many different signalling molecules; including IRAKs, TRIF and Mal (Ye et al., 2002, Sato et al., 2003, Mansell et al., 2004). The binding motif of TRAF6 has been identified as P-X-E-X-X-(aromatic/acidic residue) (Ye et al., 2002). This motif sequence is also found in CD40, TNF-related Activation-induced Cytokine Receptor (TRANCE) and IRAKs; three of these motifs in IRAK1, two in IRAK2 and one in IRAK-M (Table 1.2) (Akira and Takeda, 2004). TRAF6 has a very diverse and significant role in immunity and homeostasis, as it is involved not only in immunity, but also bone remodelling and cell survival (Lee and Lee, 2002).

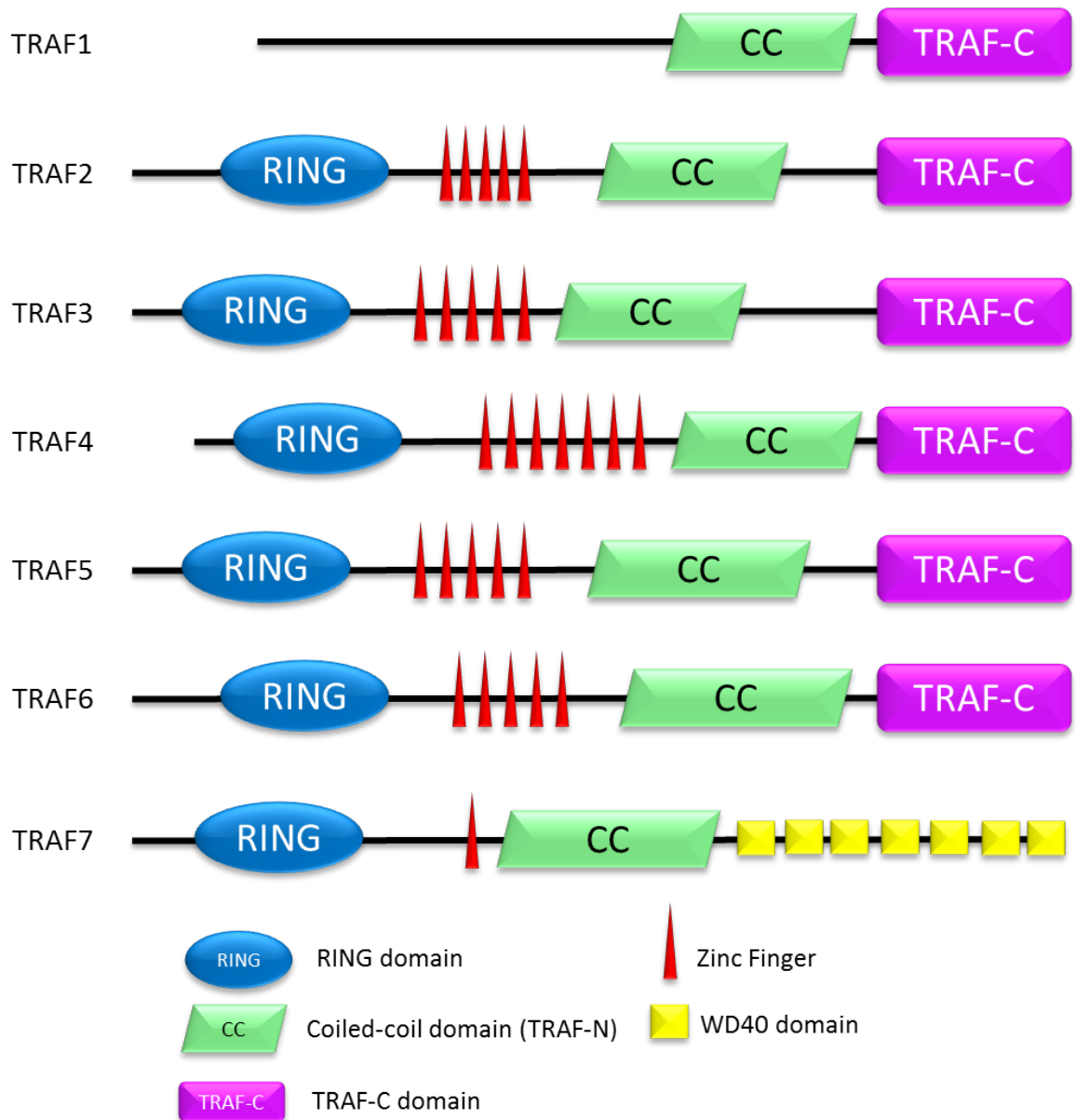


Figure 1.18: TRAF family members.

TRAF proteins contain an N-terminal zinc binding domain (containing a RING finger followed by several zinc fingers), and a C-terminal TRAF domain, that is made up of a coiled-coil domain known as the TRAF-N domain and a highly conserved TRAF-C domain.

Adapted from Kobayashi. et al. (2004). "The role of TRAF6 in signal transduction and the immune response." *Microbes and Infection*. 6: 1333-1338.

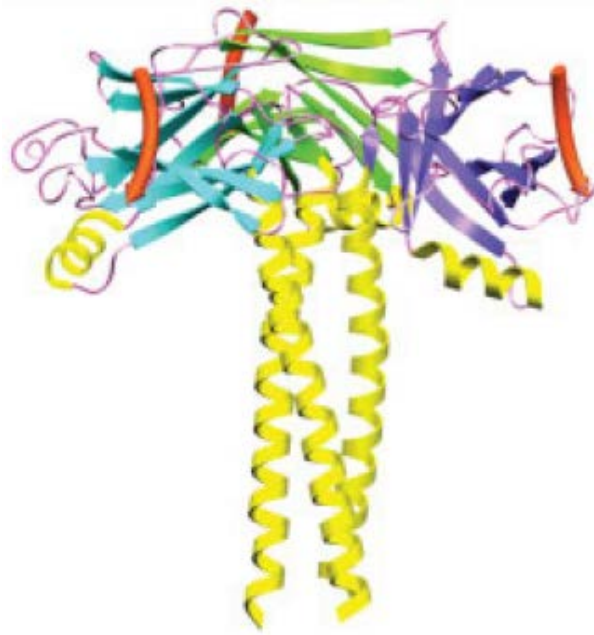


Figure 1.19: Structural analysis of TRAF6.

Example of TRAF-mediated signalling via trimerisation, and formation of the mushroom like structure.

Wu et al. (2003). "TRAF6, a molecular bridge spanning adaptive immunity, innate immunity and osteoimmunology." *Bioessays*, 25: 1096-1105.

Table 1.2: Putative TRAF6 binding motifs in immune signalling molecules.

Critical glutamic acid residue is shown in red. Ar/Ac – Aromatic/Acidic Group

TRAF6 binding motif	P	x	E	x	x	Ar/Ac	
Mal (188-196)	P	P	E	L	R	F	Mansell et al. 2004
TRAM (181-186)	P	R	E	R	T	P	
TRIF (250-255)	P	E	E	M	S	W	Sato et al. 2003 Jiang et al 2004
IRAK (1) (542-547)	P	Q	E	N	S	Y	Ye et al. 2002
IRAK (2) (585-590)	P	V	E	S	D	E	
IRAK (3) (504-509)	P	E	E	S	D	E	
IRAK2 (1) (526-531)	P	E	E	T	D	D	
IRAK2 (2) (557-562)	P	T	E	N	G	E	
IRAK-M (578-583)	P	V	E	D	D	E	
RIP2 (194-199)	P	P	E	N	Y	E	
CD40 (233-238)	P	Q	E	I	N	F	
TRANCER (1) (344-349)	P	T	E	D	E	Y	
TRANCER (2) (377-382)	P	L	E	V	G	E	
TRANCER (3) (453-458)	P	G	E	D	C	E	

TRAF6 can also activate IKK through interaction with two intermediary factors TRAF6-regulated IKK Activator 1 (TRIKA1) and TRIKA2 (Wang et al., 2001). TRIKA1 is a heterodimeric protein complex made up of the ubiquitin conjugating enzymes Ubc13 and Uev1A. The ubiquitination of proteins requires an enzyme cascade that is composed of a ubiquitin activating enzyme (E1), a ubiquitin conjugating enzyme (E2) and a ubiquitin protein ligase (E3) (Bradley and Pober, 2001).

This occurs in three steps, firstly ubiquitin is bound to E1 via a thioester bond and this process is ATP-dependent. Secondly, ubiquitin is then transferred from E1 to the active site cysteine residue of E2. Thirdly, E2 then transfers ubiquitin onto lysine residues of the target protein and this occurs with the aid of E3 (Pickart and Eddins, 2004). The RING finger domain of TRAF6 can function as an E3 ubiquitin ligase, with the complex Ubc13 and Uev1A mediating the polyubiquitination of TAK1, and subsequent activation of IKK (Akira et al., 2006). This occurs through the formation of a K63-linked polyubiquitination chain, that functions independently of a proteasome (Wang et al., 2001).

Wu and colleagues (Yin et al., 2009) have recently crystallized TRAF6 and Ubc13. TRAF6 interacts with Ubc13 through TRAF6's RING domain, residues upstream from the RING domain and the first zinc finger. The monomer structure of TRAF6 RING domain and zinc fingers 1-3 show that it resembles a golf club (Yin et al., 2009) (Figure 1.20). The RING domain forms the head of the club, while the zinc fingers make up the shaft and this structure is quite rigid. Whilst the C-terminus of TRAF6 forms a trimeric structure, the N-terminus forms a dimeric structure via its RING domain and the linker helix (Yin et al., 2009) (Figure 1.21). This dimerisation of the N-terminus is crucial for TRAF6's ability to promote polyubiquitin synthesis, autoubiquitination, NFκB activation and oligomerisation of itself. Only TRAF6 is able to interact with Ubc13 despite the fact that TRAF2 and TRAF5 can activate NFκB through K63-linked polyubiquitination, highlighting the unique role TRAF6 has in multiple signalling pathways (Pineda et al., 2007, Nakano et al., 1996).

Recently, TRAF6 was found to translocate to mitochondria following TLR1, TLR2 and TLR4 ligand stimulation (West et al., 2011). The translocation of TRAF6 from the cytoplasm to the mitochondria involved interaction with Evolutionarily Conserved Signalling Intermediate in Toll Pathways (ECSIT) and this resulted in recruitment of mitochondria to phagosomes and the generation of mitochondrial ROS (mtROS). ECSIT has been shown to interact with the chaperone NADH Dehydrogenase (ubiquinone) Complex I, Assembly Factor 1 (NDUFAF1), and is involved in

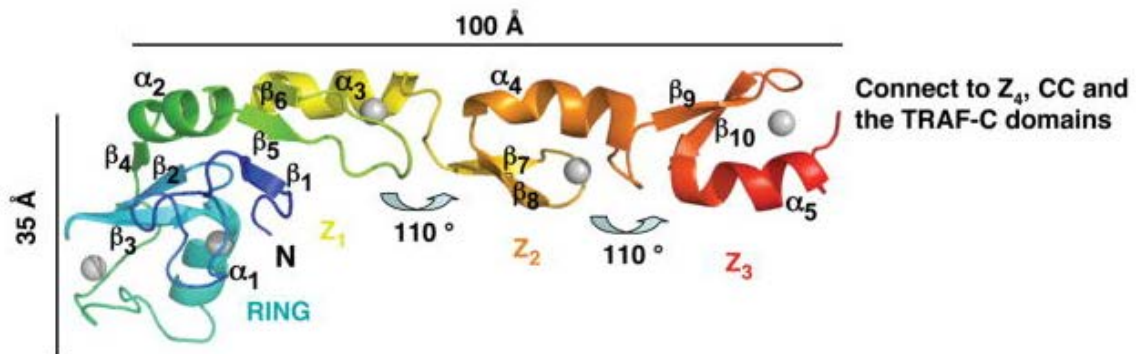


Figure 1.20: Structure of the N-terminal region of TRAF6.

Ribbon diagram of the monomer structure of TRAF6's N-terminus. The structure resembles a golf club, with the RING domain as the head and the three zinc fingers (Z1 [yellow], Z2 [orange] and Z3 [red]) as the shaft.

Yin et al. (2009). "E2 interaction and dimerization in the crystal structure of TRAF6." Nature Structural & Molecular Biology. 16: 658-66.

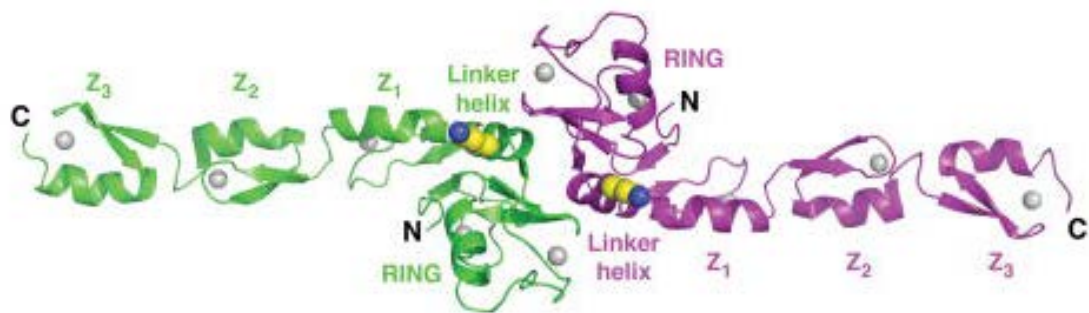


Figure 1.21: Dimerisation of the TRAF6 N-terminal domain.

The structure of TRAF6 as a dimer. The dimerisation of TRAF6 is important for its ability to promote polyubiquitination. The major site of autoubiquitination has been mapped to the K124 residue and this is depicted as a ball-and-stick model.

Yin et al. (2009). "E2 interaction and dimerization in the crystal structure of TRAF6." Nature Structural & Molecular Biology. 16: 658-66.

mitochondrial complex I assembly (Vogel et al., 2007). ECSITs interaction with TRAF6 leads to its ubiquitination, where it begins to accumulate at the mitochondrial periphery and induces mtROS production (West et al., 2011). TRAF6- and ECSIT-deficient macrophages were challenged with *Salmonella typhimurium*. Both TRAF6- and ECSIT-deficient macrophages produced lower levels of mtROS and cellular ROS. This study demonstrates a direct link between TLR signalling and mitochondria, and the emerging role mitochondria have in innate immunity.

TRAF6 therefore is critical in IL-1/TLR signalling pathways and it acts as a central signalling mediator that bifurcates signalling to the canonical and MAPK pathways, although the mechanism for them is still poorly understood. Recent studies also demonstrate that TRAF6 appears to have a role in ROS generation.

1.4.3.4 - TAK1 and TABs

The activation of NF κ B and AP-1 by TRAF6, involves TAK1 (MAP3K7), TAB1 and TAB2. TAK1 is a serine/threonine kinase that is a member of the MAPK kinase kinase (MAPKKK) family (Adhikari et al., 2007). TAK1 has been shown to participate in TNFR1 and IL-1/TLR mediated signalling (Shim et al., 2005). Three adaptor proteins that interact with TAK1 have been identified; these are TAB1, TAB2 and TAB3. Overexpression of TAB1 induces TAK1 kinase activity, revealing that TAB1 is an activator of TAK1 (Shibuya et al., 1996). The C-terminus of TAB1 facilitates interaction and activation of TAK1 (Landström, 2010). TAB2 and TAB3 associate with TAB1 and have been demonstrated to be required for TAK1 activation following TNF- α and IL-1 β stimulation. TAB2 and TAB3 have unique ubiquitin protein domains, making them distinct from TAB1. The N-terminus contains a Coupling of Ubiquitin Conjugation to ER Degradation (CUE) domain, and the C-terminus contains a Novel Zinc Finger (NZF) domain (Landström, 2010). After IL-1 stimulation TAB2 translocates from the cell membrane to the cytosol where it interacts with TAB1 and TRAF6 to activate TAK1 (Takaesu et al., 2000). The formation of the K63 ubiquitin chains by TRAF6 lead to activation of TAK1, though this process is poorly understood. Following subsequent activation by TRAF6, TAK1 phosphorylates IKK β and MKK6, which leads to the activation of NF κ B and MAPKs (Akira et al., 2006). Activated TAK1 can also phosphorylate members of the MKK family, which in turn can phosphorylate JNK and p38k (Wang et al., 2001).

1.5 - JAK-STAT pathway

The JAK-STAT pathway is used by cytokines which bind to their respective ligands, leading to rapid reprogramming of the genes being expressed in that cell. The JAK-STAT pathway is used by type I and type II IFNs as well as IL-6 (Heinrich et al., 1998). Type I IFNs however, make use of STAT1 in transducing their signals. All type I IFNs bind to a heterodimer receptor that is made up of IFNAR 1 and IFNAR2 (Uzé et al., 1990). Associated with these two receptors is the JAK proteins TYK2 and JAK1 (Figure 1.22) (Novick et al., 1994, Colamonici et al., 1994).

Binding of the ligand causes the receptors to dimerise, however unlike growth factor receptors these receptors do not have intrinsic tyrosine kinase activity, instead the kinase activity is supplied through requirement of the JAK proteins (Velazquez et al., 1992, Silvennoinen et al., 1993). Dimerisation of the receptors allows the JAKs to phosphorylate tyrosine residues on themselves and the receptor. This produces docking sites that are recognised by STAT1 and STAT2 through their Src-homology 2 (SH2) domains (Schindler, 2002, Mahieu and Libert, 2007, Murray, 2007). Once the STAT proteins bind to the phosphotyrosine sites, the STAT proteins are themselves phosphorylated on activating tyrosine residues. The activated STATs can then form homo- or heterodimers. STAT dimers are then rapidly translocated to the nucleus, where they bind to specific sequences of DNA and induce increased expression of target genes (Aaronson and Horvath, 2002). Phosphorylation of Tyr-701 alone is sufficient for STAT1 dimers to bind DNA elements. Phosphorylation of STAT1 on Ser-727 is further required for maximal transcriptional activity of STAT1 (Wen et al., 1995).

1.5.1 - STAT structure

The seven STAT proteins all share a highly conserved structure with a number of functional domains. They are comprised of a C-terminal transactivation domain (TAD), a SH2 domain, a linker domain, DNA-binding domain and a coiled-coil domain (Lim and Cao, 2006) (Figure 1.23). The N-terminal domain of STATs is involved in dimerisation (Vinkemeier et al., 1998) and the four long helical coils of the coiled-coil domain facilitate protein-protein interactions. The DNA-binding domain forms an immunoglobulin structure and binds DNA when the STAT proteins form a dimer (Horvath et al., 1995). This domain is also responsible for nuclear import of the STATs (Ma and Cao, 2006). Yang et al. (1999) demonstrated that the linker domain was required for STAT1 transcriptional activity. Of all the domains, the SH2 domain is most highly conserved and is crucial

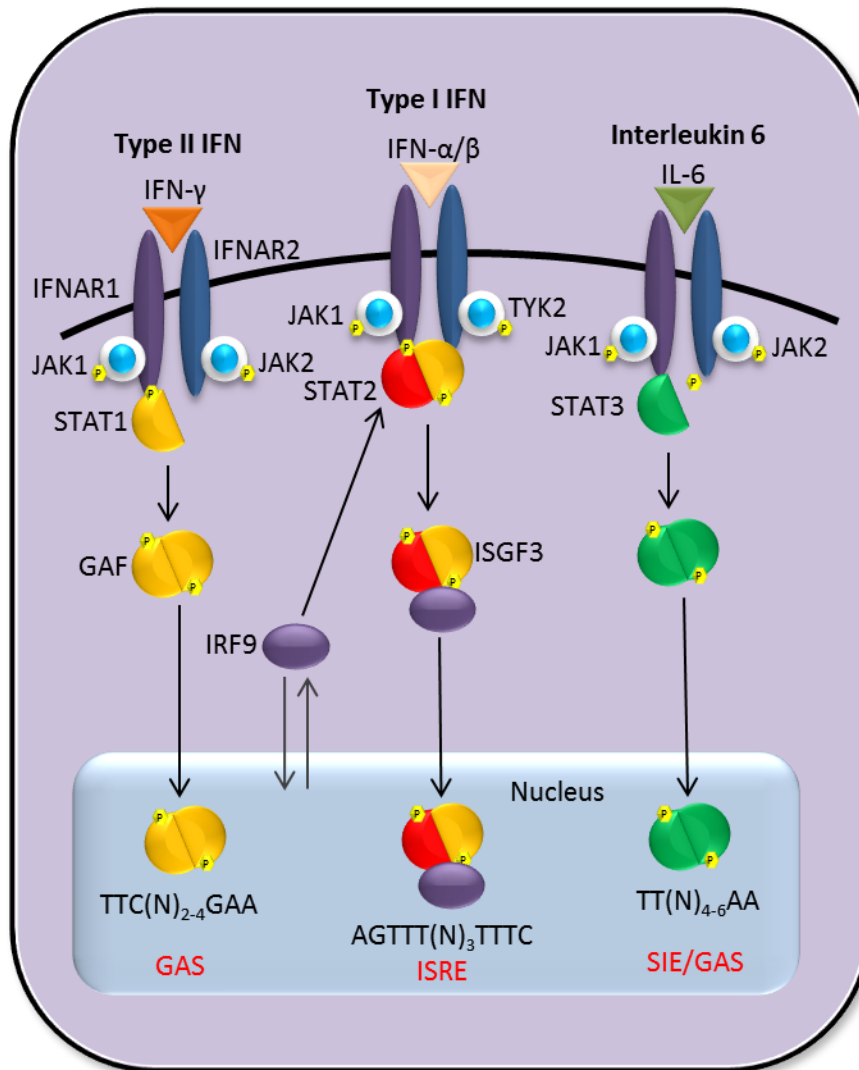


Figure 1.22: JAK-STAT signalling in type I, II interferon and interleukin-6.

Binding of IFNAR ligands leads to dimerisation of the receptor subunits, phosphorylation of JAK proteins and the receptor, and the recruitment of STAT molecules. STATs are then phosphorylated, resulting in STAT homo- or heterodimerisation and their translocation to the nucleus. STAT proteins bind specific DNA elements and induce transcription of target genes.

Adapted from Aaronson, D. S. and C. M. Horvath (2002). "A Road Map for Those Who Don't Know JAK-STAT." *Science*. 296: 1653-1655.

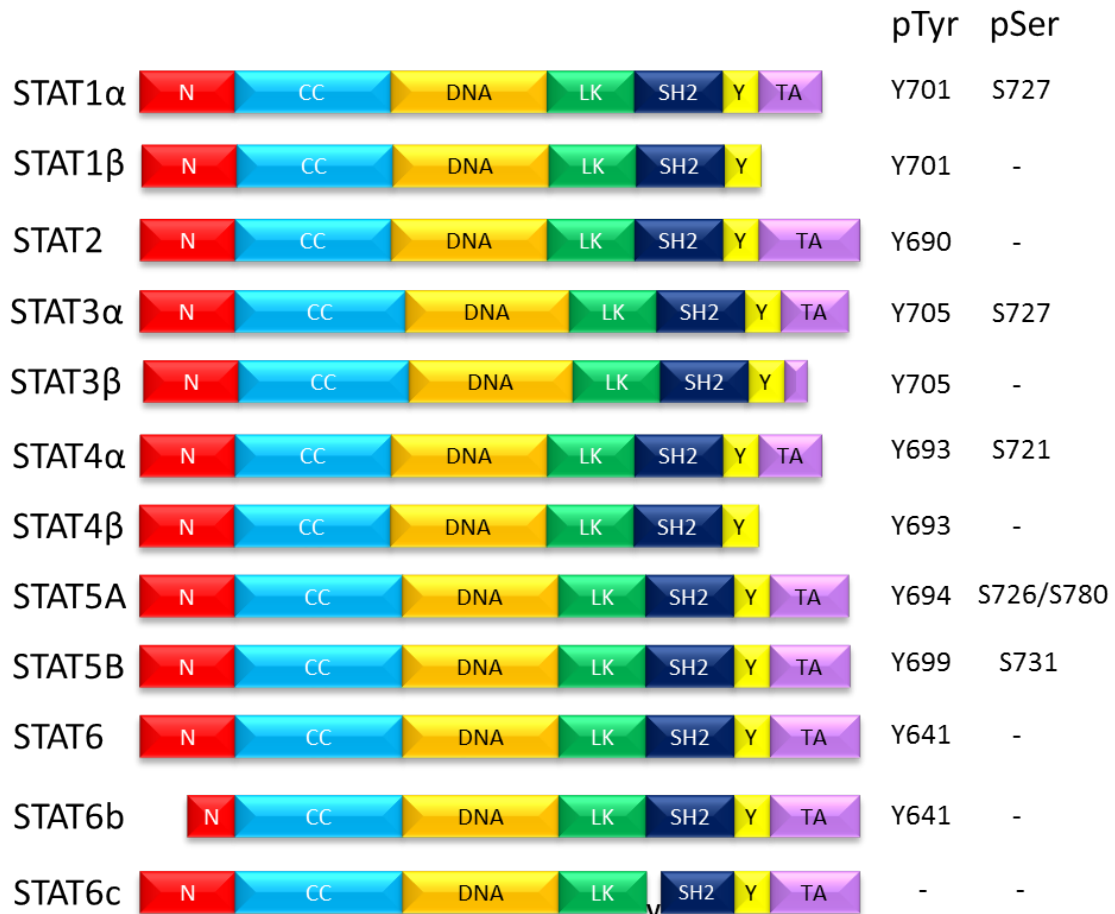


Figure 1.23: STAT domains.

N = N-terminal domain, CC = coiled-coil domain, DNA = DNA-binding domain, LK = linker domain, SH2 = SH2 domain, Y = Phosphotyrosyl tail segment, TA = transactivation domain. Splice variants generate a longer α isoform and shorter β , b and c isoforms.

Adapted from Lim and Cao. (2006) "Structure, function and regulation of STAT proteins." Molecular Biosystems. 2: 536-550.

for receptor association and dimerisation following tyrosine phosphorylation (Heim et al., 1995). The TAD is the least conserved, and in STAT1 and STAT3, contain a P-M-S-P motif where an important serine residue at 727 can be phosphorylated (Wen et al., 1995).

Crystal structures of a STAT1 homodimer bound to DNA and STAT3 β homodimer bound to DNA have been resolved. Both of these crystal structures lack N- and C-terminal domains. The STAT1 and STAT3 β homodimer crystal structure is comprised of the coiled-coil, DNA-binding, linker and SH2 domain and all four domains bind to adjacent domains and together they form a hydrophobic core. STAT1 and STAT3 bind DNA as a homodimer, and together this structure resembles a nutcracker (Chen et al., 1998, Becker et al., 1998) (Figure 1.24 and Figure 1.25). The only point of contact between two STAT molecules is at the SH2 domain, this interaction is comprised of the SH2 domains of each monomer binding to one another, forming an anti-parallel β sheet (Chen et al., 1998).

The structure of STAT1 was resolved in 2005 and displays STAT1 existing as a tetrameric complex (Mao et al., 2005). The four N-terminal domains are arranged in the centre of the tetramer, with four core fragments surrounding them (Figure 1.26). This complex contains two dimer interfaces, one between the two N-terminal domains and one between the two core fragments, which consist of the coiled-coil domain to the phosphotyrosyl tail segment (Mao et al., 2005). The unphosphorylated core fragment pairs together form a boat-like arrangement (Figure 1.27). In solution STAT1 predominately exists as a dimer, and in this state the unphosphorylated STAT1 dimer is proposed to exist in two possible conformations (Mao et al., 2005). These two conformations are termed parallel and anti-parallel, and are based on the location of the SH2 domain, the anti-parallel conformation has the SH2 domains on opposite ends of the dimer (Figure 1.28). Both dimer conformations are relatively weak compared to the tyrosine phosphorylated dimer. In the cytoplasm the anti-parallel is proposed to be the latent form of STAT1, as it is stabilised by interactions between the N-terminal domains and the core fragments (Mao et al., 2005). STAT1 adopts the parallel conformation upon stimulation as it allows an easier transition into the phosphotyrosine (pTyr) conformation. The unphosphorylated STAT3 core fragment has also been resolved and unlike STAT1 which forms tetramers, STAT3 is predominately monomeric (Ren et al., 2008) (Figure 1.29). Similar to STAT1, STAT3 does not undergo drastic conformational changes when tyrosine phosphorylated, and the domains all interact to form a hydrophobic core. For STAT1, interaction between the coiled-coil domain and

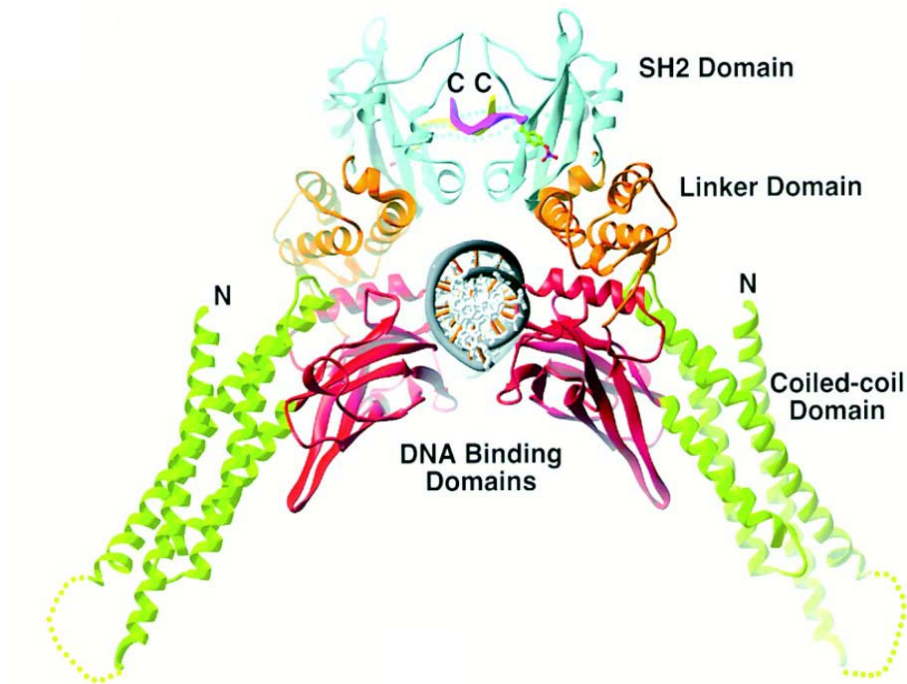


Figure 1.24: Structure of STAT1 homodimer.

Ribbon diagram displaying STAT1 homodimer bound to DNA. Coiled-coil domain is green, DNA-binding domain is red, linker domain is orange, SH2 domain is cyan and DNA is represented in grey. The C-terminal tail segment is represented in yellow and magenta. Dotted lines denote disordered loops (one in the coiled-coil domain and one in the SH2 domain). The tyrosine 705 residue is shown in stick representation. The N- and C-terminus are represented by N and C.

Chen et al. (1998). "Crystal Structure of a Tyrosine Phosphorylated STAT-1 Dimer Bound to DNA." Cell. 93: 827-839.

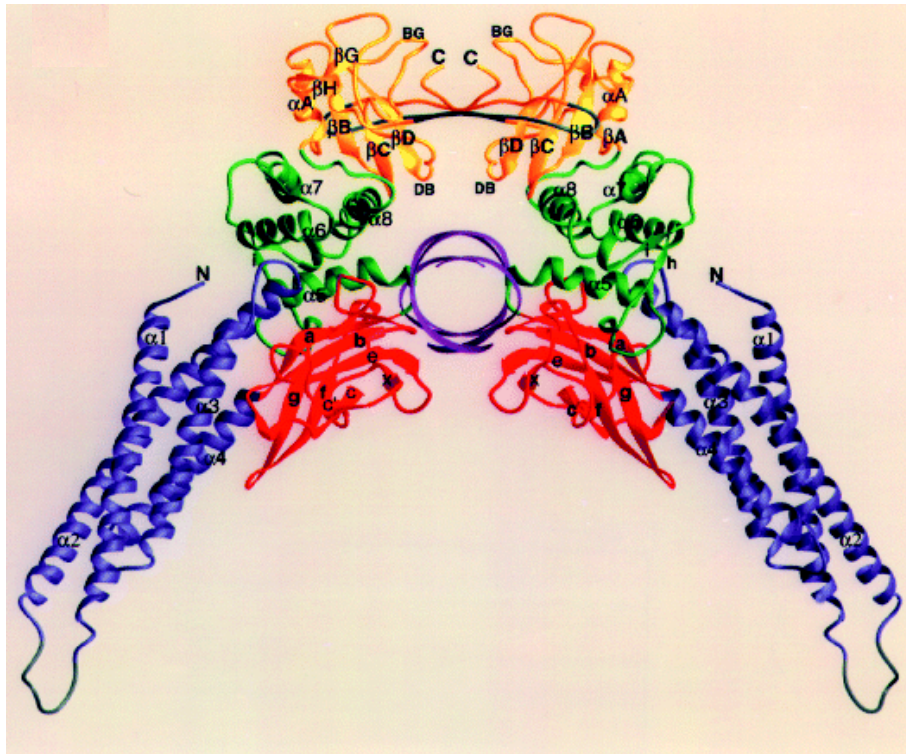


Figure 1.25: Structure of STAT3 homodimer.

Ribbon diagram displaying STAT3 homodimer bound to DNA. The coiled-coil is shown in blue, the DNA-binding domain is represented in red, the linker domain is in green, the SH2 domain is in yellow and DNA is represented in purple.

Becker et al. (1998). "Three-dimensional structure of the Stat3 β homodimer bound to DNA." *Nature*. 394: 145-151.

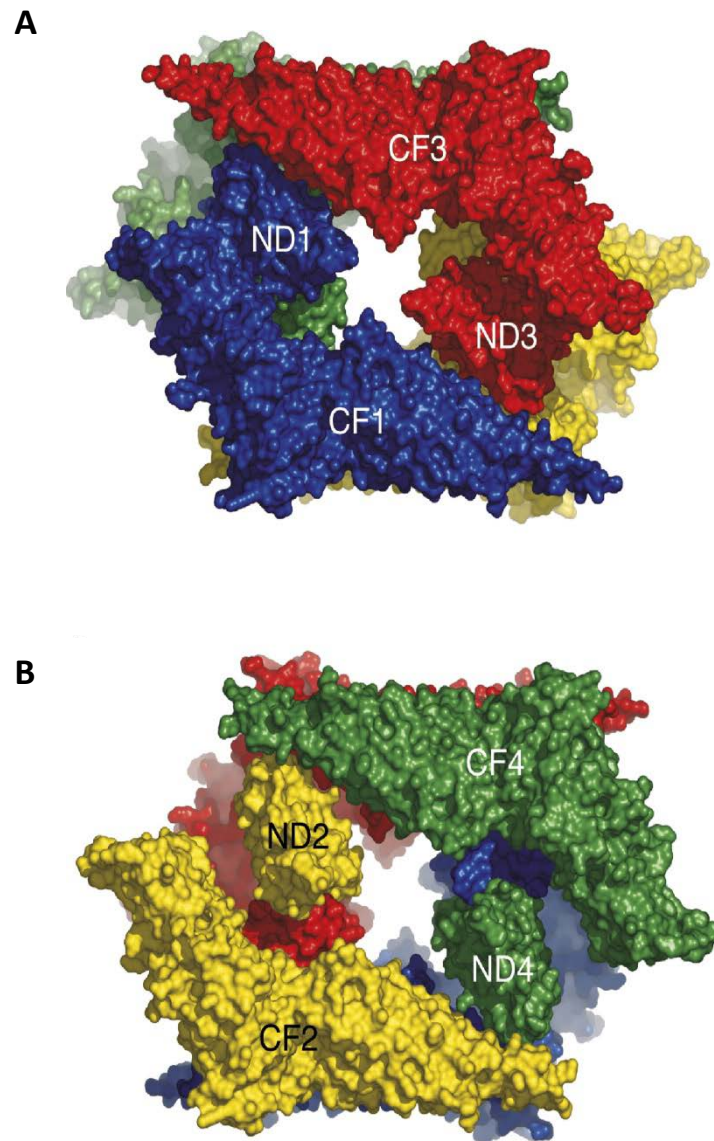


Figure 1.26: Structure of STAT1 tetramer.

(A) Front view of STAT1 tetramer. **(B)** Back view of STAT1 tetramer. STAT1 monomers are represented in red, blue, yellow and green. ND = N-terminal domain and CF = core fragment.

Mao et al. (2005). "Structural Bases of Unphosphorylated STAT1 Association and Receptor Binding." *Molecular Cell*. 17: 761-771.

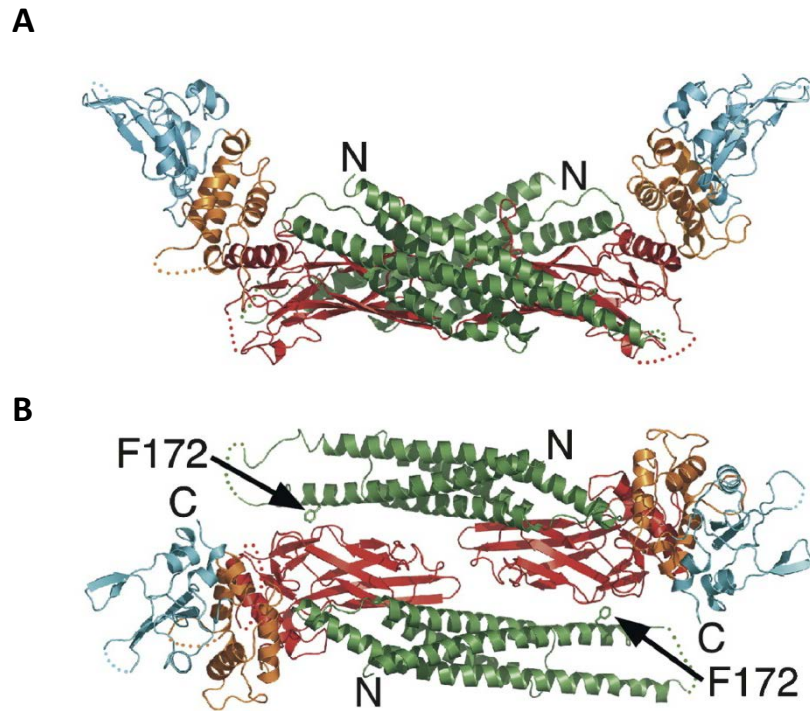


Figure 1.27: Structure of STAT1 dimer interfaces.

(A) Side view of the core fragment interface. **(B)** Top view of the core fragment interface. N = N-terminal domain and C = C-terminal domain. F172 is a hydrophobic residue located in the coiled-coil domain.

Mao et al. (2005). "Structural Bases of Unphosphorylated STAT1 Association and Receptor Binding." *Molecular Cell*. 17: 761-771.

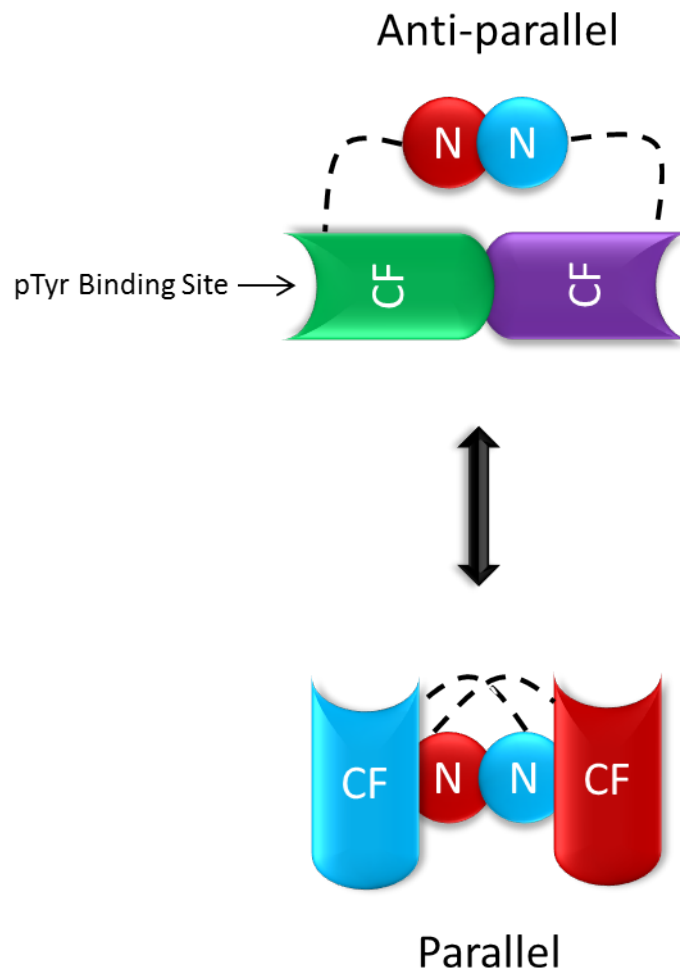


Figure 1.28: Two possible STAT1 dimer conformations.

A diagram displaying the two possible STAT1 dimer conformations, parallel and anti-parallel. N = N-terminal domain and CF = core fragment.

Adapted from Mao et al. (2005). "Structural Bases of Unphosphorylated STAT1 Association and Receptor Binding." *Molecular Cell*. 17: 761-771.

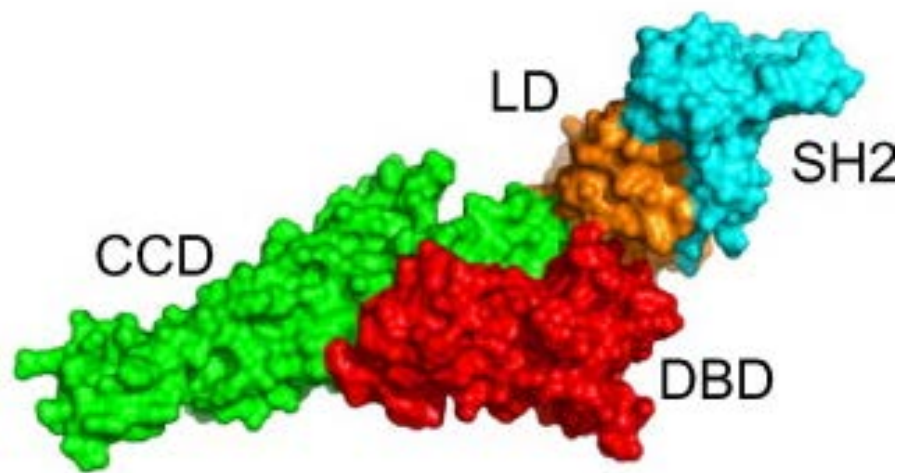


Figure 1.29: Structure of monomeric STAT3.

CCD = coiled-coil domain (green), DBD = DNA-binding domain (red), LD = linker domain (orange) and SH2 = SH2 domain (blue).

Ren et al. (2008). "Crystal structure of unphosphorylated STAT3 core fragment." Biochemical and Biophysical Research Communications. 374: 1-5.

DNA-binding domain has been demonstrated to play a role in the dephosphorylation of pTyr STAT1 (Mertens et al., 2006).

Mutations of critical residues in the core fragment dimer interface of STAT1 resulted in prolonged tyrosine activation of STAT1, in contrast mutation of the analogous STAT3 core fragment dimer interaction did not affect phosphorylation times (Ren et al., 2008). These results suggest that either STAT3 does not contain interaction of the coiled-coil domain and DNA-binding domain or that the dimer interface in STAT3 does not regulate tyrosine dephosphorylation.

1.5.2 - STAT1

STAT1 was first identified as part of the IFN-stimulated Gene Factor 3 (ISGF3) following stimulation with IFN- α (Fu et al., 1990). Subsequent studies found that STAT1 was the mediator for IFN- γ signalling (Shuai et al., 1992). Stimulation with IFN- α leads to formation of a STAT1/STAT2 heterodimer, whereas stimulation with IFN- γ results in formation of a STAT1 homodimer (Shuai et al., 1994, Schindler et al., 1992a). Other than IFNs, STAT1 can also be activated by a variety of cytokines and growth factors, including several ILs such as IL-6, IL-12, IL-21, TNF- α , Epidermal Growth Factor (EGF), Vascular Endothelial Growth Factor (VEGF) and growth hormone (Najjar and Fagard, 2010).

Unlike STAT3-deficient mice, STAT1-deficient mice are not embryonically lethal however, they are highly susceptible to infection from bacteria and viruses (Meraz et al., 1996). Despite the lack of developmental defects, STAT1 knockout mice are completely unresponsive to IFN- α and IFN- γ , though the mice respond normally when exposed to other cytokines that activate STAT1 (Meraz et al., 1996). These knockout studies demonstrate STAT1's crucial role in mediating IFN-type responses.

Alternate splicing of the STAT1 gene produces two isoforms, a STAT1 α and a truncated form STAT1 β (Schindler et al., 1992a). STAT1 β is expressed at low levels and lacks the transactivation domain, thus rendering it transcriptionally inactive (Shuai et al., 1992). This truncated form can still be tyrosine phosphorylated and both isoforms can form homo- and heterodimers that bind DNA (Vinkemeier et al., 1996). When stimulated with IFN- γ both STAT1 α and STAT1 β accumulate at the IRF1 promoter, however only STAT1 α can recruit Cyclic Adenosine Monophosphate (cAMP)

Response Element-binding Protein (CREB)/p300 and activate transcription (Zakharova et al., 2003). As STAT1 β binds to the same DNA targets as STAT1 α , overexpression of STAT1 β inhibits phosphorylation, the DNA binding ability and transcriptional activity of STAT1 α (Baran-Marszak et al., 2004). Baran-Marszak et al. (2004) also observed that the inhibition of STAT1 α phosphorylation correlated with an increase of STAT1 β phosphorylation suggesting that STAT1 β may compete with STAT1 α at the receptor level. *Leishmania* has also been found to attenuate the IFN- γ response through enhancing tyrosine phosphorylation of STAT1 β thereby negatively regulating STAT1 α transcriptional activity (Bhardwaj et al., 2005). The function of STAT1 β isoform was also investigated in a STAT1-deficient B cell line. STAT1 α was found to enhance cell death and also facilitate the phosphorylation and nuclear localisation of p53 (Najjar et al., 2008). In contrast, STAT1 β -induced cell death was independent of p53, whilst STAT1 α induced p53 nuclear localisation; p53 in STAT1 β reconstituted cells was cytoplasmically located where it had no transcriptional activity (Najjar et al., 2008).

IFN stimulation induces Tyr-701 phosphorylation of STAT1 which is required for the formation of STAT1 homodimers and STAT1/STAT2 heterodimers via the SH2 domains. Tyrosine phosphorylation alone is sufficient for STAT1 to mediate the IFN-induced responses and is required to induce the DNA binding ability of STAT1 (Larner et al., 1993, Quelle et al., 1995). Nuclear translocation of STAT1 has been shown to be dependent on the interaction of the SH2 domain with the phosphotyrosine residue of another STAT, though only active SH2 phosphotyrosine interaction is required to facilitate STAT dimerisation (Gupta et al., 1996). Blockage of the STAT1 tyrosine phosphorylation inhibits the nuclear translocation of STAT1 further demonstrating the importance of this residue for STAT1 function (Shuai et al., 1994).

Initiation of TLR signalling can induce expression of IFN- β . IFN- β can activate STAT1 at Tyr-701 through IFNAR via an autocrine mechanism in response to TLR3 and TLR4 signalling (Figure 1.30) (Kobayashi et al., 2006). Studies by Dalpke et al. (2003) have also shown interplay between IFN- γ signalling and TLR signalling. It is well-known that IFN- γ interacts with a heterodimeric type II IFN receptor, resulting in activation of JAK1 and JAK2 which leads to Tyr-701 phosphorylation of STAT1 (Dalpke et al., 2003). IFN- γ signalling can be enhanced and inhibited by stimulation with TLR ligands. Stimulation with TLR ligands results in enhanced IFN- γ production and this was attributed to the p38k phosphorylation of STAT1 Ser-727 (Dalpke et al., 2003). Additionally, it has also been reported that p38k can enhance IFN- γ signalling independently of Ser-727 phosphorylation (Ramsauer et al., 2002).

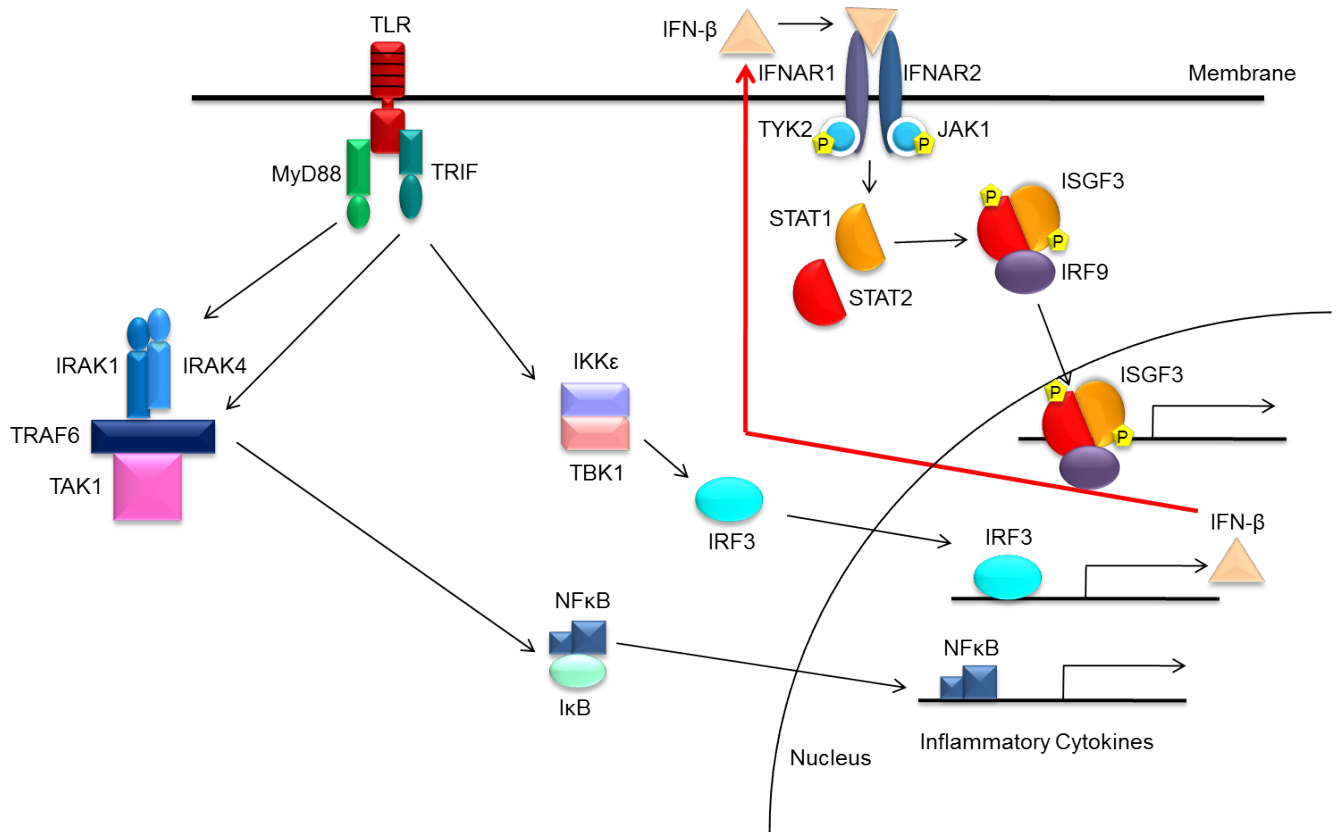


Figure 1.30: Interaction between TLR4 and IFNAR via production of IFN-β and subsequent activation of JAK-STAT signalling.

Upon TLR4 recognition of LPS, TLR4 signals via the MyD88-dependent and -independent pathways. Signalling through the MyD88-independent pathway, leads to the production of IFN-β, which via an autocrine feedback loop, binds to the IFNAR and activates JAK-STAT signalling.

Whilst tyrosine phosphorylation of STAT1 is required to induce the transcriptional activity of STAT1, serine phosphorylation has been demonstrated to activate the maximal transcriptional ability of STAT1. U3A cells, which lack STAT1, were transfected with a STAT1 S727A mutant and these cells displayed severely attenuated STAT1-mediated IFN- γ secretion (Wen et al., 1995). The increase of transcription from Ser-727 phosphorylation of STAT1 was also confirmed by Kovarik et al. (1998) who found that pre-treatment of macrophages with LPS, which only resulted in STAT1 Ser-727 phosphorylation, enhanced expression of STAT1 target genes following IFN- γ treatment. These *in vitro* studies were later validated in mice models. Mice expressing a STAT1 S727A mutant displayed significantly reduced IFN- γ production and under heavy pathogen burden were unsuccessful in clearing microbial threats (Varinou et al., 2003). This demonstrates that STAT1 serine phosphorylation is required for maintaining a sustained IFN- γ response that induces an anti-viral state and for inducing maximal transcriptional activity of STAT1.

The TLR pathway can interact with JAK-STAT signalling through the secretion of IFN- β , however previous studies have demonstrated the possibility that an alternative cross-talk may exist between the TLR and the JAK-STAT pathways. In response to TLR2 and TLR4 stimulation, STAT1 Ser-727 is rapidly phosphorylated within 10-15 minutes, whilst only TLR4 stimulation leads to Tyr-701 phosphorylation after 2 hours, presumably via IFN- β production and subsequent IFNAR activation. This activation however was delayed compared with Ser-727 STAT1 phosphorylation suggesting that Ser-727 phosphorylation is a direct consequence of TLR activation and was not reliant on IFN- β expression (Rhee et al., 2003). This study also revealed that TLR-induced STAT1 phosphorylation at Tyr-701 is Phosphoinositide 3-kinase (PI3K)-dependent; however Ser-727 phosphorylation is PI3K-independent. In contrast, TLR2 only induces STAT1 Ser-727 phosphorylation, but not Tyr-701 which is expected as TLR2 does not induce IFN- β (Rhee et al., 2003). Other studies conducted demonstrate that STAT1 Ser-727 phosphorylation can be induced through IL-1, and is dependent on IRAK1, but not the kinase activity of the IRAK1 protein (Nguyen et al., 2003). In fact this process is PI3K and p38k independent, as STAT1 Ser-727 phosphorylation was not affected by chemical inhibitors, dominant negative and constitutively active mutants of signalling proteins that activated NF κ B or activated the transcriptional activity of STAT1. (Nguyen et al., 2003). Schroder et al. (2007) further demonstrated that STAT1 can also undergo Ser-727 phosphorylation after TLR9 stimulation, occurring through the MyD88-dependent pathway, yet independent of IFN- β induced phosphorylation. The study also suggests that cytoplasmic STAT1 may play an inhibitory role in response to TLR ligands that activate p38k, but did not induce type I

IFN production (Figure 1.31) (Schroder et al., 2007). Taken together these results indicate that crosstalk may exist between the TLR and JAK-STAT pathways.

1.5.3 - STAT3

STAT3 was first identified as an IL-6-dependent transcription factor that regulates the acute-phase response (Akira et al., 1994). It is activated by a variety of cytokines and growth factors which include EGF, Platelet-derived Growth Factor (PDGF) and IL-6 (Zhong et al., 1994, Cao et al., 1996a, Akira et al., 1994). STAT3 has a very diverse role within the body, playing a role in both inflammation and cancer. STAT3 transduces signals from the IL-6, IL-10, Granulocyte Colony Stimulating Factor (G-CSF), leptin, IL-21 and IL-27 (Kisseleva et al., 2002). Of all the STATs, STAT3 knockout mice are the only ones that are embryonic lethal, demonstrating the importance of STAT3 in development (Takeda et al., 1997). Tissue specific knockouts of STAT3 provided a more comprehensive look on the significance of the role of STAT3.

STAT3-deficient T cells display severely impaired proliferation when induced by IL-6 and were not protected from apoptosis induced by Bcl-2 (Takeda et al., 1998). Takeda et al. (1999) later demonstrated that a conditional STAT3^{-/-} mice, with STAT3 disrupted in macrophages and neutrophils, expressed higher levels of proinflammatory cytokines and were highly susceptible to endotoxic shock as the anti-inflammatory effects of IL-10 was completely abolished in these mice. In keratinocytes, the lack of STAT3 affected both hair cycle and wound healing, although proliferation of keratinocytes was unaffected, their ability to migrate was dependent on STAT3 (Sano et al., 1999). Mammary gland involution in the absence of STAT3 exhibited decreased apoptosis and involution was significantly delayed (Chapman et al., 1999). Deletion of STAT3 in the liver completely abolishes IL-6 induced acute-phase response genes and this was also observed in response to LPS (Alonzi et al., 2001). All these studies demonstrate the importance and vast role of STAT3 in cellular functions.

STAT3 can be expressed as two isoforms, a full length STAT3 α and a truncated STAT3 β . STAT3 β is missing 55 aa at the C-terminal domain, but contains an additional 7 aa that STAT3 α lacks (Schaefer et al., 1995). This splice variant encodes a ~80 kDa protein that is considered to be a dominant negative form (Caldenhoven et al., 1996). Whilst STAT3 β lacks the C-terminal domain and cannot activate IL-6-induced genes, it has been shown to bind c-Jun and activate the α_2 -macroglobulin gene (Schaefer et al., 1995). When transfected into the African green monkey cell

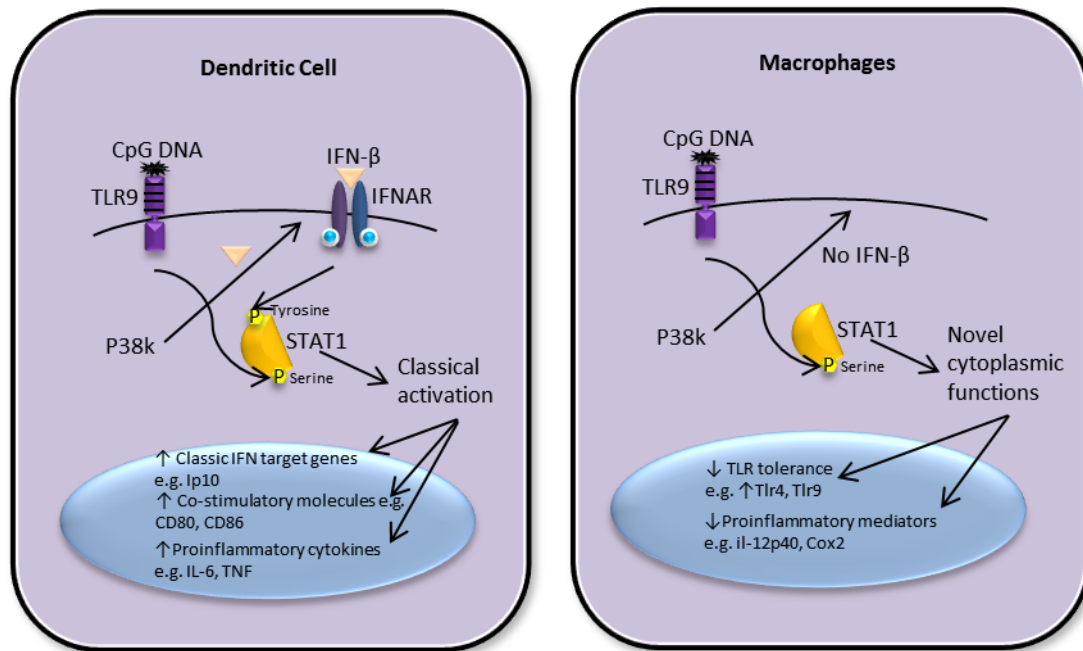


Figure 1.31: TLR9-mediated activation of STAT1 in DCs vs. macrophages.

In DCs, TLR9 signalling leads to the p38k-dependent phosphorylation of Tyr-701 and Ser-727. The double phosphorylated STAT1 dimerises and translocates to the nucleus to bind its target genes. In contrast, TLR9 signalling in macrophages only induces Ser-727 phosphorylation, and does not trigger IFN-β production. Unphosphorylated STAT1 at the Tyr-701 residue cannot dimerise and therefore cannot translocate to the nucleus. STAT1 remains in the cytoplasm and regulates gene expression.

Adapted from Schroder, K., M. Spille, et al. (2007). "Differential Effects of CpG DNA on IFN-β Induction and STAT1 Activation in Murine Macrophages versus Dendritic Cells: Alternatively Activated STAT1 Negatively Regulates TLR Signalling in Macrophages." The Journal of Immunology. 179: 3495-3503.

line, COS, both STAT3 α and STAT3 β could be activated by the same set of growth factors and cytokines, and were capable of DNA binding and inducing transcription (Schaefer et al., 1997). Whilst STAT3 α had greater transcription activity, STAT3 β had increased DNA binding and was more stable, revealing that the C-terminal tail may control STAT3 binding efficiency (Schaefer et al., 1997). Park et al. (2000) had similar results indicating that the DNA binding ability of STAT3 α and STAT3 β were markedly different, and this is explained by the C-terminal domain. Deletions in the C-terminus region of STAT3 α enhanced its DNA binding ability and its stability as a dimer (Park et al., 2000). STAT3 β knockout mice generated by Yoo et al. (2002) were able to produce normal levels of proinflammatory cytokines, but were slower to recover from endotoxic shock, illustrating STAT3 β 's role in regulating a subset of genes that may aid in recovery from endotoxin challenge. Maritano et al. (2004) next generated both STAT3 α - and STAT3 β -deficient mice and found that whilst STAT3 α mice died 24 hours post-birth, STAT3 β was able to prevent this. In fact, STAT3 β is not a dominant negative isoform of STAT3 as expression of STAT3 β can induce acute-phase gene expression; though it plays no role in development, it can still mediate inflammatory events. In contrast, STAT3 α regulates post-natal survival, maintains the acute-phase response and is required to mediate IL-10's anti-inflammatory properties (Maritano et al., 2004).

It has been reported that MyD88 may play a role in mediating STAT3 phosphorylation in response to LPS (Yamawaki et al., 2010). Injection of LPS in the hypothalamus and livers of mice induced expression of SOCS3, a negative regulator of STAT3. LPS is able to induce IL-6 production, which in turn would induce STAT3 phosphorylation and this was shown to be a MyD88-dependent process. MyD88-deficient mice produced lower levels of LPS-induced IL-6 production and this also decreased STAT3 phosphorylation (Yamawaki et al., 2010). Although LPS-induced STAT3 phosphorylation was mainly mediated by MyD88-dependent signalling, it was not completely abolished in MyD88-deficient mice livers. This revealed that LPS-induced STAT3 phosphorylation was also mediated by the MyD88-independent pathway (Yamawaki et al., 2010). As TLR4 signals through both the MyD88-dependent and -independent pathway, it is thought that both pathways act synergistically in inducing STAT3 phosphorylation.

STAT3 has also been shown to interact with TRAF6, demonstrating crosstalk between TLR and JAK-STAT signalling. TRAF6 and STAT3 were co-immunoprecipitated *in vitro*, and STAT3 was observed to have increased K63-linked ubiquitination when co-transfected with TRAF6 (Wei et al., 2012). The RING finger domain and TRAF-type zinc fingers are essential in negatively regulating

STAT3, but each domain separately failed to inhibit STAT3 transcription activity, suggesting they cooperate together for TRAF6 to exert its inhibitory effect. TRAF6 is able to downregulate STAT3 target genes as TRAF6 inhibited C-Reactive Protein (CRP) production following IFN- α stimulation (Wei et al., 2012).

Traditionally, tyrosine phosphorylated STAT3 is required for STAT3 dimerisation and nuclear translocation to initiate gene transcription, with serine phosphorylation enhancing the transcriptional activity of STAT3. This was demonstrated by Wen and colleagues (1995) who found that STAT3 S727A transfected cells had a reduced capacity to drive activation of STAT3 target genes. Shen et al. (2004) further demonstrated in STAT3 S727A homozygous mice had ~50% of the transcriptional activity of WT mice illustrating the requirement of serine phosphorylation in achieving maximal transcription. Though the serine phosphorylation of STAT3 is clearly demonstrated as essential for proper cytokine expression, recent studies have identified a new role of Ser-727 phosphorylated STAT3 that is independent of tyrosine phosphorylation.

Serine phosphorylation of STAT3 has been implicated in the regulation of other cellular functions independent from its role of inducing maximal transcriptional activity. In Ras-transformed cells, STAT3 required the Ser-727 phosphorylation site to support Ras-transformation (Gough et al., 2009). STAT3 was detected in the mitochondria of these cells, but translocation to the mitochondria didn't require the tyrosine phosphorylation site, SH2 domain or the DNA binding domains. Ras-transformed cells required STAT3 in the mitochondria for full transforming potential, and it was revealed that the loss of STAT3 in the mitochondria impaired mitochondrial function, with a 50% decrease in cellular ATP levels. Mitochondrial STAT3 thus contributes to Ras-dependent cell transformation by augmenting ETC activity and acting mainly on complexes II and V of the ETC.

Wegrzyn et al. (2009) found that in STAT3^{-/-} cells complexes I and II of the Electron Transport Chain (ETC) in mitochondria showed significantly decreased activity. Gene Associated with Retinoid-IFN-induced Mortality 19 (GRIM-19) is a component of complex I of the ETC, and has been demonstrated to directly interact with and negatively regulate STAT3 transcriptional activity (Fearnley et al., 2001, Lufei et al., 2003, Zhang et al., 2003). GRIM-19-deficient mice are embryonically lethal and GRIM-19-deficient stem cells have impaired complex I assembly. The lack of GRIM-19 also affects the assembly and function of the other complexes of the ETC (Huang et al., 2004a). Wegrzyn et al. (2009) therefore proposed that STAT3 and GRIM-19 may colocalise

in the mitochondria. STAT3 was found in mitochondrial preparations, and was shown to interact with GRIM-19 in complex I, demonstrating that STAT3's presence in the mitochondria is required for optimal function of the ETC.

Recently, STAT3 was found to interact with GRIM-19 and its translocation to the mitochondria was required for TNF- α -induced necroptosis (Shulga and Pastorino, 2012). TNF- α -induced necroptosis is in part mediated by ROS production as suppression of STAT3 inhibited both TNF- α -induced ROS production and necroptosis. Ser-727 phosphorylation of STAT3 was shown to be important in ROS generation and TNF- α -induced necroptosis. Their studies demonstrated that the RIP Kinase 1 (RIPK1) was required for Ser-727 of STAT3 during TNF- α -induced necroptosis and its translocation to the mitochondria, as suppression of RIPK1 inhibited both ROS generation and serine phosphorylation of STAT3. Phosphoserine (pSer)-727 STAT3 interacts with GRIM-19 which facilitates its mitochondrial localisation and this interaction is dependent on RIPK1 as inhibition of RIPK1 reduced this interaction (Shulga and Pastorino, 2012). Suppression of GRIM-19 and STAT3 reduced levels of STAT3 and GRIM-19 accumulation in the mitochondria, respectively. This suggests that GRIM-19 and STAT3 are dependent on each other for mitochondria translocation during TNF- α -induced necroptosis.

1.6 – Rationale and aims of my PhD project

The innate immune system is critical to the normal functioning of all organisms as it allows clearance of invading pathogens. Innate immunity was once thought of as a non-specific system however, it is now known that the innate immune system functions through a multitude of receptors which recognise many different PAMPs. The TLRs and their signalling molecules have been shown to be vital in providing a means of defence through induction of anti-pathogen inflammation and it is the elucidation of the cross-talk between different signalling pathways that will create a better understanding of innate immune regulation. Cross-talk between different signalling pathways is important as it allows fine-tuning of the immune response and the tailoring of the innate immune system to a particular insult. Therefore the need to understand the mechanisms of cross-talk is crucial in development of therapeutics as inhibition of specific proteins may potentially have drastic consequences on other signalling pathways. Critically, a mechanism of this cross-talk between STAT signalling and TLRs has not been clearly identified. From the current data, it can be proposed that TLR signalling may lead to the direct recruitment of STAT1 and STAT3 in activating the innate immune response independent of type I IFN

production and the activation of JAK-STAT signalling. Activation of a second receptor complex does not explain the rapid Ser-727 phosphorylation of STAT1 and STAT3 that is observed in previous studies. Our laboratory have previously identified that both STAT1 and STAT3 contain several putative T6BMs and I therefore propose that:

1. STAT1 and STAT3 interact with TRAF6 via T6BMs,
2. TRAF6, STAT1 and STAT3 facilitate the cross-talk between TLR and JAK-STAT signalling,
3. The recruitment of STAT1 and STAT3 modulates the TLR-mediated innate immune response.

The aims of my PhD project are to establish a mechanism of cross-talk between TLR and JAK-STAT signalling and elucidate the biological effects of this crosstalk in innate immune function.

- Demonstrate cross-talk between STAT1/TRAF6 and STAT3/TRAF6
- Characterise the biological effects of STAT1 and TRAF6 interaction
- Characterise the biological effects of STAT3 and TRAF6 interaction

Chapter 2: Materials and Methods

Chapter 2: Materials and Methods

2.1 - Tissue culture

2.1.1 - Cell line passaging

Human Embryonic Kidney 293 (HEK293), HEK293T, HT1080, WT and knockout immortalised macrophages were maintained in Dulbecco's Modified Eagle's Medium (DMEM, Life Technologies) supplemented with 10% of Fetal Bovine Serum (FBS, Life Technologies), 2 mM L-glutamine (Life Technologies), 50 U/ml penicillin and 50 mg/ml streptomycin (Life Technologies, Appendix I). The cell lines were kept at 37°C in a humidified atmosphere of 5% carbon dioxide (CO₂).

DMEM was first aspirated, cells were washed in 5 ml of Dulbecco's Phosphate Buffered Saline (DPBS pH 7.4, Life Technologies) and then detached from the flask surface using 1 ml of TrypLE express (Life Technologies), a trypsin like enzyme. Cells were resuspended in 10 ml or 20 ml of pre-warmed supplemented DMEM and then aliquoted into a 50 ml conical tube (BD Biosciences). The cell suspension is then diluted 1:4 in supplemented DMEM and added to a 75 cm² or a 175 cm² cell culture flask (BD Biosciences). Cell passaging was performed every 2-3 days.

RAW264.7 and THP1 cells were maintained in Roswell Park Memorial Institute (RPMI) 1640 medium (Life Technologies) supplemented with 10% FBS, 2 mM L-glutamine, 50 U/ml penicillin and 50 mg/ml streptomycin (Appendix I). The cell lines were kept at 37°C in a humidified atmosphere of 5% CO₂.

For RAW264.7 murine macrophages, RPMI 1640 media was first aspirated and 10 ml of fresh pre-warmed supplemented RPMI 1640 media was added to the 100 mm Petri dish (Sarstedt). Media was pipetted up and down to dislodge cells from Petri dish and transferred to a 50 ml conical tube (BD Biosciences). The cells were then seeded into a new 100 mm Petri dish diluted at 1:10 in pre-warmed supplemented RPMI 1640 media.

As THP1 cells are suspension cells, the cell suspension was transferred to a 50 ml conical tube, and then centrifuged at 1000 rpm for 5 minutes at room temperature. Media was discarded and cell pellet was resuspended in 25 ml of RPMI 1640 media. The cell suspension was then diluted 1:2 in a 175 cm² cell culture flask.

2.1.2 - Generation of Mouse Embryonic Fibroblasts (MEFs)

Mice at day 13 of gestation were culled, embryos collected and placed into PBS. In a laminar flow hood the embryos were washed in 100% ethanol (EtOH, Merck-Millipore), then separated from the amniotic sac and placenta. The liver was removed from embryos and the heads were separated for PCR genotyping. The remaining embryo was washed in DPBS to remove blood. Using scissors and/or scalpel blade embryos were then dissected into fine pieces. Embryos were added to a 15 ml conical tube (BD Biosciences) containing 1.5 ml of TrypLE express, mixed vigorously, then incubated in a humidified atmosphere for 5 minutes at 37°C, 5% CO₂. The solution containing the embryos was then pipetted through a 10 ml serological pipette (Corning), to dissociate cells and further incubated in humidified atmosphere at 37°C, 5% CO₂ for 5 minutes. This was then pipetted through a 5 ml serological pipette (Corning) to further dissociate cells and cells were transferred into a 75 cm² cell culture flask. The cells were left for 5 days incubating in a humidified atmosphere at 37°C, 5% CO₂. Cells were passaged and frozen according to protocol outlined in 2.1.1 and 2.1.5, respectively.

2.1.3 – Generation of Bone Marrow-derived Macrophages (BMMs)

Mice legs were obtained from WT C57BL/6 and STAT1 S727A mice (Courtesy of Thomas Decker, University of Vienna) aged between 6-12 weeks old. Mice were culled, sprayed with 70% EtOH and legs were dissected out by removing surrounding muscle and tissue. Hip joints were dislocated to remove legs and placed in cold supplemented DMEM media. In a laminar flow hood, legs were washed in 70% EtOH and remaining muscle was removed with scissors and kimwipes (Kimtech Science). The femur was then separated from the tibia at the knee joint and both ends of the femur and tibia were removed. Using a syringe the bones were flushed with cold DPBS into a 50 ml conical tube. Cells were pelleted at 1500 rpm for 5 minutes and DPBS decanted. 5 ml of red blood cell lysing buffer (Sigma-Aldrich) was used to resuspend cells and this was incubated for 5 minutes at room temperature. After incubation, 35 ml of supplemented DMEM was added to the cells, this was filtered through a 70 µM cell strainer (BD Biosciences) into a new 50 ml conical

tube. Centrifugation was performed at 1500 rpm for 5 minutes and the supernatant was removed. The cells were then resuspended in 10 ml of supplemented DMEM and counted using a haemocytometer (Optik Labor) and inverted research microscope (Leica DMIRB, Leica Microsystems). Cells were plated out at 1×10^6 cells/ml into a 100 mm Petri dish in 15 ml of supplemented DMEM with 20% L929-cell conditioned media. This was then incubated for 8-10 days at 37 °C in a humidified atmosphere with 5% CO₂. 3 ml of fresh L929-cell conditioned media was added on day 4. After 8-10 days the cells were passaged as described in 2.1.1 and set up for experiments 24 hours before use.

2.1.4 - Viable cell counting

After passaging confluent cells, 10 µl of the cell suspension was taken and stained with 10 µl of 0.4 % (w/v) Trypan Blue stain (Sigma-Aldrich). Cells were counted using a haemocytometer and an inverted research microscope.

2.1.5 - Thawing cells

Cells were removed from liquid nitrogen storage and then immediately thawed in a 37°C water bath. Cells were resuspended in 12 ml of pre-warmed supplemented DMEM in a 15 ml conical tube. The cell suspension was then centrifuged at 1000 rpm for 5 minutes. Media was discarded and the cell pellet resuspended in 6 ml of pre-warmed supplemented DMEM. The cell suspension was then transferred into a 25 cm² cell culture flask (BD Biosciences) and incubated at 37° in a humidified atmosphere with 5% CO₂. After 24 hours, depending on confluence of cell line, the cells were then passaged into 75 cm² or 175 cm² cell culture flask.

2.1.6 - Freezing cells

Cells were grown in either a 75 cm² or 175 cm² cell culture flasks to 80-90% confluence. Media was discarded and cells were washed with DPBS and detached from the flask using TrypLE express. Supplemented media was then added to cells and cells were pelleted by centrifugation at 1000 rpm for 5 minutes. Media was discarded and the cell pellet was resuspended in 1.5 ml of pre-chilled FBS for a 75cm² flask and 2 ml of pre-chilled FBS for a 175 cm² flask. For 75 cm² and 175 cm² flasks, respectively, 75 µl of DMSO (Sigma-Aldrich) or 100 µl of DMSO was added to the

cells, the mixture was gently pipetted up and down, then transferred into labelled cyrovials (Griener Bio-One). The cyrovials were subsequently placed into a -80°C freezer overnight. The following day cyrovials were transferred from the -80° freezer to liquid nitrogen for long term storage.

2.2 – TLR stimulation of RAW264.7 murine macrophages

2.2.1 - Preparation of RAW264.7 murine macrophages

24 hours prior to stimulation, RAW264.7 murine macrophages were seeded into a 6-well tissue culture plate (BD Biosciences) at 1×10^6 cells/ml in 3 ml of supplemented RPMI 1640 media. Cells were then stimulated over a time course of 0, 5, 10, 15, 30, and 60 minutes with the respective ligand as described in table 2.1.

2.2.2 - Cell harvesting

Note: All steps were performed at 4°C or on ice, unless otherwise stated.

Media was aspirated and wells washed with cold PBS. 80 µl of Kal B lysis buffer (Appendix I) supplemented with 1 x Ser/Thr phosphate inhibitors (Appendix I) and Sodium Vanadate (NaV, Sigma-Aldrich, Appendix I), Phenylmethylsulphonyl Fluoride (PMSF, Sigma-Aldrich, Appendix I) and a protease inhibitor cocktail tablet (Roche Diagnostics, Appendix I) was added to each well and incubated for 5 minutes. Wells were scraped using a cell scraper (TPP) and transferred to pre-chilled 1.7 ml microcentrifuge tubes (Corning). The lysates were placed on rotation for 30 minutes and centrifuged at 14,500 rpm for 5 minutes to remove cellular debris. Supernatants were transferred into new 1.7 ml microcentrifuge tubes and 20 µl of Laemmli reducing sample buffer (Appendix I) was added to each tube. The samples were subsequently boiled at 95°C for 5 minutes and stored at -20°C.

Table 2.1: TLR ligands and the concentrations used.

TLR	Ligand	Concentration	Source
2	Pam ₃ Cys	100 ng/ml	EMC Microcollections
3	Poly (I:C)	10 µg/ml	InvivoGen
4	LPS	100 ng/ml	Enzo Life Sciences
7	Loxoribine	500 µM	InvivoGen
9	CpG DNA (Class B - 1668S)	500 nM	Gene Works

2.2.3 - Nuclear protein extracts

Note: All steps were performed at 4°C or on ice, unless otherwise stated.

Media was discarded and cells washed with chilled PBS. 800 µl of PBS was then added to each well and the cells scraped using a cell scraper. Cell lysates were transferred to a pre-chilled 1.7 ml microcentrifuge tube. The tubes were centrifuged at 2000 rpm for 5 minutes, and supernatants discarded. Cell pellets were resuspended in 80 µl of plasma membrane lysis buffer (Appendix I) supplemented with 1x Ser/Thr phosphate inhibitors, 1 mM NaV and a protease inhibitor cocktail tablet. The samples were rotated for 10 minutes and further centrifuged at 14,500 rpm for 10 minutes. The plasma membrane fraction was collected and the nuclei pellets washed three times in plasma membrane lysis buffer before resuspension in 30 µl of nuclear lysis buffer (Appendix I) supplemented with 1 x Ser/Thr phosphate inhibitors, 1 mM NaV and a protease inhibitor cocktail tablet. The nuclei pellets were then rotated for 10 minutes and the nuclear fraction was clarified by centrifugation (14,500 rpm, 10 minutes). Nuclei supernatants were collected and Laemmli reducing sample buffer added to both cytoplasmic and nuclear fractions. These fractions were boiled at 95°C for 5 minutes and stored at -20°C.

2.3 – Mitochondrial isolation

2.3.1 – THP1 cell preparation

Four 175 cm² cell culture flasks of THP1 cells were pooled together and cells were seeded at 2×10^7 cells/ml into 24-well tissue culture plates (BD Bioscience) in 900 µl of THP1-conditioned media. THP1 cells were then stimulated with Pam₃Cys (100 ng/ml) or LPS (100 ng/ml) at 0, 10, 20, 30 and 60 minutes.

2.3.2 – Cell harvesting and mitochondria isolation

Note: All steps were performed at 4°C or on ice, unless otherwise stated.

THP1 cells were pelleted at 1000 rpm for 3 minutes then resuspended in 10 ml of chilled PBS. The cells were lysed in a 45 ml cell disruption vessel (Parr Instrument Company) using nitrogen cavitation at 350 psi for 1 minute. The resulting lysates were collected and using the mitochondria isolation kit (Miltenyi Biotec) mitochondria were isolated as per manufacturer's instructions. In brief, cells were pelleted at 2000 rpm for 10 minutes and then resuspended in 1 ml of lysis buffer (Miltenyi Biotec) in a 15 ml conical tube. 9 ml of 1x separation buffer (Miltenyi Biotec) was added to the lysis buffer and 50 µl of α -Translocase of the Outer Mitochondrial Membrane 22 (TOM22) microbeads (Miltenyi Biotec) were used to label mitochondria, this was then rotated for 60 minutes. LS columns (Miltenyi Biotec) were placed into a MidiMACS separation unit (Miltenyi Biotec) and the columns were rinsed with 3 ml of 1x separation buffer. Lysates were transferred into the columns and allowed to flow through. The columns were subsequently washed three times with 3 ml of 1x separation buffer. After washing, the columns were removed from the separation unit and placed into a 1.7 ml microcentrifuge tube, 1.5 ml of 1x separation buffer was added and flushed out by placing the plunger into the column. The mitochondrial suspension was further centrifuged at 13,000 rpm for 2 minutes and the supernatant decanted. 100 µl of Laemmli reducing sample buffer was added to the pellet and this was boiled at 95°C for 5 minutes then stored at -20°C.

2.4 - Sodium Dodecyl Sulfate-Polyacrylamide Gel Electrophoresis (SDS-PAGE)

Depending on size of the protein to be analysed, the density of gel was determined. Gel densities used were 8%, 10% 12% and 15%. The stacking gel was a constant 5% (Refer to table 2.2)

Gels were poured using SE 245 Dual Gel Caster (Hoefer). 20 µl of samples were loaded into each well along with a Colour-plus Pre-stained Protein Ladder (New England Biolabs). The gel was run using a SE 250 Mini-Vertical Unit (GE Healthcare Life Sciences) at 100 V until samples passed through the stacking gel and then at 150 V for approximately 60 minutes till the dye front was run off gel.

Table 2.2: Compositions of separating and stacking gels.

Separating Gel	8%	10%	12%	15%
H ₂ O	9.28 ml	7.95 ml	6.6 ml	4.6 ml
30% Polyacrylamide	5.32 ml	6.65 ml	8.08 ml	10 ml
Lower Gel Buffer	5.2 ml	5.2 ml	5.2 ml	5.2 ml
10% APS	200 µl	200 µl	200 µl	200 µl
TEMED	8 µl	8 µl	8 µl	8 µl

Stacking Gel	5%
H ₂ O	3.4 ml
30% Polyacrylamide	850 µl
Upper Gel Buffer	675 µl
10% APS	50 µl
TEMED	5 µl

2.5 - Western blot

2.5.1 - Wet transfer

After separation on SDS-PAGE was completed, proteins were transferred onto Hybond-C Extra nitrocellulose membrane (GE Healthcare Life Sciences) or Immobilon-FL transfer membrane (Merck-Millipore) using the wet transfer sandwich method and a Mini Trans-Blot Cell (Bio-Rad Laboratories).

Prior to transfer, fibre pads, filter paper and nitrocellulose membrane were soaked in pre-chilled 1 x transfer buffer (Appendix I). For PVDF membranes, these were pre-activated in methanol then rinsed in water before soaking in 1 x transfer buffer. The 'sandwich' was arranged as follows, with the black negative side of the gel cassette holder on the bottom; fibre pad, filter paper, gel, membrane, filter paper, fibre pad. The cassette was closed tightly and inserted in the Mini-Trans Blot Cell. This was run at 100 V for 1 hour on ice.

2.5.2 - Immunoblotting

Following transfer completion, membranes were blocked in 5% (w/v) powdered skim milk (Diploma) in Tris Buffered Saline (TBS) with 0.05% Tween 20 (TBST) (Sigma-Aldrich) and 1x Ser/Thr phosphate inhibitors and NaV (Appendix I) for 1 hour at room temperature. After completion of blocking, membranes were incubated with primary antibody, diluted in 5% bovine serum albumin (BSA) with 1x Ser/Thr phosphate inhibitors and NaV overnight at 4°C. The following day, membranes were washed in TBST and 2.5% (w/v) powdered skim milk with 1x Ser/Thr phosphate inhibitors and NaV (Appendix I) for 3 x 10 minute washes. The membranes were then incubated with secondary antibody diluted in supplemented 2.5% (w/v) powdered skim milk in TBST for 1 hour at room temperature. After incubation, membranes were washed in TBST and supplemented 2.5% (w/v) powdered skim milk in TBST for 3 x 10 minute washes. Membranes were again rinsed in TBST, followed by washing in MilliQ Water (MQ.H₂O, Merck-Millipore). For a list of primary and secondary antibodies used refer to table 2.3.

Table 2.3 List of antibodies and dilutions

Primary Antibody	Primary Dilution	Secondary Antibody	Secondary Dilution
α -pSTAT1 (Ser-727) (Cell Signalling Technologies)	1:1000	Goat α -rabbit HRP (Dako) or Goat α -rabbit IgG (H&L) antibody IRDye 800 CW (Rockland)	1:2000
α -pSTAT1 (Tyr-701) (Cell Signalling Technologies)	1:1000	Goat α -rabbit HRP or Goat α -rabbit IgG (H&L) antibody IRDye 800 CW	1:2000
α -STAT1 (Cell Signalling Technologies)	1:1000	Goat α -rabbit HRP or Goat α -rabbit IgG (H&L) antibody IRDye 800 CW	1:2000
α -pSTAT3 (Ser-727) (Cell Signalling Technologies)	1:1000	Goat α -rabbit IgG (H&L) antibody IRDye 800 CW	1:2000
α -pSTAT3 (Tyr-705) (Cell Signalling Technologies)	1:1000	Goat α -rabbit IgG (H&L) antibody IRDye 800 CW	1:2000
α -STAT3 (Cell Signalling Technologies)	1:1000	Goat α -rabbit HRP or Goat α -rabbit IgG (H&L) antibody IRDye 800 CW	1:2000
α -Myc (Cell Signalling Technologies)	1:1000	Rabbit α -mouse HRP (Dako) or Rabbit α - mouse IgG (H&L) antibody IRDye 800CW (Rockland)	1:2000
α -Flag (Sigma-Aldrich)	1:1000	Rabbit α -mouse HRP or Rabbit α -mouse IgG (H&L) antibody IRDye 800CW	1:2000
α -TRAF6 (H274) (Santa Cruz Biotechnology)	1:1000	Goat α -rabbit IgG (H&L) antibody IRDye 800 CW	1:2000
α -TRAF6 (D-10) (Santa Cruz Biotechnology)	1:1000	Rabbit α -mouse IgG (H&L) antibody IRDye 800CW	1:2000
α - β -Tubulin (Abcam)	1:1000	Rabbit α -mouse IgG (H&L) antibody IRDye 800CW	1:2000
α -HDAC3 (H-99) (Santa Cruz Biotechnology)	1:2000	Goat α -rabbit IgG (H&L) antibody IRDye 800 CW	1:2000
α -VDAC/Porin (Abcam)	1:1000	Goat α -rabbit IgG (H&L) antibody IRDye 800 CW	1:2000

2.5.3 - Enhanced Chemiluminescence (ECL) detection

Proteins were visualized by using the SuperSignal West Pico Chemiluminescent Substrate (Thermo Scientific). 500 μ l of luminol/enhancer was mixed with 500 μ l of stable peroxide buffer and added dropwise onto membrane, ensuring coverage of entire membrane. This was incubated for 1 min at room temperature in darkness and excess was drained off. Membranes were then exposed to X-ray film (CL-Xposure Film, Thermo Scientific) for varying time periods. The film was developed using the CP-1000 film processor (Agfa-Gevaert).

2.5.4 - Odyssey infrared system

For use of the odyssey infrared system (LI-COR Biosciences), membranes were blocked in odyssey blocking buffer (LI-COR Biosciences) for 1 hour at room temperature following transfer. After blocking, membranes were subsequently incubated in primary antibody diluted in odyssey blocking buffer for 1 hour at room temperature or overnight at 4°C. Membranes were then rinsed in PBS containing 0.05% Tween 20 (PBST) for 3 x 5 minute washes. Following washing, secondary antibody diluted in odyssey blocking buffer was added to the membrane for 1 hour at room temperature. After incubation, membranes were washed in PBST for 3 x 5 minutes. Membranes were then stored in PBST at 4°C away from light until they could be scanned by the odyssey imager. For a list of primary and secondary antibodies used refer to table 2.3.

2.5.5 - Membrane stripping

Membrane stripping was performed by rinsing membrane in PBST, followed by 3 x 10 minute washes in 1 x glycine, pH 2 (Appendix I). The membrane was further rinsed in PBST prior to blocking in 5% (w/v) milk solution or odyssey blocking buffer.

2.5.6 - Densitometry analysis

Densitometry analysis was conducted using Fiji ImageJ (version 1.48c, National Institutes of Health). Using the **Rectangular Selections** tool each lane was selected with the band of interest. The lanes were identified using the *Analyse->Gels* function and a profile plot of each lane was generated. Utilising the **Straight Line** tool the peaks in the profile plots were closed off to account for background. Next each peak was highlighted using the **Wand** tool, and the percentage of each

peak was produced using the *Analyse->Gels->Label Peaks* function. The values obtained were transferred into Excel (Microsoft Office 2010) and the relative density of the bands was normalised to an unstimulated or control sample. The relative density of bands was also adjusted against a loading control or total STAT to account for variances in protein loading where applicable. At least three immunoblots were analysed via densitometry and these values were then graphed in GraphPad Prism (version 6, GraphPad Software).

2.6 - DNA manipulation

2.6.1 - Mini-preparations of plasmid DNA

DNA purification and isolation were performed using QIAprep Spin Miniprep Kit (Qiagen) as per manufacturer's instructions. Single colonies were selected and used to inoculate 10 ml of LB (Luria-Bertani) broth (Appendix I) supplemented with 10 µl of 1000x ampicillin (Sigma-Aldrich) in a 50 ml conical tube and incubated at 37°C with shaking overnight. 1.5 ml of the culture was transferred to a 1.7 ml microcentrifuge tube and centrifuged at 14,500 rpm for 5 minutes. The supernatant was discarded and a further 1.5 ml of the culture added to the microcentrifuge tube and the process repeated. The bacterial cell pellet was resuspended in buffer P1 (Qiagen), then lysed with buffer P2 (Qiagen). In addition, Buffer N3 (Qiagen) was added to neutralise the solution and subsequently centrifuged at 13,000 rpm for 10 minutes. The resulting supernatant was transferred to a QIAprep spin column (Qiagen) and centrifuged at 14,500 rpm for 60 seconds. The spin column was washed with buffer PB (Qiagen) and buffer PE (Qiagen), both washes requiring centrifugation at 14,500 rpm for 60 seconds. Finally, DNA was eluted into a 1.7 ml microcentrifuge tube using buffer EB (Qiagen), letting stand for 1 minute and then centrifuged for a further 1 minute at 14,500 rpm to collect all eluted DNA. The concentration of DNA was then determined by utilizing a Nanodrop ND-1000 spectrophotometer (Thermo Scientific). Samples were stored at -20°C.

2.6.2 - Midi-preparations of plasmid DNA

Glycerol stocks were first grown in 10 ml of LB broth supplemented with 10 µl of 1000x ampicillin in a 37°C shaker. Approximately 6 hours later, the starter cultures were then transferred into

sterile 500 ml culture flask containing 100 ml of LB broth supplemented with 100 µl of 1000x ampicillin. The flasks were incubated overnight in a 37°C shaker at 210 rpm.

DNA isolation and purification was performed using QIAfilter Plasmid Purification Kit (Qiagen) as per manufacturer's instructions. The bacterial cells were first harvested by centrifugation at 6000 rpm for 15 minutes at 4°C using a J2-21M/E centrifuge (Beckman Coulter) and a JA 10 rotor (Beckman Coulter). The bacterial pellet was resuspended in buffer P1, lysed using buffer P2 and incubated at room temperature for 5 minutes. Following incubation, Buffer P3 (Qiagen) was used for neutralisation and the solution was incubated for 10 minutes at room temperature in a QIAfilter cartridge (Qiagen). The lysate was then filtered through a QIAGEN-tip 100 equilibrated with buffer QBT (Qiagen) and washed twice using buffer QC (Qiagen). DNA was eluted using Buffer QF (Qiagen) into a 15 ml conical tube. DNA precipitation was performed by the addition of isopropanol (Merck-Millipore) to the eluted DNA, mixed and centrifuged at 8000 rpm for 1 hour at 4°C using a Heraeus Multifuge 3SR+ centrifuge (Thermo Scientific). Isopropanol was discarded and the DNA pellet was then washed using 70% EtOH, transferred into a 1.7 ml microcentrifuge tube and centrifuged at 14,500 rpm for 5 minutes. The pellet was air dried for 5-10 minutes and resuspended in 200 µl of MQ.H₂O; the concentration of DNA was determined by using the Nanodrop. Samples were stored at -20°C.

2.6.3 – Restriction endonuclease digest

Restriction endonuclease digestion was conducted using 1-15 µg of DNA, 1x restriction enzyme buffer for enzyme of choice (Promega) and 1 U per µg of DNA of enzyme (Promega) made up to a total volume of 20 µl of MQ.H₂O. This was then incubated at 37°C for 1 hour.

2.6.4 – Agarose gel electrophoresis

Agarose powder (Promega) was weighed out and dissolved in heated 1x TAE buffer (Appendix I). After cooling solution, SYBR Safe DNA gel stain (Life Technologies) was added diluted at 1:33 to visualise DNA. The solution was then poured into a horizontal mini or wide mini-SUB CELL GT gel tray (Bio-Rad Laboratories) and allowed to set for 40 minutes.

DNA samples were diluted 1:10 in DNA loading dye (Appendix I) and a λ HindIII (Promega) DNA molecular weight marker was used to determine the size of DNA fragments. Agarose gels were run at 100 V for approximately 40 minutes in 1x TAE buffer. DNA was visualised using Safe Imager blue light transilluminator (Life Technologies) and images captured using a Quantum ST4-1000 (Vilber Lourmat). Images were printed on an UP-D987 digital graphic printer (Sony) using Type V high glossy paper (UPP-110HG, Sony).

2.6.5 – Site-directed mutagenesis

Primers were designed following manufacturer's instructions: 25 to 45 bp long, melting temperature of $>78^{\circ}\text{C}$. These were calculated by using the following formula:

$$T_m = 81.5 + 0.41 (\%GC) - \frac{675}{N} - \% \text{ Mismatch}$$

T_m = Melting temperature
 N = Length of primer in bp

Site-directed mutagenesis was performed using QuikChange II XL Site-Directed Mutagenesis Kit (Agilent Technologies) as per manufacturer's instructions. A total volume of 50 μl of solution was made up consisting of 5 μl of 10x reaction buffer, 10 ng of dsDNA template, 125 ng of oligonucleotide forward primer, 125 ng of oligonucleotide reverse primer, 1 μl of dNTP mix, 3 μl of QuikSolution reagent, and the remainder made up with MQ.H₂O. 1 μl of PfuUltra HF DNA polymerase (Agilent Technologies) was then added to each sample. Polymerase Chain Reaction (PCR) was performed using My Cyclor Thermal Cyclor (Bio-Rad Laboratories) utilising cycle parameters outlined in table 2.4. 1 μl of Dpn I restriction enzyme (Agilent Technologies) was then added to the PCR products to digest parental DNA at 37°C for approximately 2 hours. 45 μl of XL10-Gold ultra-competent cells (Agilent Technologies) were thawed on ice and then mixed with 2 μl of β -mercaptoethanol (BME, Agilent Technologies) and incubated on ice for 10 minutes. 2 μl of PCR products was then added to competent cells and further incubated on ice for 30 minutes. Cells were heat shocked at 42°C for 45 seconds, then placed on ice for another 2 minutes. Competent cells were added to 500 μl of SOC media (Appendix I) in a 15 ml conical tube and incubated at 37°C for 1 hour. 100 μl of the transformation reaction was plated out onto LB agar (Appendix I) containing appropriate antibiotics and incubated at 37°C overnight. Single colonies were selected, grown up overnight in LB broth with appropriate antibiotic selection. Bacterial

Table 2.4: Cycle parameters for PCR

Temperature	Time	Cycles
95°C	1 minute	1
95°C	50 seconds	18
60°C	50 seconds	
68°C	1 minute/kb	
68°C	7 minute	1

cultures were grown and used for DNA extraction to facilitate mini-preparations, sequencing and glycerol stocks.

2.6.6 – DNA quantification

DNA quantification was determined using a Nanodrop ND-1000 spectrophotometer. The Nanodrop was first calibrated with 2 µl of MQ.H₂O, then blanked using 2 µl of buffer that DNA is resuspended in (e.g. MQ.H₂O, TE buffer etc.). DNA concentration and purity was determined by analysing a 2 µl aliquot of sample at an absorbance of 260/280 nm and 260/230 nm.

2.6.7 - Glycerol stocks

A single colony was selected from a LB agar plate and used to inoculate 10 ml of LB broth containing appropriate antibiotic selection in a 50 ml conical tube. This was grown up overnight at 37°C with shaking. 850 µl of the bacterial culture was then added to 150 µl of glycerol in a sterile cryotube (SteriHealth), vortexed and stored at -80°C.

2.6.8 - DNA sequencing

DNA sequencing was performed by Grandel Charitable Trust Sequencing Centre, Monash Institute of Medical Research using a 16-capillary 3130x/Genetic Analyser (Life Technologies). 400 ng of DNA made up to a total volume of 15 µl with MQ.H₂O and 3.2 pM of primer was used for sequencing. Sequences were examined manually and digitally using GENTle for Windows (version 1.94, University of Cologne).

2.7 - Immunoprecipitation

2.7.1 - Cell transfection

24 hours prior to cell transfection, confluent HEK293T cells were washed with DPBS then stripped off the surface of the flask using TrypLE express. Cells were then resuspended in supplemented DMEM and counted using a haemocytometer. HEK293T cells were seeded in 10 cm cell culture

dishes (BD Biosciences) at 2×10^6 cells/ml in 10 ml of supplemented DMEM. The following DNA samples were used for immunoprecipitation STAT1-Myc, TRAF6-Flag, STAT3-Flag and TRAF6-Myc, either in combination or alone with pEFBOS as an empty backbone vector and at a concentration of 1.25 μ g. Cell transfections were carried out using Fugene-6 transfection reagent (Promega). The transfection protocol is as follows: for each sample, 7.5 μ l of Fugene-6 was added dropwise to 242.5 μ l of DMEM. This was incubated for 5 minutes at room temperature. 250 μ l of the transfection solution was then added to DNA and incubated for 20 minutes at room temperature. These solutions were then dropwise added to the cell culture dishes and incubated for 24 hours at 37°C in 5% CO₂ in a humidified atmosphere.

2.7.2 - Ectopic immunoprecipitation

Note: All steps were performed at 4°C or on ice, unless otherwise stated.

24 hours after transfection the media was aspirated and 1 ml of Kal B lysis buffer solution (Appendix I) supplemented with Sodium Fluoride (NaF, Sigma-Aldrich), NaV, PMSF and 1 tablet of protease inhibitor cocktail tablet (Appendix I) was added per dish to lyse cells for 5 minutes. The cells were scraped off using a cell scraper and transferred to a pre-chilled 1.7 ml microcentrifuge tube. Samples were rotated for 30 minutes and centrifugation was performed at 14,500 rpm for 5 minutes. The resulting supernatant was transferred to new pre-chilled microcentrifuge tubes and 20 μ l of a 50% slurry of protein G-sepharose 4 Fastflow (GE Healthcare Life Sciences) in Kal B lysis buffer was added. The samples were further rotated for 30 minutes and centrifuged at 3,000 rpm for 5 minutes. Supernatants were then transferred to new pre-chilled 1.7 ml microcentrifuge tubes. 20 μ l of the supernatant was transferred to another new pre-chilled 1.7 ml microcentrifuge tube and 10 μ l of Laemmli reducing sample buffer added. The samples were boiled at 95°C for 5 minutes to denature proteins. After boiling, samples were stored at -20°C. 20 μ l of 50% slurry of α -Flag M2 agarose beads (Sigma-Aldrich) was added to the remaining supernatants and rotated for 2 hours. The samples were then centrifuged at 3,000 rpm for 5 minutes. The supernatant was discarded and the pellet washed with 1 ml of Kal B lysis buffer, then centrifuged at 3,000 rpm for 5 minutes. This process was repeated 3 times. After the final wash, supernatants were discarded and 30 μ l of Laemmli reducing sample buffer was added to the washed beads. These were then boiled at 95°C for 5 minutes and stored at -20°C.

The samples were analysed by SDS-PAGE and immunoblot as previously described in 2.4 and 2.5. For a list of primary and secondary antibodies used refer to table 2.3.

2.7.3 – Semi-endogenous immunoprecipitation

Note: All steps were performed at 4°C or on ice, unless otherwise stated.

RAW264.7 and THP1 cells were passaged and then seeded at 2×10^6 cells/ 10 cm dish and 5×10^6 cells/10 cm dish, respectively, 24 hours before use. The cells were treated with Pam₃Cys (100 ng/ml) or LPS (100 ng/ml) over a time course, two dishes per treatment were pooled together and the cells were harvested as described in 2.7.2, using recombinant glutathione S-transferase (GST)-TRAF6 fusion protein bound to glutathione sepharose 4B beads (GE Healthcare Life Sciences) (See 2.9).

2.8 - Expression and purification of murine-GST-TRAF6 and GST

Pre-transformed rosetta strains were grown overnight from a glycerol stock in 2 x 50 ml conical tubes with 15 ml of LB broth containing 100 µg/ml of ampicillin and 100 µg/ml of chloramphenicol (Sigma-Aldrich). This was incubated at 37°C with shaking overnight. The starter cultures were then added to 1 L of LB broth containing 1 ml of 1000x ampicillin and 1 ml of 1000x chloramphenicol and incubated at 37°C with vigorous shaking until the optical density (OD) reached 0.5. Cultures were cooled to room temperature for ~3 hours. After cooling, 20 µl of 1 M isopropyl β-D-thiogalactopyranoside (IPTG) was added, along with 1 ml of 1000x ampicillin and 1 ml of 1000x chloramphenicol and the culture incubated at 18°C overnight with shaking.

Note: All steps were performed at 4°C or on ice, unless otherwise stated.

The bacterial cells were harvested by centrifugation at 6,000 rpm for 20 minutes using a J2-21M/E centrifuge and a JA 10 rotor. The supernatant was discarded and the pellet resuspended in 15 ml of Low Salt Soluble Buffer (LSSB) supplemented with 0.1 mM PMSF and 1 tablet of protease inhibitor cocktail tablet. After addition of supplemented LSSB, cells were disrupted using a 4710 series ultrasonics homogenizer (Cole-Parmer) set to a frequency of 6, performed in controlled bursts of 20 seconds on and 30 seconds off for 3-4 minutes. The lysate was subsequently rotated

for 30 minutes, before centrifugation at 12,000 rpm for 30 minutes. The supernatant was then stored at 4°C in a 50 ml conical tube and the pellet resuspended in 15 ml of High Salt Soluble Buffer (HSSB) supplemented with 0.1 mM PMSF and 1 tablet of protease inhibitor cocktail tablet. Sonication of cells was performed as previously described and rotated for 2 hours. After which the lysate was centrifuged at 18,000 rpm for 50 minutes and the supernatant pooled with the previously stored supernatant and stored at 4°C.

2.8.1 - Batch purification of proteins

300 µl of glutathione sepharose 4B beads were transferred to a 1.7 ml microcentrifuge tube and pelleted by centrifugation at 2,000 rpm for 5 minutes. The supernatant was discarded and the pellet washed with 1 ml cold HSSB and centrifuged at 2,000 rpm for 5 minutes. This was repeated a total of 3 times, finally the beads were resuspended in 300 µl of HSSB, resulting in a 50% slurry. The beads were then added to the pooled supernatant and rotated for 2 hours. The samples were subsequently centrifuged at 2,000 rpm for 5 minutes, and the supernatant stored as the unbound fraction at 4°C. The pellet was resuspended in 2 ml of HSSB and transferred to a 2 ml microcentrifuge tube (Corning). The beads were centrifuged at 2,000 rpm for 5 minutes and the supernatant discarded. Washes were repeated 10 times and the beads were resuspended in 300 µl of PBS and stored at 4°C.

2.8.2 - Coomassie R250 blue staining

To determine purity of GST-TRAF6 fusion protein bound to GST beads, the beads were analysed by SDS-PAGE using a 12% separating gel. 20 µl of the unbound fraction and 20 µl of the GST-TRAF6 beads were transferred to two 1.7 ml microcentrifuge tubes and 10 µl of Laemmli reducing sample buffer was added. The samples were then boiled at 95°C for 5 minutes and loaded onto a gel. The samples were run at 150 V for approximately 1½ hours. After which the gel was stained with a Coomassie blue stain (Appendix I) for 1 hour, then de-stained using Coomassie destain (Appendix I) overnight. The gel was then washed in Coomassie de-stain for another hour and washed in MQ.H₂O before being sealed in plastic for storage.

2.9 - GST pull-down assay

The recombinant GST-TRAF6 fusion protein bound to glutathione sepharose 4B beads were used in immunoprecipitation studies as previously described in 2.7. Note the following changes. HEK293Ts were transfected with 1.5 µg of STAT1-Myc and STAT3-Flag along with 1 µg of pEF-BOS. The recombinant GST-TRAF6 fusion protein was used for immunoprecipitation as described in 2.7.2. 20 µl of recombinant GST-TRAF6 fusion protein was added to each sample and 10 µl of recombinant GST beads was added as a control sample. Samples were analysed by SDS-PAGE and immunoblot as previously described in 2.4 and 2.5. For a list of primary and secondary antibodies used refer to table 2.3.

2.10 - Confocal microscopy

Confocal images were captured using a C1 inverted microscope with 4 excitation lasers (405 nm, 488 nm, 561 nm and 635 nm, Nikon Instruments). Images were captured using either a 60x or 100x oil objective lens. Confocal images were acquired at 1024 x 1024 pixels and are representative of at least 3 independent experiments where >100 cells were examined per condition. Image processing was performed using Fiji ImageJ (version 1.48c, National Institutes of Health) and Imaris (version 7.6.4, Bitplane).

2.10.1 - Coverslip and cell preparation

12 mm round coverslips (Thermo Scientific) were placed on a paper towel in a container then autoclaved. For HEK293Ts and HT1080s, the coverslips were coated in 1% gelatin (Appendix I), placed at an angle in a 24-well plate (BD Biosciences), and allowed to dry overnight. The coverslips were then placed flat in a 24-well plate and cells were seeded at a concentration of 5×10^4 cells/ml in 1 ml of supplemented media and incubated in a humidified atmosphere at 37°C, 5% CO₂ for 24 hours.

2.10.2 - Cell fixation

Following stimulation of cells, media was aspirated and cells were rinsed in chilled PBS twice. For cells washed in digitonin/sucrose buffer (Appendix I), this step occurs prior to cell fixation. Coverslips are washed in 250 μ l of digitonin/sucrose buffer four times for one minute with gentle agitation. Next the cells were fixed using either 4% paraformaldehyde (Sigma-Aldrich) or 10% formalin (Amber Scientific). When cells were fixed using paraformaldehyde, the paraformaldehyde was first dissolved in warm PBS, heated in a microwave, following by incubation in a 55°C oven and inverted every 15 minutes to ensure the paraformaldehyde was fully dissolved. The solution was then placed at 4°C till ready for use. 1 ml of 4% paraformaldehyde was then added to cells and incubated for 20 minutes at room temperature. The paraformaldehyde was then aspirated and cells were rinsed twice in 500 μ l of chilled PBS.

When using 10% formalin, 500 μ l of formalin was added to the cells, and then incubated at 37°C for 10 minutes. The formalin was removed and cells were washed twice in 500 μ l of chilled PBS.

2.10.3 - Cell permeabilization

After fixation, cells were permeabilized using a 0.1% Triton X-100 solution (Merck-Millipore). 500 μ l of 0.1% Triton X-100 was added to the cells then incubated for 10 minutes at room temperature. The permeabilizing solution was subsequently removed and cells were washed twice with 500 μ l of chilled PBS.

2.10.4 - Immunostaining

For nuclear staining, 500 μ l of Hoechst 33342 stain (Life Technologies) per well was used at a concentration of 1 μ g/ml. The cells were incubated in Hoechst stain for 10 minutes at room temperature in the dark. Hoechst stain was then removed, and the cells washed twice with 500 μ l of chilled PBS.

For mitochondrial staining, live cells were stained prior to fixation, as the mitochondrial dyes passively diffuse across the plasma membrane into active mitochondria. Cells were stained with either Mitotracker Red CMXRos (100nM, Life Technologies) or Mitotracker Deep Red FM (100

nM, Life Technologies). Cells were incubated for 15 minutes at 37°C in a humidified atmosphere of 5% CO₂. The mitochondrial dye was then discarded and cells washed in media and incubated for 10 minutes at 37°C in a humidified atmosphere with 5% CO₂, this was repeated five times.

Following staining, the cells were then blocked in 500 µl of 5% BSA for 2 hours away from light. Coverslips were removed from the 24-well plate, drained and inverted onto parafilm containing 100 µl of primary antibody diluted at 1:500 in 5% BSA. This was then incubated at 4°C overnight away from light. Following incubation, coverslips were drained and placed onto parafilm containing 100 µl of PBS for 5 minutes, this was repeated three times and the coverslips were drained following each wash and placed in darkness. For some samples a second primary antibody was used. Coverslips were placed onto parafilm containing 100 µl of primary antibody diluted 1:500 in 5% BSA. This was then incubated for 1 hour at room temperature away from light. Coverslips were subsequently washed as previously described.

The coverslips were then placed onto parafilm containing either Alex Fluor 594 goat anti-mouse IgG (H+L) (Life Technologies) or Alex Fluor 488 goat anti-rabbit IgG (H+L) (Life Technologies) secondary antibody diluted at 1:1000 in 5% BSA for 1 hour at room temperature in the dark. Unbound antibody was removed from the coverslips as described above. The coverslips were then mounted onto SuperFrost 76 x 26 mm slides (Menzel-Gläser) with 10 µl of fluorescent mounting media (Dako).

2.11 - High content screen

Cells were seeded at a concentration of 2×10^4 cells/well in a black 96-well plate (Corning) and incubated at 37°C, 5% CO₂ in a humidified atmosphere for 24 hours. Before cells were treated, the media was removed and replaced with 100 µl of fresh media. Cells were then treated with TLR ligands (Pam₃Cys – 200 ng/ml, poly (I:C) [transfected 10 µg/ml, untransfected 20 µg/ml] and LPS – 200 ng/ml), rotenone (10 µM, Sigma-Aldrich) then washed twice with 100 µl of PBS. Next cells were stained with both Hoechst 33342 (1 µg/ml) and Mitotracker Red CMXRos (100 nM) or dihydroethidium (DHE, 5 µM, Life Technologies) or MitoSOX (5 µM, Life Technologies). Stains were combined together and cells were incubated for 15 minutes at 37°C in a humidified atmosphere with 5% CO₂. The cells were then washed twice with fresh media and incubated for 10 minutes in a humidified atmosphere at 37°C with 5% CO₂ per wash. Following this, cells were

washed in twice in PBS and subsequently fixed in 10% formalin and incubated at 37°C for 10 minutes. Finally, cells were washed twice in PBS, then stored in PBS and kept at 4°C away from light till ready for scanning. The plates were scanned with a Cellomics ArrayScan VTI HCS Reader (Thermo Scientific) and data was analysed with ArrayScan HCS reader software (Thermo Scientific). Values were then graphed in Graphpad Prism.

2.12 - Small Interfering RNA (siRNA) transfection

Cells were passaged in antibiotic free media and seeded into a 96-well plate (BD Biosciences) at a concentration of 1×10^4 cells/well and incubated at 37°C in a humidified atmosphere with 5% CO₂ for 24 hours. The siRNA was first prepared by diluting in 1x siRNA buffer (Thermo Scientific) to a concentration of 5 µM. For each well 0.5 µl of 5 µM siRNA and 9.5 µl of serum free media was required, siRNA was then incubated for 5 minutes at room temperature. In a separate tube, 0.3 µl of DharmaFECT 4 (Thermo Scientific) and 9.7 µl of serum free media was required for each well; this solution was also incubated for 5 minutes at room temperature. The contents of both tubes were then combined, and the resulting siRNA transfection solution was incubated for 20 minutes at room temperature. 80 µl of antibiotic free media per well was added to the siRNA transfection solution, resulting in a total volume of 100 µl per well. Media from the 96-well plate was discarded and a 100 µl of siRNA transfection solution was added to the cells. The cells were then incubated for 72 hours in a humidified atmosphere at 37°C with 5% CO₂.

2.13 - Enzyme-linked Immunosorbent Assay (ELISA)

Cytokine levels of TNF-α, IL-6, RANTES and IL-12 were measured using mouse TNF-α, mouse IL-6 ELISA kits (BD Biosciences), mouse CCL5/RANTES Duoset (R&D Systems) and mouse IL-12 ELISA MAX Deluxe kit (Biolegend) as per manufacturer's instructions. In brief, 96-well plates (Thermo Scientific) were first coated in 100 µl of the appropriate capture antibody diluted in coating buffer (Appendix I). The plates were sealed and incubated at 4°C or room temperature overnight. The coating buffer was discarded and the plates were washed three times in >300 µl of PBST. The plates were then blocked in 200 µl of ELISA assay diluent (Appendix I), sealed and incubated at room temperature for 1 hour. Assay diluent was discarded and plates were washed three times in PBST. Standards were serially diluted and 100 µl of the appropriate standards were then added to the plates in duplicate with a blank control, in addition 100 µl of cell supernatant was also added

to plates. Standards and samples were diluted in assay diluent as required. Plates were then sealed and incubated at room temperature for at least 2 hours. The standards and samples were then aspirated and the plates were washed five times in PBST. The appropriate detection antibody was then diluted in assay diluent and 100 μ l was added to plates. This was sealed and incubated at room temperature for 1 hour. The wells were emptied and rinsed five times with PBST. Next, streptavidin-HRP was diluted in assay diluent and 100 μ l was added to wells. The plate was sealed and incubated for 30 minutes at room temperature in darkness. The streptavidin-HRP was then discarded and wells washed 7 times with PBST allowing the wells to soak in PBST for 30 seconds to 1 minute between each wash. Peroxidase substrate (TMB, Thermo Scientific) was then mixed at a 1:1 ratio with peroxide solution (Thermo Scientific) and 100 μ l added to wells. Colour was allowed to develop for up to 30 minutes before the reaction was stopped with 50 μ l of ELISA stop solution (Appendix I). The plates were then scanned on a FLUOstar Optima fluorescent microplate reader (BMG Labtech) at 450 nm and cytokine levels were determined on a standard curve generated with MARS data analysis software (version 1.1, BMG Labtech). Values were then graphed in Graphpad Prism.

2.14 – MTT cell proliferation assay

24 hours before assay, cells were plated out in a 96-well plate at desired concentration in supplemented media and incubated in a humidified atmosphere at 37°C with 5% CO₂. Media was discarded and MTT solution (Sigma-Aldrich) was prepared by diluting in supplemented media to a final concentration of 500 μ g/ml. Cells were incubated in 100 μ l of MTT solution, including media alone as a blank, away from light for 5 minutes on a shaker. The plate was further incubated for 4 hours at 37°C with 5% CO₂ in a humidified atmosphere. After incubation, MTT solution was aspirated and cells were resuspended in 100 μ l of DMSO, including DMSO alone as a second blank. The plate was placed on a shaker away from light for 10 minutes, then scanned at 590 nm on a FLUOstar Optima fluorescent microplate reader and data analysed using MARS data analysis software. Values were then graphed in Graphpad Prism.

2.15 - Luciferase reporter assay

HEK293T cells stably expressing TLR2 were seeded at 2×10^4 cells/well in a 96-well plate at 37°C and 5% CO₂ in a humidified atmosphere for 24 hours. Cells were then transfected following

protocol in 2.7.1. For each well, 0.8 μ l of Fugene-6 transfection reagent was added to 9.2 μ l of serum free DMEM. 10 μ l of this solution was then added to DNA. The cells were transfected with 230ng of DNA containing a Thymidine Kinase (TK)-Renilla encoding plasmid (50ng), a luciferase reporter construct (80ng, κ B-luciferase, TNF- α -luciferase and IL-6-luciferase) and/or empty vector or STAT1/3 construct (80ng).

24 hours following transfection, media was discarded and cells were lysed with 50 μ l of 1x reporter lysis buffer (Promega) diluted in MQ.H₂O. 20 μ l of cellular lysate was transferred to a white microton 96-well plate (Greiner Bio-One), and 50 μ l of TK-Renilla substrate (Promega) diluted in PBS was also added. Renilla activity was read immediately using a FLUOstar Optima fluorescent microplate reader at 415 nM. Luciferase activity was assessed by also taking 20 μ l of cellular lysates and transferring it to a white microton 96-well plate. 30 μ l of luciferase substrate solution (Promega) was then added and luciferase activity was read immediately using a FLUOstar Optima fluorescent microplate reader at 415 nM. Vector normalisation was performed by dividing the luciferase activity by TK-Renilla activity. Values were then graphed in Graphpad Prism.

2.16 – TRANSFAC promoter analysis

Using Esembl biomart (Ensembl release 73), 1500 bp upstream of the gene of interest was obtained. These promoter regions were entered into TRANSFAC MATCH (TRANSFAC Professional 2011.1) and employing the user generated profiles with a minimize false positive cut-off, promoter analysis was conducted and predicted transcription factor binding sites were obtained for genes of interest.

2.17 - Statistical analysis

All statistical analysis was performed using GraphPad Prism (version 6, GraphPad Software). Paired t-tests and one-way ANOVAs were conducted on normally-distributed data. Levels of significance are de-noted as: * P < 0.05, ** P < 0.01, *** P < 0.001 and **** P < 0.0001.

**Chapter 3: Demonstrating the
Cross-talk Between TLR and JAK-
STAT Signalling**

Chapter 3: Demonstrating the Cross-talk Between TLR and JAK-STAT Signalling

3.1 – Introduction

The activation of the TLR signalling cascade is a result of binding of its cognate ligands, leading to dimerisation of the receptor and recruitment of adaptor molecules. Ultimately, TLR signalling induces expression of proinflammatory cytokines that are required to resolve pathogen invasion. LPS stimulation of TLR4 can also result in production of IFN- β through the TLR pathway (Toshchakov et al., 2002). The secretion of IFN- β leads to autocrine activation of JAK-STAT signalling where IFN- β binds the IFNAR resulting in STAT1 Tyr-701 phosphorylation followed by homo- or hetero-dimerisation with STAT2 and translocation to the nucleus (Darnell et al., 1994). Nuclear localisation of STAT1 leads to binding of IFN-stimulated Response Elements (ISREs) as an ISGF complex resulting in expression of proinflammatory genes (Decker et al., 1991).

TLR signalling however has been shown to impact directly on STAT1 phosphorylation without the need for secretion of IFN- β . Two studies have demonstrated Ser-727 phosphorylation of STAT1 following TLR ligand stimulation. Rhee et al. (2003) found that murine macrophages underwent Ser-727 phosphorylation following Pam₃Cys (TLR2) and LPS (TLR4) stimulation. A similar result was demonstrated by Schroder et al. (2007), who found in BMMs that CpG DNA (TLR9) also induced Ser-727 phosphorylation of STAT1, but not a corresponding Tyr-701 phosphorylation that occurs following IFN stimulation.

In glycoprotein 130 (gp130)^{Y757F/Y757F} (F/F) knock-in mice, which contains a mutation that disrupts the negative feedback loop of gp130 signalling resulting in hyperactivation of STAT3 (Jenkins et al., 2005), these mice have also demonstrated a hypersensitivity to LPS (Greenhill et al., 2011). LPS hypersensitivity in F/F mice is a result of the TLR4/MyD88-dependent pathway inducing IL-6 production which in turn causes tyrosine phosphorylation of STAT3 (Greenhill et al., 2011). This tyrosine phosphorylation of STAT3 is independent of type I IFN production, as blocking the IFNAR complex with mouse IFN- α/β receptor 1 (MAR1) monoclonal antibody, which binds the extracellular domain of IFNAR1, did not affect mRNA levels of IL-6 (Greenhill et al., 2011). This study therefore suggests a mechanism of cross-talk between TLR and gp130 signalling, implying it may also be possible that STAT3 and STAT1 play a role in TLR signalling and cytokine expression independent of traditional cytokine JAK-STAT signalling.

TRAF6 is a crucial signalling molecule that is involved in a diverse range of physiological processes. TRAF1, 2, 3 and 5 recognise peptide motifs that TRAF6 cannot interact with, due to its unique TRAF-C domain. Unlike the other TRAFs, TRAF6 serves as a common signalling mediator in TNF- α and IL-1/TLR signalling, allowing translocation of signals from the cell surface and activation of NF κ B (Kobayashi et al., 2004). Overexpression of TRAF6 has been demonstrated to activate NF κ B, whilst overexpression of a dominant negative mutant of TRAF6 impairs NF κ B activation (Arch et al., 1998). Furthermore, TRAF6 knockout mice display impaired activation of NF κ B following IL-1 and LPS stimulation, reiterating TRAF6's crucial function in IL-1/TLR signalling (Lomaga et al., 1999, Naito et al., 1999). Due to TRAF6's multifaceted role in biological processes, it is not surprising that TRAF6 interacts with many different molecules.

Proteins such as CD40, TRANCE, IRAK, TRIF, TRAM and Mal all interact with TRAF6 via a T6BM identified in all these proteins (Ye et al., 2002, Sato et al., 2003, Mansell et al., 2004) (Table 3.1). The T6BM which is comprised of the aa motif P-X-E-X-X-(aromatic/acidic residue) (Ye et al., 2002), is a critical signature that when mutated renders proteins unable to interact with TRAF6 and affects downstream signalling. These findings demonstrate the importance of identifying T6BMs in signalling mediators of inflammatory pathways and TRAF6's central role in IL-1/TLR and TNF- α signalling. I have identified that STAT1 and STAT3 each contain three putative T6BMs, suggesting a possible interaction between STAT1/STAT3 and TRAF6.

The findings here form the basis for this project, investigating the interaction between STAT1/TRAF6 and STAT3/TRAF6, and the mechanisms of this interaction. The direct recruitment of STAT1 and STAT3 into TLR signalling represents a novel discovery of possible cross-talk between signalling pathways that has not previously been shown and demonstrates the potential augmentation of the immune response through synergy of TLR and JAK-STAT signalling.

Table 3.1: Putative TRAF6 binding motifs in immune signalling molecules.

Critical glutamic acid residue is shown in red. Ar/Ac – Aromatic/Acidic Group

TRAF6 binding motif	P	X	E	X	X	Ar/Ac	
Mal (188-196)	P	P	E	L	R	F	Mansell et al. 2004
TRAM (181-186)	P	R	E	R	T	P	
TRIF (250-255)	P	E	E	M	S	W	Sato et al. 2003 Jiang et al 2004
IRAK1 (542-547)	P	Q	E	N	S	Y	Ye et al. 2002
IRAK2 (585-590)	P	V	E	S	D	E	
IRAK3 (504-509)	P	E	E	S	D	E	
IRAK-2 (1) (526-531)	P	E	E	T	D	D	
IRAK-2 (2) (557-562)	P	T	E	N	G	E	
IRAK-M (578-583)	P	V	E	D	D	E	
RIP2 (194-199)	P	P	E	N	Y	E	
CD40 (233-238)	P	Q	E	I	N	F	
TRANCER (1) (344-349)	P	T	E	D	E	Y	
TRANCER (2) (377-382)	P	L	E	V	G	E	
TRANCER (3) (453-458)	P	G	E	D	C	E	

3.2 – Results

3.2.1 – Serine phosphorylation of STAT1 following TLR ligand stimulation

As Rhee et al. (2003) and Schroder et al. (2007) have previously established that STAT1 is Ser-727 phosphorylated following stimulation with Pam₃Cys (TLR2), LPS (TLR4) and CpG DNA (TLR9), I initially wished to examine multiple TLR-induced STAT1 phosphorylation in RAW264.7 murine macrophage cells as they represent a relevant biological model; as macrophages are one of the first cells to recognise and respond to foreign insults. These experiments were conducted to re-confirm previous studies and to assess the Tyr-701 and Ser-727 status of STAT1 following stimulation with other TLR agonists.

I first used IFN- α , as it is a well characterised positive control known to induce both tyrosine and serine phosphorylation of STAT1 (Schindler et al., 1992b, Kovarik et al., 1998). As can be seen in figure 3.1 STAT1 undergoes both rapid and robust Ser-727 (Figure 3.1A, panel 1) and Tyr-701 phosphorylation (Figure 3.1A, panel 2). STAT1 Ser-727 phosphorylated is first observed at 10 minutes post-stimulation with this phosphorylation sustained for up to 60 minutes post-challenge (Figure 3.1A, panel 1). In contrast, Tyr-701 phosphorylation isn't observed until 20 minutes post-stimulation though this is maintained for longer than pSer-727, up to 120 minutes (Figure 3.1A, panel 2). Densitometry analysis of the serine phosphorylation illustrates rapid activation observed at 10 minutes (31.20 ± 0.92 , $p=0.0009$), peaking at 30 minutes and diminishing from 60 minutes onwards (Figure 3.1B).

Next I examined the effect of the TLR2 ligand, Pam₃Cys on STAT1 phosphorylation. Similar to previous results, STAT1 is observed to undergo Ser-727 phosphorylation rapidly at 10 minutes post-stimulation where the serine phosphorylation was sustained for up to 120 minutes and began to diminish back to background levels (Figure 3.2A, panel 1). Pam₃Cys however, did not induce a corresponding Tyr-701 phosphorylation and this was not observed at any time point (Figure 3.2A, panel 2). Analysis of the serine phosphorylation blot via densitometry displays substantial serine phosphorylation after 10 minutes, reaching maximal effect at 20 minutes and beginning to diminish between 30 (75.88 ± 5.4 , $p=0.0053$) and 60 minutes (82.79 ± 11.43 , $p=0.0191$). By 120 minutes, serine phosphorylation of STAT1 has almost returned to basal levels (Figure 3.2B).

Stimulation with the TLR3 ligand, poly (I:C) produces a similar effect on STAT1, albeit with delayed kinetics. Unlike Pam₃Cys, poly (I:C) induces serine phosphorylation at 60 minutes and this Ser-727 phosphorylation is maintained for up to 120 minutes, where the activation of STAT1 begins to weaken (Figure 3.3A, panel 1). Tyr-701 phosphorylation of STAT1 is also observed at 120 minutes

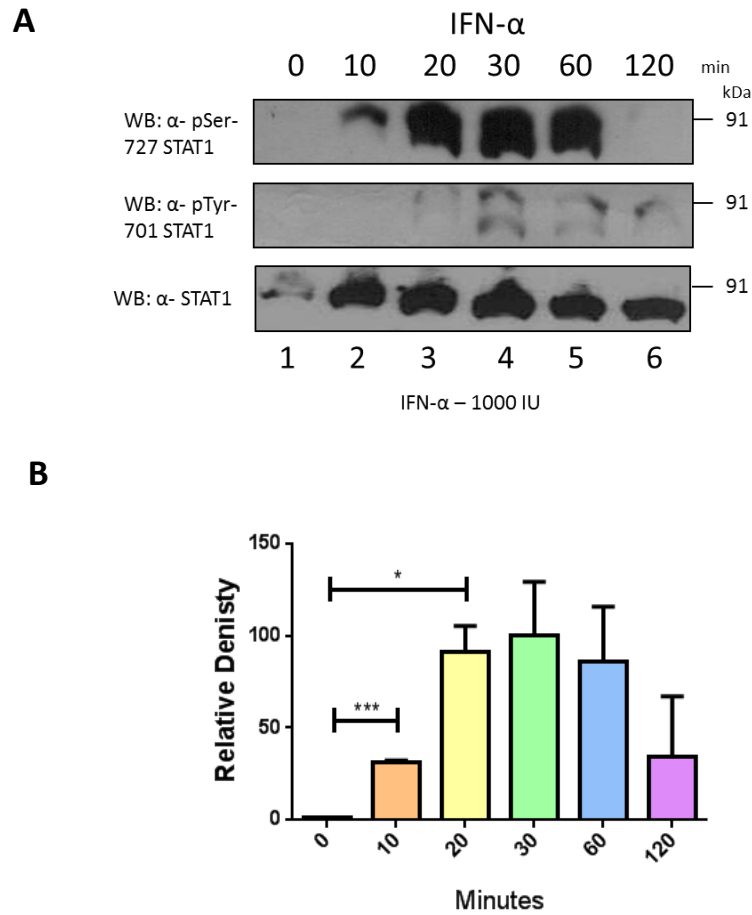


Figure 3.1: IFN- α stimulation induces rapid Ser-727 and Tyr-701 phosphorylation of STAT1.

RAW264.7 murine macrophages were seeded into a 6-well plate at 1×10^6 cells/well, 24 hours prior to stimulation. The cells were then stimulated with 1000 IU of IFN- α over a time course of 120 minutes. Following stimulation, cells were harvested in Kal B solution containing Ser/Thr phosphate inhibitors (Appendix I), subjected to 30 minutes rotation and then centrifuged to separate cellular debris (14,500 rpm, 4°C, 5 minutes). Samples were separated by gel electrophoresis and immunoblotted with α -pSTAT1 (Ser-727) antibody, α -pSTAT1 (Tyr-701) and α -STAT1 antibody. **(A)** Western blot demonstrates Tyr-701 and Ser-727 phosphorylation of STAT1. **(B)** Densitometry analysis illustrates the rapid Ser-727 phosphorylation of STAT1. These results are a representation of three individual experiments (n=3).

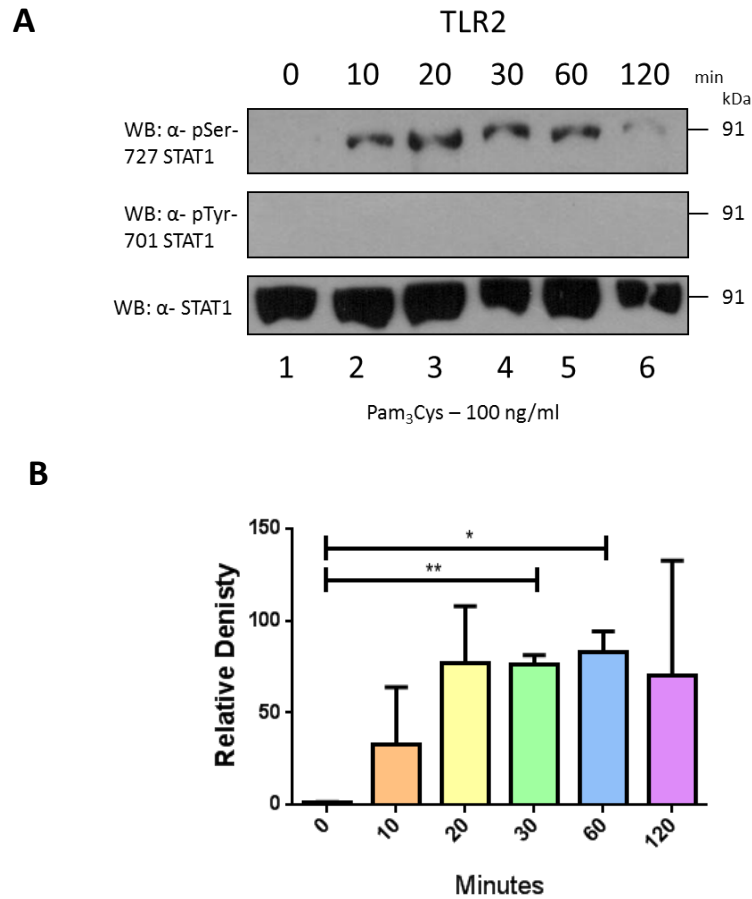


Figure 3.2: The TLR2 ligand, Pam₃Cys, induces rapid Ser-727 phosphorylation of STAT1.

RAW264.7 murine macrophages were prepared as described in figure 3.1. Cells were stimulated with 100 ng/ml of Pam₃Cys over a time course of 120 minutes. Samples were then separated by gel electrophoresis and immunoblotted with α -pSTAT1 (Ser-727) antibody, α -pSTAT1 (Tyr-701) and α -STAT1 antibody. **(A)** Western blot demonstrates rapid Ser-727 phosphorylation of STAT1. **(B)** Densitometry analysis illustrates the rapid Ser-727 phosphorylation of STAT1. These results are a representation of three individual experiments (n=3).

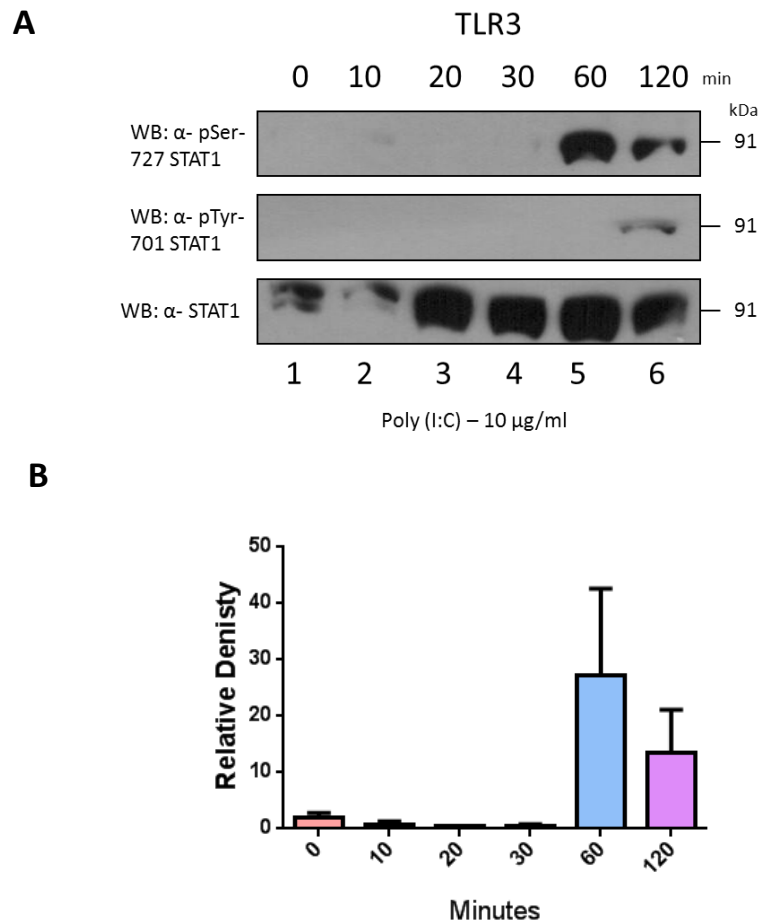


Figure 3.3: STAT1 Ser-727 phosphorylation displays delayed kinetics in response to the TLR3 ligand, poly (I:C).

RAW264.7 murine macrophages were prepared as described in figure 3.1. Cells were stimulated with 10 μ g/ml of poly (I:C) over a time course of 120 minutes. Samples were then separated by gel electrophoresis and immunoblotted with α -pSTAT1 (Ser-727) antibody, α -pSTAT1 (Tyr-701) and α -STAT1 antibody. **(A)** Western blot demonstrates Ser-727 phosphorylation of STAT1. **(B)** Densitometry analysis illustrates the Ser-727 phosphorylation of STAT1. These results are a representation of three individual experiments (n=3).

which matches the results of Rhee et al. (2003) and may be a consequence of IFN- β production (Alexopoulou et al., 2001). Similar to my initial observation of the immunoblot, densitometry confirms the delayed kinetics of STAT1 Ser-727 phosphorylation compared to TLR2. Maximum serine phosphorylation of STAT1 is not seen until 60 minutes post-challenge and the serine phosphorylation begins to decrease from 120 minutes (Figure 3.3B).

Commensurate with that observed in TLR2 stimulation, the TLR4 agonist LPS also induces rapid Ser-727 phosphorylation of STAT1, observed at 10 minutes post-stimulation with the phosphorylation sustained for 120 minutes (Figure 3.4A, panel 1). Tyr-701 phosphorylation can initially be detected at 30 minutes though this appears to be very weak. Only at 120 minutes is tyrosine phosphorylation significantly observed consistent with previous observations (Figure 3.4A, panel 2). Densitometry analysis of the immunoblot confirms these observations, demonstrating rapid serine phosphorylation of STAT1 following LPS stimulation which can be detected at 10 minutes post-stimulation (238.8 ± 48.59 , $p=0.0392$) and this serine phosphorylation is maintained over the time course, albeit with a decrease in serine phosphorylation at 30 minutes post LPS stimulation (Figure 3.4B).

Like TLR3, TLR7 and TLR9 are also endosomally located (Matsumoto et al., 2003, Heil et al., 2003, Ahmad-Nejad et al., 2002, Latz et al., 2004). Similar to the delayed kinetics observed with TLR3 stimulation, the results display a similar trend. Following stimulation with the TLR7 agonist, loxoribine, serine phosphorylation of STAT1 is observed as delayed compared to membrane TLRs such as TLR2 and TLR4, only been observed at 20 minutes and reaching its maximal phosphorylation at 60 minutes, thereafter decreasing at 120 minutes (Figure 3.5A, panel 1). In contrast to TLR3 however, loxoribine did not induce Tyr-701 phosphorylation of STAT1 over the time course (Figure 3.5A, panel 2). Further analysis of the serine phosphorylation immunoblots by densitometry confirms my initial observations. Substantial serine phosphorylation of STAT1 can be detected at 30 minutes (67.19 ± 10 , $p=0.0267$) and this gradually increases along the time course, reaching a peak at 60 minutes and beginning to diminish by 120 minutes (Figure 3.5B).

TLR9 exhibits the same phenomenon, with STAT1 undergoing delayed serine phosphorylation that is detected at 30 minutes post-stimulation and is sustained for up to 120 minutes (Figure 3.6A, panel 1). Though Ser-727 phosphorylation is sustained for over an hour, the induction of this serine phosphorylation appears to be quite weak. Comparable to TLR7, CpG DNA is also unable to induce Tyr-701 phosphorylation, which is not observed over the 120 minute time course (Figure 3.6A, panel 2). Densitometry analysis performed on the pSer-727 STAT1 immunoblots further illustrates the delayed kinetics of the endosomal TLR. Ser-727 STAT1 is detected at 30 minutes and this phosphorylation is observed to be increasing up to 120 minutes (Figure 3.6B).

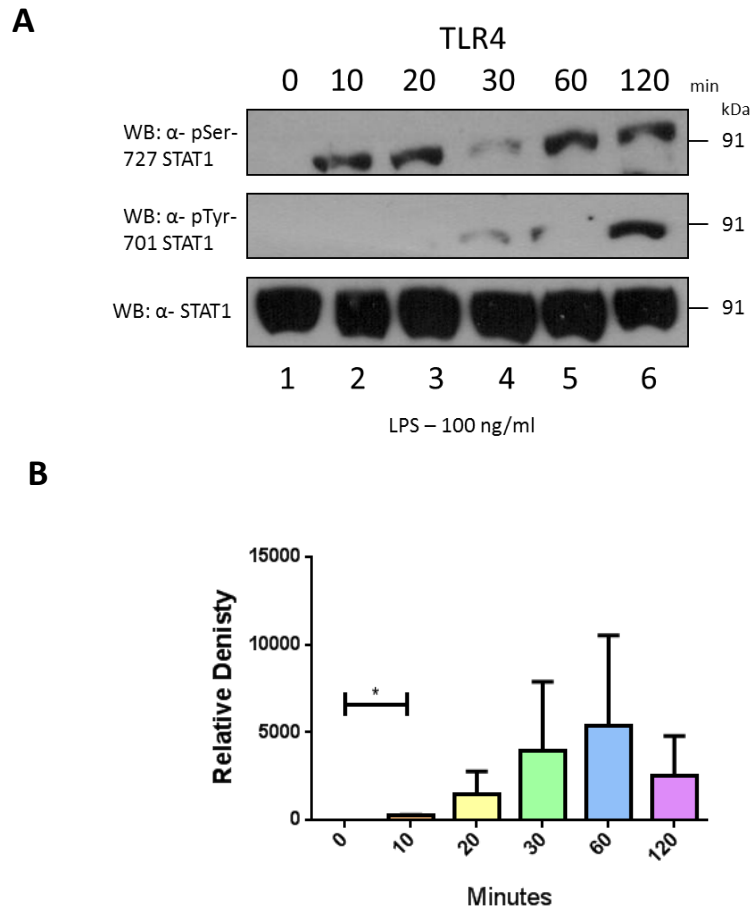


Figure 3.4: Rapid Ser-727 phosphorylation with no corresponding Tyr-701 phosphorylation is observed in RAW264.7 murine macrophages stimulated with the TLR4 ligand, LPS.

RAW264.7 murine macrophages were prepared as described in figure 3.1. Cells were stimulated with 100 ng/ml of LPS over a time course of 120 minutes. Samples were then separated by gel electrophoresis and immunoblotted with α -pSTAT1 (Ser-727) antibody, α -pSTAT1 (Tyr-701) and α -STAT1 antibody. **(A)** Western blot demonstrates rapid Ser-727 phosphorylation of STAT1. **(B)** Densitometry analysis illustrates the rapid Ser-727 phosphorylation of STAT1. These results are a representation of three individual experiments (n=3).

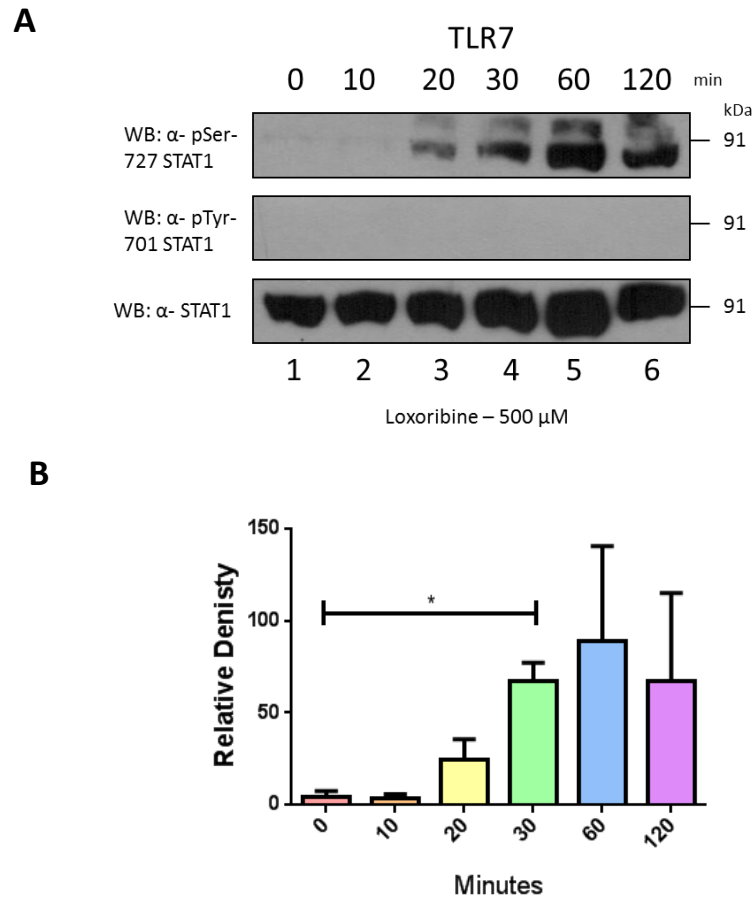


Figure 3.5: TLR7 ligand, loxoribine, induces Ser-727 phosphorylation of STAT1 albeit with delayed kinetics.

RAW264.7 murine macrophages were prepared as described in figure 3.1. Cells were stimulated with 500 μ M of loxoribine over a time course of 120 minutes. Samples were then separated by gel electrophoresis and immunoblotted with α -pSTAT1 (Ser-727) antibody, α -pSTAT1 (Tyr-701) and α -STAT1 antibody. **(A)** Western blot demonstrates rapid Ser-727 phosphorylation of STAT1. **(B)** Densitometry analysis illustrates the rapid Ser-727 phosphorylation of STAT1. These results are a representation of three individual experiments (n=3).

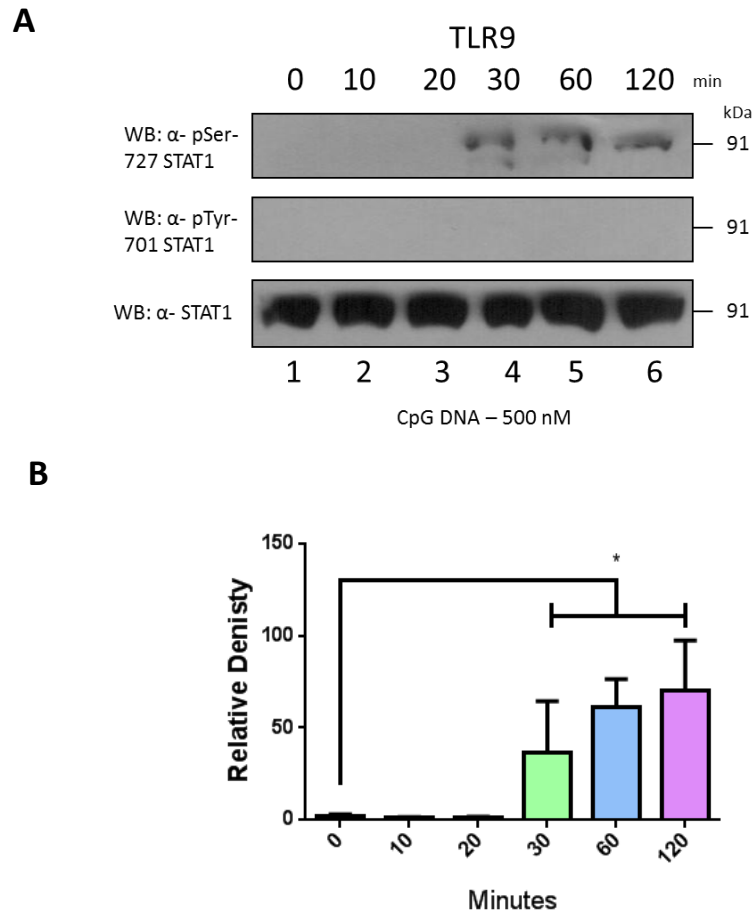


Figure 3.6: Ser-727 phosphorylation of STAT1 is delayed when stimulated with the TLR9 ligand, CpG DNA.

RAW264.7 murine macrophages were prepared as described in figure 3.1. Cells were stimulated with 500 nM of mCpG DNA over a time course of 120 minutes. Samples were then separated by gel electrophoresis and immunoblotted with α-pSTAT1 (Ser-727) antibody, α-pSTAT1 (Tyr-701) and α-STAT1 antibody. **(A)** Western blot demonstrates rapid Ser-727 phosphorylation of STAT1. **(B)** Densitometry analysis illustrates the rapid Ser-727 phosphorylation of STAT1. These results are a representation of three individual experiments (n=3).

Together these results indicate that STAT1 Ser-727 phosphorylation occurs following TLR stimulation. Interestingly, all the TLRs examined are able to induce Ser-727 phosphorylation of STAT1, though the delayed serine phosphorylation of STAT1 in TLR3, TLR7 and TLR9 ligand treated cells may be a result of cellular localisation. Though rapid Ser-727 phosphorylation of STAT1 was observed in response to all TLR ligands the corresponding Tyr-701 phosphorylation observed following IFN- α stimulation was only observed at later time points in poly (I:C) and LPS stimulated cells. This indicates that the phosphorylation of these two residues can occur independently and are not dependent on each other, suggesting that the serine phosphorylation may be regulated directly by TLR signalling.

3.2.2 - Serine phosphorylation of STAT1 is dependent on MyD88/TRIF but not IRF3/7

As STAT1 undergoes serine phosphorylation following TLR ligand stimulation, I next wanted to determine whether the serine phosphorylation of STAT1 was a direct effect of TLR signal transduction or autocrine activation due to secretion of type I IFNs.

Consistent with my earlier results in RAW264.7 murine macrophages STAT1 undergoes Ser-727 phosphorylation in response to TLR ligand stimulation in immortalised WT BMMs (Figure 3.7A, panel 1). Densitometry analysis demonstrates that all TLR ligands induce significant activation of pSer-727 STAT1 (Figure 3.7B).

To examine the requirement of TLR canonical signalling or autocrine induction of IRF-mediated type I IFN secretion on TLR-induced STAT1 Ser-727 phosphorylation, I next investigated the ability of TLR stimulation to induce phosphorylation in immortalised gene deficient BMMs. To determine that TLR signalling is crucial for STAT1's serine phosphorylation, MyD88^{-/-}/TRIF^{-/-} immortalised macrophages were used to address this question. Having previously established that all TLR ligand stimulation induces STAT1 Ser-727 phosphorylation at 60 minutes, I next stimulated MyD88^{-/-}/TRIF^{-/-} immortalised macrophages with all TLR ligands as indicated for 60 minutes. Cells were harvested and immunoblotted for pSer-727 STAT1 and total STAT1. Ser-727 STAT1 was not detected in MyD88/TRIF double knockout macrophages, although only IFN- α was able to induce serine phosphorylation of STAT1 consistent with it not requiring MyD88 or TRIF to signal (Figure 3.8, panel 1). This result demonstrates that STAT1 serine phosphorylation is dependent upon TLR signal transduction.

To determine if TLR-induced IFN activation of JAK-STAT signalling is involved in TLR-induced STAT1 serine phosphorylation, IRF3/7^{-/-} immortalised macrophages were stimulated with TLR ligands for 60 minutes and analysed for Ser-727 phosphorylated STAT1. TLR signalling is able to induce secretion of

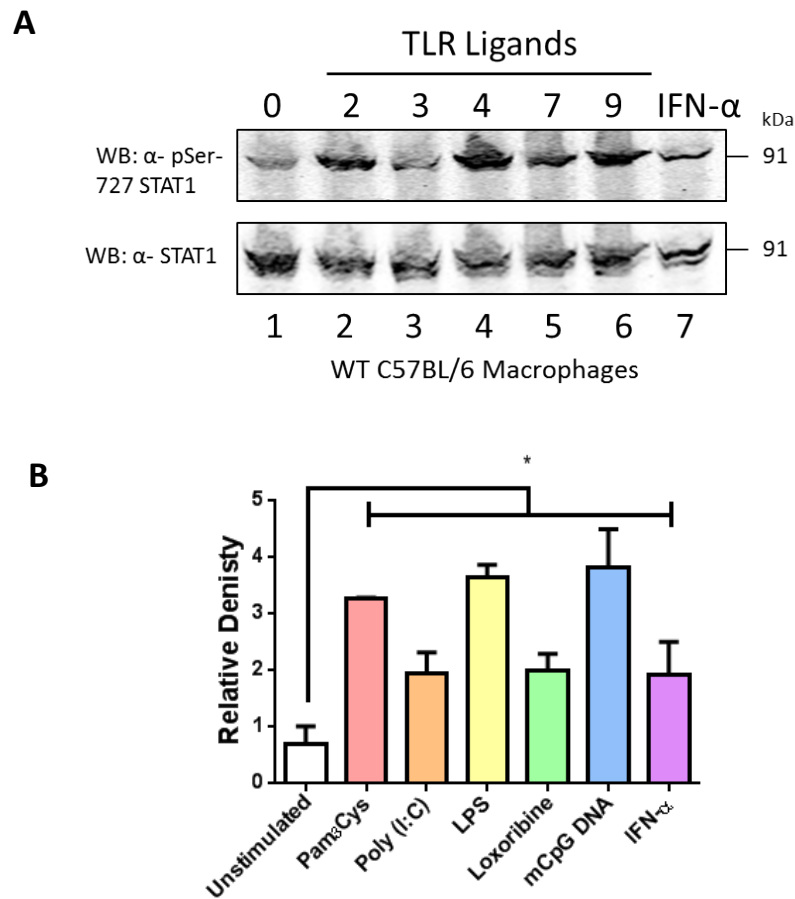


Figure 3.7: WT C57BL/6 immortalised macrophages stimulated with TLR agonists demonstrate Ser-727 phosphorylation of STAT1.

WT C57/BL6 immortalised macrophages were prepared as described in figure 3.1. Cells were stimulated with Pam₃Cys (100 ng/ml), poly (I:C) (10 μ g/ml), LPS (100 ng/ml), loxoribine (500 μ M), mCpG DNA (500 nM) and IFN- α (1000 I/U) for 60 minutes. Samples were then separated by gel electrophoresis and immunoblotted with α -pSTAT1 (Ser-727) antibody and α -STAT1 antibody. **(A)** Western blot demonstrates Ser-727 phosphorylation of STAT1. **(B)** Densitometry analysis illustrates relative density of bands compared to unstimulated sample. These results are a representation of three individual experiments (n=3).

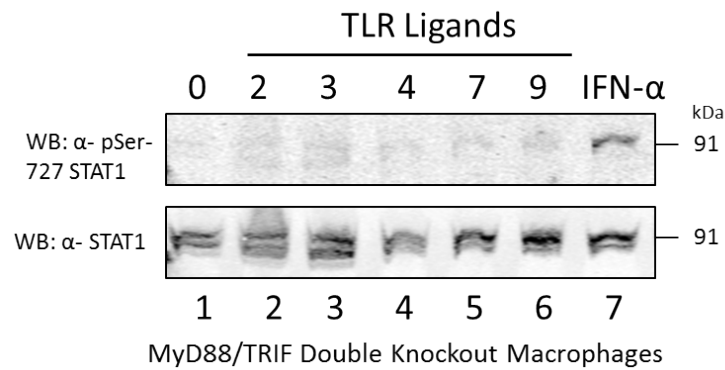


Figure 3.8: MyD88^{-/-}/TRIF^{-/-} immortalised macrophages fail to induce Ser-727 phosphorylation of STAT1 when stimulated with TLR agonists.

MyD88^{-/-}/TRIF^{-/-} immortalised macrophages were prepared as described in figure 3.1. Cells were stimulated with Pam₃Cys (100 ng/ml), poly (I:C) (10 μ g/ml), LPS (100 ng/ml), loxoribine (500 μ M), mCpG DNA (500 nM) and IFN- α (1000 I/U) for 60 minutes. Samples were then separated by gel electrophoresis and immunoblotted with α -pSTAT1 (Ser-727) antibody and α -STAT1 antibody. Western blot demonstrates lack of Ser-727 phosphorylation of STAT1. These results are a representation of three individual experiments (n=3).

type I IFNs through the MyD88-independent pathway by activation of IRF3 or IRF7 in specific cells. Thus cells lacking IRF3 and IRF7 are unable to induce type I IFN secretion, impairing their ability to activate JAK-STAT signalling. As can be observed in figure 3.9A, macrophages lacking IRF3 and IRF7 still display serine phosphorylation of STAT1 in response to TLR stimulation, demonstrating that IRF3 or IRF7 is not required for TLR-induced STAT1 phosphorylation. Densitometry analysis further confirms this observation that TLRs induce a significant increase in Ser-727 STAT1 activation. Pam₃Cys, LPS and loxoribine induced a ~4-fold activation of STAT1 compared to unstimulated cells (Figure 3.9B). CpG DNA induced a significant 4.454 ± 0.51 -fold activation of STAT1. Both poly (I:C) and IFN- α were also able to induce a 2.146 ± 0.38 -fold and 5.261 ± 2.36 -fold activation of STAT1, respectively (Figure 3.9B). The rapid serine phosphorylation of STAT1 is therefore dependent upon MyD88/TRIF-mediated TLR signalling and is not a secondary effect of IRF3/IRF7-induced type I IFN production.

3.2.3 – Serine phosphorylation of STAT3 following TLR stimulation

Having determined that STAT1 undergoes serine phosphorylation following TLR ligand stimulation, I next wished to determine if TLR's may induce a similar specificity of serine phosphorylation in STAT3.

RAW264.7 murine macrophages were first stimulated with IFN- α , as IFN- α induces both tyrosine and serine phosphorylation of STAT3 (Yang et al., 1996). Consistent with previous studies, STAT3 was observed to undergo both serine and tyrosine phosphorylation in a time-dependent manner, occurring rapidly and robustly (Figure 3.10A, panel 1 and panel 2). Densitometry analysis confirmed my initial observations where IFN- α induced 1.262 ± 0.295 -fold rapid serine phosphorylation of STAT3. The serine phosphorylation gradually increased from 20 minutes (1.142 ± 0.07) peaking at 120 minutes (2.492 ± 0.89) (Figure 3.10B).

Following stimulation with the TLR2 ligand Pam₃Cys, cells were assayed by immunoblot for Ser-727 phosphorylation of STAT3. STAT3 demonstrates rapid serine phosphorylation, initially observed at 10 minutes post-stimulation and was sustained until 120 minutes post-challenge (Figure 3.11A, panel 1). A corresponding tyrosine phosphorylation was not observed, in concordance with my STAT1 serine immunoblots (Figure 3.11A, panel 2). Further analysis via densitometry demonstrates the rapid time-dependent Ser-727 phosphorylation of STAT3 by TLR2 challenge. This can be detected at 10 minutes (1.484 ± 0.56) and reaches maximal effect at 60 minutes (2.161 ± 0.45); by 120 minutes the serine phosphorylation begins to diminish commensurate with that observed for non-stimulated cells (Figure 3.11B).

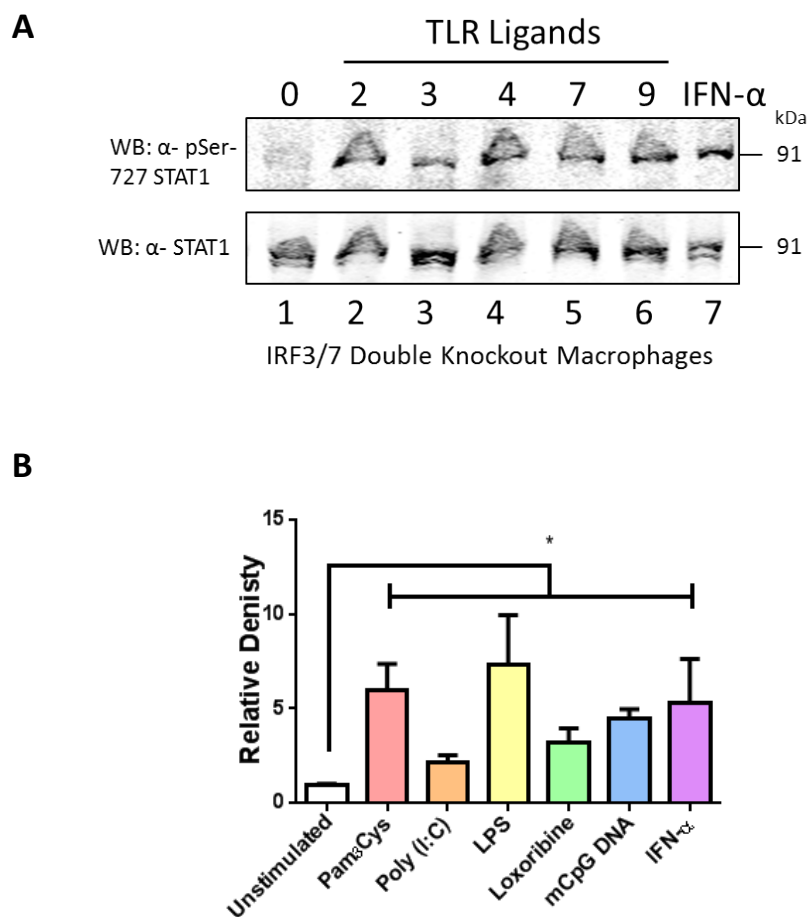


Figure 3.9: Ser-727 phosphorylation of STAT1 is independent of JAK-STAT signalling as IRF3/7^{-/-} immortalised macrophages still induce Ser-727 phosphorylation of STAT1 following TLR agonists stimulation.

IRF3/7^{-/-} immortalised macrophages were prepared as described in figure 3.1. Cells were stimulated with Pam₃Cys (100 ng/ml), poly (I:C) (10 μ g/ml), LPS (100 ng/ml), loxoribine (500 μ M), mCpG DNA (500 nM) and IFN- α (1000 I/U) for 60 minutes. Samples were then separated by gel electrophoresis and immunoblotted with α -pSTAT1 (Ser-727) antibody and α -STAT1 antibody. **(A)** Western blot demonstrates Ser-727 phosphorylation of STAT1. **(B)** Densitometry analysis illustrates relative density of bands compared to unstimulated sample. These results are a representation of three individual experiments (n=3).

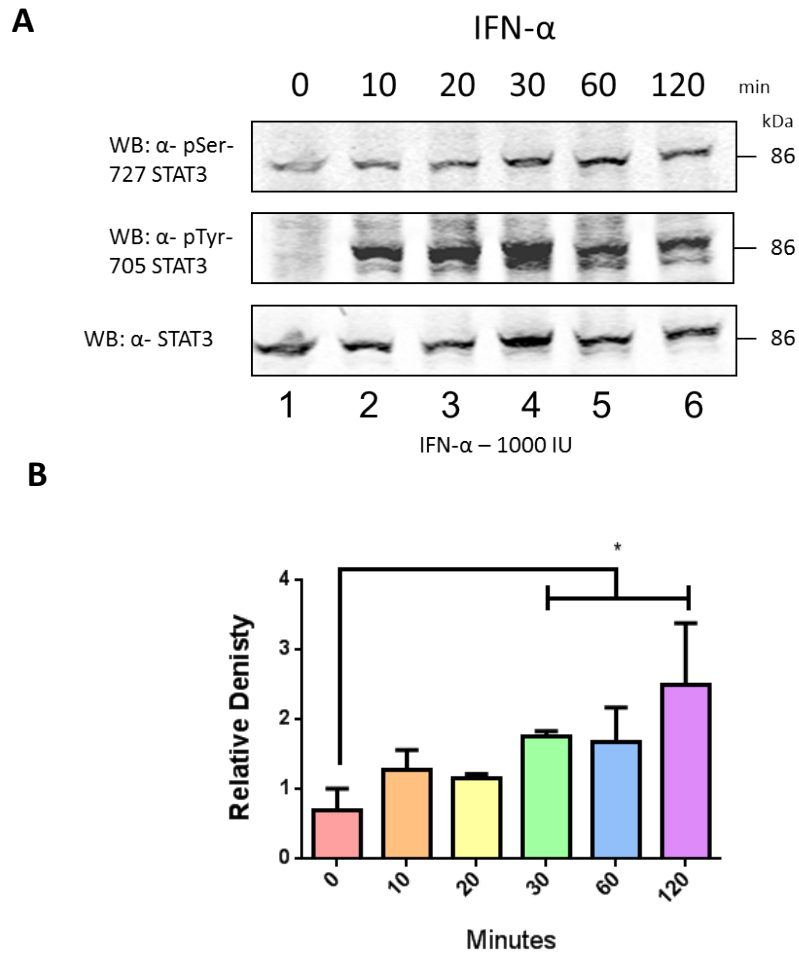


Figure 3.10: IFN- α induces rapid Tyr-705 and Ser-727 phosphorylation of STAT3.

RAW264.7 murine macrophages were prepared as described in figure 3.1. Cells were stimulated with 1000 IU of IFN- α over a time course of 120 minutes. Samples were then separated by gel electrophoresis and immunoblotted with α -pSTAT3 (Ser-727) antibody, α -pSTAT3 (Tyr-705) and α -STAT3 antibody. **(A)** Western blot demonstrates Tyr-705 and Ser-727 phosphorylation of STAT3. **(B)** Densitometry analysis illustrates the rapid Ser-727 phosphorylation of STAT3. These results are a representation of three individual experiments (n=3).

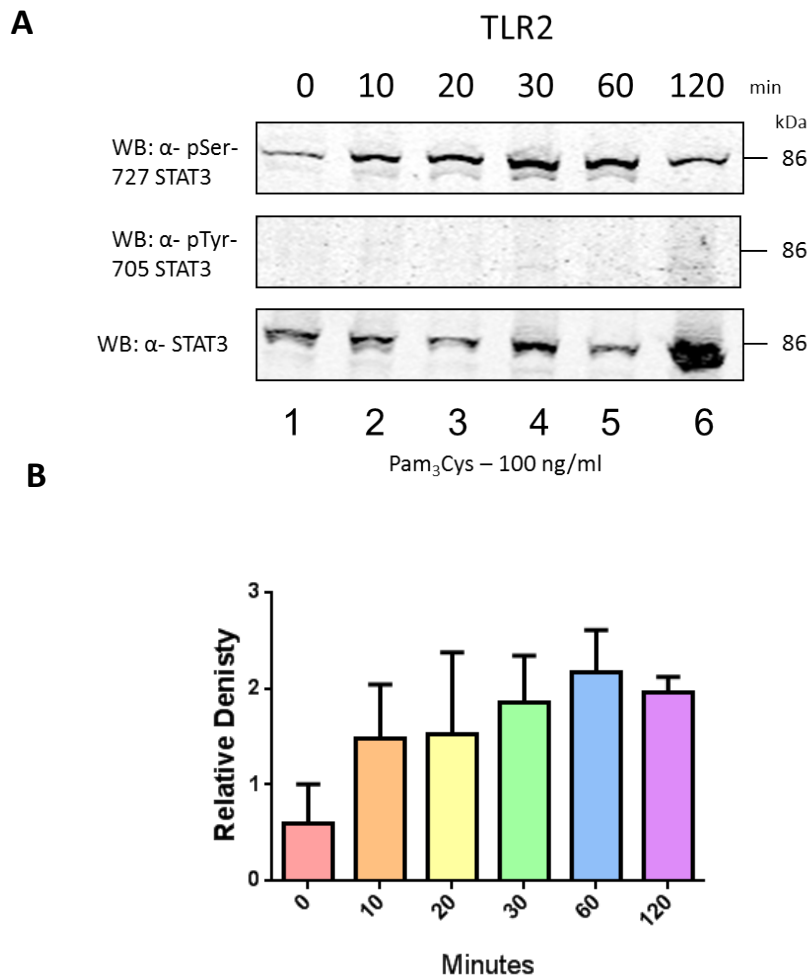


Figure 3.11: Rapid induction of pSer-727 STAT3 following stimulation with Pam₃Cys.

RAW264.7 murine macrophages were prepared as described in figure 3.1. Cells were stimulated with 100 ng/ml of Pam₃Cys over a time course of 120 minutes. Samples were then separated by gel electrophoresis and immunoblotted with α -pSTAT3 (Ser-727) antibody, α -pSTAT3 (Tyr-705) and α -STAT3 antibody. **(A)** Western blot demonstrates rapid Ser-727 phosphorylation of STAT3. **(B)** Densitometry analysis illustrates the rapid Ser-727 phosphorylation of STAT3. These results are a representation of three individual experiments (n=3).

RAW 264.7 murine macrophages were next stimulated with the TLR3 ligand poly (I:C). Comparable to my observations with pSer-727 STAT1 immunoblots, poly (I:C) induces rapid Ser-727 phosphorylation of STAT3 within 10 minutes and this is sustained up to 120 minutes post-challenge (Figure 3.12A, panel 1). Importantly, Tyr-705 phosphorylation of STAT3 was not seen until 120 minutes post-stimulation, possibly as a result of IFN- β signalling (Figure 3.12A, panel 2). Densitometry conducted on multiple pSer-727 STAT3 experiments displays the rapid Ser-727 phosphorylation of STAT3 which can be observed at 10 minutes (4.4 ± 1.14), persisting till 30 minutes and beginning to decrease from 60 minutes onwards (Figure 3.12B).

Like Pam₃Cys, the TLR4 ligand LPS also induces rapid Ser-727 phosphorylation of STAT3. This was observed at 10 minutes and serine phosphorylation was maintained for 120 minutes (Figure 3.13A panel 1). Importantly, LPS did not induce Tyr-705 phosphorylation of STAT3 from 10 minutes to 60 minutes (Figure 3.13A, panel 2). Tyrosine phosphorylation of STAT3 however, was detected at 120 minutes post-stimulation and may be a possible result of IFN- β production through activation of IRF3 (Schafer et al., 1998). I next performed densitometry analysis on the serine phosphorylation immunoblots. pSer-727 STAT3 was detected in unstimulated cells and following LPS stimulation this was sustained and elevated significantly at 30 minutes (1.172 ± 0.027), with levels of pSer-727 STAT3 declining at 120 minutes (0.697 ± 0.38) (Figure 3.13B).

Next, the TLR7 ligand, loxoribine was employed to stimulate cells. Ser-727 phosphorylation of STAT3 was initially detected at 10 minutes, gradually increasing and peaking at 60 minutes where it was sustained for the full 120 minute time course (Figure 3.14A, panel 1). Tyr-705 phosphorylation of STAT3 on the other hand, was not detected at any of the time points assessed (Figure 3.14A, panel 2). Densitometry conducted on the pSer-727 STAT3 blots illustrates the delayed kinetics of Ser-727 STAT3 phosphorylation. Ser-727 phosphorylated STAT3 was weakly activated at 10 minutes (1.356 ± 0.098), and this was demonstrated to steadily increase, peaking at 60 minutes (2.641 ± 0.77) and beginning to decrease at 120 minutes (2.846 ± 0.21) (Figure 3.14B).

The TLR9 ligand CpG DNA was also able to induce Ser-727 phosphorylation of STAT3 and matches the serine phosphorylation blots of STAT1. pSer-727 STAT3 can be found at the 10 minute time point, and persisted for up to 120 minutes (Figure 3.15A, panel 1). Similar to figure 3.14, an equivalent Tyr-705 phosphorylation of STAT3 was not observed over the time course following CpG DNA stimulation, commensurate with previous data (Figure 3.15A, panel 2). Further examination of serine phosphorylation blots by densitometry displayed pSer-727 STAT3 in unstimulated cells. Following CpG DNA treatment pSer-727 STAT3 gradually increased, reaching a maximum at 20 minutes (1.191 ± 0.16) and steadily decreasing from 60 minutes onwards (Figure 3.15B).

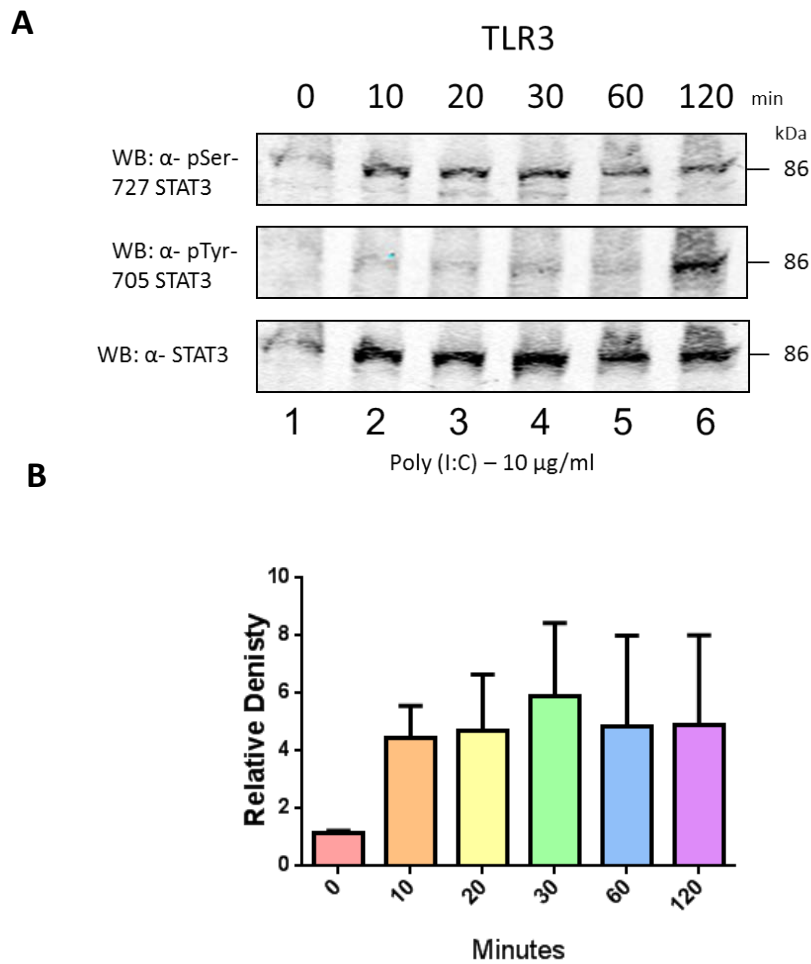


Figure 3.12: Poly (I:C) induces Ser-727 phosphorylation of STAT3 with pTyr-705 STAT3 being detected at 120 minutes post-stimulation.

RAW264.7 murine macrophages were prepared as described in figure 3.1. Cells were stimulated with 10 μ g/ml of poly (I:C) over a time course of 120 minutes. Samples were then separated by gel electrophoresis and immunoblotted with α -pSTAT3 (Ser-727) antibody, α -pSTAT3 (Tyr-705) and α -STAT3 antibody. **(A)** Western blot demonstrates rapid Ser-727 phosphorylation of STAT3. **(B)** Densitometry analysis illustrates the rapid Ser-727 phosphorylation of STAT3. These results are a representation of three individual experiments (n=3).

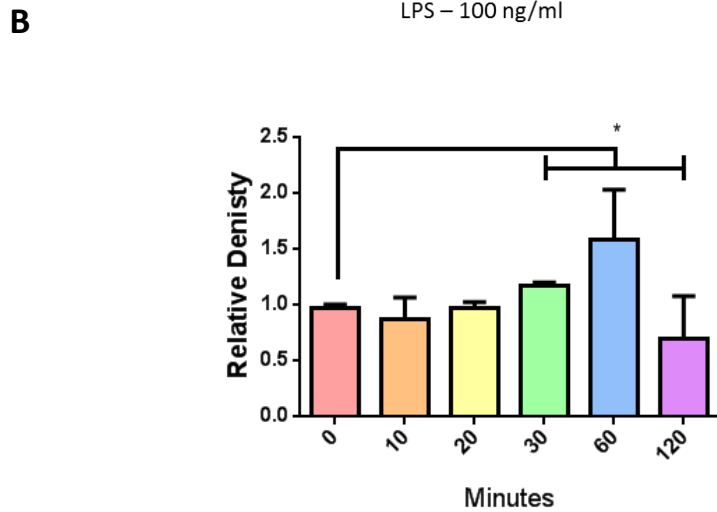
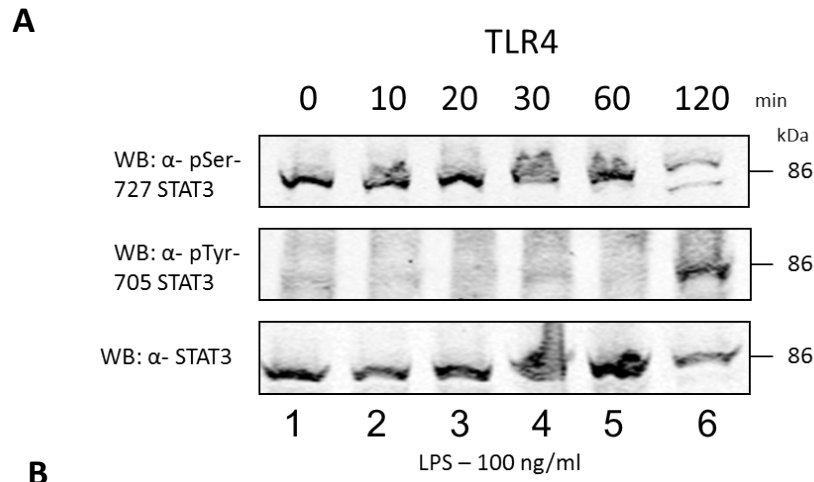


Figure 3.13: LPS induces rapid Ser-727 phosphorylation of STAT3 with a corresponding tyrosine phosphorylation observed at 120 minutes post-stimulation.

RAW264.7 murine macrophages were prepared as described in figure 3.1. Cells were stimulated with 100 ng/ml of LPS over a time course of 120 minutes. Samples were then separated by gel electrophoresis and immunoblotted with α -pSTAT3 (Ser-727) antibody, α -pSTAT3 (Tyr-705) and α -STAT3 antibody. **(A)** Western blot demonstrates rapid Ser-727 phosphorylation of STAT3. **(B)** Densitometry analysis illustrates the rapid Ser-727 phosphorylation of STAT3. These results are a representation of three individual experiments (n=3).

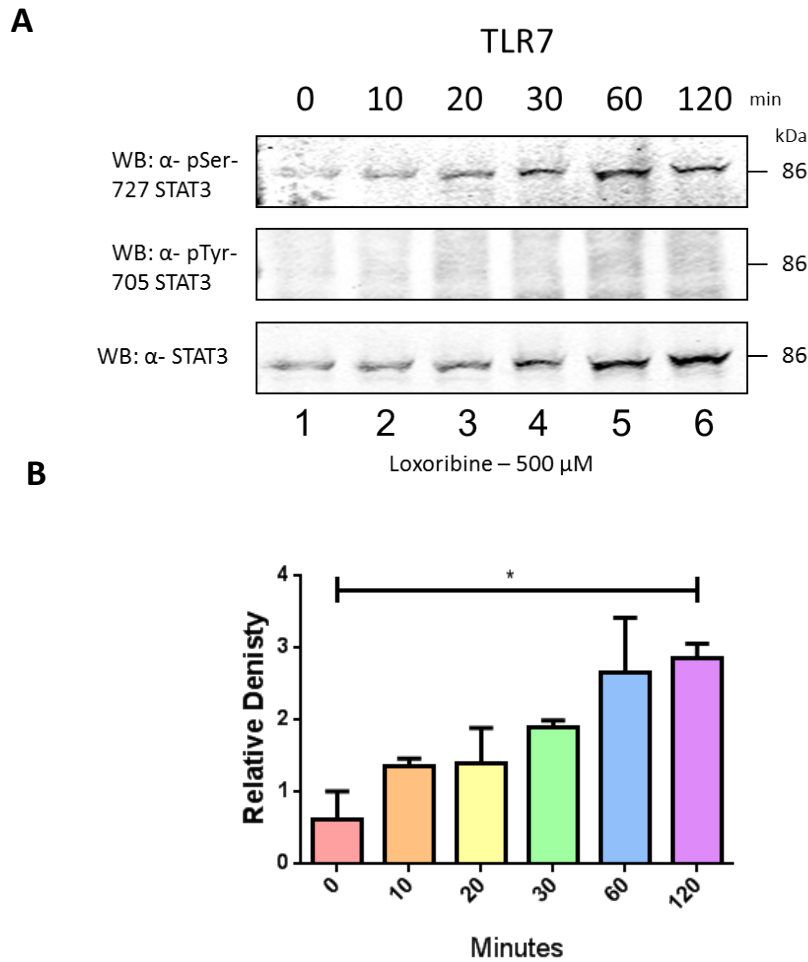


Figure 3.14: Stimulation with loxoribine induces rapid phosphorylation of STAT3 at Ser-727.

RAW264.7 murine macrophages were prepared as described in figure 3.1. Cells were stimulated with 500 μ M of loxoribine over a time course of 120 minutes. Samples were then separated by gel electrophoresis and immunoblotted with α -pSTAT3 (Ser-727) antibody, α -pSTAT3 (Tyr-705) and α -STAT3 antibody. **(A)** Western blot demonstrates rapid Ser-727 phosphorylation of STAT3. **(B)** Densitometry analysis illustrates the rapid Ser-727 phosphorylation of STAT3. These results are a representation of three individual experiments (n=3).

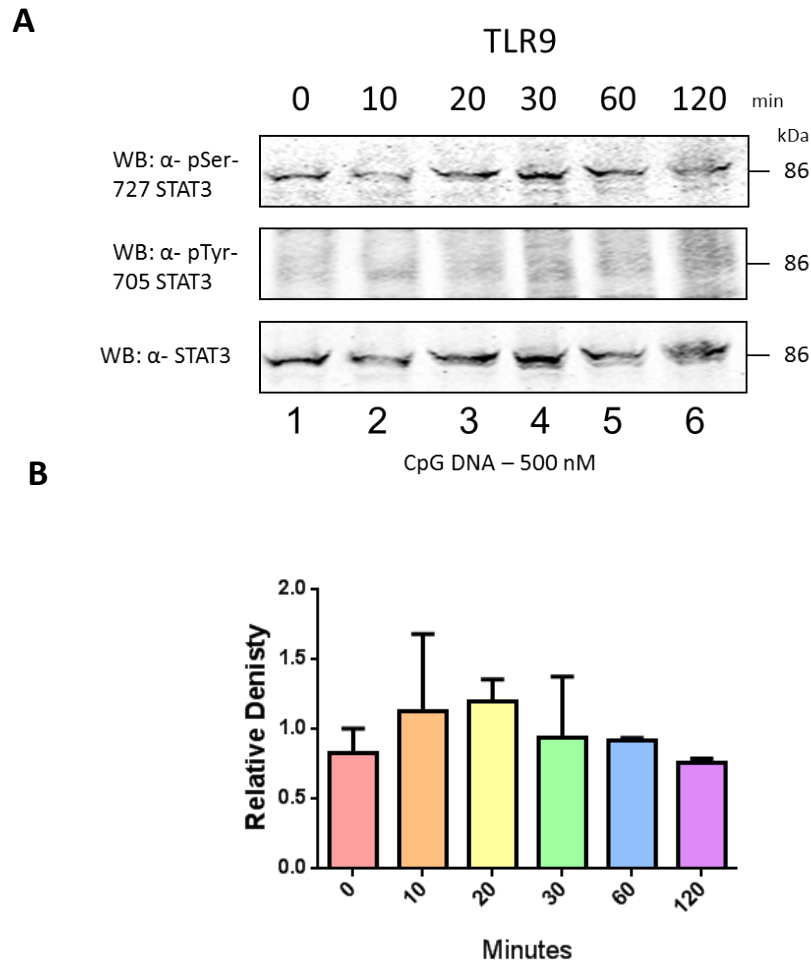


Figure 3.15: CpG DNA induces rapid Ser-727 phosphorylation of STAT3 with no corresponding Tyr-705 phosphorylation.

RAW264.7 murine macrophages were prepared as described in figure 3.1. Cells were stimulated with 500 nM of mCpG DNA over a time course of 120 minutes. Samples were then separated by gel electrophoresis and immunoblotted with α -pSTAT3 (Ser-727) antibody, α -pSTAT3 (Tyr-705) and α -STAT3 antibody. **(A)** Western blot demonstrates rapid Ser-727 phosphorylation of STAT3. **(B)** Densitometry analysis illustrates the rapid Ser-727 phosphorylation of STAT3. These results are a representation of three individual experiments (n=3).

Taken together, my novel results demonstrate that whilst STAT1 has been implicated to undergo serine phosphorylation after TLR stimulation (Rhee et al., 2003, Schroder et al., 2007); to my knowledge this is the first report identifying rapid Ser-727 phosphorylation of STAT3, with no corresponding Tyr-705 phosphorylation following TLR stimulation. These results indicate that the serine phosphorylation of STAT3 appears to be a general effect that occurs across multiple TLRs.

3.2.4 – Serine phosphorylation of STAT3 is dependent on MyD88/TRIF and not IRF3/7

Having established that STAT3 is serine phosphorylated following TLR stimulation, my next aim was to determine whether this event occurred directly downstream of TLRs or occurred indirectly as a consequence of autocrine IFN- β signalling.

Immortalised WT macrophages were first used to confirm that this serine phosphorylation was not limited to RAW264.7 murine macrophages. Cells were stimulated with a variety of TLR ligands and IFN- α and as shown in figure 3.16A, STAT3 undergoes Ser-727 phosphorylation in a time-dependent manner consistent with my earlier findings. Densitometry analysis of the serine phosphorylation blot demonstrates that most TLRs induce Ser-727 phosphorylation of STAT3 to varying degrees, with LPS inducing a 1.462 ± 0.62 -fold and IFN- α inducing a 1.77 ± 0.35 -fold increase of pSer-727 STAT3 compared to unstimulated cells (Figure 3.16B).

Macrophages lacking MyD88 and TRIF were next treated with TLR ligands and IFN- α to identify whether canonical TLR signalling was required for serine phosphorylation of STAT3. The absence of both MyD88 and TRIF completely abolished TLR-induced Ser-727 phosphorylation of STAT3 (Figure 3.17), demonstrating that the MyD88-dependent or MyD88-independent signalling is required to facilitate Ser-727 phosphorylation of STAT3.

In order to establish IFNs role in STAT3 serine phosphorylation, IRF3/7^{-/-} immortalised macrophages were employed to abolish the ability of TLR signalling in inducing IFN secretion through the IRFs. In contrast to MyD88^{-/-}/TRIF^{-/-} immortalised macrophages, IRF3/7 deficiency did not affect or diminish STAT3 serine phosphorylation (Figure 3.18A). Densitometric analysis of the pSer-727 STAT3 blots confirmed that all TLRs ligands caused an increase in induction of STAT3 serine phosphorylation. With Pam₃Cys inducing 2.227 ± 0.61 -fold activation of STAT3, the highest detected. Whereas poly (I:C) and loxoribine induced 1.745 ± 0.21 -fold and 1.686 ± 0.32 -fold STAT3 activation, respectively (Figure 3.18B). This result confirms that the rapid serine phosphorylation is a direct result of TLR signalling and doesn't require IRF3/IRF7-induced IFN secretion and activation of JAK-STAT signalling.

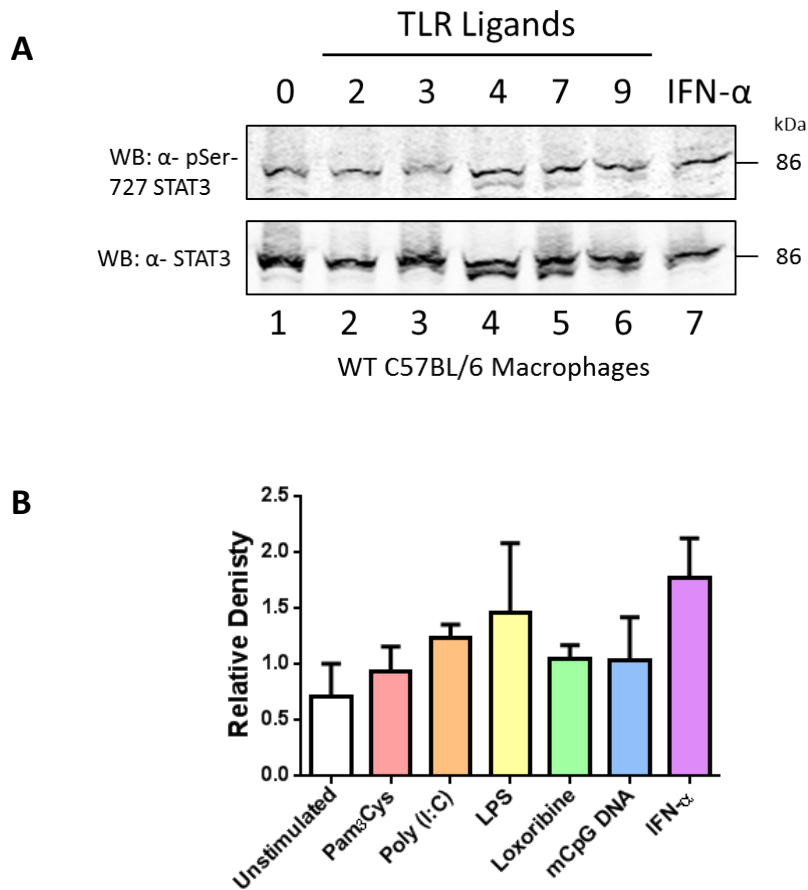


Figure 3.16: Stimulation with TLR agonists induces Ser-727 phosphorylation of STAT3 in wild-type C57BL/6 immortalised macrophages.

WT C57BL/6 immortalised macrophages were prepared as described in figure 3.1. Cells were stimulated with Pam₃Cys (100 ng/ml), poly (I:C) (10 μ g/ml), LPS (100 ng/ml), loxoribine (500 μ M), mCpG DNA (500 nM) and IFN- α (1000 I/U) for 60 minutes. Samples were then separated by gel electrophoresis and immunoblotted with α -pSTAT3 (Ser-727) antibody and α -STAT3 antibody. **(A)** Western blot demonstrates Ser-727 phosphorylation of STAT3. **(B)** Densitometry analysis illustrates relative density of bands compared to unstimulated sample. These results are a representation of three individual experiments (n=3).

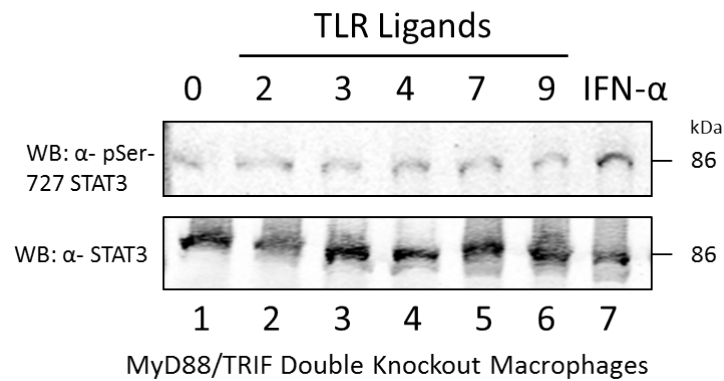


Figure 3.17: In $MyD88^{-/-}TRIF^{-/-}$ immortalised macrophages stimulation with TLR agonists fails to induce Ser-727 phosphorylation of STAT3.

$MyD88^{-/-}TRIF^{-/-}$ immortalised macrophages were prepared as described in figure 3.1. Cells were stimulated with Pam₃Cys (100 ng/ml), poly (I:C) (10 μ g/ml), LPS (100 ng/ml), loxoribine (500 μ M), mCpG DNA (500 nM) and IFN- α (1000 I/U) for 60 minutes. Samples were then separated by gel electrophoresis and immunoblotted with α -pSTAT3 (Ser-727) antibody and α -STAT3 antibody. Western blot demonstrates lack of Ser-727 phosphorylation of STAT3. These results are a representation of three individual experiments (n=3).

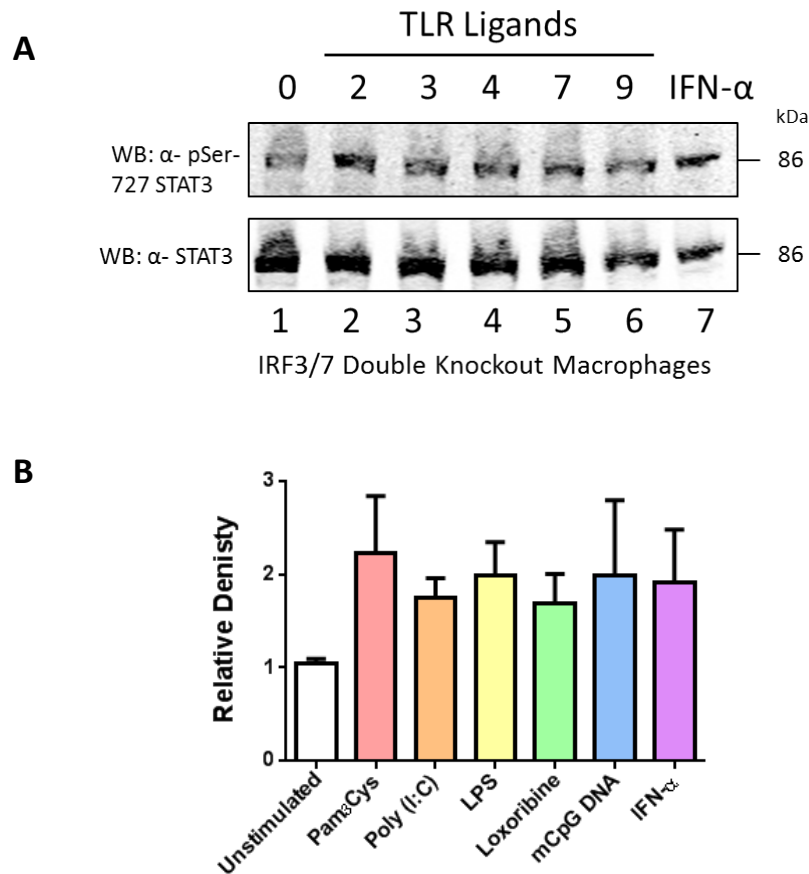


Figure 3.18: Ser-727 phosphorylation of STAT3 is not abolished in IRF3/7^{-/-} immortalised macrophages following stimulation with TLR agonists.

IRF3/7^{-/-} immortalised macrophages were prepared as described in figure 3.1. Cells were stimulated with Pam₃Cys (100 ng/ml), poly (I:C) (10 μ g/ml), LPS (100 ng/ml), loxoribine (500 μ M), mCpG DNA (500 nM) and IFN- α (1000 I/U) for 60 minutes. Samples were then separated by gel electrophoresis and immunoblotted with α -pSTAT3 (Ser-727) antibody and α -STAT3 antibody. **(A)** Western blot demonstrates Ser-727 phosphorylation of STAT3. **(B)** Densitometry analysis illustrates relative density of bands compared to unstimulated sample. These results are a representation of three individual experiments (n=3).

However, this doesn't discount IL-6 and IL-10 signalling which can also activate STAT3 (Zhong et al., 1994, Finbloom and Winestock, 1995).

3.2.5 – TRAF6 binding motifs in STAT1 and STAT3

Proteins that interact with TRAF6 all contain a T6BM that is comprised of a P-X-E-X-X-(Ar/Ac) motif. Bioinformatic analysis of the STAT1 and STAT3 sequences identified that both STAT1 and STAT3 contain three putative TRAF6 binding motifs each (Table 3.2). The motifs are homologous to the T6BM described in other TLR signalling proteins such as Mal, TRIF and TRAM, containing the critical proline, glutamic acid and aromatic/acid residues.

3.2.6 – Production of recombinant GST-TRAF6 fusion protein

I have previously established by co-ectopic immunoprecipitation studies that STAT1 could interact with TRAF6 (Luu, 2008). However, as overexpression studies occasionally demonstrate artefactual associations, I wished to further examine this interaction with a more specific protein interaction assay. GST-TRAF6 recombinant fusion protein bound to glutathione sepharose 4B beads was employed to assess the interaction between STAT1/TRAF6 and STAT3/TRAF6 respectively.

Expression of GST-TRAF6 fusion protein was performed by inducing an overnight starter culture of pGEX-6T-3-GST-TRAF6 with 50 μ M of IPTG overnight at 18°C. The cells were pelleted and harvested in both a low and high salt buffer. The fractions were combined and soluble GST-TRAF6 was purified using glutathione sepharose 4B beads in a 50% slurry in PBS. The purified GST-TRAF6 fusion protein bound to glutathione sepharose 4B beads were then assessed for purity by resolving on a 15% SDS-PAGE gel, following by Coomassie blue stain.

As can be seen in figure 3.19, a band can be observed at ~84 kDa (Figure 3.19, Lane 3) which is the theoretical size of GST-TRAF6 (GST ~25 kDa and TRAF6 ~59 kDa). Lane 2 represents the unpurified fraction and indicates the efficient one step purification of the GST-TRAF6 fusion protein bound to Glutathione Sepharose 4B beads.

3.2.7 – STAT1 and STAT3 interact with recombinant GST-TRAF6 fusion protein

As the serine phosphorylation of STAT1 and STAT3 is mediated by TLR signalling and both STATs contain putative T6BMs, I wanted to assess whether TRAF6 may interact with both STAT1 and STAT3 and recruit them into the TLR pathway. Cellular lysates of HEK293T cells ectopically expressing Myc-tagged STAT1 were probed with GST-TRAF6 fusion protein. As can be observed in figure 3.20, GST-TRAF6 was able to specifically immunoprecipitate STAT1 from cellular lysates as detect by α -Myc

Table 3.2: Putative TRAF6 binding motifs in STAT1 and STAT3

Critical glutamic acid residues are shown in red. Ar/Ac – Aromatic/Acidic Group.

TRAF6 Binding Motif	P	x	E	x	x	Ar/Ac
STAT1 (1) (27-32)	P	M	E	I	R	Q
STAT1 (2) (684-689)	P	K	E	A	P	E
STAT1 (3) (728-733)	P	E	E	F	D	E
STAT3 (1) (27-32)	P	E	E	F	D	E
STAT3 (2) (97-102)	P	M	E	I	A	R
STAT3 (3) (677-682)	P	K	E	E	A	F

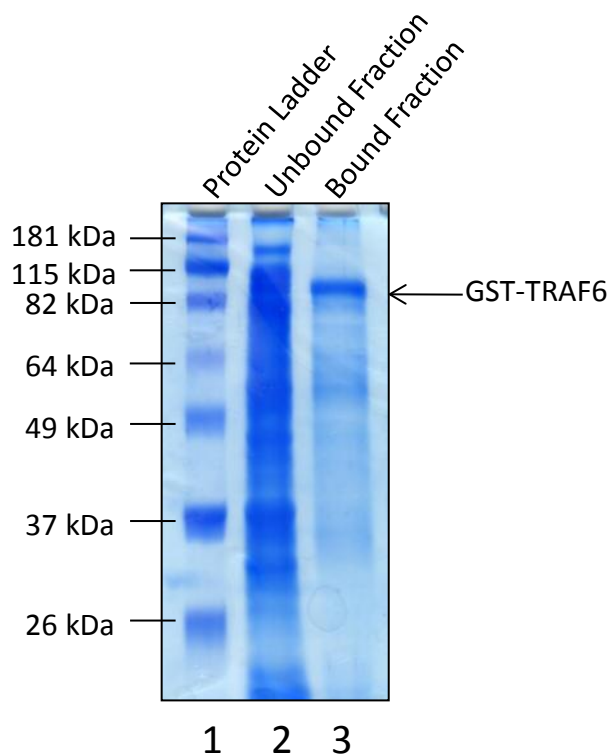


Figure 3.19: Coomassie stain of recombinant GST-TRAF6 fusion protein.

Laemmli reducing sample buffer was added to samples of GST-TRAF6 fusion protein bound to glutathione sepharose 4B beads and the unbound fraction then boiled at 95°C for 5 minutes. Samples were then separated by gel electrophoresis. Coomassie stain of a 12% SDS-PAGE gel showing the presence of recombinant GST-TRAF6 fusion protein. Expected size of GST-TRAF6 fusion protein is ~84 kDa. (TRAF6 molecular weight ~59 kDa : GST molecular weight ~25 kDa) Lane 1 contains protein ladder, lane 2 contains unbound fraction and lane 3 contains GST-TRAF6 fusion protein bound to glutathione sepharose 4B beads. These results are a representation of three individual experiments (n=3).

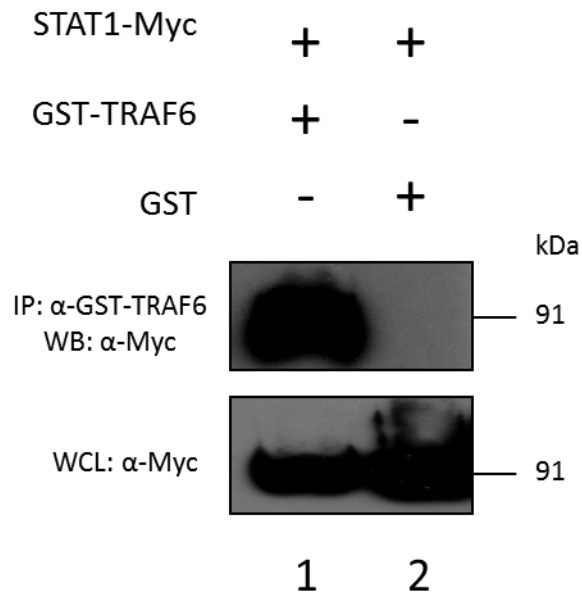


Figure 3.20: STAT1 interacts with recombinant TRAF6.

HEK293T cells were co-transfected with STAT1-Myc 24 hours prior to harvesting. Cells were harvested in Kal B solution (Appendix I), pre-cleared with glutathione sepharose 4B beads. Samples were probed with 20 μ l of GST-TRAF6 fusion protein or 10 μ l of GST to immunoprecipitate STAT1. Samples were then separated by gel electrophoresis and immunoblotted with α -Myc antibody. Lanes 1 demonstrates STAT1 interacting with recombinant GST-TRAF6 fusion protein. Lane 2 displays no non-specific interaction between STAT1-Myc and GST. These results are a representation of three individual experiments (n=3).

immunoblot (Figure 3.20, lane 1). Myc-tagged STAT1 was not detected in cellular lysates probed with GST, demonstrating exclusive interaction between STAT1 and TRAF6 (Figure 3.20, lane 2).

To assess STAT3's ability to directly interact with TRAF6, HEK293Ts were also transfected with Flag-tagged STAT3. Cellular lysates were then probed with GST-TRAF6 fusion protein and blotted with α -Flag antibody. GST-TRAF6 can be observed to specifically interact with STAT3 (Figure 3.21, lane 1), whilst no Flag-tagged STAT3 was able to be detected in cellular lysates probed with GST demonstrating the specificity of the interaction (Figure 3.21, lane 2).

Taken together, the results here illustrate that TRAF6 interacts with STAT1 and STAT3, which may facilitate their recruitment into TLR signalling pathway. The T6BMs in both STATs may facilitate this interaction between STAT1/TRAF6 and STAT3/TRAF6.

3.2.8 – Semi-endogenous immunoprecipitation of TRAF6 and STAT1

To further elucidate the specificity of the interaction between TRAF6 and STAT1, semi-endogenous immunoprecipitations were conducted on TLR-stimulated RAW264.7 cell lysates. Endogenous STAT1 was immunoprecipitated with recombinant GST-TRAF6 fusion protein following stimulation with LPS. A time-dependent increase in STAT1 TRAF6 association can be observed after LPS stimulation (Figure 3.22, panel 1). Interestingly, TRAF6 appears to recognise STAT1 prior to LPS stimulation. In its serine phosphorylated form, STAT1 was also precipitated by TRAF6 (Figure 3.22, panel 2, lane 1) and this interaction increased following LPS stimulation (Figure 3.22, panel 2, lane 2-4). This rise in pSer-727 STAT1 and TRAF6 association is likely a reflection of the increasing amount of pSer-727 STAT1 detected in cellular lysates (Figure 3.22, panel 3). STAT1 was not immunoprecipitated by GST alone probed cellular lysates (Figure 3.22, panel 1, lane 5) demonstrating that the interaction of TRAF6 and endogenous STAT1 is not a side effect of GST fused to TRAF6.

In order to assess TRAF6 and STAT1 interaction in humans, the human monocyte cell line, THP1 was used. Pam₃Cys was next used to stimulate THP1 cells thereby only activating MyD88-dependent signalling and eliminating activation of the MyD88-independent pathway and negating the possibility of IFN production. Pam₃Cys stimulation produced similar results to TLR4 stimulated cells. The interaction between the STAT1 and TRAF6 remains constant and differs to the enrichment observed in Figure 3.22, panel 1 (Figure 3.23, panel 1). Consistent with earlier results however, pSer-727 STAT1 can be observed interacting with TRAF6 pre-stimulation and this interaction is maintained post-stimulation (Figure 3.23, panel 2). Whilst levels of pSer-727 STAT1 increase in a time-dependent manner in cellular lysates post-stimulation (3.23, panel 3), this doesn't equate to an increasing

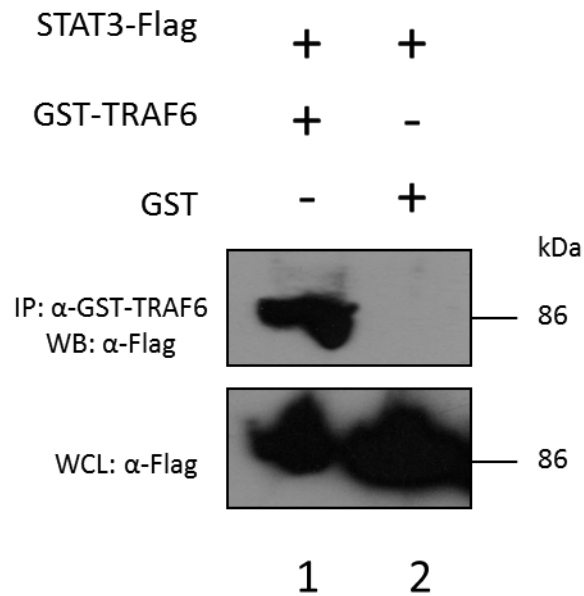


Figure 3.21: STAT3 interacts with recombinant TRAF6.

HEK293T cells were co-transfected with STAT3-Flag 24 hours prior to harvesting. Cells were harvested in Kal B solution (Appendix I), pre-cleared with glutathione sepharose 4B beads. Samples were probed with 20 μ l of GST-TRAF6 fusion protein or 10 μ l of GST to immunoprecipitate STAT3. Samples were then separated by gel electrophoresis and immunoblotted with α -Flag antibody. Lanes 1 demonstrates STAT3 interacting with recombinant GST-TRAF6 fusion protein. Lane 2 shows no non-specific interaction between STAT3-Flag and GST. These results are a representation of three individual experiments (n=3).

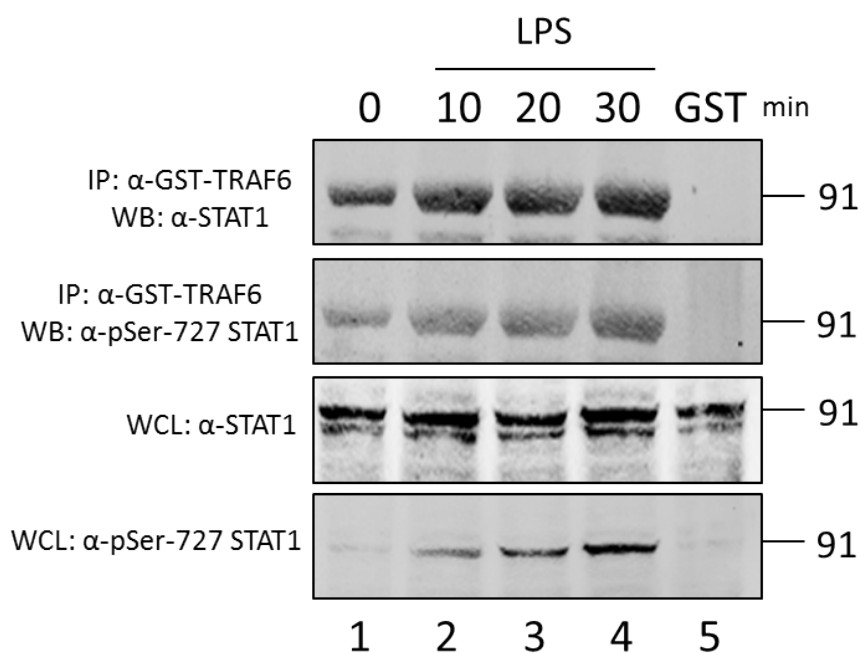


Figure 3.22: STAT1 interacts with TRAF6 at basal levels and following LPS stimulation.

RAW264.7 murine macrophages were seeded into a 10 cm dish at 2×10^6 cells per dish, 24 hours prior to stimulation. Cells were then treated with 100 ng/ml of LPS over a 30 minute time course. The cells were harvested in Kal B solution, pre-cleared with glutathione sepharose 4B beads and then probed with GST-TRAF6 beads. Samples were then separated by gel electrophoresis and immunoblotted with α -pSTAT1 (Ser-727) and α -STAT1 antibody. pSer-727 STAT1 and total STAT1 interact with GST-TRAF6 at basal levels and following stimulation. These results are a representation of three individual experiments (n=3).

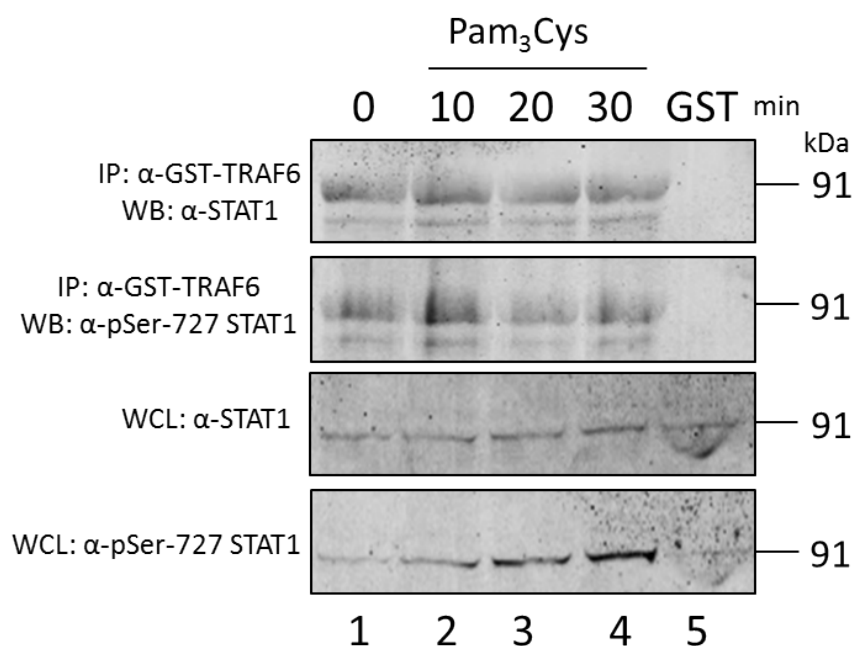


Figure 3.23: In THP1 cells, STAT1 interacts with TRAF6 in unstimulated and Pam₃Cys stimulated cells.

THP1 cells were seeded into a 10 cm dish at 5×10^6 cells per dish, 24 hours prior to stimulation. Cells were then treated with 100 ng/ml of Pam₃Cys over a 30 minute time course. The cells were harvested in Kal B solution, pre-cleared with glutathione sepharose 4B beads and then probed with GST-TRAF6 beads. Samples were then separated by gel electrophoresis and immunoblotted with α-pSTAT1 (Ser-727) and α-STAT1 antibody. pSer-727 STAT1 and total STAT1 interact with GST-TRAF6 at basal levels and following stimulation. These results are a representation of three individual experiments (n=3).

interaction between GST-TRAF6 and STAT1 (Figure 3.23, panel 2). Consistent with my earlier finding GST did not interact with STAT1 (Figure 3.23, panel 1, lane 5).

From this set of experiments, it is evident that endogenous STAT1 can interact with TRAF6, with a STAT1/TRAF6 complex detected in unstimulated cells and this interaction is sustained after TLR ligand stimulation. As the STAT1 β isoform (84 kDa) lacks the Ser-727 residue and only the 91 kDa STAT1 α isoform can be detected in the GST-TRAF6 probed lysates, it can be deduced that STAT1 α facilitates TLR and JAK-STAT cross-talk.

3.2.9 – STAT3 interaction with TRAF6 following TLR4 and TLR2 stimulation

To further confirm the specificity of the TRAF6 and STAT3 interaction, TLR-stimulated cellular lysates were probed with recombinant GST-TRAF6 fusion proteins. RAW264.7 murine macrophages were first stimulated with LPS and probed for pSer-727 STAT3. As can be seen in figure 3.24, RAW264.7 cells were stimulated with LPS over a 30 minute time course and then analysed for serine phosphorylated STAT3. STAT3 can be observed interacting with GST-TRAF6 at time 0 (Figure 3.24, panel 1, lane 1) and this interaction persisted following LPS stimulation at all time points examined (Figure 3.24, panel 1, lane 1-4). Similar to STAT1, pSer-727 STAT3 can be recognised by TRAF6 in unstimulated cells and following LPS stimulation (Figure 3.24, panel 2). STAT3 in the immunoprecipitate produced an unexplained double band in the GST only control (Figure 3.22, panel 1, lane 5). The double band is of a higher molecular weight, though its origins are unknown. Although GST probed cellular lysates did not recognise pSer-727 STAT3 this further confirms the specificity of TRAF6/STAT3 interaction (Figure 3.24, panel 2, lane 5).

To assess if TRAF6 also interacted with STAT3 in a human cell line, THP1s were used to address this. THP1 cells stimulated with Pam₃Cys displayed concurring results with RAW264.7 cells stimulated with LPS. GST-TRAF6 fusion protein was able to associate with STAT3 in unstimulated cells, though Pam₃Cys stimulation did not increase this interaction (Figure 3.25, panel 1). Akin to previous findings, pSer-727 STAT3 was observed to interact with TRAF6 at basal levels, with this interaction persisting up to 30 minutes post-stimulation (Figure 3.25, panel 2, lane 1-4). When probing for STAT3 in the immunoprecipitate, an unknown double band was also observed in the GST only control (Figure 3.25, panel 1, lane 5), suggesting some non-specific binding of the total STAT3 antibody. Serine phosphorylated STAT3 did not interact with the GST only control, further confirming the specificity of the STAT3/TRAF6 interaction (Figure 3.25, panel 2, lane 5).

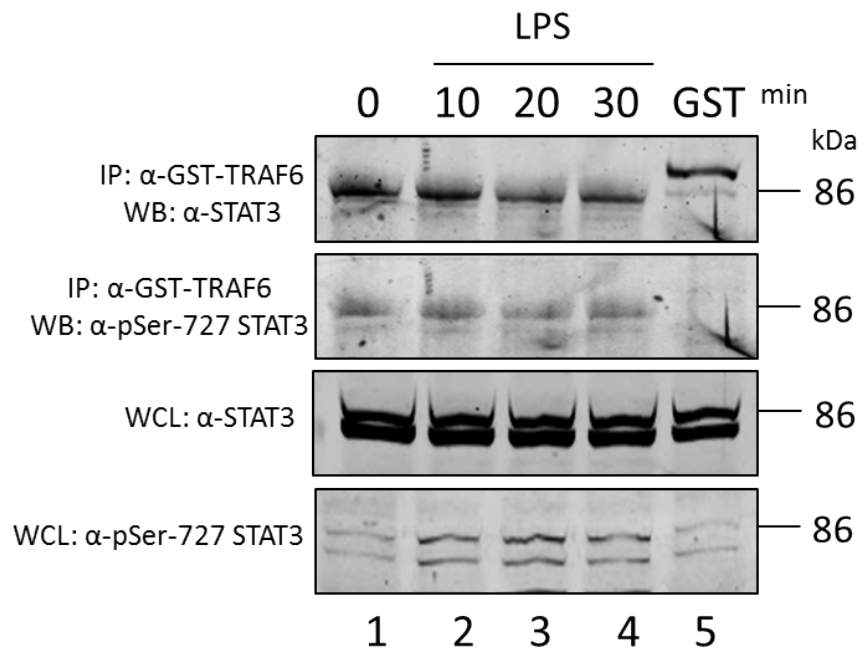


Figure 3.24: STAT3 interaction with TRAF6 occurs in resting cells and following LPS stimulation.

RAW264.7 murine macrophages were prepared as described in figure 3.22. Samples were separated by gel electrophoresis and immunoblotted with α -pSTAT3 (Ser-727) and α -STAT3 antibody. pSer-727 STAT3 and total STAT3 interact with GST-TRAF6 at basal levels and following stimulation. These results are a representation of three individual experiments (n=3).

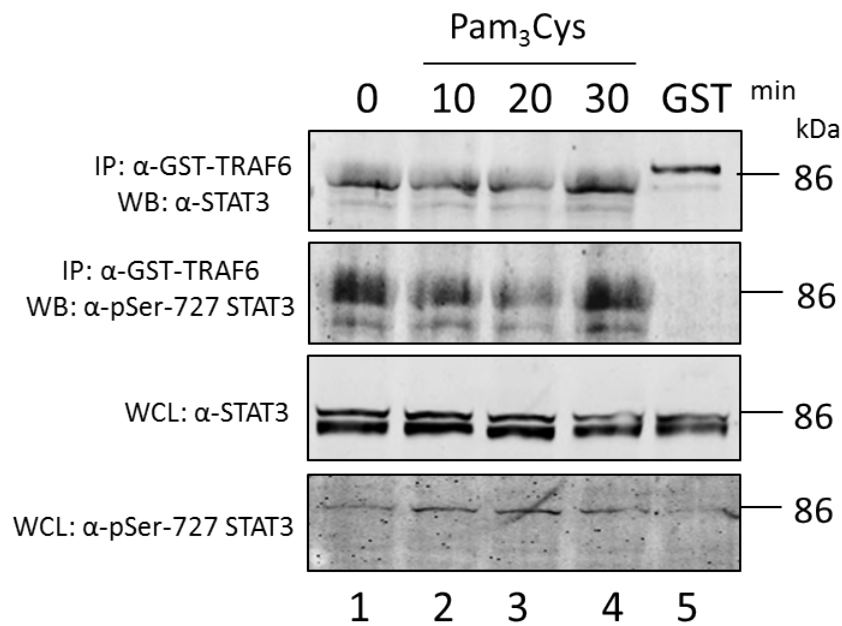


Figure 3.25: THP1 cells demonstrate interaction of STAT3 and TRAF6 in unstimulated and Pam₃Cys stimulated cells.

THP1 cells were prepared as described in figure 3.23. Samples were then separated by gel electrophoresis and immunoblotted with α-pSTAT3 (Ser-727) and α-STAT3 antibody. pSer-727 STAT3 and total STAT3 interact with GST-TRAF6 at basal levels and following stimulation. These results are a representation of three individual experiments (n=3).

Our results here further confirm the STAT3/TRAF6 interaction, demonstrating that endogenous STAT3 can interact with GST-TRAF6 fusion protein and that TRAF6 and STAT3 may potentially exist as a complex in cells.

3.2.10 – Identifying the kinase that phosphorylates STAT1 and STAT3

Though TRAF6 may facilitate the cross-talk of TLR and JAK-STAT signalling, a kinase is still required to facilitate serine phosphorylation of STAT1 and STAT3 as TRAF6 contains no intrinsic kinase activity. A number of kinases have been implicated in the serine phosphorylation of STAT1 and STAT3 such as ERK, p38k and JNK, all members of the MAPK family (Chung et al., 1997, Kovarik et al., 1999, Goh et al., 1999, Lim and Cao, 1999) (Table 3.3).

I next wished to identify the kinase that may be responsible for TLR-mediated Ser-727 phosphorylation of STAT1 and STAT3. RAW264.7 murine macrophages were first treated with U0126 (MEK 1/2 inhibitor, 10 μ M) (Aomatsu et al., 2008), SB203580 (p38k inhibitor, 100 nM) (Cuenda et al., 1995), SB600125 (JNK inhibitor, 20 μ M) (Prickett and Brautigan, 2007), wortmannin (PI3K inhibitor, 10 nM) (Arcaro and Wymann, 1993) and 2-aminopurine (Protein Kinase R (PKR) inhibitor, 10 mM) (Chuang et al., 2011) for 2 hours. The cells were then stimulated with LPS for 60 minutes, as my previous stimulation studies have demonstrated that this time point induces robust Ser-727 phosphorylation (See Figure 3.2 to 3.6 and 3.11 to 3.15). Treatment with these inhibitors did not affect the Ser-727 phosphorylation levels of STAT1 (Figure 3.26A, panel 1) as the levels of pSer-727 STAT1 were equivalent to the untreated sample (Figure 3.26A, panel 1, lane 2 compared to lanes 3-7). Densitometry analysis of the serine phosphorylation immunoblot further confirms that the kinase inhibitors had little effect on serine phosphorylation of STAT1, though the MEK1/2 inhibitor, U0126, had slightly diminished pSer-727 STAT1 levels; however this was not significant (Figure 3.26B).

Cellular lysates prepared for figure 3.26 were also immunoblotted for pSer-727 STAT3. Levels of pSer-727 STAT3 were not affected as can be observed in figure 3.27 (panel 1, lane 2 compared to lanes 3-7). In contrast, cells treated with 2-aminopurine displayed a decreased band of pSer-727 STAT3 (Figure 3.27A, panel 1, lane 7), suggesting it may play a role in the phosphorylation of STAT3 following TLR ligand stimulation. β -tubulin cellular concentration were employed to ensure equal protein loading (Figure 3.27A, panel 2). Densitometry analysis demonstrates that only the PKR inhibitor, 2-aminopurine affected serine phosphorylation of STAT3 (0.9583 ± 0.29 vs. 1.202 ± 0.2 for untreated cells), with the other kinase inhibitors having no impairment of STAT3 serine phosphorylation (Figure 3.27B).

Table 3.3: Kinases responsible for STAT1 and STAT3 Ser-727 phosphorylation.

STAT protein	Kinase	Reference
STAT1	p38k	Kovarik et al. (1999)
STAT1	p38k	Goh et al. (1999)
STAT3	JNK1	Lim and Cao (1999)
STAT3	JNK1 and p38	Turkson et al. (1999)
STAT3	ERK	Chung et al. (1997)

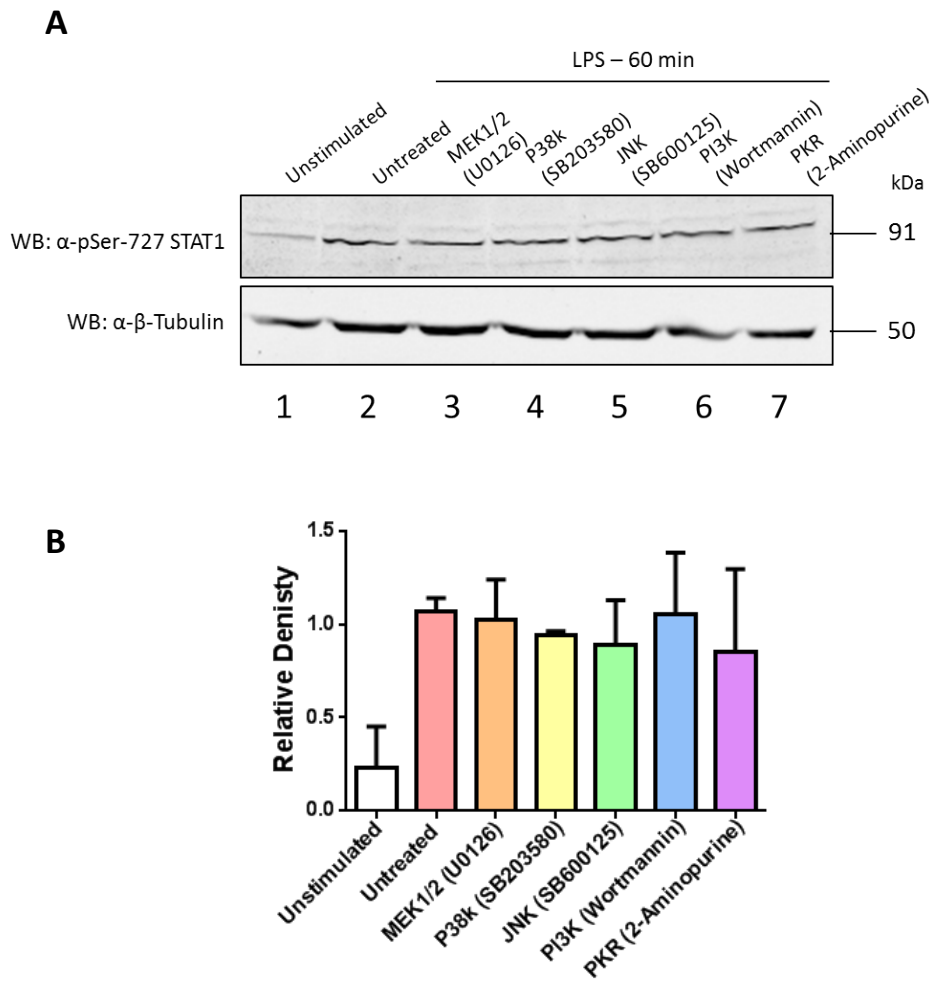


Figure 3.26: Serine phosphorylation of STAT1 is not affected by treatment with MEK1/2, p38k, JNK, PI3K and PKR inhibitors.

RAW264.7 murine macrophages were seeded in a 6-well plate at 1×10^6 cells/well, 24 hours prior to treatment. Cells were then treated with U0126 (10 μ M), SB203580 (100 nM), SB600125 (20 μ M), wortmannin (10 nM) and 2-aminopurine (10 mM) for 2 hours. Following inhibitor treatment, RAW264.7 murine macrophages were stimulated with LPS (100ng/ml) for 60 minutes, and then harvested. Samples were then separated by gel electrophoresis and immunoblotted with α -pSTAT1 (Ser-727) antibody. **(A)** Serine phosphorylation of STAT1 is not affected by inhibiting the kinases MEK1/2, p38k, JNK, PI3K and PKR. **(B)** Densitometry analysis illustrates relative density of bands compared to untreated sample. These results are a representation of three individual experiments (n=3).

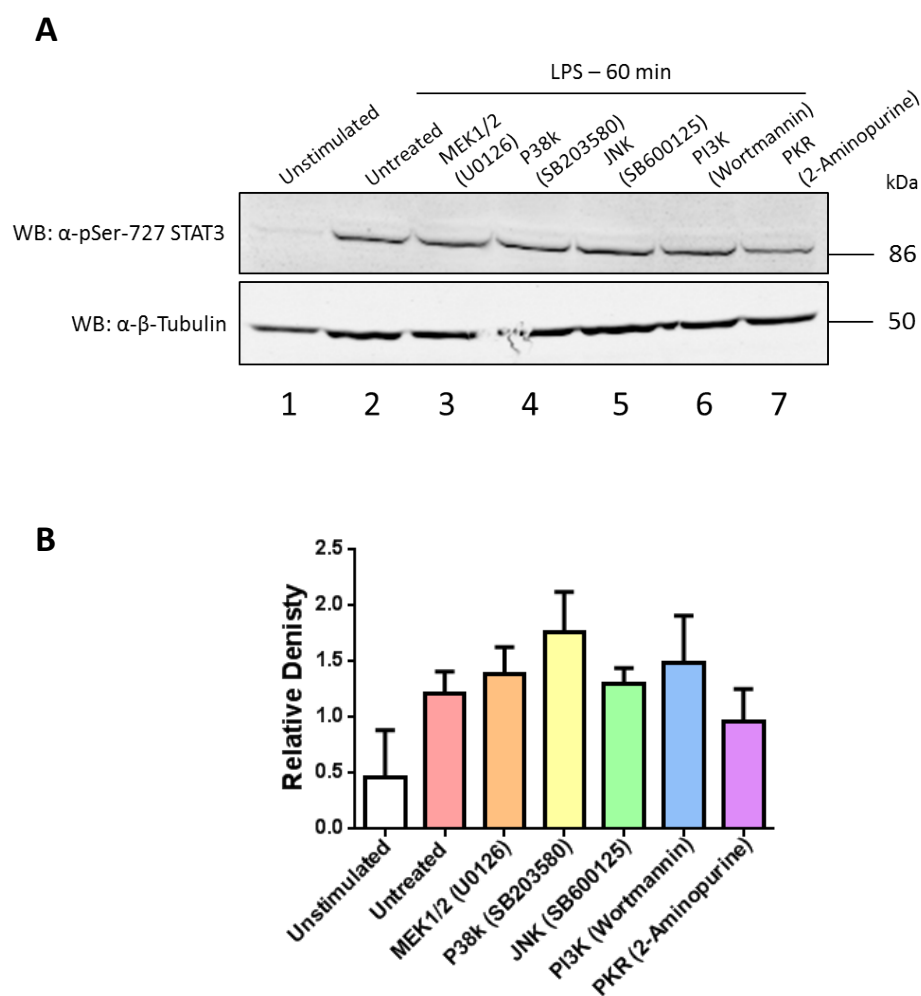


Figure 3.27: STAT3 Ser-727 phosphorylation is not affected by MEK1/2, p38k, JNK and PI3K, but PKR may be involved in STAT3 serine phosphorylation.

RAW264.7 murine macrophages were prepared as described in figure 3.26. Cells were then treated with U0126 (10 μ M), SB203580 (100 nM), SB600125 (20 μ M), wortmannin (10 nM) and 2-aminopurine (10 mM) for 2 hours. Samples were then separated by gel electrophoresis and immunoblotted with α -pSTAT3 (Ser-727) antibody. **(A)** Serine phosphorylation of STAT3 was not affected by inhibiting the kinases MEK1/2, p38k, JNK and PI3K, though PKR inhibition decreases pSer-727 STAT3. **(B)** Densitometry analysis illustrates relative density of bands compared to untreated sample. These results are a representation of three individual experiments (n=3).

3.2.11 – STAT3 Ser-727 phosphorylation is not attenuated in PKR-deficient cells

To further investigate the potential role PKR plays in TLR-induced Ser-727 phosphorylation of STAT3, PKR-deficient splenic macrophages were stimulated with TLR ligands and the phosphorylation status of STAT3 was examined.

Although inhibition of PKR in RAW264.7 murine macrophages produced a band of weaker intensity compared to the other inhibitors, as can be seen from figure 3.28, TLR ligands failed to induce STAT3 Ser-727 phosphorylation in both WT and PKR knockout cells. Densitometry analysis further confirms these observations, demonstrating the lack of STAT3 Ser-727 phosphorylation. Thus these results are inconclusive. Taken together, my results indicate that for STAT1 neither ERK, JNK, p38k, PI3K and PKR were the kinase responsible for TLR-induced STAT1 serine phosphorylation, though MEK1/2 marginally affected STAT1 Ser-727 phosphorylation. In contrast with the exception of 2-aminopurine, STAT3's serine phosphorylation was also not regulated by the kinases examined, though our results suggest that 2-aminopurine may contribute to TLR-induced STAT3 Ser-727 phosphorylation. Further analysis with PKR-deficient cells however proved inconclusive.

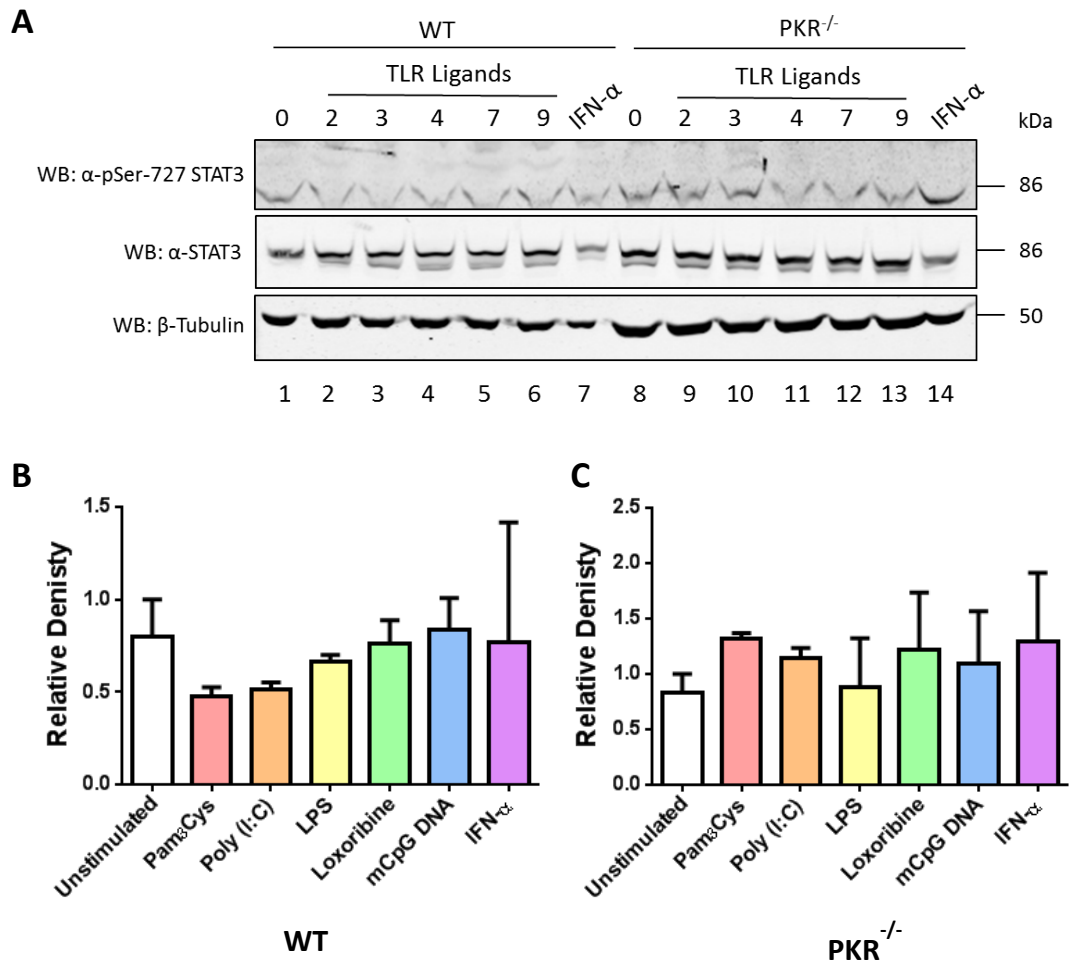


Figure 3.28: Ser-727 phosphorylation and STAT3 was not inhibited in PKR^{-/-} cells.

WT and PKR^{-/-} splenic macrophages were prepared as described in figure 3.26. Cells were stimulated with Pam₃Cys (100 ng/ml), poly (I:C) (10 μ g/ml), LPS (100 ng/ml), loxoribine (500 μ M), mCpG DNA (500 nM) and IFN- α (1000 IU) for 60 minutes. **(A)** TLR-induced STAT3 Ser-727 phosphorylation was not inhibited in PKR^{-/-} cells compared to WT cells. **(B)** WT splenic macrophages undergo low levels of STAT3 Ser-727 phosphorylation. **(C)** STAT3 Ser-727 phosphorylation is comparable to unstimulated and WT cells. These results are a representation of three individual experiments (n=3).

3.3 - Discussion

In this chapter I have established a mechanism of cross-talk between TLR and the JAK-STAT signalling pathways following TLR ligand stimulation. After TLR ligand stimulation, STAT1 and STAT3 undergoes a robust serine phosphorylation with delayed tyrosine phosphorylation occurring in cells stimulated with TLR3 and TLR4 ligands. This cross-talk is facilitated by TRAF6 interacting with both STAT1 and STAT3, potentially recruiting them into the TLR signalling pathway following ligand stimulation. The interaction of STAT1/TRAF6 and STAT3/TRAF6 is mediated directly through TLR signalling as the absence of the TLR adaptor molecules, MyD88 and TRIF, abolished STAT1 and STAT3 Ser-727 phosphorylation. Autocrine activation of the JAK-STAT signalling pathway through type I IFN production is not responsible for Ser-727 phosphorylation of STAT1 and STAT3 as IRF3/7-deficient cells did not impair the serine phosphorylation of STAT1 or STAT3. My results therefore demonstrate a novel direct TLR-mediated response with an unknown biological consequence.

Previous studies by Rhee et al. (2003) and Schroder et al. (2007) have reported STAT1 serine phosphorylation following TLR ligand stimulation, however, TLR-induced Ser-727 STAT3 phosphorylation has previously not been reported. My studies however have demonstrated that the Ser-727 phosphorylation event occurs for both STAT1 and STAT3 and is a general TLR response that is independent of the TLRs cellular location. Serine phosphorylation of STAT1 and STAT3 was observed in all cells stimulated with TLR ligands a corresponding tyrosine phosphorylation only detected in cells stimulated with poly (I:C) and LPS. Both TLR3 and TLR4 can induce production of IFN- β , therefore it is possible that the tyrosine phosphorylation of STAT1 and STAT3 is the result of the IFN- β secretion and the subsequent activation of JAK-STAT signalling pathway (Matsumoto et al., 2002, Kawai et al., 2001). The NF κ B-dependent genes, IL-6 and IL-10 can also induce tyrosine phosphorylation of STAT3, although the rapid kinetics of this STAT3 activation (e.g. within 10-20 minutes post-stimulation) suggests this is not the case. LPS stimulation has also been documented in inhibiting IL-6-induced STAT3 activation but not IL-10 (Niemand et al., 2003), further supporting my hypothesis that STAT3 tyrosine phosphorylation occurs through IFN- β secretion. The timing of tyrosine phosphorylation of STAT1 and STAT3 observed is consistent with autocrine activation of JAK-STAT signalling and secretion of IFN- β . Importantly, the tyrosine phosphorylation of both STATs is not observed in RAW264.7 murine macrophages stimulated with Pam₃Cys, as TLR2 does not induce IFN- β production, but does induce production of IL-6 and IL-10 (Toshchakov et al., 2002). Whilst TLR7 and TLR9 can induce production of IFN- β through activation of IRF7 in pDCs, the ligand loxoribine only induces weak

IFN- β mRNA expression (Al-Salleeh and Petro, 2007). Consistent with this finding, Schroder et al. (2007) found that macrophages differ to DCs in IFN- β production following TLR9 challenge. Both BMMs and RAW264.7 murine macrophages did not induce IFN- β production, whilst only bone marrow-derived DCs (BMDCs) induced IFN- β mRNA expression. Our data therefore agrees with these studies, demonstrating the lack of tyrosine phosphorylated STAT1 and STAT3 in Pam₃Cys, loxoribine and CpG DNA stimulated cells with both STATs undergoing Ser-727 phosphorylation.

Whilst Ser-727 phosphorylation of STAT1 has previously been documented, TLR-induced STAT3 Ser-727 phosphorylation is a novel finding. Although serine phosphorylation of STAT1 and STAT3 was observed, the kinetics of this differed in a few of the TLR agonists used which appeared consistent with the cellular localisation of the respective receptor. TLR2 and TLR4 are expressed on the cell surface where they can bind their ligands upon stimulation thus allowing rapid signal transduction and phosphorylation of STAT1. pSer727 STAT1 was detected at early time points (within 10 minutes) when stimulated with Pam₃Cys and LPS. Stimulation with poly (I:C), loxoribine and CpG DNA displayed a similar serine phosphorylation albeit with delayed kinetics; the serine phosphorylation was observed at approximately 30 minutes compared to 10 minutes when induced by Pam₃Cys and LPS. As TLRs 3, 7 and 9 are endosomally located (Matsumoto et al., 2003, Heil et al., 2003, Ahmad-Nejad et al., 2002, Latz et al., 2004), their ligands must first be endocytosed. The TLR ligands are shuttled into the cell via the endocytic pathway and undergo acidification. Following this process the endosomal TLRs are then recruited to endolysosomes by interacting with UNC93B1, where they are can bind their respective ligands (Tabeta et al., 2006). This explains the delayed kinetics of STAT1 Ser-727 phosphorylation observed in figures 3.3, 3.5 and 3.6. For the plasma membrane located TLR2 and TLR4, both these receptors can recognise ligands at the cell surface hence the phosphorylation of STAT1 is very rapid. The kinetics of STAT3 serine phosphorylation differs from those of STAT1, with pSer-727 STAT3 being able to be detected very rapidly post-stimulation. This could be a result of growth factors (e.g. CSF, Insulin Growth Factor (IGF) etc.) in the serum activating STAT3, thus high levels of pSer-727 STAT3 were detected in unstimulated cells. Whilst cells were serum starved overnight to reduce STAT3 activation by growth factors, this only marginally reduced basal STAT3 activation.

Having confirmed that TLR ligands induced serine phosphorylation of both STAT1 and STAT3, it was necessary to determine if IFNs were responsible for the STAT activation and validate TLR signalling's importance for STAT1 and STAT3 serine phosphorylation. Macrophages lacking both MyD88 and TRIF, which cannot signal via the MyD88-dependent and -independent pathways, are unable to induce serine phosphorylation of STAT1 and STAT3 suggesting that the Ser-727

phosphorylation observed is dependent upon TLR signalling. Both IRF3 and IRF7 are crucial to the induction of type I IFNs (Sato et al., 2000) and TLR treated IRF3/7^{-/-} macrophages were still able to phosphorylate STAT1 and STAT3 suggesting that serine phosphorylation of STAT1 and STAT3 doesn't require IFN secretion and the JAK-STAT signalling pathway. However, despite the unlikelihood, future studies could also investigate the possibility of other NFκB-dependent genes such as IL-6 or IL-10 being responsible for STAT3 Ser-727 phosphorylation. Our experiments demonstrate that the serine phosphorylation of STAT1 and STAT3 is directly mediated by the TLR signalling pathway and suggests that molecules downstream of the TLR adaptor molecules is directly involved in facilitating STAT1 and STAT3 Ser-727 phosphorylation. Taken together my results suggest a direct TLR-mediated Ser-727 phosphorylation of STAT1 and STAT3, that is independent of JAK-STAT signalling. The robust serine phosphorylation of STAT1 and STAT3 is a direct result of recruitment into the TLR signalling pathway.

TLR2, TLR4, TLR7 and TLR9 all utilize the MyD88-dependent pathway, which requires the adaptor molecule MyD88. In contrast, TLR3 is the only receptor that signals via the MyD88-independent pathway and utilises the adaptor molecule TRIF. Both MyD88- and TRIF-dependent signalling resulted in Ser-727 phosphorylation of STAT1 and STAT3 therefore these adaptor molecules are unlikely to be responsible for facilitating JAK-STAT and TLR signalling cross-talk. A common signalling molecule that connects TLR and JAK-STAT signalling must therefore act downstream of the adaptor molecules and be involved in both MyD88-dependent and -independent pathways. TRAF6 is a central signalling molecule in the TLR pathway and is involved in the both MyD88-dependent and -independent pathways.

As discussed earlier TRAF6 has been well documented to interact with many molecules. Proteins that interact with TRAF6 all contain a T6BM that has been found to be crucial for this interaction. The T6BM was identified to be P-X-E-X-X-(aromatic/acidic residue), with the proline, glutamic acid and aromatic/acidic residue determined to be critical for TRAF6 interaction (Ye et al., 2002). Mutations of the three critical residues of the T6BM in CD40 impaired NFκB reporter activity compared to WT CD40, illustrating the importance of this interaction for NFκB activation (Ye et al., 2002). TRANCER and IRAK1 were also found to contain T6BMs and mutation of the T6BM reduced activation of NFκB (Ye et al., 2002). Subsequent studies identified T6BMs in TRIF, TRAM and Mal (Sato et al., 2003, Mansell et al., 2004) and in the case of TRIF, mutations of all the T6BMs and a C-terminal truncation was required to abolish NFκB activation. Mansell et al. (2004) found that the mutation of Mal's single T6BM did not abolish interaction with TRAF6 however, the Mal mutant failed to drive NFκB activity following TLR2 and TLR4 ligand stimulation.

Furthermore, specific studies demonstrated that mutation of the single glutamic acid residue ablated signalling, interaction and cytokine production (Verstak et al., 2009). Taken together these studies demonstrate the importance of TRAF6 interaction in activating NF κ B. Though my results showed STAT1/TRAF6 and STAT3/TRAF6 interaction, further elucidation of this interaction is required to investigate the biological significance of STAT1/TRAF6 and STAT3/TRAF6 interaction on innate immune responses. As both STAT1 and STAT3 contain three T6BMs, future experiments will examine mutations of these motifs. Ye et al. (2002) and Sato et al. (2003) both found that molecules containing more than one T6BM such as IRAK1 and TRIF; that not one T6BM alone is responsible for facilitating TRAF6 interaction. In fact the T6BMs act redundantly as mutation of one of the multiple T6BMs did not abolish TRAF6 interaction (Ye et al., 2002, Sato et al., 2003). Furthermore, TRIF was also found to be able to bind TRAF6 via its N-terminus and mutation of the single T6BM in Mal failed to abolish TRAF6/Mal interaction; therefore it may be possible that STAT1 and STAT3 interact with TRAF6 via another domain or motif. It is possible that similar to TRIF, further truncations of STAT1 and STAT3 are required to ablate TRAF6 interaction. However, this approach does not identify if the T6BMs are responsible for their association and truncation would produce an inactive protein. Further studies could investigate this by mutating more residues of the T6BM, as mutation of the glutamic acid residue alone may not completely abolish association with TRAF6.

Having observed STAT1/TRAF6 and STAT3/TRAF6 interaction in our GST pull-down experiments, it was necessary to confirm these results in an endogenous protein interaction assay. This was performed in a semi-endogenous fashion using the recombinant GST-TRAF6 fusion proteins to identify STAT1 and STAT3. In resting cells, TRAF6 was observed to interact with both STAT1 and STAT3, suggesting that serine phosphorylation of STAT1 and STAT3 is not a requirement of STAT1/TRAF6 and STAT3/TRAF6 interaction. Following stimulation with Pam₃Cys or LPS, both a STAT1/TRAF6 and STAT3/TRAF6 complex was observed at all time points. This interaction did not appear to increase following stimulation, suggesting that levels of STAT1, STAT3 and TRAF6 are not altered. Although pSer-727 STAT1 levels increased following LPS stimulation, this did not translate to increased STAT1/TRAF6 association (Figure 3.22). It is interesting to note that TRAF6 is still able to interact with pSer-727 STAT1 and STAT3. Traditionally when STAT1 and STAT3 undergo tyrosine phosphorylation, these proteins form homo- or heterodimers and are transported to the nucleus (Decker and Kovarik, 2000). Whilst it is known that tyrosine phosphorylation of the STATs is required for dimerisation, Ser-727 phosphorylation of STAT1 and STAT3 is reported to provide potentiated transcriptional activity (Wen et al., 1995). Serine phosphorylation of STAT1 and STAT3 independent of tyrosine phosphorylation has been

documented (Ceresa and Pessin, 1996, Gotoh et al., 1996, Zhu et al., 1997, Kovarik et al., 1999). In Chinese Hamster Ovary (CHO) cells, STAT3 was found to exclusively undergo serine phosphorylation in response to insulin stimulation for 5 minutes, although other STAT isoforms were not affected (Ceresa and Pessin, 1996). Stimulation with steel factor (SLF) in human factor-dependent cell lines MO7e and TF-1, a cytokine involved in hematopoietic progenitor cell development also resulted in serine phosphorylation of STAT3 but not tyrosine demonstrating that phosphorylation of the tyrosine and serine residues of STAT3 is independent of each other (Gotoh et al., 1996). For STAT1, Zhu et al. (1997) demonstrated that following IFN- γ stimulation in NIH 3T3 cells, STAT1 could possibly undergo serine phosphorylation independent of tyrosine phosphorylation, though this occurred 20 minutes post-challenge and was dependent on JAK2 for IFN- γ -mediated STAT1 Ser-727 phosphorylation. It was also reported that Bac1.2F5 macrophages treated with ultraviolet (UV) irradiation and TNF- α for 25 minutes only caused Ser-727 phosphorylation of STAT1. This was demonstrated to not involve JAK-STAT signalling, but was p38k-dependent (Kovarik et al., 1999). These studies therefore show that serine phosphorylation of both STAT1 and STAT3 can occur in response to other stimuli, though the role of the serine phosphorylation is still not clearly understood.

Traditionally the serine phosphorylation of STAT1 and STAT3 has been implicated in enhancing transcriptional activity (Wen et al., 1995). Serine phosphorylation of the STATs does not induce dimerisation, a prerequisite for nuclear translocation and the role cytoplasmic Ser-727 phosphorylated STAT1 and STAT3 remains to be determined. Schroder et al. (2007) found pSer-727 STAT1 was retained in the cytoplasm and proposed that in this state, STAT1 sequesters transcription factors. Previous studies have demonstrated STAT1 interacts with IRF1, IRF2 and IRF8 (Chatterjee-Kishore et al., 2000, Rouyez et al., 2005, Unlu et al., 2007), therefore it is possible that serine phosphorylated STAT1 sequesters IRF1, IRF2 and IRF8 in the cytoplasm. Other studies have implicated Ser-727 phosphorylated STAT1 in the induction of apoptosis in cardiac myocytes (Stephanou et al., 2001). Following ischemic insult, Ser-727 phosphorylated STAT1 and not Tyr-701 phosphorylated STAT1 is crucial for the induction of Fas and Fas ligand (FasL) expression (Stephanou et al., 2001). This suggests that rather than functioning as a transcription factor like Tyr-701 phosphorylated STAT1, Ser-727 phosphorylated STAT1 may modulate other cellular functions. Perhaps the serine phosphorylation plays a role in augmenting the immune response or regulation of other organelles other than the nucleus?

In regards to STAT3, F/F mice were found to be hyperresponsive to LPS and activation of TLR4 by LPS was demonstrated to be independent of TLR-induced IFN- β production (Greenhill et al.,

2011). Interestingly, STAT3 was identified to be mediating the hyperresponsiveness to LPS, although Greenhill et al. (2011) only examined tyrosine phosphorylated STAT3. It is therefore possible that serine phosphorylated STAT3 may be driving or augmenting the initial inflammatory response to LPS. Inhibition of IFNAR and genetic ablation of type I IFN signalling failed to rescue F/F mice from LPS hypersensitivity. In contrast, deletion of Mal which is required for TLR4-induced MyD88-dependent signalling, reduced LPS hypersensitivity demonstrating a direct TLR effect on STAT3 via activation of IL-6/gp130 signalling (Greenhill et al., 2011). This matches our data where I found that cells deficient in MyD88/TRIF failed to serine phosphorylate STAT3, but IRF3/7^{-/-} cells had no effect on STAT3 Ser-727 phosphorylation. Taken together this would suggest that serine phosphorylated STAT3 may contribute to the initial immune response, with tyrosine phosphorylated STAT3 activated by IL-6 acting in the late phase, thereby mediating F/F mice LPS hypersensitivity. Recent evidence has also emerged demonstrating that STAT3 has a role outside that of a transcription factor. Unlike tyrosine phosphorylated STAT3 which translocates to the nucleus, serine phosphorylated STAT3 has been demonstrated to localise inside mitochondria. In Ras-transformed cells serine phosphorylated STAT3 were shown to be required for cellular transformation as mutation of the serine phosphorylation site or deletion of the C-terminal domain abolished STAT3 and Ras interaction (Gough et al., 2009). This indicates that serine phosphorylation of STAT3 may have another role in innate immunity other than unlocking STAT3's maximal transcriptional activity.

TRAF6 would appear to facilitate the cross-talk between TLR and JAK-STAT by functioning as a bridging protein recruiting STAT1 and STAT3 into the TLR pathway. However, TRAF6 itself does not contain any intrinsic kinase activity, therefore a serine kinase must be activated to serine phosphorylate STAT1 and STAT3. Possible candidate kinases were assembled based on previously published data that have been implicated in serine phosphorylating STATs. Previous studies have suggested that the Ser-727 phosphorylation of STAT1 is mediated by the p38k in response to stress (Kovarik et al., 1999, Goh et al., 1999). Chung et al. (1997) demonstrated that STAT1 is in fact a poor substrate for p38k both *in vivo* and *in vitro*, therefore it is unlikely that p38k is responsible for the Ser-727 phosphorylation of STAT1. Nguyen et al. (2003) also found that IL-1 mediated STAT1 serine phosphorylation does not require MAPKs. Furthermore, Cecil et al. (2004) also demonstrated that in HeLa cells the activation of p38k was not sufficient to phosphorylate STAT1 at Ser-727. Although Kovarik et al. (1999) reported that STAT1 Ser-727 phosphorylation in response to LPS, UV irradiation and TNF- α was sensitive to the p38k inhibitor in macrophages, this conflicts with previous studies conducted and my results (Figure 3.26A). In my experiments, p38k inhibition did not affect Ser-727 phosphorylation of STAT1 in macrophages following LPS

stimulation. Other members of the MAPK family that were tested produced a similar result, with no apparent reduction of Ser-727 phosphorylation of STAT1. Densitometry analysis suggested that the MEK1/2 inhibitor slightly reduced Ser-727 phosphorylation of STAT1, but this requires further investigation and the use of more specific methodology. Previous studies investigating Ser-727 phosphorylation of STAT1 primarily focused on IFN- γ treatment of cells, which may induce an alternative mechanism of STAT1 serine phosphorylation that is partly dependent on p38k (Goh et al., 1999). My experiments however, focused on examining a kinase responsible for TLR-induced Ser-727 phosphorylation of STAT1. PKC- δ has previously been implicated in the serine phosphorylation of STAT1 following TLR activation (Rhee et al., 2003). In macrophages, treatment with rottlerin, a PKC- δ inhibitor, blocked TLR4-induced STAT1 Ser-727 phosphorylation but not TLR2 (Rhee et al., 2003). However, Shoenfelt and Fenton (2006) demonstrated that murine peritoneal macrophages activated through TLR2 and TLR4 displayed rapid serine phosphorylation in the absence of PKC- δ , suggesting another kinase is responsible for TLR-induced STAT1 Ser-727 phosphorylation. These findings suggests that different stimuli and cell types may utilize different kinases to serine phosphorylate STAT1 and indicates that STAT1 may be serine phosphorylated by different kinases depending on the TLR ligand used.

In the case of STAT3, there is evidence suggesting that ERK2 is responsible for its serine phosphorylation. Chung et al. (1997) found that ERK-dependent serine phosphorylation of STAT3 appears to be induced by growth factors and not IL-6 and *in vitro* experiments demonstrated that ERK2 phosphorylated STAT3 at Ser-727. Inhibition of ERK2 with PD98059 (MEK1 inhibitor, upstream of ERK2, 50 μ M), also inhibited pSer-727 STAT3 detection, suggesting ERK2s role as a serine kinase (Chung et al., 1997). STAT3 could also be immunoprecipitated with ERK2 and mutation of the Ser-727 site diminished this interaction (Jain et al., 1998). My results however, did not agree with these studies as inhibition of MEK1/2, using the inhibitor U0126 (10 μ M), failed to abolish Ser-727 phosphorylation of STAT3. As PD98059 inhibits MEK1 more potently than MEK2 it is possible that MEK2 may serine phosphorylate STAT3 hence this was not observed when using the dual MEK1/2 inhibitor U0126. Lim and Cao (1999) demonstrated that STAT3 undergoes Ser-727 phosphorylation when induced by UV and TNF- α , although LPS induced a weaker serine phosphorylation of STAT3. JNK1 was shown to serine phosphorylate STAT3, and transfection of a constitutively active JNK kinase kinase, MEKK1, lead to Ser-727 phosphorylation of STAT3 (Lim and Cao, 1999). Though Lim and Cao (1999) found that JNK1 can serine phosphorylate STAT1 *in vitro* and *in vivo*, my results demonstrate that in response to LPS, inhibition of JNK with the inhibitor SB600125 (20 μ M), did not induce decreased Ser-727 phosphorylation of STAT3. Inhibition of other members of the MAPK family also failed to abolish

Ser-727 phosphorylation of STAT3 following TLR stimulation and this is in part supported by a study conducted Schuringa et al. (2000). In response to IL-6, STAT3 also undergoes Ser-727 phosphorylation but this was reported not be mediated by ERK, JNK or p38k (Schuringa et al., 2000). Although JNK was not found to be involved in STAT3 serine phosphorylation, the kinases upstream of JNK, ERK1 and MAPK kinase 4 were important for STAT3 Ser-727 phosphorylation. Inhibition of PKR slightly reduced Ser-727 phosphorylation of STAT3, suggesting that PKR may indirectly facilitate STAT3 Ser-727 phosphorylation, however studies conducted in WT and PKR-deficient splenic macrophages were inconclusive and will require further investigation using primary cell lines. When stimulated with PDGF, PKR has been demonstrated to interact with STAT3 and both tyrosine and serine phosphorylation of STAT3 is dependent on PKR (Deb et al., 2001). In the context of TLR signalling, PKR may have an indirect role in facilitating the Ser-727 phosphorylation of STAT3. Most studies investigating STAT3 Ser-727 phosphorylation have mainly examined treatment with IL-6, growth factors and inflammatory cytokines; it would appear though that different cell lines and different stimuli induce a unique signalling cascade that activates a kinase which phosphorylates STAT3 on Ser-727. It is possible that multiple kinases may serine phosphorylate both STAT1 and STAT3 depending on the kind of stimuli the cell is treated with and cell specificity.

Whilst I was unable to identify the kinase responsible for serine phosphorylating the STATs following TLR ligand stimulation, perhaps kinases that are activated during TLR signalling may be involved in the serine phosphorylation of STAT1 and STAT3. IRAKs and TAK1 may therefore be potential candidates. As I have demonstrated that TRAF6 can interact with the serine phosphorylated forms of STAT1 and STAT3, it is possible for TRAF6 to bring both STATs proximal to a serine kinase. TRAF6 can interact with both IRAKs and TAK1, functioning as a bridging adaptor bringing the IRAKs into contact with TAK1 and allowing TAK1 to associate with the IKK complex. As such, TRAF6-interacting kinases such as IRAKS could be responsible for the phosphorylation of STAT1. Nguyen et al. (2003) found that IRAK does interact with STAT1 *in vivo* and suggested that IRAK may not serve as the proximal serine kinase of STAT1 but may in fact recruit a kinase to STAT1. Therefore it is possible that following TLR stimulation the IRAKs could recruit TRAF6 which in turn may bind STAT1 and STAT3, bringing both molecules proximal to TAK1. IRAK1-deficient splenocytes fail to induce STAT3 Ser-727 phosphorylation and IL-10 production following LPS stimulation (Huang et al., 2004b). Interestingly, IRAK1 and STAT3 were found to interact within the nucleus, with increased levels of pSer-727 STAT3 detected in the nucleus (Huang et al., 2004b). After TLR agonist treatment, TRAF6 may remain bound to IRAK1 and could potentially bind STAT3 facilitating its serine phosphorylation. Future studies utilizing

inhibitors, knockout cells and siRNA will be employed to examine these potential candidates in the Ser-727 phosphorylation of STAT1 and STAT3. This may prove to be difficult though as disruption of IRAK would ablate canonical TLR signalling affecting downstream mediators such as TRAF6, thus potentially affecting the ability of TRAF6 to recruit STAT1/STAT3 and produce a false negative result.

There are some pathologies that have been thought to be TLR-dependent and also demonstrate increased STAT1 and STAT3 expression. Demonstrating cross-talk between TLR and JAK/STAT pathway may suggest that there are diseases which may be potentiated if STAT1 and STAT3 play a role in the biological consequences of TLR activation. In cases like sepsis and septic shock where a hyperinflammatory state is undesired, the reduction of inflammatory mediators may increase the chances of recovery and survival, therefore the biological outcomes of this cross-talk need to be fully characterised. As serine phosphorylation of the STATs is not as critical as tyrosine phosphorylation, inhibition of STAT serine phosphorylation may have fewer side effects when used to treat inflammatory diseases. Thus targeting the serine residue represents a new therapeutic target that may also not compromise the hosts' immune system.

In this chapter, I have established a means of cross-talk between TLR and JAK-STAT signalling. This cross-talk is facilitated by TRAF6 recruitment of STAT1 and STAT3 via T6BMs into the TLR signalling pathway. Both STAT1 and STAT3 undergo a robust Ser-727 phosphorylation with delayed tyrosine phosphorylation occurring in cells stimulated with TLR3 and TLR4 ligands. This serine phosphorylation is independent of autocrine signalling and type I IFN production. The interaction between STAT1/TRAF6 and STAT3/TRAF6 displays the complexity of innate immunity and also provides therapeutic potential as disrupting this cross-talk may dampen the immune response.

**Chapter 4: Ser-727 STAT3,
Mitochondria and Innate Immunity**

Chapter 4: Ser-727 STAT3, Mitochondria and Innate Immunity

4.1 – Introduction

STAT3 participates in a wide array of biological functions due to the multitude of growth factors and cytokines which activate it. STAT3 has been implicated in inflammation, survival, proliferation, angiogenesis, cellular transformation, invasion and cancer metastasis (Aggarwal et al., 2009). Enhanced STAT3 activation via phosphorylation of the Tyr-705 residue, and more recently Ser-727, can be found in many cancers (Yu and Jove, 2004, Wegrzyn et al., 2009).

Whilst tyrosine phosphorylation of STAT3 is a requirement for dimerisation, there is some controversy regarding the effect of serine phosphorylation. Wen et al. (1995) first demonstrated that like STAT1, serine phosphorylation of STAT3 also increases STAT3's transcriptional activity; however other studies found this not to be the case (Jain et al., 1998, Jain et al., 1999, Lim and Cao, 1999, Sengupta et al., 1998). Both the serine phosphorylation and tyrosine phosphorylation could be induced and regulated independently of each other (Chung et al., 1997). Additionally, EGF induced increased levels of tyrosine phosphorylation of a STAT3 S727A mutant compared to WT STAT3 suggesting that the serine residue may in fact negatively regulate tyrosine phosphorylation either by inhibiting tyrosine phosphorylation or increasing tyrosine dephosphorylation (Chung et al., 1997). Moreover, it was later observed that the absence or presence of serine phosphorylation did not affect the DNA binding ability of STAT3, implying that the enhancement of transcription may occur after DNA binding (Wen and Darnell, 1997). In fact the serine phosphorylation of STAT3 has been implicated in regulating the duration of STAT3 activity. STAT3 activity is regulated through dephosphorylation of tyrosine, and this is dependent on serine phosphorylation acting through the nuclear phosphatase, TC45. (Wakahara et al., 2012). Furthermore, STAT3 S727A mice are not embryonically lethal like STAT3^{-/-} mice, but do display ~50% less transcriptional activity, indicating the importance of the serine residue in activating STAT3's maximal transcriptional activity (Shen et al., 2004). These mice were otherwise normal but the heterozygous STAT3^{S727A/-} mice were 75% perinatal lethal, displayed slow growth and altered IGF-1 levels (Shen et al., 2004). Therefore whilst STAT3 is critical for development, only approximately 25% STAT3 activity is enough for survival of mice.

In B-cell chronic lymphocytic leukaemia (CLL), STAT3 has been identified to be constitutively Ser-727 phosphorylated (Hazan-Halevy et al., 2010). Although STAT3 could still undergo tyrosine phosphorylation in CLL cells, this was only transient; contrastingly Ser-727 phosphorylation remained for 72 hours. Hazan-Halevy et al. (2010) demonstrated that pSer-727 STAT3 localised to the nucleus

by having importin- α 3 or α 6 bind the Nuclear Localisation Sequence (NLS) of STAT3, this complex then interacts with importin- β 1 and is translocated to the nucleus. pSer-727 STAT3 was found to bind DNA of CLL cells and induce transcription of STAT3-regulated genes. Interestingly, dephosphorylation of pTyr-705 STAT3 did not inhibit STAT3 DNA binding suggesting that pSer-727 STAT3 directly interacts with DNA (Hazan-Halevy et al., 2010). STAT3 has also been demonstrated to be constitutively Ser-727 phosphorylated in melanocytes and melanoma cells (Sakaguchi et al., 2012). STAT3 Ser-727 phosphorylation was associated with increased cell survival and pSer-727 STAT3 was shown to localise to the nucleus independent of tyrosine phosphorylation. This further suggests Ser-727 STAT3 involvement in driving tumourigenesis.

More recently studies have found that STAT3 may function outside its normal role as a transcription factor. STAT3 has been detected in the mitochondria in its Ser-727 phosphorylated form, and in STAT3-deficient cells complex I and II of the ETC had reduced activity (Gough et al., 2009, Wegrzyn et al., 2009). In fact, it was demonstrated that serine phosphorylation, not DNA binding, tyrosine phosphorylation or nuclear translocation was required for Ras-dependent cellular transformation (Gough et al., 2009). These findings therefore suggest that alternative activation of STAT3 via Ser-727 phosphorylation can induce non-canonical translocation to the mitochondria and generation of ROS. As TLRs can induce both ROS production (West et al., 2011) and STAT3 Ser-727 phosphorylation, it is therefore possible that the TLR-mediated STAT3 Ser-727 phosphorylation is responsible for the generation of mitochondrial ROS (mtROS).

STAT3's role in driving gp130 inflammatory responses is very well studied, in contrast the role STAT3 plays in TLR-mediated immunity has not been examined. In particular, whilst tyrosine phosphorylation of STAT3 predominately governs the majority of STAT3's action, the part serine phosphorylation plays is to induce maximal gene transcription. In this chapter I will investigate the biological role pSer-727 STAT3 has in TLR-induced inflammation.

4.2 – Results

4.2.1 – TLR-induced mitochondrial membrane destabilisation

In order to confirm my hypothesis, I first determined if TLRs could induce mitochondrial membrane destabilisation. This was quantified by measurement of mitochondria membrane integrity through the use of high content screening. Cells were stimulated with TLR ligands and stained with Mitotracker Red. Mitotracker Red accumulates in the mitochondria of living cells and this is dependent on the mitochondrial membrane potential, if the membrane potential becomes destabilised this results in a “leaky” membrane and thus a decrease in Mitotracker Red staining intensity. The cells were imaged and either 10 fields or 500 cells were captured, images were then processed and quantified using the Cellomics ArrayScan VTi High Content Instrument.

A 24 hour time course was first conducted in order to determine the optimum time to measure mitochondrial membrane destabilisation. RAW264.7 murine macrophages were stimulated with Pam₃Cys (TLR2), transfected (RLR) and untransfected poly (I:C) (TLR3) and LPS (TLR4), stained with Hoechst stain to identify nuclei and Mitotracker Red for mitochondria then analysed for mitochondrial staining intensity. It can be observed that following treatment with the TLR ligands, Mitotracker Red intensity decreases initially during the first 2 hours however; Mitotracker Red intensity slowly begins to recover during the later time points (Figure 4.1). Interestingly, activation of the RIG-1 receptor with transfected poly (I:C) induced little mitochondrial loss of integrity suggesting specificity for TLR-induced effect.

As the first 2 hours of the time course displayed the greatest effect on Mitotracker Red intensity and may also be a direct effect of the acute immune response, I next focused on a shorter time course. In order to observe the different effects of plasma membrane and endosomal TLRs only Pam₃Cys and untransfected poly (I:C) was used to stimulate cells. In order to observe kinetic differences in TLR activation and mimic endogenous cellular environment, I utilised untransfected poly (I:C). Consistent with earlier findings, following stimulation with TLR2 and TLR3 ligands, RAW 264.7 cells exhibited a gradual decrease in Mitotracker Red intensity that is consistent with figure 4.1 (Figure 4.2).

The results here demonstrate that the TLRs can destabilize the mitochondrial membrane, resulting in the loss of Mitotracker Red staining. This appears to be a general TLR mechanism as both plasma membrane and endosomal TLR can induce this.

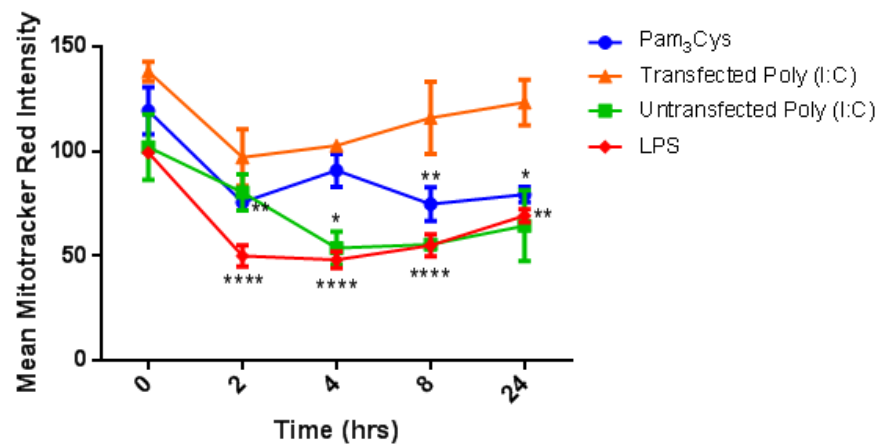


Figure: 4.1: Mean Mitotracker Red intensity decreases following TLR stimulation.

RAW264.7 murine macrophages were seeded at 2×10^4 cells/well into a 96-well plate, 24 hours before stimulation. The following day, cells were stimulated with Pam₃Cys (200 ng/ml), poly (I:C) (transfected 10 ug/ml, untransfected 20 ug/ml) and LPS (200 ng/ml). The cells were washed in PBS, fixed in 10% formalin and stained with Hoechst 33342 stain (1 μ g/ml) and Mitotracker Red CMXRos (100 μ M). After stimulation with TLR agonists, mean Mitotracker Red intensity decreased, with the greatest effect seen at 2 hours. Data is represented as mean \pm SEM and is a representation of three individual experiments (n=3).

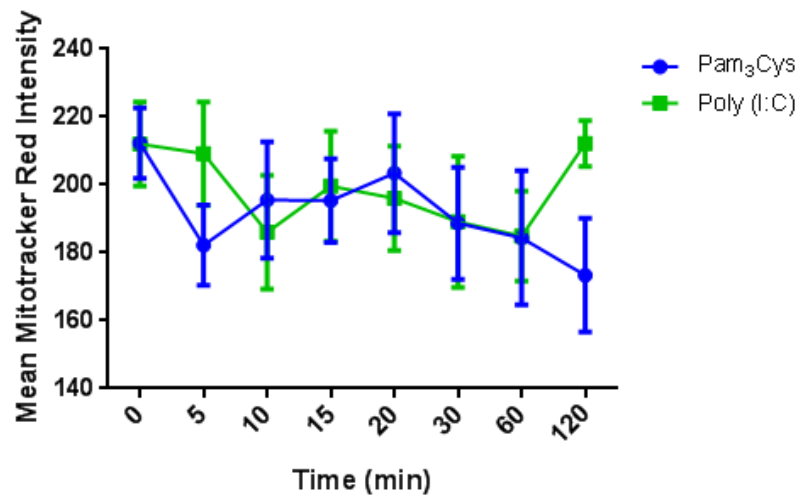


Figure: 4.2: Mean Mitotracker Red intensity decreases marginally in macrophages.

RAW264.7 murine macrophages were prepared as described in figure 4.1. Cells were stimulated with Pam₃Cys (200 ng/ml) and poly (I:C) (20 µg/ml). Following Pam₃Cys and poly (I:C) mean Mitotracker Red intensity decreased. Data is represented as mean ± SEM and is a representation of three individual experiments (n=3).

4.2.2 – TLR stimulation induces mitochondrial reactive oxygen species production

The loss of the Mitotracker Red staining is normally due to a disruption of the mitochondrial membrane potential. This can be a result of ROS production; therefore I next examined the ability of TLR ligands to induce ROS. Utilising high content analysis, cells were stimulated with Pam₃Cys and poly (I:C), ROS generation was then detected by staining with dihydroethidium (DHE). DHE detects superoxide and exhibits blue fluorescence when unoxidised. Following oxidation, DHE forms a red fluorescent protein, ethidium which binds the cell's DNA and stains the nucleus red (Rothe and Valet, 1990). Recent studies however have suggested that 2-hydroxyethidium is actually formed after DHE undergoes oxidation (Zhao et al., 2005). Cells were imaged as previously described and mean nuclear DHE intensity was determined.

Following stimulation, both Pam₃Cys and poly (I:C) induce an increase in DHE intensity in a time-dependent manner, indicating that TLR stimulation can result in cytoplasmic ROS production (Figure 4.3). The kinetics of ROS generation is also similar between the TLR agonists suggesting that the mechanism of ROS production is common among plasma membrane and endosomal TLRs.

As ROS can be detected in the cytoplasm and mitochondria are known to be the main generator of ROS, I next examined whether TLR stimulation induces mtROS production. Employing the same method as described, RAW264.7 murine macrophages were stimulated with Pam₃Cys, poly (I:C) and rotenone then stained for mtROS using MitoSOX. MitoSOX is targeted to the mitochondria and when oxidized by mitochondrial superoxide produces red fluorescence. Rotenone functions by inhibiting complex I of the ETC resulting in the formation of mtROS. As can be observed in figure 4.4, both TLR agonists and rotenone were able to induce mtROS, this occurred rapidly within 5 minutes of stimulation suggesting that the ROS detected in the cytoplasm is a result of ROS produced from the mitochondria.

My results here demonstrate that the loss of Mitotracker Red intensity is in part due to the production of TLR-induced ROS from mitochondria producing a decrease in mitochondrial membrane potential.

4.2.3 – Mitochondrial destabilisation is also observed in fibroblasts

In order to determine whether other cell lines are able to produce ROS after TLR stimulation, HT1080 cells were employed to investigate this. HT1080s are a human fibrosarcoma cell line that was utilised to examine for differences in response to TLRs and ROS production.

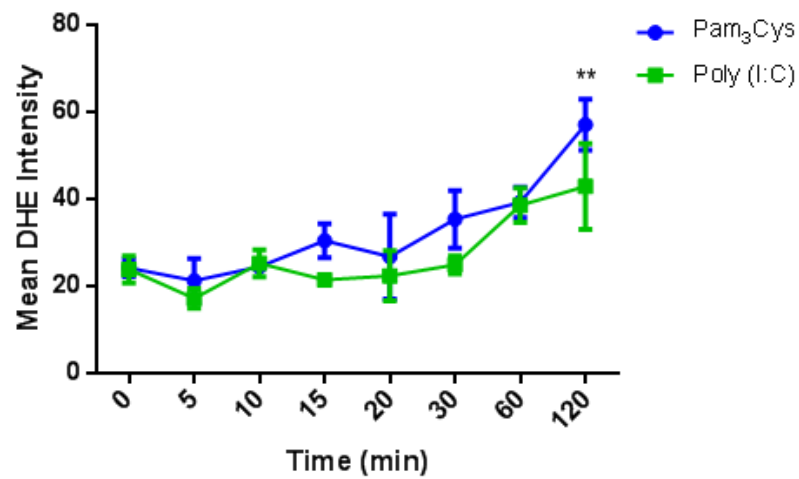


Figure: 4.3: TLR stimulation induces production of ROS.

RAW264.7 murine macrophages were prepared as described in figure 4.1, but instead of staining with Mitotracker Red CMXRos, cells were stained with dihydroethidium (DHE, 5 μ M). Mean DHE intensity increased following stimulation with Pam₃Cys and poly (I:C), demonstrating production of superoxide. Data is represented as mean \pm SEM and is a representation of three individual experiments (n=3).

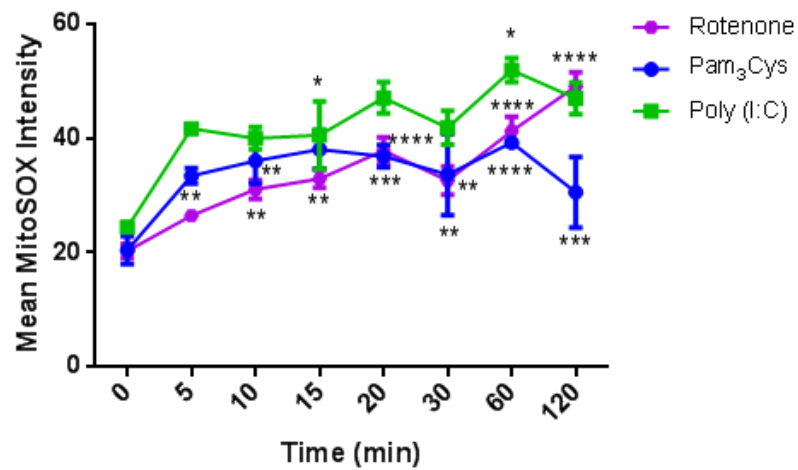


Figure: 4.4: Mitochondrial ROS increases following TLR stimulation.

RAW264.7 murine macrophages were prepared as described in figure 4.1 and were also stimulated with rotenone (10 μ M), but instead of staining with Mitotracker Red CMXRos, cells were stained with MitoSOX (5 μ M). Following stimulation with rotenone and TLR agonists, MitoSOX intensity increased, demonstrating production of superoxide in mitochondria. Data is represented as mean \pm SEM and is a representation of three individual experiments (n=3).

Consistent with earlier findings, HT1080s displayed a reduction in Mitotracker Red intensity albeit with different kinetics following stimulation with Pam₃Cys and poly (I:C). The effect of TLR ligand stimulation is much more pronounced, with a greater overall reduction in Mitotracker Red intensity (Figure 4.5). Poly (I:C) induces a rapid decrease of Mitotracker Red intensity, with Pam₃Cys inducing a slower and steady decrease of Mitotracker Red.

Though the effect of Mitotracker Red intensity reduction is much more pronounced in fibroblasts, this result further demonstrates that the TLR-induced mtROS is not restricted to macrophages and may represent a general cellular mechanism in initiating innate immune responses.

4.2.4 – TLR stimulation increases nuclear localisation of STAT3

As TLR stimulation induces STAT3 Ser-727 phosphorylation, and pSer-727 STAT3 has been documented to localise to mitochondria, the localisation of TLR-induced STAT3 serine phosphorylation was investigated. Using confocal microscopy, RAW264.7 murine macrophages were stimulated with LPS over a 60 minute time course. The nuclei stained with Hoechst stain and STAT3 was detected using an α -STAT3 antibody.

Unstimulated cells displayed a high level of basal STAT3 that can be detected in the nucleus (Figure 4.6A). Whilst cells were serum starved overnight in serum-free media to reduce this, basal nuclear STAT3 could still be detected. STAT3 is also found in the cytoplasm as is expected of a latent transcription factor. Over the 60 minutes time course there is an enrichment of STAT3 in the nucleus, demonstrating that LPS can induce nuclear localisation STAT3 (Figure 4.6B-D).

From this experiment it can be seen that RAW264.7 murine macrophages display a high basal level of STAT3 activation, with STAT3 being detected in all time points including in unstimulated cells. LPS stimulation further increases the amount of STAT3 localising to the nucleus though whether this is a Tyr-705 or Ser-727 STAT3 remains to be determined.

4.2.5 – TLR-induced pSer-727 STAT3 doesn't localise to the nucleus

Due to the high level of basal STAT3 found in the nucleus, I next wanted to investigate whether a phosphorylated form of STAT3 was responsible for the nuclear bound STAT3. Cells were prepared as described previously and stained with pSTAT3 (Ser-727) antibody.

Interestingly, increased levels of pSer-727 STAT3 was not detected throughout the 60 minute time course (Figure 4.7). Following LPS stimulation, pSer-727 STAT3 staining displays a punctate staining pattern and this appears to increase up to 60 minutes post-stimulation (Figure 4.7B-D). Overlaying of

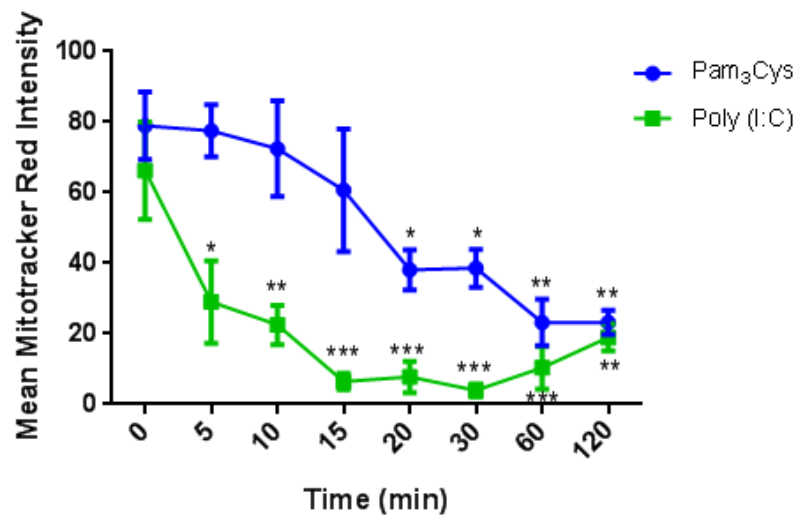


Figure: 4.5: Mean Mitotracker Red intensity decreases greatly in fibroblasts following TLR stimulation.

HT1080 cells were prepared as described in figure 4.1. Mean Mitotracker Red was observed to decrease greatly following stimulation with TLR agonists. Data is represented as mean \pm SEM and is a representation of three individual experiments (n=3).

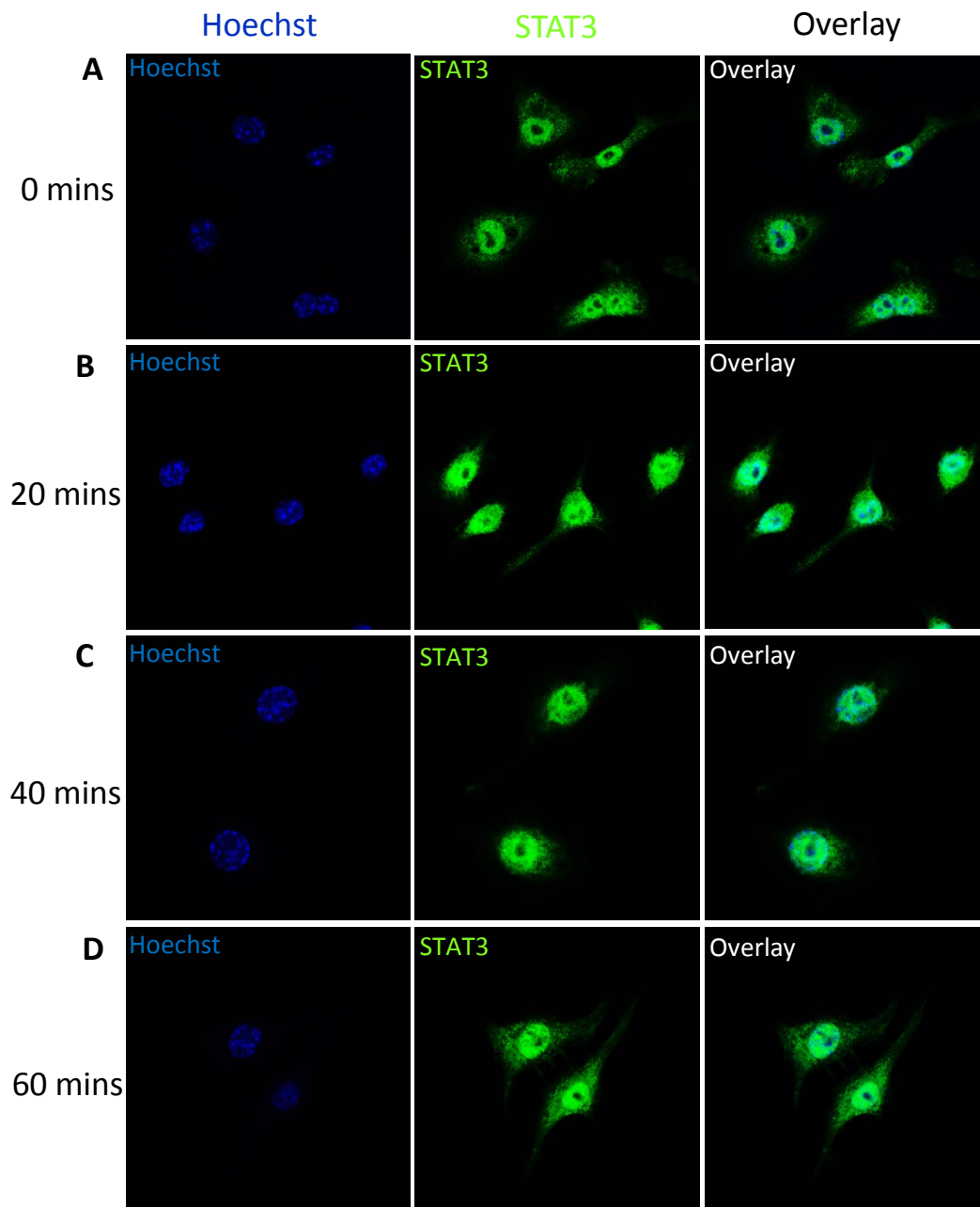


Figure: 4.6: LPS stimulation increases STAT3 detection in the cytoplasm.

RAW264.7 murine macrophages are seeded onto coverslips at 2×10^4 cells/well, 24 hours prior to stimulation. Cells were then stimulated with LPS at 100 ng/ml, fixed with 10% formalin, permeabilized with 0.1% Triton X-100 solution, nuclei stained with Hoechst 33342 (1 ug/ml) and subsequently incubated with α -STAT3 antibody. The cells were probed with an Alex Fluor 488 goat α -rabbit antibody and mounted onto slides using Dako fluorescent medium. **(A)** Unstimulated RAW264.7 murine macrophages. **(B)** LPS stimulation for 20 minutes. **(C)** LPS stimulation for 40 minutes. **(D)** LPS stimulation for 60 minutes. Unstimulated RAW264.7 murine macrophages displayed high levels of STAT3 in the nucleus, with an increase in STAT3 nuclear localisation following LPS stimulation in a time-dependent manner. All images are single confocal sections taken with a 60x oil objective lens. These results are a representation of three individual experiments (n=3), where >100 cells were examined per condition.

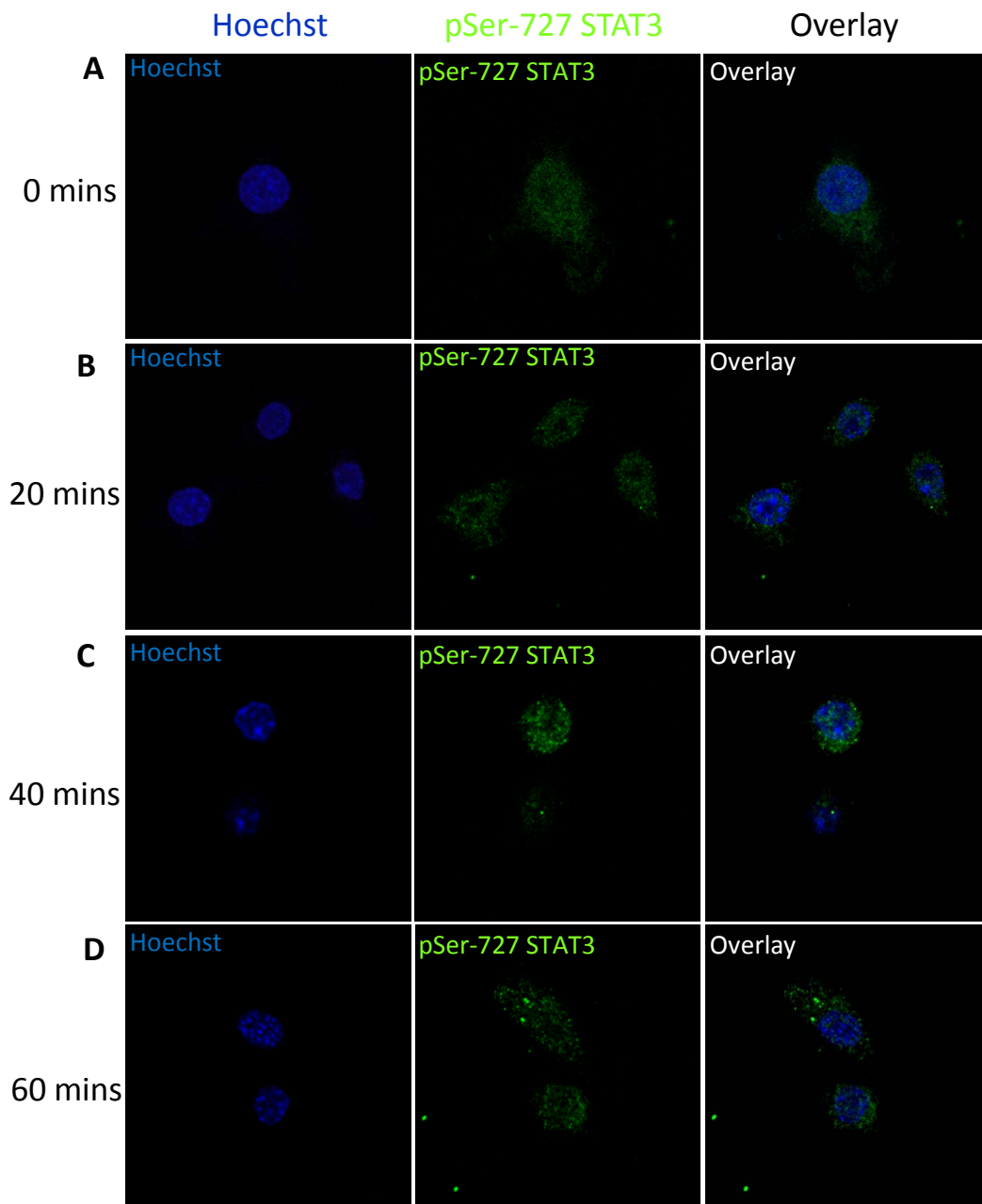


Figure: 4.7: pSer-727 STAT3 can be detected in the cytoplasm following LPS stimulation.

RAW264.7 murine macrophages were prepared as described in figure 4.6, but were probed with α -pSTAT3 (Ser-727) antibody. **(A)** Unstimulated RAW264.7 murine macrophages. **(B)** LPS (100 ng/ml) stimulation for 20 minutes. **(C)** LPS stimulation for 40 minutes. **(D)** LPS stimulation for 60 minutes. Diffuse staining of pSer-727 STAT3 is seen following LPS stimulation. All images are single confocal sections taken with a 60x oil objective lens. These results are a representation of three individual experiments (n=3), where >100 cells were examined per condition.

pSer-727 STAT3 with Hoechst stain, illustrates some pSer-727 STAT3 localised to the nucleus with the majority remaining in the cytoplasm.

These results are consistent with my earlier observations of TLR-induced specific Ser-727 phosphorylation of STAT3. Whilst LPS does induce a time-dependent increase in STAT3 Ser-727 phosphorylation, pSer-727 STAT3 is not detected in the nucleus at the levels identified in STAT3 stained cells.

4.2.6 – Rapid nuclear localisation of pTyr-705 STAT3 is not observed in TLR stimulated cells

Having found that pSer-727 STAT3 is not translocated to the nucleus post-stimulation, I next examined tyrosine phosphorylation of STAT3. RAW264.7 murine macrophages were stimulated with LPS and probed for Tyr-705 STAT3 using pSTAT3 (Tyr705) antibody.

Unstimulated cells displayed a low level of pTyr-705 STAT3 and when overlaid with Hoechst stain did not demonstrate staining characteristic of nuclear localisation (Figure 4.8A). Following LPS stimulation, pTyr-705 STAT3 staining appears to be unaltered, with the staining pattern observed to be diffuse throughout the entire cell (Figure 4.8B & C). Hoechst and pTyr-705 STAT3 overlaid images illustrated no colocalisation of STAT3 in the nucleus indicating that STAT3 detected in nuclei was not pTyr-705 STAT3 (Figure 4.8B & C, Overlay). Nuclear localisation of pTyr-705 STAT3 is observed at 60 minutes post-stimulation matching immunoblotting data from chapter 3 and is thought to be induced by type I IFN secretion.

pTyr-705 STAT3 can be detected after LPS stimulation although the levels of this do not change from unstimulated cells except at 60 minutes post-stimulation. It appears that the high level of STAT3 nuclear localisation is possibly neither pSer-727 nor pTyr-705 STAT3, but is consistent with unphosphorylated STAT3 which has previously been documented Meyer et al. (2002). However differences in antibody affinity have not been accounted for.

4.2.7 – pSer-727 STAT3 localises to mitochondria

Studies conducted by Gough et al. (2009) found that in Ras-transformed cells pSer-727 STAT3 was found to colocalise in mitochondria. From my confocal microscopy images the punctate staining of pSer-727 STAT3 in the cytoplasm may potentially colocalise to mitochondria, hence I wished to determine if LPS-induced pSer-727 STAT3 can localise to mitochondria.

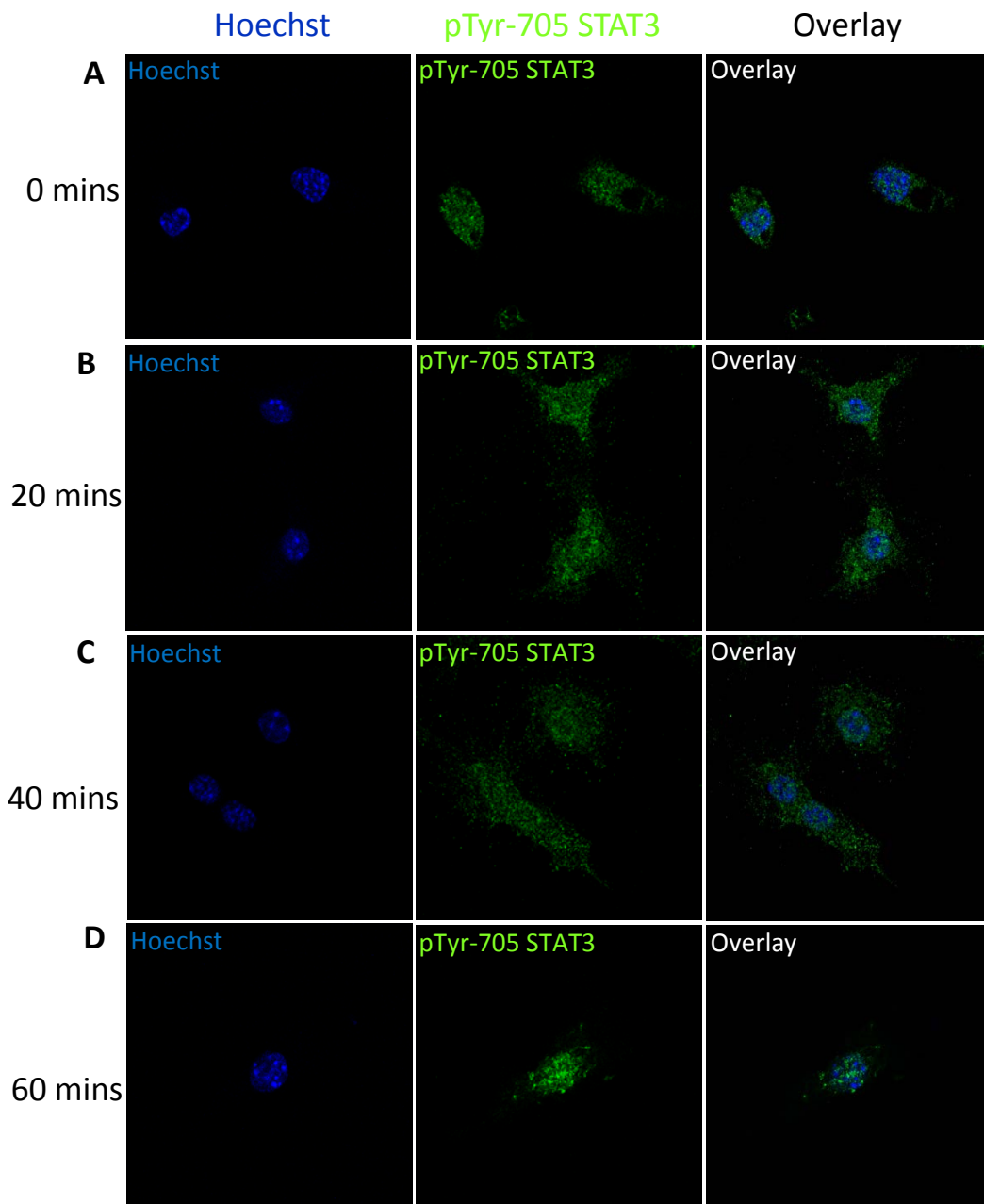


Figure: 4.8: pTyr-705 STAT3 increases following LPS stimulation and can be detected in the nucleus 60 minutes post-stimulation.

RAW264.7 murine macrophages were prepared as described in figure 4.6 and probed with α -pSTAT1 (Tyr-705) antibody. **(A)** Unstimulated RAW264.7 murine macrophages. **(B)** LPS (100 ng/ml) stimulation for 20 minutes. **(C)** LPS stimulation for 40 minutes. **(D)** LPS stimulation for 60 minutes. Diffuse staining of pTyr-705 STAT3 was seen following LPS stimulation. At 60 minutes, nuclear localisation of tyrosine phosphorylated STAT3 can be observed. All images are single confocal sections taken with a 60x oil objective lens. These results are a representation of three individual experiments ($n=3$), where >100 cells were examined per condition.

As can be observed in figure 4.9A, unstimulated cells demonstrate very low staining of pSer-727 STAT3. The reduction in background staining can be attributed to the use of digitonin to further permeabilize the cell membrane to decrease non-specific staining. Consistent with earlier results, LPS induces punctate staining of pSer-727 STAT3 and when overlaid with Mitotracker Red leads to colocalisation of pSer-727 STAT3 and mitochondria. Only a low concentration of pSer-727 STAT3 colocalises to mitochondria and this is similar to that observed by Gough et al. (2009). Mitochondrial localisation of STAT3 occurs in a time-dependent manner commensurate with my prior findings of small concentrations of pSer-727 STAT3 detected in the nucleus (Figure 4.9B-D).

To further confirm that pSer-727 STAT3 colocalised to mitochondria, intensity profile plots of colocalisation were conducted on a single plane. The histogram plot represents the intensity of individual pixels (Y-axis) along a line (X-axis) as shown in figure 4.10. As can be seen in figure 4.10A, over the 60 minute time course, colocalisation of pSer-727 STAT3 and Mitotracker Red is observed at 20, 40 (Figure 4.10B) and 60 minutes post LPS treatment (Figure 4.10C). This is confirmed by intensity profile plots which demonstrate the histogram of Mitotracker Red overlays with that of pSer-727 STAT3 and is observed to occur at all three time points.

These results demonstrate that the LPS-induced Ser-727 phosphorylation of STAT3 results in its mitochondrial localisation persisting for at least 60 minutes post-stimulation.

4.2.8 – Total STAT3 does not localise to mitochondria and remains in the nucleus

Due to the high level of basal STAT3 that was detected in figure 4.1, I next wanted to determine whether total STAT3 could also colocalise to mitochondria.

In order to remove background and non-specific staining digitonin washes were implemented and as can be observed, unstimulated RAW264.7 murine macrophages displayed no staining of STAT3 in the cytoplasm however, STAT3 can be detected in the nucleus (Figure 4.11A). Cells were serum starved overnight in serum-free media to reduce basal STAT3 activation, though STAT3 can still be observed in nuclei suggesting the RAW264.7 murine macrophages have an increased level of basal STAT3 activation. Consistent with earlier results, stimulation with LPS induces a time-dependent enrichment of STAT3 nuclear localisation, although STAT3 is not detected in the cytoplasm, except at 60 minutes (Figure 4.11D). The overlaid images with Hoechst and Mitotracker Red illustrates that STAT3 is only detected in the nucleus, with no colocalisation of STAT3 and Mitotracker Red (Figure 4.11). The punctate staining in the cytoplasm observed at 60 minutes post LPS stimulation is consistent with the staining pattern observed in figure 4.9 indicating pSer-727 STAT3 is found in the cytoplasm.

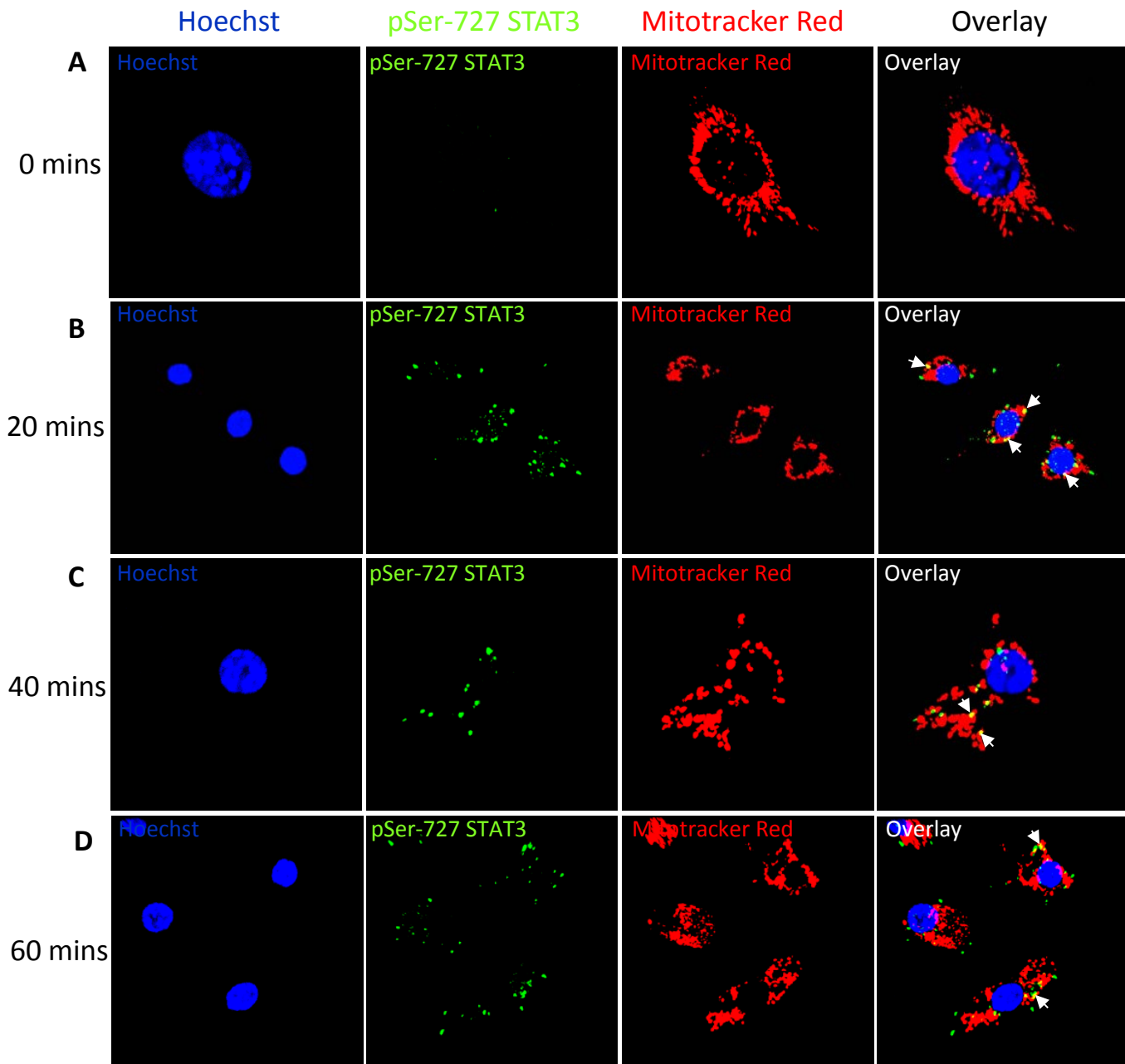


Figure: 4.9: LPS stimulation results in pSer-727 STAT3 colocalisation with mitochondria.

RAW264.7 murine macrophages were prepared as described in figure 4.6. Mitochondria was stained using Mitotracker Red CMXRos (100 nM) prior to fixation and cells were probed with α -pSTAT1 (Ser-727) antibody **(A)** Unstimulated RAW264.7 murine macrophages. **(B)** LPS (100 ng/ml) stimulation for 20 minutes. **(C)** LPS stimulation for 40 minutes. **(D)** LPS stimulation for 60 minutes. Punctate staining of pSer-727 STAT3 can be observed following LPS stimulation. When overlaid with Mitotracker Red it can be seen that pSer-727 STAT3 colocalises with mitochondria (Arrows indicate colocalisation). All images are single confocal sections taken from a Z-stack with a 60x oil objective lens. These results are a representation of three individual experiments (n=3), where >100 cells were examined per condition.

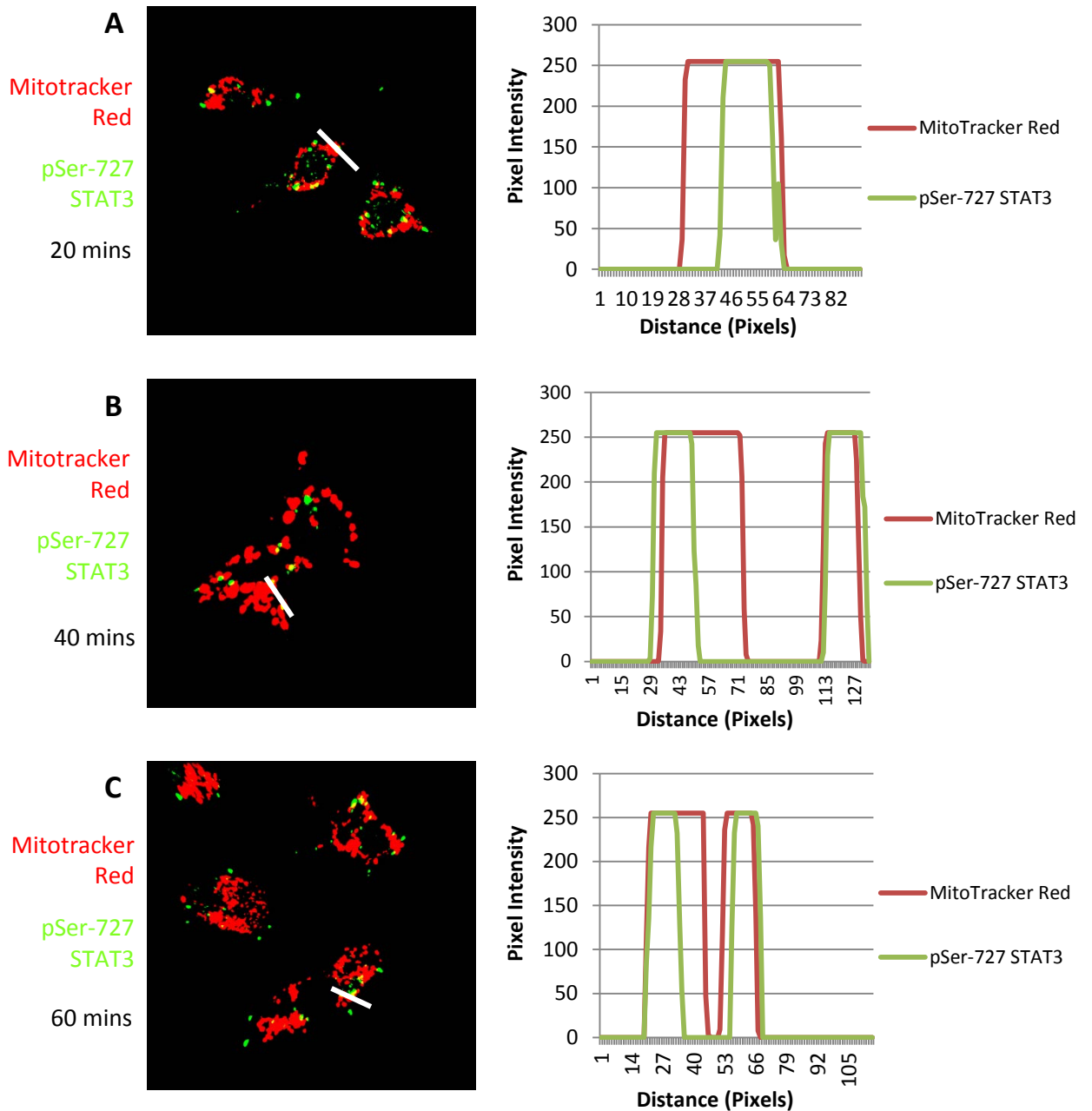


Figure: 4.10: Intensity profile plot demonstrates colocalisation of Mitotracker Red and pSer-727 STAT3.

Images from figure 4.9 were analysed using an intensity profile plot. Histograms depict colocalisation of pixels from different channels over a distance. Colocalisation of pixels from Mitotracker Red and pSer-727 STAT3 can be observed. The white line indicates the area examined for colocalisation. **(A)** 20 minutes post LPS stimulation. **(B)** 40 minutes post LPS stimulation. **(C)** 60 minutes post LPS stimulation.

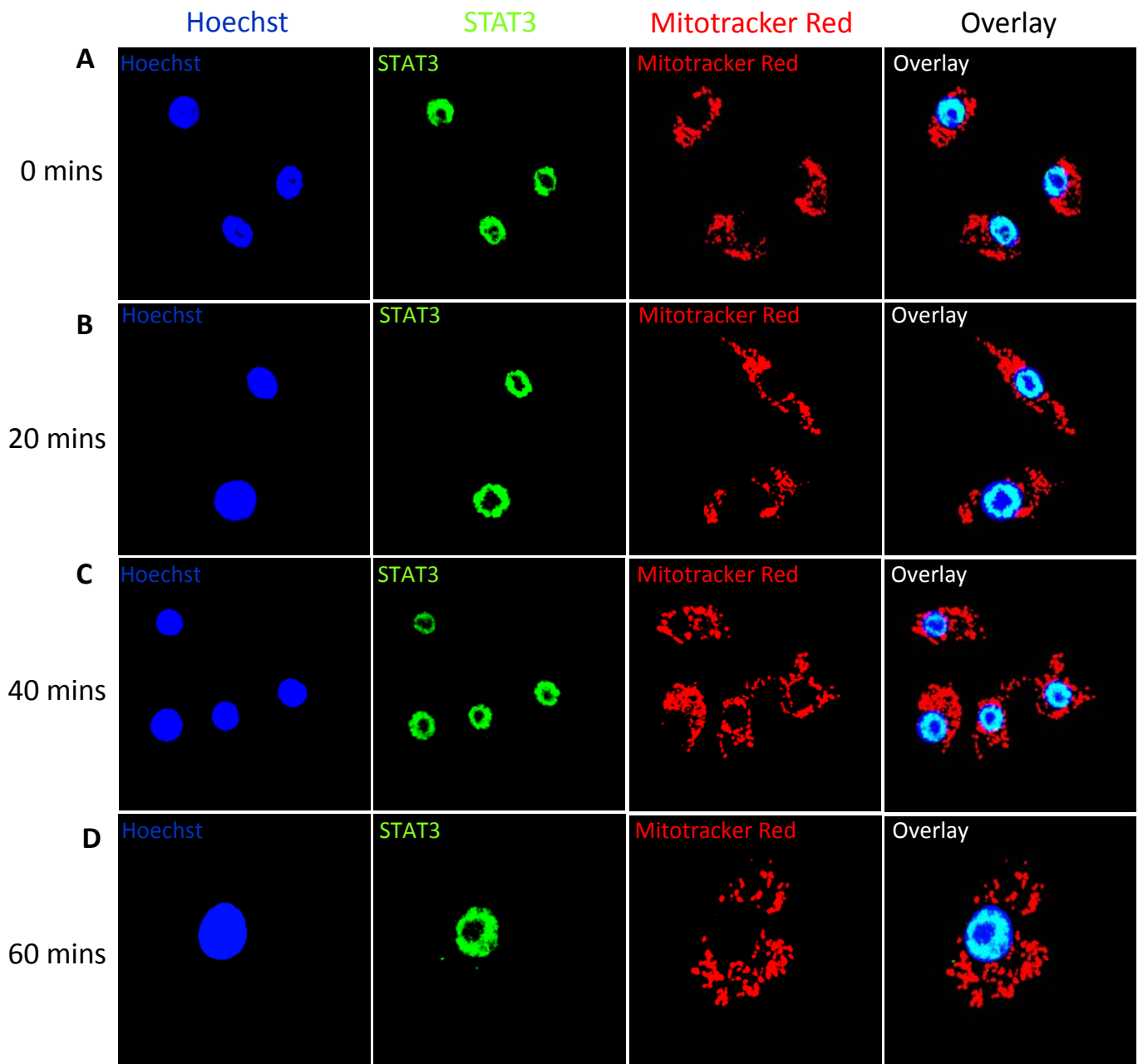


Figure 4.11: STAT3 does not colocalise with mitochondria.

RAW264.7 murine macrophages were prepared as described in figure 4.6. **(A)** Unstimulated RAW264.7 murine macrophages. **(B)** LPS stimulation for 20 minutes. **(C)** LPS stimulation for 40 minutes. **(D)** LPS stimulation for 60 minutes. High basal levels of STAT3 can be observed localised in the nucleus in unstimulated cells. Following LPS stimulation, nuclear levels of STAT3 remain consistent. All images are single confocal sections taken from a Z-stack with a 60x oil objective lens.

These results are a representation of three individual experiments (n=3), where >100 cells were examined per condition.

My results demonstrate that there is a basal level of STAT3 that is localised in the nucleus and this persisted after LPS stimulation. STAT3 is not detected in mitochondria which concurs with observations made by Gough et al. (2009), who demonstrated that only pSer-727 STAT3 localises to mitochondria. The punctate staining of STAT3 in the cytoplasm matches with staining of pSer-727 STAT3 suggesting that pSer-727 STAT3 localises to mitochondria.

4.2.9 – TRAF6 colocalises with pSer-727 STAT3, but this complex is not detected in mitochondria

As I have previously demonstrated that STAT3 interacts with TRAF6 and following TLR ligand stimulation STAT3 undergoes serine phosphorylation localising to the mitochondria to potentially generate ROS through disruption of the ETC. I therefore wanted to determine if STAT3 localises to the mitochondria in conjunction with TRAF6. During my studies, it was reported by West et al. (2011) that TRAF6 can also be found localised to mitochondria following TLR agonists stimulation. Therefore I investigated the ability of pSer-727 STAT3/TRAF6 to localise to mitochondria.

RAW264.7 murine macrophages were stimulated with LPS over a 60 minute time course and stained with Hoechst stain, Mitotracker Deep Red, a TRAF6 antibody and a pSer-727 STAT3 antibody. As both TRAF6 and pSer-727 STAT3 are detected at their highest concentrations at 30 and 60 minutes, respectively, my confocal microscopy experiments focused on these time points. In unstimulated cells, TRAF6 and STAT3 do not appear to colocalise and pSer-727 STAT3 is only detected at very low levels (Figure 4.12A). Merging of the channels illustrates a lack of mitochondrial localisation of both TRAF6 and pSer-727 STAT3 agreeing with my previous data, suggesting a stimulus is required before translocation of these proteins occur. After stimulation with LPS for 30 minutes however colocalisation between pSer-727 STAT3 and TRAF6 can be observed (Figure 4.12B). Both pSer-727 STAT3 and TRAF6 can be observed to localise to the mitochondria independently. Although a pSer-727 STAT3/TRAF6 complex doesn't appear to localise to the mitochondria. The same pattern of interaction can also be seen 60 minutes post-stimulation. Individually pSer-727 STAT3 and TRAF6 can be found to localise to mitochondria, but this complex cannot be identified in mitochondria. Intensity profile plots further confirm my observations, displaying cointensities of fluorescence between pSer-727 STAT3/TRAF6 (Figure 4.13A), Mitotracker Deep Red/pSer-727 STAT3 (Figure 4.13B) and Mitotracker Deep Red/TRAF6 (Figure 4.13C).

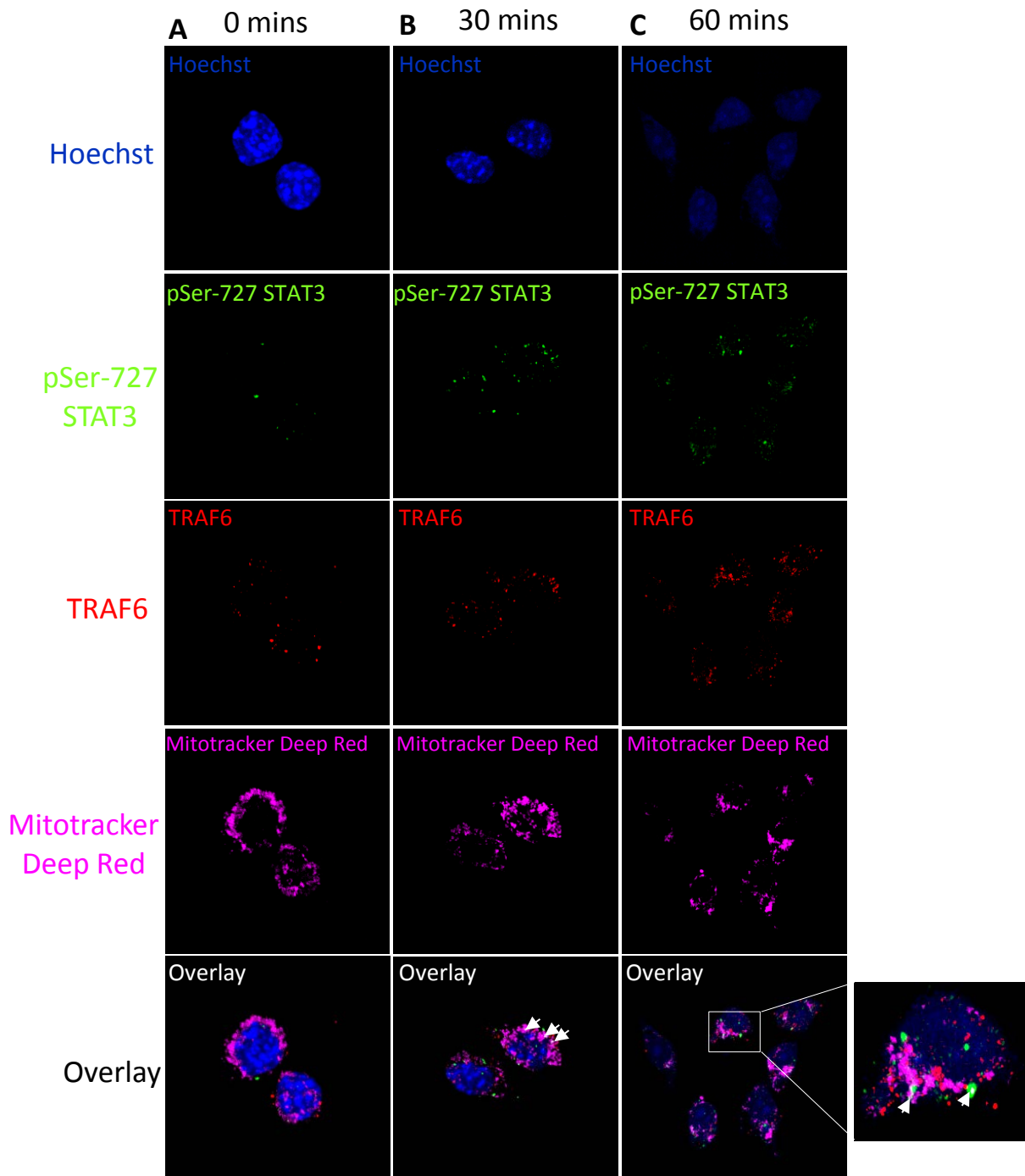


Figure: 4.12: LPS stimulation results in pSer-727 STAT3 colocalisation with TRAF6 and pSer-727 STAT3 and TRAF6 can be observed to colocalise with mitochondria individually.

RAW264.7 murine macrophages were prepared as described in figure 4.6. Before fixation cells were stained with Mitotracker Deep Red (100 nM) then probed with α -TRAF6 and α -pSTAT3 (Ser-727) antibody. **(A)** Unstimulated RAW 264.7 murine macrophages. **(B)** LPS stimulation for 30 minutes. **(C)** LPS stimulation for 60 minutes. pSer-727 STAT3 and TRAF6 is not observed to colocalise in unstimulated cells, but following LPS stimulation pSer-727 STAT3/TRAF6 colocalisation was seen. The pSer-727 STAT3/TRAF6 complex was not observed to be localising in mitochondria, even after LPS stimulation. All images are single confocal sections taken from a Z-stack with a 100x oil objective lens. These results are a representation of three individual experiments (n=3), where >100 cells were examined per condition.

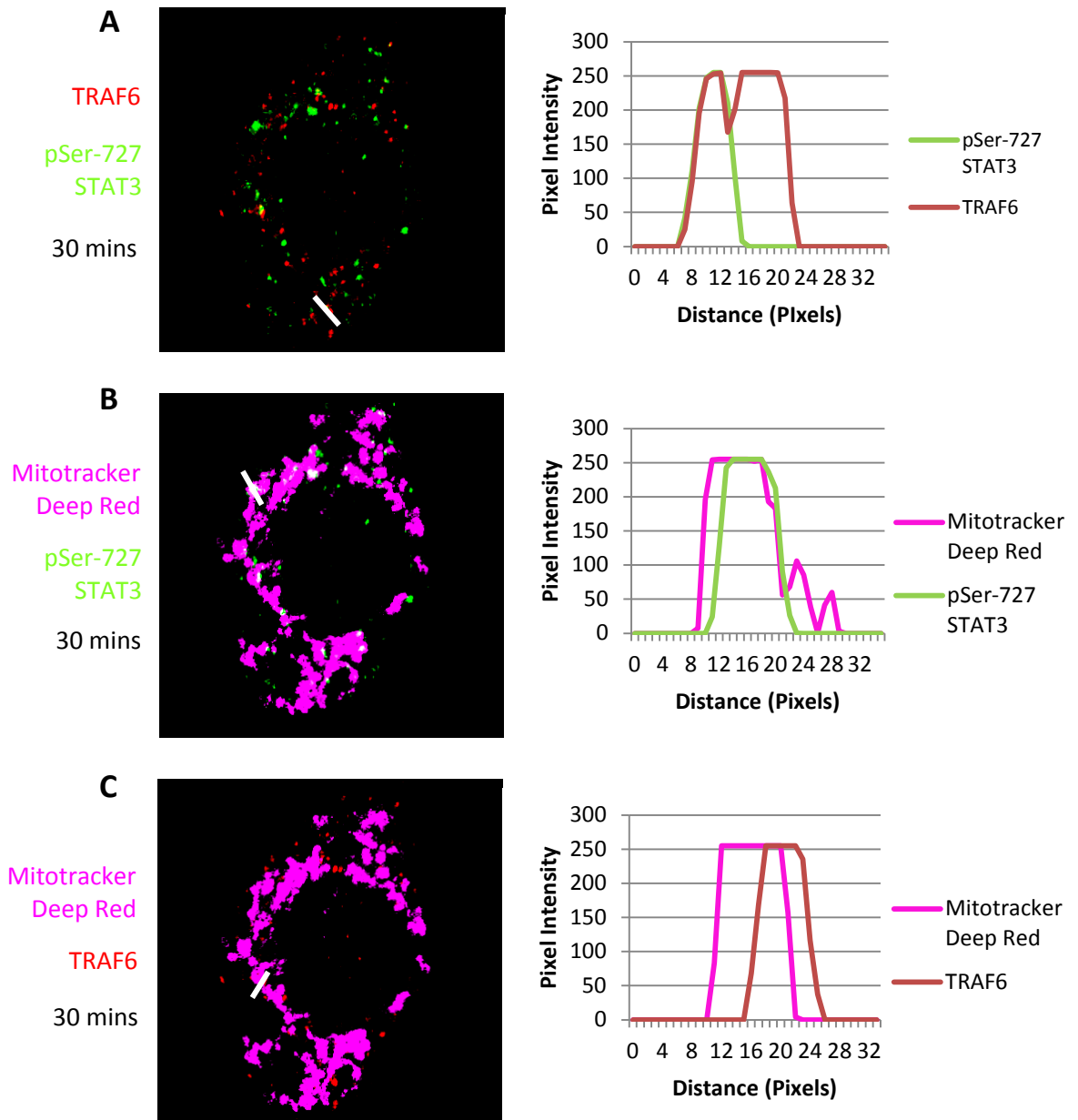


Figure: 4.13: pSer-727 STAT3 colocalises with TRAF6 and mitochondria, TRAF6 also colocalises with mitochondria however of a complex of pSer-727 STAT3/TRAF6 in mitochondria was not observed.

Images from figure 4.12 were analysed using line profile plot analysis. **(A)** Colocalisation of TRAF6 and pSer-727 STAT3 can be observed in LPS stimulated cells. **(B)** Similar to previous findings, pSer-727 STAT3 colocalises to mitochondria after stimulation **(C)** Following LPS treatment, TRAF6 was also illustrated to localise to mitochondria.

Whilst STAT3 undergoes serine phosphorylation and interacts with TRAF6, the complex of pSer-727 STAT3 and TRAF6 does not localise to the mitochondria together. Instead, pSer-727 STAT3 and TRAF6 individually localise to mitochondria.

4.2.10 – pSer-727 STAT3 and TRAF6 can be detected in mitochondrial extracts

In order to validate the confocal microscopy data, I next purified mitochondrial extracts and probed for pSer-727 STAT3 and TRAF6. As THP1 cells were demonstrated in chapter 3 to exhibit pSer-727 STAT3/TRAF6 interaction and the ease of growing large quantities, these cells were elected for this experiment. THP1 cells were stimulated with Pam₃Cys and LPS, lysed using nitrogen cavitation and mitochondria were purified using α -TOM22 (outer mitochondria membrane protein) magnetic microbeads. Mitochondrial extracts were then probed with α -TRAF6 and α -pSer-727 STAT3 antibodies.

Consistent with figure 4.13, both pSer-727 STAT3 and TRAF6 can be detected in mitochondria, interestingly, both proteins are also found in unstimulated cells although these cells were not serum starved (Figure 4.14). In Pam₃Cys stimulated THP1 cells, both TRAF6 and pSer-727 STAT3 concentrations remain consistent throughout the time course (Figure 4.14A). In contrast, LPS treated cells displayed a time-dependent enrichment of pSer-727 STAT3, with the levels of pSer-727 STAT3 peaking at 30 minutes (Figure 4.14B). However, the concentration of TRAF6 exhibits little variation from 0 to 60 minutes.

These results demonstrate that both pSer-727 STAT3 and TRAF6 can localised to mitochondria and confirm my observations from confocal microscopy images.

4.2.11 –STAT3 S727A mutant inhibits NF κ B activation

STAT3 traditionally acts as a transcription factor following Tyr-705 phosphorylation, although it is unknown whether just Ser-727 phosphorylation alone can induce gene transcription. Hence I generated a STAT3 mutant containing a serine to alanine mutation at the 727 residue in order to examine the potential ability of pSer-727 STAT3 in driving promoter activation.

HEK293 cells stably expressing TLR2 were transfected with an NF κ B fused to a luciferase construct along with STAT3 or STAT3 S727A. Following stimulation with Pam₃Cys, STAT3 was able to drive production of NF κ B promoter activity. In contrast, STAT3 S727A transfected cells displayed reduced activation of the NF κ B promoter suggesting that STAT3 S727A is acting as a dominant negative inhibitor (Figure 4.15).

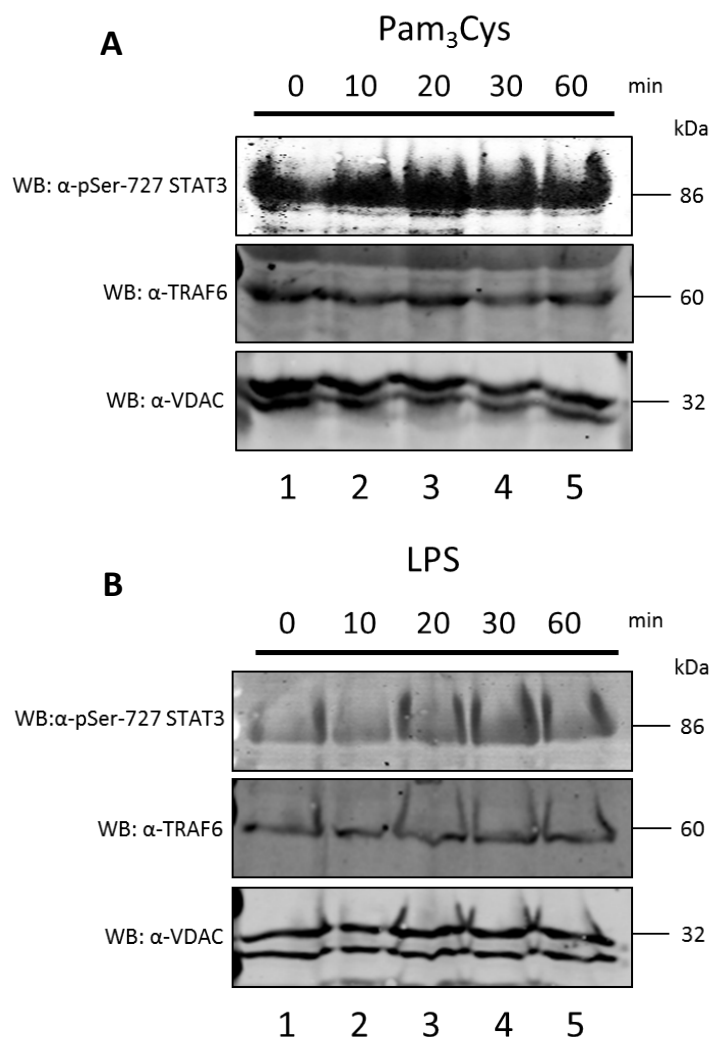


Figure: 4.14: pSer-727 STAT3 and TRAF6 can be detected in mitochondria.

THP1 cells were seeded at 2×10^7 cells/well, 24 hours prior to stimulation with TLR ligands as indicated. Cells were harvested in 10 ml of PBS and subjected to nitrogen cavitation. Cellular lysates were labelled with α -TOM22 magnetic microbeads and rotated for 60 minutes at 4°C. Mitochondria were isolated through column purification and subjected to gel electrophoresis and probed with α -pSTAT3 (Ser-727) (panel 1), α -TRAF6 (panel 2) and α -VDAC (panel 3) antibodies. THP1 cells were stimulated with **(A)** Pam₃Cys (100 ng/ml) stimulation. Both pSer-727 STAT3 and TRAF6 can be detected in mitochondria in unstimulated and stimulated cells, though levels of either protein are not enriched after stimulation. **(B)** LPS (100 ng/ml) stimulation. Similar to (A), pSer-727 STAT3 and TRAF6 were found in the mitochondria. After LPS stimulation levels of pSer-727 STAT3 can be observed to increase, but TRAF6 levels remained constant. These results are a representation of three individual experiments (n=3).

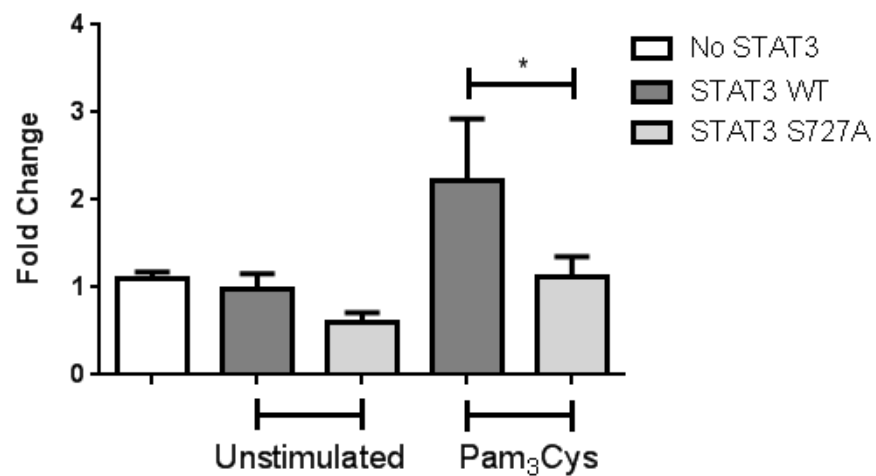


Figure: 4.15: STAT3 S727A acts as a dominant negative inhibiting activation of Nfkb.

HEK293 cells stably expressing TLR2 were seeded at 2×10^4 cells/well in a 96-well plate, 24 hours prior to transfection with Fugene-6 transfection reagent. The cells were transfected with NF κ B promoter fused to a luciferase vector and either STAT3 WT or STAT3 S727A mutant. 24 hours later, cells were stimulated with Pam₃Cys (100 ng/ml) for 6 hours. In response to Pam₃Cys stimulation, the mutant STAT3 demonstrated impaired NF κ B promoter activation compared to WT STAT3. Transfection efficiency was determined by comparing to a constitutively expressed reporter gene, TK Renilla. Pooled data is represented as mean \pm SEM of three independent experiments (n=3).

Taken together these results demonstrate that the Ser-727 residue of STAT3 is important in driving promoter activation as the STAT3 S727A mutant decreases NF κ B activation.

4.2.12 – STAT3 depletion using siRNA

As STAT3 Ser-727 phosphorylation is able to drive NF κ B activation, I next wanted to knockdown STAT3 to examine their ability to induce cytokine expression.

RAW264.7 murine macrophages were transfected with a control or STAT3 siRNA and then incubated for 72 hours before harvesting. Cell lysates were separated on a 10% SDS-PAGE gel and probed for STAT3. Immunoblotting illustrates that STAT3 has been successfully depleted in RAW264.7 murine macrophages, with β -tubulin confirming equal protein loading (Figure 4.16).

4.2.13 – IL-6 is attenuated in STAT3-depleted macrophages, but TNF- α production is not affected

RAW264.7 murine macrophages depleted of STAT3 were next stimulated using Pam₃Cys, LPS and CpG DNA. These ligands were selected to examine for differences between plasma membrane and endosomal TLRs, and also the use of MyD88-dependent or –independent signalling or both pathways in regards to TLR4.

As can be observed, IL-6 production is significantly ablated in STAT3-depleted macrophages. This attenuation of IL-6 secretion can be seen following stimulation with Pam₃Cys, LPS and CpG DNA suggesting that STAT3 is involved in the induction of IL-6 through all TLR ligands and is consistent with immunoblotting data from chapter 3 (Figure 4.17).

Next, I examined TNF- α , a proinflammatory cytokine that is activated during TLR signalling. Production of TNF- α is unaffected in STAT3 siRNA transfected cells in comparison to control siRNA transfected cells (Figure 4.18A). It appears that STAT3 plays a minimal role in TLR-induced TNF- α secretion.

A study conducted by Hoentjen et al. (2005) found that in BMDCs, STAT3 may also regulate IL-12 production. My experiments show that TLR stimulation did not induce IL-12, and knockdown of STAT3 had no effect on IL-12 production (Figure 4.18B).

Taken together these results demonstrate that STAT3 plays a role in TLR-mediated IL-6 production, but not TNF- α .

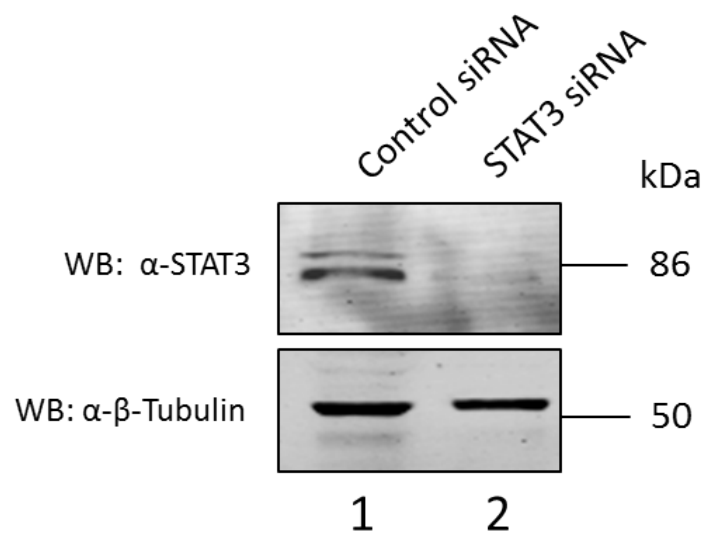


Figure: 4.16: STAT3 can be effectively silenced in macrophages.

RAW264.7 murine macrophages were seeded at 1×10^4 cells/well in a 96-well plate, 24 hours before transfection. Cells were transfected with 5 μ M of control siRNA or STAT3 siRNA and incubated for 72 hours. Cells were then harvested and separated on a 10% SDS-PAGE gel. STAT3 is demonstrated to be depleted 72 hours post-transfection compared with control siRNA. These results are a representation of three individual experiments (n=3).

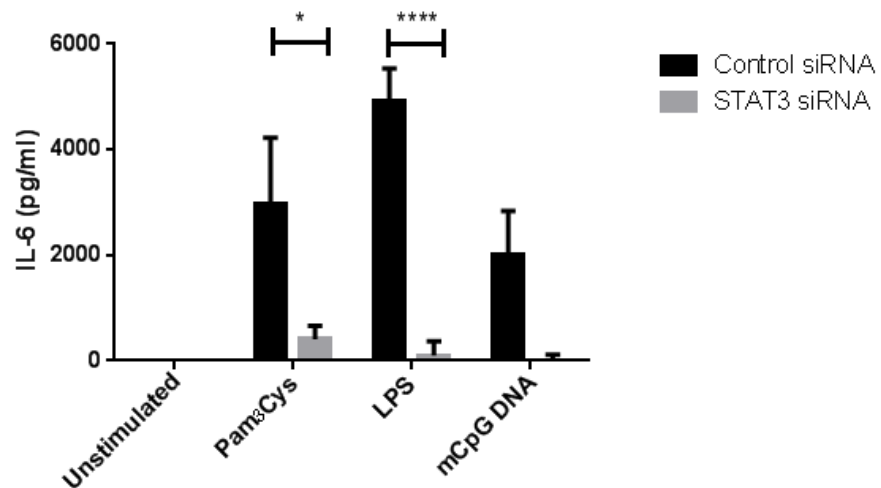


Figure: 4.17: IL-6 production is significantly decreased in STAT3-depleted RAW264.7 murine macrophages.

STAT3 depletion was performed as described in figure 4.16. RAW264.7 murine macrophages were then stimulated with Pam₃Cys (100 ng/ml), LPS (100 ng/ml) and mCpG DNA (500 nM) for 16 hours. Supernatants were collected and IL-6 production was measured by ELISA. Production of IL-6 was impaired in STAT3-depleted cells in comparison to control siRNA cells following TLR agonist stimulation. Pooled data is presented as mean \pm SEM of three independent experiments (n=3).

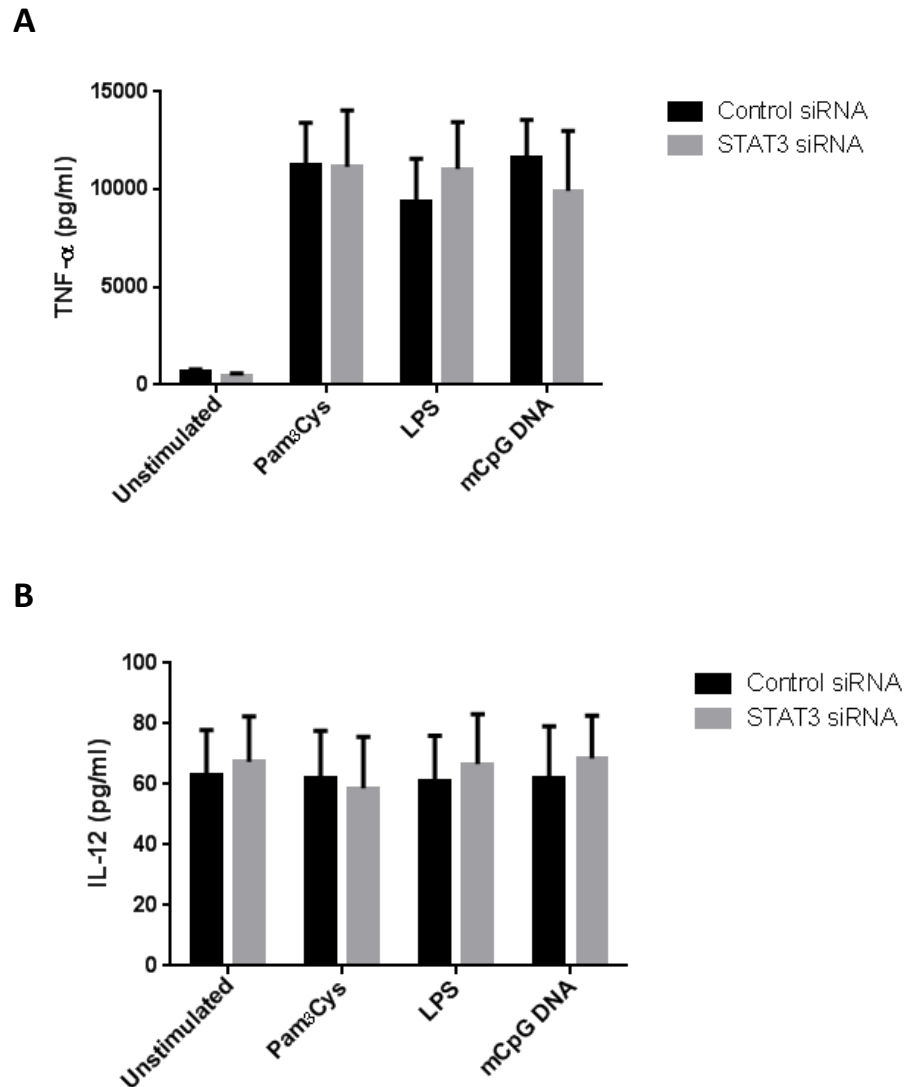


Figure: 4.18: TNF- α production is not diminished in STAT3 knockdown RAW264.7 murine macrophages, whilst TLR stimulation fails to induce IL-12 production.

RAW264.7 murine macrophages were prepared as described in figure 4.17. **(A)** Production of TNF- α was not affected in STAT3-depleted macrophages in comparison to control siRNA cells following stimulation with TLR agonists. **(B)** However, TLR stimulated cells failed to induce IL-12 secretion. Pooled data is presented as mean \pm SEM of three independent experiments (n=3).

4.3 - Discussion

The aims of this chapter are to further characterise the role of STAT3 in TLR signalling. Following TLR ligand stimulation, mitochondrial staining intensity can be observed to decrease indicative of a loss membrane potential. This may be a result of ROS production. TLR ligand stimulation was also able to induce production of ROS; specifically superoxide (DHE) and mtROS (MitoSOX). This is proposed to be due to STAT3 mitochondrial localisation as pSer-727 STAT3 can be found localised to mitochondria. Whilst STAT3 does interact with TRAF6, this complex is not seen localising to mitochondria, although both proteins can be detected in mitochondrial extracts. STAT3 S727A mutants inhibited activation of the NF κ B promoter and depletion of STAT3 resulted in decreased IL-6 production, but not TNF- α . Taken together my results suggest that following TLR ligand stimulation, STAT3 is Ser-727 phosphorylated, localises to mitochondria and induces ROS production. pSer-727 STAT3 can also regulate gene expression and STAT3 is required for inducing an optimal TLR-induced IL-6 response.

The ability of TLR signalling to influence mitochondria function was first demonstrated by West et al. (2011) who found translocation of TRAF6 to mitochondria via interaction with ECSIT, induced production of mtROS following TLR stimulation. Similar to these findings, my results also demonstrated that TLRs induced mtROS production. Although West et al. (2011) did not observe poly (I:C)-mediated mtROS, my results contradict this. TLR3 stimulation was able to induce ROS generation in both cytoplasmic and mitochondrial fractions; furthermore, levels of ROS production were comparable to Pam₃Cys stimulation. This suggest that poly (I:C) can induce production of ROS and the discrepancy between my findings and West and co-workers (2011) may be due to the time points examined. As can be observed in figure 4.1, after 24 hours of stimulation, Mitotracker Red can be observed to recover from the initial loss of staining at 2 hours. Thus it is possible that when West et al. (2011) examined mtROS at 16 hours post-stimulation the cells may have neutralised the mtROS produced. TLR3 stimulation has been documented to induce ROS generation, although this was demonstrated to result in both tyrosine and serine phosphorylation of STAT1 and its subsequent nuclear localisation (Yang et al., 2013). As ROS production was detected in the cytoplasm, it is likely that the main source of it originated from mitochondria. As I have demonstrated that pSer-727 STAT3 can interact with TRAF6 and pSer-727 STAT3 has been implicated to localise to mitochondria and interact with the ETC, it is therefore possible that Ser-727 phosphorylated STAT3 may also play a role in mtROS generation (Gough et al., 2009, Wegrzyn et al., 2009). Despite TRAF6 and STAT3 interaction observed in the cytoplasm (Figure 4.12) and the detection of both components in mitochondrial extracts (Figure

4.14), this complex was not detected in mitochondria. As discussed earlier, this suggests that whilst TRAF6 may facilitate STAT3 Ser-727 phosphorylation it does not transport pSer-727 STAT3 to mitochondria. It is likely that following STAT3 Ser-727 phosphorylation, both TRAF6 and STAT3 disengaged where, as illustrated by West et al. (2011) TRAF6 interacts with ECSIT and localises to the outer mitochondrial membrane. In contrast, STAT3 may interact with GRIM-19, a subunit of complex I of the ETC. *In vitro* studies demonstrated that GRIM-19 facilitated STAT3 mitochondrial import and a substitution of the Ser-727 residue to alanine reduced STAT3 recruitment to mitochondria (Tammineni et al., 2013). Taken together this suggests that TLR stimulation induces recruitment of STAT3 via TRAF6, resulting in its Ser-727 phosphorylation. After STAT3 serine phosphorylation, the STAT3/TRAF6 complex disassociates, TRAF6 interacts with ECSIT, whereas pSer-727 STAT3 may interact with GRIM-19, both complexes are then imported into mitochondria. Further studies are still required to determine the underlying mechanisms which regulate TLR-induced pSer-727 STAT3 mitochondrial localisation.

Purification of mitochondria and probing with pSer-727 STAT3 and TRAF6 antibodies further demonstrated mitochondrial localisation of Ser-727 phosphorylated STAT3 and TRAF6. Interestingly, both Ser-727 STAT3 and TRAF6 were detected in unstimulated cells which differs to West et al. (2011) who detected TRAF6 mitochondrial localisation at 5 minutes post TLR2 and TLR4 stimulation. The dissimilarity may be accounted for by the different methods employed in isolating mitochondria. The use of superparamagnetic microbeads conjugated to α -TOM22 antibody has been reported to isolate higher yields of mitochondria compared to differential centrifugation and ultra-centrifugation, hence the different results obtained by immunoblot (Hornig-Do et al., 2009). However, enrichment of TRAF6 was not observed following TLR2 or TLR4 stimulation and may be a result of different cell lines used. In contrast, similar to data shown by Gough et al. (2009) and Wegrzyn et al. (2009) pSer-727 STAT3 was detected in unstimulated cells. In Pam₃Cys stimulated cells, Ser-727 phosphorylated STAT3 was consistently high, although LPS stimulation resulted in time-dependent enrichment of pSer-727 STAT3 in mitochondria. The enrichment of Ser-727 phosphorylated STAT3 correlates with serine phosphorylation observed in immunoblotting data in chapter 3. This further confirms my results indicating that TLR stimulation induces mitochondrial localisation of pSer-727 STAT3.

Interestingly, a recent paper has demonstrated that TRAF6 binds STAT3 however, this was found to downregulate JAK-STAT signalling (Wei et al., 2012). TRAF6 interaction with STAT3 mediates its K63-linked ubiquitination, which is known to induce non-proteolytic functions (Chen and Sun, 2009). West and colleagues (2011) also showed that ECSIT underwent K63-linked ubiquitination

following TLR stimulation suggesting that it is possible that TRAF6-mediated ubiquitination may play a role in mitochondrial import. More work however, is still required to determine the role ubiquitination has in mitochondrial import of proteins.

Consistent with findings made by West and co-workers (2011), I demonstrated that TLR ligands can induce a reduction in Mitotracker Red staining which is thought to be a result of mtROS production. Interestingly, mitochondria membrane depolarisation was more profound in HT1080s and this may be a result of differing responses in myeloid and non-myeloid cell lines. The difference in kinetics may be explained by the fact that macrophages are able to utilise the respiratory burst, hence they are more resistant to the effects of ROS and in fact incorporate ROS in activation of proinflammatory cytokines and members of the MAPK family (Iles and Forman, 2002). Staining with the cytoplasmic superoxide detector, DHE and the mitochondrial ROS detector, MitoSOX confirmed that Pam₃Cys and LPS can induce mtROS production. The reduction of Mitotracker Red staining and generation of ROS correlates with the detection of pSer-727 STAT3 from my immunoblotting data; this suggests that Ser-727 phosphorylated STAT3 may induce ROS generation. This is supported by previous studies that have identified pSer-727 STAT3 in mitochondria (Gough et al., 2009, Wegrzyn et al., 2009). pSer-727 STAT3 was found to be highly enriched in murine mitochondria compared to cytoplasmic fractions and in STAT3^{-/-} cells mitochondrial oxidation rates were reduced by 70%, suggesting that STAT3 regulates mitochondrial respiration (Wegrzyn et al., 2009). This study was complemented by Gough et al. (2009) who found that pSer-727 STAT3 was required for Ras-transformation and mitochondrial function was dependent on Ser-727 phosphorylated STAT3. This demonstrates a requirement for STAT3 in mitochondrial function therefore the induction of pSer-727 STAT3 may induce ROS secretion. It is possible that Ser-727 phosphorylated STAT3 increases oxidative phosphorylation, which in turn induces ROS generation through the production of ATP, the increase in energy would therefore allow activation of other cellular functions to combat infection. (Cadenas and Davies, 2000). Thus the activation of STAT3 through TLR stimulation may not only induce inflammatory responses but the resulting ROS production has also been implicated to induce other cellular signalling pathways (Chandel et al., 1998, Janssen-Heininger et al., 2008, Kamata et al., 2005). In addition, ROS generation can also activate the prototypic proinflammatory transcription factor, NFκB, as pSer-727 STAT3's induction of ROS may augment the acute immune response (Schreck et al., 1991). Production of ROS by TLRs has previously been reported on. In root canal infections, macrophages stimulated with *Fusobacterium nucleatum* and *Peptostreptococcus anaerobius* produced high levels of NO and ROS (Marcato et al., 2008). Ryan et al. (2004) also reported that TLR4-induced NFκB activation and IL-8 production could be

inhibited by antioxidants, illustrating the emerging role ROS has in innate immune signal transduction. Induction of IL-12 by *Lactobacillus* was also reported to be dependent on ROS generation and MyD88 indicating the importance of ROS in TLR signalling. These studies and mine further demonstrate the emerging role ROS production plays in inflammatory responses, although further research into the mechanisms of STAT3-mediated ROS generation is still required to determine the functional role ROS has in innate immune responses.

Basal levels of STAT3 were high in unstimulated cells and STAT3 accumulated in both cytoplasmic and nuclear fractions. Staining for Tyr-705 and Ser-727 STAT3 however demonstrated that neither phosphorylated form of STAT3 accounted for the high amount of nuclear STAT3 detected. This suggests that the STAT3 detected could possibly be unphosphorylated STAT3. As STAT3 can be activated by growth factors it is possible that secretion of growth factors into media induced basal STAT3 activity. However, cells were serum starved overnight before stimulation in order to minimise basal STAT3 activation suggesting that RAW264.7 murine macrophages have increased levels of nuclear localised STAT3. Traditionally, STAT3 must first be activated by tyrosine phosphorylation, before dimerisation and its subsequent nuclear translocation. Meyer et al. (2002) however, identified that in unstimulated cells, both STAT1 and STAT3 were found to localise to the nucleus independent of tyrosine phosphorylation. STAT3 was also reported to dynamically shuttle between the cytoplasm and nucleus, and has been detected in nuclei in a range of immortalised and primary cells even following serum starvation (Liu et al., 2005). Nuclear translocation of STAT3 was demonstrated to be independent of tyrosine phosphorylation but instead required aa 150-162 which was necessary for interaction with importin- α 3. Importin- α 3 was found to bind STAT3 regardless of its phosphorylation state suggesting that pSer-727 STAT3 could also be transported into the nucleus.

The enrichment of total STAT3 observed in the nucleus may possibly suggest that unphosphorylated STAT3 may also regulate gene expression. Unphosphorylated STAT3 has been demonstrated to interact with NF κ B to bind specific κ B DNA motifs and this is dependent on the C-terminus of TRAF6 (Yoshida et al., 2003). Overexpression of TRAF6 was found to drive the p65 homodimer reporter, demonstrating that TRAF6s involvement may enhance the STAT3/p65 gene expression (Yoshida et al., 2003). The p50 subunit of NF κ B was also illustrated to interact with STAT3, whilst p65/STAT3 interaction inhibited GAS motif interaction, p50/STAT3 interaction can co-operate with STAT3 in binding to GAS elements (Yoshida et al., 2003). This suggests that TLR-induced recruitment of TRAF6 may drive STAT3/p65 gene expression and may explain the enrichment of total STAT3 observed in LPS stimulated cells. Further evidence in support of

unphosphorylated STAT3 gene expression has found that IL-1 and IL-6 stimulation induces STAT3/p65 formation and transcription of serum amyloid A, an indicator of the acute-phase response (Hagihara et al., 2005). Interestingly, Hagihara et al. (2005) found that Ser-727 phosphorylation of STAT3 was required for maximal transcription of serum amyloid A, suggesting that it is possible that pSer-727 STAT3 can potentially bind the p65 subunit of NFκB and is required to initiate maximum gene expression. Studies conducted by Yang and colleagues (2007a) further examined gene induction by STAT3 and NFκB. A STAT3 mutant containing a substitution of the Tyr-705 residue to phenylalanine was demonstrated to bind NFκB and κB elements in promoters, demonstrating that STAT3 nuclear localisation was independent of Tyr-705 phosphorylation. These studies therefore indicate that it is possible that pSer-727 STAT3 can be transported to the nucleus via interaction with NFκB. Recently, it has been demonstrated that unphosphorylated STAT3 can bind both γ-activated GAS sites as well as AT-rich DNA structures (Timofeeva et al., 2012). Interestingly, unphosphorylated STAT3 was able to bind GAS elements as both a monomer and dimer; furthermore unphosphorylated STAT3 also recognised DNA structures such as 4-way junctions and DNA crossings suggesting it may regulate chromatin structure. Whether Ser-727 phosphorylation of STAT3 alters the binding sites of STAT3 is unknown, however Ser-727 phosphorylation of STAT3 has been shown to be required for association with p300, a transcriptional co-activating protein (Schuringa et al., 2000). Taken together these studies demonstrate the ability of unphosphorylated STAT3 in regulating gene expression. As Ser-727 phosphorylation of STAT3 does not induce conformational changes it is possible that pSer-727 STAT3 may also bind NFκB. However, Ser-727 phosphorylation of STAT3 can potentially alter the DNA binding sites it recognises by binding other co-factors therefore further work is required to determine if pSer-727 STAT3 localises to the nucleus, the proteins it interacts with and the DNA binding sites that pSer-727 STAT3 recognises.

Only a small percentage of pSer-727 STAT3 was observed to localise in mitochondria and as STAT3 dynamically shuttles between the cytoplasm and nucleus, it is possible that Ser-727 phosphorylated STAT3 exhibits similar properties. This is also consistent with previous observations regulating Ras oncogene activation of pSer-727 STAT3 (D. Gough; personal communication) (Gough et al., 2009). Thus the ability of pSer-727 STAT3 to drive gene expression was investigated using a STAT3 mutant containing a substitution of the Ser-727 residue to alanine. Compared to WT STAT3, STAT3 S727A behaved as a dominant negative, inhibiting activation of the NFκB promoter following Pam₃Cys stimulation. This suggests the Ser-727 residue may regulate gene expression in response to TLR2 ligands. Other studies have also reported similar findings, with the most convincing being a mouse line in which the serine 727 residue was

substituted with alanine. Fibroblasts harvested from the mice only had ~50% of the transcriptional response compared to WT cells (Shen et al., 2004). In CLL cells, STAT3 was found to be constitutively phosphorylated on Ser-727 but not Tyr-705 and Ser-727 STAT3 was able to translocate to the nucleus and bind DNA (Hazan-Halevy et al., 2010). This suggests that pSer-727 STAT3 may also function as a transcription factor. As discussed earlier, unphosphorylated STAT3 can bind NF κ B and translocate to the nucleus. As serine phosphorylation is not known to induce a conformational change in STAT3 it is possible that pSer-727 STAT3 binds NF κ B and regulates gene expression (Yoshida et al., 2003). The requirement for Ser-727 in driving promoter activation could also be dependent on pSer-727 STAT3 recruitment of p300 (Schuringa et al., 2000). Whether this complex increases the DNA binding affinity of pSer-727 STAT3 is unknown, however it is possible that pSer-727 requires the recruitment of other co-factors to stabilize this interaction. My experiments and previous studies therefore suggest that the Ser-727 residue of STAT3 does modulate gene expression through a currently unknown mechanism.

To further investigate the role of STAT3 in TLR signalling, I next examined whether siRNA depletion of STAT3 affected induction of proinflammatory genes. In response to Pam₃Cys, LPS and CpG DNA, reduction of STAT3 severely impaired induction of IL-6. As STAT3 is the main mediator of IL-6 signalling (Akira et al., 1994), it is not unexpected that knockdown of STAT3 impairs IL-6 production. Greenhill et al. (2011) found that IL-6 trans-signalling was regulated by STAT3 in F/F mice stimulated with LPS. F/F mice crossed with STAT3^{+/-} mice alleviated LPS hypersensitivity and also reduced levels of IL-6 induced by LPS. My data concurs with this study and further demonstrates the role of STAT3 in TLR and JAK-STAT cross-talk not only through TLR4/LPS, but also through TLR2/Pam₃Cys and TLR9/CpG DNA. In contrast to IL-6 production, TNF- α secretion was not affected in STAT3-depleted cells. TNF- α levels were comparable to control siRNA treated cells, suggesting that STAT3 is not involved in TNF- α regulation. In response to LPS, STAT3 has been documented as a poor regulator of TNF- α in human monocytes as STAT3 does not directly inhibit I κ B degradation or TNF- α production, however STAT3 does suppress LPS-induced TNF- α production through activation of IL-10 (Prele et al., 2007). In concordance with this study, my results display a similar finding, STAT3 does not appear to regulate TNF- α production in response to TLR stimulation. Whilst TNF- α secretion was not affected in STAT3-depleted macrophages, TLR stimulation failed to induce production of IL-12p40. IL-12 is an important cytokine that serves as a bridge connecting the innate and adaptive immune response by inducing the maturation of type I T helper cells (Trinchieri, 1995). Although IL-12 can be induced by TLR stimulation (Brightbill et al., 1999), my results demonstrate that in RAW264.7 murine macrophages IL-12 stimulation does not appear to be induced by TLRs. However, further studies may explain this phenomenon in other

cell types such as DCs, fibroblasts, epithelial cells etc. In an IL-10-deficient enterocolitis mice model STAT3 activation has been demonstrated to reduce IL-12p40 expression by inducing production of SOCS3 (Kobayashi et al., 2003). Hoentjen et al. (2005) also reported that constitutively active STAT3 was able to inhibit LPS-induced IL-12p40 expression. This suggests that STAT3 functions by negatively regulating IL-12p40 production and this process is dependent on IL-10 signalling. Tyrosine phosphorylation appears to play a major role in this IL-10-dependent negative feedback loop, though whether Ser-727 phosphorylated STAT3 can negatively regulate IL-12p40 expression remains to be investigated. Taken together this suggests TLR-induced STAT3 activation regulates IL-6, but not TNF- α production. Whether Ser-727 phosphorylation of STAT3 plays a role in IL-6 secretion remains to be determined. Future studies would investigate cytokine expression in particular IL-6 in STAT3 S727A cells when available and whether STAT3 S727A can localise to mitochondria and induce mtROS production.

Constitutive STAT3 activation and unregulated STAT3 signalling has been implicated in the progression of many forms of cancer (Yu et al., 2009). Therefore understanding cross-talk between inflammatory signalling pathways may provide further insights into the activation of STAT3. In recent years, TLR signalling has also been implicated in driving the development of cancers. Tye and colleagues (2012) demonstrated in the F/F mice model that STAT3 directly upregulated expression of TLR2, which was found to promote both cell survival and proliferation in gastric cancer. This further demonstrates the importance of inflammation in cancers and represents potential therapeutic opportunities. A recent study has also demonstrated the role of mtROS in driving tumour survival (Yuan et al., 2013). Aggressive gastric tumours were identified to highly express TLR4 and this correlated with enhanced cell proliferation. The TLR4-induced mtROS generation is associated with increased cell survival and thus represents a new mechanism in regulating tumour growth. Mitochondrial STAT3 is known to upregulate ETC function and thus increase mtROS generation. Zhang and co-workers (2013) found in the breast cancer cell line 4T1, transfected with STAT3 S727D, had enhanced tumour growth, increased complex I activity and reduced ROS production. In contrast, STAT3 S727A transfected cells exhibited the opposite characteristics displaying slower tumour growth, decreased complex I activity and an increase in ROS production when under hypoxic conditions. Thus this suggests that mitochondrial located pSer-727 STAT3 could play a role in promoting tumour growth and demonstrates the potential role constitutive serine phosphorylated STAT3 has in cancer. My studies, combined with these previous works suggest that whilst the TLR-induced Ser-727 phosphorylation of STAT3 may augment the innate immune response, deregulation of this signalling pathway may have drastic consequences by producing an inflammatory milieu that favours tumour growth and/or

progression. Thus tight regulation of this inflammatory pathway is required by reducing inflammation through decreasing STAT3 Ser-727 phosphorylation, mtROS generation and IL-6 production may offer potential therapeutic benefits. Further research is still required to fully elucidate the mechanisms behind TLR-mediated STAT3-driven tumourigenesis.

In summary, this chapter provides an insight into the biological role pSer-727 STAT3 plays in innate immunity. Upon TLR ligand stimulation, STAT3 is rapidly serine phosphorylated and localises in mitochondria, there it induces production of mtROS. The generation of mtROS may therefore augment the innate immune response by activating secondary pathways. My results further demonstrate the importance of STAT3 and the Ser-727 residue in expression of cytokines as depletion of STAT3 or mutation of the Ser-727 residue impairs expression of specific proinflammatory cytokines. Future studies will be required to further elucidate the mechanisms of STAT3 mitochondria localisation, ROS production and how the pSer-727 STAT3 modulates the innate inflammatory response.

Chapter 5 – The Role of STAT1 Ser-727 in TLR-mediated Inflammation

Chapter 5 - The Role of STAT1 Ser-727 in TLR-mediated Inflammation

5.1 - Introduction

The functions attributed to STAT1 primarily relate to its role in mediating the effects of IFNs. Studies conducted with STAT1-deficient cells and STAT1 knockout mice have demonstrated that STAT1 has antiproliferative and pro-apoptotic effects when activated by IFNs (Durbin et al., 1996, Meraz et al., 1996, Bromberg et al., 1996, Kumar et al., 1997, Ramana et al., 2000). STAT1 was first identified to be recruited to the IFN- γ receptor, following activation of JAK1 and JAK2, the C-terminus of the IFN- γ receptor and JAKs become tyrosine phosphorylated, STAT1 is then recruited to the receptor where it undergoes tyrosine phosphorylation allowing its subsequent nuclear translocation and transcription of IFN- γ -dependent genes (Igarashi et al., 1994). It was also found that lymphocyte proliferation and survival required a transcriptionally active STAT1 however, it was only partially dependent on IFN- γ signalling (Lee et al., 2000). STAT1's involvement in cancer was demonstrated through the use of STAT1-deficient mice that were highly susceptible to chemically-induced and transplanted tumours, suggesting that STAT1 may potentially function as a tumour suppressor (Kaplan et al., 1998, Durbin et al., 1996).

The effect of Ser-727 phosphorylation on STAT1 was first shown by Wen et al. (1995) to be required for maximal transcriptional activity as STAT1 S727A mutants induced 80% less IFN- γ -dependent genes. It appears however that tyrosine phosphorylation is not a prerequisite for serine phosphorylation, as both residues can undergo phosphorylation independent of one another (Zhu et al., 1997). Levels of serine phosphorylated STAT1 are higher than that of tyrosine phosphorylated STAT1 suggesting that pSer-727 STAT1 may potentially exist as a monomer (Zhu et al., 1997). Kovarik et al. (1998) observed that following stimulation with LPS, UV irradiation and TNF- α , STAT1 also undergoes rapid Ser-727 phosphorylation independent of tyrosine phosphorylation, and this serine phosphorylation was demonstrated to increase STAT1-dependent gene transcription. Interestingly, although the Ser-727 phosphorylation of STAT1 increases its transcriptional activity, it does not increase its ability to bind DNA suggesting that Ser-727 phosphorylation does not induce conformational changes to STAT1 (Wen and Darnell, 1997). Mice expressing a mutant STAT1 S727A were challenged with *Listeria monocytogenes* and had increased mortality compared to WT mice (Varinou et al., 2003). These mice displayed impaired clearance of bacteria from the liver and spleen, although they were less susceptible to LPS-induced septic shock syndrome (Varinou et al., 2003). The expression of IFN- γ -dependent genes was also greatly reduced in these mice, though STAT1 S727A

chromatin binding was not affected. This study illustrates the role of serine phosphorylation in macrophage activation and induction of IFN- γ -dependent gene expression.

Previous studies have demonstrated pSer-727 STAT1's role in modulating gene expression. In human fibroblasts, TNF- α stimulation greatly enhanced apoptosis and STAT1 was found to be required for the constitutive expression of the caspase-1, caspase-2 and caspase-3 (Kumar et al., 1997). STAT1 Y701F mutants re-constituted into U3A cells, which lack STAT1, were sensitive to TNF- α -induced apoptosis, although expression of caspase-2 and caspases-3 were only slightly lower when compared to WT cells indicating that STAT1 dimerisation is not crucial for the regulation of these caspases. In contrast, the STAT1 S727A mutant were resistant to TNF- α -induced apoptosis and whilst levels of caspase-1 were comparable to WT cells, caspase-3 expression was reduced substantially suggesting that pSer-727 STAT1 may regulate the constitutive expression of specific genes. Further evidence demonstrating the importance STAT1 Ser-727 phosphorylation comes from a study which found that in Wilms' tumour, a paediatric solid cancer, STAT1 was identified to be constitutively phosphorylated on Ser-727 in 19 of 21 Wilms' tumour samples, in contrast Tyr-701 phosphorylation of STAT1 was not detected (Timofeeva et al., 2006). Ser-727 phosphorylated STAT1 was resistant to apoptosis through upregulating expression of HSP27 and anti-apoptotic protein Myeloid Cell Leukaemia Sequence 1 (MCL-1). It was also identified that the serine/threonine kinase Casein Kinase 2 (CK2) was responsible for serine phosphorylating STAT1 as inhibition of CK2 blocked anchorage-independent growth of cells and caused them to be more vulnerable to growth stresses thus resulting in apoptosis (Timofeeva et al., 2006). These studies indicate the Ser-727 phosphorylated STAT1 may also be a marker of disease.

STAT1 has been implicated in disease progression of atherosclerosis as it forms a point of convergence for TLR4/LPS and IFN- γ signalling (Sikorski et al., 2011a, Sikorski et al., 2011b). The synergism between LPS and IFN- γ signalling resulted in enhanced STAT1 phosphorylation, the expression of proinflammatory cytokines and the upregulation of Intracellular Adhesion Molecule 1 (ICAM-1) and chemokine IFN- γ -induced Protein 10 kDa (IP-10), both chronic inflammatory indicators (Sikorski et al., 2011a). Human Microvascular Endothelial Cells (HMECs) jointly stimulated with LPS and IFN- γ and subsequently treated with the STAT1 inhibitor, fludarabine, displayed reduced expression of ICAM-1 and IP-10, thus demonstrating STAT1's involvement in the initial onset of atherosclerotic plaque formation (Sikorski et al., 2011a). Additionally, in salivary gland cells STAT1 Ser-727 phosphorylation also appears to play an important role in IFN- γ -induced apoptosis (Tsuboi et al., 2011). Human salivary gland cells ectopically expressing STAT1 Y701F, expression of IP-10, IRF1 and Fas was increased following IFN- γ stimulation (Tsuboi et al., 2011). In contrast, cells transfected with STAT1 S727A and stimulated with IFN- γ only displayed an increase in IP-10 mRNA expression thus further demonstrating pSer-727 STAT1's ability to regulate specific gene expression. Following

IFN- γ treatment, STAT1 Y701F cells which can only undergo Ser-727 phosphorylation also exhibited increases in apoptosis, demonstrating that serine phosphorylation of STAT1 can have a role in inducing cellular functions (Tsuboi et al., 2011).

Recently it has been found that pSer-727 STAT1 may have a role in cells that express the antigen presenting molecule Human Leukocyte Antigen-subtypes B*2701-2759 (HLA-B27) (Ruuska et al., 2013). HLA-B27 has been implicated in increased disease susceptibility, although the mechanisms are still unknown. It is thought other than its role as an antigen presenting molecule, HLA-B27 may also modulate inflammatory responses further increasing susceptibility to spondylarthropathies, a chronic inflammatory joint disease of the vertebral column (Vahamiko et al., 2005). In U937 human monocytic cells transfected with HLA-B27, then infected with *Salmonella enteritidis*, STAT1 Ser-727 phosphorylation was prolonged and believed to exacerbate the inflammatory response. Whilst inhibition of PKR can block Tyr-701 phosphorylation (Ruuska et al., 2012), Ser-727 phosphorylation was not inhibited and STAT1 was demonstrated to localise into the nucleus in the infected HLA-B27 cells (Ruuska et al., 2013). STAT1's role in the pathogenesis of spondylarthropathies therefore appears to be dependent on STAT1 Ser-727 phosphorylation, its nuclear localisation and may be a result of excessive inflammation from the induction of proinflammatory genes.

TNF- α is well documented to be pivotal in driving the development of arthritis in patients and anti-TNF- α therapy has been revolutionary in the treatment of these chronic inflammatory joint diseases (Moelants et al., 2013, Olivieri et al., 2013). In patients with Reactive Arthritis (RecA), who are also HLA-B27 positive, LPS can be detected in their joints. LPS was found to enhance TNF- α production in HLA-B27 positive patients and this was determined to be the result of rapid and increased degradation of I κ B. (Penttinen et al., 2002). It is therefore possible that the prolonged STAT1 Ser-727 phosphorylation may contribute to macrophage activation and inflammatory cytokine expression ultimately leading to the development of spondylarthritis. Thus understanding the role pSer-727 STAT1 plays in inflammation is important for developing new therapies to alleviate symptoms or cure diseases.

The role of STAT1 in inflammation, in particular the role of TLR-induced pSer-727 STAT1 has not been fully explored. My finding that STAT1 interacts with TRAF6 and undergoes rapid Ser-727 phosphorylation following TLR stimulation suggests that STAT1 may play a role in TLR-mediated inflammation and modulation of macrophages. Whilst previous studies have demonstrated that TLR2 and TLR4 induced Ser-727 phosphorylation of STAT1, a biological function for the serine phosphorylation was not described. However Schroder and co-workers (2007) demonstrated a regulatory role for STAT1 serine phosphorylation differentially in DCs and macrophages. This chapter will examine the biological consequences of TLR stimulation in the absence of STAT1 and the

mutation of the Ser-727 residue to alanine rendering the phosphorylation site of STAT1 inactive. These studies will provide insights into the role STAT1 serine phosphorylation plays in TLR-induced proinflammatory responses.

5.2 – Results

5.2.1 – STAT1 localises to the nucleus following LPS stimulation

Having established a mechanism of cross-talk between TLR and JAK-STAT signalling via interaction of TRAF6 and STAT1, I wished to determine what the biological implications were of serine phosphorylation. Traditionally tyrosine phosphorylation leads to STAT1 dimerisation and its translocation to the nucleus where it acts as a transcription factor, serine phosphorylation also occurs in the cytoplasm but is delayed compared to tyrosine phosphorylation (Zhu et al., 1997). The role that serine phosphorylation plays and the cellular location of TLR-induced pSer-727 STAT1 have not been investigated. Therefore, I first examined the cellular location of LPS-induced STAT1 by fluorescence microscopy. LPS was chosen as it a very potent and immunogenic molecule that signals through TLR4 activating both the MyD88-dependent and –independent pathways.

RAW264.7 murine macrophages were stimulated with LPS at 0, 20, 40 and 60 minutes; time points I have previously demonstrated to induce strong STAT1 Ser-727 phosphorylation. Cells were then stained with Hoechst and probed for total STAT1 localisation. Unstimulated cells displayed STAT1 located in the cytoplasm with no STAT1 detected in the nucleus (Figure 5.1A). Following 20 minutes stimulation with LPS however, STAT1 can be detected translocating to the nucleus (Figure 5.1B). STAT1 accumulation in the nucleus was observed to increase in a time-dependent manner with detectable STAT1 increasing at 40 minutes (Figure 5.1C) with the majority of STAT1 translocated to the nucleus at 60 minutes (Figure 5.1D).

Taken together, this result demonstrates that TLR4 induces STAT1 nuclear localisation in a time-dependent manner.

5.2.2 – LPS induces pSer-727 STAT1 nuclear translocation

I next wanted to identify the phosphorylation state of nuclear localising STAT1. My studies and those conducted by Kovarik et al. (1999) and Rhee et al. (2003) demonstrated that LPS stimulation resulted in rapid Ser-727 phosphorylation with delayed tyrosine phosphorylation observed 2 hours post-stimulation, it is therefore possible that the nuclear localisation of STAT1 is a result of serine phosphorylation and not tyrosine phosphorylation.

As can be observed in Figure 5.2A, resting cells display little pSer-727 STAT1, similar to my earlier immunoblot data. LPS stimulation however, induces rapid nuclear localisation of pSer-727 STAT1, within 20 minutes, consistent to that observed for STAT1 (Figure 5.2B). Nuclear localised pSer-727

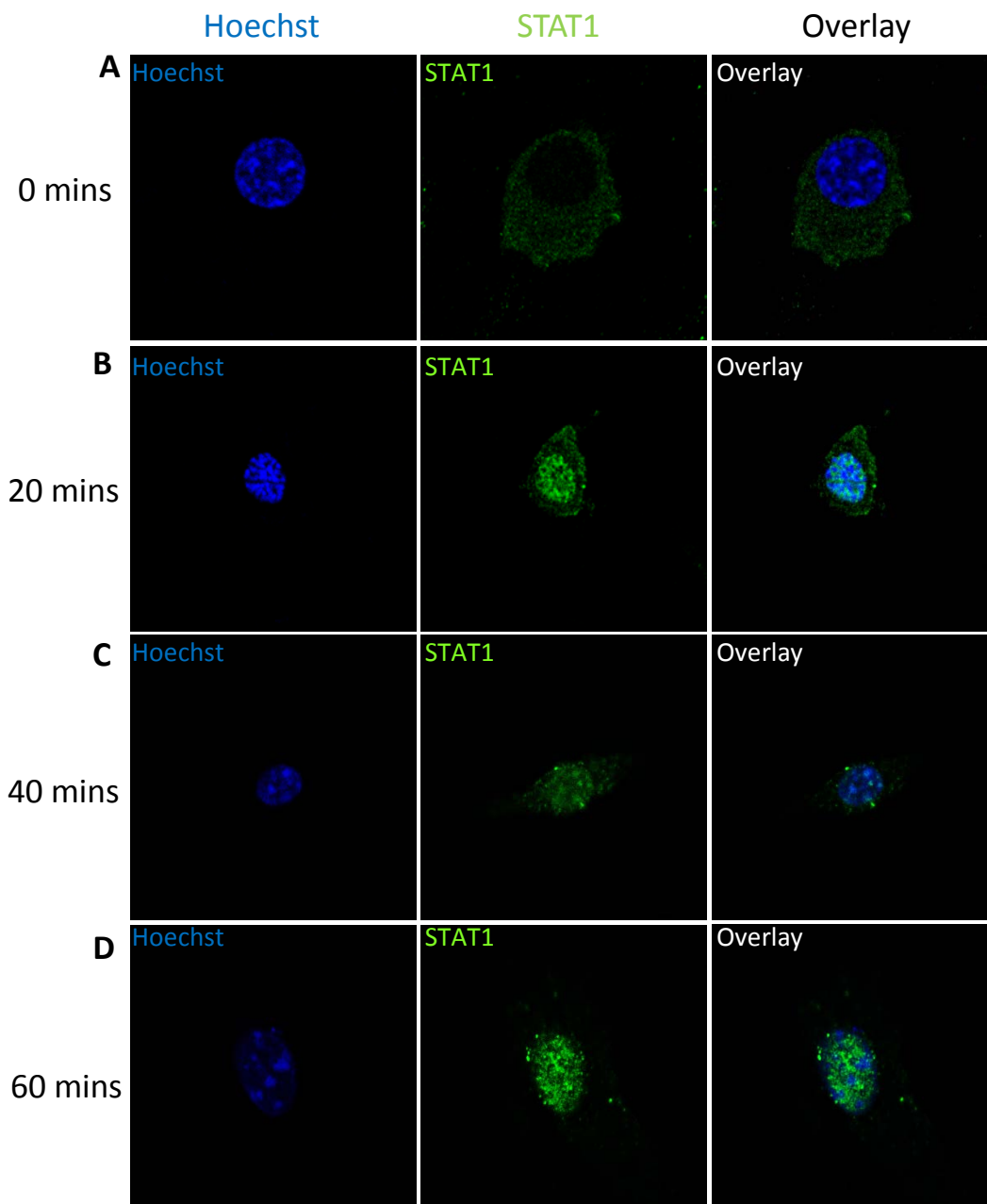


Figure 5.1: LPS stimulation induces nuclear localisation of STAT1.

RAW264.7 murine macrophages were seeded onto coverslips at 2×10^4 cells/well, 24 hours prior to stimulation. Cells were stimulated with LPS at 100 ng/ml for indicated time, fixed with 10% formalin, permeabilize with 0.1% Triton X-100 solution and stained with Hoechst 33342 (1 μ g/ml) and α -STAT1 antibody. STAT1 was visualised with Alexa Fluor 488 goat α -rabbit antibody and mounted onto slides using Dako fluorescent medium. **(A)** Unstimulated RAW264.7 murine macrophages. **(B)** LPS stimulation for 20 minutes. **(C)** LPS stimulation for 40 minutes. **(D)** LPS stimulation for 60 minutes. Following LPS stimulation, STAT1 can be seen to localise to the nucleus **(B-D)**. All images are single confocal sections taken with a 60x oil objective lens. These results are a representation of three individual experiments (n=3), where >100 cells were examined per condition.

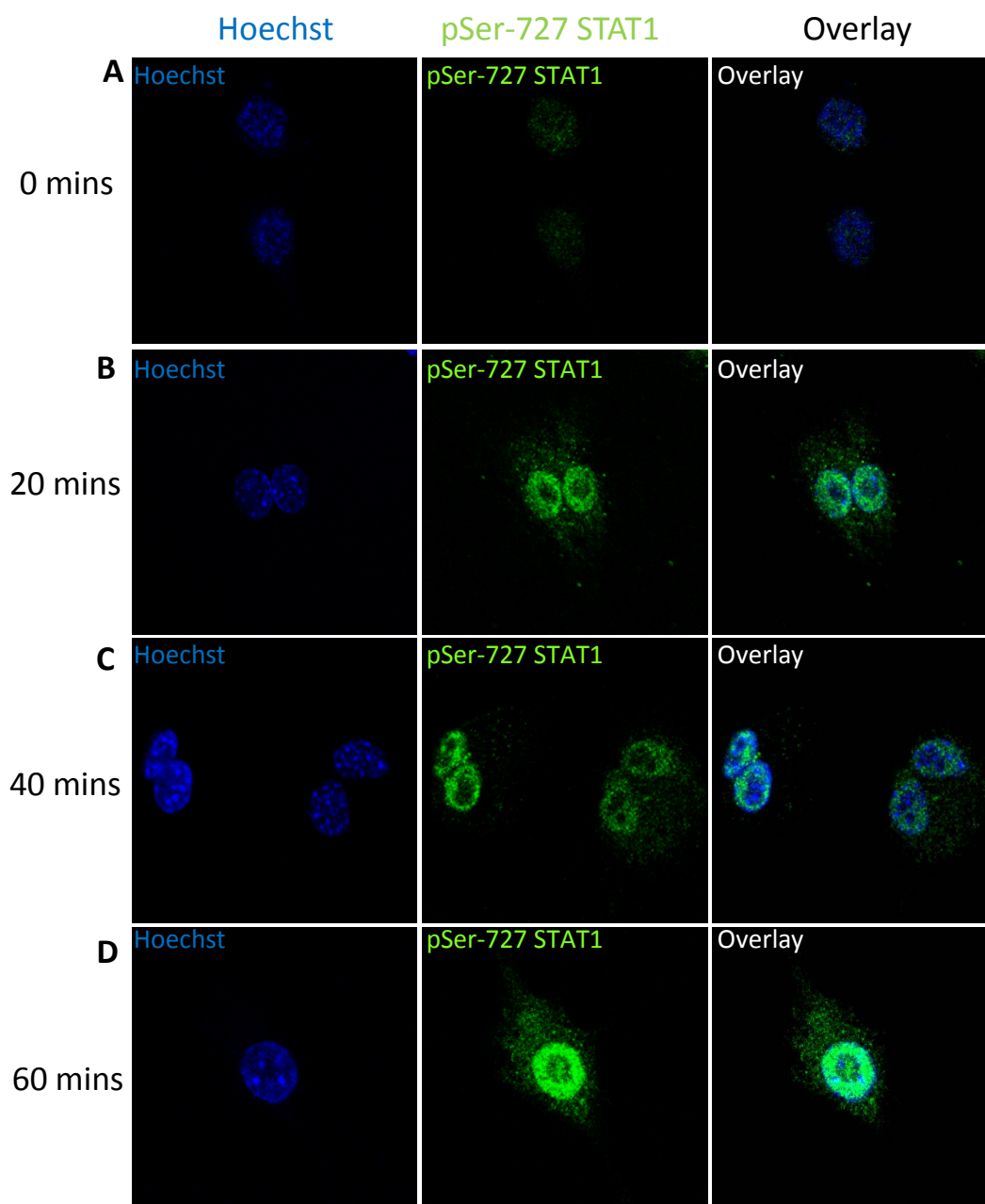


Figure 5.2: Rapid nuclear localisation of pSer-727 STAT1 following LPS stimulation.

RAW264.7 murine macrophages were prepared as described in figure 5.1, with α -pSTAT1 (Ser-727) antibody used to probe cells. **(A)** Unstimulated RAW264.7 murine macrophages. **(B)** LPS stimulation for 20 minutes. **(C)** LPS stimulation for 40 minutes. **(D)** LPS stimulation for 60 minutes. pSer-727 STAT1 is observed to localise into the nucleus following LPS stimulation **(B-D)**. This nuclear localisation occurs as early as 20 minutes and increased in a time-dependent manner. All images are single confocal sections taken with a 60x oil objective lens on. These results are a representation of three individual experiments ($n=3$), where >100 cells were examined per condition.

STAT1 levels increased in the nucleus in a time-dependent manner with the highest accumulation of nuclear pSer-727 STAT1 detected at 60 minutes post-LPS challenge (Figure 5.2C & D).

Typically, serine phosphorylation is not known to induce nuclear translocation of STAT1; therefore tyrosine phosphorylation must also be examined to determine if LPS can induce Tyr-701 phosphorylated STAT1 in RAW264.7 murine macrophages.

5.2.3 – Nuclear pTyr-701 STAT1 is only detected 60 minutes post-LPS stimulation

Having demonstrated that pSer-727 STAT1 rapidly localises to the nucleus, it is necessary to determine if pTyr-701 STAT1 also undergoes TLR4-induced nuclear translocation. Traditionally STAT1 requires tyrosine phosphorylation in order to dimerise and translocate to the nucleus. Therefore it is essential to establish if Ser-727 phosphorylation and nuclear translocation occurs following TLR4 stimulation independent of tyrosine phosphorylation.

Consistent with my earlier results, unstimulated macrophages display virtually no pTyr-701 STAT1 (Figure 5.3A). Stimulation of RAW264.7 murine macrophages for 20 minutes did not induce detectable pTyr-701 STAT1 (Figure 5.3B), although tyrosine phosphorylated STAT1 was detected at 40 minutes (Figure 5.3C), this was not observed to be localised to nuclei like pSer-727 STAT1, as observed in figure 5.2C. pTyr-701 STAT1 detected at 60 minutes post-LPS stimulation was consistent with my earlier observations of STAT1 activation determined by immunoblot (Figure 5.3D).

My results suggest that that following LPS stimulation early nuclear localisation of STAT1 is specifically Ser-727 phosphorylated STAT1. The serine phosphorylation of STAT1 resulting in nuclear localisation has not been documented before and represents a novel mechanism for TLR-induced STAT1 nuclear localisation.

5.2.4 – pSer-727 STAT1 does not colocalise with mitochondria

My studies have found that TLR activation can induce STAT3 translocation to the mitochondria and regulate mitochondrial dysfunction and ROS production, which was also demonstrated in Ras-transformed cells (Gough et al., 2009). Whilst I have established that pSer-727 STAT1 translocates to the nucleus following TLR stimulation I also wished to determine if STAT1 may also localise to the mitochondria commensurate with my observations with STAT3.

RAW264.7 murine macrophages were stimulated with LPS over a 60 minute time course and nuclei stained with Hoechst, Mitotracker Red to identify mitochondria and probed for pSer-727 STAT1. Unstimulated cells displayed a small amount of pSer-727 STAT1 in the nucleus which concurs with my

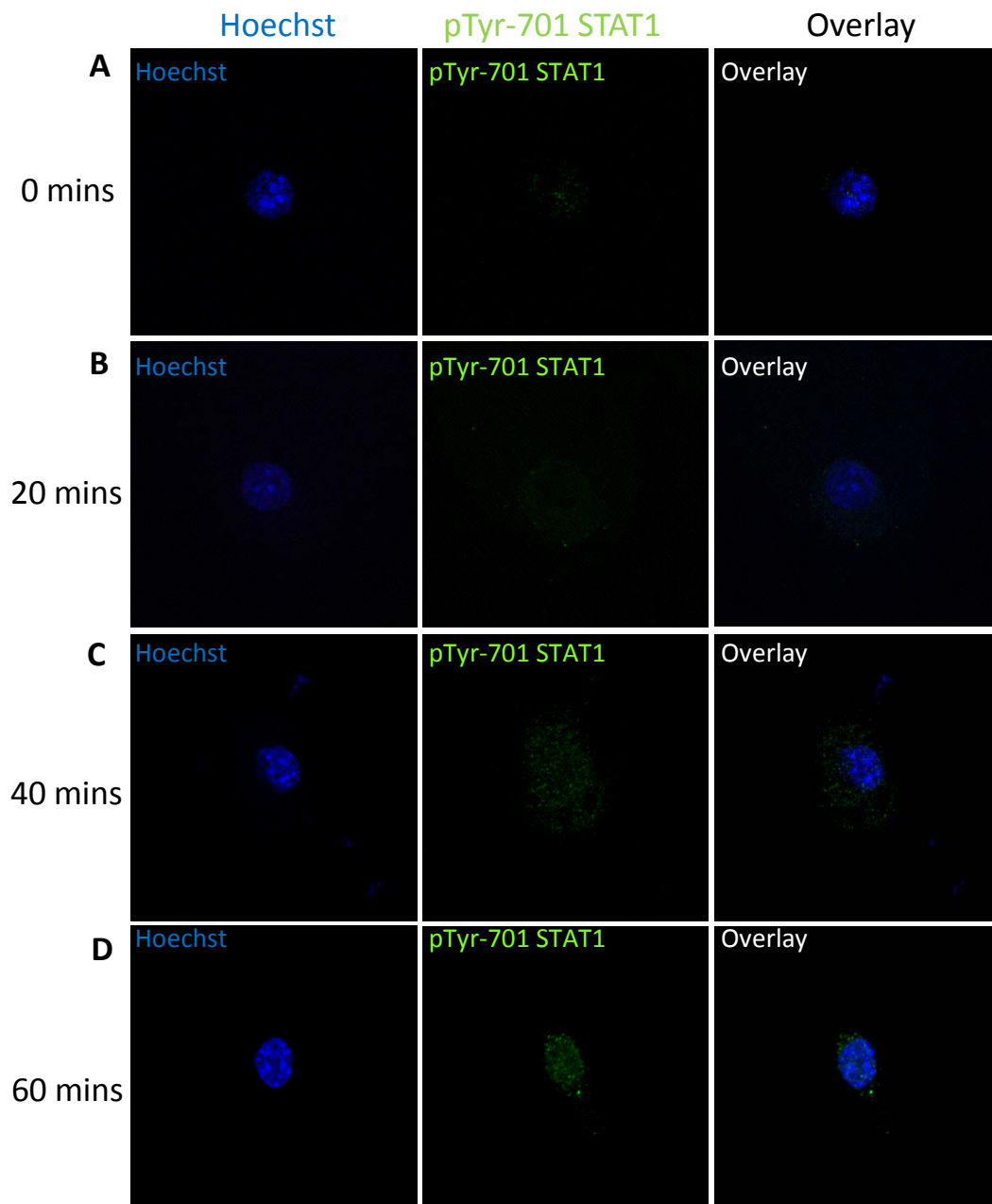


Figure 5.3: Nuclear localisation of pTyr-701 STAT1 is only induced 60 minutes post LPS stimulation.

RAW264.7 murine macrophages were prepared as described in figure 5.1. α -pSTAT1 (Tyr-701) antibody was used to probe cells. **(A)** Unstimulated RAW264.7 murine macrophages. **(B)** LPS stimulation for 20 minutes. **(C)** LPS stimulation for 40 minutes. **(D)** LPS stimulation for 60 minutes. Tyrosine phosphorylation of STAT1 is not detected at 20 and 40 minutes after LPS stimulation **(B-C)**. Nuclear localisation of pTyr-701 STAT1 can be seen at the 60 minute time point **(D)**. All images are single confocal sections taken with a 60x oil objective lens. These results are a representation of three individual experiments (n=3), where >100 cells were examined per condition.

previous data (Figure 5.4A). Stimulation with LPS resulted in a marked increase of pSer-727 STAT1 localised to the nucleus (Figure 5.4B). However, when overlaid with Hoechst stain and Mitotracker Red, it was observed that pSer-727 STAT1 was predominately localised to the nucleus at all time points, whilst cytoplasmic serine phosphorylated STAT1 remains diffuse throughout the cell (Figure 5.4B-D). Serine phosphorylated STAT1 were not observed to colocalise with mitochondria as determined by Mitotracker Red staining.

LPS-induced STAT1 Ser-727 phosphorylation translocates to the nucleus unlike STAT3 which localises to mitochondria following LPS stimulation.

5.2.5 – Nuclear localisation of pSer-727 STAT1 can be induced by multiple TLRs

To support my finding that TLR4-induced STAT1 nuclear localisation, I next stimulated RAW264.7 murine macrophages with TLR2 (Pam₃Cys), TLR3 (poly (I:C)), TLR7 (Ixoribine), TLR9 (CpG DNA) ligands and IFN- α , a known inducer of STAT1 Ser-727 phosphorylation and nuclear localisation. Cellular lysates were then separated into cytoplasmic and nuclear fractions and probed for pSer-727 STAT1 by immunoblot following 60 minute stimulation.

Consistent with my earlier findings, all TLR ligands induced Ser-727 phosphorylation of STAT1 in the cytoplasm fraction (Figure 5.5A). Cytoplasmic fractionation was confirmed by immunoblotting for β -tubulin. This was supported by densitometry analysis demonstrating significant serine phosphorylation of STAT1 above that of the unstimulated cells (Figure 5.5B). IFN- α induced STAT1 Ser-727 phosphorylation that was detected strongly in both cytoplasmic and nuclear fractions (Figure 5.5A, lane 7 and C, lane 7). Confocal microscopy illustrated LPS-induced pSer-727 STAT1 nuclear localisation and this is confirmed by immunoblotting the nuclear fractions (Figure 5.5C, lane 4). It can also be observed that all TLRs induced pSer-727 STAT1 nuclear localisation albeit at lower levels for TLR3 and TLR7 stimulation (Figure 5.5C). Nuclear fractionation was confirmed by analysis of Histone Deacetylase 3 (HDAC3). Nuclear localisation by all TLRs was supplemented by densitometry analysis of multiple nuclear fractionation experiments (Figure 5.5D).

These findings further support my initial observation from fluorescent microscopy where I observed nuclear localisation of TLR4-induced pSer-727 STAT1 and demonstrate that TLR-induced pSer-727 STAT1 nuclear localisation is a general TLR mechanism.

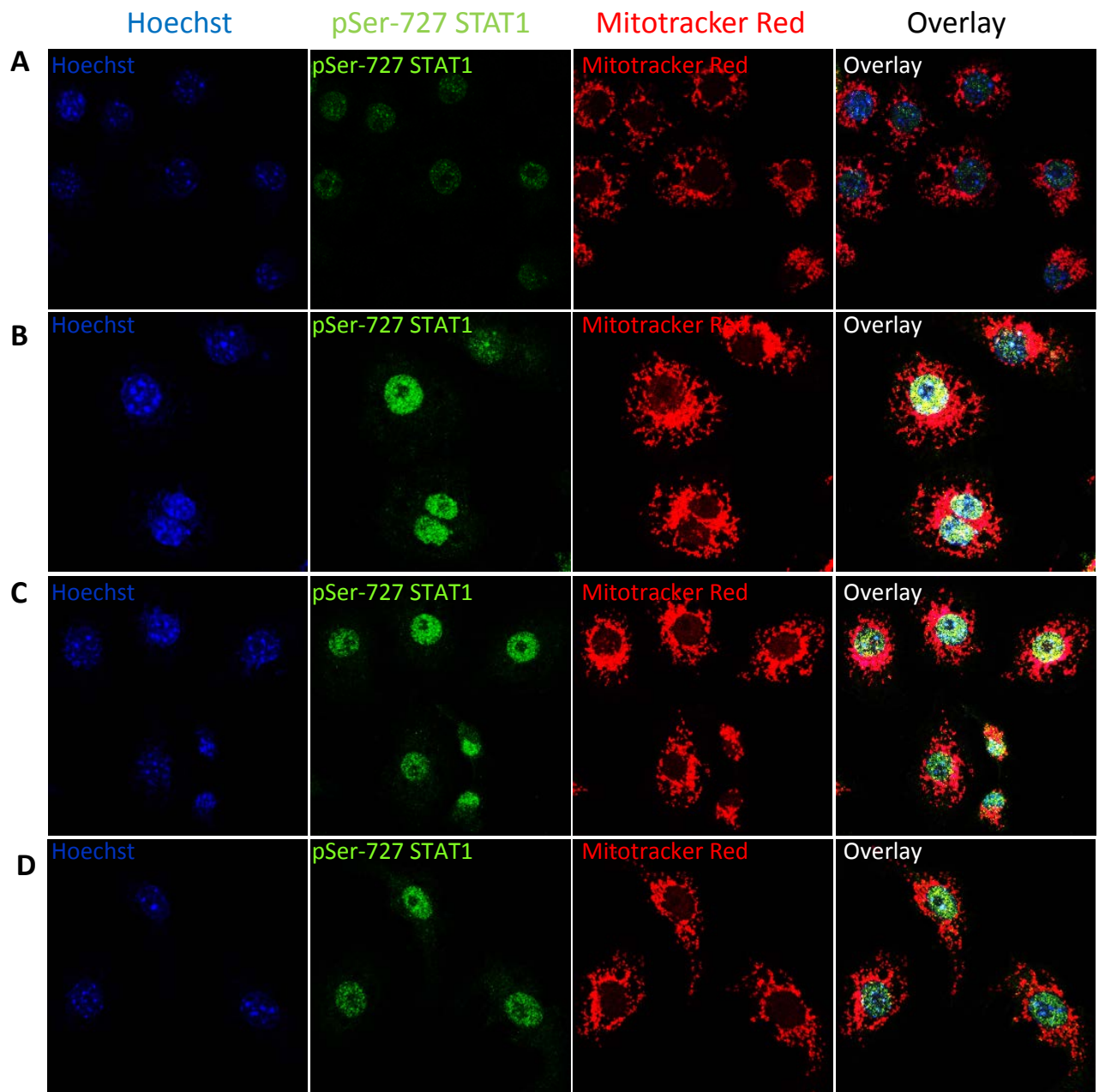


Figure 5.4: pSer-727 STAT1 does not localise to mitochondria following LPS stimulation.

Cells were prepared as described in figure 5.1. Mitotracker Red (100 nM) was used to stain cells prior to fixation and cells were probed with α -pSTAT1 (Ser-727) antibody. **(A)** Unstimulated RAW264.7 murine macrophages. **(B)** LPS stimulation for 20 minutes. **(C)** LPS stimulation for 40 minutes. **(D)** LPS stimulation for 60 minutes. Following LPS stimulation, pSer-727 STAT1 is observed to accumulate in the nucleus, with no STAT1 localising in mitochondria at all time points **(B-D)**. All images are single confocal sections from a Z-stack taken with a 60x oil objective lens. These results are a representation of three individual experiments (n=3), where >100 cells were examined per condition.

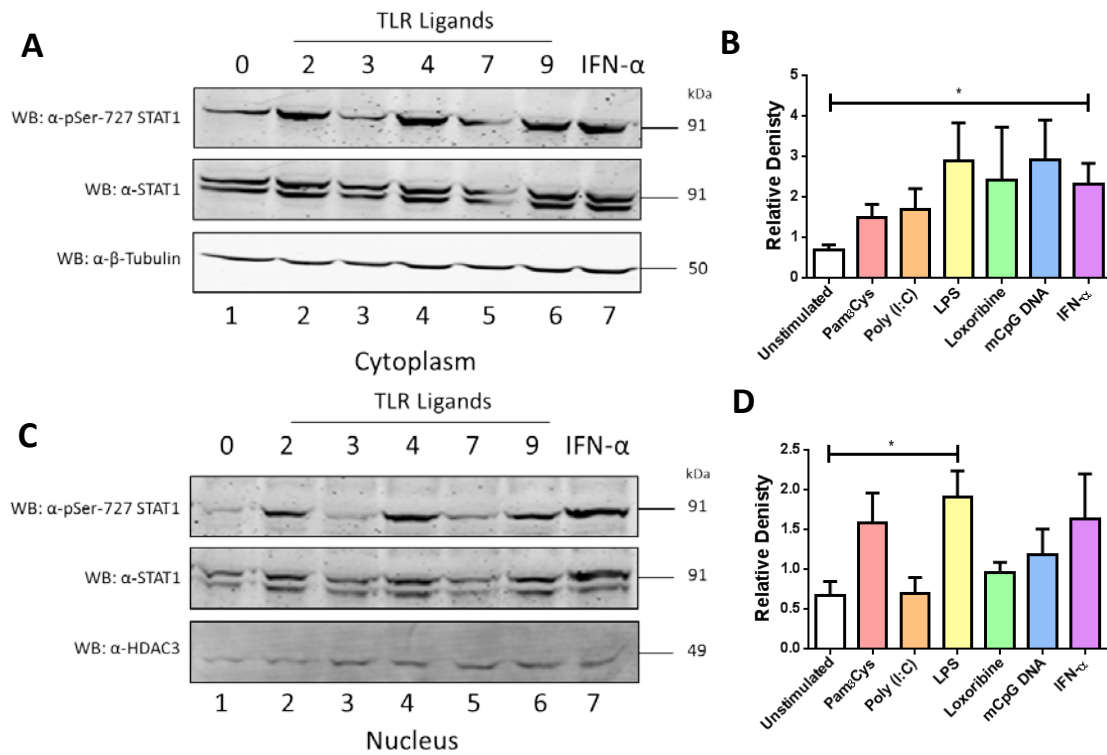


Figure 5.5: pSer-727 STAT1 can be detected in both cytoplasmic and nuclear fractions following TLR stimulation.

RAW264.7 murine macrophages were seeded at 1×10^6 cells/well in a 6-well plate, 24 hours before stimulation. Cells were then stimulated with Pam₃Cys (100 ng/ml), poly (I:C) (10 μ g/ml), LPS (100 ng/ml), loxoribine (500 μ M), mCpG DNA (500 nM) and IFN- α (1000 IU) for 60 minutes. Cells were harvested in plasma membrane lysis buffer, the nuclear pellet removed and nuclear extraction buffer used to fractionate the respective components. Proteins were separated on a 10% SDS-PAGE gel transferred and PVDF membrane visualised by enhanced fluorescence. Membranes were incubated with α -pSTAT1 (Ser-727) antibody (1/1000) and total STAT1 antibody. **(A)** Following TLR agonist stimulation, STAT1 undergoes serine phosphorylation in the cytoplasm and **(C)** serine phosphorylated STAT1 can also be detected in the nucleus. Densitometry conducted on the **(B)** cytoplasmic and **(D)** nuclear lysates demonstrates the ability of TLR ligands to induce Ser-727 phosphorylation of STAT1. These results are a representation of three individual experiments (n=3).

5.2.6 – Hyperactive F/F MEFs display decreased cytokine expression in the absence of STAT1.

Previous studies in our laboratory conducted by Greenhill et al. (unpublished data) have found that F/F mice when treated with LPS display a hyperinflammatory phenotype. STAT3 has been implicated to drive IL-6 production in these mice further exacerbating the systemic immune response. These mice however, also display increased expression of STAT1 (Jenkins et al., 2005). As my results have demonstrated that STAT1 localises to the nucleus upon TLR stimulation, it is possible that STAT1 contributes to the hyperinflammatory phenotype of the F/F mice through increased STAT1 activation. Thus I examined whether F/F STAT1^{-/-} mice display diminished activation of inflammatory cytokines compared to F/F mice following TLR stimulation.

Cytokine analysis of the supernatants of the F/F MEFs vs. F/F STAT1^{-/-} illustrates that STAT1-deficiency reduces production of TNF- α following stimulation with TLR ligands (Figure 5.6). In response to Pam₃Cys (TLR2) and LPS (TLR4), F/F STAT1^{-/-} MEFs display significantly reduced production of TNF- α , suggesting STAT1 may play a role in mediating the proinflammatory response following TLR ligand stimulation (Figure 5.6A & B). CpG DNA (TLR9) stimulation on the other hand slightly diminished TNF- α secretion (though not significant) demonstrating that STAT1 may also regulate TLR9-induced responses (Figure 5.6C).

In contrast to the effect of STAT1-deficiency on TNF- α production, IL-6 secretion however is unaffected in STAT1-deficient MEFs. F/F STAT1^{-/-} MEFs produce comparable levels of IL-6 compared to F/F MEFs following Pam₃Cys and LPS treatment (Figure 5.7A & B). Interestingly however, CpG DNA stimulation results in decreased IL-6 production (Figure 5.7C).

These results therefore suggest that STAT1 plays a role in the specific expression of TNF- α in response to TLR stimulation. IL-6 secretion however, appears to be regulated by another factor, although optimal TLR9-mediated IL-6 responses do require STAT1.

5.2.7 – STAT1 S727A mutant suppresses TLR2-mediated NF κ B promoter activity.

Taken together my data suggests that the Ser-727 residue in STAT1 is important in the regulation of nuclear translocation of STAT1 following TLR stimulation. As F/F STAT1^{-/-} MEFs had reduced TNF- α production, I next wished to investigate the role STAT1 Ser-727 has in inducing activation of the prototypic inflammatory transcription factor, NF κ B. A substitution of the Ser-727 residue to alanine was performed and used to determine the role of the mutant STAT1 in activation of TLR-induced proinflammatory gene promoter activity compared to WT STAT1.

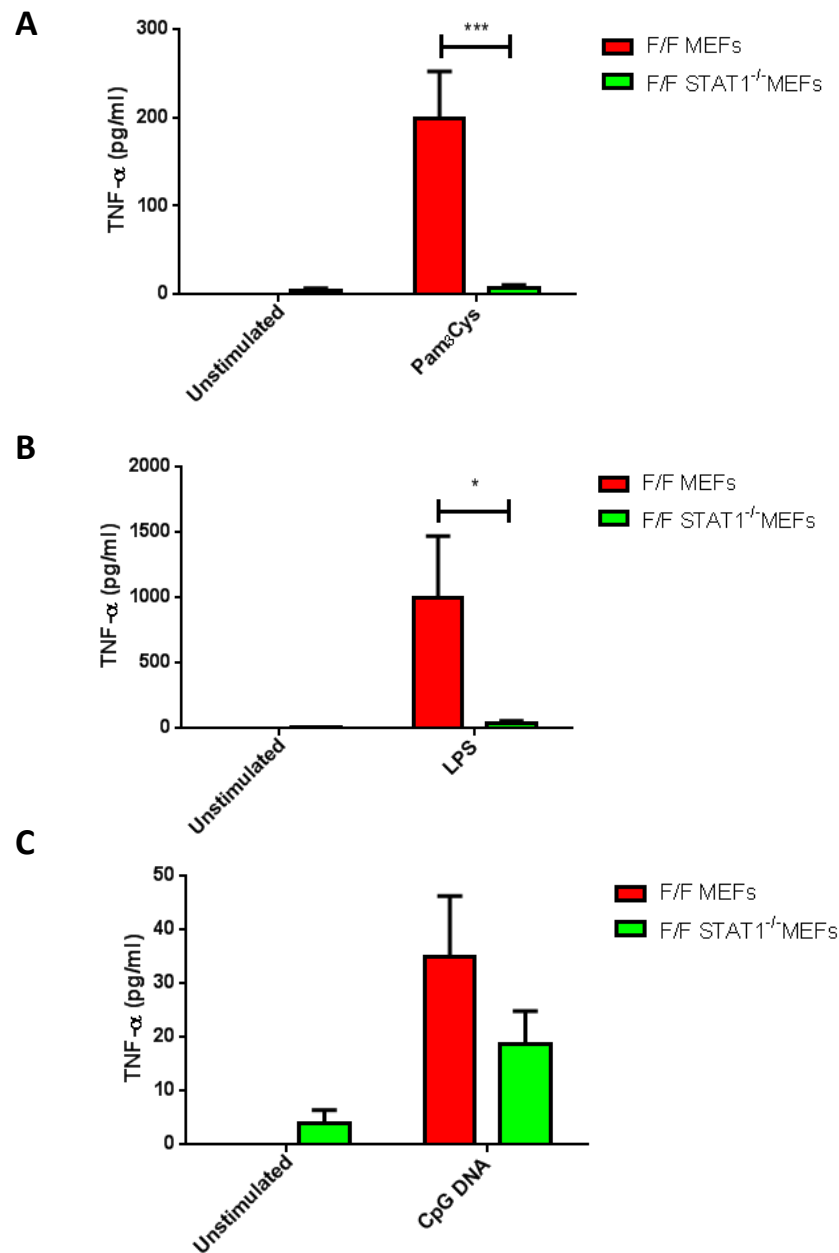


Figure 5.6: F/F STAT1^{-/-} MEFs are impaired in their ability to induce TNF- α production in response to TLR stimulation.

F/F MEFs vs F/F STAT1^{-/-} MEFs were seeded at 2×10^4 cells/well in a 96-well plate, 24 hours prior to stimulation. Cells were stimulated with **(A)** Pam₃Cys (10 ng/ml), **(B)** LPS (10ng/ml) and **(C)** mCpG DNA (100 nM) for 16 hours. Supernatants were collected and TNF- α production measured by ELISA. In response to TLR agonists, F/F STAT1^{-/-} MEFs displayed impaired production of TNF- α compared to F/F MEFs. Pooled data is presented as mean \pm SEM of three independent experiments (n=3).

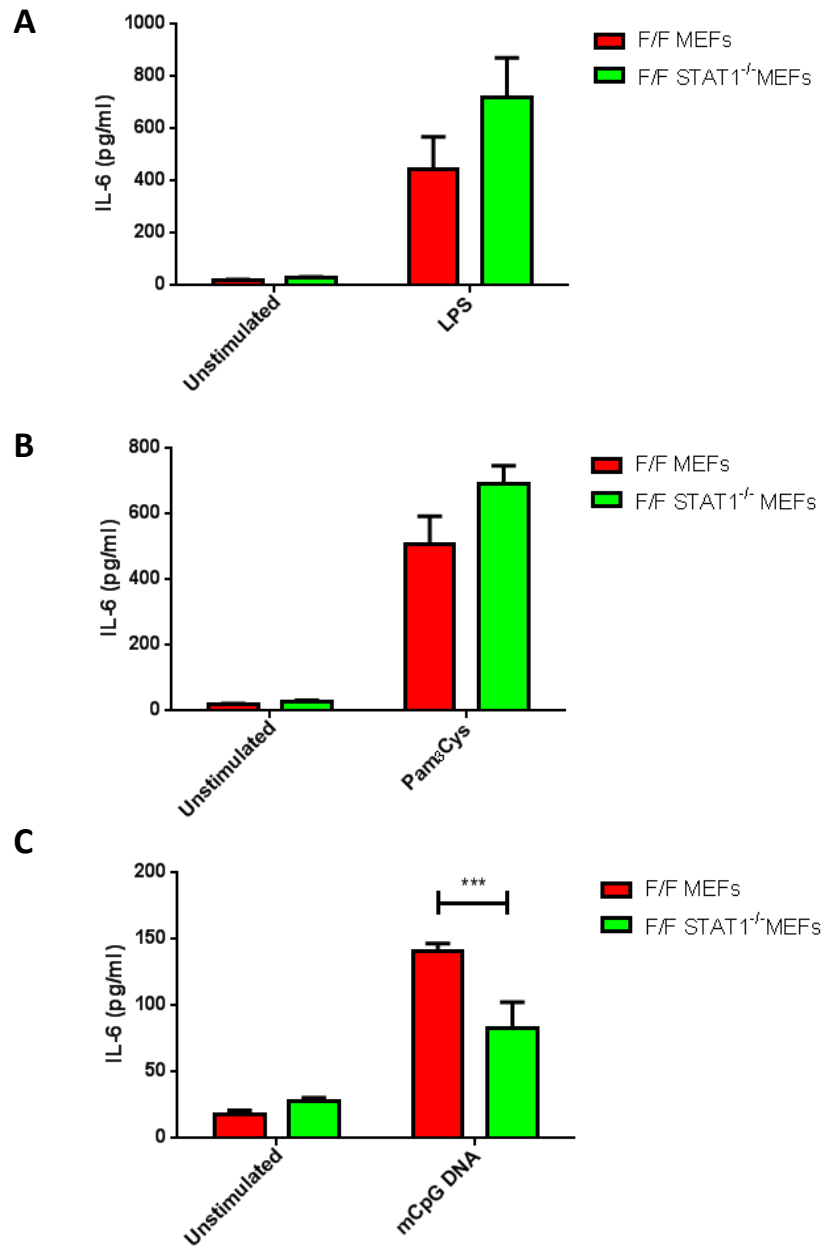


Figure 5.7: IL-6 production is not reduced in F/F STAT1^{-/-} MEFs in response to Pam₃Cys and LPS except following CpG DNA treatment.

Cells were prepared as described in figure 5.6. Cells were stimulated with **(A)** Pam₃Cys (10 ng/ml), **(B)** LPS (10 ng/ml) and **(C)** mCpG DNA (100 nM) for 16 hours. Supernatants were collected and IL-6 production measured by ELISA. In response to TLR agonists, F/F STAT1^{-/-} MEFs produced increased levels of IL-6 compared to F/F MEFs. Though CpG DNA-induced IL-6 production is diminished in F/F STAT1^{-/-} MEFs. Pooled data is presented as mean ± SEM of three independent experiments (n=3).

HEK293s stably expressing TLR2 were transfected with an NFκB promoter luciferase construct in conjunction with STAT1 WT or STAT1 S727A. Cells were then stimulated with increasing concentrations of Pam₃Cys to isolate responses to MyD88-dependent TLR signalling. In TLR2 responsive cells, HEK293s expressing WT STAT1 displayed a dose-dependent increase in NFκB-luciferase promoter activity (Figure 5.8). Conversely, whilst STAT1 S727A expressing HEK293 cells also displayed a dose-dependent increase in NFκB promoter activity, the response was significantly decreased compared to WT STAT1 (Figure 5.8).

Having demonstrated STAT1 selectivity for TNF-α expression in the previous section I next evaluated the effect STAT1 S727A has in activating the TNF-α promoter following TLR2 stimulation. Interestingly, whilst both STAT1 WT and STAT1 S727A displayed a dose-dependent increase in TNF-α-luciferase promoter activity, STAT1 S727A did not inhibit activation of the TNF-α promoter (Figure 5.9).

Conversely, analysis of IL-6 expression in response to Pam₃Cys treatment displays STAT1 S727A significantly inhibiting activation of IL-6 promoter activity (Figure 5.10). Consistent with earlier results WT STAT1 exhibits a dose-dependent increase in IL-6 promoter activation (Figure 5.10).

Taken together these results suggests that STAT1 S727A has diminished transactivator function suppressing TLR2-induced responses, implicating a role for STAT1 Ser-727 phosphorylation in mediating TLR-induced activation of NFκB and IL-6.

5.2.8 – Nuclear localisation of STAT1 is not affected in STAT1 S727A BMMs

My earlier confocal microscopy studies demonstrated that it was the pSer-727 form of STAT1 that was detectable in the cytoplasm following TLR stimulation. Therefore I next wished to determine if Ser-727 phosphorylation was required for nuclear localisation of STAT1. BMMs were generated from femurs of mice expressing STAT1 S727A; these mice have impaired clearance of bacteria and are less susceptible to LPS-induced septic shock (Varinou et al., 2003). Multi-planar images were taken of WT and STAT1 S727A BMMs either unstimulated or treated with Pam₃Cys (TLR2), LPS (TLR4) or CpG DNA (TLR9) for 30 and 60 minutes. Quantification of Z-stacks was conducted using Imaris imaging software (Bitplane ver. 7.6.4).

Contrasting from earlier results which demonstrated a potential role for pSer-727 STAT1 in mediating TLR2-induced responses, both unstimulated WT and STAT1 S727A BMMs displayed high basal levels of STAT1 nuclear localisation (Figure 5.11A & B). Pam₃Cys stimulation however, did not induce an increase in STAT1 nuclear translocation at 30 minutes in both WT and STAT1 S727A BMMs (Figure 5.11D & E), nor was this observed at 60 minutes (Figure 5.11E & F).

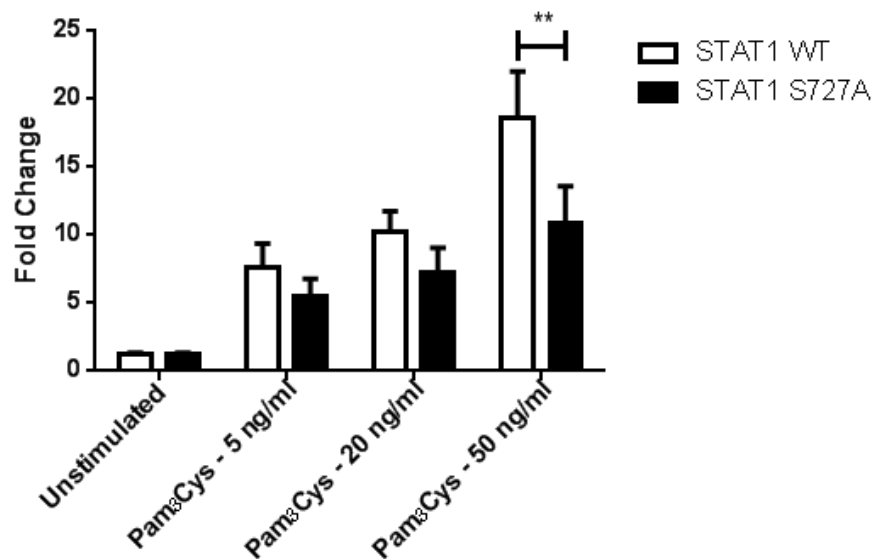


Figure 5.8: STAT1 S727A mutant suppresses TLR2-mediated NFκB activation.

HEK293 cells stably expressing TLR2 were seeded at 2×10^4 cells/well in a 96-well plate, 24 hours before transfection. The cells were transfected with a firefly luciferase reporter gene under the control an NFκB promoter and either STAT1 WT or STAT1 S727A mutant. 24 hours after transfection, cells were stimulated with Pam₃Cys (5 ng/ml, 20 ng/ml and 50 ng/ml) for 6 hours. Cells were harvested and luciferase activity determined. Transfection efficiency was determined by comparing to a constitutively expressed reporter gene, TK Renilla. In response to various concentrations of Pam₃Cys, STAT1 S727A has diminished transactivator function and suppresses activation of NFκB in comparison to STAT1 WT transfected cells. Pool data is represented as mean \pm SEM of four independent experiments (n=4).

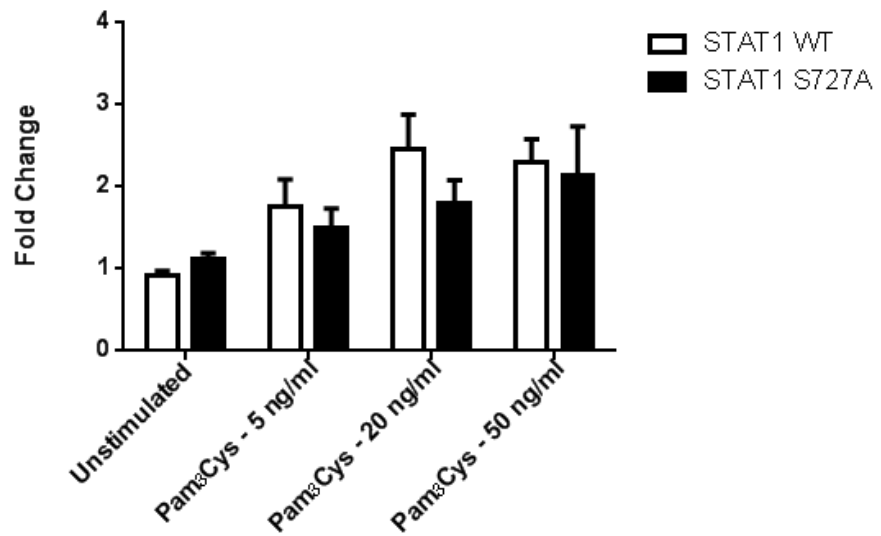


Figure 5.9: STAT1 S727A does not suppress TLR2-induced TNF- α activation.

Cells were prepared as described in figure 5.8. HEK293s stably expressing TLR2 were transfected with a firefly luciferase reporter gene under the control a TNF- α promoter and either STAT1 WT or STAT1 S727A mutant. Following stimulation with Pam₃Cys, STAT1 S727A transfected cells did not suppress TNF- α activation compared to WT STAT1. Pooled data is represented as mean \pm SEM of four independent experiments (n=4).

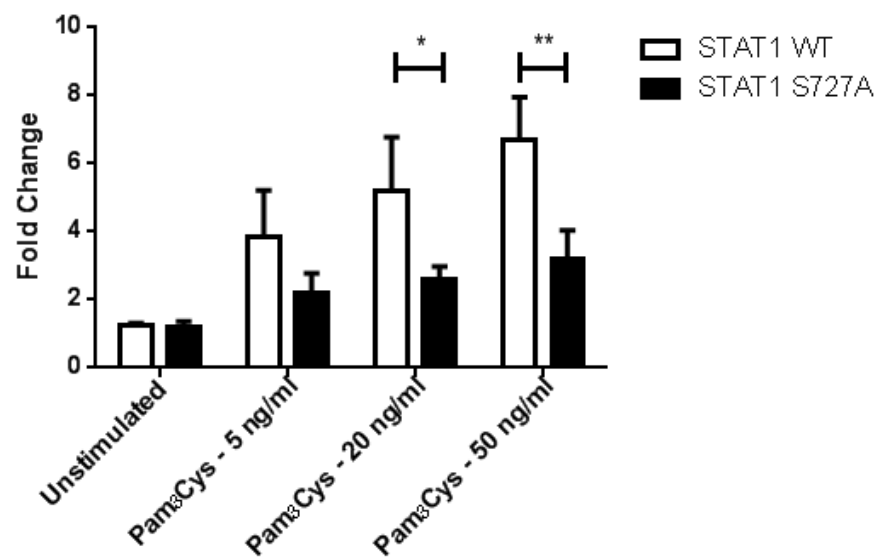


Figure 5.10: S727A mutation suppresses the ability of STAT1 to drive IL-6 promoter activity following Pam₃Cys challenge.

Cells were prepared as described in figure 5.8. HEK293s were transfected with firefly luciferase reporter gene under the control an IL-6 promoter and either STAT1 WT or STAT1 S727A mutant. In response to various concentrations of Pam₃Cys, STAT1 S727A transfected cells displayed suppressed activation of IL-6 in comparison to STAT1 WT transfected cells. Pooled data is represented as mean \pm SEM of four independent experiments (n=4).

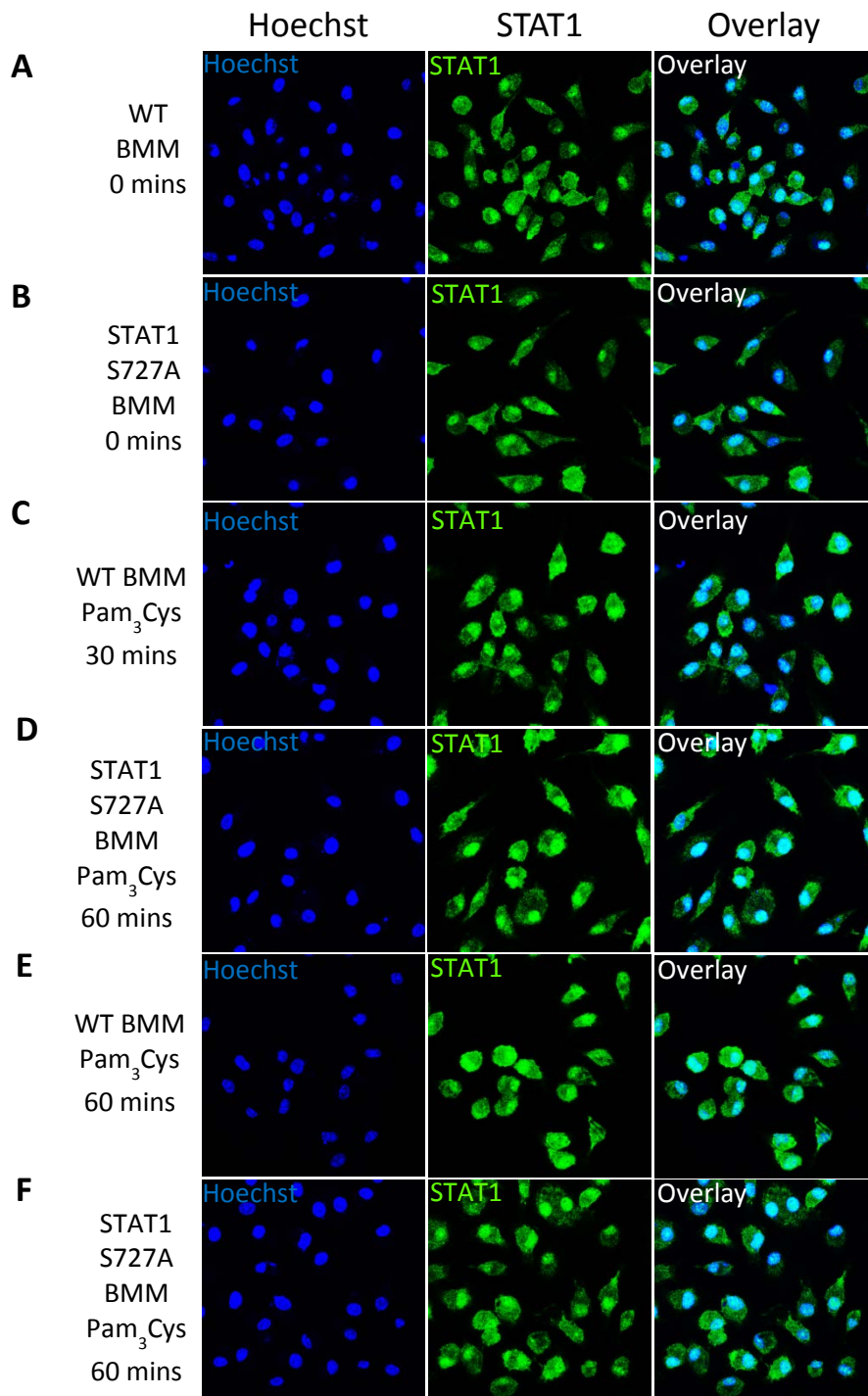


Figure 5.11: Nuclear localisation of STAT1 can be observed in both WT and STAT1 S727A BMMs following Pam₃Cys stimulation.

BMMs were prepared as described in figure 5.1. BMMs were stimulated with 100 ng/ml of Pam₃Cys and probed with α -STAT1 antibody. **(A)** WT BMMs, unstimulated. **(B)** STAT1 S727A BMMs, unstimulated. **(C)** WT BMMs, 30 minute Pam₃Cys stimulation. **(D)** STAT1 S727A BMMs, 30 minute Pam₃Cys stimulation. **(E)** WT BMMs, 60 minute Pam₃Cys stimulation. **(F)** STAT1 S727A BMMs, 60 minute Pam₃Cys stimulation. Following stimulation with Pam₃Cys, no observable difference can be detected in the nuclear localisation of STAT1. All images are single confocal sections from Z-stacks taken with a 100x oil objective lens. These results are a representation of three individual experiments (n=3), where >100 cells were examined per condition.

LPS stimulation which was demonstrated to induce rapid and strong Ser-727 phosphorylation of STAT1 also illustrated a comparable result, levels of STAT1 translocating to the nucleus were not dissimilar between WT and STAT1 S727A BMMs at 30 minutes (Figure 5.12C & D) and this remained unchanged at the 60 minute time point (Figure 5.12E & F).

Following CpG DNA stimulation F/F STAT1^{-/-} MEFs exhibited decreased IL-6 and TNF- α production suggesting that STAT1 may be required for optimal TLR9-induced responses, it is therefore possible that STAT1 S727A BMMs may also display lowered levels of STAT1 nuclear translocation. CpG DNA treatment however displayed analogous concentrations of STAT1 translocation to the nucleus at both 30 (Figure 5.13C & D) and 60 minutes (Figure 5.13E & F), respectively.

To further determine if differences were observed of STAT1 nuclear localisation between WT and STAT1 S727A BMMs, Z-stacks were quantified using Imaris imaging software where staining of STAT1 in the nucleus was determined. As can be observed in figure 5.14, only slight variations of nuclear localisation can be observed between WT BMMs and STAT1 S727A BMMs when stained for total STAT1. Stimulation with Pam₃Cys did not induced differing levels of STAT1 nuclear localisation (Figure 5.14A). In addition, LPS treatment produced similar results with no observable change of STAT1 nuclear localisation between WT and STAT1 S727A BMMs (Figure 5.14B). Quantification of images taken from BMMs stimulated with CpG DNA also demonstrated little variation between WT and STAT1 S727A BMMs nor was there any significant differences that can be observed at 30 and 60 minutes post-stimulation (Figure 5.14C).

My results here demonstrate no difference in nuclear localisation between WT and STAT1 S727A BMMs following TLR stimulation, although it is possible that the lack of variation observed is due to the inability to directly visualise pSer-727 STAT1.

5.2.9 – TNF- α , but not IL-6 or RANTES production is diminished in STAT1 S727A BMMs

To determine the biological requirement of Ser-727 phosphorylation of STAT1 in TLR-induced inflammation I next used BMMs generated from WT and STAT1 S727A mice and assessed cytokine expression.

As can be observed in Figure 5.15, WT BMMs displayed a concentration-dependent increase in TNF- α protein expression following stimulation with multiple TLR agonists (Figure 5.15A-E). Importantly, macrophages expressing STAT1 S727A displayed significantly reduced TNF- α expression in response to all TLR ligands assigned. This was particularly evident at the higher doses of TLR stimulation suggesting STAT1 Ser-727 phosphorylation is required for optimal TLR-induced TNF- α expression.

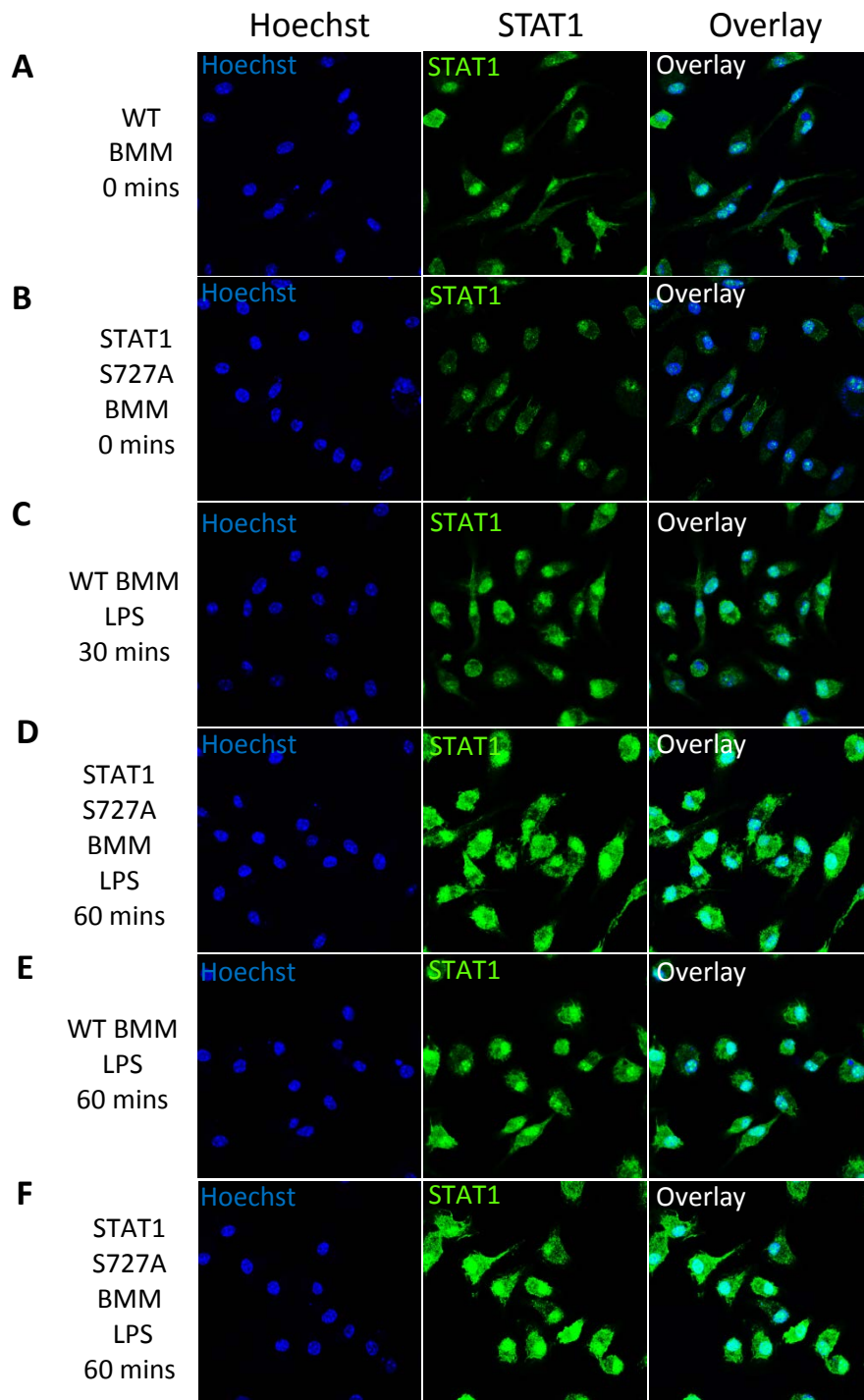


Figure 5.12: Following LPS stimulation, STAT1 is observed to translocate to nuclei in both WT and STAT1 S727A BMMs.

BMMs were prepared as described in figure 5.1. BMMs were stimulated with 100 ng/ml of LPS and probed with α -STAT1 antibody. **(A)** WT BMMs, unstimulated **(B)** STAT1 S727A BMMs, unstimulated. **(C)** WT BMMs, 30 minute LPS stimulation. **(D)** STAT1 S727A BMMs, 30 minute LPS stimulation. **(E)** WT BMMs, 60 minute LPS stimulation. **(F)** STAT1 S727A BMMs, 60 minute LPS stimulation. LPS stimulation does not induce a difference in STAT1 nuclear translocation between WT and STAT1 S727A BMMs. All images are single confocal sections from Z-stacks taken with a 100x oil objective lens. These results are a representation of three individual experiments (n=3), where >100 cells were examined per condition.

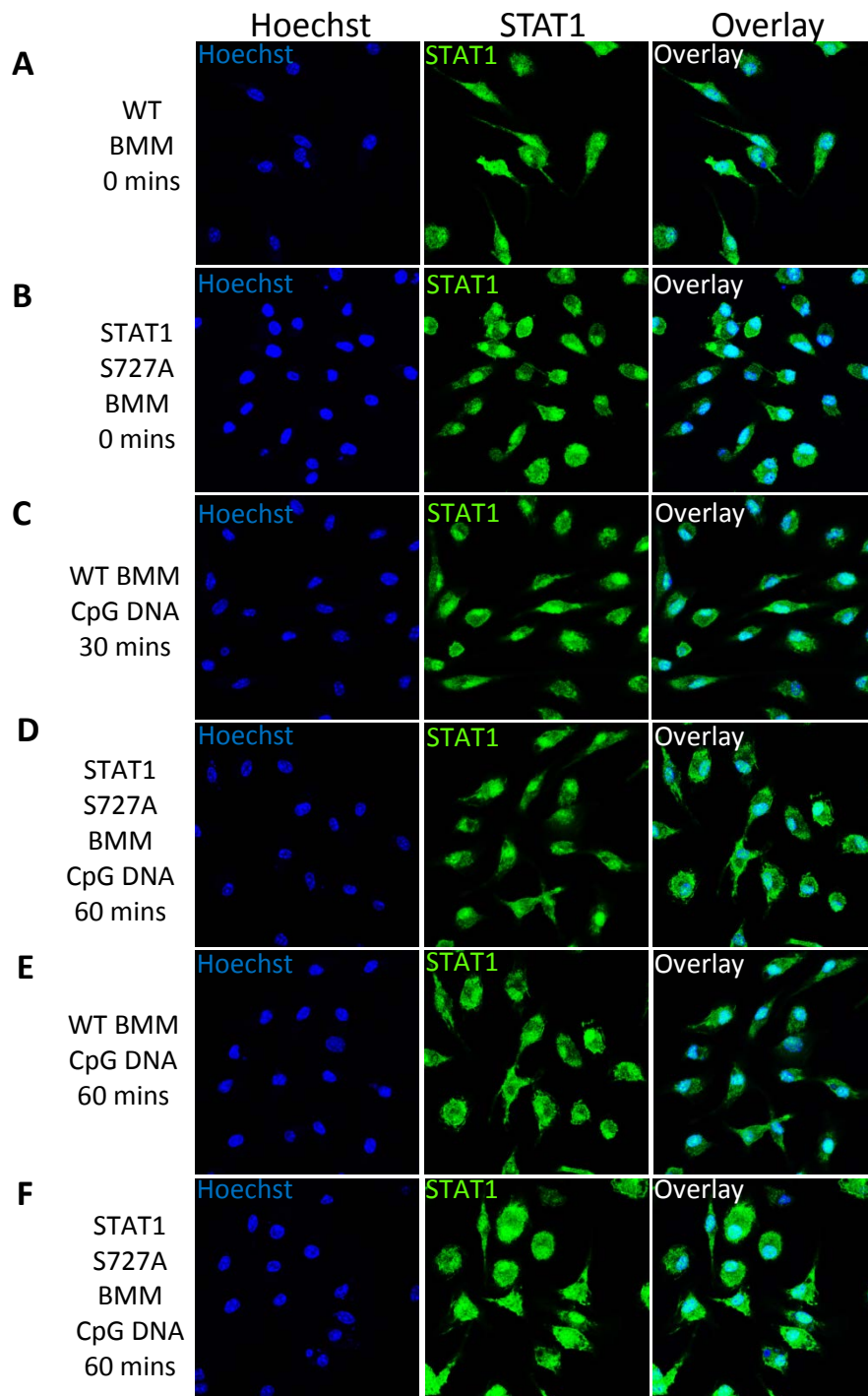


Figure 5.13: Nuclear localisation of STAT1 is similar between WT and STAT1 S727A BMMs post-CpG DNA stimulation.

BMMs were prepared as described in figure 5.1. BMMs were stimulated with 500 nM of CpG DNA and probed with α -STAT1 antibody. **(A)** WT BMMs, unstimulated. **(B)** STAT1 S727A BMMs, unstimulated. **(C)** WT BMMs, 30 minute CpG DNA stimulation. **(D)** STAT1 S727A BMMs, 30 minute CpG DNA stimulation. **(E)** WT BMMs, 60 minute CpG DNA stimulation. **(F)** STAT1 S727A BMMs, 60 minute CpG DNA stimulation. STAT1 Nuclear localisation profiles are similar between WT and STAT1 S727A BMMs following CpG DNA stimulation. All images are single confocal sections from Z-stacks taken with a 100x oil objective lens. These results are a representation of three individual experiments (n=3), where >100 cells were examined per condition.

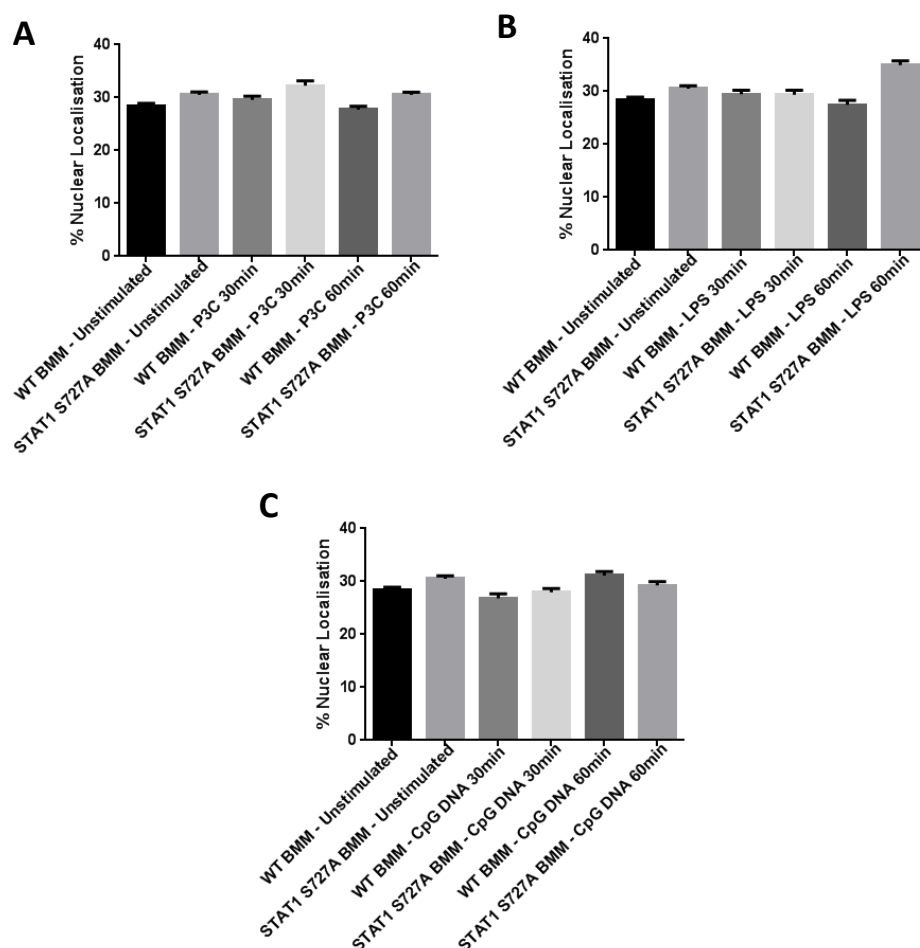


Figure 5.14: Nuclear localisation of STAT1 is not affected in STAT1 S727A BMMs.

Z stacks were subjected to analysis using Imaris imaging software, where total STAT1 intensity and nuclear STAT1 intensity was determined and expressed as a percentage. BMMs were stimulated with **(A)** Pam₃Cys (100 ng/ml) **(B)** LPS (100 ng/ml) **(C)** CpG DNA (500 nm) for 30 and 60 minutes. Following stimulation with TLR ligands, nuclear localisation of STAT1 did not differ between WT and STAT1 S727A BMMs, suggesting that the detection of total STAT1, which consists of unphosphorylated and phosphorylated STAT1, may have obscured results. Pooled data is represented as mean \pm SEM of three independent experiments where >100 cells were examined. (n=3)

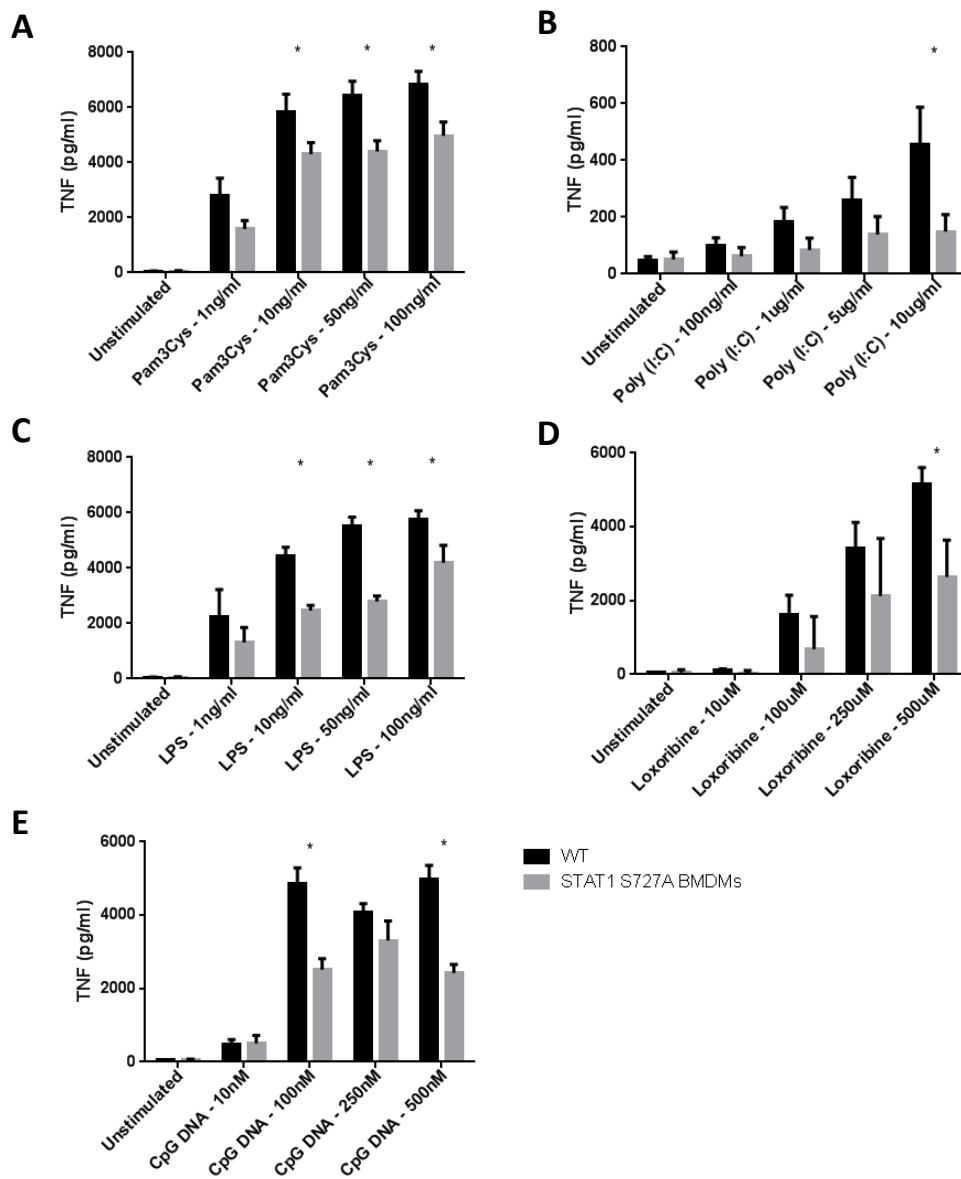


Figure 5.15: TNF-α production in STAT1 S727A BMDMs is attenuated in response to TLR ligands.

WT and STAT1 S727A BMDMs were seeded at 2×10^4 cells/well, 24 hours prior to stimulation. BMDMs were then stimulated with a selection of TLR ligands at the indicated concentrations for 16 hours. Supernatants were collected and measured by ELISA. BMDMs were stimulated with (A) Pam₃Cys (B) poly (I:C) (C) LPS (D) loxoribine (E) CpG DNA. Following stimulation with TLR ligands, TNF-α production is attenuated in STAT1 S727A BMDMs in comparison to WT BMDMs. Pooled data is represented as mean ± SEM of three independent experiments (n=3).

In contrast, IL-6 production was not diminished in STAT1 S727A BMMs. Whilst poly (I:C) stimulation failed to induce IL-6 secretion in WT and STAT1 S727A BMMs, all other TLR ligands tested induced comparable levels of IL-6 in both sets of BMMs (Figure 5.16A-E). At higher concentrations, TLR4-induced IL-6 production was greater in WT BMMs, though this was not observed when stimulating with other TLR agonists. This suggests a minimal role for TLR-induced IL-6 expression, although LPS-mediated inflammation may require Ser-727 phosphorylation of STAT1.

Consistent with figure 5.16, production of RANTES was also not affected in STAT1 S727A BMMs. In WT BMMs, stimulation with TLR ligands induced a concentration-dependent increase in RANTES protein expression (Figure 5.17A-E). However, RANTES secretion in STAT1 S727A BMMs was comparable when treated with TLR agonists. Similar to IL-6 production, TLR-induced RANTES expression appears to not required STAT1 serine phosphorylation.

Interestingly, whilst TLRs are known inducers of IL-12 in DCs (Qi et al., 2003) and TLR-induced STAT1 activation has been reported to be required for optimal IL-12 production (Gautier et al., 2005) TLR stimulation of both WT and STAT1 S727A BMMs failed to induce significant production of IL-12 above non-stimulated cells (Figure 5.18A-E).

The results here demonstrate that whilst the pSer-727 STAT1 is not critical to the innate immune response it appears to function as a mechanism of fine-tuning the inflammatory reaction. pSer-727 STAT1 may sculpt the inflammatory response through regulation of TNF- α production.

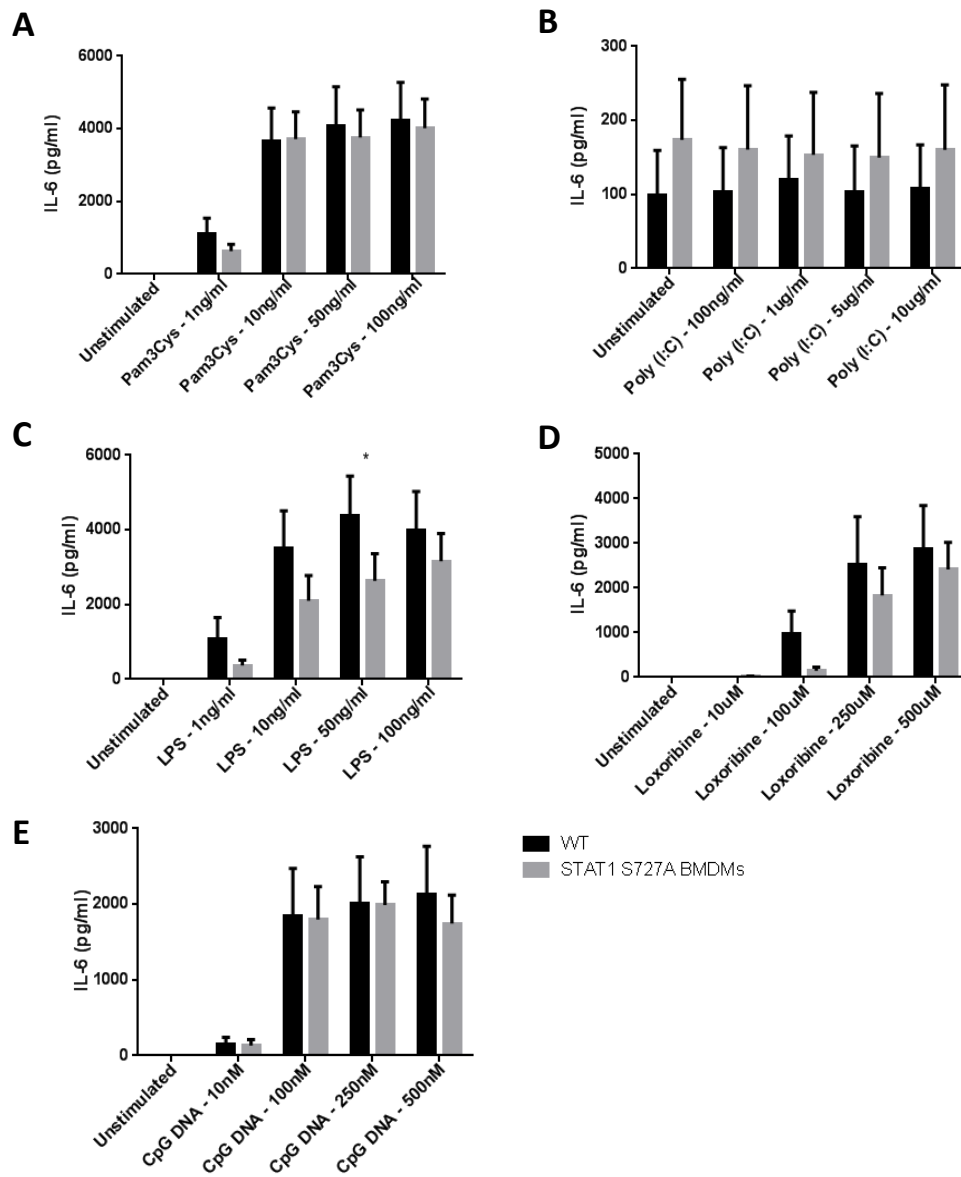


Figure 5.16: Production of IL-6 is not affected in STAT1 S727A BMM compared to WT BMMs when stimulated with TLR ligands.

BMMs were prepared as described figure 5.15. **(A)** Pam₃Cys **(B)** poly (I:C) **(C)** LPS **(D)** loxoribine **(E)** CpG DNA. Similar to WT BMMs, production of IL-6 following TLR stimulation was not attenuated, except in LPS stimulated BMMs where IL-6 levels were diminished. Pooled data is represented as mean ± SEM of three independent experiments (n=3).

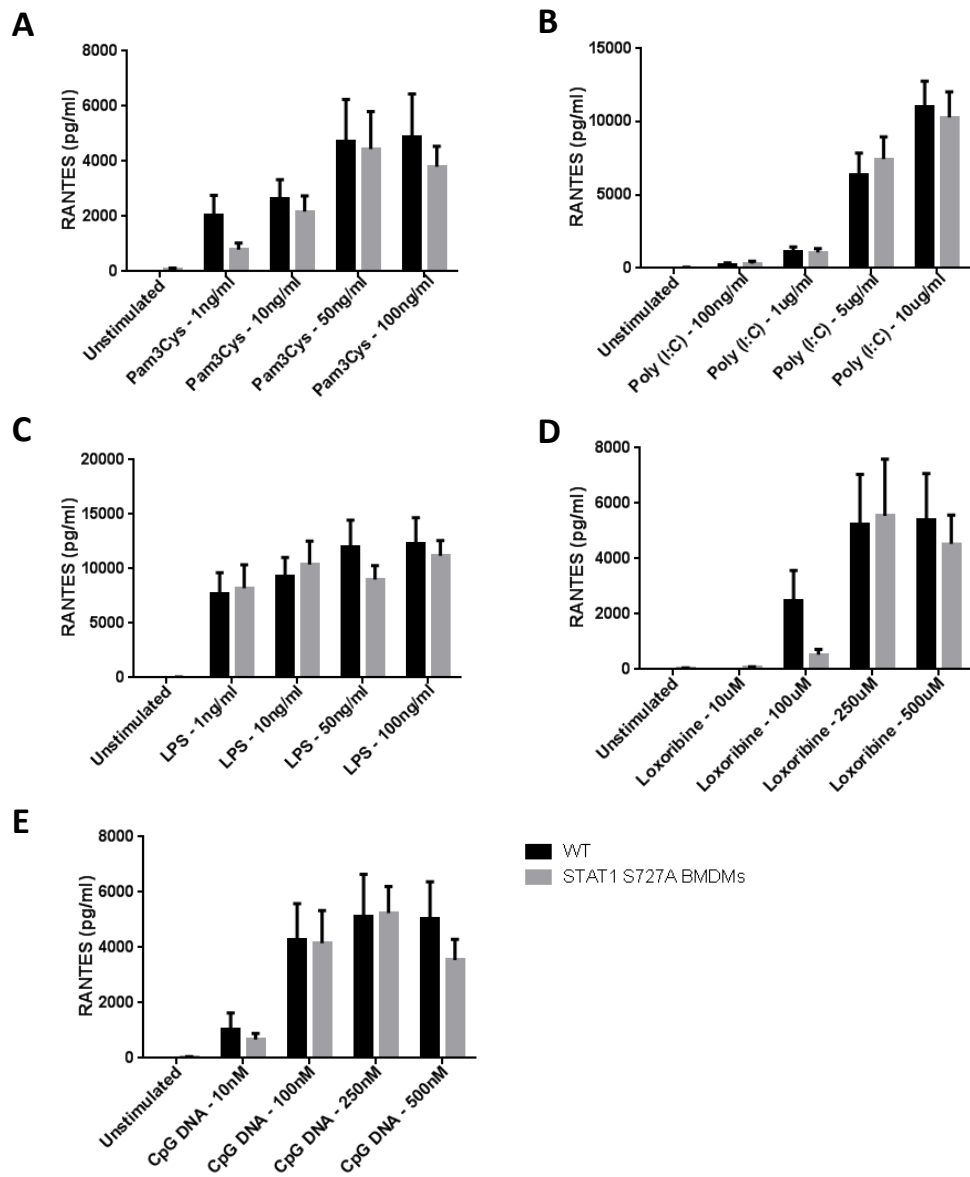


Figure 5.17: RANTES production is not inhibited in STAT1 S727A BMDMs in response to TLR stimulation.

BMDMs were prepared as described figure 5.15. **(A)** Pam₃Cys **(B)** poly (I:C) **(C)** LPS **(D)** loxoribine **(E)** CpG DNA. In response to TLR stimulation, RANTES production in STAT1 S727A BMDMs is comparable to WT BMDMs. Pooled data is represented as mean ± SEM of three independent experiments (n=3).

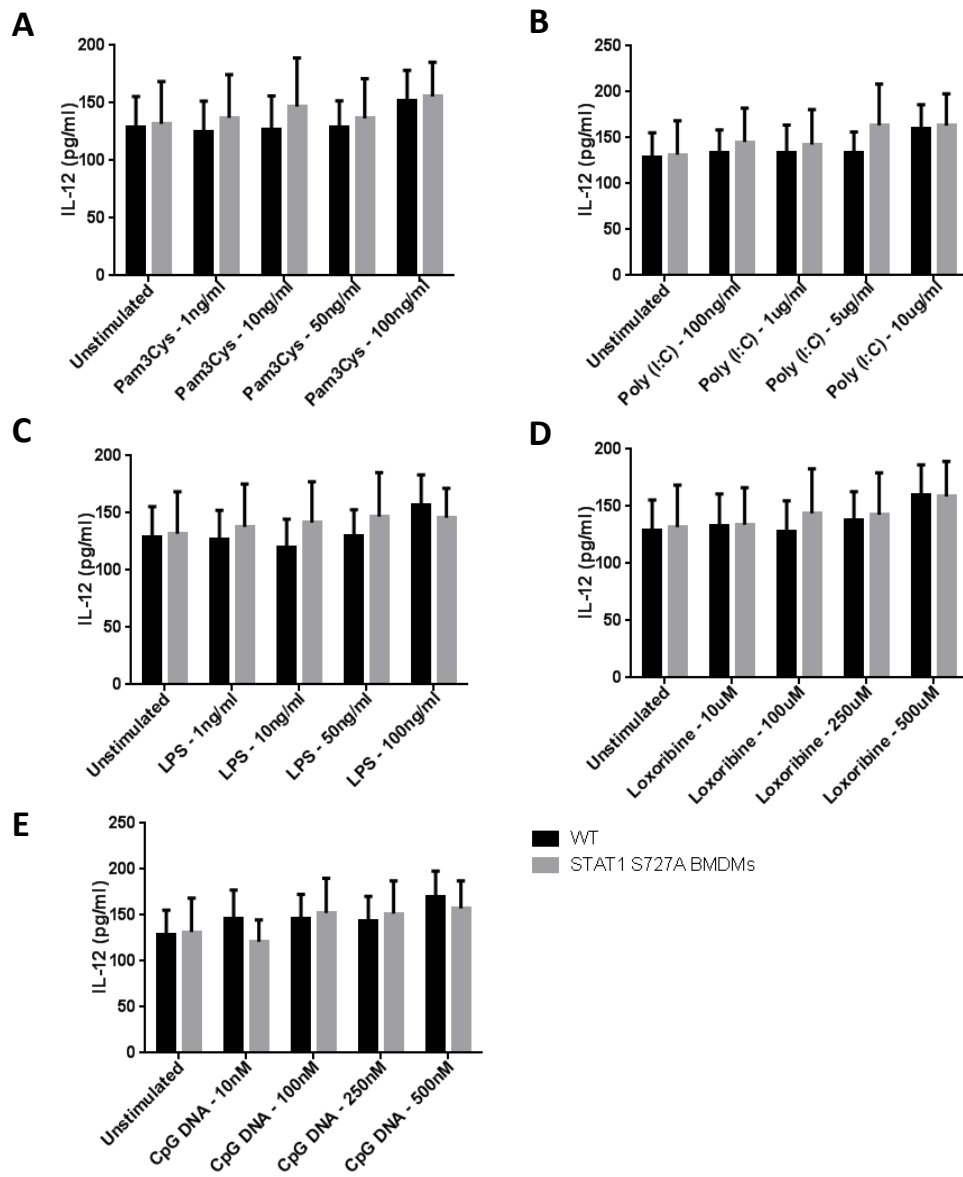


Figure 5.18: TLR stimulation does not induce IL-12 production in BMMs.

BMMs were prepared as described figure 5.15. **(A)** Pam₃Cys **(B)** poly (I:C) **(C)** LPS **(D)** loxoribine **(E)** CpG DNA. TLR stimulation failed to induce production of IL-12 in both WT and STAT1 S727A BMMs. Pooled data is represented as mean ± SEM of three independent experiments (n=3).

5.3 - Discussion

In this chapter I have demonstrated that pSer-727 STAT1 localises to the nucleus following TLR ligand stimulation. This occurs rapidly and appears to be independent of Tyr-701 phosphorylation. In contrast to STAT3, STAT1 does not localise to mitochondria, but exclusively to the nucleus. Nuclear fractionation further demonstrates that STAT1 can be detected in the nucleus supporting my confocal microscopy studies. Importantly, STAT1 appears to require Ser-727 phosphorylation and mutation of serine to alanine inhibited TLR2-induced NF κ B promoter activity. Furthermore, TLR stimulation of STAT1 S727A BMMs displayed specific attenuation of TNF- α production compared to WT BMMs. Contrastingly, STAT1 nuclear localisation was not inhibited in STAT1 S727A BMMs yet further studies are required to determine if the serine residue effects nuclear translocation. Together these studies demonstrate Ser-727 phosphorylation of STAT1 plays an important role in sculpting the innate immune response through specific regulation of TNF- α secretion.

Having established a mechanism of cross-talk between TLR and JAK-STAT signalling, it was next necessary to establish the biological significance of serine phosphorylated STAT1. Classically, STAT1 activation leads to its Tyr-701 phosphorylation which induces dimerisation and subsequent translocation to the nucleus to bind DNA and initiate gene transcription (Shuai et al., 1992). Serine phosphorylation on the other hand initiates the full transcriptional activity of STAT1 (Wen and Darnell, 1997) and has not been documented to induce nuclear translocation of STAT1. My results are the first to demonstrate TLR-dependent pSer-727 STAT1 nuclear localisation. TLR-induced STAT1 Ser-727 phosphorylation was detected in the nucleus as early as 20 minutes suggesting the TLR recruitment of STAT1 bypasses canonical IFN-induced activation of JAK-STAT signalling.

Recently, pSer-727 STAT3 has been detected localising to mitochondria (Wegrzyn et al., 2009, Gough et al., 2009), and in chapter 4 my results also found pSer-727 STAT3 in the mitochondria following LPS stimulation. This therefore prompted me to investigate if STAT1 would also localise to mitochondria following LPS stimulation. My experiments demonstrated that pSer-727 STAT1 exclusively localises to the nucleus, with STAT1 not being detected in mitochondria. It appears mitochondrial localisation is exclusively a pSer-727 STAT3 mechanism, and pSer-727 STAT1 has another role in the cell. Although my studies did not demonstrate STAT1 colocalising to mitochondria, similar to STAT3, previous studies have implicated STAT1 in ROS production. Macrophages treated with the pan-caspase inhibitor, benzyloxycarbonyl-Val-Ala-Asp (zVAD) and

LPS underwent rapid cell death resulting from the generation of superoxide (Kim and Lee, 2005). In STAT1-deficient macrophages however, superoxide levels were diminished and these macrophages were resistant to zVAD/LPS-induced death (Kim and Lee, 2005). This process of cell death was found to be mediated by p38k-induced Ser-727 phosphorylation of STAT1 as inhibition of p38k with SB203580, abolished STAT1 Ser-727 phosphorylation, reduced ROS production and zVAD/LPS-induced macrophage death. This suggests that whilst the tyrosine phosphorylation of STAT1 allows it to behave as a transcription factor, serine phosphorylation of STAT1 may induce STAT1's secondary functions. Whilst I found that inhibition of p38k did inhibit TLR-induced STAT1 Ser-727 phosphorylation, it is possible that different kinases that may serine phosphorylate STAT1 can potentially activate ancillary roles of STAT1. This could be a general mechanism present for all STATs, as discussed in chapter 4, STAT3 can also undergo Ser-727 phosphorylation where it has been demonstrated to localise to mitochondria (Gough et al., 2009). This suggests that the serine phosphorylation of STATs activates secondary mechanisms in regulating cellular function.

It is also possible that the cellular location pSer-727 may dictate its role. As hypothesized by Schroder et al. (2007); in the cytoplasm STAT1 may indirectly modulate gene expression either by sequestering other transcription factors or by binding to them and inducing nuclear transport of the complex. This differs to the role that tyrosine phosphorylated STAT1 dimer has in the nucleus, where serine phosphorylation results in enhancing its transcriptional activity (Wen et al., 1995). My findings also demonstrated that nuclear localisation which is dependent on tyrosine phosphorylation is not a prerequisite for STAT1 Ser-727 phosphorylation. Consistent with observations made by Zhu et al. (1997), both serine and tyrosine phosphorylation occurred independently, with rapid Ser-727 phosphorylation detected before Tyr-701 phosphorylation. In the context of TLR signalling it appears that STAT1 may be recruited into TLR signalling and serine phosphorylated inducing an early phase immune response. Tyrosine phosphorylation occurs later into the response mediated by IFN possibly sustaining this inflammatory state (Noppert et al., 2007).

As pSer-727 STAT1 was detected in the nucleus of cells following LPS stimulation, I wanted to further demonstrate that nuclear pSer-727 STAT1 could be induced by other TLRs. pSer-727 STAT1 could be identified in both cytoplasmic and nuclear fractions suggesting that not all pSer-727 STAT1 localises to the nucleus. Although pSer-727 STAT1 was detected at lower concentrations in TLR3 stimulated cells this may be due to the kinetics of TLR3-induced STAT1 Ser-727 phosphorylation. All other TLRs examined induced STAT1 Ser-727 phosphorylation at 10-20 minutes, in contrast, TLR3-induced STAT1 Ser-727 phosphorylation occurred at 60 minutes

therefore pSer-727 STAT1 may not have translocated to the nucleus at this time point. It has previously been reported that in macrophages, whilst LPS and CpG DNA induced Ser-727 phosphorylation of STAT1, pSer-727 STAT1 is retained in the cytoplasm unless it is also tyrosine phosphorylated (Schroder et al., 2007). My results differ from this study though as STAT1 was demonstrated to translocate to the nucleus independent of tyrosine phosphorylation and this was proven to be a general TLR response. Canonical activation of JAK-STAT signalling results in Tyr-701 phosphorylation of STAT1 and its subsequent translocation to the nucleus and this chain of events was found to be prerequisites for IFN-induced STAT1 serine phosphorylation (Sadzak et al., 2008). My findings however, reveal that the TLR activation of STAT1 bypasses the canonical activation of STAT1, as Ser-727 phosphorylation of STAT1 occurred rapidly before Tyr-701 phosphorylation was detected. Importantly, in response to TLRs that do not induce type I IFNs, I did not detect any pTyr-701 STAT1 (Figure 3.2, 3.5 & 3.6) Traditionally STAT1 localises to the nucleus via the formation of STAT1 homodimers or heterodimers with STAT2 or STAT3 (Qureshi et al., 1995, Tian et al., 1994). Although I have shown pSer-727 STAT1 in nuclei, it remains to be determined whether pSer-727 STAT1 exists as a monomer, dimer or bound to another cofactor. Unphosphorylated STAT1 has been demonstrated to bind IRF1 and constitutively regulate expression of Low Molecular Mass Polypeptide 2 (LMP2), a subunit of the 20S proteasome (Chatterjee-Kishore et al., 2000). As the serine phosphorylation of STAT1 does not induce conformation changes, STAT1 may remain bound to IRF1 and modulate expression of proinflammatory cytokines. In addition, unphosphorylated STAT1 was demonstrated to bind DNA *in vitro* (Chatterjee-Kishore et al., 2000), suggesting pSer-727 STAT1 can also bind DNA. How pSer-727 STAT1 is transported in the nucleus remains unclear, as tyrosine phosphorylation is required to expose the NLS of STAT1, pSer-727 STAT1 may bind other cofactors or form a complex with unphosphorylated STAT1 that is translocated to the nucleus.

As unphosphorylated STAT1 has been demonstrated to regulate gene expression, pSer-727 STAT1 localisation to the nucleus may also be an indication of transcriptional regulation (Chatterjee-Kishore et al., 2000, Cheon and Stark, 2009). Thus I investigated this using a luciferase reporter assay utilising STAT1 WT and a STAT1 S727A mutant. My results demonstrated that STAT1 S727A is impaired in driving the promoters of NF κ B and IL-6, but not TNF- α in response to Pam₃Cys. These results suggest that pSer-727 STAT1 is able to modulate proinflammatory gene expression but are contradictory to my findings in BMMs. Although there are discrepancies between the BMM and luciferase reporter assay, the ability of pSer-727 STAT1 to drive gene expression has previously been reported (Timofeeva et al., 2006, McLaren et al., 2007, Ramsauer et al., 2007). In Epstein-Barr Virus (EBV) infected cells and Wilms' tumour, STAT1 is found to be constitutively Ser-

727 phosphorylated and has been demonstrated to upregulate specific genes (McLaren et al., 2007, Timofeeva et al., 2006). Furthermore, STAT1 S727A expressing cells were found to have a reduced ability in recruiting CREB-binding Protein (CBP) to the *Guanylate Binding Protein 2 (Gbp2)* promoter (Ramsauer et al., 2007). Taken together this indicates pSer-727 STAT1 can directly regulate gene expression, though further assays are required to determine if TLR-mediated STAT1 Ser-727 phosphorylation also induces its ability to interact with DNA.

Further assessment of the nuclear localisation of STAT1 was performed in WT and STAT1 S727A BMMs, as distinct nuclear localisation of pSer-727 STAT1 was observed in RAW264.7 murine macrophages. The nuclear localisation profile of STAT1 S727A BMMs did not differ from WT BMMs and may be a result of the antibody used. As an antibody against pSer-727 STAT1 could not be utilised to stain for STAT1 in STAT1 S727A BMMs, use of a total STAT1 antibody did not provide a clear means of determining nuclear localisation difference. Unphosphorylated STAT1 has been reported to interact with IRF1 and translocate to the nucleus, thus the lack of difference between WT and STAT1 S727A BMMs may be a result of nuclear localised unphosphorylated STAT1 (Chatterjee-Kishore et al., 2000). Whether unphosphorylated STAT1 plays a role in maintaining innate immune responses remains to be studied. Future experiments examining the nuclear localisation of STAT1 in STAT1 S727A BMMs are necessary to fully elucidate the importance of the Ser-727 residue in STAT1 nuclear translocation.

A previous student in our laboratory has identified that in the F/F mice model, STAT1 was found to be hyperactivated following stimulation with LPS (Greenhill, 2011). I therefore investigated cytokine expression in MEFs generated from F/F mice and MEFs that were also deficient in STAT1 (F/F STAT1^{-/-}). My findings demonstrated that whilst production of TNF- α is impaired (Figure 5.6), IL-6 production in F/F STAT1^{-/-} MEFs was increased except in response to CpG DNA (Figure 5.7). In F/F mice, STAT3 is known to drive LPS hypersensitivity and IL-6 production, therefore STAT1-deficiency is not expected to affect IL-6 production (Greenhill et al., 2011). It is uncertain why IL-6 protein expression is increased in F/F STAT1^{-/-} MEFs and whether STAT1 suppresses TLR2- and TLR4-induced IL-6 secretion remains to be investigated. However, the increase in IL-6 production has been documented in STAT1 KO mice infected with Lymphocytic Choriomeningitis Virus (LCMV) and constitutively active STAT1 has been illustrated to attenuate IL-6-induced STAT3 activity demonstrating the opposing effects STAT1 has on STAT3 (Hofer et al., 2012, Dimberg et al., 2012). In contrast to IL-6, TNF- α appears to be reliant on pSer-727 STAT1 and this agrees with the STAT1-deficient mice model used, which exhibited lower levels of TNF- α mRNA expression when infected with *Mycobacterium tuberculosis* (Sugawara et al., 2004). This suggests that in F/F

mice following TLR stimulation, STAT1 primarily regulates production of TNF- α , whereas IL-6 is dependent on STAT3 (see chapter 4), providing a point of divergence for STAT1 and STAT3 in TLR signalling. CpG-induced IL-6 production however, appears to utilize another mechanism which is reliant on STAT1. Previous studies by Schroder et al. (2007) and others have identified that CpG DNA induces an alternative pattern of signalling that can activate STAT1 (Takauji et al., 2002, Schmitz et al., 2007). In pDCs, CpG DNA is thought to induce p38k-dependent STAT1 tyrosine and serine phosphorylation independent of IFN- α/β , which results in ISGF3 formation and transcription of IRF7 (Takauji et al., 2002). The ablated IL-6 production in CpG DNA stimulated F/F STAT1^{-/-} MEFs may therefore be a consequence of STAT1's absence, suggesting that CpG DNA responses require STAT1 in order to fully activate the inflammatory response. In addition, CpG DNA stimulation of myeloid DCs (mDCs) results in IRF1-dependent IFN- β secretion and activation of IFN-stimulated genes further signifying STAT1's role in TLR9-induced responses (Schmitz et al., 2007). My results add further to this specificity of activation by demonstrating that STAT1 regulates TLR-induced TNF- α production, but not IL-6.

To further investigate the role of pSer-727 STAT1 in the modulation of TLR-induced inflammation I examined TNF- α , IL-6, IL-12 and RANTES protein expression following multiple TLR challenge. STAT1 S727A mice, which are unable to undergo Ser-727 phosphorylation due to an alanine substitution have previously been shown to be refractory to LPS-induced lethality, although this was attributed to diminished IFN- γ -induced gene expression (Varinou et al., 2003). Macrophages derived from these mice displayed a clear specificity in the requirement of STAT1 Ser-727 phosphorylation for generation of TNF- α following TLR stimulation. This suggests that in addition to reduced IFN- γ signalling in STAT1 S727A mice, the phenotype observed in these mice may also be a result of diminished TNF- α secretion. Both IFN- γ and TNF- α have been demonstrated to act synergistically in inducing many proinflammatory genes and this is dependent on cross-talk between STAT1 and NF κ B (Ohmori et al., 1997). As both IFN- γ -induced genes and TNF- α levels are reduced in STAT1 S727A mice this may explain the impaired clearance of bacteria. Taken together this illustrates the importance of STAT1 Ser-727 phosphorylation in regulating TNF- α production.

The use of a primary cell line represents a more accurate biological representation of *in vivo* responses hence the discrepancies observe in my luciferase reporter assay and BMM data. The different cell lines used may also contribute to the differences observed in my luciferase reporter assay and ELISA experiments. HEK293s which are non-myeloid in origin may have alternative mechanisms of propagating signal transduction therefore direct comparisons may not be valid. Commensurate with the F/F STAT1^{-/-} MEFs, IL-6 production in response to TLR ligands in STAT1

S727A BMMs was only slightly diminished and is expected as STAT3 is known to be the primary effector of IL-6 (Akira et al., 1994). CpG DNA-induce IL-6 production was not decreased suggesting that whilst STAT1 is required to fully activate TLR9-mediated responses, the Ser-727 residue is not involved in inducing IL-6 secretion. In contrast, IL-6 production is reduced in LPS stimulated STAT1 S727A BMMs, signifying that the Ser-727 residue may contribute to the increase in transcription of IL-6. Although STAT1 can be activated by IL-6 resulting in the formation of STAT1/STAT3 heterodimers, it plays a minimal role in IL-6 signalling (Sanz et al., 2008). Astrocytes in the central nervous system of transgenic mice (Glial Fibrillary (GF)-IL-6) vs. STAT1^{-/-} GF-IL-6 mice, displayed only minor differences in inflammatory phenotype. The absence of STAT1 did not affect transcription of IL-6 mRNA in STAT1^{-/-} GF-IL-6 mice demonstrating the minimal role STAT1 plays in IL-6 signalling. STAT1 serine phosphorylation also appears to follow a similar fashion, with the substitution of the Ser-727 residue to alanine having a minor effect on IL-6 production. RANTES production was also not affected by STAT1 S727A mutation, although STAT1 has been implicated in the regulation of RANTES in response to type I IFNs, this is dependent on Tyr-701 phosphorylation of STAT1, the formation of ISGF3 and signalling through a non-classical ISRE pathway (Cremer et al., 2002). As RANTES is also dependent on NFκB and IRF3 (Moriuchi et al., 1997, Lin et al., 1999, Wietek et al., 2003) STAT1 may not be required in inducing RANTES secretion because endosomal TLR signalling activates both NFκB and IRF3 activation. Whilst I did not detect IL-12p40 expression in my stimulated macrophages, in DCs however, TLR ligands can induce production of IL-12p70. (Gautier et al., 2005). IL-12p70 secretion correlated with a strong type I IFN response and IFNAR^{-/-} mice failed to tyrosine phosphorylate STAT1 or secrete IL-12p70 suggesting that IL-12 production is dependent on tyrosine phosphorylation but not serine phosphorylation of STAT1. This also further suggests cell type specificity of activation as macrophages and DCs differentially activate STAT1. In STAT1 S727A BMMs, Schroder et al. (2007) detected increased expression of IL-12p40 mRNA after CpG DNA stimulation, however as observed in my results CpG DNA fails to induce IL-12 production. Although mRNA levels do not correlate to protein levels, why increased IL-12 is not detected remains to be investigated. From my data, it can be observed that only TNF-α production is affected in STAT1 S727A BMMs. This would therefore suggest that STAT1 localises to the nucleus and modulates TNF-α production. Schroder and co-workers (2007) proposed that in BMMs, STAT1 undergoing Ser-727 phosphorylation remains in the cytoplasm where it may indirectly modulate gene expression through the sequestration of other transcription factors. My results however are contrary, as pSer-727 STAT1 was demonstrated to localise to the nucleus where it appears to regulate expression of TNF-α. This suggests that in response to TLR stimulation, STAT1 Ser-727

phosphorylation only targets a very specific subset of genes to induce an anti-pathogenic state. Whilst STAT1 S727A BMMs only displayed attenuation of TNF- α , in contrast, IL-6 and RANTES generation was comparable to WT BMMs, suggesting that rather than playing a critical role in inflammatory responses, pSer-727 STAT1 may potentially fine-tune the innate immune response. In inflammatory responses, STAT1 is well documented in regulating IFN and TLR macrophage activation through feed-forward and feedback mechanisms (Hu et al., 2008). The sculpting of the innate immune response occurs through maintaining a balance between activation of STAT1 by IFN- γ and the anti-inflammatory properties of IL-10 and STAT3. Thus this equilibrium is critical in sustaining appropriate inflammatory responses. pSer-727 STAT1 may therefore also have similar properties in instigating the initial immune reaction through the regulation of TNF- α production.

Preliminary bioinformatic analysis of 1500 bp upstream of the mouse *Tnf- α* gene (Table 5.1) reveals that this promoter sequence contains a STAT1 half-site. A STAT1 site would represent a homodimer of STAT1 binding to DNA, whereas this non-canonical STAT1 half-site suggests that STAT1 may bind to the mouse *Tnf- α* promoter as a monomer or as a heterodimer bound to another cofactor. As it is unknown what configuration pSer-727 STAT1 adopts when entering the nucleus, this analysis proposes two possible scenarios. The first is that pSer-727 STAT1 localises to the nucleus as a monomer where it binds the *Tnf- α* promoter. In support of this STAT1 has been implicated in binding to the LMP2 promoter and overexpression of unphosphorylated STAT1 maintained transcription of IFN-induced genes, although whether monomeric pSer-727 STAT1 directly binds DNA has not been documented (Chatterjee-Kishore et al., 2000, Cheon and Stark, 2009). Serine phosphorylation of STAT1 however, is not known to induce a conformational change in STAT1 unlike tyrosine phosphorylation which results in a conformational change and dimerisation. Therefore as unphosphorylated STAT1 can bind DNA albeit weaker than a pTyr-701 STAT1 dimer, it can be postulated that Ser-727 phosphorylated STAT1 may also exhibit similar properties to unphosphorylated STAT1. The second possibility would be that pSer-727 STAT1 binds another cofactor allowing this heterodimeric complex to undergo nuclear importation thus allowing it to bind DNA and initiate transcription. Unphosphorylated STAT1 has been documented to bind IRF1 (Chatterjee-Kishore et al., 2000), whether pSer-727 STAT1 binds to another cofactor remains to be investigated. It is possible that pSer-727 STAT1 mimics unphosphorylated STAT1 and binds another transcription factor allowing its subsequent translocation to the nucleus. Ouchi et al. (2000) identified that Ser-727 phosphorylated STAT1 was able to bind Breast Cancer 1, Early Onset (BRCA1) and mediate IFN- γ -dependent transcription of p21WAF1 gene. Mutation of the Ser-727 residue reduced interaction of BRCA1 suggesting that pSer-727 STAT1 can bind other

Table 5.1: Promoter analysis indicating potential STAT1 binding sites.

1500 bp upstream of the mouse *Tnf*, *Il-6*, *Rantes* and *Il-12* promoter was selected and promoter analysis conducted with TRANSFAC Match (version 2011.1). Generic STAT and STAT1 sites were identified. STAT1 half-sites indicate that the STAT1 binds the promoter either as a monomer or bound to another co-factor.

Promoter	Matrix Identifier	Position (strand)	Core Match	Matrix Match	Sequence (+) - strand	Factor Name
TNF	V\$STAT1_02	764 (+)	0.999	0.997	cacTTCCC	STAT1 (half-site)
TNF	V\$STAT_Q6	805 (-)	0.994	0.986	tccAAGAActcaa	STAT
TNF	V\$STAT_Q6	1413 (-)	1.000	0.999	tccCAGAAaagca	STAT
IL-6	-	-	-	-	-	-
RANTES	V\$STAT_Q6	37 (-)	0.994	0.989	tccAAGAActtac	STAT
IL-12a (p35)	-	-	-	-	-	-
IL-12b (p40)	V\$STAT1_02	1435 (+)	0.999	0.999	catTTCCC	STAT1 (half-site)
IL-12b (p40)	V\$STAT1_03	1435 (+)	1.000	0.999	caTTTCCc	STAT1 (half-site)

proteins and regulate gene expression. Analysis of the *Il-6* promoter (Table 5.1) reveals no identifiable STAT1 binding sites further supporting my BMM results that STAT1 does not regulate IL-6 production. The *Rantes* promoter also lacks distinct STAT1 sites supporting the lack of a role of STAT1 in regulating expression of RANTES. Two STAT1 half-sites were also found in the *Il-12b* promoter whilst none were identified in the *Il-12a* promoter. As discussed earlier the *Il-12b* promoter transcribes the p40 subunit of IL-12 and Schroder et al. (2007) was able to detect increases in expression of mRNA IL-12p40 following CpG DNA stimulation in STAT1 S727A BMMs. However, in my experiments TLR stimulation failed to induce IL-12 production in both WT and STAT1 S727A BMMs, suggesting that stimuli other than TLR ligands may induce STAT1-dependent activation of the *Il-12b* promoter. Although previous studies conducted in macrophages have demonstrated that TLR stimulation results in IL-12p40 production (Cowdery et al., 1999) a subsequent study has reported this to be independent of IFN- γ and LPS signalling (Bradford et al., 2002). The identification of STAT1 half-sites in *Il-12b* does lend credence that STAT1 is able to regulate IL-12 production but not in the context that I have examined it in or in the cell line used. It would appear that in response to TLR stimulation, pSer-727 STAT1 plays a dominant role in regulating TNF production, although further investigation into how this sculpts the innate and adaptive immune response is required to determine the importance of STAT1 serine phosphorylation in immune function.

Inflammation has a pivotal role in pathogen clearance and injury. This mechanism of defence is tightly regulated as uncontrolled inflammation can be a precursor to the development of chronic inflammation and diseases such as cancer, arthritis and atherosclerosis. Therefore my study represents a preliminary step into understanding the regulation of inflammation through cross-talk of immune signalling pathways. As pSer-727 STAT1 appears to specifically regulate a subset of genes such as TNF- α secretion, it therefore represents the therapeutic potential in reducing inflammatory cytokines levels without compromising the bodies' ability to deal with pathogens. Further research is still required in understanding TLR-induced STAT1-dependent TNF- α production and how pSer-727 STAT1 may sculpt the innate inflammatory response. Future experiments would examine the conformation STAT1 adopts when translocating to the nucleus, potential DNA binding sites for pSer-727 STAT1 and whether STAT1 S727A alleviates inflammation in disease models.

In conclusion, I have demonstrated the biological significance of pSer-727 STAT1 in TLR-mediated innate immune inflammatory responses. The novel finding that pSer-727 STAT1 localises to the nucleus following TLR stimulation has to my knowledge not previously been reported and it

appears to specifically regulate TNF- α gene transcription. Thus, pSer-727 STAT1 appears to fine-tune the acute inflammatory response through specifically regulating inflammatory genes. Further research is still required to elucidate the mechanisms behind TLR and JAK-STAT cross-talk and the way it modulates the innate immune response.

Chapter 6: Discussion and Conclusion

Chapter 6: Discussion and Conclusion

The TLRs are fundamental to initiating the innate immune response when combating infection. Although inflammatory signal transduction pathways have been extensively studied, the cross-talk between these pathways is much less understood. Interaction among signalling pathways adds another level of complexity to these already intricate pathways, but also allows further layers of control and potentially, specificity to the immune response. Thus understanding these interactions and complexities allows for a more targeted approach when developing therapeutics to control inflammatory responses.

Traditionally, the TLR and JAK-STAT signalling pathways intersect through the induction of type I IFN secretion resulting in binding of the IFNAR complex, tyrosine phosphorylation of STAT1 and transcription of IRGs (Noppert et al., 2007). The direct recruitment of STAT1 and STAT3 into TLR signalling however represents a novel mechanism where STAT1 and STAT3 appear to fine-tune the innate inflammatory response through regulation of TNF- α and IL-6 production, respectively. This is the first demonstration of serine phosphorylated STAT1 and STAT3 regulating TLR-mediated innate immune responses. Whilst tyrosine phosphorylation of STAT1 and STAT3 predominately regulates their cellular functions, here I have established a novel mechanism whereby serine phosphorylation appears to specifically mediate TLR-induced inflammation independent of STAT tyrosine phosphorylation. The data presented in this thesis therefore identifies a unique method of modulating innate immune responses where pSer-727 STAT1 localises to the nucleus independent of tyrosine phosphorylation. STAT3 on the other hand, in its Ser-727 phosphorylated form localises to mitochondria where it may potentially interact with the ETC inducing ROS production, which can further activate ROS-dependent signalling. There is increasing evidence in the literature demonstrating that ROS generation can activate and modulate innate immune signalling. My findings further extend these studies and suggest that STAT3 may modulate inflammatory pathways via this method (Gloire et al., 2006, Zhou et al., 2010, West et al., 2011). These findings therefore significantly enhance our understanding of the role Ser-727 phosphorylated STAT1 and STAT3 plays in TLR signalling. Importantly, this novel mechanism of innate immune signalling regulation provides a unique insight into the cross-talk between these inflammatory signalling pathways with emphases on TRAF6:STAT interaction and serine phosphorylation.

STAT1 has previously been demonstrated to undergo Ser-727 phosphorylation following Pam₃Cys, LPS, CpG DNA stimulation and UV irradiation. (Kovarik et al., 1999, Rhee et al., 2003, Schroder et al.,

2007). My results however, are the first to demonstrate that STAT1 Ser-727 phosphorylation can be induced by all TLRs, irrespective of their cellular location and use of adaptor molecules. To the best of my knowledge, this thesis also assigns a biological role to TLR-induced STAT1 Ser-727 phosphorylation. As discussed in chapter 5, pSer-727 STAT1 translocates to the nucleus where it specifically regulates TNF- α production. Rather than augmenting the innate immune response, STAT1 Ser-727 phosphorylation appears to sculpt the inflammatory reaction by regulating expression of TNF- α upon TLR stimulation. Following TLR stimulation STAT3 was also observed to undergo Ser-727 phosphorylation, but this results in its mitochondrial localisation. Importantly, TLR-induced STAT3 Ser-727 phosphorylation was found to regulate IL-6 production, but not other cytokines, providing a distinct point of divergence between the roles of STAT1 and STAT3 in modulating specific TLR-induced inflammatory mediators.

TRAF6 is a key molecule in TLR signalling, functioning as both a bridging adaptor and a point of bifurcation of signal transduction. The ability of proteins to interact with TRAF6 is attributed to the presence of a T6BM (P-X-E-X-X-(aromatic/acidic residue) in interacting proteins which associate with the TRAF domain of TRAF6. (Ye et al., 2002). Both STAT1 and STAT3 each contain three T6BMs and it is thought that this motif facilitates the TRAF6 interaction I have demonstrated. Future studies identifying the specific T6BM are required to further demonstrate the importance of this interaction in mediating the actions of STAT1 and STAT3. It is possible however, that all three T6BMs are required for TRAF6 interaction, as shown by Sato et al. (2003), only mutation of all three of TRAF6's T6BMs and truncation of the C-terminal region was TRAF6 interaction abrogated. It is thought that TRAF6 functions as a bridging adaptor, bringing STAT1 and STAT3 into proximity to a serine/threonine kinase. Interestingly, a recent paper described the interaction of TRAF6 and STAT3, where STAT3 is negatively regulated through ubiquitination (Wei et al., 2012). TLR-induced NF κ B activation requires the autoubiquitination of TRAF6 through the addition of K63-linked polyubiquitin chains (Lamothe et al., 2007). Thus the interaction of STAT1 and STAT3 with TRAF6 may potentially result in their K63-linked ubiquitination. Whether this is required for TLR-induced pSer-727 STAT1 and pSer-727 STAT3 function remains to be determined. Further research into whether inhibition of TRAF6-mediated K63-linked ubiquitination affects pSer-727 STAT1 and pSer-727 STAT3 actions may provide additional insights into TLR-mediated inflammation.

The identification of the serine kinase responsible for STAT1 and STAT3 Ser-727 phosphorylation may also be important in the development of therapeutics. Without inhibiting the pleiotropic effects of tyrosine phosphorylated STAT1 and STAT3, hindering STAT serine phosphorylation could potentially reduce inflammation without compromising the body's innate immune signalling pathways. Although

I was unsuccessful in identifying the serine kinase, other kinases remain that could potentially serine phosphorylate STAT1 and STAT3. As STAT1 and STAT3 are recruited into the TLR pathway it is therefore possible that serine kinases upstream and downstream of this pathway are capable of activating STAT1 and STAT3. TAK1 which lies downstream of TRAF6, serine phosphorylates the IKK complex allowing NF κ B nuclear translocation (Kaisho and Akira, 2006). As TRAF6 functions as a bridging protein facilitating contact between TAK1 and the IKK complex, it is possible that TRAF6 serves a similar role, bringing TAK1 into proximity to STAT1 and STAT3. Further studies utilising inhibitors of TAK1 and TAK1-deficient cells however, are still required to fully elucidate the role TAK1 plays in STAT serine phosphorylation. The IRAKs which lie upstream of TRAF6 may also serine phosphorylate STAT1 and STAT3 however investigating this will encounter some difficulties. Inhibition of the IRAKs will potentially ablate canonical TLR signalling thus obstructing the TLR-induced TRAF6 recruitment of STAT1 and STAT3. Recently, CDK8 has been implicated in the Ser-727 phosphorylation of STAT1 following IFN- γ stimulation (Bancerek et al., 2013). Based on my findings however, it appears unlikely that CDK8 serine phosphorylates STAT1 and STAT3, as CDK8 is a nuclear kinase, whereas I have demonstrated that both STAT1 and STAT3 undergoes Ser-727 phosphorylation whilst remaining within the cytoplasm. Future work investigating the serine kinase that phosphorylates STAT1 and STAT3 is important for the development of therapeutics to decrease STAT activity and reduce inflammatory mediators.

In recent years emerging evidence has suggested that the immune system is contributing to cancer development. In particular, TLR-mediated inflammation has been implicated in driving carcinogenesis (Rakoff-Nahoum and Medzhitov, 2009). The idea that TLRs can enhance tumorigenesis originated from studies which found that LPS treatment augments tumour growth and survival in adoptively transferred tumours (Pidgeon et al., 1999, Harmey et al., 2002). This direct cross-talk between TLR and JAK-STAT signalling that I have demonstrated represents an alternative method for deregulated innate immune signalling that may create an inflammatory milieu for cancer cells to thrive in. Recent studies utilising a gastric cancer mice model demonstrated that cross-talk between TLR2 and STAT3 contributed to the pathogenesis of gastric cancer (Tye et al., 2012). The oncogenicity of STAT3 in part drives gastric cancer development however, unexpectedly TLR2 was found to promote cell survival and proliferation. In gastric cells, the ability of TLR2 to induce STAT3 Ser-727 phosphorylation which in turn drives IL-6 production suggests that this cross-talk may augment tumour growth. The production of ROS has also recently been demonstrated to promote gastric cancer through TLR4 (Yuan et al., 2013). TLR4 stimulation enhanced tumour cell proliferation, whereas inhibition of TLR4-induced mtROS decreased cell viability. This further highlights the emerging role TLRs play in the pathogenesis of cancer. The localisation of pSer-727 STAT3 in the mitochondria and its ability to

regulate the ETC leading to mtROS production could indicate that the cross-talk of TLR4 and STAT3 may exacerbate carcinogenesis. In normal cells the controlled cross-talk of TLR and JAK-STAT signalling allows for fine-tuning of the innate immune response to clear infection; however deregulated signalling can lead to excessive cytokine and ROS production which further amplifies inflammatory signalling. The oncogenic properties of mitochondrial pSer-727 STAT3 was recently demonstrated in the growth of breast cancer in mice (Zhang et al., 2013). STAT3 containing a mitochondrial localisation sequence and substitution of the Ser-727 to an alanine residue displayed slower tumour growth in 4T1 breast cancer cells. In addition, these cells exhibited decreased complex I activity and increased ROS generation in hypoxic conditions. These results therefore suggest that mitochondrial localised pSer-727 STAT3 plays a role in pathogenesis of 4T1 cancer cells independent of tyrosine phosphorylation. Taken together, these studies and my results indicate that under normal conditions, Ser-727 phosphorylation of STAT3 is required for shaping the initial innate immune response however constitutive Ser-727 phosphorylation of STAT3 can have detrimental effects. The creation of the inflammatory milieu creates an optimal environment for tumourigenesis, whilst excess ROS generation further enhances tumour growth. Thus careful regulation of STAT3 is required in order to maintain homeostasis.

An increasing body of evidence has demonstrated the importance of ROS in innate immunity (Matsuzawa et al., 2005, West et al., 2011, Yang et al., 2013). The ability of STAT3 to induce mtROS production therefore suggests that this could activate other inflammatory signalling pathways. Recent studies have demonstrated that mtROS production can induce activation of the NLRP3 inflammasome (Zhou et al., 2010), an oligomeric complex consisting of NLRP3, Apoptosis-associated Speck-like Protein Containing a CARD (ASC), Cardinal and caspase-1 that cleaves pro-IL-1 β and pro-IL-18 into their respective mature forms IL-1 β and IL-18 (Agostini et al., 2004). The inflammasome requires two signals to become activated; the first to increase expression of inflammasome components and the second to activate caspases. A subsequent study verified the requirement of mtROS in inducing NLRP3 inflammasome activation and Voltage-dependent Anion Channels 1 (VDAC1) was demonstrated to be essential for inflammasome activation (Zhou et al., 2011). Whether TLR-induced STAT3-dependent mtROS generation can activate the inflammasome remains to be determined however, TLR4-induced STAT3 Ser-727 phosphorylation would induce ROS activation which in turn may potentially trigger interaction of the NLRP3 inflammasome with Thioredoxin-interacting Protein (TXNIP) (Zhou et al., 2010). It remains to be determined if the TLR-induced pSer-727 STAT3-mediated ROS production is sufficient to induce this interaction and how mtROS can regulate inflammasome function. However, inhibition of mitophagy, the process of removing damaged ROS-generating mitochondria, has been demonstrated to activate the NLRP3

inflammasome (Zhou et al., 2011, Nakahira et al., 2011). Collectively, these studies suggest a role for mtROS in activating the inflammasome.

The tight control of these inflammatory pathways is critical to their function, as unregulated inflammatory signalling can result in autoimmune and inflammatory disease like arthritis and also the initiation of tumourigenesis (Marshak-Rothstein, 2006, Papadimitraki et al., 2007, Mantovani et al., 2008, Ben-Neriah and Karin, 2011). The constitutive activation of STAT1 and STAT3 has been implicated in several cancers such as Wilms' tumour, gastric cancer and colon cancer (Timofeeva et al., 2006, Jenkins et al., 2005, Corvinus et al., 2005). Both STAT1 and STAT3 have been found to be constitutively active and it was demonstrated by Tye et al. (2012) that TLR2 promoted gastric tumour proliferation. My studies demonstrating TLRs "bridging" STAT1 and STAT3 may therefore provide the link between TLR signalling and tumourigenesis. Both STAT1 and STAT3 have opposing roles in cellular function. Although STAT1 has not been implicated in the cross-talk of TLR signalling and cancer, it has been associated with many types of cancer where it can either be pro-carcinogenic or anti-carcinogenic. (Frank et al., 1997, Kaplan et al., 1998, Bowman et al., 2000). Interestingly, STAT1 Ser-727 phosphorylation was found to affect both Natural Killer (NK) cell cytotoxicity and tumour surveillance (Putz et al., 2013). Against cancer cells, NK cell toxicity was enhanced in STAT1 S727A mice and this translated to increased protection to tumour formation. This data suggests that in NK cells CDK8-mediated STAT1 Ser-727 phosphorylation has an inhibitory effect on NK cell activity. STAT1 is constitutively Ser-727 phosphorylated in NK cells and this may function as a protective feature as NK cells from STAT1 S727A mice are hyperactivated (Putz et al., 2013). Whether pSer-727 STAT1 is pro-survival or pro-apoptosis in cancer remains to be determined and future studies examining tumour development in STAT1 S727A mice challenged with TLR ligands may provide further insights into the role Ser-727 STAT1 plays in the cross-talk of TLR signalling and cancer. It is important to note that it has previously been shown that STAT1 S727A mice were protected from LPS-induced lethality, although this was attributed to deregulation of IFN- γ signalling.

STAT1-deficient mice were demonstrated to be more susceptible to infection by microbial pathogens due to a defective IFN- γ -mediated immune response (Durbin et al., 1996). However, these mice displayed no developmental defects, but developed spontaneous tumours. Crossing these mice with mice deficient in the key tumour suppressor gene, p53, results in increased tumour formation (Kaplan et al., 1998) and interaction with p53 is required to induce apoptosis in response to DNA damage (Townsend et al., 2004). This therefore suggests that STAT1 plays an important role in regulating proliferation and may function as a tumour suppressor gene. STAT1 has also been implicated in inducing TNF- α -mediated apoptotic cell death in U3A cells and is required for the

constitutive expression of caspase-1, caspase-2 and caspase-3 (Kumar et al., 1997). STAT1's ability to drive apoptosis was demonstrated to be dependent on the phosphorylation of Ser-727 residue in cardiac myocytes (Stephanou et al., 2001). Furthermore, STAT1^{-/-} cells were found to have defects in the checkpoints of the cell cycle (Townsend et al., 2005). These studies therefore suggest that STAT1 plays an important role in inducing cell death in response to specific stimuli. Contrastingly, in Wilms' tumour, 19 of 21 primary tumour samples were found to have constitutive STAT1 Ser-727 phosphorylation (Timofeeva et al., 2006). STAT1 Ser-727 phosphorylation inhibited apoptosis by upregulating production of HSP27 and the anti-apoptotic protein MCL-1. This therefore suggests that in normal cells, activation of STAT1 can induce both apoptosis of DNA damaged cells and arrest cell cycle progression. In contrast, constitutive Ser-727 phosphorylation of STAT1 results in upregulation of anti-apoptotic genes leading to apoptotic resistance and suppression of the cytotoxic response. Why constitutively Ser-727 phosphorylated STAT1 leads to adverse cellular effects may be attributable to the induction of other proinflammatory genes. As I have demonstrated in chapter 5, TLR stimulation can also induce STAT1 Ser-727 phosphorylation leading to secretion of TNF- α . Deregulated TNF- α production can have deleterious effects and is associated with autoimmune and inflammatory diseases such as rheumatoid arthritis, septic shock and inflammatory bowel disease (Feldmann et al., 1995, Beutler and Cerami, 1989, Kollias et al., 1999). Accordingly, this suggests that in diseases that exhibit constitutive STAT1 or STAT3 serine phosphorylation targeting IL-6 or TNF- α production may potentially alleviate disease progression.

In contrast to STAT1, STAT3 is implicated in many cancers where it has been shown to be constitutively active and anti-apoptotic (Garcia and Jove, 1998). The Epidermal Growth Factor Receptor (EGFR), Platelet-derived Growth Factor Receptor (PDGFR) and the non-tyrosine kinase, Src, lie upstream of STAT3 and in many solid tumour cancers are overexpressed leading to persistent activation of STAT3 (Zhong et al., 1994, Bowman et al., 2001, Yu et al., 1995). Furthermore, STAT3 was found to behave as an oncogene in nude mice resulting in tumour formation (Bromberg et al., 1999). Moreover, a constitutively active form of STAT3 (STAT3C) was found to be sufficient to mediate cell transformation by v-Src (Bromberg et al., 1998). This therefore demonstrates unregulated STAT3 signalling can initiate tumourigenesis and enhance cell proliferation. STAT3's anti-apoptotic properties are thought to be activated through interaction with the proto-oncogene, c-Jun. Ivanov et al. (2001) demonstrated that STAT3/c-Jun interaction reduced expression of Fas, thus decreasing the apoptotic potential of Fas/FasL pathway. These studies further exhibit the oncogenic nature of STAT3 by enhancing cell proliferation, down regulating apoptosis and inducing cellular transformation.

As observed from my results in chapter 3, STAT3 interacts with TRAF6, though this complex isn't detected in mitochondria, indicating that STAT3 may localise to mitochondria as a monomer or bound to another cofactor. As STAT3 does not contain a mitochondrial localisation sequence it is likely that it is bound to another protein that facilitates its mitochondrial localisation. Recent studies have implicated GRIM-19 in binding STAT3 and transporting it into mitochondria (Tammineni et al., 2013). GRIM-19, a component of complex I of the ETC was demonstrated to interact with Ser-727 phosphorylated STAT3 and chaperone pSer-727 STAT3 into the inner mitochondrial membrane (Tammineni et al., 2013). This consequently suggests that STAT3 interacts with complex I of the ETC to induce mtROS production. Wegrzyn et al. (2009) observed in STAT3-deficient cells, activities of complex I and complex II were decreased, and when reconstituted with a mitochondrial targeted STAT3 S727D, a mimetic of constitutively serine phosphorylated STAT3, activities of complex I and II were restored, signifying the importance of the Ser-727 residue in regulating cellular respiration. A similar finding was reported by Gough et al. (2009) who found decreased complex II and V activity in Ras-transformed STAT3^{-/-} cells. The mitochondrial function of STAT3 is dependent on Ser-727 suggesting that the ability of STAT3 to interact with and regulate mitochondrial activity is reliant upon serine phosphorylation. Further investigation of pSer-727 STAT3's role in cellular respiration may provide additional insights into the progression of normal cells to cancer cells as well as the induction of mtROS in pathogen clearance.

TLR stimulation results in mtROS generation which is in concordance with observations from West et al. (2011). Although STAT3 is thought to induce ROS production, further experiments are required to definitively demonstrate this. Future work will involve examining mtROS generation and cytokine expression in STAT3 S727A macrophages. STAT3 S727A's ability to localise to mitochondria will also be observed to determine if the serine residue is crucial for TLR-induced STAT3 mitochondrial localisation. These experiments will provide further insights into the role Ser-727 plays in TLR-induced inflammation. Infection models can also be utilised to further investigate the biological role STAT serine phosphorylation plays. If available STAT1 S727A and STAT3 S727A mice will be used as infection models to fully elucidate Ser-727 phosphorylation in innate immune pathways.

Understanding the cellular processes that STAT1 and STAT3 are involved in is particularly important in the development of therapeutics. Due to the contrasting nature of these two molecules the accidental inhibition of either STAT can ultimately lead to drastic consequences in patient outcomes. There are few inhibitors of STAT1 reported in the literature, on the other hand due to many cancers that display constitutive STAT3 activation, STAT3 remains a primary drug target. Due to the importance of tyrosine phosphorylation and STAT3 dimerisation the majority of inhibitors focus on

targeting these aspects of STAT3 (Turkson and Jove, 2000, Turkson, 2004). The current approach to STAT signalling inhibition targets four aspects of STAT function. Firstly, Peptidomimetic Inhibitors (PMI) and Small-molecule Dimerisation Disruptors (SMDDs) work via inhibition of pTyr-SH2 interaction, thereby disrupting STAT dimer formation (Turkson et al., 2001). Compared to SMDDs however, peptide inhibitors have had less clinical success due to their poor cell permeability and instability making them a less viable therapeutic (Miklossy et al., 2013). Due to the importance of tyrosine phosphorylation in inducing STAT dimerisation, the use of tyrosine kinase inhibitors represents another STAT inhibition strategy; these however can affect multiple STATs and lack the specificity of other approaches (Yue and Turkson, 2009). Equally, protein tyrosine phosphatases have been identified to be activated and the dephosphorylation of STATs results in downregulation of their signalling, demonstrating an alternative method of STAT inhibition (Miklossy et al., 2013). The last strategy involves the use of oligodeoxynucleotide (ODN) decoys to inhibit STAT DNA binding domains (Sen et al., 2009, Sen et al., 2012). These ODN decoys compete with endogenous DNA promoter sequences thus suppressing gene expression and are able to discriminate between STAT1 and STAT3 (Souissi et al., 2012). Recently the use of Antisense Oligonucleotides (ASOs), which bind to the RNA that transcribes the target protein, have shown great promise in pre-clinical toxicology studies (Burel et al., 2013). Despite the many STAT inhibitors that are being currently studied, only tyrosine kinase inhibitors are presently being utilised in clinical settings (Cheng et al., 2009, Muhammad et al., 2012). These however, do not directly target the STATs. Therefore the potential benefits in STAT inhibition have not been fully realised. As I have demonstrated in my findings that serine phosphorylation of STAT1 and STAT3 allow them to regulate the expression of specific genes, this represents potential drug targets. In contrast to tyrosine phosphorylation, Ser-727 phosphorylation is not crucial for STAT activation. Therefore inhibition of STAT serine phosphorylation may sufficiently impair its function and provides specificity in therapy as opposed to affecting STAT tyrosine phosphorylation and its pleiotropic effects. Although further research into this area is still required to fully elucidate the role STAT1 and STAT3 Ser-727 phosphorylation have in cellular function and the effects this has on carcinogenesis.

Overall the findings in this thesis provide further insight into inflammatory signal cross-talk. The recruitment of STAT1 and STAT3 into the TLR pathway and their subsequent Ser-727 phosphorylation represents a novel mechanism in fine-tuning the innate immune response. Further biological implications of STAT serine phosphorylation remain to be investigated and may offer potential therapeutics in treating cancer and inflammatory diseases.

Appendix I - Formulation of Buffers and Solutions

Appendix I – Formulation of Buffers and Solutions

10% Ammonium Persulphate (APS)

0.1 g APS (Bio-Rad Laboratories)

1 ml MQ.H₂O (Merck-Millipore)

Stored at -20°C.

5% Bovine Serum Albumin (BSA)

5% (w/v) BSA (Sigma-Aldrich)

50 ml 1 x TBST

Coomassie R-250 Blue Dye

0.25% (w/v) Brilliant Blue G (Sigma)

50% (v/v) Methanol (MeOH, Chem-Supply)

10% (v/v) Glacial Acetic Acid (AR grade, Merck-Millipore)

Made up to a total volume of 500 ml with MQ.H₂O.

Coomassie De-stain Solution

20% (v/v) MeOH

7% (v/v) Glacial Acetic Acid

3% (v/v) Glycerol (Amresco)

Made up to a total volume of 500 ml with MQ.H₂O.

Digitonin/Sucrose Buffer

2 µM Digitonin (Sigma-Aldrich)

300 mM Sucrose (Sigma-Aldrich)

10 mM HEPES (pH 7.4, Merck-Millipore)

10 mM Sodium Chloride (NaCl)

3 mM Magnesium Chloride (MgCl₂, Sigma-Aldrich)

1 mM Dithiothreitol (DTT, Sigma-Aldrich)

0.4 mM Phenylmethylsulphonyl Fluoride (PMSF, Sigma-Aldrich)

0.1 mM Sodium Vanadate (NaV, Sigma-Aldrich)

Made up to a total volume of 50 ml with MQ.H₂O.

Stored at 4°C.

DNA Loading Dye

0.2% (w/v) Bromophenol Blue (Sigma-Aldrich)
0.2% (w/v) Xylene Cyanol (Sigma-Aldrich)
10 mM Ethylenediaminetetraacetic acid (EDTA, pH 8.0)
20% (v/v) Glycerol

Made up to a total volume of 10 ml with MQ.H₂O.

Dulbecco's Modified Eagle's Medium (DMEM) - Supplemented

10% (v/v) Fetal Bovine Serum (FBS, Life Technologies)
2 mM L-Glutamine (Life Technologies)
50 U/ml and 50 µg/ml Penicillin- Streptomycin (Life Technologies)
In 500 ml of DMEM (Life Technologies).

0.5 M EDTA

186.12 g EDTA (Chem-Supply)
pH to 8.0 with 10 M NaOH
Made up to a total volume of 1 L with MQ.H₂O.

ELISA Stop Solution

2N Sulphuric Acid (H₂SO₄, Merck-Millipore)
Made up to a total volume of 100 ml with MQ.H₂O.

70% Ethanol (EtOH)

70% (v/v) Absolute EtOH (Chem-Supply)
Made up to a total volume of 1 L with MQ.H₂O.

1% Gelatin

1% (w/v) Gelatin (Sigma-Aldrich)
Made up to a total volume of 100 ml with MQ.H₂O, then autoclaved.

10 x Glycine Stripping Buffer

250 mM Glycine-HCl (pH 2)
Made up to a total volume of 500 ml with MQ.H₂O.

1 x Glycine Stripping Buffer

50 ml 10 x Glycine Stripping Buffer

450 ml MQ.H₂O

1 M HEPES

23.83 g HEPES

pH adjusted to 7.4 with NaOH.

Made up to a total volume of 100 ml with MQ.H₂O.

High Salt Soluble Buffer (HSSB)

50 mM HEPES (pH 7.6)

500 mM NaCl (Merck-Millipore)

0.5 mM EDTA (pH 8.0)

0.5% (v/v) Triton X-100 (Merck-Millipore)

Made up to a total volume of 500 ml with MQ.H₂O.

IL-6 & TNF ELISA Assay Diluent

10% (v/v) FBS

Made up to a total volume of 50 ml with PBS pH 7.4.

IL-6 ELISA Coating Buffer

85 mM Sodium Hydrogen Carbonate (NaHCO₃)

15 mM Sodium Carbonate (Na₂CO₃)

Made up to a total volume of 100 ml with MQ.H₂O.

pH adjusted to 9.5 with Sodium hydroxide (NaOH).

Stored at 4°C.

1 M Isopropyl-β-D-Thiogalactopyranoside (IPTG)

0.1191 g IPTG (Promega)

Dissolved in 5 ml of MQ.H₂O.

Kal B Stock Solution

50 mM Tris-HCl (pH 7.4, Amresco)

150 mM NaCl

1% (v/v) Triton X-100

1 mM EDTA (pH 8.0)

Made up to a total volume of 1 L with MQ.H₂O.

Stored at 4°C.

Kal B Lysis Buffer – Supplemented

1 Complete Mini, EDTA-free protease inhibitor cocktail tablet (Roche Diagnostics)

1 mM Sodium Fluoride (NaF, Lancaster)

1 mM NaV

1 mM PMSF

Made up to a total volume of 50 ml with Kal B Solution.

Stored at 4°C.

Kal B Lysis Buffer with Ser/Thr Phosphate Inhibitors - Supplemented

Shaving of Complete Mini, EDTA-free protease inhibitor cocktail tablet

20 µl 50 x Ser/Thr Phosphate Inhibitors

1 mM NaV

1 mM PMSF

Made up to a total volume of 1 ml with Kal B Solution.

Stored at 4°C.

Laemmli Reducing Sample Buffer

90% (v/v) 5 x SDS-PAGE Buffer

10% (v/v) 2-Mercaptoethanol (BME, Sigma-Aldrich)

Low Salt Soluble buffer (LSSB)

50 mM HEPES (pH 7.6)

50 mM NaCl

0.5 mM EDTA (pH 8.0)

Made up to a total volume of 500 ml with MQ.H₂O.

Luria Bertani (LB) Agar

- 1% (w/v) Bacto-Tryptone (BD Biosciences)
- 0.5% (w/v) Bacto-Yeast Extract (BD Biosciences)
- 170 mM NaCl
- 1.5% (w/v) Agar (Oxiod)

Made up to a total volume of 1 L with MQ.H₂O and autoclaved.

LB Ampicillin Plates

100 ml of solidified LB agar were melted and cooled to ~50°C, 100 µg/ml ampicillin was added to the agar and the solution poured into 10 cm plates. The plates were allowed to dry under Bunsen burner flame then stored at 4°C.

LB Broth

- 1% (w/v) Bacto-Tryptone
- 0.5% (w/v) Bacto-Yeast Extract
- 170 mM NaCl

Made up to a total volume of 1 L with MQ.H₂O and autoclaved.

1 M Magnesium Chloride (MgCl₂)

20.33 g MgCl₂.6H₂O (Sigma-Aldrich)

Made up to a total volume of 100 ml with MQ.H₂O.

Nuclei Lysis Buffer

- 20 mM HEPES (pH 7.8)
- 420 mM NaCl
- 20% (v/v) Glycerol
- 0.2 mM EDTA (pH 8.0)
- 1.5 mM MgCl₂

Made up to a total volume of 100 ml with MQ.H₂O.

Store at 4°C.

10x Phosphate Buffered Saline (PBS)

1400 mM NaCl

30 mM Potassium Chloride (KCl, Merck-Millipore)

100 mM Disodium Hydrogen Phosphate (Na_2HPO_4 , Merck-Millipore)

18 mM Potassium Dihydrogen Phosphate (KH_2KPO_4 , Merck-Millipore)

Made up to a total volume of 5 L with MQ.H₂O.

1x Phosphate Buffered Saline (PBS, 7.4)

500 ml 10x PBS

4.5 L MQ.H₂O

pH adjusted to 7.4.

0.5% PBS-Tween (PBST)

1 L 1x PBS

0.5% (v/v) Tween 20 (Sigma-Aldrich)

100 nM Phenylmethylsulphonyl Fluoride (PMSF)

174.2 mg PMSF

10 ml Isopropanol (Merck-Millipore)

Stored at 4°C.

Plasma Membrane Lysis Buffer

10 mM HEPES pH 7.4

1.5 mM MgCl_2

10 mM KCl

0.1% (v/v) Nonidet P-40 (Sigma-Aldrich)

Made up to a total volume of 100 ml with MQ.H₂O.

Store at 4°C.

1 M Potassium Chloride (KCl)

7.4 g KCl (Sigma-Aldrich)

Made up to a total volume of 100 ml with MQ.H₂O.

RANTES ELISA Assay Diluent

1% (w/v) BSA

50 ml PBS

RPMI Media 1640 – Supplemented

10% (v/v) FCS

2 mM L-Glutamine

50 U/ml and 50 µg/ml Penicillin- Streptomycin

In 500 ml of RPMI 1640 Medium (Life Technologies).

5 × SDS-PAGE Loading Dye

60mM 1M Tris-HCl

25% (v/v) Glycerol

2% (w/v) SDS (Merck-Millipore)

0.1% (w/v) Bromophenol Blue

Made up to a total volume of 100 ml with MQ.H₂O.

SDS-PAGE Lower Gel Buffer

1.5 M Tris-HCl (pH 8.8)

0.4% (w/v) SDS

Made up to a total volume of 1 L with MQ.H₂O.

10x SDS-PAGE Running Buffer

250 mM Tris-HCl (pH 8.3)

1920 mM Glycine

1% (w/v) SDS

Made up to a total volume of 10 L with MQ.H₂O.

1 × SDS-PAGE Running Buffer

100 ml 10x SDS-PAGE Running Buffer

900 ml MQ.H₂O

SDS-PAGE Upper Gel Buffer (pH 6.8)

500 mM Tris-HCl (pH 6.8)

0.4% (w/v) SDS

Made up to a total volume of 500 ml with MQ.H₂O.

50 x Serine/Threonine Phosphate Inhibitors

50 mM Sodium Pyrophosphate (Sigma-Aldrich)

50 mM Sodium Molybdate (Merck-Millipore)

500 mM NaF

Make up to a total volume of 500 ml with MQ.H₂O .

Stored at 4°C.

1% Skim Milk Solution

0.5 g Skim Milk Powder (Diploma)

50 ml 0.5% PBST

Stored at 4°C.

2.5% Skim Milk Solution with Ser/Thr Phosphate Inhibitors

7.5 g Skim Milk Powder

6 ml 50 x Ser/Thr Phosphate Inhibitors

1 mM NaV

300 ml 1 x TBST

Stored at 4°C.

5% Skim Milk Solution

2.5 g Skim Milk Powder

50 ml 0.5% PBST

Stored at 4°C.

5% Skim Milk Solution with Ser/Thr Phosphate Inhibitors

15 g Skim Milk Powder
6 ml 50 x Ser/Thr Phosphate Inhibitors
1 mM NaV
300 ml 1 x TBST

Stored at 4°C.

SOC Medium

2% (w/v) Bacto-Tryptone
0.5% (w/v) Bacto-Yeast Extract
0.01 M NaCl
2.5 mM KCl

Made up to a total volume of 490 ml with MQ.H₂O.

Autoclave, cool and add:

10 mM MgCl₂
10 mM Magnesium Sulphate (MgSO₄, Merck-Millipore)
10 mM Glucose (Merck-Millipore)

5 M Sodium Chloride (NaCl)

146.1 g NaCl

Made up to a total volume of 500 ml with MQ.H₂O

1 M Sodium Fluoride (NaF)

4.2 g NaF
2 ml MQ.H₂O
Stored at -20°C.

10 M Sodium Hydroxide (NaOH)

200 g NaOH (Panreac)
Made up to a total volume of 500 ml with MQ.H₂O.

1 M Sodium Vanadate (NaV)

1.839 g Sodium Othrovanadate (Sigma-Aldrich)

Made up to a total volume of 100 ml with MQ.H₂O.

pH adjusted to 10.0 with HCl and boil until colourless then allow to cool to room temperature.

pH adjusted to 10.0 with NaOH and boil until colourless then allow to cool to room temperature.

Store at -80°C.

50x Tris Acetate EDTA Buffer (TAE)

2 M Tris-acetate (pH 8.3)

0.05 M EDTA (pH 8.0)

Made up to a total volume of 10 L with MQ.H₂O.

1x TAE

400 ml 50x TAE buffer

1.6 L MQ.H₂O

10x Tris Buffered Saline- Tween (TBST)

100 mM Tris-HCl (pH 8)

1.5 M NaCl

0.5% (v/v) Tween 20

Made up to a total volume of 1 L with MQ.H₂O.

1x TBST

100 ml 10 x TBST

900 ml MQ.H₂O

TNF- α ELISA Coating Buffer

100 mM NaHCO₃

34 mM Na₂CO₃

Made up to a total volume of 100 ml with MQ.H₂O.

pH adjusted to 9.5.

Stored at 4°C.

10x Transfer Buffer

15.6 mM Tris-HCl (pH 8.3)

120 mM Glycine

Made up to a total volume of 1 L with MQ.H₂O.

1x Transfer Buffer

80 ml 10 x Transfer Buffer

160 ml MeOH

560 ml MQ.H₂O

Cool to 4°C prior to use.

0.1% Triton X-100

0.1% (v/v) Triton X-100

Made up to a total volume of 100 ml with MQ.H₂O.

Appendix II - Primer Sequences

Appendix II – Primer Sequences

Site-directed mutagenesis primers

STAT1 sense S727A

5'-AACCTGCTCCCATGGCTCCTGAGGAGTTTG-3'

STAT1 anti-sense S727A

5'-CAAACCTCCTCAGGAGCCATGGGGAGCAGGTT-3'

STAT3 sense S727A

5'-GACCTGCCGATGGCCCCCGCACTT-3'

STAT3 anti-sense S727A

5'-AAGTGCGGGGGCCATCGGCAGGTC-3'

Sequencing primers

STAT1

5'-TGTCTCAGTGGTCGAACTTCAG-3'

5'-CAGGCTCAGTCGGGGAATATTC-3'

5'-AGTGAAGCGGAGACAGCAGA -3'

5'-CCCCTGACATCATTGCAATTAC-3'

5'-CGACAGTATGATGAACACAG-3'

STAT3

5'-CTGCTAATGACGTTATCCAG-3'

5'-ACAGATTGCCTGCATTGGAGG-3'

5'-CTGCCAGTGTAGTCAGCTG-3'

5'-CCAATTGGAACCTGGGATC-3'

5'-GAAGAGCTGGCTGACTGGAA-3'

5'-CAGATGCCAAATGCTTGGGCA-3'

**Appendix III - List of
Manufacturers**

Appendix III – List of Manufacturers

Manufacturer	Location
Agfa-Gevaert	Mortsel, Belgium
Agilent Technologies	Mulgrave, VIC, Australia
Amber Scientific	Midvale, WA, Australia
Amresco	Solon, OH, USA
Applied Biosystems	Foster City, CA, USA
BD Biosciences	North Ryde, NSW, Australia
Beckman Coulter	Lane Cove, NSW, Australia
Biolegend	San Diego, CA, USA
Bio-Rad Laboratories	Gladesville, NSW, Australia
Bitplane	Zurich, Switzerland
BMG Labtech	Mornington, VIC, Australia
Chem-Supply	Port Adelaide, SA, Australia
Cole-Parmer	Vernon Hills, IL, USA
Corning	Tewksbury, MA, USA
Dako	Campbellfield, VIC, Australia
EMC Microcollections	Tübingen, Germany
Enzo Life Sciences	Farmingdale, NY, USA
GE Healthcare Life Sciences	Rydalmere, NSW, Australia
Gene Works	Hindmarsh, SA, Australia
Graphpad Software	La Jolla, CA, USA
Griener Bio-One	Frickenhausen, Germany
Hofer	Holliston, MA, USA
Invivogen	San Diego, CA, USA
Kimtech Science	Milsons Point, NSW, Australia
Leica Microsystems	North Ryde, NSW, Australia
LI-COR Biosciences	Lincoln, NE, USA
Life Technologies	Mulgrave, VIC, Australia
Menzel-Gläser	Brunswick, Germany
Merck-Millipore	Kilsyth, VIC, Australia
Miltenyi Biotech	Macquarie Park, NSW, Australia
New England Biolabs	Ipswich, MA, USA

Nikon Instruments	Melville, NY, USA
Optik Labor	Lancing, UK
Panreac	Barcelona, Spain
Parr Instrument Company	Moline, IL, USA
Promega	Alexandria, NSW, Australia
Qiagen	Chadstone, VIC, Australia
R&D Systems	Minneapolis, MN, USA
Roche Diagnostics	Castle Hill, NSW, Australia
Rockland	Gilbertsville, PA, USA
Santa Cruz Biotechnology	Dalla, TX, USA
Sarstedt	Technology Park, SA, Australia
Sigma-Aldrich	Sydney, NSW, Australia
Sony	Clayton, VIC, Australia
SteriHealth	Dandenong South, VIC, Australia
Thermo Scientific	Scoresby, VIC, Australia
TPP	Trasadingen, Switzerland
Vilber Lourmat	Marne-la-Vallée, France

Bibliography

Bibliography

- AARONSON, D. S. & HORVATH, C. M. 2002. A road map for those who don't know JAK-STAT. *Science*, 296, 1653-1655.
- ADACHI, O., KAWAI, T., TAKEDA, K., MATSUMOTO, M., TSUTSUI, H., SAKAGAMI, M., NAKANISHI, K. & AKIRA, S. 1998. Targeted disruption of the MyD88 gene results in loss of IL-1- and IL-18-mediated function. *Immunity*, 9, 143-50.
- ADEREM, A. & ULEVITCH, R. J. 2000. Toll-like receptors in the induction of the innate immune response. *Nature*, 406, 782-7.
- ADHIKARI, A., XU, M. & CHEN, Z. J. 2007. Ubiquitin-mediated activation of TAK1 and IKK. *Oncogene*, 26, 3214-26.
- AGGARWAL, B. B., KUNNUMAKKARA, A. B., HARIKUMAR, K. B., GUPTA, S. R., THARAKAN, S. T., KOCA, C., DEY, S. & SUNG, B. 2009. Signal Transducer and Activator of Transcription-3, Inflammation, and Cancer. *Annals of the New York Academy of Sciences*, 1171, 59-76.
- AGOSTINI, L., MARTINON, F., BURNS, K., MCDERMOTT, M. F., HAWKINS, P. N. & TSCHOPP, J. 2004. NALP3 forms an IL-1beta-processing inflammasome with increased activity in Muckle-Wells autoinflammatory disorder. *Immunity*, 20, 319-25.
- AHMAD-NEJAD, P., HÄCKER, H., RUTZ, M., BAUER, S., VABULAS, R. M. & WAGNER, H. 2002. Bacterial CpG-DNA and lipopolysaccharides activate Toll-like receptors at distinct cellular compartments. *European Journal of Immunology*, 32, 1958-1968.
- AKASHI, S., SAITOH, S.-I., WAKABAYASHI, Y., KIKUCHI, T., TAKAMURA, N., NAGAI, Y., KUSUMOTO, Y., FUKASE, K., KUSUMOTO, S., ADACHI, Y., KOSUGI, A. & MIYAKE, K. 2003. Lipopolysaccharide Interaction with Cell Surface Toll-like Receptor 4-MD-2: Higher Affinity than That with MD-2 or CD14. *The Journal of Experimental Medicine*, 198, 1035-1042.
- AKIRA, S., NISHIO, Y., INOUE, M., WANG, X.-J., WE, S., MATSUSAKA, T., YOSHIDA, K., SUDO, T., NARUTO, M. & KISHIMOTO, T. 1994. Molecular cloning of APRF, a novel IFN-stimulated gene factor 3 p91-related transcription factor involved in the gp130-mediated signaling pathway. *Cell*, 77, 63-71.
- AKIRA, S. & TAKEDA, K. 2004. Toll-like receptor signalling. *Nat Rev Immunol*, 4, 499-511.
- AKIRA, S., TAKEDA, K. & KAISHO, T. 2001. Toll-like receptors: critical proteins linking innate and acquired immunity. *Nat Immunol*, 2, 675-80.
- AKIRA, S., UEMATSU, S. & TAKEUCHI, O. 2006. Pathogen recognition and innate immunity. *Cell*, 124, 783-801.

- AKIRA, S., YAMAMOTO, M. & TAKEDA, K. 2003. Role of adapters in Toll-like receptor signalling. *Biochem Soc Trans*, 31, 637-42.
- AL-SALLEEH, F. & PETRO, T. M. 2007. TLR3 and TLR7 are involved in expression of IL-23 subunits while TLR3 but not TLR7 is involved in expression of IFN- β by Theiler's virus-infected RAW264.7 cells. *Microbes and Infection*, 9, 1384-1392.
- ALEXOPOULOU, L., HOLT, A. C., MEDZHITOV, R. & FLAVELL, R. A. 2001. Recognition of double-stranded RNA and activation of NF- κ B by Toll-like receptor 3. *Nature*, 413, 732-738.
- ALONZI, T., MARITANO, D., GORGONI, B., RIZZUTO, G., LIBERT, C. & POLI, V. 2001. Essential Role of STAT3 in the Control of the Acute-Phase Response as Revealed by Inducible Gene Activation in the Liver. *Molecular and Cellular Biology*, 21, 1621-1632.
- ANANTHARAMAN, V. & ARAVIND, L. 2002. The GOLD domain, a novel protein module involved in Golgi function and secretion. *Genome Biol*, 3, research0023.
- AOMATSU, K., KATO, T., FUJITA, H., HATO, F., OSHITANI, N., KAMATA, N., TAMURA, T., ARAKAWA, T. & KITAGAWA, S. 2008. Toll-like receptor agonists stimulate human neutrophil migration via activation of mitogen-activated protein kinases. *Immunology*, 123, 171-80.
- ARCARO, A. & WYMAN, M. P. 1993. Wortmannin is a potent phosphatidylinositol 3-kinase inhibitor: the role of phosphatidylinositol 3,4,5-trisphosphate in neutrophil responses. *Biochem J*, 296 (Pt 2), 297-301.
- ARCH, R. H., GEDRICH, R. W. & THOMPSON, C. B. 1998. Tumor necrosis factor receptor-associated factors (TRAFs)—a family of adapter proteins that regulates life and death. *Genes & Development*, 12, 2821-2830.
- ASEHNOUNE, K., STRASSHEIM, D., MITRA, S., KIM, J. Y. & ABRAHAM, E. 2004. Involvement of reactive oxygen species in Toll-like receptor 4-dependent activation of NF- κ B. *J Immunol*, 172, 2522-9.
- BANCEREK, J., POSS, ZACHARY C., STEINPARZER, I., SEDLYAROV, V., PFAFFENWIMMER, T., MIKULIC, I., DÖLKEN, L., STROBL, B., MÜLLER, M., TAATJES, DYLAN J. & KOVARIK, P. 2013. CDK8 Kinase Phosphorylates Transcription Factor STAT1 to Selectively Regulate the Interferon Response. *Immunity*, 38, 250-262.
- BARAN-MARSZAK, F., FEUILLARD, J., NAJJAR, I., LE CLORENNEC, C., BECHET, J. M., DUSANTER-FOURT, I., BORNKAMM, G. W., RAPHAEL, M. & FAGARD, R. 2004. Differential roles of STAT1 α and STAT1 β in fludarabine-induced cell cycle arrest and apoptosis in human B cells. *Blood*, 104, 2475-83.

- BARBALAT, R., LAU, L., LOCKSLEY, R. M. & BARTON, G. M. 2009. Toll-like receptor 2 on inflammatory monocytes induces type I interferon in response to viral but not bacterial ligands. *Nat Immunol*, 10, 1200-7.
- BARTON, G. M., KAGAN, J. C. & MEDZHITOV, R. 2006. Intracellular localization of Toll-like receptor 9 prevents recognition of self DNA but facilitates access to viral DNA. *Nat Immunol*, 7, 49-56.
- BAUMANN, C. L., ASPALTER, I. M., SHARIF, O., PICHLMAIR, A., BLUML, S., GREBIEN, F., BRUCKNER, M., PASIERBEK, P., AUMAYR, K., PLANYAVSKY, M., BENNETT, K. L., COLINGE, J., KNAPP, S. & SUPERTI-FURGA, G. 2010. CD14 is a coreceptor of Toll-like receptors 7 and 9. *J Exp Med*, 207, 2689-701.
- BEAMER, L. J., CARROLL, S. F. & EISENBERG, D. 1999. The three-dimensional structure of human bactericidal/permeability-increasing protein: implications for understanding protein-lipopolysaccharide interactions. *Biochem Pharmacol*, 57, 225-9.
- BECKER, S., GRONER, B. & MULLER, C. W. 1998. Three-dimensional structure of the Stat3[beta] homodimer bound to DNA. *Nature*, 394, 145-151.
- BELINDA, L. W.-C., WEI, W. X., HANH, B. T. H., LEI, L. X., BOW, H. & LING, D. J. 2008. SARM: a novel Toll-like receptor adaptor, is functionally conserved from arthropod to human. *Molecular Immunology*, 45, 1732-1742.
- BELL, J. K., ASKINS, J., HALL, P. R., DAVIES, D. R. & SEGAL, D. M. 2006a. The dsRNA binding site of human Toll-like receptor 3. *Proceedings of the National Academy of Sciences*, 103, 8792-8797.
- BELL, J. K., BOTOS, I., HALL, P. R., ASKINS, J., SHILOACH, J., DAVIES, D. R. & SEGAL, D. M. 2006b. The molecular structure of the TLR3 extracellular domain. *J Endotoxin Res*, 12, 375-378.
- BELL, J. K., BOTOS, I., HALL, P. R., ASKINS, J., SHILOACH, J., SEGAL, D. M. & DAVIES, D. R. 2005. The molecular structure of the Toll-like receptor 3 ligand-binding domain. *Proc Natl Acad Sci U S A*, 102, 10976-80.
- BELL, J. K., MULLEN, G. E. D., LEIFER, C. A., MAZZONI, A., DAVIES, D. R. & SEGAL, D. M. 2003. Leucine-rich repeats and pathogen recognition in Toll-like receptors. *Trends in Immunology*, 24, 528-533.
- BELLA, J., HINDLE, K. L., MCEWAN, P. A. & LOVELL, S. C. 2008. The leucine-rich repeat structure. *Cellular and Molecular Life Sciences*, 65, 2307-2333.
- BEN-NERIAH, Y. & KARIN, M. 2011. Inflammation meets cancer, with NF-kappaB as the matchmaker. *Nat Immunol*, 12, 715-23.

- BEUTLER, B. & CERAMI, A. 1989. The biology of cachectin/TNF--a primary mediator of the host response. *Annu Rev Immunol*, 7, 625-55.
- BHARDWAJ, N., ROSAS, L. E., LAFUSE, W. P. & SATOSKAR, A. R. 2005. Leishmania inhibits STAT1-mediated IFN- γ signaling in macrophages: increased tyrosine phosphorylation of dominant negative STAT1 β by Leishmania mexicana. *International Journal for Parasitology*, 35, 75-82.
- BONIFACINO, J. S. & TRAUB, L. M. 2003. Signals for sorting of transmembrane proteins to endosomes and lysosomes. *Annu Rev Biochem*, 72, 395-447.
- BONIZZI, G., PIETTE, J., MERVILLE, M. P. & BOURS, V. 2000. Cell type-specific role for reactive oxygen species in nuclear factor-kappaB activation by interleukin-1. *Biochem Pharmacol*, 59, 7-11.
- BOTOS, I., SEGAL, DAVID M. & DAVIES, DAVID R. 2011. The Structural Biology of Toll-like Receptors. *Structure*, 19, 447-459.
- BOUTIN, J. A. 1997. Myristoylation. *Cellular Signalling*, 9, 15-35.
- BOWIE, A. & O'NEILL, L. A. 2000. The interleukin-1 receptor/Toll-like receptor superfamily: signal generators for pro-inflammatory interleukins and microbial products. *Journal of Leukocyte Biology*, 67, 508-14.
- BOWMAN, T., BROOME, M. A., SINIBALDI, D., WHARTON, W., PLEDGER, W. J., SEDIVY, J. M., IRBY, R., YEATMAN, T., COURTNEIDGE, S. A. & JOVE, R. 2001. Stat3-mediated Myc expression is required for Src transformation and PDGF-induced mitogenesis. *Proc Natl Acad Sci U S A*, 98, 7319-24.
- BOWMAN, T., GARCIA, R., TURKSON, J. & JOVE, R. 2000. STATs in oncogenesis. *Oncogene*, 19, 2474 - 2488.
- BRADFORD, M., SCHROEDER, A., MORSE, H. C., 3RD, VOGEL, S. N. & COWDERY, J. S. 2002. CpG DNA induced IL-12 p40 gene activation is independent of STAT1 activation or production of interferon consensus sequence binding protein. *J Biomed Sci*, 9, 688-96.
- BRADLEY, J. R. & POBER, J. S. 2001. Tumor necrosis factor receptor-associated factors (TRAFs). *Oncogene*, 20, 6482-91.
- BRIGHTBILL, H. D., LIBRATY, D. H., KRUTZIK, S. R., YANG, R. B., BELISLE, J. T., BLEHARSKI, J. R., MAITLAND, M., NORGARD, M. V., PLEVY, S. E., SMALE, S. T., BRENNAN, P. J., BLOOM, B. R., GODOWSKI, P. J. & MODLIN, R. L. 1999. Host defense mechanisms triggered by microbial lipoproteins through toll-like receptors. *Science*, 285, 732-6.

- BRINKMANN, M. M., SPOONER, E., HOEBE, K., BEUTLER, B., PLOEGH, H. L. & KIM, Y. M. 2007. The interaction between the ER membrane protein UNC93B and TLR3, 7, and 9 is crucial for TLR signaling. *J Cell Biol*, 177, 265-75.
- BROMBERG, J., WRZESZCZYNSKA, M., DEVGAN, G., ZHAO, Y., PESTELL, R., ALBANESE, C. & DARNELL, J. 1999. Stat3 as an oncogene. *Cell*, 98, 295 - 303.
- BROMBERG, J. F., HORVATH, C. M., BESSER, D., LATHAM, W. W. & DARNELL, J. E., JR. 1998. Stat3 activation is required for cellular transformation by v-src. *Mol Cell Biol*, 18, 2553-8.
- BROMBERG, J. F., HORVATH, C. M., WEN, Z., SCHREIBER, R. D. & DARNELL, J. E., JR. 1996. Transcriptionally active Stat1 is required for the antiproliferative effects of both interferon alpha and interferon gamma. *Proc Natl Acad Sci U S A*, 93, 7673-8.
- BUREL, S. A., HAN, S. R., LEE, H. S., NORRIS, D. A., LEE, B. S., MACHEMER, T., PARK, S. Y., ZHOU, T., HE, G., KIM, Y., MACLEOD, A. R., MONIA, B. P., LIO, S., KIM, T. W. & HENRY, S. P. 2013. Preclinical evaluation of the toxicological effects of a novel constrained ethyl modified antisense compound targeting signal transducer and activator of transcription 3 in mice and cynomolgus monkeys. *Nucleic Acid Ther*, 23, 213-27.
- CADENAS, E. & DAVIES, K. J. A. 2000. Mitochondrial free radical generation, oxidative stress, and aging. *Free Radical Biology and Medicine*, 29, 222-230.
- CALDENHOVEN, E., VAN DIJK, T. B., SOLARI, R., ARMSTRONG, J., RAAIJMAKERS, J. A. M., LAMMERS, J.-W. J., KOENDERMAN, L. & DE GROOT, R. P. 1996. STAT3 β , a Splice Variant of Transcription Factor STAT3, Is a Dominant Negative Regulator of Transcription. *Journal of Biological Chemistry*, 271, 13221-13227.
- CALVO, D., DOPAZO, J. & VEGA, M. A. 1995. The CD36, CLA-1 (CD36L1), and LIMPII (CD36L2) gene family: cellular distribution, chromosomal location, and genetic evolution. *Genomics*, 25, 100-6.
- CAO, X., TAY, A., GUY, G. R. & TAN, Y. H. 1996a. Activation and association of Stat3 with Src in v-Src-transformed cell lines. *Mol Cell Biol*, 16, 1595-603.
- CAO, Z., HENZEL, W. J. & GAO, X. 1996b. IRAK: a kinase associated with the interleukin-1 receptor. *Science*, 271, 1128-31.
- CARPENTER, S., CARLSON, T., DELLACASAGRANDE, J., GARCIA, A., GIBBONS, S., HERTZOG, P., LYONS, A., LIN, L. L., LYNCH, M., MONIE, T., MURPHY, C., SEIDL, K. J., WELLS, C., DUNNE, A. & O'NEILL, L. A. 2009. TRIL, a functional component of the TLR4 signaling complex, highly expressed in brain. *J Immunol*, 183, 3989-95.
- CARPENTER, S., WOCHAL, P., DUNNE, A. & O'NEILL, L. A. 2011. Toll-like receptor 3 (TLR3) signaling requires TLR4 Interactor with leucine-rich REPeats (TRIL). *J Biol Chem*, 286, 38795-804.

- CARTY, M., GOODBODY, R., SCHRODER, M., STACK, J., MOYNAGH, P. N. & BOWIE, A. G. 2006. The human adaptor SARM negatively regulates adaptor protein TRIF-dependent Toll-like receptor signaling. *Nat Immunol*, 7, 1074-1081.
- CECIL, A. A. & KLEMSZ, M. J. 2004. p38 activation through Toll-like receptors modulates IFN γ induced expression of the Tap-1 gene only in macrophages. *Journal of Leukocyte Biology*, 75, 560-568.
- CERESA, B. P. & PESSIN, J. E. 1996. Insulin stimulates the serine phosphorylation of the signal transducer and activator of transcription (STAT3) isoform. *J Biol Chem*, 271, 12121-4.
- CHANDEL, N. S., MALTEPE, E., GOLDWASSER, E., MATHIEU, C. E., SIMON, M. C. & SCHUMACKER, P. T. 1998. Mitochondrial reactive oxygen species trigger hypoxia-induced transcription. *Proc Natl Acad Sci U S A*, 95, 11715-20.
- CHANG, M., JIN, W. & SUN, S. C. 2009. Peli1 facilitates TRIF-dependent Toll-like receptor signaling and proinflammatory cytokine production. *Nat Immunol*, 10, 1089-95.
- CHAPMAN, R. S., LOURENCO, P. C., TONNER, E., FLINT, D. J., SELBERT, S., TAKEDA, K., AKIRA, S., CLARKE, A. R. & WATSON, C. J. 1999. Suppression of epithelial apoptosis and delayed mammary gland involution in mice with a conditional knockout of Stat3. *Genes & Development*, 13, 2604-2616.
- CHATTERJEE-KISHORE, M., WRIGHT, K. L., TIANG, J. P. Y. & STARK, G. R. 2000. How Start1 mediates constitutive gene expression: a complex of unphosphorylated Start1 and IRF1 supports transcription of the LMP2 gene. *EMBO J*, 19, 4855-4855.
- CHEN, X., VINKEMEIER, U., ZHAO, Y., JERUZALMI, D., DARNELL JR, J. E. & KURIYAN, J. 1998. Crystal Structure of a Tyrosine Phosphorylated STAT-1 Dimer Bound to DNA. *Cell*, 93, 827-839.
- CHEN, Z. J. & SUN, L. J. 2009. Nonproteolytic functions of ubiquitin in cell signaling. *Mol Cell*, 33, 275-86.
- CHENG, A.-L., KANG, Y.-K., CHEN, Z., TSAO, C.-J., QIN, S., KIM, J. S., LUO, R., FENG, J., YE, S., YANG, T.-S., XU, J., SUN, Y., LIANG, H., LIU, J., WANG, J., TAK, W. Y., PAN, H., BUROCK, K., ZOU, J., VOLIOTIS, D. & GUAN, Z. 2009. Efficacy and safety of sorafenib in patients in the Asia-Pacific region with advanced hepatocellular carcinoma: a phase III randomised, double-blind, placebo-controlled trial. *The Lancet Oncology*, 10, 25-34.
- CHENG, H., ADDONA, T., KESHISHIAN, H., DAHLSTRAND, E., LU, C. F., DORSCH, M., LI, Z., WANG, A. L., OCAIN, T. D., LI, P., PARSONS, T. F., JAFFEE, B. & XU, Y. J. 2007. Regulation of IRAK-4 kinase activity via autophosphorylation within its activation loop. *Biochemical and Biophysical Research Communications*, 352, 609-616.

- CHEON, H. & STARK, G. R. 2009. Unphosphorylated STAT1 prolongs the expression of interferon-induced immune regulatory genes. *Proc Natl Acad Sci U S A*, 106, 9373-8.
- CHOE, J., KELKER, M. S. & WILSON, I. A. 2005. Crystal Structure of Human Toll-Like Receptor 3 (TLR3) Ectodomain. *Science*, 309, 581-585.
- CHRISTENSEN, S. R., SHUPE, J., NICKERSON, K., KASHGARIAN, M., FLAVELL, R. A. & SHLOMCHIK, M. J. 2006. Toll-like receptor 7 and TLR9 dictate autoantibody specificity and have opposing inflammatory and regulatory roles in a murine model of lupus. *Immunity*, 25, 417-28.
- CHUANG, C.-F. & BARGMANN, C. I. 2005. A Toll-interleukin 1 repeat protein at the synapse specifies asymmetric odorant receptor expression via ASK1 MAPKKK signaling. *Genes & Development*, 19, 270-281.
- CHUANG, J. H., CHUANG, H. C., HUANG, C. C., WU, C. L., DU, Y. Y., KUNG, M. L., CHEN, C. H., CHEN, S. C. & TAI, M. H. 2011. Differential toll-like receptor 3 (TLR3) expression and apoptotic response to TLR3 agonist in human neuroblastoma cells. *J Biomed Sci*, 18, 65.
- CHUNG, J., UCHIDA, E., GRAMMER, T. C. & BLENIS, J. 1997. STAT3 serine phosphorylation by ERK-dependent and -independent pathways negatively modulates its tyrosine phosphorylation. *Mol Cell Biol*, 17, 6508-16.
- CHUNG, J. Y., PARK, Y. C., YE, H. & WU, H. 2002. All TRAFs are not created equal: common and distinct molecular mechanisms of TRAF-mediated signal transduction. *Journal of Cell Science*, 115, 679-688.
- COBAN, C., IGARI, Y., YAGI, M., REIMER, T., KOYAMA, S., AOSHI, T., OHATA, K., TSUKUI, T., TAKESHITA, F., SAKURAI, K., IKEGAMI, T., NAKAGAWA, A., HORII, T., NUNEZ, G., ISHII, K. J. & AKIRA, S. 2010. Immunogenicity of whole-parasite vaccines against Plasmodium falciparum involves malarial hemozoin and host TLR9. *Cell Host Microbe*, 7, 50-61.
- COLAMONICI, O., YAN, H., DOMANSKI, P., HANDA, R., SMALLEY, D., MULLERSMAN, J., WITTE, M., KRISHNAN, K. & KROLEWSKI, J. 1994. Direct binding to and tyrosine phosphorylation of the alpha subunit of the type I interferon receptor by p135tyk2 tyrosine kinase. *Molecular and Cellular Biology*, 14, 8133-8142.
- CONZE, D. B., WU, C. J., THOMAS, J. A., LANDSTROM, A. & ASHWELL, J. D. 2008. Lys63-linked polyubiquitination of IRAK-1 is required for interleukin-1 receptor- and toll-like receptor-mediated NF-kappaB activation. *Mol Cell Biol*, 28, 3538-47.
- CORVINUS, F. M., ORTH, C., MORIGGL, R., TSAREVA, S. A., WAGNER, S., PFITZNER, E. B., BAUS, D., KAUFMANN, R., HUBER, L. A., ZATLOUKAL, K., BEUG, H., OHLSCHLAGER, P., SCHUTZ, A.,

- HALBHUBER, K. J. & FRIEDRICH, K. 2005. Persistent STAT3 activation in colon cancer is associated with enhanced cell proliferation and tumor growth. *Neoplasia*, 7, 545-55.
- COUILLAULT, C., PUJOL, N., REBOUL, J., SABATIER, L., GUICHOU, J. F., KOHARA, Y. & EWBANK, J. J. 2004. TLR-independent control of innate immunity in *Caenorhabditis elegans* by the TIR domain adaptor protein TIR-1, an ortholog of human SARM. *Nat Immunol*, 5, 488-94.
- COWDERY, J. S., BOERTH, N. J., NORIAN, L. A., MYUNG, P. S. & KORETZKY, G. A. 1999. Differential Regulation of the IL-12 p40 Promoter and of p40 Secretion by CpG DNA and Lipopolysaccharide. *The Journal of Immunology*, 162, 6770-6775.
- CREMER, I., GHYSDAEL, J. & VIEILLARD, V. 2002. A non-classical ISRE/ISGF3 pathway mediates induction of RANTES gene transcription by type I IFNs. *FEBS Letters*, 511, 41-45.
- CROSTON, G. E., CAO, Z. & GOEDDEL, D. V. 1995. NF- κ B Activation by Interleukin-1 (IL-1) Requires an IL-1 Receptor-associated Protein Kinase Activity. *Journal of Biological Chemistry*, 270, 16514-16517.
- CUENDA, A., ROUSE, J., DOZA, Y. N., MEIER, R., COHEN, P., GALLAGHER, T. F., YOUNG, P. R. & LEE, J. C. 1995. SB 203580 is a specific inhibitor of a MAP kinase homologue which is stimulated by cellular stresses and interleukin-1. *FEBS Lett*, 364, 229-33.
- DALPKE, A. H., ECKERLE, S., FREY, M. & HEEG, K. 2003. Triggering of Toll-like receptors modulates IFN- γ signaling: involvement of serine 727 STAT1 phosphorylation and suppressors of cytokine signaling. *European Journal of Immunology*, 33, 1776-1787.
- DARNELL, J. E., JR., KERR, I. M. & STARK, G. R. 1994. Jak-STAT pathways and transcriptional activation in response to IFNs and other extracellular signaling proteins. *Science*, 264, 1415-21.
- DEB, A., ZAMANIAN-DARYOUSH, M., XU, Z., KADEREIT, S. & WILLIAMS, B. R. G. 2001. Protein kinase PKR is required for platelet-derived growth factor signaling of c-fos gene expression via Erks and Stat3. *EMBO J*, 20, 2487-2496.
- DECKER, T. & KOVARIK, P. 2000. Serine phosphorylation of STATs. *Oncogene*, 19, 2628-37.
- DECKER, T., LEW, D. J., MIRKOVITCH, J. & DARNELL, J. E., JR. 1991. Cytoplasmic activation of GAF, an IFN-gamma-regulated DNA-binding factor. *EMBO J*, 10, 927-32.
- DIDONATO, J. A., HAYAKAWA, M., ROTHWARF, D. M., ZANDI, E. & KARIN, M. 1997. A cytokine-responsive I κ B kinase that activates the transcription factor NF- κ B. *Nature*, 388, 548-554.
- DIEBOLD, S. S., KAISHO, T., HEMMI, H., AKIRA, S. & REIS E SOUSA, C. 2004. Innate antiviral responses by means of TLR7-mediated recognition of single-stranded RNA. *Science*, 303, 1529-31.

- DIMBERG, L. Y., DIMBERG, A., IVARSSON, K., FRYKNAS, M., RICKARDSON, L., TOBIN, G., EKMAN, S., LARSSON, R., GULLBERG, U., NILSSON, K., OBERG, F. & WIKLUND, H. 2012. Stat1 activation attenuates IL-6 induced Stat3 activity but does not alter apoptosis sensitivity in multiple myeloma. *BMC Cancer*, 12, 318.
- DURBIN, J. E., HACKENMILLER, R., SIMON, M. C. & LEVY, D. E. 1996. Targeted disruption of the mouse Stat1 gene results in compromised innate immunity to viral disease. *Cell*, 84, 443-50.
- DZIARSKI, R., TAPPING, R. I. & TOBIAS, P. S. 1998. Binding of bacterial peptidoglycan to CD14. *J Biol Chem*, 273, 8680-90.
- ERMOLAEVA, M. A., MICHALLET, M. C., PAPADOPOULOU, N., UTERMOHLEN, O., KRANIDIOTI, K., KOLLIAS, G., TSCHOPP, J. & PASPARAKIS, M. 2008. Function of TRADD in tumor necrosis factor receptor 1 signaling and in TRIF-dependent inflammatory responses. *Nat Immunol*, 9, 1037-46.
- FEARNLEY, I. M., CARROLL, J., SHANNON, R. J., RUNSWICK, M. J., WALKER, J. E. & HIRST, J. 2001. GRIM-19, a cell death regulatory gene product, is a subunit of bovine mitochondrial NADH:ubiquinone oxidoreductase (complex I). *J Biol Chem*, 276, 38345-8.
- FEINSTEIN, E., KIMCHI, A., WALLACH, D., BOLDIN, M. & VARFOLOMEEV, E. 1995. The death domain: a module shared by proteins with diverse cellular functions. *Trends Biochem Sci*, 20, 342-4.
- FELDMANN, M., BRENNAN, F. M., WILLIAMS, R. O., ELLIOTT, M. J. & MAINI, R. N. 1995. Cytokine expression and networks in rheumatoid arthritis: rationale for anti-TNF alpha antibody therapy and its mechanism of action. *J Inflamm*, 47, 90-6.
- FINBLOOM, D. S. & WINESTOCK, K. D. 1995. IL-10 induces the tyrosine phosphorylation of tyk2 and Jak1 and the differential assembly of STAT1 alpha and STAT3 complexes in human T cells and monocytes. *The Journal of Immunology*, 155, 1079-90.
- FITZGERALD, K. A., PALSSON-MCDERMOTT, E. M., BOWIE, A. G., JEFFERIES, C. A., MANSELL, A. S., BRADY, G., BRINT, E., DUNNE, A., GRAY, P., HARTE, M. T., MCMURRAY, D., SMITH, D. E., SIMS, J. E., BIRD, T. A. & O'NEILL, L. A. J. 2001. Mal (MyD88-adaptor-like) is required for Toll-like receptor-4 signal transduction. *Nature*, 413, 78-83.
- FITZGERALD, K. A., ROWE, D. C., BARNES, B. J., CAFFREY, D. R., VISINTIN, A., LATZ, E., MONKS, B., PITHA, P. M. & GOLENBOCK, D. T. 2003. LPS-TLR4 Signaling to IRF-3/7 and NF- κ B Involves the Toll Adapters TRAM and TRIF. *The Journal of Experimental Medicine*, 198, 1043-1055.

- FRANK, D. A., MAHAJAN, S. & RITZ, J. 1997. B lymphocytes from patients with chronic lymphocytic leukemia contain signal transducer and activator of transcription (STAT) 1 and STAT3 constitutively phosphorylated on serine residues. *J Clin Invest*, 100, 3140-8.
- FU, X. Y., KESSLER, D. S., VEALS, S. A., LEVY, D. E. & DARNELL, J. E. 1990. ISGF3, the transcriptional activator induced by interferon alpha, consists of multiple interacting polypeptide chains. *Proceedings of the National Academy of Sciences*, 87, 8555-8559.
- FUJIHARA, M., MUROI, M., TANAMOTO, K.-I., SUZUKI, T., AZUMA, H. & IKEDA, H. 2003. Molecular mechanisms of macrophage activation and deactivation by lipopolysaccharide: roles of the receptor complex. *Pharmacology & Therapeutics*, 100, 171-194.
- FUKUI, R., SAITOH, S., MATSUMOTO, F., KOZUKA-HATA, H., OYAMA, M., TABETA, K., BEUTLER, B. & MIYAKE, K. 2009. Unc93B1 biases Toll-like receptor responses to nucleic acid in dendritic cells toward DNA- but against RNA-sensing. *J Exp Med*, 206, 1339-50.
- GANGULY, D., CHAMILOS, G., LANDE, R., GREGORIO, J., MELLER, S., FACCHINETTI, V., HOMEY, B., BARRAT, F. J., ZAL, T. & GILLIET, M. 2009. Self-RNA-antimicrobial peptide complexes activate human dendritic cells through TLR7 and TLR8. *J Exp Med*, 206, 1983-94.
- GAO, B. & TSAN, M. F. 2003. Endotoxin contamination in recombinant human heat shock protein 70 (Hsp70) preparation is responsible for the induction of tumor necrosis factor alpha release by murine macrophages. *J Biol Chem*, 278, 174-9.
- GARCIA, R. & JOVE, R. 1998. Activation of STAT transcription factors in oncogenic tyrosine kinase signaling. *J Biomed Sci*, 5, 79-85.
- GAUTIER, G., HUMBERT, M., DEAUVIEAU, F., SCUILLER, M., HISCOTT, J., BATES, E. E. M., TRINCHIERI, G., CAUX, C. & GARRONE, P. 2005. A type I interferon autocrine–paracrine loop is involved in Toll-like receptor-induced interleukin-12p70 secretion by dendritic cells. *The Journal of Experimental Medicine*, 201, 1435-1446.
- GAY, N. J. & KEITH, F. J. 1991. Drosophila Toll and IL-1 receptor. *Nature*, 351, 355-6.
- GLOIRE, G., LEGRAND-POELS, S. & PIETTE, J. 2006. NF- κ B activation by reactive oxygen species: Fifteen years later. *Biochemical Pharmacology*, 72, 1493-1505.
- GOH, K. C., HAQUE, S. J. & WILLIAMS, B. R. G. 1999. p38 MAP kinase is required for STAT1 serine phosphorylation and transcriptional activation induced by interferons. *Embo Journal*, 18, 5601-5608.
- GOHDA, J., MATSUMURA, T. & INOUE, J.-I. 2004. Cutting Edge: TNFR-Associated Factor (TRAF) 6 Is Essential for MyD88-Dependent Pathway but Not Toll/IL-1 Receptor Domain-Containing Adaptor-Inducing IFN- β (TRIF)-Dependent Pathway in TLR Signaling. *The Journal of Immunology*, 173, 2913-2917.

- GOTOH, A., TAKAHIRA, H., MANTEL, C., LITZ-JACKSON, S., BOSWELL, H. S. & BROXMEYER, H. E. 1996. Steel factor induces serine phosphorylation of Stat3 in human growth factor-dependent myeloid cell lines. *Blood*, 88, 138-45.
- GOUGH, D. J., CORLETT, A., SCHLESSINGER, K., WEGRZYN, J., LARNER, A. C. & LEVY, D. E. 2009. Mitochondrial STAT3 supports Ras-dependent oncogenic transformation. *Science*, 324, 1713-6.
- GRAY, P., DUNNE, A., BRIKOS, C., JEFFERIES, C. A., DOYLE, S. L. & O'NEILL, L. A. 2006. MyD88 adapter-like (Mal) is phosphorylated by Bruton's tyrosine kinase during TLR2 and TLR4 signal transduction. *J Biol Chem*, 281, 10489-95.
- GREENHILL, C. J. 2011. *IL-6 trans-signalling modulates TLR4-dependent inflammatory responses via STAT1 and STAT3*. PhD thesis, Monash University.
- GREENHILL, C. J., ROSE-JOHN, S., LISSILAA, R., FERLIN, W., ERNST, M., HERTZOG, P. J., MANSELL, A. & JENKINS, B. J. 2011. IL-6 Trans-Signaling Modulates TLR4-Dependent Inflammatory Responses via STAT3. *The Journal of Immunology*, 186, 1199-1208.
- GUAN, Y., RANOA, D. R. E., JIANG, S., MUTHA, S. K., LI, X., BAUDRY, J. & TAPPING, R. I. 2010. Human TLRs 10 and 1 Share Common Mechanisms of Innate Immune Sensing but Not Signaling. *The Journal of Immunology*, 184, 5094-5103.
- GUPTA, S., YAN, H., WONG, L. H., RALPH, S., KROLEWSKI, J. & SCHINDLER, C. 1996. The SH2 domains of Stat1 and Stat2 mediate multiple interactions in the transduction of IFN-alpha signals. *EMBO J*, 15, 1075-84.
- HACKER, H., REDECKE, V., BLAGOEV, B., KRATCHMAROVA, I., HSU, L. C., WANG, G. G., KAMPS, M. P., RAZ, E., WAGNER, H., HACKER, G., MANN, M. & KARIN, M. 2006. Specificity in Toll-like receptor signalling through distinct effector functions of TRAF3 and TRAF6. *Nature*, 439, 204-207.
- HAGIHARA, K., NISHIKAWA, T., SUGAMATA, Y., SONG, J., ISOBE, T., TAGA, T. & YOSHIZAKI, K. 2005. Essential role of STAT3 in cytokine-driven NF- κ B-mediated serum amyloid A gene expression. *Genes to Cells*, 10, 1051-1063.
- HAILMAN, E., LICHENSTEIN, H. S., WURFEL, M. M., MILLER, D. S., JOHNSON, D. A., KELLEY, M., BUSSE, L. A., ZUKOWSKI, M. M. & WRIGHT, S. D. 1994. Lipopolysaccharide (LPS)-binding protein accelerates the binding of LPS to CD14. *J Exp Med*, 179, 269-77.
- HARMEY, J. H., BUCANA, C. D., LU, W., BYRNE, A. M., MCDONNELL, S., LYNCH, C., BOUCHIER-HAYES, D. & DONG, Z. 2002. Lipopolysaccharide-induced metastatic growth is associated with increased angiogenesis, vascular permeability and tumor cell invasion. *Int J Cancer*, 101, 415-22.

- HARTE, M. T., HAGA, I. R., MALONEY, G., GRAY, P., READING, P. C., BARTLETT, N. W., SMITH, G. L., BOWIE, A. & O'NEILL, L. A. 2003. The poxvirus protein A52R targets Toll-like receptor signaling complexes to suppress host defense. *J Exp Med*, 197, 343-51.
- HASAN, U., CHAFFOIS, C., GAILLARD, C., SAULNIER, V., MERCK, E., TANCREDI, S., GUIET, C., BRIERE, F., VLACH, J., LEBECQUE, S., TRINCHIERI, G. & BATES, E. E. 2005. Human TLR10 is a functional receptor, expressed by B cells and plasmacytoid dendritic cells, which activates gene transcription through MyD88. *J Immunol*, 174, 2942-50.
- HASHIMOTO, C., HUDSON, K. L. & ANDERSON, K. V. 1988. The Toll gene of *Drosophila*, required for dorsal-ventral embryonic polarity, appears to encode a transmembrane protein. *Cell*, 52, 269-79.
- HAYASHI, F., SMITH, K. D., OZINSKY, A., HAWN, T. R., YI, E. C., GOODLETT, D. R., ENG, J. K., AKIRA, S., UNDERHILL, D. M. & ADEREM, A. 2001. The innate immune response to bacterial flagellin is mediated by Toll-like receptor 5. *Nature*, 410, 1099-1103.
- HAYDEN, M. S., WEST, A. P. & GHOSH, S. 2006. NF-kappaB and the immune response. *Oncogene*, 25, 6758-80.
- HAZAN-HALEVY, I., HARRIS, D., LIU, Z., LIU, J., LI, P., CHEN, X., SHANKER, S., FERRAJOLI, A., KEATING, M. J. & ESTROV, Z. 2010. STAT3 is constitutively phosphorylated on serine 727 residues, binds DNA, and activates transcription in CLL cells. *Blood*, 115, 2852-2863.
- HEIL, F., AHMAD-NEJAD, P., HEMMI, H., HOCHREIN, H., AMPENBERGER, F., GELLERT, T., DIETRICH, H., LIPFORD, G., TAKEDA, K., AKIRA, S., WAGNER, H. & BAUER, S. 2003. The Toll-like receptor 7 (TLR7)-specific stimulus loxoribine uncovers a strong relationship within the TLR7, 8 and 9 subfamily. *European Journal of Immunology*, 33, 2987-2997.
- HEIL, F., HEMMI, H., HOCHREIN, H., AMPENBERGER, F., KIRSCHNING, C., AKIRA, S., LIPFORD, G., WAGNER, H. & BAUER, S. 2004. Species-specific recognition of single-stranded RNA via toll-like receptor 7 and 8. *Science*, 303, 1526-9.
- HEIM, M. H., KERR, I. M., STARK, G. R. & DARNELL, J. E., JR. 1995. Contribution of STAT SH2 groups to specific interferon signaling by the Jak-STAT pathway. *Science*, 267, 1347-9.
- HEINRICH, P. C., BEHRMANN, I., MULLER-NEWEN, G., SCHAPER, F. & GRAEVE, L. 1998. Interleukin-6-type cytokine signalling through the gp130/Jak/STAT pathway. *Biochemical Journal*, 334, 297-314.
- HERMANCE, N. C., KHURANA, S. & LEE, T. H. 2005. Rip1 Mediates the Trif-dependent Toll-like Receptor 3- and 4-induced NF- B Activation but Does Not Contribute to Interferon Regulatory Factor 3 Activation. *Journal of Biological Chemistry*, 280, 36560-36566.

- HIROTANI, T., YAMAMOTO, M., KUMAGAI, Y., UEMATSU, S., KAWASE, I., TAKEUCHI, O. & AKIRA, S. 2005. Regulation of lipopolysaccharide-inducible genes by MyD88 and Toll/IL-1 domain containing adaptor inducing IFN-beta. *Biochem Biophys Res Commun*, 328, 383-92.
- HIRSCHFELD, M., MA, Y., WEIS, J. H., VOGEL, S. N. & WEIS, J. J. 2000. Cutting edge: Repurification of lipopolysaccharide eliminates signaling through both human and murine toll-like receptor 2. *Journal of Immunology*, 165, 618-622.
- HOCHREIN, H., SCHLATTER, B., O'KEEFE, M., WAGNER, C., SCHMITZ, F., SCHIEMANN, M., BAUER, S., SUTER, M. & WAGNER, H. 2004. Herpes simplex virus type-1 induces IFN-alpha production via Toll-like receptor 9-dependent and -independent pathways. *Proc Natl Acad Sci U S A*, 101, 11416-21.
- HOEBE, K., DU, X., GEORGEL, P., JANSSEN, E., TABETA, K., KIM, S. O., GOODE, J., LIN, P., MANN, N., MUDD, S., CROZAT, K., SOVATH, S., HAN, J. & BEUTLER, B. 2003. Identification of Lps2 as a key transducer of MyD88-independent TIR signalling. *Nature*, 424, 743-8.
- HOENTJEN, F., SARTOR, R. B., OZAKI, M. & JOBIN, C. 2005. STAT3 regulates NF-kB recruitment to the IL-12p40 promoter in dendritic cells. *Blood*, 105, 689-696.
- HOFER, M. J., LI, W., MANDERS, P., TERRY, R., LIM, S. L., KING, N. J. C. & CAMPBELL, I. L. 2012. Mice Deficient in STAT1 but Not STAT2 or IRF9 Develop a Lethal CD4+ T-Cell-Mediated Disease following Infection with Lymphocytic Choriomeningitis Virus. *Journal of Virology*, 86, 6932-6946.
- HONDA, K., OHBA, Y., YANAI, H., NEGISHI, H., MIZUTANI, T., TAKAOKA, A., TAYA, C. & TANIGUCHI, T. 2005. Spatiotemporal regulation of MyD88-IRF-7 signalling for robust type-I interferon induction. *Nature*, 434, 1035-40.
- HONDA, K., YANAI, H., MIZUTANI, T., NEGISHI, H., SHIMADA, N., SUZUKI, N., OHBA, Y., TAKAOKA, A., YEH, W. C. & TANIGUCHI, T. 2004. Role of a transductional-transcriptional processor complex involving MyD88 and IRF-7 in Toll-like receptor signaling. *Proc Natl Acad Sci U S A*, 101, 15416-21.
- HORNG, T., BARTON, G. M., FLAVELL, R. A. & MEDZHITOV, R. 2002. The adaptor molecule TIRAP provides signalling specificity for Toll-like receptors. *Nature*, 420, 329-33.
- HORNG, T., BARTON, G. M. & MEDZHITOV, R. 2001. TIRAP: an adapter molecule in the Toll signaling pathway. *Nat Immunol*, 2, 835-841.
- HORNIG-DO, H. T., GUNTHER, G., BUST, M., LEHNARTZ, P., BOSIO, A. & WIESNER, R. J. 2009. Isolation of functional pure mitochondria by superparamagnetic microbeads. *Anal Biochem*, 389, 1-5.

- HORNUNG, V., GUENTHNER-BILLER, M., BOURQUIN, C., ABLASSER, A., SCHLEE, M., UEMATSU, S., NORONHA, A., MANOHARAN, M., AKIRA, S., DE FOUGEROLLES, A., ENDRES, S. & HARTMANN, G. 2005. Sequence-specific potent induction of IFN-alpha by short interfering RNA in plasmacytoid dendritic cells through TLR7. *Nat Med*, 11, 263-70.
- HORVATH, C. M., WEN, Z. & DARNELL, J. E. 1995. A STAT protein domain that determines DNA sequence recognition suggests a novel DNA-binding domain. *Genes & Development*, 9, 984-994.
- HU, X., CHAKRAVARTY, S. D. & IVASHKIV, L. B. 2008. Regulation of interferon and Toll-like receptor signaling during macrophage activation by opposing feedforward and feedback inhibition mechanisms. *Immunol Rev*, 226, 41-56.
- HUANG, G., LU, H., HAO, A., NG, D. C., PONNIAH, S., GUO, K., LUFELI, C., ZENG, Q. & CAO, X. 2004a. GRIM-19, a cell death regulatory protein, is essential for assembly and function of mitochondrial complex I. *Mol Cell Biol*, 24, 8447-56.
- HUANG, Y., LI, T., SANE, D. C. & LI, L. 2004b. IRAK1 Serves as a Novel Regulator Essential for Lipopolysaccharide-induced Interleukin-10 Gene Expression. *Journal of Biological Chemistry*, 279, 51697-51703.
- HUSEBYE, H., HALAAS, O., STENMARK, H., TUNHEIM, G., SANDANGER, O., BOGEN, B., BRECH, A., LATZ, E. & ESPEVIK, T. 2006. Endocytic pathways regulate Toll-like receptor 4 signaling and link innate and adaptive immunity. *EMBO J*, 25, 683-92.
- HUYTON, T., ROSSJOHN, J. & WILCE, M. 2007. Toll-like receptors: structural pieces of a curve-shaped puzzle. *Immunol Cell Biol*, 85, 406-410.
- IGARASHI, K., GAROTTA, G., OZMEN, L., ZIEMIECKI, A., WILKS, A. F., HARPUR, A. G., LARNER, A. C. & FINBLOOM, D. S. 1994. Interferon-gamma induces tyrosine phosphorylation of interferon-gamma receptor and regulated association of protein tyrosine kinases, Jak1 and Jak2, with its receptor. *J Biol Chem*, 269, 14333-6.
- ILES, K. E. & FORMAN, H. J. 2002. Macrophage signaling and respiratory burst. *Immunol Res*, 26, 95-105.
- IOVINE, N., EASTVOLD, J., ELSBACH, P., WEISS, J. P. & GIOANNINI, T. L. 2002. The carboxyl-terminal domain of closely related endotoxin-binding proteins determines the target of protein-lipopolysaccharide complexes. *J Biol Chem*, 277, 7970-8.
- IP, W. K., TAKAHASHI, K., MOORE, K. J., STUART, L. M. & EZEKOWITZ, R. A. 2008. Mannose-binding lectin enhances Toll-like receptors 2 and 6 signaling from the phagosome. *J Exp Med*, 205, 169-81.

- IVANOV, S., DRAGOI, A. M., WANG, X., DALLACOSTA, C., LOUTEN, J., MUSCO, G., SITIA, G., YAP, G. S., WAN, Y., BIRON, C. A., BIANCHI, M. E., WANG, H. & CHU, W. M. 2007. A novel role for HMGB1 in TLR9-mediated inflammatory responses to CpG-DNA. *Blood*, 110, 1970-81.
- IVANOV, V. N., BHOUMIK, A., KRASILNIKOV, M., RAZ, R., OWEN-SCHAUB, L. B., LEVY, D., HORVATH, C. M. & RONAI, Z. 2001. Cooperation between STAT3 and c-jun suppresses Fas transcription. *Mol Cell*, 7, 517-28.
- JAIN, N., ZHANG, T., FONG, S. L., LIM, C. P. & CAO, X. 1998. Repression of Stat3 activity by activation of mitogen-activated protein kinase (MAPK). *Oncogene*, 17, 3157-67.
- JAIN, N., ZHANG, T., KEE, W. H., LI, W. & CAO, X. 1999. Protein Kinase C δ Associates with and Phosphorylates Stat3 in an Interleukin-6-dependent Manner. *Journal of Biological Chemistry*, 274, 24392-24400.
- JANSSEN-HEININGER, Y. M., MOSSMAN, B. T., HEINTZ, N. H., FORMAN, H. J., KALYANARAMAN, B., FINKEL, T., STAMLER, J. S., RHEE, S. G. & VAN DER VLIET, A. 2008. Redox-based regulation of signal transduction: principles, pitfalls, and promises. *Free Radic Biol Med*, 45, 1-17.
- JANSSENS, S. & BEYAERT, R. 2002. A universal role for MyD88 in TLR/IL-1R-mediated signaling. *Trends in Biochemical Sciences*, 27, 474-482.
- JEFFERIES, C. A., DOYLE, S., BRUNNER, C., DUNNE, A., BRINT, E., WIETEK, C., WALCH, E., WIRTH, T. & O'NEILL, L. A. 2003. Bruton's tyrosine kinase is a Toll/interleukin-1 receptor domain-binding protein that participates in nuclear factor kappaB activation by Toll-like receptor 4. *J Biol Chem*, 278, 26258-64.
- JENKINS, B. J., GRAIL, D., NHEU, T., NAJDOVSKA, M., WANG, B., WARING, P., INGLESE, M., MCLOUGHLIN, R. M., JONES, S. A., TOPLEY, N., BAUMANN, H., JUDD, L. M., GIRAUD, A. S., BOUSSIOUTAS, A., ZHU, H.-J. & ERNST, M. 2005. Hyperactivation of Stat3 in gp130 mutant mice promotes gastric hyperproliferation and desensitizes TGF- β signaling. *Nat Med*, 11, 845-852.
- JIANG, Z., GEORGEL, P., LI, C., CHOE, J., CROZAT, K., RUTSCHMANN, S., DU, X., BIGBY, T., MUDD, S., SOVATH, S., WILSON, I. A., OLSON, A. & BEUTLER, B. 2006. Details of Toll-like receptor:adapter interaction revealed by germ-line mutagenesis. *Proc Natl Acad Sci U S A*, 103, 10961-6.
- JIANG, Z., ZAMANIAN-DARYOUSH, M., NIE, H., SILVA, A. M., WILLIAMS, B. R. & LI, X. 2003. Poly(I-C)-induced Toll-like receptor 3 (TLR3)-mediated activation of NFkappa B and MAP kinase is through an interleukin-1 receptor-associated kinase (IRAK)-independent pathway employing the signaling components TLR3-TRAF6-TAK1-TAB2-PKR. *J Biol Chem*, 278, 16713-9.

- JIN, M. S., KIM, S. E., HEO, J. Y., LEE, M. E., KIM, H. M., PAIK, S. G., LEE, H. & LEE, J. O. 2007. Crystal structure of the TLR1-TLR2 heterodimer induced by binding of a tri-acylated lipopeptide. *Cell*, 130, 1071-82.
- JIN, M. S. & LEE, J. O. 2008. Structures of the toll-like receptor family and its ligand complexes. *Immunity*, 29, 182-91.
- JOHNSEN, I. B., NGUYEN, T. T., RINGDAL, M., TRYGGESTAD, A. M., BAKKE, O., LIEN, E., ESPEVIK, T. & ANTHONSEN, M. W. 2006. Toll-like receptor 3 associates with c-Src tyrosine kinase on endosomes to initiate antiviral signaling. *EMBO J*, 25, 3335-46.
- JOHNSON, G. B., BRUNN, G. J., KODAIRA, Y. & PLATT, J. L. 2002. Receptor-mediated monitoring of tissue well-being via detection of soluble heparan sulfate by Toll-like receptor 4. *J Immunol*, 168, 5233-9.
- KAGAN, J. C. & MEDZHITOV, R. 2006. Phosphoinositide-mediated adaptor recruitment controls Toll-like receptor signaling. *Cell*, 125, 943-55.
- KAGAN, J. C., SU, T., HORNG, T., CHOW, A., AKIRA, S. & MEDZHITOV, R. 2008. TRAM couples endocytosis of Toll-like receptor 4 to the induction of interferon-[beta]. *Nat Immunol*, 9, 361-368.
- KAISER, W. J. & OFFERMANN, M. K. 2005. Apoptosis induced by the toll-like receptor adaptor TRIF is dependent on its receptor interacting protein homotypic interaction motif. *J Immunol*, 174, 4942-52.
- KAISHO, T. & AKIRA, S. 2006. Toll-like receptor function and signaling. *Journal of Allergy and Clinical Immunology*, 117, 979-987.
- KAJAVA, A. V. 1998. Structural diversity of leucine-rich repeat proteins. *J Mol Biol*, 277, 519-27.
- KAMATA, H., HONDA, S., MAEDA, S., CHANG, L., HIRATA, H. & KARIN, M. 2005. Reactive oxygen species promote TNFalpha-induced death and sustained JNK activation by inhibiting MAP kinase phosphatases. *Cell*, 120, 649-61.
- KANG, J. Y., NAN, X., JIN, M. S., YOUN, S.-J., RYU, Y. H., MAH, S., HAN, S. H., LEE, H., PAIK, S.-G. & LEE, J.-O. 2009. Recognition of Lipopeptide Patterns by Toll-like Receptor 2-Toll-like Receptor 6 Heterodimer. *Immunity*, 31, 873-884.
- KAPLAN, D. H., SHANKARAN, V., DIGHE, A. S., STOCKERT, E., AGUET, M., OLD, L. J. & SCHREIBER, R. D. 1998. Demonstration of an interferon gamma-dependent tumor surveillance system in immunocompetent mice. *Proc Natl Acad Sci U S A*, 95, 7556-61.
- KAWAGOE, T., SATO, S., MATSUSHITA, K., KATO, H., MATSUI, K., KUMAGAI, Y., SAITOH, T., KAWAI, T., TAKEUCHI, O. & AKIRA, S. 2008. Sequential control of Toll-like receptor-dependent responses by IRAK1 and IRAK2. *Nat Immunol*, 9, 684-91.

- KAWAI, T., ADACHI, O., OGAWA, T., TAKEDA, K. & AKIRA, S. 1999. Unresponsiveness of MyD88-deficient mice to endotoxin. *Immunity*, 11, 115-22.
- KAWAI, T. & AKIRA, S. 2006. Innate immune recognition of viral infection. *Nat Immunol*, 7, 131-137.
- KAWAI, T. & AKIRA, S. 2007. Signaling to NF- κ B by Toll-like receptors. *Trends in Molecular Medicine*, 13, 460-469.
- KAWAI, T. & AKIRA, S. 2010. The role of pattern-recognition receptors in innate immunity: update on Toll-like receptors. *Nat Immunol*, 11, 373-384.
- KAWAI, T., SATO, S., ISHII, K. J., COBAN, C., HEMMI, H., YAMAMOTO, M., TERAJ, K., MATSUDA, M., INOUE, J., UEMATSU, S., TAKEUCHI, O. & AKIRA, S. 2004. Interferon-alpha induction through Toll-like receptors involves a direct interaction of IRF7 with MyD88 and TRAF6. *Nat Immunol*, 5, 1061-8.
- KAWAI, T., TAKEUCHI, O., FUJITA, T., INOUE, J.-I., MÜHLRADT, P. F., SATO, S., HOSHINO, K. & AKIRA, S. 2001. Lipopolysaccharide Stimulates the MyD88-Independent Pathway and Results in Activation of IFN-Regulatory Factor 3 and the Expression of a Subset of Lipopolysaccharide-Inducible Genes. *The Journal of Immunology*, 167, 5887-5894.
- KEATING, S. E., MALONEY, G. M., MORAN, E. M. & BOWIE, A. G. 2007. IRAK-2 participates in multiple toll-like receptor signaling pathways to NFkappaB via activation of TRAF6 ubiquitination. *J Biol Chem*, 282, 33435-43.
- KELLEY, S. L., LUKK, T., NAIR, S. K. & TAPPING, R. I. 2012. The Crystal Structure of Human Soluble CD14 Reveals a Bent Solenoid with a Hydrophobic Amino-Terminal Pocket. *The Journal of Immunology*.
- KESSENBROCK, K., FROHLICH, L., SIXT, M., LAMMERMANN, T., PFISTER, H., BATEMAN, A., BELAAOUAJ, A., RING, J., OLLERT, M., FASSLER, R. & JENNE, D. E. 2008. Proteinase 3 and neutrophil elastase enhance inflammation in mice by inactivating antiinflammatory progranulin. *J Clin Invest*, 118, 2438-47.
- KHAN, J. A., BRINT, E. K., O'NEILL, L. A. & TONG, L. 2004. Crystal structure of the Toll/interleukin-1 receptor domain of human IL-1RAPL. *J Biol Chem*, 279, 31664-70.
- KIM, H. M., PARK, B. S., KIM, J. I., KIM, S. E., LEE, J., OH, S. C., ENKHBAYAR, P., MATSUSHIMA, N., LEE, H., YOO, O. J. & LEE, J. O. 2007a. Crystal structure of the TLR4-MD-2 complex with bound endotoxin antagonist Eritoran. *Cell*, 130, 906-17.
- KIM, H. S. & LEE, M. S. 2005. Essential role of STAT1 in caspase-independent cell death of activated macrophages through the p38 mitogen-activated protein kinase/STAT1/reactive oxygen species pathway. *Mol Cell Biol*, 25, 6821-33.

- KIM, S., TAKAHASHI, H., LIN, W. W., DESCARGUES, P., GRIVENNIKOV, S., KIM, Y., LUO, J. L. & KARIN, M. 2009. Carcinoma-produced factors activate myeloid cells through TLR2 to stimulate metastasis. *Nature*, 457, 102-6.
- KIM, Y.-M., BRINKMANN, M. M., PAQUET, M.-E. & PLOEGH, H. L. 2008. UNC93B1 delivers nucleotide-sensing toll-like receptors to endolysosomes. *Nature*, 452, 234-238.
- KIM, Y., ZHOU, P., QIAN, L., CHUANG, J.-Z., LEE, J., LI, C., IADECOLA, C., NATHAN, C. & DING, A. 2007b. MyD88-5 links mitochondria, microtubules, and JNK3 in neurons and regulates neuronal survival. *The Journal of Experimental Medicine*, 204, 2063-2074.
- KISSELEVA, T., BHATTACHARYA, S., BRAUNSTEIN, J. & SCHINDLER, C. W. 2002. Signaling through the JAK/STAT pathway, recent advances and future challenges. *Gene*, 285, 1-24.
- KLUNE, J. R., DHUPAR, R., CARDINAL, J., BILLIAR, T. R. & TSUNG, A. 2008. HMGB1: endogenous danger signaling. *Mol Med*, 14, 476-84.
- KOBAYASHI, M., KWEON, M. N., KUWATA, H., SCHREIBER, R. D., KIYONO, H., TAKEDA, K. & AKIRA, S. 2003. Toll-like receptor-dependent production of IL-12p40 causes chronic enterocolitis in myeloid cell-specific Stat3-deficient mice. *J Clin Invest*, 111, 1297-308.
- KOBAYASHI, T., TAKAESU, G. & YOSHIMURA, A. 2006. Mal-function of TLRs by SOCS. *Nat Immunol*, 7, 123-4.
- KOBAYASHI, T., WALSH, M. C. & CHOI, Y. 2004. The role of TRAF6 in signal transduction and the immune response. *Microbes Infect*, 6, 1333-8.
- KOLLEWE, C., MACKENSEN, A. C., NEUMANN, D., KNOP, J., CAO, P., LI, S., WESCHE, H. & MARTIN, M. U. 2004. Sequential autophosphorylation steps in the interleukin-1 receptor-associated kinase-1 regulate its availability as an adapter in interleukin-1 signaling. *J Biol Chem*, 279, 5227-36.
- KOLLIAS, G., DOUNI, E., KASSIOTIS, G. & KONTOYIANNIS, D. 1999. On the role of tumor necrosis factor and receptors in models of multiorgan failure, rheumatoid arthritis, multiple sclerosis and inflammatory bowel disease. *Immunol Rev*, 169, 175-94.
- KOVARIK, P., STOIBER, D., EYERS, P. A., MENGHINI, R., NEININGER, A., GAESTEL, M., COHEN, P. & DECKER, T. 1999. Stress-induced phosphorylation of STAT1 at Ser727 requires p38 mitogen-activated protein kinase whereas IFN-gamma uses a different signaling pathway. *Proc Natl Acad Sci U S A*, 96, 13956-13961.
- KOVARIK, P., STOIBER, D., NOVY, M. & DECKER, T. 1998. Stat1 combines signals derived from IFN-gamma and LPS receptors during macrophage activation. *EMBO J*, 17, 3660-8.

- KRASITY, B. C., TROLL, J. V., WEISS, J. P. & MCFALL-NGAI, M. J. 2011. LBP/BPI proteins and their relatives: conservation over evolution and roles in mutualism. *Biochem Soc Trans*, 39, 1039-44.
- KRUG, A., LUKER, G. D., BARCHET, W., LEIB, D. A., AKIRA, S. & COLONNA, M. 2004. Herpes simplex virus type 1 activates murine natural interferon-producing cells through toll-like receptor 9. *Blood*, 103, 1433-1437.
- KUBO-MURAI, M., HAZEKI, K., NIGORIKAWA, K., OMOTO, T., INOUE, N. & HAZEKI, O. 2008. IRAK-4-dependent degradation of IRAK-1 is a negative feedback signal for TLR-mediated NF- κ B activation. *Journal of Biochemistry*, 143, 295-302.
- KUMAR, A., COMMANE, M., FLICKINGER, T., HORVATH, C. & STARK, G. 1997. Defective TNF- α -induced apoptosis in STAT1-null cells due to low constitutive levels of caspases. *Science*, 278, 1630 - 1632.
- LAMOTHE, B., WEBSTER, W. K., GOPINATHAN, A., BESSE, A., CAMPOS, A. D. & DARNAY, B. G. 2007. TRAF6 ubiquitin ligase is essential for RANKL signaling and osteoclast differentiation. *Biochem Biophys Res Commun*, 359, 1044-9.
- LANDE, R., GREGORIO, J., FACCHINETTI, V., CHATTERJEE, B., WANG, Y. H., HOMEY, B., CAO, W., SU, B., NESTLE, F. O., ZAL, T., MELLMAN, I., SCHRODER, J. M., LIU, Y. J. & GILLIET, M. 2007. Plasmacytoid dendritic cells sense self-DNA coupled with antimicrobial peptide. *Nature*, 449, 564-9.
- LANDER, H. M. 1997. An essential role for free radicals and derived species in signal transduction. *FASEB J*, 11, 118-24.
- LANDSTRÖM, M. 2010. The TAK1–TRAF6 signalling pathway. *The International Journal of Biochemistry & Cell Biology*, 42, 585-589.
- LARNER, A. C., DAVID, M., FELDMAN, G. M., IGARASHI, K., HACKETT, R. H., WEBB, D. S., SWEITZER, S. M., PETRICOIN, E. F., 3RD & FINBLOOM, D. S. 1993. Tyrosine phosphorylation of DNA binding proteins by multiple cytokines. *Science*, 261, 1730-3.
- LATZ, E., SCHOENEMEYER, A., VISINTIN, A., FITZGERALD, K. A., MONKS, B. G., KNETTER, C. F., LIEN, E., NILSEN, N. J., ESPEVIK, T. & GOLENBOCK, D. T. 2004. TLR9 signals after translocating from the ER to CpG DNA in the lysosome. *Nat Immunol*, 5, 190-8.
- LATZ, E., VERMA, A., VISINTIN, A., GONG, M., SIROIS, C. M., KLEIN, D. C. G., MONKS, B. G., MCKNIGHT, C. J., LAMPHIER, M. S., DUPREX, W. P., ESPEVIK, T. & GOLENBOCK, D. T. 2007. Ligand-induced conformational changes allosterically activate Toll-like receptor 9. *Nat Immunol*, 8, 772-779.

- LATZ, E., VISINTIN, A., LIEN, E., FITZGERALD, K. A., MONKS, B. G., KURT-JONES, E. A., GOLENBOCK, D. T. & ESPEVIK, T. 2002. Lipopolysaccharide rapidly traffics to and from the Golgi apparatus with the toll-like receptor 4-MD-2-CD14 complex in a process that is distinct from the initiation of signal transduction. *J Biol Chem*, 277, 47834-43.
- LEE, C. C., AVALOS, A. M. & PLOEGH, H. L. 2012. Accessory molecules for Toll-like receptors and their function. *Nat Rev Immunol*, 12, 168-179.
- LEE, C. K., SMITH, E., GIMENO, R., GERTNER, R. & LEVY, D. E. 2000. STAT1 affects lymphocyte survival and proliferation partially independent of its role downstream of IFN-gamma. *J Immunol*, 164, 1286-92.
- LEE, H. K., DUNZENDORFER, S., SOLDAU, K. & TOBIAS, P. S. 2006. Double-stranded RNA-mediated TLR3 activation is enhanced by CD14. *Immunity*, 24, 153-63.
- LEE, N. K. & LEE, S. Y. 2002. Modulation of life and death by the tumor necrosis factor receptor-associated factors (TRAFs). *Journal of Biochemistry and Molecular Biology*, 35, 61-66.
- LEIFER, C. A., BROOKS, J. C., HOELZER, K., LOPEZ, J., KENNEDY, M. N., MAZZONI, A. & SEGAL, D. M. 2006. Cytoplasmic targeting motifs control localization of toll-like receptor 9. *J Biol Chem*, 281, 35585-92.
- LEMAITRE, B., NICOLAS, E., MICHAUT, L., REICHHART, J. M. & HOFFMANN, J. A. 1996. The dorsoventral regulatory gene cassette spatzle/Toll/cactus controls the potent antifungal response in Drosophila adults. *Cell*, 86, 973-83.
- LEONARD, J. N., GHIRLANDO, R., ASKINS, J., BELL, J. K., MARGULIES, D. H., DAVIES, D. R. & SEGAL, D. M. 2008. The TLR3 signaling complex forms by cooperative receptor dimerization. *Proc Natl Acad Sci U S A*, 105, 258-63.
- LEULIER, F. & LEMAITRE, B. 2008. Toll-like receptors--taking an evolutionary approach. *Nat Rev Genet*, 9, 165-78.
- LI, Q., HARRAZ, M. M., ZHOU, W., ZHANG, L. N., DING, W., ZHANG, Y., EGGLESTON, T., YEAMAN, C., BANFI, B. & ENGELHARDT, J. F. 2006. Nox2 and Rac1 regulate H₂O₂-dependent recruitment of TRAF6 to endosomal interleukin-1 receptor complexes. *Mol Cell Biol*, 26, 140-54.
- LI, Q., LU, Q., BOTTERO, V., ESTEPA, G., MORRISON, L., MERCURIO, F. & VERMA, I. M. 2005. Enhanced NF-kappaB activation and cellular function in macrophages lacking IkappaB kinase 1 (IKK1). *Proc Natl Acad Sci U S A*, 102, 12425-30.
- LI, S., STRELOW, A., FONTANA, E. J. & WESCHE, H. 2002. IRAK-4: a novel member of the IRAK family with the properties of an IRAK-kinase. *Proc Natl Acad Sci U S A*, 99, 5567-72.

- LIBERATI, N. T., FITZGERALD, K. A., KIM, D. H., FEINBAUM, R., GOLENBOCK, D. T. & AUSUBEL, F. M. 2004. Requirement for a conserved Toll/interleukin-1 resistance domain protein in the *Caenorhabditis elegans* immune response. *Proc Natl Acad Sci U S A*, 101, 6593-8.
- LILJEROOS, M., VUOLTEENAHO, R., MORATH, S., HARTUNG, T., HALLMAN, M. & OJANIEMI, M. 2007. Bruton's tyrosine kinase together with PI 3-kinase are part of Toll-like receptor 2 multiprotein complex and mediate LTA induced Toll-like receptor 2 responses in macrophages. *Cell Signal*, 19, 625-33.
- LIM, C. P. & CAO, X. 1999. Serine Phosphorylation and Negative Regulation of Stat3 by JNK. *Journal of Biological Chemistry*, 274, 31055-31061.
- LIM, C. P. & CAO, X. 2006. Structure, function, and regulation of STAT proteins. *Molecular BioSystems*, 2, 536-550.
- LIN, R., HEYLBROECK, C., GENIN, P., PITHA, P. M. & HISCOTT, J. 1999. Essential Role of Interferon Regulatory Factor 3 in Direct Activation of RANTES Chemokine Transcription. *Molecular and Cellular Biology*, 19, 959-966.
- LIN, S. C., LO, Y. C. & WU, H. 2010. Helical assembly in the MyD88-IRAK4-IRAK2 complex in TLR/IL-1R signalling. *Nature*, 465, 885-90.
- LIN, Y., LEE, H., BERG, A. H., LISANTI, M. P., SHAPIRO, L. & SCHERER, P. E. 2000. The lipopolysaccharide-activated toll-like receptor (TLR)-4 induces synthesis of the closely related receptor TLR-2 in adipocytes. *J Biol Chem*, 275, 24255-63.
- LIU, B., DAI, J., ZHENG, H., STOILOVA, D., SUN, S. & LI, Z. 2003. Cell surface expression of an endoplasmic reticulum resident heat shock protein gp96 triggers MyD88-dependent systemic autoimmune diseases. *Proceedings of the National Academy of Sciences*, 100, 15824-15829.
- LIU, B. & LI, Z. 2008. Endoplasmic reticulum HSP90b1 (gp96, grp94) optimizes B-cell function via chaperoning integrin and TLR but not immunoglobulin. *Blood*, 112, 1223-30.
- LIU, B., YANG, Y., QIU, Z., STARON, M., HONG, F., LI, Y., WU, S., HAO, B., BONA, R., HAN, D. & LI, Z. 2010. Folding of Toll-like receptors by the HSP90 paralogue gp96 requires a substrate-specific cochaperone. *Nat Commun*, 1, 79.
- LIU, L., BOTOS, I., WANG, Y., LEONARD, J. N., SHILOACH, J., SEGAL, D. M. & DAVIES, D. R. 2008. Structural Basis of Toll-Like Receptor 3 Signaling with Double-Stranded RNA. *Science*, 320, 379-381.
- LIU, L., MCBRIDE, K. M. & REICH, N. C. 2005. STAT3 nuclear import is independent of tyrosine phosphorylation and mediated by importin-alpha3. *Proc Natl Acad Sci U S A*, 102, 8150-5.

- LOMAGA, M. A., YE H, W. C., SAROSI, I., DUNCAN, G. S., FURLONGER, C., HO, A., MORONY, S., CAPPARELLI, C., VAN, G., KAUFMAN, S., VAN DER HEIDEN, A., ITIE, A., WAKEHAM, A., KHOO, W., SASAKI, T., CAO, Z. D., PENNINGER, J. M., PAIGE, C. J., LACEY, D. L., DUNSTAN, C. R., BOYLE, W. J., GOEDEL, D. V. & MAK, T. W. 1999. TRAF6 deficiency results in osteopetrosis and defective interleukin-1, CD40, and LPS signaling. *Genes & Development*, 13, 1015-1024.
- LORICK, K. L., JENSEN, J. P., FANG, S., ONG, A. M., HATAKEYAMA, S. & WEISSMAN, A. M. 1999. RING fingers mediate ubiquitin-conjugating enzyme (E2)-dependent ubiquitination. *Proc Natl Acad Sci U S A*, 96, 11364-9.
- LOTZE, M. T. & TRACEY, K. J. 2005. High-mobility group box 1 protein (HMGB1): nuclear weapon in the immune arsenal. *Nat Rev Immunol*, 5, 331-342.
- LU, J. & SUN, P. D. 2012. The Structure of the TLR5-Flagellin Complex: A New Mode of Pathogen Detection, Conserved Receptor Dimerization for Signaling. *Sci. Signal.*, 5, pe11-.
- LUFELI, C., MA, J., HUANG, G., ZHANG, T., NOVOTNY-DIERMAYR, V., ONG, C. T. & CAO, X. 2003. GRIM-19, a death-regulatory gene product, suppresses Stat3 activity via functional interaction. *EMBO J*, 22, 1325-35.
- LUND, J., SATO, A., AKIRA, S., MEDZHITOV, R. & IWASAKI, A. 2003. Toll-like receptor 9-mediated recognition of Herpes simplex virus-2 by plasmacytoid dendritic cells. *Journal of Experimental Medicine*, 198, 513-20.
- LUU, K. 2008. *Investigating the Interaction Between TRAF6 and STAT1*. Bachelor of Biomedical Science Honours, Monash University.
- MA, J. & CAO, X. 2006. Regulation of Stat3 nuclear import by importin α 5 and importin α 7 via two different functional sequence elements. *Cellular Signalling*, 18, 1117-1126.
- MAHIEU, T. & LIBERT, C. 2007. Should We Inhibit Type I Interferons in Sepsis? *Infection and Immunity*, 75, 22-29.
- MANSELL, A., BRINT, E., GOULD, J. A., O'NEILL, L. A. & HERTZOG, P. J. 2004. Mal interacts with tumor necrosis factor receptor-associated factor (TRAF)-6 to mediate NF-kappaB activation by toll-like receptor (TLR)-2 and TLR4. *J Biol Chem*, 279, 37227-30.
- MANSELL, A., SMITH, R., DOYLE, S. L., GRAY, P., FENNER, J. E., CRACK, P. J., NICHOLSON, S. E., HILTON, D. J., O'NEILL, L. A. J. & HERTZOG, P. J. 2006. Suppressor of cytokine signaling 1 negatively regulates Toll-like receptor signaling by mediating Mal degradation. *Nat Immunol*, 7, 148-155.
- MANTOVANI, A., ALLAVENA, P., SICA, A. & BALKWILL, F. 2008. Cancer-related inflammation. *Nature*, 454, 436-44.

- MAO, X., REN, Z., PARKER, G. N., SONDERMANN, H., PASTORELLO, M. A., WANG, W., MCMURRAY, J. S., DEMELER, B., DARNELL, J. E. & CHEN, X. 2005. Structural Bases of Unphosphorylated STAT1 Association and Receptor Binding. *Molecular cell*, 17, 761-771.
- MARCATO, L. G., FERLINI, A. P., BONFIM, R. C., RAMOS-JORGE, M. L., ROPERT, C., AFONSO, L. F., VIEIRA, L. Q. & SOBRINHO, A. P. 2008. The role of Toll-like receptors 2 and 4 on reactive oxygen species and nitric oxide production by macrophage cells stimulated with root canal pathogens. *Oral Microbiol Immunol*, 23, 353-9.
- MARITANO, D., SUGRUE, M. L., TINININI, S., DEWILDE, S., STROBL, B., FU, X., MURRAY-TAIT, V., CHIARLE, R. & POLI, V. 2004. The STAT3 isoforms [alpha] and [beta] have unique and specific functions. *Nat Immunol*, 5, 401-409.
- MARSHAK-ROTHSTEIN, A. 2006. Toll-like receptors in systemic autoimmune disease. *Nat Rev Immunol*, 6, 823-35.
- MARTIN, M. U. & KOLLEWE, C. 2001. Interleukin-1 receptor-associated kinase-1 (IRAK-1): A self-regulatory adapter molecule in the signaling cascade of the Toll/IL-1 receptor family. *Signal Transduction*, 1, 37-50.
- MARTINON, F., MAYOR, A. & TSCHOPP, J. 2009. The Inflammasomes: Guardians of the Body. *Annu Rev Immunol*, 27, 229-265.
- MATSUMOTO, F., SAITOH, S., FUKUI, R., KOBAYASHI, T., TANIMURA, N., KONNO, K., KUSUMOTO, Y., AKASHI-TAKAMURA, S. & MIYAKE, K. 2008. Cathepsins are required for Toll-like receptor 9 responses. *Biochem Biophys Res Commun*, 367, 693-9.
- MATSUMOTO, M., FUNAMI, K., TANABE, M., OSHIUMI, H., SHINGAI, M., SETO, Y., YAMAMOTO, A. & SEYA, T. 2003. Subcellular Localization of Toll-Like Receptor 3 in Human Dendritic Cells. *The Journal of Immunology*, 171, 3154-3162.
- MATSUMOTO, M., KIKKAWA, S., KOHASE, M., MIYAKE, K. & SEYA, T. 2002. Establishment of a monoclonal antibody against human Toll-like receptor 3 that blocks double-stranded RNA-mediated signaling. *Biochemical and Biophysical Research Communications*, 293, 1364-1369.
- MATSUZAWA, A., SAEGUSA, K., NOGUCHI, T., SADAMITSU, C., NISHITOH, H., NAGAI, S., KOYASU, S., MATSUMOTO, K., TAKEDA, K. & ICHIJO, H. 2005. ROS-dependent activation of the TRAF6-ASK1-p38 pathway is selectively required for TLR4-mediated innate immunity. *Nat Immunol*, 6, 587-92.
- MATZINGER, P. 1994. Tolerance, danger, and the extended family. *Annu Rev Immunol*, 12, 991-1045.
- MATZINGER, P. 2002. The danger model: a renewed sense of self. *Science*, 296, 301-5.

- MCGETTRICK, A. F., BRINT, E. K., PALSSON-MCDERMOTT, E. M., ROWE, D. C., GOLENBOCK, D. T., GAY, N. J., FITZGERALD, K. A. & O'NEILL, L. A. 2006. Trif-related adapter molecule is phosphorylated by PKC{epsilon} during Toll-like receptor 4 signaling. *Proc Natl Acad Sci U S A*, 103, 9196-201.
- MCGETTRICK, A. F. & O'NEILL, L. A. 2010. Localisation and trafficking of Toll-like receptors: an important mode of regulation. *Curr Opin Immunol*.
- MCLAREN, J., ROWE, M. & BRENNAN, P. 2007. Epstein–Barr virus induces a distinct form of DNA-bound STAT1 compared with that found in interferon-stimulated B lymphocytes. *Journal of General Virology*, 88, 1876-1886.
- MCWHIRTER, S. M., FITZGERALD, K. A., ROSAINS, J., ROWE, D. C., GOLENBOCK, D. T. & MANIATIS, T. 2004. IFN-regulatory factor 3-dependent gene expression is defective in Tbk1-deficient mouse embryonic fibroblasts. *Proc Natl Acad Sci U S A*, 101, 233-8.
- MEDZHITOV, R. 2001. Toll-like receptors and innate immunity. *Nat Rev Immunol*, 1, 135-45.
- MEDZHITOV, R., PRESTON-HURLBURT, P. & JANEWAY, C. A., JR. 1997. A human homologue of the *Drosophila* Toll protein signals activation of adaptive immunity. *Nature*, 388, 394-7.
- MERAZ, M. A., WHITE, J. M., SHEEHAN, K. C., BACH, E. A., RODIG, S. J., DIGHE, A. S., KAPLAN, D. H., RILEY, J. K., GREENLUND, A. C., CAMPBELL, D., CARVER-MOORE, K., DUBOIS, R. N., CLARK, R., AGUET, M. & SCHREIBER, R. D. 1996. Targeted disruption of the Stat1 gene in mice reveals unexpected physiologic specificity in the JAK-STAT signaling pathway. *Cell*, 84, 431-42.
- MERTENS, C., ZHONG, M., KRISHNARAJ, R., ZOU, W., CHEN, X. & DARNELL, J. E., JR. 2006. Dephosphorylation of phosphotyrosine on STAT1 dimers requires extensive spatial reorientation of the monomers facilitated by the N-terminal domain. *Genes Dev*, 20, 3372-81.
- MEYER, T., GAVENIS, K. & VINKEMEIER, U. 2002. Cell type-specific and tyrosine phosphorylation-independent nuclear presence of STAT1 and STAT3. *Exp Cell Res*, 272, 45-55.
- MEYLAN, E., BURNS, K., HOFMANN, K., BLANCHETEAU, V., MARTINON, F., KELLIHER, M. & TSCHOPP, J. 2004. RIP1 is an essential mediator of Toll-like receptor 3-induced NF-kappa B activation. *Nat Immunol*, 5, 503-507.
- MEYLAN, E. & TSCHOPP, J. 2008. IRAK2 takes its place in TLR signaling. *Nat Immunol*, 9, 581-2.
- MIDWOOD, K., SACRE, S., PICCININI, A. M., INGLIS, J., TREBAUL, A., CHAN, E., DREXLER, S., SOFAT, N., KASHIWAGI, M., OREND, G., BRENNAN, F. & FOXWELL, B. 2009. Tenascin-C is an endogenous activator of Toll-like receptor 4 that is essential for maintaining inflammation in arthritic joint disease. *Nat Med*, 15, 774-80.

- MIGGIN, S. M., PALSSON-MCDERMOTT, E., DUNNE, A., JEFFERIES, C., PINTEAUX, E., BANAHAN, K., MURPHY, C., MOYNAGH, P., YAMAMOTO, M., AKIRA, S., ROTHWELL, N., GOLENBOCK, D., FITZGERALD, K. A. & O'NEILL, L. A. 2007. NF-kappaB activation by the Toll-IL-1 receptor domain protein MyD88 adapter-like is regulated by caspase-1. *Proc Natl Acad Sci U S A*, 104, 3372-7.
- MIKLOSSY, G., HILLIARD, T. S. & TURKSON, J. 2013. Therapeutic modulators of STAT signalling for human diseases. *Nat Rev Drug Discov*, 12, 611-29.
- MINK, M., FOGELGREN, B., OLSZEWSKI, K., MAROY, P. & CSISZAR, K. 2001. A novel human gene (SARM) at chromosome 17q11 encodes a protein with a SAM motif and structural similarity to Armadillo/beta-catenin that is conserved in mouse, Drosophila, and Caenorhabditis elegans. *Genomics*, 74, 234-44.
- MOELANTS, E. A. V., MORTIER, A., VAN DAMME, J. & PROOST, P. 2013. Regulation of TNF-[alpha] with a focus on rheumatoid arthritis. *Immunol Cell Biol*, 91, 393-401.
- MORIUCHI, H., MORIUCHI, M. & FAUCI, A. S. 1997. Nuclear factor-kappa B potently up-regulates the promoter activity of RANTES, a chemokine that blocks HIV infection. *The Journal of Immunology*, 158, 3483-91.
- MOTSHWENE, P. G., MONCRIEFFE, M. C., GROSSMANN, J. G., KAO, C., AYALURU, M., SANDERCOCK, A. M., ROBINSON, C. V., LATZ, E. & GAY, N. J. 2009. An oligomeric signaling platform formed by the Toll-like receptor signal transducers MyD88 and IRAK-4. *J Biol Chem*, 284, 25404-11.
- MUHAMMAD, S., JIANG, Z., LIU, Z., KAUR, K. & WANG, X. 2012. The role of EGFR monoclonal antibodies (MoABs) cetuximab/panitumab, and BRAF inhibitors in BRAF mutated colorectal cancer. *Journal of Gastrointestinal Oncology*, 4, 72-81.
- MULERO, J., BOYLE, B., BRADLEY, S., BRIGHT, J., NELKEN, S., HO, T., MIZE, N., CHILDS, J., BALLINGER, D., FORD, J. & RUPP, F. 2002. Three new human members of the lipid transfer/lipopolysaccharide binding protein family (LT/LBP). *Immunogenetics*, 54, 293-300.
- MULLICK, A. E., TOBIAS, P. S. & CURTISS, L. K. 2005. Modulation of atherosclerosis in mice by Toll-like receptor 2. *J Clin Invest*, 115, 3149-56.
- MURRAY, P. J. 2007. The JAK-STAT Signaling Pathway: Input and Output Integration. *The Journal of Immunology*, 178, 2623-2629.
- MUZIO, M., NI, J., FENG, P. & DIXIT, V. M. 1997. IRAK (Pelle) family member IRAK-2 and MyD88 as proximal mediators of IL-1 signaling. *Science*, 278, 1612-1615.

- NAGAI, Y., AKASHI, S., NAGAFUKU, M., OGATA, M., IWAKURA, Y., AKIRA, S., KITAMURA, T., KOSUGI, A., KIMOTO, M. & MIYAKE, K. 2002. Essential role of MD-2 in LPS responsiveness and TLR4 distribution. *Nat Immunol*, 3, 667-672.
- NAITO, A., AZUMA, S., TANAKA, S., MIYAZAKI, T., TAKAKI, S., TAKATSU, K., NAKAO, K., NAKAMURA, K., KATSUKI, M., YAMAMOTO, T. & INOUE, J. 1999. Severe osteopetrosis, defective interleukin-1 signalling and lymph node organogenesis in TRAF6-deficient mice. *Genes Cells*, 4, 353-62.
- NAJJAR, I. & FAGARD, R. 2010. STAT1 and pathogens, not a friendly relationship. *Biochimie*, 92, 425-444.
- NAJJAR, I., SCHISCHMANOFF, P. O., BARAN-MARSZAK, F., DEGLESNE, P.-A., YOULYOUZ-MARFAK, I., PAMPIN, M., FEUILLARD, J., BORNKAMM, G. W., CHELBI-ALIX, M. K. & FAGARD, R. 2008. Novel function of STAT1 β in B cells: induction of cell death by a mechanism different from that of STAT1 α . *Journal of Leukocyte Biology*, 84, 1604-1612.
- NAKAHIRA, K., HASPEL, J. A., RATHINAM, V. A., LEE, S. J., DOLINAY, T., LAM, H. C., ENGLERT, J. A., RABINOVITCH, M., CERNADAS, M., KIM, H. P., FITZGERALD, K. A., RYTER, S. W. & CHOI, A. M. 2011. Autophagy proteins regulate innate immune responses by inhibiting the release of mitochondrial DNA mediated by the NALP3 inflammasome. *Nat Immunol*, 12, 222-30.
- NAKANO, H., OSHIMA, H., CHUNG, W., WILLIAMS-ABBOTT, L., WARE, C. F., YAGITA, H. & OKUMURA, K. 1996. TRAF5, an activator of NF-kappaB and putative signal transducer for the lymphotoxin-beta receptor. *J Biol Chem*, 271, 14661-4.
- NAKATA, T., YASUDA, M., FUJITA, M., KATAOKA, H., KIURA, K., SANO, H. & SHIBATA, K. 2006. CD14 directly binds to triacylated lipopeptides and facilitates recognition of the lipopeptides by the receptor complex of Toll-like receptors 2 and 1 without binding to the complex. *Cell Microbiol*, 8, 1899-909.
- NAKATSU, F. & OHNO, H. 2003. Adaptor protein complexes as the key regulators of protein sorting in the post-Golgi network. *Cell Struct Funct*, 28, 419-29.
- NEGISHI, H., FUJITA, Y., YANAI, H., SAKAGUCHI, S., OUYANG, X., SHINOHARA, M., TAKAYANAGI, H., OHBA, Y., TANIGUCHI, T. & HONDA, K. 2006. Evidence for licensing of IFN-gamma-induced IFN regulatory factor 1 transcription factor by MyD88 in Toll-like receptor-dependent gene induction program. *Proc Natl Acad Sci U S A*, 103, 15136-41.
- NEWTON, K., MATSUMOTO, M. L., WERTZ, I. E., KIRKPATRICK, D. S., LILL, J. R., TAN, J., DUGGER, D., GORDON, N., SIDHU, S. S., FELLOUSE, F. A., KOMUVES, L., FRENCH, D. M., FERRANDO, R. E., LAM, C., COMPAAN, D., YU, C., BOSANAC, I., HYMOWITZ, S. G., KELLEY, R. F. & DIXIT,

- V. M. 2008. Ubiquitin chain editing revealed by polyubiquitin linkage-specific antibodies. *Cell*, 134, 668-78.
- NGUYEN, H., CHATTERJEE-KISHORE, M., JIANG, Z., QING, Y., RAMANA, C. V., BAYES, J., COMMANE, M., LI, X. & STARK, G. R. 2003. IRAK-dependent phosphorylation of Stat1 on serine 727 in response to interleukin-1 and effects on gene expression. *J Interferon Cytokine Res*, 23, 183-92.
- NIEMAND, C., NIMMESGERN, A., HAAN, S., FISCHER, P., SCHAPER, F., ROSSAINT, R., HEINRICH, P. C. & MÜLLER-NEWEN, G. 2003. Activation of STAT3 by IL-6 and IL-10 in Primary Human Macrophages Is Differentially Modulated by Suppressor of Cytokine Signaling 3. *The Journal of Immunology*, 170, 3263-3272.
- NILSEN, N. J., DEININGER, S., NONSTAD, U., SKJELDAL, F., HUSEBYE, H., RODIONOV, D., VON AULOCK, S., HARTUNG, T., LIEN, E., BAKKE, O. & ESPEVIK, T. 2008. Cellular trafficking of lipoteichoic acid and Toll-like receptor 2 in relation to signaling; role of CD14 and CD36. *Journal of Leukocyte Biology*, 84, 280-291.
- NISHIYA, T., KAJITA, E., MIWA, S. & DEFRANCO, A. L. 2005. TLR3 and TLR7 are targeted to the same intracellular compartments by distinct regulatory elements. *J Biol Chem*, 280, 37107-17.
- NOLAN, G. P., GHOSH, S., LIOU, H.-C., TEMPST, P. & BALTIMORE, D. 1991. DNA binding and I^αB inhibition of the cloned p65 subunit of NF- κ B, a rel-related polypeptide. *Cell*, 64, 961-969.
- NOPERT, S. J., FITZGERALD, K. A. & HERTZOG, P. J. 2007. The role of type I interferons in TLR responses. *Immunol Cell Biol*, 85, 446-57.
- NOVICK, D., COHEN, B. & RUBINSTEIN, M. 1994. The human interferon $\alpha\beta$ receptor: Characterization and molecular cloning. *Cell*, 77, 391-400.
- NYMAN, T., STENMARK, P., FLODIN, S., JOHANSSON, I., HAMMARSTROM, M. & NORDLUND, P. 2008. The crystal structure of the human toll-like receptor 10 cytoplasmic domain reveals a putative signaling dimer. *J Biol Chem*, 283, 11861-5.
- O'NEILL, L. A., FITZGERALD, K. A. & BOWIE, A. G. 2003. The Toll-IL-1 receptor adaptor family grows to five members. *Trends Immunol*, 24, 286-90.
- O'NEILL, L. A. J. 2006. How Toll-like receptors signal: what we know and what we don't know. *Current Opinion in Immunology*, 18, 3-9.
- OGANESYAN, G., SAHA, S. K., GUO, B., HE, J. Q., SHAHANGIAN, A., ZARNEGAR, B., PERRY, A. & CHENG, G. 2006. Critical role of TRAF3 in the Toll-like receptor-dependent and -independent antiviral response. *Nature*, 439, 208-11.

- OHMORI, Y., SCHREIBER, R. D. & HAMILTON, T. A. 1997. Synergy between interferon-gamma and tumor necrosis factor-alpha in transcriptional activation is mediated by cooperation between signal transducer and activator of transcription 1 and nuclear factor kappaB. *J Biol Chem*, 272, 14899-907.
- OLIVIERI, I., D'ANGELO, S., PADULA, A., LECCESE, P., NIGRO, A. & PALAZZI, C. 2013. Can we reduce the dosage of biologics in spondyloarthritis? *Autoimmunity Reviews*, 12, 691-693.
- ORDUREAU, A., SMITH, H., WINDHEIM, M., PEGGIE, M., CARRICK, E., MORRICE, N. & COHEN, P. 2008. The IRAK-catalysed activation of the E3 ligase function of Pellino isoforms induces the Lys63-linked polyubiquitination of IRAK1. *Biochem J*, 409, 43-52.
- OSHIUMI, H., MATSUMOTO, M., FUNAMI, K., AKAZAWA, T. & SEYA, T. 2003a. TICAM-1, an adaptor molecule that participates in Toll-like receptor 3-mediated interferon-[beta] induction. *Nat Immunol*, 4, 161-167.
- OSHIUMI, H., SASAI, M., SHIDA, K., FUJITA, T., MATSUMOTO, M. & SEYA, T. 2003b. TICACM-2: a bridging adapter recruiting to Toll-like receptor 4 TICAM-1 that induces interferon-beta. *J Biol. Chem.*, M305820200.
- OUCHI, T., LEE, S. W., OUCHI, M., AARONSON, S. A. & HORVATH, C. M. 2000. Collaboration of signal transducer and activator of transcription 1 (STAT1) and BRCA1 in differential regulation of IFN- γ target genes. *Proceedings of the National Academy of Sciences*, 97, 5208-5213.
- OZINSKY, A., UNDERHILL, D. M., FONTENOT, J. D., HAJJAR, A. M., SMITH, K. D., WILSON, C. B., SCHROEDER, L. & ADEREM, A. 2000. The repertoire for pattern recognition of pathogens by the innate immune system is defined by cooperation between toll-like receptors. *Proc Natl Acad Sci U S A*, 97, 13766-71.
- PALSSON-MCDERMOTT, E. M., DOYLE, S. L., MCGETTRICK, A. F., HARDY, M., HUSEBYE, H., BANAHAN, K., GONG, M., GOLENBOCK, D., ESPEVIK, T. & O'NEILL, L. A. 2009. TAG, a splice variant of the adaptor TRAM, negatively regulates the adaptor MyD88-independent TLR4 pathway. *Nat Immunol*, 10, 579-86.
- PANDEY, S. & AGRAWAL, D. K. 2006. Immunobiology of Toll-like receptors: emerging trends. *Immunol Cell Biol*, 84, 333-41.
- PAPADIMITRAKI, E. D., BERTSIAS, G. K. & BOUMPAS, D. T. 2007. Toll like receptors and autoimmunity: a critical appraisal. *J Autoimmun*, 29, 310-8.
- PARK, B., BRINKMANN, M. M., SPOONER, E., LEE, C. C., KIM, Y. M. & PLOEGH, H. L. 2008. Proteolytic cleavage in an endolysosomal compartment is required for activation of Toll-like receptor 9. *Nat Immunol*, 9, 1407-14.

- PARK, B., BUTI, L., LEE, S., MATSUWAKI, T., SPOONER, E., BRINKMANN, M. M., NISHIHARA, M. & PLOEGH, H. L. 2011. Granulin is a soluble cofactor for toll-like receptor 9 signaling. *Immunity*, 34, 505-13.
- PARK, B. S., SONG, D. H., KIM, H. M., CHOI, B.-S., LEE, H. & LEE, J.-O. 2009. The structural basis of lipopolysaccharide recognition by the TLR4-MD-2 complex. *Nature*, 458, 1191-1195.
- PARK, H. S., JUNG, H. Y., PARK, E. Y., KIM, J., LEE, W. J. & BAE, Y. S. 2004. Cutting edge: direct interaction of TLR4 with NAD(P)H oxidase 4 isozyme is essential for lipopolysaccharide-induced production of reactive oxygen species and activation of NF-kappa B. *J Immunol*, 173, 3589-93.
- PARK, O. K., SCHAEFER, L. K., WANG, W. & SCHAEFER, T. S. 2000. Dimer Stability as a Determinant of Differential DNA Binding Activity of Stat3 Isoforms. *Journal of Biological Chemistry*, 275, 32244-32249.
- PARK, Y. C., BURKITT, V., VILLA, A. R., TONG, L. & WU, H. 1999. Structural basis for self-association and receptor recognition of human TRAF2. *Nature*, 398, 533-8.
- PENG, J., YUAN, Q., LIN, B., PANNEERSELVAM, P., WANG, X., LUAN, X. L., LIM, S. K., LEUNG, B. P., HO, B. & DING, J. L. 2010. SARM inhibits both TRIF- and MyD88-mediated AP-1 activation. *European Journal of Immunology*, 40, 1738-1747.
- PENTTINEN, M. A., HOLMBERG, C. I., SISTONEN, L. & GRANFORS, K. 2002. HLA-B27 modulates nuclear factor kappaB activation in human monocytic cells exposed to lipopolysaccharide. *Arthritis Rheum*, 46, 2172-80.
- PETER, M. E., KUBARENKO, A. V., WEBER, A. N. & DALPKE, A. H. 2009. Identification of an N-terminal recognition site in TLR9 that contributes to CpG-DNA-mediated receptor activation. *J Immunol*, 182, 7690-7.
- PICARD, C., VON BERNUTH, H., GHANDIL, P., CHRABIEH, M., LEVY, O., ARKWRIGHT, P. D., MCDONALD, D., GEHA, R. S., TAKADA, H., KRAUSE, J. C., CREECH, C. B., KU, C. L., EHL, S., MARODI, L., AL-MUHCEN, S., AL-HAJJAR, S., AL-GHONAIUM, A., DAY-GOOD, N. K., HOLLAND, S. M., GALLIN, J. I., CHAPEL, H., SPEERT, D. P., RODRIGUEZ-GALLEGO, C., COLINO, E., GARTY, B. Z., ROIFMAN, C., HARA, T., YOSHIKAWA, H., NONOYAMA, S., DOMACHOWSKIE, J., ISSEKUTZ, A. C., TANG, M., SMART, J., ZITNIK, S. E., HOARAU, C., KUMARARATNE, D. S., THRASHER, A. J., DAVIES, E. G., BETHUNE, C., SIRVENT, N., DE RICAUD, D., CAMCIOGLU, Y., VASCONCELOS, J., GUEDES, M., VITOR, A. B., RODRIGO, C., ALMAZAN, F., MENDEZ, M., AROSTEGUI, J. I., ALSINA, L., FORTUNY, C., REICHENBACH, J., VERBSKY, J. W., BOSSUYT, X., DOFFINGER, R., ABEL, L., PUEL, A. & CASANOVA, J. L. 2010.

- Clinical features and outcome of patients with IRAK-4 and MyD88 deficiency. *Medicine (Baltimore)*, 89, 403-25.
- PICCININI, A. M. & MIDWOOD, K. S. 2010. DAMPening inflammation by modulating TLR signalling. *Mediators Inflamm*, 2010.
- PICKART, C. M. & EDDINS, M. J. 2004. Ubiquitin: structures, functions, mechanisms. *Biochim Biophys Acta*, 1695, 55-72.
- PIDGEON, G. P., HARMEY, J. H., KAY, E., DA COSTA, M., REDMOND, H. P. & BOUCHIER-HAYES, D. J. 1999. The role of endotoxin/lipopolysaccharide in surgically induced tumour growth in a murine model of metastatic disease. *Br J Cancer*, 81, 1311-7.
- PINEDA, G., EA, C. K. & CHEN, Z. J. 2007. Ubiquitination and TRAF signaling. *Adv Exp Med Biol*, 597, 80-92.
- POBEZINSKAYA, Y. L., KIM, Y. S., CHOKSI, S., MORGAN, M. J., LI, T., LIU, C. & LIU, Z. 2008. The function of TRADD in signaling through tumor necrosis factor receptor 1 and TRIF-dependent Toll-like receptors. *Nat Immunol*, 9, 1047-54.
- POLTORAK, A., HE, X. L., SMIRNOVA, I., LIU, M. Y., VAN HUFFEL, C., DU, X., BIRDWELL, D., ALEJOS, E., SILVA, M., GALANOS, C., FREUDENBERG, M., RICCIARDI-CASTAGNOLI, P., LAYTON, B. & BEUTLER, B. 1998. Defective LPS signaling in C3H/HeJ and C57BL/10ScCr mice: Mutations in Tlr4 gene. *Science*, 282, 2085-2088.
- PRELE, C. M., KEITH-MAGEE, A. L., MURCHA, M. & HART, P. H. 2007. Activated signal transducer and activator of transcription-3 (STAT3) is a poor regulator of tumour necrosis factor-alpha production by human monocytes. *Clin Exp Immunol*, 147, 564-72.
- PRICKETT, T. D. & BRAUTIGAN, D. L. 2007. Cytokine activation of p38 mitogen-activated protein kinase and apoptosis is opposed by alpha-4 targeting of protein phosphatase 2A for site-specific dephosphorylation of MEK3. *Mol Cell Biol*, 27, 4217-27.
- PUTZ, E. M., GOTTHARDT, D., HOERMANN, G., CSISZAR, A., WIRTH, S., BERGER, A., STRAKA, E., RIGLER, D., WALLNER, B., JAMIESON, A. M., PICKL, W. F., ZEBEDIN-BRANDL, E. M., MULLER, M., DECKER, T. & SEXL, V. 2013. CDK8-Mediated STAT1-S727 Phosphorylation Restrains NK Cell Cytotoxicity and Tumor Surveillance. *Cell Rep*, 4, 437-44.
- QI, H., DENNING, T. L. & SOONG, L. 2003. Differential Induction of Interleukin-10 and Interleukin-12 in Dendritic Cells by Microbial Toll-Like Receptor Activators and Skewing of T-Cell Cytokine Profiles. *Infection and Immunity*, 71, 3337-3342.
- QUELLE, F. W., THIERFELDER, W., WITTHUHN, B. A., TANG, B., COHEN, S. & IHLE, J. N. 1995. Phosphorylation and Activation of the DNA Binding Activity of Purified Stat1 by the Janus

- Protein-tyrosine Kinases and the Epidermal Growth Factor Receptor. *Journal of Biological Chemistry*, 270, 20775-20780.
- QURESHI, S. A., SALDITT-GEORGIEFF, M. & DARNELL, J. E., JR. 1995. Tyrosine-phosphorylated Stat1 and Stat2 plus a 48-kDa protein all contact DNA in forming interferon-stimulated-gene factor 3. *Proc Natl Acad Sci U S A*, 92, 3829-33.
- RAETZ, C. R. 1990. Biochemistry of endotoxins. *Annu Rev Biochem*, 59, 129-70.
- RAKOFF-NAHOUM, S. & MEDZHITOV, R. 2009. Toll-like receptors and cancer. *Nat Rev Cancer*, 9, 57-63.
- RAMANA, C. V., CHATTERJEE-KISHORE, M., NGUYEN, H. & STARK, G. R. 2000. Complex roles of Stat1 in regulating gene expression. *Oncogene*, 19, 2619-27.
- RAMSAUER, K., FARLIK, M., ZUPKOVITZ, G., SEISER, C., KROGER, A., HAUSER, H. & DECKER, T. 2007. Distinct modes of action applied by transcription factors STAT1 and IRF1 to initiate transcription of the IFN-gamma-inducible gbp2 gene. *Proc Natl Acad Sci U S A*, 104, 2849-54.
- RAMSAUER, K., SADZAK, I., PORRAS, A., PILZ, A., NEBRED, A. R., DECKER, T. & KOVARIK, P. 2002. p38 MAPK enhances STAT1-dependent transcription independently of Ser-727 phosphorylation. *Proc Natl Acad Sci U S A*, 99, 12859-64.
- RANDOW, F. & SEED, B. 2001. Endoplasmic reticulum chaperone gp96 is required for innate immunity but not cell viability. *Nat Cell Biol*, 3, 891-6.
- REN, Z., MAO, X., MERTENS, C., KRISHNARAJ, R., QIN, J., MANDAL, P. K., ROMANOWSKI, M. J., MCMURRAY, J. S. & CHEN, X. 2008. Crystal structure of unphosphorylated STAT3 core fragment. *Biochemical and Biophysical Research Communications*, 374, 1-5.
- RHEE, S. H., JONES, B. W., TOSHCHAKOV, V., VOGEL, S. N. & FENTON, M. J. 2003. Toll-like receptors 2 and 4 activate STAT1 serine phosphorylation by distinct mechanisms in macrophages. *J Biol Chem*, 278, 22506-12.
- ROBINSON, M. J., SANCHO, D., SLACK, E. C., LEIBUNDGUT-LANDMANN, S. & SOUSA, C. R. E. 2006. Myeloid C-type lectins in innate immunity. *Nat Immunol*, 7, 1258-1265.
- ROELOFS, M. F., BOELEN, W. C., JOOSTEN, L. A., ABDOLLAHI-ROODSAZ, S., GEURTS, J., WUNDERINK, L. U., SCHREURS, B. W., VAN DEN BERG, W. B. & RADSTAKE, T. R. 2006. Identification of small heat shock protein B8 (HSP22) as a novel TLR4 ligand and potential involvement in the pathogenesis of rheumatoid arthritis. *J Immunol*, 176, 7021-7.
- ROSS, K., YANG, L., DOWER, S., VOLPE, F. & GUESDON, F. 2002. Identification of threonine 66 as a functionally critical residue of the interleukin-1 receptor-associated kinase. *J Biol Chem*, 277, 37414-21.

- ROTHER, G. & VALET, G. 1990. Flow cytometric analysis of respiratory burst activity in phagocytes with hydroethidine and 2',7'-dichlorofluorescein. *J Leukoc Biol*, 47, 440-8.
- ROTHER, M., SARMA, V., DIXIT, V. M. & GOEDDEL, D. V. 1995. TRAF2-mediated activation of NF-kappa B by TNF receptor 2 and CD40. *Science*, 269, 1424-7.
- ROUYEZ, M. C., LESTINGI, M., CHARON, M., FICHELSON, S., BUZYN, A. & DUSANTER-FOURT, I. 2005. IFN regulatory factor-2 cooperates with STAT1 to regulate transporter associated with antigen processing-1 promoter activity. *J Immunol*, 174, 3948-58.
- ROWE, D. C., MCGETTRICK, A. F., LATZ, E., MONKS, B. G., GAY, N. J., YAMAMOTO, M., AKIRA, S., O'NEILL, L. A., FITZGERALD, K. A. & GOLENBOCK, D. T. 2006. The myristoylation of TRIF-related adaptor molecule is essential for Toll-like receptor 4 signal transduction. *Proc Natl Acad Sci U S A*, 103, 6299-304.
- RUCKDESCHEL, K., PFAFFINGER, G., HAASE, R., SING, A., WEIGHARDT, H., HACKER, G., HOLZMANN, B. & HEESEMANN, J. 2004. Signaling of apoptosis through TLRs critically involves toll/IL-1 receptor domain-containing adapter inducing IFN-beta, but not MyD88, in bacteria-infected murine macrophages. *J Immunol*, 173, 3320-8.
- RUUSKA, M., SAHLBERG, A. S., COLBERT, R. A., GRANFORS, K. & PENTTINEN, M. A. 2012. Enhanced phosphorylation of STAT-1 is dependent on double-stranded RNA-dependent protein kinase signaling in HLA-B27-expressing U937 monocytic cells. *Arthritis Rheum*, 64, 772-7.
- RUUSKA, M., SAHLBERG, A. S., GRANFORS, K. & PENTTINEN, M. A. 2013. Phosphorylation of STAT-1 serine 727 is prolonged in HLA-B27-expressing human monocytic cells. *PLoS One*, 8, e50684.
- RYAN, K. A., SMITH, M. F., JR., SANDERS, M. K. & ERNST, P. B. 2004. Reactive oxygen and nitrogen species differentially regulate Toll-like receptor 4-mediated activation of NF-kappa B and interleukin-8 expression. *Infect Immun*, 72, 2123-30.
- SADZAK, I., SCHIFF, M., GATTERMEIER, I., GLINITZER, R., SAUER, I., SAALMÜLLER, A., YANG, E., SCHALJO, B. & KOVARIK, P. 2008. Recruitment of Stat1 to chromatin is required for interferon-induced serine phosphorylation of Stat1 transactivation domain. *Proceedings of the National Academy of Sciences*, 105, 8944-8949.
- SAKAGUCHI, M., OKA, M., IWASAKI, T., FUKAMI, Y. & NISHIGORI, C. 2012. Role and regulation of STAT3 phosphorylation at Ser727 in melanocytes and melanoma cells. *J Invest Dermatol*, 132, 1877-85.
- SANDOR, F. & BUC, M. 2005. Toll-like receptors. I. Structure, function and their ligands. *Folia Biol (Praha)*, 51, 148-57.

- SANLIOGLU, S., WILLIAMS, C. M., SAMAVATI, L., BUTLER, N. S., WANG, G., MCCRAY, P. B., JR., RITCHIE, T. C., HUNNINGHAKE, G. W., ZANDI, E. & ENGELHARDT, J. F. 2001. Lipopolysaccharide induces Rac1-dependent reactive oxygen species formation and coordinates tumor necrosis factor-alpha secretion through IKK regulation of NF-kappa B. *J Biol Chem*, 276, 30188-98.
- SANO, S., ITAMI, S., TAKEDA, K., TARUTANI, M., YAMAGUCHI, Y., MIURA, H., YOSHIKAWA, K., AKIRA, S. & TAKEDA, J. 1999. Keratinocyte-specific ablation of Stat3 exhibits impaired skin remodeling, but does not affect skin morphogenesis. *EMBO J*, 18, 4657-4668.
- SANZ, E., HOFER, M. J., UNZETA, M. & CAMPBELL, I. L. 2008. Minimal role for STAT1 in interleukin-6 signaling and actions in the murine brain. *Glia*, 56, 190-9.
- SASAI, M., LINEHAN, M. M. & IWASAKI, A. 2010. Bifurcation of Toll-Like Receptor 9 Signaling by Adaptor Protein 3. *Science*, 329, 1530-1534.
- SASAI, M., OSHIUMI, H., MATSUMOTO, M., INOUE, N., FUJITA, F., NAKANISHI, M. & SEYA, T. 2005. Cutting Edge: NF-kappaB-activating kinase-associated protein 1 participates in TLR3/Toll-IL-1 homology domain-containing adapter molecule-1-mediated IFN regulatory factor 3 activation. *J Immunol*, 174, 27-30.
- SATO, M., SUEMORI, H., HATA, N., ASAGIRI, M., OGASAWARA, K., NAKAO, K., NAKAYA, T., KATSUKI, M., NOGUCHI, S., TANAKA, N. & TANIGUCHI, T. 2000. Distinct and essential roles of transcription factors IRF-3 and IRF-7 in response to viruses for IFN-alpha/beta gene induction. *Immunity*, 13, 539-48.
- SATO, S., SUGIYAMA, M., YAMAMOTO, M., WATANABE, Y., KAWAI, T., TAKEDA, K. & AKIRA, S. 2003. Toll/IL-1 Receptor Domain-Containing Adaptor Inducing IFN- β (TRIF) Associates with TNF Receptor-Associated Factor 6 and TANK-Binding Kinase 1, and Activates Two Distinct Transcription Factors, NF- κ B and IFN-Regulatory Factor-3, in the Toll-Like Receptor Signaling. *The Journal of Immunology*, 171, 4304-4310.
- SCHAEFER, L., BABELOVA, A., KISS, E., HAUSSER, H. J., BALIOVA, M., KRZYZANKOVA, M., MARSCHE, G., YOUNG, M. F., MIHALIK, D., GOTTE, M., MALLE, E., SCHAEFER, R. M. & GRONE, H. J. 2005. The matrix component biglycan is proinflammatory and signals through Toll-like receptors 4 and 2 in macrophages. *J Clin Invest*, 115, 2223-33.
- SCHAEFER, T. S., SANDERS, L. K. & NATHANS, D. 1995. Cooperative transcriptional activity of Jun and Stat3 beta, a short form of Stat3. *Proceedings of the National Academy of Sciences*, 92, 9097-9101.
- SCHAEFER, T. S., SANDERS, L. K., PARK, O. K. & NATHANS, D. 1997. Functional differences between Stat3alpha and Stat3beta. *Molecular and Cellular Biology*, 17, 5307-16.

- SCHAFFER, S. L., LIN, R., MOORE, P. A., HISCOTT, J. & PITHA, P. M. 1998. Regulation of Type I Interferon Gene Expression by Interferon Regulatory Factor-3. *Journal of Biological Chemistry*, 273, 2714-2720.
- SCHINDLER, C., FU, X. Y., IMPROTA, T., AEBERSOLD, R. & DARNELL, J. E., JR. 1992a. Proteins of transcription factor ISGF-3: one gene encodes the 91-and 84-kDa ISGF-3 proteins that are activated by interferon alpha. *Proc Natl Acad Sci U S A*, 89, 7836-9.
- SCHINDLER, C., SHUAI, K., PREZIOSO, V. R. & DARNELL, J. E., JR. 1992b. Interferon-dependent tyrosine phosphorylation of a latent cytoplasmic transcription factor. *Science*, 257, 809-13.
- SCHINDLER, C. W. 2002. JAK-STAT signaling in human disease. *Journal of Clinical Investigation*, 109, 1133-1137.
- SCHMITZ, F., HEIT, A., GUGGEMOOS, S., KRUG, A., MAGES, J., SCHIEMANN, M., ADLER, H., DREXLER, I., HAAS, T., LANG, R. & WAGNER, H. 2007. Interferon-regulatory-factor 1 controls Toll-like receptor 9-mediated IFN- β production in myeloid dendritic cells. *European Journal of Immunology*, 37, 315-327.
- SCHNARE, M., BARTON, G. M., HOLT, A. C., TAKEDA, K., AKIRA, S. & MEDZHITOV, R. 2001. Toll-like receptors control activation of adaptive immune responses. *Nat Immunol*, 2, 947-950.
- SCHOONBROODT, S., FERREIRA, V., BEST-BELPOMME, M., BOELAERT, J. R., LEGRAND-POELS, S., KORNER, M. & PIETTE, J. 2000. Crucial role of the amino-terminal tyrosine residue 42 and the carboxyl-terminal PEST domain of I kappa B alpha in NF-kappa B activation by an oxidative stress. *J Immunol*, 164, 4292-300.
- SCHRECK, R., RIEBER, P. & BAEUERLE, P. A. 1991. Reactive oxygen intermediates as apparently widely used messengers in the activation of the NF-kappa B transcription factor and HIV-1. *EMBO J*, 10, 2247-58.
- SCHRODER, K., SPILLE, M., PILZ, A., LATTIN, J., BODE, K. A., IRVINE, K. M., BURROWS, A. D., RAVASI, T., WEIGHARDT, H., STACEY, K. J., DECKER, T., HUME, D. A., DALPKE, A. H. & SWEET, M. J. 2007. Differential Effects of CpG DNA on IFN- β Induction and STAT1 Activation in Murine Macrophages versus Dendritic Cells: Alternatively Activated STAT1 Negatively Regulates TLR Signaling in Macrophages. *The Journal of Immunology*, 179, 3495-3503.
- SCHURINGA, J. J., JONK, L. J., DOKTER, W. H., VELLENGA, E. & KRUIJER, W. 2000. Interleukin-6-induced STAT3 transactivation and Ser727 phosphorylation involves Vav, Rac-1 and the kinase SEK-1/MKK-4 as signal transduction components. *Biochem. J.*, 347, 89-96.

- SCHWANDNER, R., DZIARSKI, R., WESCHE, H., ROTHE, M. & KIRSCHNING, C. J. 1999. Peptidoglycan- and lipoteichoic acid-induced cell activation is mediated by toll-like receptor 2. *Journal of Biological Chemistry*, 274, 17406-17409.
- SEN, M., THOMAS, S. M., KIM, S., YEH, J. I., FERRIS, R. L., JOHNSON, J. T., DUVVURI, U., LEE, J., SAHU, N., JOYCE, S., FREILINO, M. L., SHI, H., LI, C., LY, D., RAPIREDDY, S., ETTER, J. P., LI, P. K., WANG, L., CHIOSEA, S., SEETHALA, R. R., GOODING, W. E., CHEN, X., KAMINSKI, N., PANDIT, K., JOHNSON, D. E. & GRANDIS, J. R. 2012. First-in-human trial of a STAT3 decoy oligonucleotide in head and neck tumors: implications for cancer therapy. *Cancer Discov*, 2, 694-705.
- SEN, M., TOSCA, P. J., ZWAYER, C., RYAN, M. J., JOHNSON, J. D., KNOSTMAN, K. A., GICLAS, P. C., PEGGINS, J. O., TOMASZEWSKI, J. E., MCMURRAY, T. P., LI, C., LEIBOWITZ, M. S., FERRIS, R. L., GOODING, W. E., THOMAS, S. M., JOHNSON, D. E. & GRANDIS, J. R. 2009. Lack of toxicity of a STAT3 decoy oligonucleotide. *Cancer Chemother Pharmacol*, 63, 983-95.
- SENGUPTA, T. K., TALBOT, E. S., SCHERLE, P. A. & IVASHKIV, L. B. 1998. Rapid inhibition of interleukin-6 signaling and Stat3 activation mediated by mitogen-activated protein kinases. *Proceedings of the National Academy of Sciences*, 95, 11107-11112.
- SHARMA, S., TENOEVER, B. R., GRANDVAUX, N., ZHOU, G.-P., LIN, R. & HISCOTT, J. 2003. Triggering the Interferon Antiviral Response Through an IKK-Related Pathway. *Science*, 300, 1148-1151.
- SHEEDY, F. J., GREBE, A., RAYNER, K. J., KALANTARI, P., RAMKHELAWON, B., CARPENTER, S. B., BECKER, C. E., EDIRIWEERA, H. N., MULLICK, A. E., GOLENBOCK, D. T., STUART, L. M., LATZ, E., FITZGERALD, K. A. & MOORE, K. J. 2013. CD36 coordinates NLRP3 inflammasome activation by facilitating intracellular nucleation of soluble ligands into particulate ligands in sterile inflammation. *Nat Immunol*, 14, 812-20.
- SHEN, Y., SCHLESSINGER, K., ZHU, X., MEFFRE, E., QUIMBY, F., LEVY, D. E. & DARNELL, J. E., JR. 2004. Essential role of STAT3 in postnatal survival and growth revealed by mice lacking STAT3 serine 727 phosphorylation. *Mol Cell Biol*, 24, 407-19.
- SHIBUYA, H., YAMAGUCHI, K., SHIRAKABE, K., TONEGAWA, A., GOTOH, Y., UENO, N., IRIE, K., NISHIDA, E. & MATSUMOTO, K. 1996. TAB1: An Activator of the TAK1 MAPKKK in TGF- β Signal Transduction. *Science*, 272, 1179-1182.
- SHIM, J. H., XIAO, C. C., PASCHAL, A. E., BAILEY, S. T., RAO, P., HAYDEN, M. S., LEE, K. Y., BUSSEY, C., STECKEL, M., TANAKA, N., YAMADA, G., AKIRA, S., MATSUMOTO, K. & GHOSH, S. 2005. TAK1, but not TAB1 or TAB2, plays an essential role in multiple signaling pathways in vivo. *Genes & Development*, 19, 2668-2681.

- SHOENFELT, J. L. & FENTON, M. J. 2006. TLR2- and TLR4-dependent activation of STAT1 serine phosphorylation in murine macrophages is protein kinase C-delta-independent. *J Endotoxin Res*, 12, 231-240.
- SHUAI, K., HORVATH, C. M., HUANG, L. H. T., QURESHI, S. A., COWBURN, D. & DARNELL JR, J. E. 1994. Interferon activation of the transcription factor Stat91 involves dimerization through SH2-phosphotyrosyl peptide interactions. *Cell*, 76, 821-828.
- SHUAI, K., SCHINDLER, C., PREZIOSO, V. R. & DARNELL, J. E., JR. 1992. Activation of transcription by IFN-gamma: tyrosine phosphorylation of a 91-kD DNA binding protein. *Science*, 258, 1808-12.
- SHULGA, N. & PASTORINO, J. G. 2012. GRIM-19 Mediated Translocation of STAT3 to Mitochondria is Necessary for TNF Induced Necroptosis. *Journal of Cell Science*.
- SIKORSKI, K., CHMIELEWSKI, S., PRZYBYL, L., HEEMANN, U., WESOLY, J., BAUMANN, M. & BLUYSSSEN, H. A. 2011a. STAT1-mediated signal integration between IFNgamma and LPS leads to increased EC and SMC activation and monocyte adhesion. *Am J Physiol Cell Physiol*, 300, C1337-44.
- SIKORSKI, K., CZERWONIEC, A., BUJNICKI, J. M., WESOLY, J. & BLUYSSSEN, H. A. 2011b. STAT1 as a novel therapeutical target in pro-atherogenic signal integration of IFNgamma, TLR4 and IL-6 in vascular disease. *Cytokine Growth Factor Rev*, 22, 211-9.
- SILVENNOINEN, O., IHLE, J. N., SCHLESSINGER, J. & LEVY, D. E. 1993. Interferon-induced nuclear signalling by Jak protein tyrosine kinases. *Nature*, 366, 583-585.
- SLACK, J. L., SCHOOLEY, K., BONNERT, T. P., MITCHAM, J. L., QWARNSTROM, E. E., SIMS, J. E. & DOWER, S. K. 2000. Identification of Two Major Sites in the Type I Interleukin-1 Receptor Cytoplasmic Region Responsible for Coupling to Pro-inflammatory Signaling Pathways. *Journal of Biological Chemistry*, 275, 4670-4678.
- SONG, D. H. & LEE, J.-O. 2012. Sensing of microbial molecular patterns by Toll-like receptors. *Immunological Reviews*, 250, 216-229.
- SOUISSI, I., LADAM, P., COGNET, J., LE COQUIL, S., VARIN-BLANK, N., BARAN-MARSZAK, F., METELEV, V. & FAGARD, R. 2012. A STAT3-inhibitory hairpin decoy oligodeoxynucleotide discriminates between STAT1 and STAT3 and induces death in a human colon carcinoma cell line. *Mol Cancer*, 11, 12.
- STEPHANOU, A., SCARABELLI, T. M., BRAR, B. K., NAKANISHI, Y., MATSUMURA, M., KNIGHT, R. A. & LATCHMAN, D. S. 2001. Induction of Apoptosis and Fas Receptor/Fas Ligand Expression by Ischemia/Reperfusion in Cardiac Myocytes Requires Serine 727 of the STAT-1

- Transcription Factor but Not Tyrosine 701. *Journal of Biological Chemistry*, 276, 28340-28347.
- SUGAWARA, I., YAMADA, H. & MIZUNO, S. 2004. STAT1 knockout mice are highly susceptible to pulmonary mycobacterial infection. *Tohoku J Exp Med*, 202, 41-50.
- SUZUKI, N., SUZUKI, S., DUNCAN, G. S., MILLAR, D. G., WADA, T., MIRTSOS, C., TAKADA, H., WAKEHAM, A., ITIE, A., LI, S., PENNINGER, J. M., WESCHE, H., OHASHI, P. S., MAK, T. W. & YEH, W. C. 2002. Severe impairment of interleukin-1 and Toll-like receptor signalling in mice lacking IRAK-4. *Nature*, 416, 750-6.
- SWANTEK, J. L., TSEN, M. F., COBB, M. H. & THOMAS, J. A. 2000. IL-1 receptor-associated kinase modulates host responsiveness to endotoxin. *J Immunol*, 164, 4301-6.
- TABETA, K., HOEBE, K., JANSSEN, E. M., DU, X., GEORGEL, P., CROZAT, K., MUDD, S., MANN, N., SOVATH, S., GOODE, J., SHAMEL, L., HERSKOVITS, A. A., PORTNOY, D. A., COOKE, M., TARANTINO, L. M., WILTSHIRE, T., STEINBERG, B. E., GRINSTEIN, S. & BEUTLER, B. 2006. The Unc93b1 mutation 3d disrupts exogenous antigen presentation and signaling via Toll-like receptors 3, 7 and 9. *Nat Immunol*, 7, 156-164.
- TAKAESU, G., KISHIDA, S., HIYAMA, A., YAMAGUCHI, K., SHIBUYA, H., IRIE, K., NINOMIYA-TSUJI, J. & MATSUMOTO, K. 2000. TAB2, a novel adaptor protein, mediates activation of TAK1 MAPKKK by linking TAK1 to TRAF6 in the IL-1 signal transduction pathway. *Mol Cell*, 5, 649-58.
- TAKAHASHI, K., SHIBATA, T., AKASHI-TAKAMURA, S., KIYOKAWA, T., WAKABAYASHI, Y., TANIMURA, N., KOBAYASHI, T., MATSUMOTO, F., FUKUI, R., KOURO, T., NAGAI, Y., TAKATSU, K., SAITOH, S. & MIYAKE, K. 2007. A protein associated with Toll-like receptor (TLR) 4 (PRAT4A) is required for TLR-dependent immune responses. *J Exp Med*, 204, 2963-76.
- TAKAOKA, A., YANAI, H., KONDO, S., DUNCAN, G., NEGISHI, H., MIZUTANI, T., KANO, S., HONDA, K., OHBA, Y., MAK, T. W. & TANIGUCHI, T. 2005. Integral role of IRF-5 in the gene induction programme activated by Toll-like receptors. *Nature*, 434, 243-9.
- TAKAUJI, R., IHO, S., TAKATSUKA, H., YAMAMOTO, S., TAKAHASHI, T., KITAGAWA, H., IWASAKI, H., IIDA, R., YOKOCHI, T. & MATSUKI, T. 2002. CpG-DNA-induced IFN-alpha production involves p38 MAPK-dependent STAT1 phosphorylation in human plasmacytoid dendritic cell precursors. *J Leukoc Biol*, 72, 1011-9.
- TAKEDA, K. & AKIRA, S. 2004. TLR signaling pathways. *Semin Immunol*, 16, 3-9.

- TAKEDA, K., CLAUSEN, B. E., KAISHO, T., TSUJIMURA, T., TERADA, N., FÖRSTER, I. & AKIRA, S. 1999. Enhanced Th1 Activity and Development of Chronic Enterocolitis in Mice Devoid of Stat3 in Macrophages and Neutrophils. *Immunity*, 10, 39-49.
- TAKEDA, K., KAISHO, T., YOSHIDA, N., TAKEDA, J., KISHIMOTO, T. & AKIRA, S. 1998. Stat3 Activation Is Responsible for IL-6-Dependent T Cell Proliferation Through Preventing Apoptosis: Generation and Characterization of T Cell-Specific Stat3-Deficient Mice. *The Journal of Immunology*, 161, 4652-4660.
- TAKEDA, K., NOGUCHI, K., SHI, W., TANAKA, T., MATSUMOTO, M., YOSHIDA, N., KISHIMOTO, T. & AKIRA, S. 1997. Targeted disruption of the mouse Stat3 gene leads to early embryonic lethality. *Proceedings of the National Academy of Sciences*, 94, 3801-3804.
- TAKEUCHI, M., ROTHE, M. & GOEDEL, D. V. 1996. Anatomy of TRAF2. *Journal of Biological Chemistry*, 271, 19935-19942.
- TAKEUCHI, O., KAWAI, T., MUHLRADT, P. F., MORR, M., RADOLF, J. D., ZYCHLINSKY, A., TAKEDA, K. & AKIRA, S. 2001. Discrimination of bacterial lipoproteins by Toll-like receptor 6. *Int Immunol*, 13, 933-40.
- TAKEUCHI, O., SATO, S., HORIUCHI, T., HOSHINO, K., TAKEDA, K., DONG, Z., MODLIN, R. L. & AKIRA, S. 2002. Cutting edge: role of Toll-like receptor 1 in mediating immune response to microbial lipoproteins. *J Immunol*, 169, 10-4.
- TAMMINENI, P., ANUGULA, C., MOHAMMED, F., ANJANEYULU, M., LARNER, A. C. & SEPURI, N. B. V. 2013. The Import of the Transcription Factor STAT3 into Mitochondria Depends on GRIM-19, a Component of the Electron Transport Chain. *Journal of Biological Chemistry*, 288, 4723-4732.
- TANIMURA, N., SAITOH, S., MATSUMOTO, F., AKASHI-TAKAMURA, S. & MIYAKE, K. 2008. Roles for LPS-dependent interaction and relocation of TLR4 and TRAM in TRIF-signaling. *Biochem Biophys Res Commun*, 368, 94-9.
- TERMEER, C., BENEDIX, F., SLEEMAN, J., FIEBER, C., VOITH, U., AHRENS, T., MIYAKE, K., FREUDENBERG, M., GALANOS, C. & SIMON, J. C. 2002. Oligosaccharides of Hyaluronan activate dendritic cells via toll-like receptor 4. *J Exp Med*, 195, 99-111.
- THOMAS, J. A., ALLEN, J. L., TSEN, M., DUBNICOFF, T., DANAOK, J., LIAO, X. C., CAO, Z. D. & WASSERMAN, S. A. 1999. Impaired cytokine signaling in mice lacking the IL-1 receptor-associated kinase. *Journal of Immunology*, 163, 978-984.
- TIAN, J., AVALOS, A. M., MAO, S. Y., CHEN, B., SENTHIL, K., WU, H., PARROCHE, P., DRABIC, S., GOLENBOCK, D., SIROIS, C., HUA, J., AN, L. L., AUDOLY, L., LA ROSA, G., BIERHAUS, A.,

- NAWORTH, P., MARSHAK-ROTHSTEIN, A., CROW, M. K., FITZGERALD, K. A., LATZ, E., KIENER, P. A. & COYLE, A. J. 2007. Toll-like receptor 9-dependent activation by DNA-containing immune complexes is mediated by HMGB1 and RAGE. *Nat Immunol*, 8, 487-96.
- TIAN, S. S., LAMB, P., SEIDEL, H. M., STEIN, R. B. & ROSEN, J. 1994. Rapid activation of the STAT3 transcription factor by granulocyte colony-stimulating factor. *Blood*, 84, 1760-4.
- TIMOFEEVA, O. A., CHASOVSKIKH, S., LONSKAYA, I., TARASOVA, N. I., KHAVRUTSKII, L., TARASOV, S. G., ZHANG, X., KOROSTYSHEVSKIY, V. R., CHEEMA, A., ZHANG, L., DAKSHANAMURTHY, S., BROWN, M. L. & DRITSCHILO, A. 2012. Mechanisms of Unphosphorylated STAT3 Transcription Factor Binding to DNA. *Journal of Biological Chemistry*, 287, 14192-14200.
- TIMOFEEVA, O. A., PLISOV, S., EVSEEV, A. A., PENG, S., JOSE-KAMPFNER, M., LOVVORN, H. N., DOME, J. S. & PERANTONI, A. O. 2006. Serine-phosphorylated STAT1 is a prosurvival factor in Wilms' tumor pathogenesis. *Oncogene*, 25, 7555-64.
- TOSHCHAKOV, V., JONES, B. W., PERERA, P. Y., THOMAS, K., CODY, M. J., ZHANG, S., WILLIAMS, B. R., MAJOR, J., HAMILTON, T. A., FENTON, M. J. & VOGEL, S. N. 2002. TLR4, but not TLR2, mediates IFN-beta-induced STAT1alpha/beta-dependent gene expression in macrophages. *Nat Immunol*, 3, 392-8.
- TOWNSEND, P., SCARABELLI, T., DAVIDSON, S., KNIGHT, R., LATCHMAN, D. & STEPHANOU, A. 2004. STAT-1 interacts with p53 to enhance DNA damage-induced apoptosis. *J Biol Chem*, 279, 5811 - 5820.
- TOWNSEND, P. A., CRAGG, M. S., DAVIDSON, S. M., MCCORMICK, J., BARRY, S., LAWRENCE, K. M., KNIGHT, R. A., HUBANK, M., CHEN, P. L., LATCHMAN, D. S. & STEPHANOU, A. 2005. STAT-1 facilitates the ATM activated checkpoint pathway following DNA damage. *J Cell Sci*, 118, 1629-39.
- TRIAANTAFILOU, M., GAMPER, F. G., HASTON, R. M., MOURATIS, M. A., MORATH, S., HARTUNG, T. & TRIANTAFILOU, K. 2006. Membrane sorting of toll-like receptor (TLR)-2/6 and TLR2/1 heterodimers at the cell surface determines heterotypic associations with CD36 and intracellular targeting. *J Biol Chem*, 281, 31002-11.
- TRIAANTAFILOU, M., MIYAKE, K., GOLENBOCK, D. T. & TRIANTAFILOU, K. 2002. Mediators of innate immune recognition of bacteria concentrate in lipid rafts and facilitate lipopolysaccharide-induced cell activation. *J Cell Sci*, 115, 2603-11.
- TRINCHIERI, G. 1995. Interleukin-12: a proinflammatory cytokine with immunoregulatory functions that bridge innate resistance and antigen-specific adaptive immunity. *Annu Rev Immunol*, 13, 251-76.

- TSENG, P. H., MATSUZAWA, A., ZHANG, W., MINO, T., VIGNALI, D. A. & KARIN, M. 2010. Different modes of ubiquitination of the adaptor TRAF3 selectively activate the expression of type I interferons and proinflammatory cytokines. *Nat Immunol*, 11, 70-5.
- TSUBOI, H., WAKAMATSU, E., IIZUKA, M., NAKAMURA, Y., SUGIHARA, M., SUZUKI, T., OGISHIMA, H., HAYASHI, T., GOTO, D., ITO, S., MATSUMOTO, I. & SUMIDA, T. 2011. Importance of serine727 phosphorylated STAT1 in IFN γ -induced signaling and apoptosis of human salivary gland cells. *International Journal of Rheumatic Diseases*, 14, 86-91.
- TURKSON, J. 2004. STAT proteins as novel targets for cancer drug discovery. *Expert Opin Ther Targets*, 8, 409-22.
- TURKSON, J., BOWMAN, T., ADNANE, J., ZHANG, Y., DJEU, J. Y., SEKHARAM, M., FRANK, D. A., HOLZMAN, L. B., WU, J., SEBTI, S. & JOVE, R. 1999. Requirement for Ras/Rac1-Mediated p38 and c-Jun N-Terminal Kinase Signaling in Stat3 Transcriptional Activity Induced by the Src Oncoprotein. *Molecular and Cellular Biology*, 19, 7519-7528.
- TURKSON, J. & JOVE, R. 2000. STAT proteins: novel molecular targets for cancer drug discovery. *Oncogene*, 19, 6613-26.
- TURKSON, J., RYAN, D., KIM, J. S., ZHANG, Y., CHEN, Z., HAURA, E., LAUDANO, A., SEBTI, S., HAMILTON, A. D. & JOVE, R. 2001. Phosphotyrosyl peptides block Stat3-mediated DNA binding activity, gene regulation, and cell transformation. *J Biol Chem*, 276, 45443-55.
- TYE, H., KENNEDY, C. L., NAJDOVSKA, M., MCLEOD, L., MCCORMACK, W., HUGHES, N., DEV, A., SIEVERT, W., OOI, C. H., ISHIKAWA, T. O., OSHIMA, H., BHATHAL, P. S., PARKER, A. E., OSHIMA, M., TAN, P. & JENKINS, B. J. 2012. STAT3-driven upregulation of TLR2 promotes gastric tumorigenesis independent of tumor inflammation. *Cancer Cell*, 22, 466-78.
- UEMATSU, S. & AKIRA, S. 2007. Toll-like receptors and Type I interferons. *J Biol Chem*, 282, 15319-23.
- UEMATSU, S., SATO, S., YAMAMOTO, M., HIROTANI, T., KATO, H., TAKESHITA, F., MATSUDA, M., COBAN, C., ISHII, K. J., KAWAI, T., TAKEUCHI, O. & AKIRA, S. 2005. Interleukin-1 receptor-associated kinase-1 plays an essential role for Toll-like receptor (TLR)7- and TLR9-mediated interferon- α induction. *J Exp Med*, 201, 915-23.
- UNDERHILL, D. M., OZINSKY, A., HAJJAR, A. M., STEVENS, A., WILSON, C. B., BASSETTI, M. & ADEREM, A. 1999. The Toll-like receptor 2 is recruited to macrophage phagosomes and discriminates between pathogens. *Nature*, 401, 811-5.
- UNLU, S., KUMAR, A., WATERMAN, W. R., TSUKADA, J., WANG, K. Z., GALSON, D. L. & AURON, P. E. 2007. Phosphorylation of IRF8 in a pre-associated complex with Spi-1/PU.1 and non-

- phosphorylated Stat1 is critical for LPS induction of the IL1B gene. *Mol Immunol*, 44, 3364-79.
- UZÉ, G., LUTFALLA, G. & GRESSER, I. 1990. Genetic transfer of a functional human interferon α receptor into mouse cells: Cloning and expression of its c-DNA. *Cell*, 60, 225-234.
- VABULAS, R. M., AHMAD-NEJAD, P., GHOSE, S., KIRSCHNING, C. J., ISSELS, R. D. & WAGNER, H. 2002a. HSP70 as endogenous stimulus of the Toll/interleukin-1 receptor signal pathway. *J Biol Chem*, 277, 15107-12.
- VABULAS, R. M., BRAEDEL, S., HILF, N., SINGH-JASUJA, H., HERTER, S., AHMAD-NEJAD, P., KIRSCHNING, C. J., DA COSTA, C., RAMMENSEE, H. G., WAGNER, H. & SCHILD, H. 2002b. The endoplasmic reticulum-resident heat shock protein Gp96 activates dendritic cells via the Toll-like receptor 2/4 pathway. *J Biol Chem*, 277, 20847-53.
- VAHAMIKO, S., PENTTINEN, M. A. & GRANFORS, K. 2005. Aetiology and pathogenesis of reactive arthritis: role of non-antigen-presenting effects of HLA-B27. *Arthritis Res Ther*, 7, 136-41.
- VALLABHAPURAPU, S., MATSUZAWA, A., ZHANG, W., TSENG, P.-H., KEATS, J. J., WANG, H., VIGNALI, D. A. A., BERGSAGEL, P. L. & KARIN, M. 2008. Nonredundant and complementary functions of TRAF2 and TRAF3 in a ubiquitination cascade that activates NIK-dependent alternative NF- κ B signaling. *Nat Immunol*, 9, 1364-1370.
- VARINO, L., RAMSAUER, K., KARAGHIOSOFF, M., KOLBE, T., PFEFFER, K., MULLER, M. & DECKER, T. 2003. Phosphorylation of the Stat1 transactivation domain is required for full-fledged IFN-gamma-dependent innate immunity. *Immunity*, 19, 793-802.
- VELAZQUEZ, L., FELLOUS, M., STARK, G. R. & PELLEGRINI, S. 1992. A protein tyrosine kinase in the interferon alpha/beta signaling pathway. *Cell*, 70, 313-22.
- VERMEULEN, L., DE WILDE, G., NOTEBAERT, S., VANDEN BERGHE, W. & HAEGEMAN, G. 2002. Regulation of the transcriptional activity of the nuclear factor- κ B p65 subunit. *Biochemical Pharmacology*, 64, 963-970.
- VERSTAK, B., HERTZOG, P. & MANSELL, A. 2007. Toll-like receptor signalling and the clinical benefits that lie within. *Inflamm Res*, 56, 1-10.
- VERSTAK, B., NAGPAL, K., BOTTOMLEY, S. P., GOLENBOCK, D. T., HERTZOG, P. J. & MANSELL, A. 2009. MyD88 adapter-like (Mal)/TIRAP interaction with TRAF6 is critical for TLR2- and TLR4-mediated NF- κ B proinflammatory responses. *J Biol Chem*, 284, 24192-203.
- VINKEMEIER, U., COHEN, S. L., MOAREFI, I., CHAIT, B. T., KURIYAN, J. & DARNELL, J. E., JR. 1996. DNA binding of in vitro activated Stat1 alpha, Stat1 beta and truncated Stat1: interaction between NH2-terminal domains stabilizes binding of two dimers to tandem DNA sites. *EMBO J*, 15, 5616-26.

- VINKEMEIER, U., MOAREFI, I., DARNELL, J. E., JR. & KURIYAN, J. 1998. Structure of the amino-terminal protein interaction domain of STAT-4. *Science*, 279, 1048-52.
- VOGEL, R. O., JANSSEN, R. J., VAN DEN BRAND, M. A., DIETEREN, C. E., VERKAART, S., KOOPMAN, W. J., WILLEMS, P. H., PLUK, W., VAN DEN HEUVEL, L. P., SMEITINK, J. A. & NIJTMANS, L. G. 2007. Cytosolic signaling protein Ecsit also localizes to mitochondria where it interacts with chaperone NDUFAF1 and functions in complex I assembly. *Genes Dev*, 21, 615-24.
- VON BERNUTH, H., PICARD, C., JIN, Z., PANKLA, R., XIAO, H., KU, C. L., CHRABIEH, M., MUSTAPHA, I. B., GHANDIL, P., CAMCIOGLU, Y., VASCONCELOS, J., SIRVENT, N., GUEDES, M., VITOR, A. B., HERRERO-MATA, M. J., AROSTEGUI, J. I., RODRIGO, C., ALSINA, L., RUIZ-ORTIZ, E., JUAN, M., FORTUNY, C., YAGUE, J., ANTON, J., PASCAL, M., CHANG, H. H., JANNIERE, L., ROSE, Y., GARTY, B. Z., CHAPEL, H., ISSEKUTZ, A., MARODI, L., RODRIGUEZ-GALLEGO, C., BANCHEREAU, J., ABEL, L., LI, X., CHAUSSABEL, D., PUEL, A. & CASANOVA, J. L. 2008. Pyogenic bacterial infections in humans with MyD88 deficiency. *Science*, 321, 691-6.
- VON BERNUTH, H., PICARD, C., PUEL, A. & CASANOVA, J.-L. 2012. Experimental and natural infections in MyD88- and IRAK-4-deficient mice and humans. *European Journal of Immunology*, 42, 3126-3135.
- WAKABAYASHI, Y., KOBAYASHI, M., AKASHI-TAKAMURA, S., TANIMURA, N., KONNO, K., TAKAHASHI, K., ISHII, T., MIZUTANI, T., IBA, H., KOURO, T., TAKAKI, S., TAKATSU, K., ODA, Y., ISHIHAMA, Y., SAITOH, S. & MIYAKE, K. 2006. A protein associated with toll-like receptor 4 (PRAT4A) regulates cell surface expression of TLR4. *J Immunol*, 177, 1772-9.
- WAKAHARA, R., KUNIMOTO, H., TANINO, K., KOJIMA, H., INOUE, A., SHINTAKU, H. & NAKAJIMA, K. 2012. Phospho-Ser727 of STAT3 regulates STAT3 activity by enhancing dephosphorylation of phospho-Tyr705 largely through TC45. *Genes to Cells*, 17, 132-145.
- WANG, C., DENG, L., HONG, M., AKKARAJU, G. R., INOUE, J. & CHEN, Z. J. 2001. TAK1 is a ubiquitin-dependent kinase of MKK and IKK. *Nature*, 412, 346-351.
- WANG, H., BLOOM, O., ZHANG, M., VISHNUBHAKAT, J. M., OMBRELLINO, M., CHE, J., FRAZIER, A., YANG, H., IVANOVA, S., BOROVIKOVA, L., MANOGUE, K. R., FAIST, E., ABRAHAM, E., ANDERSSON, J., ANDERSSON, U., MOLINA, P. E., ABUMRAD, N. N., SAMA, A. & TRACEY, K. J. 1999. HMG-1 as a late mediator of endotoxin lethality in mice. *Science*, 285, 248-51.
- WANG, J., SHAO, Y., BENNETT, T. A., SHANKAR, R. A., WIGHTMAN, P. D. & REDDY, L. G. 2006. The functional effects of physical interactions among Toll-like receptors 7, 8, and 9. *J Biol Chem*, 281, 37427-34.
- WANG, Y., LIU, L., DAVIES, D. R. & SEGAL, D. M. 2010. Dimerization of Toll-like receptor 3 (TLR3) is required for ligand binding. *J Biol Chem*, 285, 36836-41.

- WEGRZYN, J., POTLA, R., CHWAE, Y. J., SEPURI, N. B., ZHANG, Q., KOECK, T., DERECKA, M., SZCZEPANEK, K., SZELAG, M., GORNICKA, A., MOH, A., MOGHADDAS, S., CHEN, Q., BOBBILI, S., CICHY, J., DULAK, J., BAKER, D. P., WOLFMAN, A., STUEHR, D., HASSAN, M. O., FU, X. Y., AVADHANI, N., DRAKE, J. I., FAWCETT, P., LESNEFSKY, E. J. & LARNER, A. C. 2009. Function of mitochondrial Stat3 in cellular respiration. *Science*, 323, 793-7.
- WEI, J., YUAN, Y., JIN, C., CHEN, H., LENG, L., HE, F. & WANG, J. 2012. The Ubiquitin Ligase TRAF6 Negatively Regulates the JAK-STAT Signaling Pathway by Binding to STAT3 and Mediating Its Ubiquitination. *PLoS ONE*, 7, e49567.
- WEN, Z. & DARNELL, J. E., JR. 1997. Mapping of Stat3 serine phosphorylation to a single residue (727) and evidence that serine phosphorylation has no influence on DNA binding of Stat1 and Stat3. *Nucleic Acids Res*, 25, 2062-7.
- WEN, Z., ZHONG, Z. & DARNELL, J. E., JR. 1995. Maximal activation of transcription by Stat1 and Stat3 requires both tyrosine and serine phosphorylation. *Cell*, 82, 241-50.
- WERTS, C., GIRARDIN, S. E. & PHILPOTT, D. J. 2006. TIR, CARD and PYRIN: three domains for an antimicrobial triad. *Cell Death Differ*, 13, 798-815.
- WERTZ, I. E., O'ROURKE, K. M., ZHOU, H., EBY, M., ARAVIND, L., SESHAGIRI, S., WU, P., WIESMANN, C., BAKER, R., BOONE, D. L., MA, A., KOONIN, E. V. & DIXIT, V. M. 2004. De-ubiquitination and ubiquitin ligase domains of A20 downregulate NF-kappaB signalling. *Nature*, 430, 694-9.
- WESCHE, H., GAO, X., LI, X., KIRSCHNING, C. J., STARK, G. R. & CAO, Z. 1999. IRAK-M is a novel member of the Pelle/interleukin-1 receptor-associated kinase (IRAK) family. *J Biol Chem*, 274, 19403-10.
- WESCHE, H., HENZEL, W. J., SHILLINGLAW, W., LI, S. & CAO, Z. D. 1997. MyD88: An adapter that recruits IRAK to the IL-1 receptor complex. *Immunity*, 7, 837-847.
- WEST, A. P., BRODSKY, I. E., RAHNER, C., WOO, D. K., ERDJUMENT-BROMAGE, H., TEMPST, P., WALSH, M. C., CHOI, Y., SHADEL, G. S. & GHOSH, S. 2011. TLR signalling augments macrophage bactericidal activity through mitochondrial ROS. *Nature*, 472, 476-80.
- WHEELER, D. S., CHASE, M. A., SENFT, A. P., POYNTER, S. E., WONG, H. R. & PAGE, K. 2009. Extracellular Hsp72, an endogenous DAMP, is released by virally infected airway epithelial cells and activates neutrophils via Toll-like receptor (TLR)-4. *Respir Res*, 10, 31.
- WIETEK, C., MIGGIN, S. M., JEFFERIES, C. A. & O'NEILL, L. A. 2003. Interferon regulatory factor-3-mediated activation of the interferon-sensitive response element by Toll-like receptor (TLR) 4 but not TLR3 requires the p65 subunit of NF-kappa. *J Biol Chem*, 278, 50923-31.

- WINDHEIM, M., STAFFORD, M., PEGGIE, M. & COHEN, P. 2008. Interleukin-1 (IL-1) induces the Lys63-linked polyubiquitination of IL-1 receptor-associated kinase 1 to facilitate NEMO binding and the activation of I κ B kinase. *Mol Cell Biol*, 28, 1783-91.
- WONG, S. W., KWON, M. J., CHOI, A. M., KIM, H. P., NAKAHIRA, K. & HWANG, D. H. 2009. Fatty acids modulate Toll-like receptor 4 activation through regulation of receptor dimerization and recruitment into lipid rafts in a reactive oxygen species-dependent manner. *J Biol Chem*, 284, 27384-92.
- WU, H. & ARRON, J. R. 2003. TRAF6, a molecular bridge spanning adaptive immunity, innate immunity and osteoimmunology. *Bioessays*, 25, 1096-105.
- XU, Y., TAO, X., SHEN, B., HORNG, T., MEDZHITOV, R., MANLEY, J. L. & TONG, L. 2000. Structural basis for signal transduction by the Toll/interleukin-1 receptor domains. *Nature*, 408, 111-5.
- YAMAMOTO, M., SATO, S., HEMMI, H., HOSHINO, K., KAISHO, T., SANJO, H., TAKEUCHI, O., SUGIYAMA, M., OKABE, M., TAKEDA, K. & AKIRA, S. 2003a. Role of adaptor TRIF in the MyD88-independent toll-like receptor signaling pathway. *Science*, 301, 640-643.
- YAMAMOTO, M., SATO, S., HEMMI, H., SANJO, H., UEMATSU, S., KAISHO, T., HOSHINO, K., TAKEUCHI, O., KOBAYASHI, M., FUJITA, T., TAKEDA, K. & AKIRA, S. 2002a. Essential role for TIRAP in activation of the signalling cascade shared by TLR2 and TLR4. *Nature*, 420, 324-9.
- YAMAMOTO, M., SATO, S., HEMMI, H., UEMATSU, S., HOSHINO, K., KAISHO, T., TAKEUCHI, O., TAKEDA, K. & AKIRA, S. 2003b. TRAM is specifically involved in the Toll-like receptor 4-mediated MyD88-independent signaling pathway. *Nat Immunol*, 4, 1144-1150.
- YAMAMOTO, M., SATO, S., MORI, K., HOSHINO, K., TAKEUCHI, O., TAKEDA, K. & AKIRA, S. 2002b. Cutting edge: A novel toll/IL-1 receptor Domain containing adapter that preferentially activates the IFN-beta promoter in the toll-like receptor signaling. *Journal of Immunology*, 169, 6668-6672.
- YAMAMOTO, M., TAKEDA, K. & AKIRA, S. 2004. TIR domain-containing adaptors define the specificity of TLR signaling. *Molecular Immunology*, 40, 861-868.
- YAMAWAKI, Y., KIMURA, H., HOSOI, T. & OZAWA, K. 2010. MyD88 plays a key role in LPS-induced Stat3 activation in the hypothalamus. *American Journal of Physiology - Regulatory, Integrative and Comparative Physiology*, 298, R403-R410.
- YAMIN, T. T. & MILLER, D. K. 1997. The interleukin-1 receptor-associated kinase is degraded by proteasomes following its phosphorylation. *J Biol Chem*, 272, 21540-7.
- YANG, C.-H., SHI, W., BASU, L., MURTI, A., CONSTANTINESCU, S. N., BLATT, L., CROZE, E., MULLERSMAN, J. E. & PFEFFER, L. M. 1996. Direct Association of STAT3 with the IFNAR-1

- Chain of the Human Type I Interferon Receptor. *Journal of Biological Chemistry*, 271, 8057-8061.
- YANG, C. S., KIM, J. J., LEE, S. J., HWANG, J. H., LEE, C. H., LEE, M. S. & JO, E. K. 2013. TLR3-Triggered Reactive Oxygen Species Contribute to Inflammatory Responses by Activating Signal Transducer and Activator of Transcription-1. *J Immunol*, 190, 6368-77.
- YANG, E., WEN, Z., HASPEL, R. L., ZHANG, J. J. & DARNELL, J. E. 1999. The Linker Domain of Stat1 Is Required for Gamma Interferon-Driven Transcription. *Molecular and Cellular Biology*, 19, 5106-5112.
- YANG, J., LIAO, X., AGARWAL, M. K., BARNES, L., AURON, P. E. & STARK, G. R. 2007a. Unphosphorylated STAT3 accumulates in response to IL-6 and activates transcription by binding to NFkappaB. *Genes Dev*, 21, 1396-408.
- YANG, Y., LIU, B., DAI, J., SRIVASTAVA, P. K., ZAMMIT, D. J., LEFRANCOIS, L. & LI, Z. 2007b. Heat shock protein gp96 is a master chaperone for toll-like receptors and is important in the innate function of macrophages. *Immunity*, 26, 215-26.
- YE, H., ARRON, J. R., LAMOTHE, B., CIRILLI, M., KOBAYASHI, T., SHEVDE, N. K., SEGAL, D., DZIVENU, O. K., VOLOGODSKAIA, M., YIM, M., DU, K., SINGH, S., PIKE, J. W., DARNAY, B. G., CHOI, Y. & WU, H. 2002. Distinct molecular mechanism for initiating TRAF6 signalling. *Nature*, 418, 443-7.
- YI, A. K., TUETKEN, R., REDFORD, T., WALDSCHMIDT, M., KIRSCH, J. & KRIEG, A. M. 1998. CpG motifs in bacterial DNA activate leukocytes through the pH-dependent generation of reactive oxygen species. *J Immunol*, 160, 4755-61.
- YIN, Q., LIN, S. C., LAMOTHE, B., LU, M., LO, Y. C., HURA, G., ZHENG, L., RICH, R. L., CAMPOS, A. D., MYSZKA, D. G., LENARDO, M. J., DARNAY, B. G. & WU, H. 2009. E2 interaction and dimerization in the crystal structure of TRAF6. *Nat Struct Mol Biol*, 16, 658-66.
- YONEYAMA, M. & FUJITA, T. 2007. RIG-I family RNA helicases: Cytoplasmic sensor for antiviral innate immunity. *Cytokine & Growth Factor Reviews*, 18, 545-551.
- YOO, J.-Y., HUSO, D. L., NATHANS, D. & DESIDERIO, S. 2002. Specific Ablation of Stat3 β Distorts the Pattern of Stat3-Responsive Gene Expression and Impairs Recovery from Endotoxic Shock. *Cell*, 108, 331-344.
- YOON, S.-I., KURNASOV, O., NATARAJAN, V., HONG, M., GUDKOV, A. V., OSTERMAN, A. L. & WILSON, I. A. 2012. Structural Basis of TLR5-Flagellin Recognition and Signaling. *Science*, 335, 859-864.

- YOSHIDA, Y., KUMAR, A., KOYAMA, Y., PENG, H., ARMAN, A., BOCH, J. A. & AURON, P. E. 2003. IL-1 activates Stat3/NF-kappa B cross-talk via a unique TRAF6 and p65-dependent mechanism. *J. Biol. Chem.*, M311498200.
- YOUN, H. S., LEE, J. Y., FITZGERALD, K. A., YOUNG, H. A., AKIRA, S. & HWANG, D. H. 2005. Specific inhibition of MyD88-independent signaling pathways of TLR3 and TLR4 by resveratrol: Molecular targets are TBK1 and RIP1 in TRIF complex. *Journal of Immunology*, 175, 3339-3346.
- YU, C. L., MEYER, D. J., CAMPBELL, G. S., LARNER, A. C., CARTER-SU, C., SCHWARTZ, J. & JOVE, R. 1995. Enhanced DNA-binding activity of a Stat3-related protein in cells transformed by the Src oncoprotein. *Science*, 269, 81-3.
- YU, H. & JOVE, R. 2004. The STATs of cancer [mdash] new molecular targets come of age. *Nat Rev Cancer*, 4, 97-105.
- YU, H., PARDOLL, D. & JOVE, R. 2009. STATs in cancer inflammation and immunity: a leading role for STAT3. *Nat Rev Cancer*, 9, 798-809.
- YUAN, X., ZHOU, Y., WANG, W., LI, J., XIE, G., ZHAO, Y., XU, D. & SHEN, L. 2013. Activation of TLR4 signaling promotes gastric cancer progression by inducing mitochondrial ROS production. *Cell Death Dis*, 4, e794.
- YUE, P. & TURKSON, J. 2009. Targeting STAT3 in cancer: how successful are we? *Expert Opin Investig Drugs*, 18, 45-56.
- ZAKHAROVA, N., LYMAR, E. S., YANG, E., MALIK, S., ZHANG, J. J., ROEDER, R. G. & DARNELL, J. E. 2003. Distinct Transcriptional Activation Functions of STAT1 α and STAT1 β on DNA and Chromatin Templates. *Journal of Biological Chemistry*, 278, 43067-43073.
- ZANETTI, M., GENNARO, R. & ROMEO, D. 1997. The cathelicidin family of antimicrobial peptide precursors: a component of the oxygen-independent defense mechanisms of neutrophils. *Ann N Y Acad Sci*, 832, 147-62.
- ZHANG, J., YANG, J., ROY, S. K., TINININI, S., HU, J., BROMBERG, J. F., POLI, V., STARK, G. R. & KALVAKOLANU, D. V. 2003. The cell death regulator GRIM-19 is an inhibitor of signal transducer and activator of transcription 3. *Proc Natl Acad Sci U S A*, 100, 9342-7.
- ZHANG, Q., RAJE, V., YAKOVLEV, V. A., YACOUB, A., SZCZEPANEK, K., MEIER, J., DERECKA, M., CHEN, Q., HU, Y., SISLER, J., HAMED, H., LESNEFSKY, E. J., VALERIE, K., DENT, P. & LARNER, A. C. 2013. Mitochondrial-Localized Stat3 Promotes Breast Cancer Growth via Phosphorylation of Serine 727. *Journal of Biological Chemistry*.
- ZHAO, H., JOSEPH, J., FALES, H. M., SOKOLOSKI, E. A., LEVINE, R. L., VASQUEZ-VIVAR, J. & KALYANARAMAN, B. 2005. Detection and characterization of the product of

- hydroethidine and intracellular superoxide by HPLC and limitations of fluorescence. *Proc Natl Acad Sci U S A*, 102, 5727-32.
- ZHONG, Z., WEN, Z. & DARNELL, J. E., JR. 1994. Stat3: a STAT family member activated by tyrosine phosphorylation in response to epidermal growth factor and interleukin-6. *Science*, 264, 95-8.
- ZHOU, R., TARDIVEL, A., THORENS, B., CHOI, I. & TSCHOPP, J. 2010. Thioredoxin-interacting protein links oxidative stress to inflammasome activation. *Nat Immunol*, 11, 136-40.
- ZHOU, R., YAZDI, A. S., MENU, P. & TSCHOPP, J. 2011. A role for mitochondria in NLRP3 inflammasome activation. *Nature*, 469, 221-225.
- ZHU, J., NATHAN, C., JIN, W., SIM, D., ASHCROFT, G. S., WAHL, S. M., LACOMIS, L., ERDJUMENT-BROMAGE, H., TEMPST, P., WRIGHT, C. D. & DING, A. 2002. Conversion of proepithelin to epithelins: roles of SLPI and elastase in host defense and wound repair. *Cell*, 111, 867-78.
- ZHU, J. G., HUANG, X. P. & YANG, Y. P. 2007. Innate immune response to adenoviral vectors is mediated by both Toll-like receptor-dependent and -independent pathways. *Journal of Virology*, 81, 3170-3180.
- ZHU, X., WEN, Z., XU, L. Z. & DARNELL, J. E., JR. 1997. Stat1 serine phosphorylation occurs independently of tyrosine phosphorylation and requires an activated Jak2 kinase. *Mol Cell Biol*, 17, 6618-23.